PO Box 2345, Beijing 100023, China
Fax: +86-10-85381893
E-mail: wjg@wjgnet.com www.wjgnet.com

World J Gastroenterol 2004;10(23):3389-3393
World Journal of Gastroenterology
Copyright © 2004 by The WJG Press ISSN 1007-9327

• ESOPHAGEAL CANCER •

GSTM1, *GSTT1*, *GSTP1* and *CYP1A1* genetic polymorphisms and susceptibility to esophageal cancer in a French population: Different pattern of squamous cell carcinoma and adenocarcinoma

Ahmed Abbas, Karine Delvinquière, Mathilde Lechevrel, Pierre Lebailly, Pascal Gauduchon, Guy Launoy, François Sichel

Ahmed Abbas, Karine Delvinquière, Mathilde Lechevrel, Pierre Lebailly, Pascal Gauduchon, François Sichel, GRECAN-EA1772, UFR des Sciences Pharmaceutiques, Université de Caen Basse-Normandie et Centre François Baclesse, Avenue du Général Harris, 14076 Caen cedex 05, France
Guy Launoy, GRECAN-EA1772, Université de Caen Basse-Normandie et Registre des Tumeurs Digestives du Calvados, UFR de Médecine, Avenue de la Côte de Nacre, 14032 Caen cedex, France
Supported by the Grants From Ligue Nationale Contre le Cancer, Comités Départementaux de la Manche, de l'Orne et du Calvados and from Université de Metz
Correspondence to: François Sichel, GRECAN-EA1772, UFR des Sciences Pharmaceutiques, Université de Caen Basse-Normandie et Centre François Baclesse, Avenue du Général Harris, 14076 Caen cedex 05, France. f.sichel@baclesse.fr
Telephone: +33-231-455070 **Fax:** +33-231-455172
Received: 2004-02-20 **Accepted:** 2004-04-27

Abstract

AIM: To evaluate the association between *CYP1A1* and *GSTs* genetic polymorphisms and susceptibility to esophageal squamous cell carcinoma (SCC) and esophageal adenocarcinoma (ADC) in a high risk area of northwest of France.

METHODS: A case-control study was conducted to investigate the genetic polymorphisms of these enzymes (*CYP1A1*2C* and *GSTP1* exon 7 Val alleles, *GSTM1*2/*2* and *GSTT1*2/*2* null genotypes). A total of 79 esophageal cancer cases and 130 controls were recruited.

RESULTS: *GSTM1*2/*2* and *CYP1A1*1A/*2C* genotype frequencies were higher among squamous cell carcinomas at a level close to statistical significance (OR = 1.83, 95% CI 0.88-3.83, $P = 0.11$; OR = 3.03, 95% CI 0.93-9.90, $P = 0.07$, respectively). For *GSTP1* polymorphism, no difference was found between controls and cases, whatever their histological status. Lower frequency of *GSTT1* deletion was observed in ADC group compared to controls with a statistically significant difference (OR = 13.31, 95% CI 1.66-106.92, $P<0.01$).

CONCLUSION: In SCC, our results are consistent with the strong association of this kind of tumour with tobacco exposure. In ADC, our results suggest 3 distinct hypotheses: (1) activation of exogenous procarcinogens, such as small halogenated compounds by *GSTT1*; (2) contribution of *GSTT1* to the inflammatory response of esophageal mucosa, which is known to be a strong risk factor for ADC, possibly through leukotriene synthesis; (3) higher sensitivity to the inflammatory process associated with intracellular depletion of glutathione.

Abbas A, Delvinquière K, Lechevrel M, Lebailly P, Gauduchon P, Launoy G, Sichel F. *GSTM1*, *GSTT1*, *GSTP1* and *CYP1A1* genetic polymorphisms and susceptibility to esophageal cancer in a French population: Different pattern of squamous cell carcinoma and adenocarcinoma. *World J Gastroenterol* 2004; 10(23): 3389-3393
http://www.wjgnet.com/1007-9327/10/3389.asp

INTRODUCTION

One of the highest incidences of esophageal cancer in Europe is observed in the Northwest of France[1-4]. There are two predominant histological forms of this cancer: squamous cell carcinoma (SCC) and adenocarcinoma (ADC)[4,5]. Recent epidemiological observations showed an important decrease in the incidence of SCC whilst ADC was slightly increased[2,4].

In Western countries, smoking tobacco and drinking alcohol are the main risk factors for SCC. For ADC, exogenous risk factors are not well known. A link was found between this pathology, esophageal reflux and Barret's esophagus[5].

Tobacco smoke contains many carcinogens such as polycyclic aromatic hydrocarbons (PAH) and *N*-nitrosamines that can be activated or deactivated by phase I (cytochromes P-450) and phase II enzymes (glutathione S-transferases). Cytochromes P450 (CYP) are a widely expressed enzyme family, some members of which present genetic polymorphisms (e.g. *CYP1A1*, *2E1*, *2D6*). *CYP1A1* is expressed in esophageal mucosa, which means that activation of tobacco carcinogens can happen *in situ*[6]. Benzo[a]pyrene is activated by *CYP1A1* to diol-epoxide, which is a reactive and carcinogenic product. Four main genetic polymorphisms are described for *CYP1A1*. One of the most studied is Ile/Val polymorphism in exon 7 (*CYP1A1*2C* allele). One study reported that Val-type could be associated with a higher aryl hydrocarbon hydroxylase activity[7].

Many studies have reported the association of *CYP1A1* polymorphisms with lung cancer[8], particularly with SCC of the lung[9,10]. The level of DNA adducts was found to be linked to *CYP1A1*2C* polymorphism[11]. All these results suggest that susceptibility to tobacco-related cancers could be modified by *CYP1A1* polymorphisms.

The glutathione S-transferases are a family of phase II enzymes, which catalyse the conjugation of many endogenous and exogenous electrophilic compounds to glutathione. GSTM1 and GSTP1 are able to detoxify benzopyrene diol-epoxide[12], whereas GSTT1 can conjugate oxidised lipids and halogenated compounds[12]. Both *GSTM1*, *P1* and *T1* are expressed in esophageal mucosa[13,14]. GSTP1 is the mainly expressed GST in this tissue[15]. *GSTP1* presents a substitution polymorphism in exon 7 that results in a substitution of Ile by Val at amino acid position 104[16]. Val variants were found to have a lower activity towards 1-chloro-2, 4-dinitrobenzene[17]. *GSTM1* and *GSTT1* present deletion polymorphisms (*GSTM1*2/*2* and *GSTT1*2/*2*), which are currently at about 50% and 20% among Caucasians, respectively[18,19]. *GSTM1*2/*2* polymorphism has been found to increase the frequency of chromosome aberrations after tobacco-specific *N*-nitrosamine exposure *in vitro*[20]. Many studies have shown that this deletion increases the susceptibility conferred by the *CYP1A1*2C* allele for tobacco-associated cancer[21]. While *GSTT1*2/*2* genotypes have not been clearly

associated with susceptibility to tobacco-linked cancers, an interaction with *GSTM1*2/*2* has often been found[22,23].

The aim of our work was to evaluate the susceptibility conferred by *CYP1A1* and *GSTs* genetic polymorphisms to SCC and ADC of esophagus in a high risk European area.

MATERIALS AND METHODS

Controls and cases were from the geographic area of Basse-Normandie, France. Patients were recruited after endoscopic and histologic diagnosis of primary esophageal cancer. All cases were newly diagnosed and previously untreated patients. Controls were required to be free of any chronic diseases, having no cancer history and living in Basse-Normandie. They were matched with cases in sex and age. Alcohol and tobacco consumption were also evaluated during the recruitment of cases and controls by means of a questionnaire.

The research protocol was approved by the Comité Consultatif pour la Protection des Personnes dans la Recherche Biomédical en Basse-Normandie. A 20 mL sample of venous blood was taken and DNA extraction was performed by phenol/chloroform method.

The primer sequences and product sizes of each gene amplification are shown in Table 1. *GSTM1* and *GSTT1* multiplex PCR was performed according to the Lin *et al*. method[24], with some modifications. A final mixture volume of 25 µL was prepared containing 0.100 µg of DNA, 0.25 µmol/L of dNTP, 0.4 µmol/L of primer for *GSTM1*, 0.8 µmol/L of primer *GSTT1*, 0.8 µmol/L of primer albumin, 5 µL of 10× buffer, 2 mmol/L of $MgCl_2$ and 0.5 U per sample of DNA Gold *Taq* polymerase (Applied Biosystem, Coutaboeuf, France). The first step was performed for 15 min at 95℃ followed by 35 cycles: at 94 ℃ for 1 min (denaturation), at 58 ℃ for 1 min (annealing), at 72 ℃ for 1 min (elongation). PCR ended a final extension for 10 min at 72 ℃. PCR products were visualised on 20 g/L agarose gel with ethidium bromide staining.

Table 1 Primer sequences and length of PCR products

Gene	Primer sequence	Size of PCR product (bp)	Reference
GSTM1	5'-GAACTCCCTGAAAAGCTAAAGC-3'	219	Lin *et al*, 1998[24]
	5'-GTTGGGCTCAAATATACGGTGG-3'		
GSTT1	5'-TTCCTTACTGGTCCTCACATCTC-3'	459	
	5'-TCACCGGATCATGGCCAGCA-3'		
Albumin	5'-GCCCTCTGCTAACAAGTCCTAC-3'	350	
	5'-GCCCTAAAAAGAAAATCCCCAATC-3'		
GSTP1	5'-ACCCCAGGGCTCTATGGGAA-3'	176	Harries *et al*, 1997[16]
	5'-TGAGGGCACAAGAAGCCCCT-3'		
CYP1A1	5'-GGCTGAGCAATCTGACCCTA-3'	206	Cascorbi *et al*, 1996[8]
	5'-TTCCACCCGTTGCAGCAGGATAGCC-3'		

GSTP1 PCR restriction fragment length polymorphism (rflp) was performed using a method adopted by Harries *et al*.[16] with slight modifications. The final mixture (40 µL) was prepared containing 0.100-0.500 µg of DNA, 0.25 µmol/L of dNTP, 0.25 µmol/L of each of the primers, 1.25 µmol/L of $MgCl_2$, 4 µL of 10× buffer, 4 µL of DMSO, 1.5 U of *Taq* polymerase (Eurobio, Les Ulis, France). Briefly, the samples were denatured at 94 ℃ for 5 min and submitted to 30 cycles of amplification as follows: for 30 s at 94 ℃ (denaturation), for 30 s at 55 ℃ (annealing), for 30 s at 72 ℃ (extension) and a final extension at 72 ℃ for 5 min. PCR product of 12 µL was digested by 5 U Alw26 I restriction enzyme (Eurogentec, Seraing, Belgium) for 12 h at 37 ℃. Migration was performed on low melting 40 g/L agarose gel (Eurobio, Les Ulis, France), stained with ethidium bromide, in order to separate the 85 and 91 bp fragments.

*CYP1A1*2C* polymorphism was determined by PCR-RFLP as previously described[8].

Each PCR analysis was performed twice in double blind.

Statistical analysis

Chi-square test and *P* value estimation were performed using Stata software (STATA Corporation, college Station, TX). Odds ratio was also evaluated using StataÒ software and adjusted for age, sex and histological type.

RESULTS

The populations of controls and cases are described in Table 2. The patient group consisted of 52 SCCs and 27 ADCs. The mean ages for cases and controls were 62 and 56 years respectively. Unfortunately, we obtained tobacco and alcohol exposure data for only 48 cases. This was insufficient to allow us to study interaction between exposure and polymorphisms. As it could be expected, the vast majority of SCCs were smokers (93%, all with more than 20 years of tobacco consumption) and heavy drinkers (86% drinking more than 229 g/wk). Fewer ADCs were smokers (78%, of which 67 % with more than 20 years of tobacco consumption) and only 50% were heavy drinkers (Table 2).

Table 2 Description of control and case populations

	Control *n* (%)	Case *n* (%)	SCC *n* (%)	ADC *n* (%)
Male	87 (0.67)	69 (0.87)	44 (0.85)	25 (0.93)
Female	43 (0.33)	10 (0.13)	8 (0.15)	2 (0.07)
Mean age (yr)	56 [19; 87]	62 [40; 85]	60 [40; 78]	66 [51; 85]
Tobacco duration[1,2]				
(*years of smoking*)				
Non-smokers	66 (0 .66)	6 (0.13)	2 (0.07)	4 (0.22)
1-19	13 (0.13)	2 (0.04)	0 (-)	2 (0.11)
+20	21 (0.21)	40 (0.83)	28 (0.93)	12 (0.67)
Alcohol consumption[3,4]				
(*g of ethanol per week*)				
0-228	11 (0.64)	13 (0.28)	4 (0.14)	9 (0.50)
228.5 - / + 470	6 (0.36)	35 (0.72)	26 (0.86)	9 (0.50)

[1]Tobacco duration (year); [2]Data were available for 77% of controls, 61% of cases, including 58% of SCC and 67% of ADC; [3]Alcohol consumption (gram of ethanol per week); [4]Data for alcohol consumption were available for only 13% of controls, 61% of cases, including 58% of SCC and 67% of ADC.

Frequencies of the different genetic polymorphisms in the control group were 0.06 for *CYP1A1*A/*2C* (no homozygous **2C/*2C* subject was found), 0.45 and 0.07 for Ile/Val and Val/Val *GSTP1* genotypes, 0.49 for *GSTM1*2/*2* and 0.26 for *GSTT1*2/*2* (Tables 3, 4).

A high frequency of *CYP1A1*1A/*2C* genotype was found in SCC cancer patients (Table 3). However, the difference did not reach statistical significance (with a *P* value of 0.06). The ADC patient group did not show any significant difference compared to the control group.

*GSTM1*2/*2* genotype (*GST M1* null) was increased among the cases compared to the controls, particularly among SCC patients (Table 4), but this difference was not statistically significant (OR = 1.83; 95% CI = 0.88-3.83). The distribution of *GSTM1*2/*2* genotype among ADCs did not differ from the controls.

The frequency of *GSTT1*2/*2* genotype (*GSTT1* null) was not different between cases and controls (Table 5). However, the ADC group showed a greatly decreased frequency of *GSTT1*2/*2* genotype (4%) compared to the control population (26%) and SCCs (29%) (OR = 13.31, 95 % CI = 1.66-106.92).

Distribution of the *GSTP1* genotype did not differ between SCC, ADC and control groups (Table 6).

Table 3 Repartition of *CYP1A1* genotypes among controls and cases

	n	CYP1A1*1A/*1A		CYP1A1*1A/*2C			OR[1]	95% CI
		n	(%)	*n*	(%)			
Controls	107	101	(94)	6	(6)			
Cases	70	61	(87)	9	(13)	All cases *vs* controls[2]	2.63	[0.84-8.28]
SCC	47	40	(85)	7	(15)	SCC *vs* controls[3]	3.03	[0.93-9.90][5]
ADC	23	21	(91)	2	(9)	ADC *vs* controls[4]	2.06	[0.33-13.04]

[1]Adjusted OR for age and sex; [2]Comparison of *CYP1A1*1A/*2C* genotype repartition in controls *vs* all cases; [3]Comparison of *CYP1A1*1A/*2C* genotype repartition in controls *vs* SCCs; [4]Comparison of *CYP1A1*1A/*2C* genotype repartition in controls *vs* ADCs; [5]$P = 0.067$.

Table 4 Repartition of *GSTM1* genotypes among controls and cases

	n	*GSTM1*2/*2*			OR[1]	95% CI
		n	(%)			
Controls	120	59	(49)			
Cases	68	39	(57)	All cases *vs* controls[2]	1.43	[0.76-2.69]
SCC	43	27	(63)	SCC *vs* controls[3]	1.83	[0.88-3.83][5]
ADC	25	12	(48)	ADC *vs* controls[4]	0.95	[0.38-2.41]

[1]Adjusted OR for age and sex; [2]Comparison of *GSTM1*2/*2* genotype repartition in controls *vs* all cases; [3]Comparison of *GSTM1*2/*2* genotype repartition in controls *vs* SCCs; [4]Comparison of *GSTM1*2/*2* genotype repartition in controls *vs* ADCs; [5]$P = 0.108$.

Table 5 Repartition of *GSTT1* genotypes among controls and cases

	n	*GSTT1*2/*2*			OR[1]	95% CI
		n	(%)			
Controls	115	30	(26)			
Cases	70	14	(20)	All cases *vs* controls[2]	1.78	[0.84-3.80]
SCC	44	13	(29)	SCC *vs* controls[3]	1.03	[0.46-2.27]
ADC	26	1	(4)	ADC *vs* controls[4]	13.31	[1.66-106.92][a]

[1]Adjusted OR for age and sex; [2]Comparison of *GSTT1*2/*2* genotype repartition in controls *vs* all cases; [3]Comparison of *GSTT1*2/*2* genotype repartition in controls *vs* SCCs; [4]Comparison of *GSTT1*2/*2* genotype repartition in controls *vs* ADCs; [a]$P<0.05$.

Table 6 Repartition of *GSTP1* genotypes among controls and cases

	n	*GSTP1*							OR[1,2]	95% CI
		Ile/Ile		Ile/Val		Val/Val				
		n	(%)	*n*	(%)	*n*	(%)			
Controls	124	59	(48)	56	(45)	9	(7)			
Cases	70	31	(44)	33	(47)	6	(9)	All cases *vs* controls[3]	1.02	[0.55-1.89]
SCC	45	21	(47)	21	(47)	3	(6)	SCC *vs* controls[4]	0.95	[0.47-1.91]
ADC	25	10	(40)	12	(48)	3	(12)	ADC *vs* controls[5]	1.17	[0.46-2.97]

[1]Adjusted OR for age and sex; [2]Ile/Val and Val/Val genotypes were compared to Ile/Ile genotype; [3]Comparison of *GSTP1* Ile/Val and Val/Val genotype repartition in controls versus all cases; [4]Comparison of *GSTP1* Ile/Val and Val/Val genotype repartition in controls *vs* SCCs; [5]Comparison of *GSTP1* Ile/Val and Val/Val genotype repartition in controls *vs* ADCs.

DISCUSSION

Esophageal cancer presents a very variable incidence in different regions and ethnic groups. In France, different levels of environmental exposure to carcinogens could not fully explain this high variability[25-27], a fact which suggests a genetic susceptibility. Many epidemiological studies have established that exposure to tobacco smoke and alcohol is a major risk factor for SCC in Western countries, whereas ADC is not strongly linked to exogenous factors. As far as we know, only one study concerning the genetic susceptibility to esophageal cancer was performed among Caucasians[28]. Moreover, the cases for this study were recruited in a low risk area in Europe.

The repartition of different polymorphisms in our control group agrees with available data for a Caucasian population[8,16,18,19,29]. Recently, frequencies of these polymorphisms among a healthy population were evaluated and published by International Collaborative Study on Genetic Susceptibility to Environmental Carcinogens (GSEC)[18].

Among SCC cases, *CYP1A1*2A/*2C* frequency was increased when compared to controls and adjusted OR was 3.03 (95% CI 0.93-9.90), however this result was not statistically significant ($P = 0.067$). The deletion of *GSTM1* gene was also more frequent among SCC cases when compared to controls (63% and 49% respectively, OR = 1.83; 0.88-3.83). But this result was also not statistically significant ($P = 0.108$). *CYP1A1*2A/*2C* and *GSTM1*2/*2* genotypes were found to increase the risk of SCC in a previous study in an Asian population, particularly among cases with higher tobacco consumption. However, some studies did not find *CYP1A1* and *GSTM1* gene polymorphisms to be related to SCC. No association was found between other genetic polymorphisms studied (*GSTT1*, *GSTP1)* and esophageal SCC, which is in accordance with the data in literature[24,30,31]. It should be emphasized that, concerning *GSTT1*, our study is the first report about a Caucasian population.

No differences were found among ADC cases regarding the

frequencies of *CYP1A1*, *GSTM1* and *GSTP1* polymorphisms when compared to controls. This observation is in accordance with the weak association of tobacco smoke, alcohol consumption and ADC. In the ADC group, an unexpected protective effect of *GSTT1* deletion was found (OR = 13.31; 95% CI 1.66-106.92). Such results have been previously described for other sites such as renal or prostate carcinoma[32,33]. It is well known that the risk of renal carcinoma is increased by exposure to small halogenated compounds such as dicholoromethane or trichloroethylene. Activation of these compounds in electrophilic species implies GSTT1[29], which could explain these results. However, to our knowledge, no studies have demonstrated a role of small halogenated compounds in esophageal ADC carcinogenesis. Exposure to these compounds is possible through occupational factors, chlorinated tap water consumption or tobacco smoke. The latter, which is a weakly associated risk factor for ADC, contains methyl chloride[34]. However, our present data did not allow us to estimate exposure to halogenated compounds in our population.

Another hypothesis is that GST could participate in chronic inflammation through leukotriene synthesis[35]. In particular, leukotriene A4 to C4 (LTC4) conversion requires GST activity. Inflammation is a major etiologic factor for ADC and leukotrienes have been found to be mediators implicated in this process[5]. Furthermore, leukotriene LTD4, which is biosynthesized from LTC4, was found to induce contraction of the oesophagus and lower esophageal sphincter in animal models[35,36]. This phenomenon is likely to be involved in gastro-oesophageal reflux, which constitutes the strongest risk factor for ADC. However, though GSTT1 is also expressed in esophageal mucosa[14], it remains unclear whether this enzyme contributes to LTC4 synthesis in this tissue.

The association between susceptibility to cancer and *GSTT1* genotypes could be also explained by depletion in intracellular glutathione in the presence of GSTT1 enzyme. In this case, cells would be more sensitive to radical species produced during the inflammatory process observed among adenocarcinoma patients.

In conclusion, our study shows a different pattern of susceptibility to SCC and ADC of esophagus in a European high risk population. Whereas a slight susceptibility to SCC could be conferred by *CYP1A1*1A/*2C* and *GSTM1*2/*2* genotypes, a high frequency of *GSTT1*1/*1* genotype was found among ADC. These results are consistent with the association of SCC with tobacco exposure, as other tobacco-related cancers such as lung cancer were found to be moderately linked to *CYPA1A1*2C* allele and *GSTM1*2/*2* genotype. In ADC, our results suggest 3 distinct hypotheses. (1) The activation of exogenous procarcinogens, such as small halogenated compounds (to which ways of exposure remain to be identified), by GSTT1. Unlike tobacco, the evaluation of exposure to small halogenated compounds remains difficult because of the wide distribution of these compounds. (2) The contribution of GSTT1 to the inflammatory response of esophageal mucosa, which is known to be a strong risk factor for ADC, possibly by way of leukotriene synthesis. (3) Higher sensitivity to the inflammatory process associated with intracellular depletion of glutathione. A new study focusing on esophageal ADC with a larger recruitment would allow us to investigate these issues.

ACKNOWLEDGEMENTS

We thank Dr Dominique Arsène and Pr Marc Gignoux (Services de Gastroentérologie et de Chirurgie Digestive, CHU de Caen) for assistance in case recruitment. We thank Jacques Marnay and Dr Jacques Chasles (Laboratoire d'Anatomie Pathologique, Centre François Baclesse, Caen) for help in the histological diagnosis of tumors. We thank Marie Ingouf, Jocelyne Dannetot and Anne Leclerc for technical assistance.

REFERENCES

1 Cancer incidence in five continents. Volume VII. *IARC Sci Publ* 1997: 478-481
2 **Desoubeaux N**, Le Prieur A, Launoy G, Maurel J, Lefevre H, Guillois JM, Gignoux M. Recent time trends in cancer of the oesophagus and gastric cardia in the region of Calvados in France, 1978-1995: a population based study. *Eur J Cancer Prev* 1999; **8**: 479-486
3 **Tuyns AJ**. Oesophageal cancer in non-smoking drinkers and in non-drinking smokers. *Int J Cancer* 1983; **32**: 443-444
4 **Gignoux M**, Launoy G. Recent epidemiologic trends in cancer of the esophagus. *Rev Prat* 1999; **49**: 1154-1158
5 **Chen X**, Yang CS. Esophageal adenocarcinoma: a review and perspectives on the mechanism of carcinogenesis and chemoprevention. *Carcinogenesis* 2001; **22**: 1119-1129
6 **Lechevrel M**, Casson AG, Wolf CR, Hardie LJ, Flinterman MB, Montesano R, Wild CP. Characterization of cytochrome P450 expression in human oesophageal mucosa. *Carcinogenesis* 1999; **20**: 243-248
7 **Kawajiri K**, Watanabe J, Hayashi S. Identification of allelic variants of the human CYP1A1 gene. *Methods Enzymol* 1996; **272**: 226-232
8 **Cascorbi I**, Brockmoller J, Roots I. A C4887A polymorphism in exon 7 of human CYP1A1: population frequency, mutation linkages, and impact on lung cancer susceptibility. *Cancer Res* 1996; **56**: 4965-4969
9 **Song N**, Tan W, Xing D, Lin D. CYP 1A1 polymorphism and risk of lung cancer in relation to tobacco smoking: a case-control study in China. *Carcinogenesis* 2001; **22**: 11-16
10 **Lin P**, Wang SL, Wang HJ, Chen KW, Lee HS, Tsai KJ, Chen CY, Lee H. Association of CYP1A1 and microsomal epoxide hydrolase polymorphisms with lung squamous cell carcinoma. *Br J Cancer* 2000; **82**: 852-857
11 **Bartsch H**, Nair U, Risch A, Rojas M, Wikman H, Alexandrov K. Genetic polymorphism of CYP genes, alone or in combination, as a risk modifier of tobacco-related cancers. *Cancer Epidemiol Biomarkers Prev* 2000; **9**: 3-28
12 **Seidegard J**, Ekstrom G. The role of human glutathione transferases and epoxide hydrolases in the metabolism of xenobiotics. *Environ Health Perspect* 1997; **105**(Suppl 4): 791-799
13 **Chen YK**, Lin LM. Immunohistochemical demonstration of epithelial glutathione S- transferase isoenzymes in normal, benign, premalignant and malignant human oral mucosa. *J Oral Pathol Med* 1995; **24**: 316-321
14 **de Bruin WC**, Wagenmans MJ, Peters WH. Expression of glutathione S-transferase alpha, P1-1 and T1-1 in the human gastrointestinal tract. *Jpn J Cancer Res* 2000; **91**: 310-316
15 **van Lieshout EM**, van Haelst UJ, Wobbes T, Peters WH. Immunohistochemical localization of glutathione S-transferase alpha and pi in human esophageal squamous epithelium, Barrett's epithelium and carcinoma. *Jpn J Cancer Res* 1999; **90**: 530-535
16 **Harries LW**, Stubbins MJ, Forman D, Howard GC, Wolf CR. Identification of genetic polymorphisms at the glutathione S-transferase Pi locus and association with susceptibility to bladder, testicular and prostate cancer. *Carcinogenesis* 1997; **18**:641-644
17 **Zimniak P**, Nanduri B, Pikula S, Bandorowicz-Pikula J, Singhal SS, Srivastava SK, Awasthi S, Awasthi YC. Naturally occurring human glutathione S-transferase GSTP1-1 isoforms with isoleucine and valine in position 104 differ in enzymic properties. *Eur J Biochem* 1994; **224**: 893-899
18 **Taioli E**. International collaborative study on genetic susceptibility to environmental carcinogens. *Cancer Epidemiol Biomarkers Prev* 1999; **8**: 727-728
19 **Nelson HH**, Wiencke JK, Christiani DC, Cheng TJ, Zuo ZF, Schwartz BS, Lee BK, Spitz MR, Wang M, Xu X. Ethnic differences in the prevalence of the homozygous deleted genotype of glutathione S-transferase theta. *Carcinogenesis* 1995; **16**: 1243-1245
20 **Salama SA**, Abdel-Rahman SZ, Sierra-Torres CH, Hamada

FA, Au WW. Role of polymorphic GSTM1 and GSTT1 genotypes on NNK-induced genotoxicity. *Pharmacogenetics* 1999; **9**: 735-743

21 **Lazarus P**, Sheikh SN, Ren Q, Schantz SP, Stern JC, Richie JP Jr, Park JY. p53, but not p16 mutations in oral squamous cell carcinomas are associated with specific CYP1A1 and GSTM1 polymorphic genotypes and patient tobacco use. *Carcinogenesis* 1998; **19**: 509-514

22 **Landi S**. Mammalian class theta GST and differential susceptibility to carcinogens: a review. *Mutat Res* 2000; **463**: 247-283

23 **Saarikoski ST**, Voho A, Reinikainen M, Anttila S, Karjalainen A, Malaveille C, Vainio H, Husgafvel-Pursiainen K, Hirvonen A. Combined effect of polymorphic GST genes on individual susceptibility to lung cancer. *Int J Cancer* 1998; **77**: 516-521

24 **Lin DX**, Tang YM, Peng Q, Lu SX, Ambrosone CB, Kadlubar FF. Susceptibility to esophageal cancer and genetic polymorphisms in glutathione S-transferases T1, P1, and M1 and cytochrome P450 2E1. *Cancer Epidemiol Biomarkers Prev* 1998; **7**: 1013-1018

25 **Launoy G**, Milan C, Day NE, Faivre J, Pienkowski P, Gignoux M. Oesophageal cancer in France: potential importance of hot alcoholic drinks. *Int J Cancer* 1997; **71**: 917-923

26 **Launoy G**, Milan C, Day NE, Pienkowski MP, Gignoux M, Faivre J. Diet and squamous-cell cancer of the oesophagus: a French multicentre case-control study. *Int J Cancer* 1998; **76**: 7-12

27 **Launoy G**, Milan CH, Faivre J, Pienkowski P, Milan CI, Gignoux M. Alcohol, tobacco and oesophageal cancer: effects of the duration of consumption, mean intake and current and former consumption. *Br J Cancer* 1997; **75**: 1389-1396

28 **van Lieshout EM**, Tiemessen DM, Witteman BJ, Jansen JB, Peters WH. Low glutathione and glutathione S-transferase levels in Barrett's esophagus as compared to normal esophageal epithelium. *Jpn J Cancer Res* 1999; **90**: 81-85

29 **Pemble S**, Schroeder KR, Spencer SR, Meyer DJ, Hallier E, Bolt HM, Ketterer B, Taylor JB. Human glutathione S-transferase theta (GSTT1): cDNA cloning and the characterization of a genetic polymorphism. *Biochem J* 1994; **300**(Pt 1): 271-276

30 **Roth MJ**, Dawsey SM, Wang G, Tangrea JA, Zhou B, Ratnasinghe D, Woodson KG, Olivero OA, Poirier MC, Frye BL, Taylor PR, Weston A. Association between GSTM1*0 and squamous dysplasia of the esophagus in the high risk region of Linxian, China. *Cancer Lett* 2000; **156**: 73-81

31 **van Lieshout EM**, Roelofs HM, Dekker S, Mulder CJ, Wobbes T, Jansen JB, Peters WH. Polymorphic expression of the glutathione S-transferase P1 gene and its susceptibility to Barrett's esophagus and esophageal carcinoma. *Cancer Res* 1999; **59**: 586-589

32 **Longuemaux S**, Delomenie C, Gallou C, Mejean A, Vincent-Viry M, Bouvier R, Droz D, Krishnamoorthy R, Galteau MM, Junien C, Beroud C, Dupret JM. Candidate genetic modifiers of individual susceptibility to renal cell carcinoma: a study of polymorphic human xenobiotic-metabolizing enzymes. *Cancer Res* 1999; **59**: 2903-2908

33 **Kelada SN**, Kardia SL, Walker AH, Wein AJ, Malkowicz SB, Rebbeck TR. The glutathione S-transferase-mu and -theta genotypes in the etiology of prostate cancer: genotype-environment interactions with smoking. *Cancer Epidemiol Biomarkers Prev* 2000; **9**: 1329-1334

34 **Guerin MR**, Jenkins RA, Tomkins BA. The Chemistry of Environmental Tobacco Smoke: composition and Measurement. Boca Raton, FL: *Lewis Publishers* 1992: 43-62

35 **Kim N**, Cao W, Song IS, Kim CY, Sohn UD, Harnett KM, Biancani P. Leukotriene D4-induced contraction of cat esophageal and lower esophageal sphincter circular smooth muscle. *Gastroenterology* 1998; **115**: 919-928

36 **Kim N**, Sohn UD, Mangannan V, Rich H, Jain MK, Behar J, Biancani P. Leukotrienes in acetylcholine-induced contraction of esophageal circular smooth muscle in experimental esophagitis. *Gastroenterology* 1997; **112**: 1548-1558

Edited by Chen WW, Zhu LH and Wang XL **Proofread by** Xu FM

PO Box 2345, Beijing 100023, China
Fax: +86-10-85381893
E-mail: wjg@wjgnet.com www.wjgnet.com

World J Gastroenterol 2004;10(23):3394-3398
World Journal of Gastroenterology
Copyright © 2004 by The WJG Press ISSN 1007-9327

• GASTRIC CANCER •

Expression of Dnmt1, demethylase, MeCP2 and methylation of tumor-related genes in human gastric cancer

Jing-Yuan Fang, Zhong-Hua Cheng, Ying-Xuan Chen, Rong Lu, Li Yang, Hong-Yin Zhu, Lun-Gen Lu

Jing-Yuan Fang, Zhong-Hua Cheng, Ying-Xuan Chen, Rong Lu, Li Yang, Hong-Yin Zhu, Lun-Gen Lu, Shanghai Institute of Digestive Disease, Shanghai Second Medical University Renji Hospital, Shanghai 200001, China
Supported by National Natural Science Foundation of China, No. 30170413; Foundation for the Author of National Excellent Doctoral Dissertation of China, No.199946 and the Key Project Funds of Shanghai Education Committee
Correspondence to: Dr. Jing-Yuan Fang, Shanghai Institute of Digestive Disease, 145 Shandong Zhong Road, Shanghai 200001, China. jingyuanfang@yahoo.com
Telephone: +86-21-63200874 **Fax:** +86-21-63266027
Received: 2004-03-27 **Accepted:** 2004-04-16

Abstract

AIM: To explore the effect of DNA methyltransferase, demethylase and methyl-CpG binding protein MeCP2 on the expressions and methylation of hMSH2 and proto-oncogene in human gastric cancer.

METHODS: Paired samples of primary gastric cancer and corresponding para-cancerous, non-cancerous gastric mucosae were obtained from surgically resected specimens of 28 patients. Transcription levels of Dnmt1, mbd2, MeCP2, $p16^{INK4A}$, hMSH2 and c-myc were detected by using real-time PCR or RT-PCR. Promoter methylation of $p16^{INK4A}$, c-myc and hMSH2 genes was assayed by methylation-specific PCR (MSP) and sequencing (mapping). Their relationships were analyzed by Fisher's exact test using the software SPSS.

RESULTS: The average mRNA level of Dnmt1 gene from cancerous tissue was higher and that of mbd2 gene from cancerous tissue was lower than that from non-cancerous tissue, respectively. mbd2 was lower in cancerous tissue than in non-cancerous tissue in 14 (50.0%) of patients but higher in 3 cases (10.7%) of non-cancerous gastric tissue ($P<0.001$). c-myc expression was up-regulated in cancer tissues ($P<0.05$). The up-regulation of mbd2 was found in all patients with hypomethylated c-myc. The transcriptional levels of $p16^{INK4A}$ and MeCP2 genes did not display any difference between gastric cancerous and matched non-cancerous tissues. There were down-regulation and hypermethylation of hMSH2 in cancer tissues, and the hypermethylation of hMSH2 coexisted with down-regulated transcription. However, the transcription level of the above genes was not associated with biological behaviours of gastric cancers.

CONCLUSION: The up-regulation of proto-oncogene may be the consequence of epigenetic control of gene expression by demethylase, and mbd2 is involved in the regulation of hMSH2 expression in human gastric cancer.

Fang JY, Cheng ZH, Chen YX, Lu R, Yang L, Zhu HY, Lu LG. Expression of Dnmt1, demethylase, MeCP2 and methylation of tumor-related genes in human gastric cancer. *World J Gastroenterol* 2004; 10(23): 3394-3398
http://www.wjgnet.com/1007-9327/10/3394.asp

INTRODUCTION

Methylation of gene regulatory elements, a well-known epigenetic change, acts as an important alternative to genetic alteration for gene inactivation. DNA methyltransferase (Dnmt) and DNA demethylase are the enzymes potentially affecting promoter methylation status. Human DNA demethylase has been cloned[1]. The inactivity of demethylase may play a role in production and maintenance of regional DNA hypermethylation, which frequently results in reduced expression of tumor suppressor genes in human cancers.

Gastric cancer is the second most common malignant tumor in Asia, with a much higher incidence than in Western countries. During gastric carcinogenesis, hypomethylation of c-myc and c-Ha-ras proto-oncogenes was frequently seen[2,3], however the average level of mRNA for Dnmt1 was significantly higher in gastric cancers than in corresponding non-cancerous mucosa[4]. mbd2 has been proposed to be a DNA demethylase, and the average level of mbd2 mRNA was significantly lower in gastric cancer than in non-cancerous mucosa. But there was no significant association between DNA demethylase mRNA level and malignant potential in gastric cancers[5]. The mRNA expression levels for pro-methylation of Dnmt1, Dnmt3a and Dnmt3b and mbd2 are not the critical determinant of tumor-specific promoter hypermethylation of hMLH1, $p16^{INK4A}$ or CDH1 in gastric cancer[6]. However, little is known about the relationship between mbd2 or Dnmt1 and the methylation status of proto-oncogene or hMSH2, another important mismatch repair (MMR) gene. Furthermore, up-to date, there has not been any report about methyl-CpG binding protein MeCP2 associated with tumor-related genes in gastric cancer.

In the present study, we examined the methylation and transcriptional level of tumor-related genes including $p16^{INK4A}$, hMSH2 and c-myc, and detected the expression of Dnmt1, mbd2 and MeCP2. We therefore analyzed their relationship in normal and cancerous stomach tissues.

MATERIALS AND METHODS

Patients

Paired samples of histologically verified primary gastric cancer and corresponding para-cancerous (3-5 cm from cancer margin) and non-cancerous gastric mucosae were obtained immediately from surgically resected specimens of 28 patients (C1-C28) treated at Renji Hospital, Shanghai, China. A complete written informed consent was obtained from all patients. They were all diagnosed pathologically by HE-stained sections and classified according to WHO's histological classifications of gastric carcinoma. The histological characteristics in para-cancerous area were chronic gastritis or intestinal metaplasia, and dysplasia was present in ten cases. The clinico-pathological features of each patient were reviewed and recorded (Table 1). The mean age of patients (19 men and 9 women) at resection was 58 (range 45-79) years. A portion of the tissues (approximately 1-3 g) was snap-frozen on dry ice and kept in liquid nitrogen until used for DNA or RNA extraction. Other portions were used for histological examination.

RNA extraction and reverse-transcription polymerase chain reaction (RT-PCR)

First, mRNA expression of tumor-related genes in cancerous, para-cancerous and non-cancerous tissues from each patient was detected by using RT-PCR and real-time PCR. Total RNA was extracted using a commercial kit (Trizol) according to the manufacturer's instructions (Gibco BRL). RT reactions using 5 μg of total RNA in 20 μL of reaction buffer were performed with Superscript II reverse transcriptase (Life Technologies, Inc). mRNA transcription levels of mbd2, MeCP2, $p16^{INK4A}$ and c-myc genes were evaluated by using RT-PCR. The sequence and PCR reaction for each primer are shown in Table 2. For control of RT-PCR, a 612 bp fragment of β-actin cDNA was also amplified. At the end of 40 cycles, reaction products were separated electrophoretically on a 3% agarose gel and stained with ethidium bromide for visual confirmation of PCR products. The density of bands in RT-PCR in each lane was normalized to the amount of total RNA as determined by the density of the band in RT-PCR for β-actin[7]. RT-PCR analysis was repeated at least thrice.

Real-time quantitative PCR for Dnmt1 and hMSH2

mRNA levels of Dnmt1 and hMSH2 were measured using a real-time quantitative PCR system. Relative quantitation using the comparative Ct method with the data from ABI PRISM 7700 sequence detection system (version 1.6 software) was performed according to the manufacturer's protocol.

Real-time PCR was also performed with Taqman β-actin to normalize each of the extracts for amplifiable human DNA. The results were expressed as the ratio of copies of each gene to β-actin, respectively. The Ct values were measured, and the average Ct value of triplicate samples was calculated. Alteration of mRNA expression was defined as a 3-fold difference in the expression level[8]. The primers and the Taqman fluorogenic probes for Dnmt1, hMSH2 and β-actin were provided by Jikang Company, Shanghai, China.

The sequences of all primers and probes, as well as PCR programs are shown in Table 3.

Table 1 Relationship between Dnmt1 and pathological change in patients with gastric cancer (case number, %)

		Subtotal	Dnmt1 transcription			*P*
			Up-regulated	Normal	Down-regulated	
Total or subtotal		28 (100.0)	9 (32.14)	9 (32.14)	10 (35.72)	
Age (yr)	>50	18 (64.30)	7 (38.89)	4 (22.22)	7 (38.89)	0.30
	<50	10 (35.70)	2 (20.00)	5 (50.00)	3 (30.00)	
Size of tumor	>5 cm	14 (50.00)	4 (28.57)	5 (35.71)	5 (35.71)	0.88
	<5 cm	14 (50.00)	4 (28.57)	5 (35.71)	5 (35.71)	
Borrmann	II	6 (21.43)	2 (33.33)	0 (0.00)	4 (66.67)	0.34
	III	15 (53.57)	5 (33.33)	6 (40.00)	4 (26.67)	
	IV	7 (25.00)	2 (28.57)	3 (42.86)	2 (28.57)	
Lymph node invasion	Positive	21 (75.00)	6 (28.57)	8 (38.10)	7 (33.33)	0.49
	Negative	7 (25.00)	3 (42.86)	1 (14.29)	3 (42.86)	

Table 2 Primer sequences and PCR conditions for RT-PCR, MSP and sequencing

Primers	Sense (5'→3')	Antisense (5'→3')	Product size (bp) PCR program	GenBank accession number
β-Actin	GGA GTC CTG TGG CAT CCA CG	CTA GAA GCA TTT GCG GTG GA	322 bp 94 ℃ 30 s, 60 ℃ 1 min, 72 ℃ 1 min, 27 cycles	BC023204
$p16^{INK4A}$ RT-PCR	CCC GCT TTC GTA GTT TTC AT	TTA TTT GAG CTT TGG TTC TG	355 bp 94 ℃ 1 min, 58 ℃ 1 min, 72 ℃, 1 min, 35 cycles	L27211
c-myc RT-PCR	CCA ACA GGA GCT ATG ACC TC	CTC GGT CAC CAT CTC CAG CT	290 bp 94 ℃ 1 min, 52 ℃ 1 min, 72 ℃ 1 min, 35 cycles	V00568
MeCP2 RT-PCR	ACT CCT CAG AAT ACA CCT TGC TT	TGA GGC CCT GGA GGT CCT	112 bp 95 ℃ 1 min, 50 ℃ 1 min, 72 ℃ 1 min, 35 cycles	MCB, 2000; 20: 3316
mbd2 RT-PCR	AAC CCT GCT GTT TGC TTA AC	CGT ACT TGC TGT ACT CGC TCT TC	101 bp 94 ℃ 1 min, 60 ℃ 1 min, 72 ℃ 1 min, 40 cycles	AF072242
$p16^{INK4A}$ M-MSP	TTA TTA GAG GGT GGG GCG GAT CGC	GAC CCC GAA CCG CGA CCG TAA	150 bp 95 ℃ 30 s, 65 ℃ 30 s, 72 ℃ 1 min, 40 cycles	X94154
$p16^{INK4A}$ UM-MSP	TTA TTA GAG GGT GGG GTG GAT TGT	CAA CCC CAA ACC ACA ACC ATA A	151 bp 95 ℃ 30 s, 60 ℃ 30 s, 72 ℃ 1 min, 40 cycles	X94154
c-myc M-MSP	TAG AAT TGG ATC GGG GTA AA	CGA CCG AAA ATC AAC GCG AAT	131 bp 95 ℃ 30 s, 56 ℃ 30 s, 72 ℃ 1 min, 40 cycles	AF002859
c-myc UM-MSP	TAG AAT TGG ATT GGG GTA AA	CCA ACC AAA AAT CAA CAT GAA T	132 bp 95 ℃ 30 s, 56 ℃ 30 s, 72 ℃ 1 min, 40 cycles	AF002859
hMSH2 sequencing 1st round	TGT TTA GAA AGA AAA AGG GA	AAA CCT CCT CAC CTC CT	94 ℃ 1 min, 55 ℃ 1 min, 72 ℃ 1 min, 35 cycles	AB006445
hMSH2 sequencing 2nd round	AAA TAT TGG GAG GAG GAG GA	ACC CAC TAA ACT ATT TCC CA	327 bp 94 ℃ 1 min, 55 ℃ 1 min, 72 ℃ 1 min, 35 cycles	AB006445

Table 3 Sequence of primers and probes for real-time PCR

Gene	Sense (5'→3')	Antisense (5'→3')	Probe	GenBank No
Dnmt1	GCA CCT CAT TTG CCG AAT ACA	TCT CCT GCA TCA GCC CAA ATA	AGT CCC GAG TAT GCG C	XM_017218
hMSH2	ATC CAA GGA GAA TGA TTG GTA TTT G	CAA AGA GAA TGT CTT CAA ACT GAG AGA	CAT ATA AGG CTT CTC CTG GC	HSU04045
β-actin	CTG GCA CCC AGC ACA ATG	GGA CAG CGA GGC CAG GAT	ATC ATT GCT CCT CCT GAG	BC016045

Methyl-specific PCR (MSP) for p16^{INK4A} and c-myc genes

To amplify the promoters of p16^{INK4A} and c-myc genes, we carried out bisulfite modification[9] and MSP.

Bisulfite could convert unmethylated cytosine residues to uracil, but methylated cytosines remained non-reactive. PCR amplified uracil as thymine while methylated cytosines were only amplified as cytosines. Two micrograms of total genomic DNA (from at least two independent treatments corresponding to RT-PCR experiments) were isolated by using QIAamp DNA blood mini kit (QIAGEN Inc.), then denatured by NaOH and modified by sodium bisulfite solution (2.35 mol/L) containing hydroquinone (40 mmol/L) freshly prepared. The bisulfite-treated DNA was desalted using Wizard DNA clean up kit (Promega) and amplified by PCR using primers specific for methylated and unmethylated p16^{INK4A} and c-myc promoters. PCR reaction buffer contained 0.1 mmol/L dNTP, 2.0 mmol/L $MgCl_2$, and 0.5 μmol/L primers. PCR products were directly loaded onto 3% agarose gels and electrophoresed. The gel was stained with ethidium bromide and directly visualized under UV illumination. Furthermore, the primers for wild-type p16^{INK4A} and c-myc were used to monitor complete conversion of DNA obtained in the bisulfite reaction.

Bisulfite modification and sequencing (mapping) for hMSH2

Primers were designed in the region without CpG dinucleotides to amplify both methylated and unmethylated alleles in hMSH2. The PCR products were recovered using QIA quick gel extraction kit (Gibco). Direct sequencing was performed by using ABI PRISM BigDye terminator kit (PE Biosystems, Foster City, CA). The products of sequencing PCR included 22 CpG sites in promoter of hMSH2 gene.

The sequences of all primers and PCR programs are shown in Table 2.

Statistical analysis

Results were representative of at least three independent experiments performed in triplicate and presented as mean±SD. Comparisons between groups were made using Student's paired *t* test. Their relationship was analyzed by Fisher's exact test using the software SPSS.

RESULTS

Expressions of Dnmt1, mbd2 and MeCP2 genes in cancerous and non-cancerous gastric tissues

After quantitative PCR, the specific products visually confirmed on agarose gels were about 101- and 96 bp, and no non-specific products were obtained upon amplification of Dnmt1 and β-actin, respectively. In all cancerous, para-cancerous and non-cancerous tissues, their mRNA expressions were detected, and 32.2% (9/28) of cancerous tissues over-expressed Dnmt1, and the copies of Dnmt1 were higher than in non-cancerous tissues (5.08 *vs* 1).

mbd2 was expressed in all samples. However, mbd2 was down-regulated in 50% (14/28) of gastric cancer tissues, up-regulated in 10.7% (3/28) cases, and no significant change in 3.39% (11/28), respectively. Average value of mbd2 mRNA expression was lower in cancerous tissues than in non-cancerous tissue (Figures 1, 2). In 11 patients, mbd2 mRNA level in gastric cancer was particularly low, being reduced by 50% or more when compared with that in the corresponding non-cancerous mucosae. However, we did not find association between expressions of MeCP2 and Dnmt1 and mbd2.

In addition, we did not find the association of overall aberrant methylation and expressions of Dnmt1, MeCP2, mbd2 with the age of patients.

Examination of mRNA expression of tumor-related genes and status of promoter methylation in primary gastric cancers

Figure 1 shows the results from RT-PCR and real-time PCR, and Figure 2 shows the relative mRNA levels of each gene after normalization with the signal of β-actin. These data demonstrated that the expressions of p16^{INK4A} and hMSH2 (data not shown) were down-regulated in cancerous tissues from 11 cases (39.3%) and 10 cases (35.7%) respectively, but there was no significant difference between cancerous and non-cancerous tissues. As shown in Figure 2, c-myc transcription level was up-regulated in 14 patients with gastric cancer, and the mean value of expression in cancerous tissues was greater than that in non-cancerous tissues ($P<0.05$).

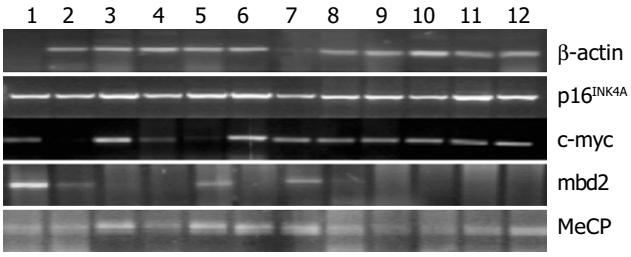

Figure 1 mRNA expression of p16^{INK4A}, c-myc, mbd2 and MeCP2 in cancerous (lanes 1, 4, 7 and 10), para-cancerous (lanes 2, 5, 8 and 11) and non-cancerous (lanes 3, 6, 9 and 12) tissues from patients with gastric cancer by using RT-PCR.

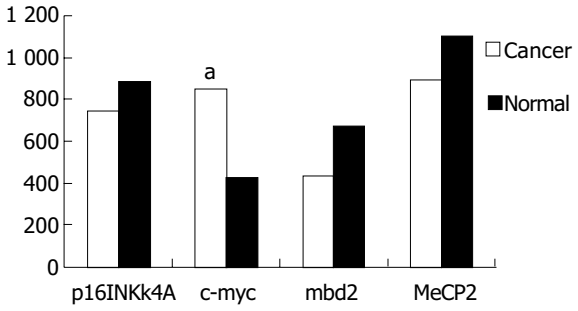

Figure 2 Density of bands from RT-PCR in each lane normalized to the total RNA as determined by the density of bands in RT-PCR for β-actin. Assuming β-actin was 4 562.39 units (pixels of brightness), the calculation [4 562.39 / (density of actin)]×(density of each gene) equals each gene normalized to β-actin. Data shown are representative of three separate experiments. $^aP<0.05$.

To determine whether the expression of p16^{INK4A}, hMSH2 and c-myc genes in gastric cancer was associated with methylation, we selected the samples from cancerous, para-cancerous and non-cancerous tissues in ten patients for MSP or genomic bisulfite sequencing. Each tissue showed a positive 150 bp and a 151 bp band for methylated and unmethylated specific primer sets for p16^{INK4A}, indicating that the p16^{INK4A} gene was partially methylated in human gastric cancer. The methylated bands for the p16^{INK4A} gene in the cancerous and para-cancerous tissues were consistently stronger than the products of non-cancerous tissues (Figure 3A). Regarding c-myc gene, the methylated product (131 bp) was significantly lower and the unmethylated product (132 bp) was higher in cancerous and para-cancerous tissues than in non-cancerous tissues. Figure 3B displays representative examples of MSP products analyzed by electrophoresis on an agarose gel.

Bisulfite genomic sequencing of the representative PCR products of hMSH2 showed that all cytosines at non-CpG sites were converted to thymine. This excluded the possibility that successful amplification could be attributable to incomplete bisulfite conversion. Interestingly, methylation occurred at the -166 CpG site only (Figure 4).

Taken together, the results from MSP, sequencing, RT-PCR and real-time PCR indicated that hypermethylation of hMSH2

might be induced, inactivation and activation of c-myc were associated with its hypomethylation in human gastric cancer.

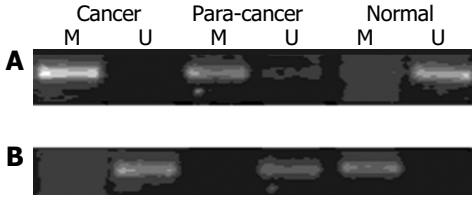

Figure 3 Hypermethylation of p16^{INK4A} promoter (A) and hypomethylation of proto-oncogene c-myc promoter (B) in gastric cancer tissue indicated by MSP. U: unmethylation-specific PCR; M: methylation-specific PCR.

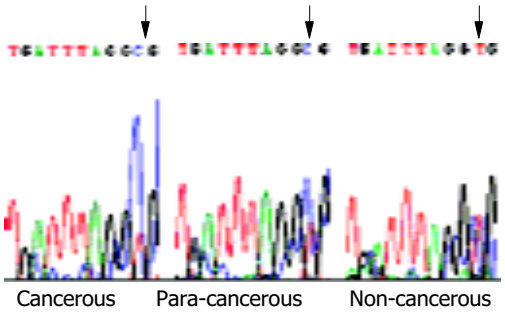

Figure 4 Methylation analysis of hMSH2 gene promoter by bisulfite sequencing. The arrows indicate the changes of CG to TG in promoters of non-cancerous and para-cancerous tissue, but CG remained in cancerous tissues.

Correlation between mRNA expression of Dnmt1, mbd2 and DNA methylation

Dnmt1 was not associated with the methylation status of p16^{INK4A} or c-myc gene.

Among Dnmt1 down-regulated cases, 6 (60%) had over-expression of c-myc in cancerous tissues. In the cancer cases with up-regulated mbd2, all 3 had an expression of c-myc. We also found that there was a positive correlation in the expression of c-myc and mbd2 ($r = 0.59$, $P = 0.026$), MeCP2 ($r = 0.64$, $P = 0.02$), but c-myc had no positive correlation with Dnmt1.

In contrast to cancer tissues, all normal tissues had a positive association of p16^{INK4A} with MeCP2 ($r = 0.483$, $P = 0.02$) or mbd2 ($r = 0.483$, $P = 0.027$).

Among the 10 cases with down-regulated hMSH2, 6 cases had a decreased mbd2 mRNA, but there was no significant association between expressions of Dnmt1 and hMSH2.

Association of Dnmt1, mbd2 and histological change

There was no significant association between Dnmt1, mbd2 mRNA level and clinico-pathological parameters of the tumors, such as histological differentiation, size of tumor and lymph node metastasis. These data failed to indicate their aberrant expression as an early event in gastric cancer.

DISCUSSION

Generally, the global DNA methylation level is lower in cancer cells than in normal cells, and some loci tend to show hypomethylation of proto-oncogene in human gastrointestinal cancers[10]. Recent studies demonstrated that DNA methylation could contribute to inactivation of tumor suppressor genes, a key event in tumorigenesis of a wide spectrum of human tumors[11,12].

Three enzymes are responsible for DNA methylation. The carboxy-terminal domain of Dnmt1 could catalyse the methylation of DNA containing hemi-methylated CpG dinucleotides more efficiently than unmethylated DNA *in vitro*[13]. DNA demethylase was first identified by Szyf's group, and they demethylated both fully methylated and hemimethylated DNA, showing dinucleotide specificity, and could demethylate mCpG in different sequence contexts[5]. The shortest form of methyl- CpG binding domain (MBD)2, mbd2b, has been proposed to be a DNA demethylase which has been cloned and characterized[14]. MeCP2 is the first true member of the family of proteins that could selectively recognize methylated CpG[15]. It is a single polypeptide characterized by an MBD and a transcriptional repression domain[16,17]. Aberrant methylation in tumor-related genes was frequently detected in gastric intestinal metaplasia of both cancer and non-cancer patients, suggesting their early involvement in the multi-step progression of gastric carcinogenesis[18]. However, little is known about the relationship of Dnmt1, demethylase, MeCP2 with tumor-related genes.

We found that the average mRNA level of Dnmt1 gene in cancerous tissue was higher and that of mbd2 gene was lower than that in non-cancerous tissue. Regarding Dnmt1 expression, these results are consistent with a study by Kanai[4]. On the other hand, Patra found that MBD2 protein expression was significantly higher in benign prostatic hyperplasia BPH-1 cells and deficient in prostate cancer cell lines and in BPH tissues[19]. For mbd2, our result is consistent with another experiment of gastrointestinal cancer[3]. They suggested that the average levels of demethylase mRNA expression normalized to GAPDH mRNA were significantly lower in colorectal (0.81±0.55) and gastric (2.88±0.23) cancers than in the non-cancerous mucosae (1.90±0.16 and 5.11±0.34, respectively, $P < 0.0001$). However, up to date, we have not found any report about the expression of MeCP2 in gastric cancer. Darwanto found that colonic mucinous adenocarcinomas showed a strong MeCP2 expression[20], and Muller observed a higher expression level of MeCP2 mRNA in breast cancer tissues than in non-cancerous tissues[21].

Previous studies indicated that the mRNA expression level for Dnmt1 and mbd2 was not a critical determinant of promoter hypermethylation of tumor-suppressor gene p16^{INK4A} in gastric cancer[6,22]. Regarding the hMLH1, the result was different in different studies[6,23]. During gastric carcinogenesis, hypomethylation of c-myc proto-oncogene is common, and it has not been linked to Dnmt1, mbd2 or MeCP2, or hMSH2. In the present study, we demonstrated that there was a positive association of mbd2 and c-myc proto-oncogene in gastric cancerous tissues. The up-regulation of mbd2 was found in all patients with hypomethylated c-myc. The correlation of mbd2 expression with unmethylation of c-myc promoter suggests that c-myc may be a target for demethylation by the enzymes.

Another interesting gene we tested was hMSH2. The second important finding in this study was the decrease of mbd2 mRNA in most patients with down-regulated hMSH2, but we did not find any correlation between hMSH2 and Dnmt1 or MeCP2. It suggests that mbd2 is also involved in the regulation of hMSH2 expression in human gastric cancer. We did not test the promoter region of hMLH1 gene, because the promoter was not associated with Dnmt1[6,23] and mbd2[6] in human gastric cancer.

In addition, the data from our study demonstrated that the transcription level of Dnmt1, mbd2 and MeCP2 might not be associated with biological behaviours in human gastric cancer. Kanai also suggested there was no significant association between DNA demethylase mRNA level and malignant potential in gastric cancers[5]. Although the mbd2 expression was lower both in early and in advanced cancers, we could not demonstrate a definitive relationship between the histology and mbd2 expression due to the small number of patients studied.

In conclusion, the up-regulation of proto-oncogene may be the consequence of epigenetic control of gene expression by demethylase, and mbd2 is also involved in the regulation of hMSH2 expression in human gastric cancer.

ACKNOWLEDGEMENTS

Thanks are given to Dr. Yao Shi and Xiao-Yu Chen, Ms. Hong-Yin Zhu and Ms. Wei-Qi Gu for performing the diagnosis of pathology, MSP and real-time PCR.

REFERENCES

1 **Bhattacharya SK**, Ramchandani S, Cervoni N, Szyf M. A mammalian protein with specific demethylase activity for mCpG DNA. *Nature* 1999; **397**: 579-583

2 **Fang JY,** Zhu SS, Xiao SD, Jiang SJ, Shi Y, Chen XY, Zhou XM, Qian LF. Studies on the hypomethylation of c-myc, c-Ha-ras oncogenes and histopathological changes in human gastric carcinoma. *J Gastroenterol Hepatol* 1996; **11:** 1079-1082

3 **Fang J,** Zhu S, Xiao S, Shi Y, Jiang S, Zhou X, Qian L. Alterations of level of total genomic DNA methylation and pattern of c-Myc, c-Ha-ras oncogene methylation in human gastric carcinogenesis. *Chin Med J* 1996; **109:** 787-791

4 **Kanai Y,** Ushijima S, Kondo Y, Nakanishi Y, Hirohashi S. DNA methyltransferase expression and DNA methylation of CPG islands and peri-centromeric satellite regions in human colorectal and stomach cancers. *Int J Cancer* 2001; **91:** 205-212

5 **Kanai Y,** Ushijima S, Saito Y, Nakanishi Y, Sakamoto M, Hirohashi S. MRNA expression of genes altered by 5-azacytidine treatment in cancer cell lines is associated with clinicopathological parameters of human cancers. *J Cancer Res Clin Oncol* 2001; **127**: 697-706

6 **Oue N,** Shigeishi H, Kuniyasu H, Yokozaki H, Kuraoka K, Ito R, Yasui W. Promoter hypermethylation of MGMT is associated with protein loss in gastric carcinoma. *Int J Cancer* 2001; **93**: 805-809

7 **Fang JY,** Mikovits JA, Bagni R, Petrow-Sadowski CL, Ruscetti FW. Infection of lymphoid cells by integration-defective human immunodeficiency virus type 1 increases de novo methylation. *J Virol* 2001; **75**: 9753-9761

8 **Scanlan MJ,** Welt S, Gordon CM, Chen YT, Gure AO, Stockert E, Jungbluth AA, Ritter G, Jager D, Jager E, Knuth A, Old LJ. Cancer-related serological recognition of human colon cancer: identification of potential diagnostic and immunotherapeutic targets. *Cancer Res* 2002; **62:** 4041-4047

9 **Xiong Z,** Laird PW. COBRA: a sensitive and quantitative DNA methylation assay. *Nucleic Acids Res* 1997; **25:** 2532-2534

10 **Fang JY,** Xiao SD. Alteration of DNA methylation in gastrointestinal carcinogenesis. *J Gastroenterol Hepatol* 2001; **16:** 960-968

11 **Jones PA,** Takai D. The role of DNA methylation in mammalian epigenetics. *Science* 2001; **293:** 1068-1070

12 **Baylin SB,** Herman JG. DNA hypermethylation in tumorigenesis: epigenetics joins genetics. *Trends Genet* 2000; **16:** 168-174

13 **Bestor TH.** Activation of mammalian DNA methyltransferase by cleavage of a Zn binding regulatory domain. *EMBO J* 1992; **11:** 2611-2617

14 **Ramchandani S,** Bhattacharya SK, Cervoni N, Szyf M. DNA methylation is a reversible biological signal. *Proc Natl Acad Sci U S A* 1999; **96:** 6107-6112

15 **Nan X,** Meehan RR, Bird A. Dissection of the methyl-CpG binding domain from the chromosomal protein MeCP2. *Nucleic Acids Res* 1993; **21:** 4886-4892

16 **Ng HH,** Zhang Y, Hendrich B, Johnson CA, Turner BM, Erdjument-Bromage H, Tempst P, Reinberg D, Bird A. MBD2 is a transcriptional repressor belonging to the MeCP1 histone deacetylase complex. *Nat Genet* 1999; **23:** 58-61

17 **Nan X,** Campoy FJ, Bird A. MeCP2 is a transcriptional repressor with abundant binding sites in genomic chromatin. *Cell* 1997; **88:** 471-481

18 **To KF,** Leung WK, Lee TL, Yu J, Tong JH, Chan MW, Ng EK, Chung SC, Sung JJ. Promoter hypermethylation of tumor-related genes in gastric intestinal metaplasia of patients with and without gastric cancer. *Int J Cancer* 2002; **102:** 623-628

19 **Patra SK,** Patra A, Zhao H, Dahiya R. DNA methyltransferase and demethylase in human prostate cancer. *Mol Carcinog* 2002; **33:** 163-171

20 **Darwanto A,** Kitazawa R, Maeda S, Kitazawa S. MeCP2 and promoter methylation cooperatively regulate E-cadherin gene expression in colorectal carcinoma. *Cancer Sci* 2003; **94:** 442-447

21 **Muller HM,** Fiegl H, Goebel G, Hubalek MM, Widschwendter A, Muller-Holzner E, Marth C, Widschwendter M. MeCP2 and MBD2 expression in human neoplastic and non-neoplastic breast tissue and its association with oestrogen receptor status. *Br J Cancer* 2003; **89:** 1934-1939

22 **Sato M,** Horio Y, Sekido Y, Minna JD, Shimokata K, Hasegawa Y. The expression of DNA methyltransferases and methyl-CpG-binding proteins is not associated with the methylation status of p14(ARF), p16(INK4a) and RASSF1A in human lung cancer cell lines. *Oncogene* 2002; **21:** 4822-4829

23 **Etoh T,** Kanai Y, Ushijima S, Nakagawa T, Nakanishi Y, Sasako M, Kitano S, Hirohashi S. Increased DNA methyltransferase 1 (DNMT1) protein expression correlates significantly with poorer tumor differentiation and frequent DNA hypermethylation of multiple CpG islands in gastric cancers. *Am J Pathol* 2004; **164:** 689-699

Edited by Wang XL **Proofread by** Zhu LH and Xu FM

PO Box 2345, Beijing 100023, China
Fax: +86-10-85381893
E-mail: wjg@wjgnet.com www.wjgnet.com

World J Gastroenterol 2004;10(23):3399-3404
World Journal of Gastroenterology
Copyright © 2004 by The WJG Press ISSN 1007-9327

• GASTRIC CANCER •

Transabdominal ultrasonography in preoperative staging of gastric cancer

Sheng-Ri Liao, Ying Dai, Ling Huo, Kun Yan, Lin Zhang, Hui Zhang, Wen Gao, Min-Hua Chen

Sheng-Ri Liao, Ying Dai, Ling Huo, Kun Yan, Lin Zhang, Hui Zhang, Wen Gao, Min-Hua Chen, Department of Ultrasonography, School of Oncology, Peking University, Beijing 10036, China
Supported by the Hospital Medicine Development Foundation, No. ZD 199909
Correspondence to: Min-Hua Chen, Department of Ultrasonography, School of Oncology, Peking University, Beijing 10036, China. shengri@sina.com
Telephone: +86-10-88121122 Ext. 2139
Received: 2004-02-28 **Accepted:** 2004-04-05

Abstract

AIM: To investigate the value of transabdominal ultrasonography (US) in the preoperative staging of gastric cancer.

METHODS: A total of 198 patients with gastric cancer underwent preoperatively transabdominal US, depth of tumor infiltration was assessed in 125 patients, and lymph node metastasis was assessed in 106 patients.

RESULTS: The staging accuracy of transabdominal US was 55.6%, 75.0%, 87.3% and 71.1% in T1, T2, T3 and T4 carcinomas, respectively. The overall accuracy was 77.6%. The detection rate for pancreatic invasion and liver invasion was 77.4%, 71.4%, respectively. The sensitivity, specificity, accuracy of transabdominal US in assessment of lymph node metastasis were 77.6%, 64.1%, 72.6%, respectively. Various shapes such as round, ovoid, spindle were encountered in benign and malignant lymph nodes. Majority of both benign and malignant lymph nodes were hyperechoic and had a distinct border. Benign lymph nodes were smaller than malignant lymph nodes in length and width (P = 0.000, 0.005). Irregular shape, fusional shape, infiltrative signs, inhomogenous echo were seen mainly in malignant lymph nodes (P = 0.045, 0.006, 0.027, 0.006).

CONCLUSION: Transabdominal US is useful for preoperative staging in gastric cancer, although it is difficult to differentiate benign from malignant lymph nodes.

Liao SR, Dai Y, Huo L, Yan K, Zhang L, Zhang H, Gao W, Chen MH. Transabdominal ultrasonography in preoperative staging of gastric cancer. *World J Gastroenterol* 2004; 10 (23): 3399-3404
http://www.wjgnet.com/1007-9327/10/3399.asp

INTRODUCTION

Gastric cancer is one of the most prevalent malignant tumors[1,2]. An accurate preoperative staging is helpful for the prediction of prognosis and establishment of the individualized therapy. Although endoscopy and upper gastrointestinal series with double-contrast study have significantly improved the diagnostic accuracy in gastric cancer, they neither allow the assessment of the depth of tumor infiltration nor visualize perigastric lymph nodes[3,4]. Currently, endoscopic ultrasonography (EUS) has been considered as a useful modality for the preoperative staging of gastric cancer, and the accuracy of EUS in the assessment of the depth of tumor infiltration and lymph node metastasis is 67-92% and 63-78%[5-11], respectively. However, EUS procedure is relatively complex, and can not be performed successfully in some patients, due to marked obstruction of gastric lumen caused by tumor or noticeable discomfort during examination.

Transabdominal ultrasonography (US) is applied widely in clinical practice. When condition of patients is suitable, transabdominal US can detect lymph nodes with a diameter of 5 mm, and the normal wall of fluid-filled stomach after the patients drank water can be described as a 5-layer structure[12-14], which contributes to the assessment of the depth of tumor infiltration. Literature on the preoperative staging with transabdominal US is sparse[15,16]. The aim of our study was to further assess the accuracy and limitations of transabdominal US in preoperative staging of the depth of tumor infiltration and lymph node metastasis.

MATERIALS AND METHODS

Between January 2000 to July 2003, 198 patients with gastric cancer confirmed by endoscopic biopsy underwent transabdominal US preoperatively. Patients with preoperative transabdominal US findings and detailed operative and pathological findings were included in this study. The depth of tumor infiltration was assessed in 125 patients (78 males, 47 females, ranged 27-78 years). Lymph node metastasis was assessed in 106 patients (66 males, 40 females, ranged 31-78 years).

All patients were required to drink water to fill stomach for the assessment of the depth of tumor infiltration. Transabdominal US was performed 3-5 min after 500-700 mL boiled water was drunk. Patients were examined usually in the supine position. Sitting position, left or right lateral decubitus position might be taken for visualization of lesions according to different locations of tumors.

The wall of fluid-filled stomach is described as a 5-layer structure[12-14]. The innermost hyperechoic layer (the first layer) corresponds to the superficial mucosa, the second hypoechoic layer corresponds to the deep mucosa, the third hyperechoic layer corresponds to the submucosa plus the acoustic interface between the submucosa and muscularis propria, the fourth hypoechoic layer corresponds to the muscularis propria minus the acoustic interface between the submucosa and muscularis propria, the fifth hyperechoic layer corresponds to the subserosal fat and serosa.

According to the TNM (UICC) classification[17], the depth of tumor infiltration was divided into 4 categories. T1 = tumor confined to mucosa or submucosa. For mucosal carcinoma, tumor located in the first and second layers, the third layers (submucosa) was intact; for submucosal carcinoma, layers 1 to 3 were interrupted or thickened and the fourth and fifth layers were normal sonographically (Figure 1A). T2 = tumor invading muscularis propria (the fourth layer) which became thicken, and the fifth layer was intact sonographically (Figure 1B). T3 = tumor invading serosa (the fifth layer), with interruption

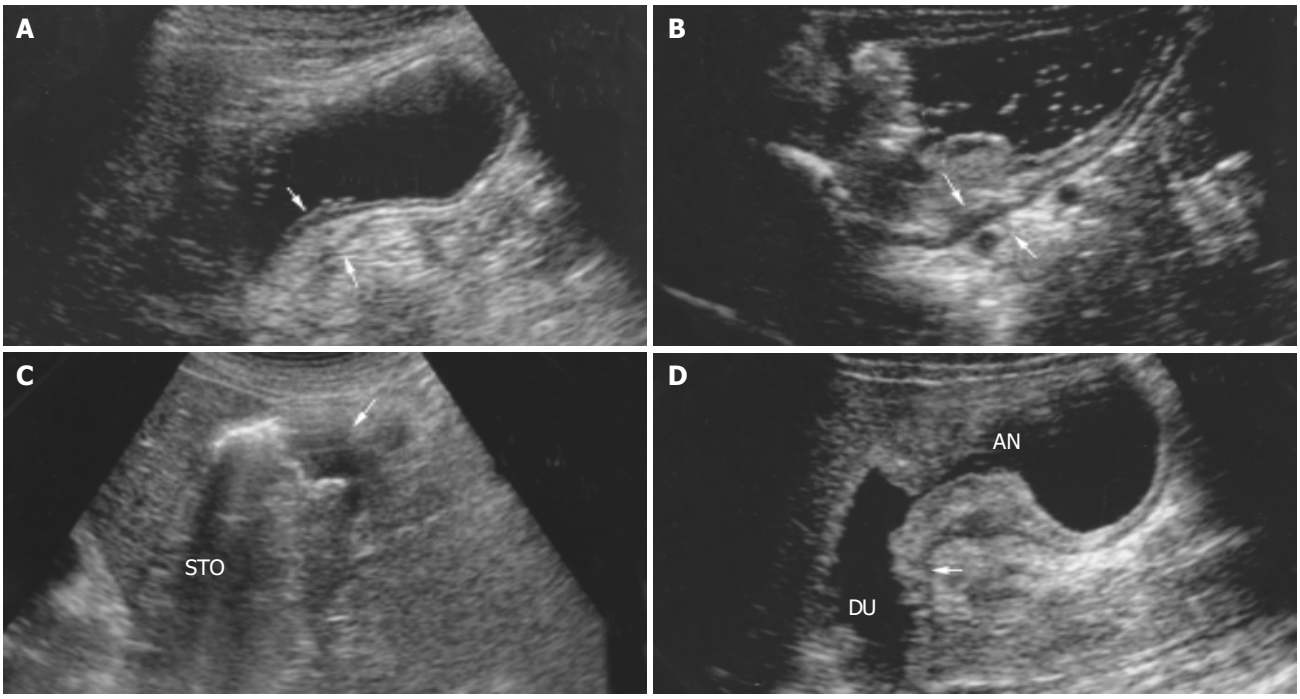

Figure 1 Sonograms of T1-T4 carcinoma. A: Submucosal carcinoma (T1) in gastric antrum. Arrow indicates segmental thickening of layers 1-3 of the posterior wall, triangle indicates normal layers 4-5. B: T2 carcinoma. The posterior wall of Gastric body is thickening. Arrow indicates the third hyperechoic layer is obliterated and the fourth hypoechoic layer is thickening, triangle indicates normal layer 5. C: T3 carcinoma. Tumor located in the greater curvature of stomach (STO) is hypoechoic with disappearance of wall all layer (arrow). D: T4 carcinoma. Sonogram shows tumor located in antrum (AN) infiltrating duodenum. Arrow indicates the segmental wall thickening of duodenal bulb.

or disappearance of all layers of wall sonographically (Figure 1C). T4 = tumor invading adjacent organs which had an indistinct border and was indistinguishable from involved organs sonographically (Figure 1D).

Assessment of regional lymph node metastasis was performed in a fasting state before water was drunk for evaluation of tumor infiltration. Regional lymph nodes around the following organs or structures were examined: stomach, liver, pancreas, gallbladder, aorta, hilum of spleen, comma hepatic aorta, superior mesenteric artery, celiac artery, and recorded number, size, shape, border, and echogenicity of lymph nodes.

Lymph nodes with a length of 5 mm or greater were considered metastatic. Regional lymph node staging was classified as N0 (no lymph node metastasis) and N+ (lymph node metastasis).

Lymph nodes detected with transabdominal US were divided into 3 groups according to their shapes: regular, irregular, fusional. Regular lymph nodes were classified into 3 categories of shape: spindle: width $\leqslant$ half the length of the lymph node; ovoid: width $\leqslant$ three quarters of the length of the lymph node; round: width > three quarters of the length of the lymph node[18].

The followings were considered as "infiltrative signs" of lymph nodes: ill-defined border, indistinguishable from the adjacent structures or loss of movement.

Sonographic examinations were performed with commercially available real time image units (Toshiba 6000, Aloka 2000, DU-6), and transducer frequency varied between 3.5-6.0 MHz.

Data were analyzed with SPSS10.0 software. $P<0.05$ was considered statistically significant.

RESULTS

Assessment of depth of tumor infiltration

Table 1 summarizes the findings of transabdominal US and operative or pathological findings in 125 patients with gastric cancer. The accuracy of transabdominal US in staging of T1 carcinomas was 55.6%, 75.0% in T2 carcinomas, 87.3% in T3 carcinomas, and 71.1% in T4 carcinomas. The overall accuracy was 77.6%.

Tumors were overstaged in 8 patients. T1 carcinoma was overstaged as a T2 carcinoma in 3 patients and as a T3 carcinoma in 1 patient (Figure 2), and T2 carcinoma was overstaged as a T3 carcinoma in 4 patients. Tumors were understaged in 20 patients. T3 carcinoma was understaged as a T2 carcinoma in 7 patients. T4 carcinoma was understaged as a T2 carcinoma in 2 patients and as a T3 carcinoma in 11 patients.

Invasion of adjacent organs confirmed by operative or pathologic findings was as follows (Table 2): pancreas (31 patients), liver (7 patients), spleen and hilum of spleen (3 patients), transverse colon (3 patients), diaphragm (2 patients), and duodenum (9 patients). The detection rate for pancreas and liver invasion with transabdominal US was 77.4% and 71.4%, respectively, whereas the detection rate for the invasion of other organs was low.

Figure 2 Mucosal carcinoma (T1) was overstaged as a T3 carcinoma with transabdominal US. Sonogram of gastric body shows hypoechoic wall thickening with ulcer (arrow), loss of wall five-layer structure (triangle).

Table 1 Accuracy of transabdominal US in assessing the depth of tumor invasion in 125 patients

Stage	*n*	Staged by operative and pathological findings			
		T1	T2	T3	T4
T1	7	5	0	0	0
T2	34	3	12	7	2
T3	80	1	4	48	11
T4	38	0	0	0	32
Accuracy (%)		55.6 (5/9)	75.0 (12/16)	87.3 (48/55)	71.1 (32/45)

Table 2 Detection rate of tumor invasion with transabdominal US

Involved organs	*n*	Cases detected with transabdominal US	Detection rate (%)
Pancreas	31	24	77.4
Liver	7	5	71.4
Spleen and hilum of spleen	3	1	33.3
Transverse colon	3	1	33.3
Diaphragm	2	0	0
Duodenum	9	4	44.4

Assessment of regional lymph node metastasis

Accuracy of assessment of regional lymph metastasis Swollen lymph nodes were found pathologically in 106 patients. Lymph node metastasis was confirmed in 67 of 106 patients. Swollen lymph nodes were detected in 66 of 106 patients with transabdominal US. All lymph nodes detected sonographically had a length of 5 mm or greater, and were considered as metastatic. Of the 66 patients, lymph node metastasis was confirmed by pathological examination in 52 patients, and swollen lymph nodes were benign in the remaining 14 patients. No swollen lymph nodes were detected sonographically in 40 of 106 patients, and lymph node metastasis was confirmed in 15 of these 40 patients. The sensitivity of transabdominal US in the assessment of lymph node metastasis was 77.6% (52 of 67 patients). The specificity was 64.1% (25 of 39 patients). The accuracy was 72.6% (77 of 106 patients) (Table3).

Table 3 Accuracy of transabdominal US in assessing lymph node metastasis in 106 patients

Diagnosis with transabdominal US	Pathological findings (*n*)	
	N+	N0
N+	52	14
N0	15	25

Sensitivity: 77.6% (52/67); Specificity: 64.1% (25/39); Accuracy: 72.6% (77/106).

Sonographic features of benign and malignant lymph nodes All lymph nodes in 14 of 66 patients with swollen lymph nodes detected with transabdominal US were confirmed benign (lymph node without metastasis), and transabdominal US detected 46 lymph nodes in these patients. All lymph nodes in 11 of 52 patients with lymph node metastasis were confirmed malignant (metastatic), and transabdominal US detected 48 lymph nodes in these patients. Forty-six benign lymph nodes had a mean length of 1.26 cm and a mean width of 0.84 cm, 48 malignant lymph nodes had a mean length of 1.79 cm and a mean width of 1.25 cm. According to size, shape, echogenicity, and border, sonographic features of these benign and malignant lymph nodes were further analyzed (Table 4). The length and width of benign lymph nodes were significantly smaller than those of malignant lymph nodes (P = 0.000, 0.005). Sonographic features such as irregular or fusional shape, infiltrative signs, and inhomogenous echoes were found mainly in malignant lymph nodes (Figure 3). There was a significant difference between benign and malignant lymph nodes (P = 0.045, 0.006, 0.027, 0.006).

Table 4 Sonographic features of 46 benign and 48 malignant lymph nodes

Sonographic feature	Pathologic findings		*P*
	Benign lymph nodes (%)	Malignant lymph nodes (%)	
Length (cm)			0.000
<0.5	0	0	
0.5-1.0	26 (56.5)	9 (18.8)	
1.1-1.5	9 (19.6)	16 (33.3)	
1.6-2.0	9 (19.6)	8 (16.7)	
⩾2.1	2 (4.3)	15 (31.2)	
Length (cm)			0.000
<0.5	0	0	
0.5-1.0	26 (56.5)	9 (18.8)	
1.1-1.5	9 (19.6)	16 (33.3)	
1.6-2.0	9 (19.6)	8 (16.7)	
⩾2.1	2 (4.3)	15 (31.2)	
Width (cm)			0.005
<0.5	5 (10.9)	2 (4.2)	
0.5-1.0	34 (73.9)	22 (45.8)	
1.1-1.5	4 (8.7)	10 (20.8)	
1.6-2.0	3 (6.5)	11 (22.9)	
⩾2.1	0 (0)	3 (6.3)	
Shape			
Spindle	9 (19.6)	5 (10.4)	
Ovoid	15 (32.6)	10 (20.8)	
Round	20 (43.5)	17 (35.4)	
Irregular	2 (4.3)	8 (16.7)	0.045
Fusional	0 (0)	8 (16.7)	0.006
Border			
Distinct	34 (73.9)	29 (60.4)	
Indistinct	12 (26.1)	13 (27.1)	
Infiltrative signs	0 (0)	6 (12.5)	0.027
Echogenicity			
Hypoechoic	40 (87.0)	38 (79.1)	
Slightly hyperechoic	6 (13.0)	2 (4.2)	
Inhomogenous	0	8 (16.6)	0.006

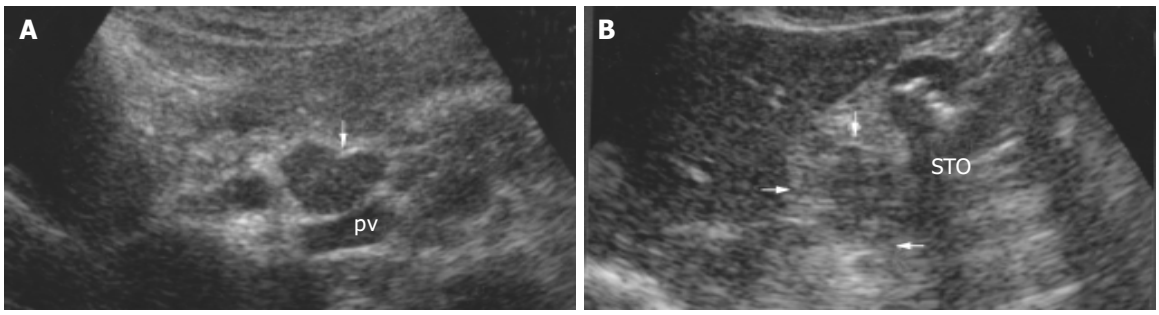

Figure 3 Metastatic lymph node. A: Sonogram shows a irregular lymph node (arrow) adjacent to the portal vein (PV) with a distinct border and 2.1×1.7 cm in size. B: Sonogram shows fusional-shaped lymph node (arrow) (4×3 cm) adjacent to the stomach (STO), invading adjacent tissues and having an indistinct border.

DISCUSSION

Assessment of the depth of tumor invasion in gastric cancer

Compared with the operative and pathological findings, the accuracy of transabdominal US for T1, T2, T3, T4 was 55.6%, 75.0%, 87.3%, 71.1%, respectively, and the overall accuracy was 77.6% (Table 1).

Although the accuracy of transabdominal US in staging of T1 carcinoma was low (55.6%), T2, T3, and T4 staging results were compared favorably with those of EUS T staging. Lim *et al*.[15] reported the accuracy of staging in early-stage carcinoma was 66.7% (10 of 15 patients) with transabdominal US. In the study of Segura *et al*.[16], the accuracy of transabdominal US for T1, T2, T3, T4 was 100%, 50%, 87%, 81%, respectively. Due to the small number of patients with early stage carcinoma (2 patients), the results of T1 staging required further investigation.

In our study, the accuracy for T3 carcinomas was the highest (87.3%) among the four groups with different depths of infiltration. The normal serosal layer was a thin and smooth hyperechoic band sonographically. When tumor invaded into the serosal layer, this band was interrupted or disappeared, which could be assessed easily with transabdominal US.

In our study, the accuracy for T1 carcinomas was most unfavorable (55.6%) because of overstaging in 4 patients, of which 3 had ulcerative carcinoma. Similarly, misdiagnosis was made in 4 patients with T2 carcinoma due to overstaging as a T3 carcinoma, and these 4 patients also had ulcerative carcinoma. Previous studies showed that the hyperechoic submucosal layer became hypoechoic because of inflammation or edema around the tumor, which was similar to echogenicity of muscularis propria and tumor. It was difficult to differentiate 3 layers with transabdominal US[19], so T1 carcinoma might be overstaged as T2 carcinoma (tumor invading muscularis propria). On the other hand, the ulcer in gastric cancer may cause gastric wall fibrosis and scar, which lead to wall thickening, loss of wall layers, and even interruption or disappearance of serosal layer, therefore, overstaging as T3 carcinoma may occur in T1 or T2 carcinoma (Figure 2). Difficulties in differentiation between tumors and peritumor inflammation or scar may be an important source of overstaging[5,6,15,20-23].

As shown in Table 1, misdiagnosis was made in T1 and T2 carcinomas because of overstaging. On the contrary, misdiagnosis was made in T3 and T4 carcinomas because of understaging. The possible reasons for understaging were as follows: (1) The procedure did not practise adequately, because transabdominal US was technically difficult to perform and may fail to guarantee a correct diagnosis for tumors locating in gastric fundus, greater curvature or cardia[15]. Tumors in 8 of 20 understaged patients located in the above locations, respectively. (2) Location of involved organs also affected the diagnosis, because it was difficult to clearly visualize hilum of spleen, diaphragm, and the tail of pancreas. Invasions of the tail of pancreas (4 patients), diaphragm (2 patients), spleen and hilum of spleen (2 patients) were not detected with transabdominal US. (3) Microscopic tumor invasion undetected with transabdominal US was another cause of understaging[6], which occurred in 2 patients with T3 carcinoma.

Assessment of adjacent organ invasion with transabdominal US

The fact that gastric cancer invaded into adjacent organs would decrease surgical resectability, so it is important to assess preoperatively if organs are invaded by gastric cancer.

In our study, the followings were taken as the diagnostic criteria for gastric cancer invading into organs: interruption of the serosal layer of gastric wall, indistinguishable from adjacent organs, tumor and organs moving synchronously slow or no moving as breath changed.

Pancreas was the most common organ invaded by tumor, the detection rate in this study was 77.4%. In 3 of 7 patients undetected by transabdominal US, pancreas was invaded slightly, and the boundary between pancreas and tumor seemed to exist on sonogram, thus leading to understaging. In the remaining 4 patients, the tail of pancreas was invaded, which was not detected by transabdominal US due to interference of bowel gas and ribs.

The detection rate for liver invasion was higher (71.4%). Tumors invading liver located in anterior wall of stomach or lesser curvature and were close to the liver. The relationship between tumor and liver could be visualized clearly by using ultrasonographic beam through liver without interference of bowel gases.

Transverse colon was invaded in three patients, of them, correct diagnosis was made in 1 patient because complete circumference of transverse colon was invaded and marked tumor was detected. In two others undetected by transabdominal US, transverse colon was slightly invaded and bowel gases interfered severely. Correct diagnosis was made preoperatively in 1 of 3 patients with spleen and its hilum invasion. None was diagnosed preoperatively for diaphragm invasion. Spleen and its hilum, and diaphragm could not be observed completely with transabdominal US, leading to the low detection rate.

Correct diagnosis was made preoperatively in 4 of 9 patients with duodenum invasion. It was necessary to fill duodenum by drinking water for the assessment of duodenum. Because tumor caused gastric lumen obstruction, duodenum was not filled adequately and visualized clearly, leading to misdiagnosis of duodenum invasion.

Assessment of lymph node metastasis and differentiation between benign and malignant lymph nodes

The sensitivity of transabdominal US for lymph node metastasis was 77.6%, and the false positive rate was 13.2% (14 of 106 patients). The results showed transabdominal US did not permit the differentiation between benign and (metastatic) malignant lymph nodes in gastric cancer (Figures 4, 5).

Benign swollen lymph nodes due to immune reaction in patients with tumor are misdiagnosed easily as malignant lymph nodes. According to the analysis of sonographic features of lymph nodes (Table 4), benign lymph nodes were smaller than malignant lymph nodes in length and width (P = 0.000, 0.005). From Table 5, if the length $\geqslant$1.1 cm or 1.6 cm was defined as diagnostic criteria of malignant lymph nodes, the sensitivity was 81.3% and 47.9%, respectively, and the specificity was 56.5% and 76.1%, respectively. Hence the criteria could not differentiate benign from malignant lymph nodes. If the length $\geqslant$2.1 cm or the width $\geqslant$1.6 cm was defined as diagnostic criteria of malignant lymph nodes, the sensitivity was 33.3% and 29.2%, respectively, and the specificity was 95.7% and 93.5%, respectively. This result showed that lymph node with a length $\geqslant$2.1 cm or width $\geqslant$1.6 cm increased significantly the probability of metastasis. From the literature and our study, although benign lymph nodes were smaller than malignant lymph nodes, it is clear that there was a considerable overlap in size between benign and malignant lymph nodes; therefore, the value of lymph node size is limited for discriminating benign lymph nodes from malignant lymph node[18,24,25].

In our study (Table 2), benign and malignant lymph nodes in round shape were encountered most commonly (Figures 4, 5) and spindle and ovoid lymph nodes were also seen , there was no significant difference between two kinds of lymph nodes. Malignant lymph nodes in irregular shape were mostly seen, and all fusional-shaped lymph nodes were malignant (Figure 3), there was a significant difference between benign and malignant lymph nodes (P = 0.045, 0.006). It was reported that

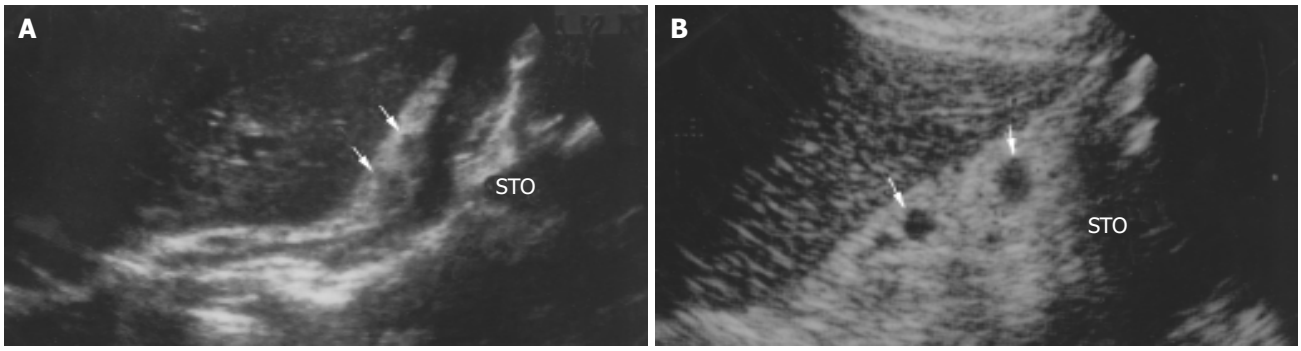

Figure 4 Differentiation between benign and metastatic lymph nodes. A: Benign lymph nodes. Sonogram shows multiple small lymph nodes (arrow) adjacent to the lesser curvature of stomach (STO). These hypoechoic lymph nodes are 5-8 mm, and misdiagnosed as metastatic with transabdominal US; Pathologic examination confirms that all theses lymph nodes are reactive and noncancerous. B: Metastatic lymph nodes. Sonogram is similar to figure A. Multiple hypoechoic small lymph nodes (arrow) adjacent to the lesser curvature of stomach (STO) are 5-9 mm, and confirmed metastatic by pathologic examination.

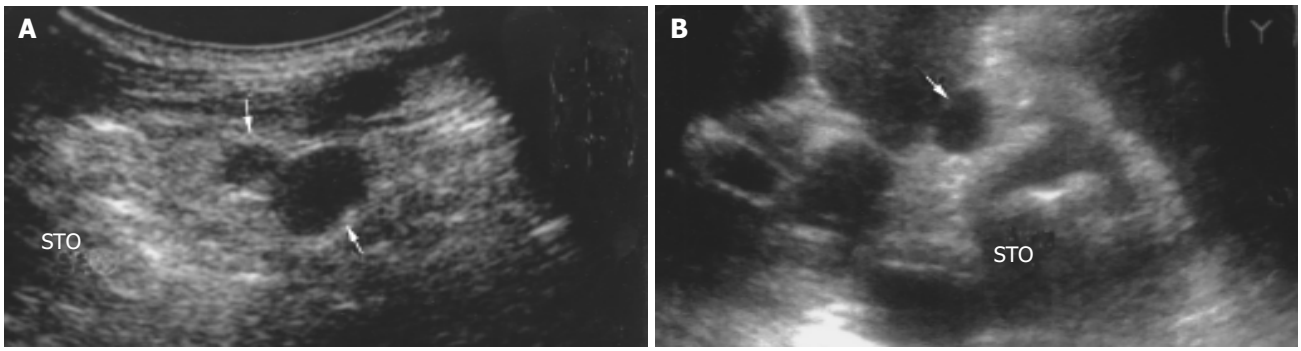

Figure 5 Differentiation between benign and metastatic lymph nodes. A: Benign lymph nodes. Sonogram shows multiple hypoechoic lymph nodes (arrow) adjacent to the greater curvature of stomach (STO). Of them, the largest is 1.8 cm with a distinct border. These lymph nodes are misdiagnosed as metastatic with transabdominal US. Pathologically, all theses lymph nodes are reactive and noncancerous. B: Metastatic lymph node. Sonogram shows hypoechoic lymph node (arrow) adjacent to the lesser curvature of stomach (STO) with 1.6 cm in size and a distinct border. Pathologic examination confirms this lymph node is metastatic.

abdominal malignant lymph nodes were round or ovoid in shape, conversely, benign lymph nodes in people who were healthy or affected by benign disease were spindle or flat in shape[9,18,24,26-30]. However in our study, both benign and malignant lymph nodes were mostly round in shape, and round shape did not allow the correct differentiation between benign and malignant lymph nodes. Immune reaction caused by tumor was different from that caused by benign diseases such as hepatitis or entities, which may be a cause for difficulties in differentiation between benign and malignant lymph nodes.

In our study the majority of benign and malignant lymph nodes had a distinct border (Figure 5), without statistical difference between them (Table 4). "Infiltrative signs" of lymph nodes were seen only in malignant lymph nodes (P = 0.027), which were typical and helpful for diagnosing malignant lymph nodes. Heintz *et al*.[31] reported that both benign and malignant lymph nodes had an indistinct or distinct border by studying surgical resection specimens of patients with esophageal and gastric carcinomas. The study reported by Akahoshi *et al*.[29,32] showed that malignant lymph nodes had a distinct border.

Table 4 shows that both benign and malignant lymph nodes were hypoechoic mostly (Figures 3-5), and the small number of lymph nodes was hyperechoic. There was no difference between benign and malignant lymph nodes. Inhomogenous echogenicity was seen only in malignant lymph nodes, there was a significant difference between benign and malignant lymph nodes (P = 0.006) and majority of inhomogenous lymph nodes were 2 cm greater in length. Contradictory data were published for echogenicity of lymph nodes. Heintz *et al*.[31] stressed that echogenicity did not allow the correct differentiation between benign and malignant lymph nodes. Other authors[24,33] reported that most malignant lymph nodes were hypoechoic, and most benign lymph nodes were isoechoic or slightly hyperechoic. The different results might result from different patients studied.

In our study, the following 4 sonographic features were taken as the diagnostic criteria of malignant lymph nodes (Table 5): irregular shape, fusional shape, infiltrative signs, and inhomogenous echo. The sensitivity of the criteria was lower than 20 percent, and the specificity was higher than 90 percent. One of these 4 features was helpful to suggest malignant, however the similar sonographic features were observed in abdominal tuberculosis. Differential diagnosis was made on the basis of medical history.

Table 5 Diagnostic results of 46 benign and 48 malignant lymph nodes

Criterion	Sensitivity (%)	Specificity (%)
Length ⩾1.1cm	81.3 (39/48)	56.5 (26/46)
⩾1.6 cm	47.9 (23/48)	76.1 (35/46)
⩾2.1 cm	33.3 (15/48)	95.7 (44/46)
Width ⩾1.1 cm	50.0 (24/48)	84.8 (39/46)
⩾1.6 cm	29.2 (14/48)	93.5 (43/46)
Irregular	16.7 (8/48)	95.7 (44/46)
Fusional	16.7 (8/48)	100 (46/46)
Infiltrative signs	12.5 (6/48)	100 (46/46)
Inhomogenous	16.7 (8/48)	100 (46/46)

Swollen lymph nodes were found pathologically in 106 patients. But no swollen lymph nodes were detected with transabdominal US in 40 of 106 patients, and lymph nodes metastases were confirmed pathologically in 15 of these 40 patients. Missing lymph nodes were associated with the size of lymph nodes mainly. Lymph nodes less than 5 mm in size were usually undetectable with transabdominal US. In addition, obesity and bowel gas were unfavorable for detection of lymph nodes.

In conclusion, transabdominal US is useful for preoperative staging of gastric cancer, especially for assessment of advanced gastric cancer invasion. Although it is difficult to differentiate benign from malignant lymph nodes, typical sonographic features might contribute to diagnosis.

REFERENCES

1 **Sipponen P**, Jarvi O, Kekki M, Siurala M. Decreased incidences of intestinal and diffuse types of gastric carcinoma in Finland during a 20-year period. *Scand J Gastroenterol* 1987; **22**: 865-871

2 **Silverberg E**. Cancer statistics, 1980. *CA Cancer J Clin* 1980; **30**: 23-38

3 **Gelfand DW**, Ott DJ. Single-*vs* double-contrast gastrointestinal studies: critical analysis of reported statistics. *Am J Roentgenol* 1981; **137**: 523-528

4 **White RM**, Levine MS, Enterline HT, Laufer I. Early gastric cancer. Recent experience. *Radiology* 1985; **155**: 25-27

5 **Xi WD**, Zhao C, Ren GS. Endoscopic ultrasonography in preoperative staging of gastric cancer: determination of tumor invasion depth, nodal involvement and surgical resectability. *World J Gastroenterol* 2003; **9**: 254-257

6 **Wang JY**, Hsieh JS, Huang YS, Huang CJ, Hou MF, Huang TJ. Endoscopic ultrasonography for preoperative locoregional staging and assessment of resectability in gastric cancer. *Clin Imaging* 1998; **22**: 355-359

7 **Rosch T**. Endosonographic staging of gastric cancer .a review of literature results. *Gastrointest Endosc Clin N Am* 1995; **5**: 549-557

8 **Ohashi S**, Nakazawa S, Yoshino J. Endoscopic ultrasonography in the assessment of invasive gastric cancer. *Scand J Gastroenterol* 1989; **24**: 1039-1048

9 **Botet JF**, Lightdale CJ, Zauber AG, Gerdes H, Winawer SJ, Urmacher C, Brennan MF. Preoperative staging of gastric cancer: comparison of endoscopic US and dynamic CT. *Radiology* 1991; **181**: 426-432

10 **Bolondi L**, Casanova P, Caletti GC, Grigioni W, Zani L, Barbara L. Primary gastric lymphoma versus gastric carcinoma: endoscopic US evaluation. *Radiology* 1987; **165**: 821-826

11 **Puylaert JB**. Acute appendicitis: US evaluation using graded compression. *Radiology* 1986; **158**: 355-360

12 **Kimmey MB**, Martin RW, Haggitt RC, Wang KY, Franklin DW, Silverstein FE. Histologic correlates of gastrointestinal Ultrasound images. *Gastroenterology* 1989; **96**(2 Pt 1): 433-441

13 **Wiersema MJ**, Wiersema LM. High-resolution 25-megahertz ultrasonography of the gastrointestinal wall: histologic correlates. *Gastrointest Endosc* 1993; **39**: 499-504

14 **Lim JH**, Jeong YM. Sonography of the stomach: an *in vitro* study to determine the anatomic cause of inner hyperechoic and hypoechoic layers of the gastric wall. *Am J Roentgenol* 1994; **162**: 335-338

15 **Lim JH**, Ko YT, Lee DH. Transabdominal US staging of gastric cancer. *Abdom lmaging* 1994; **19**: 527-531

16 **Segura JM**, Olveira A, Conde P, Erdozain JC, Suarez J. Hydrogastric sonography in the preoperative staging of gastric cancer. *J Clin Ultrasound* 1999; **27**: 499-504

17 **Sobin LH**, Hermanek P, Hutter RV. TNM classification of malignant tumors. A comparison between the new(1987) and the old editions. *Cancer* 1998; **61**: 2310-2314

18 **Smeets AJ**, Zonderland HM, van der Voorde F, Lameris JS. Evaluation of abdominal lymph nodes by ultrasound. *J Ultrasound Med* 1990; **9**: 325-331

19 **Tio TL**, Coene PP, Schouwink MH, Tytgat GN. Esophagogastric carcinoma: preoperative TNM classification with endosonography. *Radiology* 1989; **173**: 411-417

20 **Grimm H**, Binmoeller KF, Hamper K, Koch J, Henne-Bruns D, Soehendra N. Endosonography for preoperative locoregional staging of esophageal and gastric cancer. *Endoscopy* 1993; **25**: 224-230

21 **Dittler HJ**, Siewert JR. Role of endoscopic ultrasonography in gastric carcinoma. *Endoscopy* 1993; **25**: 162-166

22 **Tio TL**, Coene PP, Luiken GJ, Tytgat GN. Endosonography in the clinical staging of esophagogastric carcinoma. *Gastrointest Endosc* 1990; **36**(2 Suppl): S2-10

23 **Yanai H**, Matsumoto Y, Harada T, Nishiaki M, Tokiyama H, Shigemitsu T, Tada M, Okita K. Endoscopic ultrasonography and endoscopy for staging depth of invasion in early gastric cancer: a pilot study. *Gastrointest Endosc* 1997; **46**: 212-216

24 **Gimondo P**, Mirk P, Messina G, Pizzi C. Abdominal lymphadenopathy in benign diseases: sonographic detection and clinical significance. *J Ultrasound Med* 1996; **15**: 353-359

25 **Dorfman RE**, Alpern MB, Gross BH, Sandler MA. Upper abdominal lymph nodes: criteria for normal size determined with CT. *Radiology* 1991; **180**: 319-322

26 **Sutton RT**, Reading CC, Charboneau JW, James EM, Grant CS, Hay ID. US-guided biopsy of neck masses in postoperative management of patients with thyroid cancer. *Radiology* 1988; **168**: 769-772

27 **Sakai F**, Kiyono K, Sone S, Kondo Y, Oguchi M, Watanabe T, Sakai Y, Imai Y, Takeda S, Yamamoto K. Ultrasonic evaluation of cervical metastatic lymphadenopathy. *J Ultrasound Med* 1988; **7**: 305-310

28 **Vassallo P**, Wernecke K, Roos N, Peters PE. Differentiation of benign from malignant superficial lymphadenopathy: the role of high–resolution US. *Radiology* 1992; **183**: 215-220

29 **Akahoshi K**, Misawa T, Fujishima H, Chijiiwa Y, Nawata H. Regional lymph node metastasis in gastric cancer: evaluation with endoscopic US. *Radiology* 1992; **182**: 559-564

30 **Subramanyam BR**, Balthazar EJ, Horii SC, Hilton S. Abdominal lymphadenopathy in intravenous drug addicts: sonographic features andclinical significance. *Am J Roentgenol* 1985; **144**: 917-920

31 **Heintz A**, Mildenberger P, Georg M, Braunstein S, Junginger T. Endoscopic ultrasonography in the diagnosis of regional lymph nodes in esophageal and gastric cancer-results of studies *in vitro*. *Endoscopy* 1993; **25**: 231-235

32 **Francois E**, Peroux J, Mouroux J, Chazalle M, Hastier P, Ferrero J, Simon J, Bourry J. Preoperative endosonographic staging of cancer of the cardia. *Abdom Imaging* 1996; **21**: 483-487

33 **Metreweli C**, Ward SC. Ultrasound demonstration of lymph nodes in the hepatoduodenal ligament ('Daisy Chain nodes') in normal subjects. *Clin Radiol* 1995; **50**: 99-101

Edited by Wang XL and Chen WW **Proofread by** Xu FM

PO Box 2345, Beijing 100023, China
Fax: +86-10-85381893
E-mail: wjg@wjgnet.com www.wjgnet.com

World J Gastroenterol 2004;10(23):3405-3408
World Journal of Gastroenterology
Copyright © 2004 by The WJG Press ISSN 1007-9327

• GASTRIC CANCER •

Surgical treatment and prognosis of gastric cancer in 2 613 patients

Xiang-Fu Zhang, Chang-Ming Huang, Hui-Shan Lu, Xing-Yuan Wu, Chuang Wang, Guo-Xian Guang, Jian-Zhong Zhang, Chao-Hui Zheng

Xiang-Fu Zhang, Chang-Ming Huang, Hui-Shan Lu, Xing-Yuan Wu, Chuang Wang, Guo-Xian Guang, Jian-Zhong Zhang, Chao-Hui Zheng, Department of Oncology, Affiliated Union Hospital of Fujian Medical University, Fuzhou 350001, Fujian Province, China
Correspondence to: Dr. Xiang-Fu Zhang, Department of Oncology, Affiliated Union Hospital, Fujian Medical University, Xingchun Road No.11, Fuzhou 350001, Fujian Province, China. zjzchina@vipsina.com
Telephone: +86-591-3320856 **Fax:** +86-591-3321970
Received: 2003-12-10 **Accepted:** 2004-01-08

Abstract

AIM: To analyze the factors influencing the prognosis of patients with gastric cancer after surgical treatment, in order to optimize the surgical procedures.

METHODS: A retrospective study of 2 613 consecutive patients with gastric cancer was performed. Of these patients, 2 301 (88.1%) received operations; 196 explorative laparotomy (EL), 130 by-pass procedure (BPP), and 1 975 surgical resection of the tumors (891 palliative resection and 1 084 curative resection). The survival rate was calculated by the actuarial life table method, and the prognostic factors were evaluated using the Cox regression proportional hazard model.

RESULTS: Of the patients, 2 450 (93.8%) were followed-up. The median survival period was 4.6 mo for patients without operation, 5.2 mo for EL, 6.4 mo for BPP, and 15.2 mo for palliative resection (P = 0.0001). Of the patients with surgical resection of the tumors, the overall 1, 3 and 5-year survival rates after were 82.7%, 46.3% and 31.1%, respectively, with the 5-year survival rate being 51.2% in patients with curative resection, and 7.8% for those with palliative resection. The 5-year survival rate was 32.5% for patients with total gastrectomy, and 28.3% for those with total gastrectomy plus resection of the adjacent organs. The factors that independently correlated with poor survival included advanced stage, upper third location, palliative resection, poor differentiation, type IV of Borrmann classification, tumor metastasis (N_3), tumor invasion into the serosa and contiguous structure, proximal subtotal gastrectomy for upper third carcinoma and D_1 lymphadenectomy after curative treatment.

CONCLUSION: The primary lesion should be resected as long as the local condition permitted for stage III and IV tumors, in order to prolong the patients' survival and improve their quality of life after operation. Total gastrectomy is indicated for carcinomas in the cardia and fundus, and gastric cancer involving the adjacent organs without distant metastasis requires gastrectomy with resection of the involved organs.

Zhang XF, Huang CM, Lu HS, Wu XY, Wang C, Guang GX, Zhang JZ, Zheng CH. Surgical treatment and prognosis of gastric cancer in 2 613 patients. *World J Gastroenterol* 2004; 10(23): 3405-3408
http://www.wjgnet.com/1007-9327/10/3405.asp

INTRODUCTION

Although the mortality rate of gastric cancer has been dramatically decreased in the western country since 1930[1], cancer of the stomach remains the second most frequent malignancy in the world[2,3], and an estimate of more than 1 million new cases were identified worldwide in 1997[4]. From 1990 to 1992, the mortality rate of gastric cancer in China remained at a high level of 25.2/100 000, taking up 23.2% of the total cancer-related death, and claiming the largest death toll in cancer patients[5]. As the generally acknowledged primary treatment modality for gastric cancer, surgical interventions[6-9] give rise to many controversies concerning (1) the decision on palliative resection, by-pass procedure or avoidance of operation for advanced gastric cancer (including stage III_B or IV), (2) the optimal extent to be resected in patients with gastric cancer in the upper third, by total gastrectomy (TG) or proximal subtotal gastrectomy (PSTG), and (3) the optimal surgical resection for gastric cancer involving the neighboring organs. The aim of this retrospective study was to analyze the factors influencing the patients' prognosis after surgical treatment, curative or palliative, of gastric cancer, and find answers to above questions.

MATERIALS AND METHODS

Clinical data

This study included 2 613 patients with primary gastric cancer admitted in Department of Oncology, Affiliated Union Hospital of Fujian Medical University, during the period of June 1972 to June 2000. There were 2 059 male and 554 female patients whose ages ranged from 19 to 85 years with a mean of 55.6±2.48 years. The tumors were found in the gastric cardia and fundus in 871 cases, in the gastric body in 544 cases, in the gastric antrum in 1 069 cases and involving the entire stomach in 129 cases. The dimension (maximum diameter) of the tumor was smaller than 3 cm in 254 cases, between 3.1 and 6 cm in 1 290 cases and more than 6 cm in 1 069 cases. The tumors were histologically classified according to WHO classification criteria, and staged according to the TNM system used since 1989 in China[10], as listed in Table 1.

Table 1 Histological classification of the tumors in the 2 613 patients with gastric cancer

Histological classification	Number	Percentage (%)
Well differentiated adenocarcinoma	528	20.2
Moderately differentiated adenocarcinoma	1102	42.2
Mucinous adenocarcinoma	560	21.4
Poorly differentiated adenocarcinoma	277	10.6
Others	146	5.6
Borrmann's classification		
Type I	179	6.9
Type II	477	18.3
Type III	1683	64.4
Type IV	129	4.9
Early-stage cancer	145	5.6

Methods

Of all those patients, 312 had not received any previous surgical intervention, and 2 301 (88.1%) had undergone operations. Among the patients with a history of previous operations, 196 had explorative laparotomy (EL), 130 had by-pass procedure (BPP), 1 975 underwent surgical resection of the tumor, of whom 891 received palliative resection. The tumor resection was considered palliative on the basis of the presence of residual tumor or distant metastasis or both at the end of surgery. A total of 1 084 patients underwent curative resection, making up 54.9%. The surgical procedure was defined as curative when no grossly visible tumor tissue (metastasis or lymph node involvement) remained after the resection and the resection margins were histologically normal.

In all the 1 975 surgical patients, distal subtotal gastrectomy (DSTG) was performed in 894 patients, total gastrectomy (TG) in 615, and proximal subtotal gastrectomy (PSG) in 466. Among the patients undergoing curative resection, limited D_1 nodal dissection was performed in 159 patients (during the period of 1 972 to 1 979), extended D_2/D_2^+ in 846 and extended D_3 in 79. The clinical data of the 1 975 patients with surgical tumor resection are shown in Table 2. Metastases involving such organs as the esophagus, spleen, pancreas, colon and the duodenum were identified in 439 patients.

Table 2 Clinical data of the 1 975 patients with surgical resection of the tumor

Characteristics	Number	Percentage (%)
Type of resection		
Radical resection	1 084	54.9
Palliative resection	891	45.1
Depth of invasion (T)		
Mucosa/submucosa (PT_1)	145	7.3
Muscularis (PT_2)	347	17.6
Serosa (PT_3)	978	49.5
Serosa and contiguous structure (PT_4)	505	25.6
Lymph node involvement (N)		
N_0	207	10.5
N_1	343	17.4
N_2	936	47.4
N_3	489	24.7
Stage		
I_A	125	6.3
I_B	131	6.6
II	251	12.7
III_A	404	20.5
III_B	442	22.4
IV	622	31.5
Type of nodal dissection (radical resection)		
D_1	159	14.7
D_2/D_2^+	846	78.0
D_3	79	7.3

The 5-year cumulative survival was calculated after both curative and palliative tumor resection by actuarial life-table method. Statistical analysis was carried out by using Chi-square test and Wilcoxon rank sum test. Multivariate analysis was applied using the Cox regression proportional hazard model. The SPSS 10.0 for Windows was used for all the statistical analyses.

RESULTS

Among the 2 613 patients with gastric cancer, 163 failed to be followed-up with the follow up rate of 93.8%. Postoperative complications arose in 189 cases with an incidence of 9.6%. Death within one month after operation occurred in 41 cases (2.1%).

The survival rate was calculated in 1 498 patients with surgical resection, curative and palliative, of the tumors. Univariate and multivariate analyses were used to evaluate 5-year survival rate with respect to the main clinicopathologic and treatment variables after both curative and palliative treatment. The overall 5-year survival after surgical resection (operative mortality excluded) was 31.6%, 51.2% for curative treatment, and 7.8% for palliative resection; 91.1% for stage I_A, 86.7% for stage I_B, 51.1% for stage II, 34.5% for stage III_A, 29.1% for stage III_B, and 5.9% for stage IV (Figure 1, Table 3). The median survival period was 4.6 mo after NO, 5.2 mo after EL, 6.4 mo after BPP, and 15.2 mo after palliative resection (P = 0.0001). The 5-year survival rate was 32.5% for patients with total gastrectomy, and 28.3% for those with total gastrectomy plus resection of the adjacent organs. Univariate and multivariate survival analyses showed that the variables independently correlated with poor survival included advanced stage, upper third location, palliative resection, poorly differentiated adenocarcinoma, type IV of Borrmann classification, tumor metastasis (N_3), tumor invasion into the serosa and contiguous structure, proximal subtotal gastrectomy for upper third carcinoma and D_1 lymphadenectomy after curative treatment (Table 4).

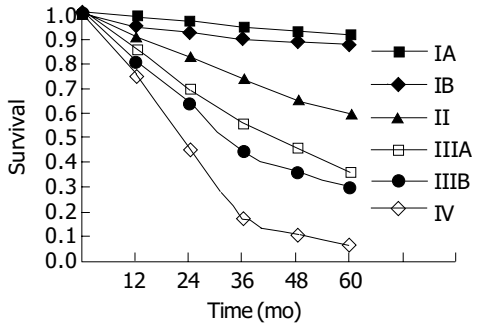

Figure 1 Survival curves of the 1 498 patients of different clinical stages undergoing surgical resection (radical and palliative) with operative death excluded.

Table 3 Univariate survival analysis of clinical and pathologic variables after surgical treatment in 1 498 cases with gastric carcinoma

Parameter	Number	5-yr survival rate (%)	P
Age (yr)			
≤30	19	21.0	0.05
30 to 60	926	29.2	
>60	553	36.2	
Tumor location			
C (upper third)	499	22.6	0.001
M (middle third)	312	35.3	
A (lower third)	613	40.9	
MCA (whole stomach)	74	2.7	
Tumor size (cm)			
<3	146	53.1	0.047
3 to 6	739	40.9	
>6	613	15.3	
Histological classification			
Well differentiated adenocarcinoma	303	38.3	0.001

Moderately differentiated adenocarcinoma	631	36.7	
Mucinous adenocarcinoma	321	28.3	
Poorly differentiated adenocarcinoma	159	15.7	
Others	84	13.1	
Type of operation			
DSTG	678	37.2	0.001
TG	466	32.4	
PSG	354	20.1	
Borrmann's classification			
Type I	103	61.1	0.001
Type II	274	45.2	
Type III	964	20.1	
Type IV	74	2.7	
Early cancer	83	90.0	
Type of resection			
Radical resection	822	51.2	0.001
Palliative resection	676	7.8	
Extent of nodal dissection			
D_1	120	34.5	0.001
D_2 to D_2^+	641	53.5	
D_3	61	50.8	
Depth of cancer invasion			
T_1	110	90.4	0.001
T_2	263	55.2	
T_3	742	25.9	
T_4	383	10.0	
Lymph node involvement			
N_0	157	86.1	0.001
N_1	260	58.1	
N_2	710	23.3	
N_3	371	5.9	

Table 4 Multivariate analysis of prognostic variables for survival

Variables	Regression coefficient	*P*
Type of resection	0.45729	0.00081[1]
Extent of nodal dissection	0.35851	0.00479[1]
Borrmann's classification	0.42583	0.00295[1]
Tumor location	0.25409	0.15204
Depth of cancer invasion	0.43839	0.00283[1]
Lymph node involvement	0.26738	0.14962
Type of operation	0.25016	0.15978
Tumour size	0.00421	0.97279

[1]Significant difference.

DISCUSSION

Surgical treatment of gastric cancer has been universally recognized as the most effective way of treatment, and the 5-year survival rate of curative resection in this study reached 51.2%. Although curative resection for gastric cancer is most effective, most cases are in stage III and IV on identification in China[11-13], as seen from the high rate of 74.9% in this study, and many of them were ineligible for radical treatment. Ekbom *et al*.[14] reported that BPP in advanced cases only resulted in the average survival period of 5.9 mo, and none of the patients survived for more than one year, similar to the results of without tumor resection[15]. The average survival periods of patients without operation, with EL and BPP in China, as reported by National Gastric Cancer Cooperation Organization, were 4.1, 4.7, and 5.5 mo, respectively[11], comparable with our findings (4.6, 5.2, and 6.4 mo, respectively, $P>0.05$). In this study, the survival period after palliative resection was 15.2 mo with a 5-year survival rate reaching 7.8%, significantly higher than that in patients without operation or with EL and BPP ($P<0.01$). Therefore, for stage III and IV gastric cancer, resection of the primary focus should be performed as much as possible. After the resection, the patient's condition might be improved to tolerate postoperative chemotherapy, immunotherapy and comprehensive treatment by traditional Chinese medicine, and the survival period of the patients might consequently be prolonged and quality of life improved[16-20].

There is still controversy over the impact of the extent of resection for tumors located in the upper third of the stomach (including cardia and fundus)[21]. Some researchers[22-25] advocate the performance of PSG so as to possibly retain the stomach even partially, and proper digestive function. It also enables patients to avoid the late stage complications following TG. However, Fujimaki and Lin discovered in their respective research that the rate of lymphatic metastasis of group 5 and 6 might reach up to 24.0% to 29.0% in some cases[26,27]. It is difficult to eliminate all tumor tissues without performing TG. The incidence of postoperative regurgitant esophagitis is high and volume of residual stomach is small, and TG may overcome these defects to improve the 5-year survival rate[28-31]. According to the review of our 28-year experience with the treatment of gastric cancer, two types of resection for cancer of the cardia (the upper 1/3 location) irrespective of the tumor stage contributed to a 5-year survival rate after TG of up to 32.5%, while the 5-year survival rate after PSG was only 20.1%, showing significant difference ($P<0.05$). Following great improvements in surgical techniques, postoperative care and measures of digestive tract reconstruction, postoperative complication and death rate have been remarkably decreased[32-34]. The incidence of complication was only 12.7% and death rate 2.9% in the 615 patients receiving TG in this study. In recent years, we attempted routine TG for treating cancer of the upper 1/3 location as long as the patients' general condition permitted, and of all gastrectomy cases, 31.1% were received TG in the study.

In approximately 15.5-22.3% of patients with advanced gastric cancer, the malignancy had already invaded the neighboring organs when the diagnosis was established[11,35,36], requiring critical decisions on the treatment for the best interests of the patients. In this study, 439 cases (22.9% of those with surgical resection) had combined resection of the involved organs, and the total 5-year survival rate was 28.3%. In these cases extensive radical resection of gastric cancer combined with resection of the spleen and the body and tail of pancreas was found to produce the best therapeutic effect, yielding a 5-year survival rate of 43.2%. For treatment of 28 cases of advanced gastric cancer involving multiple neighboring organs, left upper abdominal evisceration (LUAE) and resection of the total stomach, lower end of esophagus, left lobe of liver, spleen, body and tail of pancreas, transverse colon and partial suprarenal gland were performed, resulting in a 5-year survival rate of up to 16.7%. One of the patients has survived for 10 years. Pessimism toward gastric cancer invading nearby organs is not reasonable. For gastric cancer with metastasis to adjacent organs, but without incurable factors such as liver metastasis, peritoneal dissemination (P_2 and P_3) and widespread nodal involvement, complete excision of the invaded organs should be performed as much as possible, irrespective of the number or site of the invaded organs. Cure is possible in some cases of advanced gastric cancer. In cases with incurable factors, partial resection of the involved organs is not recommended, as it almost invariably fails to prolong the patients' survival in comparison with simple resection of the primary focus of gastric cancer, but increases the sufferings of the patient and prolongs the operation time.

Palliative operation to resect the primary focus might be a better alternative, for it not only relieves obstruction, hemorrhage and pain, but also prepares favorable condition for other postoperative treatments and at the same time, improves the quality of life and prolongs the survival period of the patient.

REFERENCES

1 **Abeloff MD,** Armitage JO, Lichter AS, Niederhuber JE. Clinical Oncology. Second edition. *China Science Press Harcourt Asia China* 2001: 1545-1585

2 **Price P,** Sikore K, Treatment of cancer. 4th edition London. *New york NewDeLHI Arnold press* 2002: 583-599

3 **Pisani P,** Parkin DM, Bray F, Ferlay J. Erratum: Estimates of the worldwide mortality from 25 cancers in 1990. *Int J Cancer* 1999; **83**: 870-873

4 World Health Organization, *the world health report. Geneva* WHO 1997

5 **Sun X,** Mu R, Zhou Y, Dai X, Qiao Y, Zhang S, Huangfu X, Sun J, Li L, Lu F. 1990-1992 mortality of sstomach cancer in China. *Zhonghua Zhongliu Zazhi* 2002; **24**: 4-8

6 **Furukawa H,** Imamura H, Kodera Y. The role of surgery in the current treatment of gastric carcinoma. *Gastric Cancer* 2002; **5** (Suppl 1): 13-16

7 **Souhami RL,** Tannock I, Hohenberger P, Horiot JC. Oxford textbook of oncology. Second edition. *Newyork Oxford University Press* 2002: 1617-1635

8 **Wu CW,** Lo SS, Shen KH, Hsieh MC, Lui WY, P'eng FK. Surgical mortality, survival, and quality of life after resection for gastric cancer in the elderly. *World J Surg* 2000; **24**: 465-472

9 **Bland KJ,** Daly JM, Karakousis CP, Surgical oncology. *Newyork, sanfrancisco, AUCKland. McGRAN-Hill Medical Publishing Dividion* 2001: 623-625

10 **Zhang TZ, Xu GW.** Zhongliuxue. First edition, *Tianjing. Tianjing Science-Technology Publishing Dividion* 1996: 1421-1505

11 National gastric cancer cooperative groups, Surgical operation of gastric cancer (analyse of 11 734 cases). *Zhonghua Waike Zazhi* 1982; **20**: 577-580

12 **Zhang RG,** Fang DK, Zhang DW, Wang LJ, Zhang DC, Yang L, Cheng GY, Meng PJ, Sun KL, Liu XY, Li J, Li WX, Huang JF. Surgical treatment results for carcinoma of the gastric cardia in 1832 cases. *Zhonghua Zhongliu Zazhi* 1998; **40**: 140-142

13 **Wang QS,** Lin MB, Su BH, Gao SY, Cui TJ, Xie JQ, Lin ZW, Lin ZH, Ye SQ, Lin XY, Tong GQ. Studies on therapeutic efficacy of surgical treatment in 1629 cases of gastric cancer. *Zhongguo Zhongliu Linchuang* 1995; **22**: 17-20

14 **Ekbom GA,** Gleysteen IJ. Gastric malignancy: resection for palliation. *Surgery* 1980; **88**: 476-481

15 **Moreaux J,** Msika S. Carcinoma of the gastric cardia: surgical management and long-term survival. *World J Surg* 1988; **12**: 229-235

16 **Maehara Y,** Sugimachi K, Akagi M, Kakegawa T, Shimazu H, Tomita M. Early postoperative chemotherapy following noncurative resection for patients with advanced gastric cancer. *Br J Cancer* 1992; **65**: 413-416

17 **Zhang XF,** Lu HS, Yin FS, Feng YM, Zheng ZW, Wu XY, Huang CM, Wu JG. Clinical experience in the treatment of 1108 patients with gastric carcinoma. *Zhonghua Zhongliu Zazhi* 1990; **12**: 49-51

18 **Maehara Y,** Moriguchi S, Sakaguchi Y, Emi Y, Kohnoe S, Tsujitani S, Sugimachi K. Adjuvant chemotherapy enhances long-term survival of patients with advanced gastric cancer following curative resection. *J Surg Oncol* 1990; **45**: 169-172

19 **Kim JP,** Yu HJ, Lee JH. Results of immunochemo-surgery for gastric carcinoma. *Hepatogastroenterology* 2001: **48**: 1227-1230

20 **Tas F,** Aykan NF, Aydiner A, Uygun K, Basaran M, Camlica H, Topuz E. The roles of chemotherapy and surgery in gastric carcinoma and the influence of prognostic factors on survival. *Am J Clin Oncol* 2000; **23**: 53-57

21 **Hansson LE,** Ekstrom AM, Bergstrom R, Nyren O. Surgery for stomach cancer in a defined Swedish population: current practices and operative results. Swedish gastric cancer study group. *World J Surg* 2000; **166**: 787-795

22 **Zhang DW,** Cheng GY, Huang GJ, Zhang RG, Zhang DC, Wang LJ, Xu PZ, Yang L, Liu JS, Chen YH, Sun KL, Peng L, Fang DK, Liu XY, Yang LH, He J, Mao YS, Li J. Surgical management of adenocarcinoma of the gastric cardia experience in 937 patients. *Zhonghua Zhongliu Zazhi* 1988; **10**: 376-378

23 **Harrison LE,** Karpeh MS, Brennan MF. Total gastrectomy is not necessary for proximal gastric cancer. *Surgery* 1998; **123**: 127-130

24 **Jakl RJ,** Miholic J, Koller R, Markis E, Wolner E. Prognostic factors in adenocarcinoma of the cardia. *Am J Surg* 1995; **169**: 316-319

25 **McNeer G,** Bowden L, Booner RJ, McPeak CJ. Elective total gastrectomy for cancer of the stomach: end results. *Ann Surg* 1974; **180**: 252-256

26 **Fujimaki M,** Soga J, Wada K, Tani H, Aizawa O. Total gastrectomy for gastric cancer. Clinical considerations on 431 cases. *Cancer* 1972: **30**: 660-664

27 **Lin YZ,** Extended radical operation for gastric cancer. *Shiyong Waike Zazhi* 1985; **5**: 63-64

28 **Wang SB**. Thirty-seven-year clinical experience on gastric cancer-a report of 2326 cases. *Zhongguo Zhongliu Linchuang* 1999; **26**: 325-329

29 **Jackson JW,** Cooper DK, Guvendik L, Reece-Smith H. The surgical management of malignant tumours of the oesophagus and cardia: a review of the results in 292 patients treated over a 15-year period (1961-1975). *Br J Surg* 1979; **66**: 98-104

30 **Shao QS,** Chen XY, Zou SC. Biological behavior of cardial cancer and its effect on surgical management. *Zhonghua Waike Zazhi* 2003; **41**: 738-740

31 **Huang CM,** Zhang XF, Lu HS, Zhang JZ, Wu XY, Guan GX, Wang C. Long-term therapeutic effects of total gastrectomy in cancer of the cardia and stomach fundus. *Zhonghua Waike Zazhi* 2003; **41**: 729-732

32 **Kishimoto H,** Koga S. Evaluation of gastrectomy combined with resection of other organs in the treatment of gastric cancer. *Jpn J Surg* 1979; **9**: 173-179

33 **Nagata T,** Ikeda M, Nakayama F. Changing state of gastric cancer in Japan. Histologic perspective of the past 76 years. *Am J Surg* 1983; **145**: 226-233

34 **Zhang JZ,** Lu HS, Huang CM, Wu XY, Guan GX, Wang C, Zheng CH, Zhang XF. Long-term effect of total gastrectomy on 615 cases with gastric cancer. *Zhonghua Weichang Waike Zazhi* 2002; **5**: 13-16

35 **Zhang XF,** Huang CM, Yin FS, Lu HS, Feng YM, Wu TG, Zheng ZW, Wu ZY, Guan GX. Evaluation of surgical resection for gastric cancer extending to adjacent organs. *Zhonghua Waike Zazhi* 1995; **33**: 603-605

36 **Korenaga D,** Okamura T, Bada H, Saito A, Sugimachi K. Results of resection of gastric cancer extending to adjacent organs. *Br J Surg* 1988; **75**: 12-15

Edited by Chen WW and Zhu LH **Proofread by** Xu FM

PO Box 2345, Beijing 100023, China
Fax: +86-10-85381893
E-mail: wjg@wjgnet.com www.wjgnet.com

World J Gastroenterol 2004;10(23):3409-3413
World Journal of Gastroenterology
Copyright © 2004 by The WJG Press ISSN 1007-9327

• LIVER CANCER •

Epstein-Barr virus in hepatocellular carcinogenesis

Wei Li, Bao-An Wu, Yong-Ming Zeng, Guang-Can Chen, Xin-Xin Li, Jun-Tian Chen, Yu-Wen Guo, Man-Hong Li, Yi Zeng

Wei Li, Bao-An Wu, Yong-Ming Zeng, Guang-Can Chen, Xin-Xin Li, Jun-Tian Chen, Yu-Wen Guo, Department of General Surgery, the First Affiliated Hospital of Shantou University Medical College, Shantou 515041, Guangdong Province, China
Man-Hong Li, Department of Pathology, the First Affiliated Hospital of Shantou University Medical College, Shantou 515041, Guangdong Province, China
Yi Zeng, Oncogenic Virus Laboratory, Institute for Viral Disease Prevention and Control, Chinese Center for Disease Control and Prevention (China CDC), Beijing 100052, China
Supported by the Technology Program of Guangdong Province, China, No. 2KM04504s
Correspondence to: Wei Li, Department of General Surgery, the First Affiliated Hospital of Shantou University Medical College, No. 57, Changping Road, Shantou 515041, Guangdong Province, China. lwmail@medmail.com.cn
Telephone: +86-754-8258290-3256
Received: 2004-04-14 **Accepted:** 2004-05-09

Abstract

AIM: In recent years, studies have suggested that Epstein-Barr virus (EBV) is associated with HCC. The present study was to determine the prevalence of EBV in HCC patients, and whether EBV acted synergistically with hepatitis viruses in HCC carcinogenesis.

METHODS: Liver tissue 115 HCC patients and 26 non-carcinoma patients were studied. Polymerase chain reaction (PCR) was performed to detect EBV *Bam*HI W DNA, EBV LMP1 DNA, HBV X DNA, and HBV S DNA. Reverse transcription PCR (RT-PCR) was performed to detect HCV RNA and HDV RNA. Immunohistochemistry was performed to detect LMP1, HBsAg, HBcAg and HCV. The positive ratios were compared between HCC group and control group by χ^2 test.

RESULTS: Totally, 78 HCC samples whose β-globulin DNA was positively detected by amplified PCR were selected. PCR was performed in all cases for EBV DNA and HBV DNA. RT-PCR was performed in 18 cases for HCV RNA and HDV RNA. EBV *Bam*HI W and EBV LMP1 were positive in 18 and 6 cases, respectively. HBV X gene and HBV S gene were positive in 42 and 27 cases respectively. HCV was positive in one of the 18 cases, and none was positive for HDV. The positive rates were 28.2% (22 of 78) for EBV DNA (*Bam*HI W and/or LMP1) and 56.4% (44 of 78) for HBV DNA (X gene and/or S gene) respectively. In addition, 12 cases were positive for both EBV DNA and HBV DNA. Among the 26 cases in the control group, 2 cases were positive for EBV *Bam*HI W, 4 positive for HBV X gene and 3 positive for HBV S gene. The positive rates were 8.0% (2 of 26) and 23.1% (6 of 26), respectively, for EBV DNA and HBV DNA. The result of DNA sequencing of *Bam*HI W was 100% homologous with the corresponding sequence of B95-8. There was significant difference in EBV infection rate between HCC patients and controls (χ^2 = 4.622, P<0.05). The difference in HBV infection rate was also significant (χ^2 = 8.681, P<0.05). However, there was no obvious correlation between HBV and EBV in HCC patients (χ^2 = 0.835, P>0.05). LMP1, HBV (HBsAg, HBcAg) and HCV were detected positively in 25, 45 and 6 of 78 cases of HCC tissues respectively. In the 26 control cases, the corresponding positive cases were 2, 4 and 0. The difference in EBV infection rate between HCC patients and control cases was statistically significant (χ^2 = 6.02, P<0.05). The difference in HBV infection rate was also statistically significant (χ^2 = 10.03, P<0.05). In the 25 cases with positive LMP1 expression, 6 were in the nuclei of tumor cells, 9 in the cytoplasm of tumor cells and 10 in mesenchymal lymphocyte cytoplasm.

CONCLUSION: The existence of EBV infection in HCC tissues suggests that EBV may be involved in the hepatocellular carcinogenesis in China. HBV infection may be a major cause of HCC. There is no correlation between EBV and HBV in the development of HCC. The prevalence of HCV infection is low in our area, and HDV appears not to play a direct role in hepatocellular carcinogenesis.

Li W, Wu BA, Zeng YM, Chen GC, Li XX, Chen JT, Guo YW, Li MH, Zeng Y. Epstein-Barr virus in hepatocellular carcinogenesis. *World J Gastroenterol* 2004; 10(23): 3409-3413
http://www.wjgnet.com/1007-9327/10/3409.asp

INTRODUCTION

Hepatocellular carcinoma (HCC) is one of the most frequent malignant tumors. It possesses the characteristics of high malignancy, rapid progress and poor prognosis. In recent years, studies have suggested that Epstein-Barr virus (EBV) is associated with HCC although opposite results have been subsequently reported. The present study was to determine the prevalence of EBV in hepatocellular carcinoma (HCC) patients, and whether EBV acted synergistically with hepatitis viruses in HCC carcinogenesis.

MATERIALS AND METHODS

Patients and tissue samples

HCC samples from 115 patients, which were resected in the First Affiliated Hospital of Medical College, Shantou University and Shantou Central Hospital between October 1997 and October 2001, were fixed in 40 g/L neutral formaldehyde and embedded in paraffin. Of these, 78 samples satisfied the criteria that their β-globulin DNA presented positive. The patients consisted of 59 men and 19 women. Their ages ranged from 22 to 76 years (average 50.2±2.4 years). According to the Edmondson (1956) HCC morphology standard, two, 34, 30 and 12 cases belonged to the levels I, II, III and IV, respectively. AFP was detected in 48 cases; the level was lower than 0.14 ng/mL in four cases, between 0.14 ng/mL and 5.6 ng/mL in 14 cases and higher than 5.6 ng/mL in 12 cases. Anti-hepatitis B virus (HBV) assay was performed by enzyme-linked immunosorbent assay (ELISA) in 62 cases, and 54 were positive. Anti- hepatitis C virus (HCV) assay was carried out in 58 cases and anti-EBV EA-IgA and VCA-IgA assays in 43 cases. The control group consisted of 20 cases with hepatolithiasis and lobectomy of liver, three cases with hepatic adenoma and three cases with hepatocyte focal nodular hyperplasia. HBV was positive in 10 cases. HCV and EBV were negative in all cases.

Reagents

Taq DNA polymerase, dNTP mixture, AMV reverse transcriptase XL, RNase inhibitor, random primer and DNA marker were purchased from TaKaRa® Biotechnology Co., Ltd (Dalian, China). The Trizol total RNA separating medium was purchased from Gibcobrl® Co., Ltd (Grand Island, NY, USA). LMP1 monoclonal antibody (Clone CS1-4), HBsAg monoclonal antibody (Clone ZMHB5), HBcAg polyclonal antibody, the immediately-used-type of the second generation immunohistochemistry Elivision™ plus broad spectrum test kit were from Maixin Co., Ltd (Fuzhou, China). Rat-anti-human HCV monoclonal antibody (Clone TORDJI-22) was from Zhongshan Biotechnology Co. Ltd (Beijing, China).

PCR, DNA sequencing and RT PCR

We downloaded the gene sequences of EBV, HBV, HCV and hepatitis D virus (HDV) from the GenBank. Each included four strains, and the homogeneity was compared among the strains by the Vector NTI suite7 software. The primers were designed by Oligo software (Table 1, LMP1[1] and β-globulin[2] primer sequences were adopted from literature) within the homogeneous gene regions, and synthesized in Shenggong Co., Ltd (Shanghai, China). The positive controls of EBV, HBV and HCV were, respectively, B95-8 cell line, PSDHBV-1 (HBV complete sequence plasmid, 7.8 k) and an HCV-positive serum. The HDV positive control could not be obtained. Fetal liver tissues served as the negative controls. Blank control was established. Primers flanking β-globulin gene were used as a positive control for DNA preservation. Full details of the sequences and genome coordinates of primers and amplification programs of PCR are given in Table 1. The PCR products were electrophoresed in 15 g/L agarose gel, stained with ethidium bromide (Et-Br), and photographed under a UV-transilluminator. After being retrieved and purified, PCR product was ligated with pMD 18-T vector, and then transfected *E.coli* competent cells. The clones were selected and identified. Sequencing of the positive clones was performed by Shenggong Co., Ltd. Bacteriophage M13 cloning vector was used to ligate the fragments. RNA extracts were prepared from paraffin sections. The tissue specimens were deparaffinized with xylene, then washed with ethanol. RNA was extracted using TRIZOL total RNA separating medium. Reverse transcription was performed using AMV reverse transcriptase XL with cDNA synthesis performed for 1 h at 42 ℃. Then nested PCR was carried out using the resulting cDNA as template. The detail is shown in Table 1.

Immunohistochemistry

We used a two-step method according to the instructions provided with the reagent kits. LMP1 located in nucleus or cytoplasm. HCV located in nucleus. HBsAg located in cytoplasm. HBcAg located in nucleus or cytoplasm. Positive cells were defined when there were clear small particles or granuloreticular reddening in cytoplasm or nucleus. The positive control was the positive tissue section provided by the company. Negative control was the sample of lobectomy of liver due to hepatolithiasis. Blank control was tissue section without addition of the first antibody.

Statistical analysis

The positive ratios were compared between HCC group and control group by means of χ^2 test. $P<0.05$ was considered as statistically significant. The statistical software used was SPSS 10.0.

RESULTS

PCR and RT-PCR

Totally, 78 HCC samples whose β-globulin DNA was positively detected by amplified PCR were selected; PCR and RT-PCR were performed in all cases for EBV and HBV, and in 18 cases for HCV and HDV. EBV *Bam*HI W and EBV LMP1 were positive in 18 and six cases, respectively. HBV X gene and HBV S gene were positive in 42 and 27 cases respectively. HCV was positive in 1 of the 18 cases, and none was positive for HDV. The positive rates were 28.2% (22 of 78) for EBV DNA (*Bam*HI W and/or LMP1) and 56.4% (44 of 78) for HBV DNA (X gene and/or S gene) respectively. In addition, 12 cases were positive for both EBV DNA and HBV DNA. Among the 26 cases in the control group, 2 cases were positive for EBV *Bam*HI W, four

Table 1 Primer sequences and amplification programs of PCR and RT-PCR detection

Transcript	Product size	Genomic coordinates in GenBank	Primer sequence (5‘-3‘)	Amplification program
EBV	337 bp	B95-8	GAGTGTGTGCCAGTTAAGGT (168 056-16 8075 20 bp)	94 ℃ 3 min (94 ℃ 30 s 55 ℃
LMP1[1]		V01555	CTAGCGACTCTGCTGGAAAT (168 373-16 8392 20 bp)	40 s 72 ℃ 1 min) ×40 72 ℃ 8 min
EBV	130 bp	B95-8	CATCACCGTCGCTGACT (14 525-14 541 17 bp)	95 ℃ 3 min (94 ℃ 30 s 52 ℃
*Bam*HI W		V01555	GTTGGGCTTAGCAGAAA(14 638-14 654 17 bp)	40 s 72 ℃ 45 s) ×40, 72 ℃ 7 min
HBV	198 bp	HBV	AGGTATGTTGCCCGTTTGT (457-475 19 bp)	95 ℃ 5 min (94 ℃ 30 s 52 ℃
S gene		AB073856	GAGGCCCACTCCCATAGG (637-654 18 bp)	40 s 72 ℃ 50s) ×35, 72 ℃ 7 min
HBV	232 bp	HBV	TGTGCTGCCAACTGGATCCT (1 387-1 406 20 bp)	95 ℃ 3 min (94 ℃ 30 s 55 ℃
X gene		AB073856	GTGGTCTCCATGCGACGTG (1600-1618 19 bp)	40 s 72 ℃ 45 s) ×37 72 ℃ 7 min
HCV	165 bp	HCV	GCGGAACCGGTGAGTACAC (138-156 19 bp)	95 ℃ 5 min, (94 ℃ 30 s 55 ℃
cDNA		NC_001433	GCACTCGCAAGCACCCTATC (283-302 20 bp)	40 s 72 ℃ 50 s) ×40 72 ℃ 7 min
Outer				
HCV	142 bp	HCV	GGAATTGCCAGGACGACC (158-175 18 bp)	95 ℃ 5 min (94 ℃ 30 s, 55 ℃
cDNA		NC_001433	CTCGCAAGCACCCTATCAG (281-299 19 bp)	40 s 72 ℃ 50 s) ×40 72 ℃ 7 min
Inner				
HDV	216 bp	HDV	GCGGGTCCGTCGTTCCAT (653-670 18 bp)	95 ℃ 5 min (94 ℃ 30 s 55 ℃
cDNA		AB037947	GTCCGACCTGGGCATCCGT (850-868 19 bp)	40 s 72 ℃ 50 s) × 35, 72 ℃ 7 min
Outer				
HDV	114 bp	HDV	TCGAGAATCGGCAAATG (752-768 17 bp)	95 ℃ 5 min (94 ℃ 30 s 52 ℃
cDNA		AB037947	GACCTGGGCATCCGTAAG (847-864 18 bp)	40 s 72 ℃ 50 s) × 35, 72 ℃ 7 min
Inner				
β-globulin	210 bp	Beta-globin	ACACAACTGTGTTCACTAGC (120-139 20 bp)	94 ℃ 5 min (94 ℃ 30 s 55 ℃
(PCO3-PCO5)[2]		human	GAAACCCAAGAGTCTTCTCT (310-329,20bp)	40 s 72 ℃ 1 min) ×35 72 ℃ 8 min
		DNA AY128650		

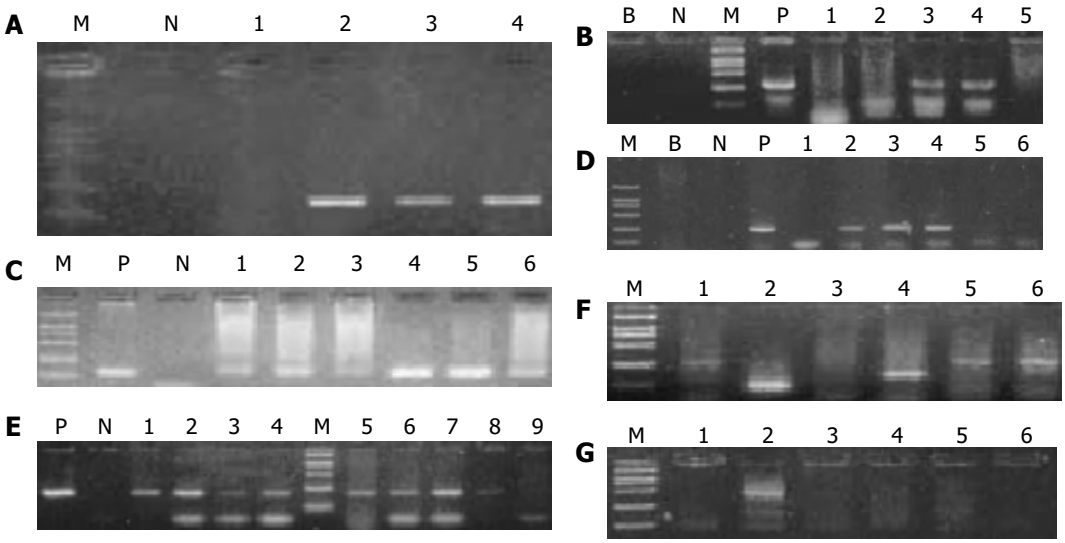

Figure 1 Results of PCR. P, positive control; N, negative control; B, blank control; M, marker of molecular mass. The sizes of the six bands of the marker are 2 000 bp, 1 000 bp, 750 bp, 500 bp, 250 bp, 100 bp, respectively. A: β-Globulin (Positive: Lanes 2-4, 210 bp), B: LMP 1 (Positive: Lanes 3 and 4, 337 bp), C: *Bam*HI W (Positive: Lanes 1-6, 130 bp), D: X gene (Positive: Lanes 2-4, 232 bp), E: S gene (Positive: Lanes 1-8, 198 bp), F: HCV (Positive: Lane 4, other lanes are nonspecific, 142bp), G: HDV (All are negative, Lane 5 is nonspecific).

positive for HBV X gene and three positive for HBV S gene. The positive rates were 8.0% (2 of 26) and 23.1% (6 of 26), respectively, for EBV DNA and HBV DNA (Figures 1A-G). The result of DNA sequencing of *Bam*HI W was 100% homologous with the corresponding sequence of B95-8 (Figure 2). There was significant difference in EBV infection rate between HCC patients and controls (χ^2 = 4.622, P<0.05). The difference in HBV infection rate was also significant (χ^2 = 8.681, P<0.05). However, there was no obvious correlation between HBV and EBV in HCC patients (χ^2 = 0.835).

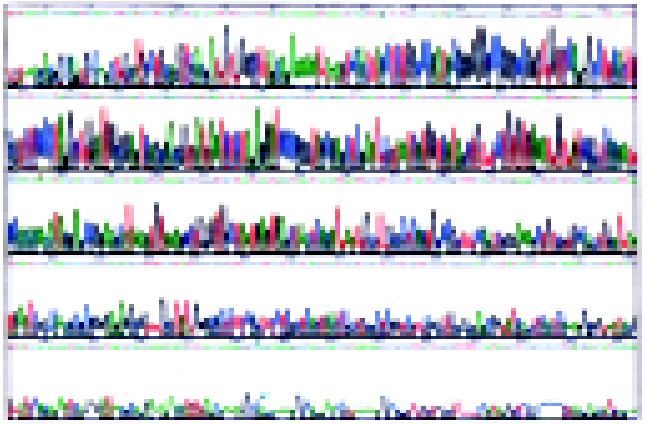

Figure 2 Sequencing results.

Immunohistochemistry

The immunohistochemical detection was performed for LMP1, HBV (HBsAg, HBcAg) and HCV in tissues of 78 cases of HCC, with 25, 45 and six cases positive, respectively. In the 26 control cases, the corresponding positive cases were two, four and zero. The difference in EBV infection rate between HCC patients and control cases was statistically significant (χ^2 = 6.02, P<0.05). The difference in HBV infection rate was also statistically significant (χ^2 = 10.03, P<0.05). In the 25 cases with positive LMP1 expression, six presented in the nuclei of tumor cells, nine in the cytoplasm of tumor cells and 10 in mesenchymal lymphocyte cytoplasm (Figures 3A-H).

DISCUSSION

EBV is considered as the first virus associated with human malignancies including Burkitt's lymphoma[3], T cell lymphoma[4], parotid lymphoepithelioma[5,6], nasopharyngeal carcinoma[7], Hodgkin's disease[8], gastric carcinoma[9] and breast carcinoma[10]. The virus proteins including EBNA1, 2, 3A, 3C, and LMP1 take part in the virus transformation and immortalization. Whether EBV has relation to HCC and whether it plays a role in the genesis of HCC has become the research focus of this field in recent years. However, the results so far are conflicting.

In Japan, Sugawara *et al*.[11-13] found that the positive rate of EBNA1 in HCC was 37% and that cells infected by EBV could facilitate the replication of HCV. The positive rate of *Bam*HI W in HCC was 33% detected by PCR. Among patients with positive *Bam*HI W, anti-HCV positive rate was 40% and HBsAg positive rate was 14%, whereas the control subjects were all negative for anti-HCV and HBsAg. Moreover, EBV DNA load in HCC tissues was 1 000 times that in peripheral blood mononuclear cells of the healthy EBV-seropositive individuals. The authors concluded that EBV accelerates the onset of HCC and plays a role in oncogenesis of HCC, probably by promoting HCV replication, exacerbating inflammatory processes in liver tissue, promoting the proliferation of carcinoma cells or directly influencing tumorigenic potential. In China, Cheng *et al*.[14] used EBV to transform the hepatitis C virus from an HCV positive patient to permanent lymphoblastoid cell lines. They found that HCV might exist and remain functional in a cultured cell line for a long period with the help of EBV. However, Chu *et al*.[15] studied 41 cases of HCC from Los Angeles area in the United States, for evidence of EBV infection. Among these patients, one was positive for EBER1 by *in situ* hybridization, and none was positive for LMP1 and EBNA4 by PCR. The authors concluded that there is no association between EBV and genesis of HCC. In addition, later studies carried out in Germany, United Kingdom and The Netherlands[16-19] reported very low detection rates of EBV in HCC patients, further suggesting that EBV has little relation to hepatocellular carcinogenesis.

In our study, EBV DNA was detected in 28.2% of the HCC tissues by PCR while the positive rate of HBV DNA was 56.4%. HCV RNA was detected in 5.6% of the HCC tissues by RT-PCR while HDV RNA was not detected in all of 18 cases. The positive rate of LMP1 was 32.1% of the HCC tissues by immunohistochemistry. The positive signals of LMP1 were mainly localized in tumor cells. The infection rate of EBV was significantly higher in HCC patients than in control patients.

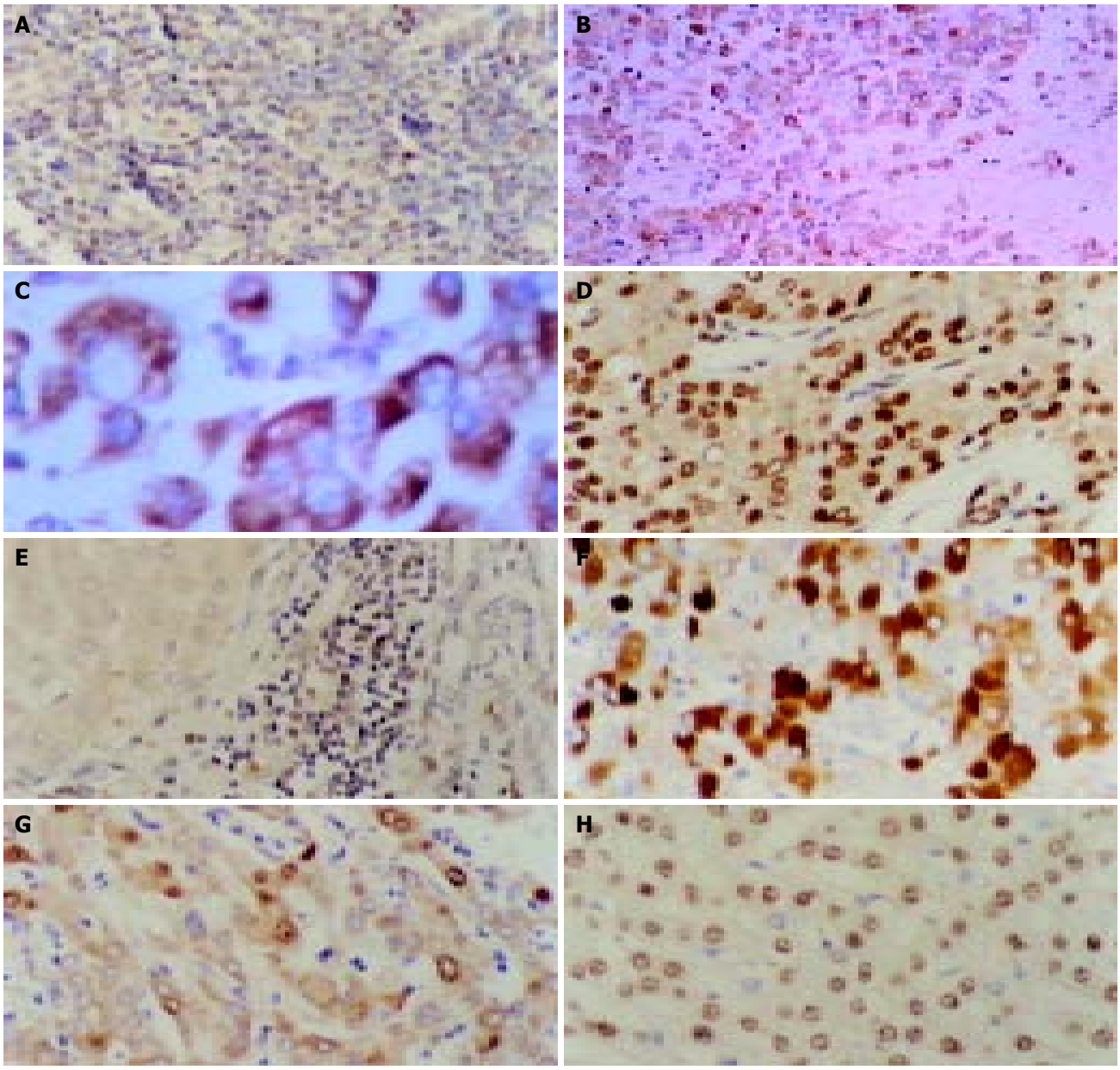

Figure 3 Results of immunohistochemistry. A: Positive-control of LMP1 from the tonsil tissue. The cytoplasm of lymphocytes showed positive signals. ×400, B: Immunohistochemical staining with anti-LMP1 antibody of an HCC specimen. The positive signals were localized in the cytoplasm and membrane of neoplasm cells. ×100, C: Immunohistochemical staining with anti-LMP1 antibody of an HCC specimen. The positive signals were localized in the cytoplasm and membrane of neoplasm cells. ×400, D: Immunohistochemical staining with anti-LMP1 antibody of an HCC specimen. The positive signals were localized in the nuclei of neoplasm cells. ×400, E: Immunohistochemical staining with anti-LMP1 antibody of an HCC specimen. The positive signals were localized in the interstitial lymphocytes but no clear positive signals were present in the adjacent neoplasm cells. ×400, F: Immunohistochemical staining with anti-HBsAg antibody of an HCC specimen. The positive signals were localized in the cytoplasm of neoplasm cells. ×400, G: Immunohistochemical staining with anti-HBcAg antibody of an HCC specimen. The positive signals were localized in the cytoplasm and nuclei of neoplasm cells. ×400, H: Immunohistochemical staining with anti-HCV antibody of an HCC specimen. The positive signals were localized in the nuclei of neoplasm cells. ×400.

These results are similar to those obtained by Sugawara *et al*. Moreover, we observed LMP1 expression in cytoplasm of interstitial lymphocytes in a large proportion of HCC tissues. Experiments *in vitro* have demonstrated that EBV can infect human B-lymphocytes, combine with C3d receptor on the surface of B lymphocyte and enter the cells, escape from the immune surveillance of the host, and then transform the cells. We postulate that EBV, which infects lymphocytes, can promote the genesis and development of HCC in an unidentified way.

Why the results of Sugawara *et al.* and ours are different from those of others? Previous studies produced controversial results on whether EBV played a role in the genesis and development of malignant tumors like breast cancer[20-23], esophageal cancer[24,25], gastric cancer and colorectal cancer. It has been reported that the correlation between EBV and tumor incidence is stronger in Japan and Taiwan than in the western countries. Therefore, we assume that the significance of EBV in HCC may vary because of regional and racial differences. Further studies are required to reveal the underlying mechanism by which EBV contributes to hepatocellular carcinogenesis.

It has been confirmed that HBV and HCV play a certain part in hepatocellular carcinogenesis. Our study showed that EBV and HBV had no synergistic action in HCC, which is consistent with the report by Yuan *et al.*[26]. Because the infection rate of HCV in our region is much lower than that in Japan, the issue whether HCV interacts with EBV in hepatocellular carcinogenesis

should be studied further. HDV is one kind of defective virus that can deteriorate the patient's condition if co-infected with HBV. It has been suggested that HDV also plays a role in hepatocellular carcinogenesis to some extent. But our study did not support such a point of view.

The method using paraffin-imbedded samples for a retrospective molecular epidemiological study may be affected, to some extent, by sample processing and conservation. In this experiment, β-globulin gene was selected as an inner control in PCR amplification. Some cases in which DNA had been seriously degraded were excluded in order to reduce the false-negative rate. To increase the detectable rate, several indexes were used for each virus. *Bam*HI W is regarded as a sensitive index as it repeats 7 to 12 times in EBV genome. LMP1, as a major virus transform protein, is detected in tumors that are related to EBV such as nasopharyngeal carcinoma, Burkitt's lymphoma and other tumors. The primers and reaction conditions are also the important factors. We took advantage of the Internet and biology software to process sequence search, primer design and reaction condition simulation, and achieved a good performance.

The relationship between EBV and the malignant tumors including HCC is very complex and controversial. More studies with larger sample sizes are required to draw a scientific and precise conclusion. If the hypothesis that there is a relation between EBV and HCC comes into existence, then, research and development of EBV vaccines will become a more significant issue, and gene therapy aiming at EBV will be an important approach in the treatment of HCC.

ACKNOWLEDGEMENTS

The authors wish to acknowledge Professor Shu-Fang Tian from Heredity Laboratory, Institute for Viral Disease Prevention and Control, China CDC for kindly providing PSDHBV-1 plasmid. We also acknowledge Dr. Yi-Shu Yang, Dr. Shu-Hui Wang, and Dr. Hai-Jun Du from Oncogenic Virus Laboratory, Institute for Viral Disease Prevention and Control, China CDC for excellent assistance in the study.

REFERENCES

1 **Huang YP,** Guo XC, He ZG, Zhao J, Zeng Y. Epstein-Barr virus induced thymus malignant T cell lymphoma. *Bindu Xuebao* 2001; **17**: 289-294

2 **Saiki RK,** Scharf S, Faloona F, Mullis KB, Horn GT, Erlich HA, Arnheim N. Enzymatic amplification of beta-globin genomic sequences and restriction site analysis for diagnosis of sickle cell anemia. *Science* 1985; **230**: 1350-1354

3 **Bell A,** Rickinson AB. Epstein-Barr virus, the TCL-1 oncogene and Burkitt's lymphoma. *Trends Microbiol* 2003; **11**: 495-497

4 **Yachie A,** Kanegane H, Kasahara Y. Epstein-Barr virus-associated T-/natural killer cell lymphoproliferative diseases. *Semin Hematol* 2003; **40**: 124-132

5 **Kuo T,** Hsueh C. Lymphoepithelioma-like salivary gland carcinoma in Taiwan: a clinicopathological study of nine cases demonstrating a strong association with Epstein-Barr virus. *Histopathology* 1997; **31**: 75-82

6 **Mok MY,** Shek WH, Wong RW. Lymphoepithelioma-like carcinoma of the parotid gland in a patient with rheumatoid arthritis. *Clin Exp Rheumatol* 2002; **20**: 848-850

7 **Thorley-Lawson DA,** Gross A. Persistence of the Epstein-Barr virus and the origins of associated lymphomas. *N Engl J Med* 2004; **350**: 1328-1337

8 **Gandhi MK,** Tellam JT, Khanna R. Epstein-Barr virus-associated Hodgkin's lymphoma. *Br J Haematol* 2004; **125**: 267-281

9 **Mladenova I,** Pellicano R. Infectious agents and gastric tumours. An increasing role for Epstein-Barr virus. *Panminerva Med* 2003; **45**: 183-188

10 **Wakiguchi H.** Overview of epstein-barr virus-associated diseases in Japan. *Crit Rev Oncol Hematol* 2002; **44**: 193-202

11 **Sugawara Y,** Mizugaki Y, Uchida T, Torii T, Imai S, Makuuchi M, Takada K. Detection of Epstein-Barr virus (EBV) in hepatocellular carcinoma tissue: a novel EBV latency characterized by the absence of EBV-encoded small RNA expression. *Virology* 1999; **256**: 196-202

12 **Sugawara Y,** Makuuchi M, Kato N, Shimotohno K, Takada K. Enhancement of hepatitis C virus replication by epstein-barr virus-encoded nuclear antigen 1. *EMBO J* 1999; **18**: 5755-5760

13 **Sugawara Y,** Makuuchi M, Takada K. Detection of Epstein-Barr virus DNA in hepatocellular carcinoma tissues from hepatitis C-positive patients. *Scand J Gastroenterol* 2000; **35**: 981-984

14 **Cheng JL,** Liu BL, Zhang Y, Tong WB, Yan Z, Feng BF. Hepatitis C virus in human B lymphocytes transformed by Epstein-Barr virus *in vitro* by *in situ* reverse transcriptase-polymerase chain reaction. *World J Gastroenterol* 2001; **7**: 370-375

15 **Chu PG,** Chen YY, Chen W, Weiss LM. No direct role for Epstein-Barr virus in American hepatocellular carcinoma. *Am J Pathol* 2001; **159**: 1287-1292

16 **Akhter S,** Liu H, Prabhu R, DeLucca C, Bastian F, Garry RF, Schwartz M, Thung SN, Dash S. Epstein-Barr virus and human hepatocellular carcinoma. *Cancer Lett* 2003; **192**: 49-57

17 **Junying J,** Herrmann K, Davies G, Lissauer D, Bell A, Timms J, Reynolds GM, Hubscher SG, Young LS, Niedobitek G, Murray PG. Absence of Epstein-Barr virus DNA in the tumor cells of european hepatocellular carcinoma. *Virology* 2003; **306**: 236-243

18 **Zur Hausen A,** van Beek J, Bloemena E, ten Kate FJ, Meijer CJ, van den Brule AJ. No role for Epstein-Barr virus in Dutch hepatocellular carcinoma: a study at the DNA, RNA and protein levels. *J Gen Virol* 2003; **84**(Pt 7): 1863-1869

19 **Herrmann K,** Niedobitek G. Epstein-Barr virus-associated carcinomas: facts and fiction. *J Pathol* 2003; **199**: 140-145

20 **Bonnet M,** Guinebretiere JM, Kremmer E, Grunewald V, Benhamou E, Contesso G, Joab I. Detection of Epstein-Barr virus in invasive breast cancers. *J Natl Cancer Inst* 1999; **91**: 1376-1381

21 **Chu PG,** Chang KL, Chen YY, Chen WG, Weiss LM. No significant association of Epstein-Barr virus infection with invasive breast carcinoma. *Am J Pathol* 2001; **159**: 571-578

22 **Touitou R,** Bonnet-Duquenoy M, Joab I. Association of Epstein-Barr virus with human mammary carcinoma. Pros and cons. *Dis Markers* 2001; **17**: 163-165

23 **Preciado MV.** Lack of evidence for an association of Epstein-Barr virus infection with breast carcinoma-another point of view. *Breast Cancer Res* 2003; **5**: E6

24 **Wang LS,** Chow KC, Wu YC, Li WY, Huang MH. Detection of Epstein-Barr virus in esophageal squamous cell carcinoma in Taiwan. *Am J Gastroenterol* 1999; **94**: 2834-2839

25 **Kijima Y,** Hokita S, Takao S, Baba M, Natsugoe S, Yoshinaka H, Aridome K, Otsuji T, Itoh T, Tokunaga M, Eizuru Y, Aikou T. Epstein-Barr virus involvement is mainly restricted to lymphoepithelial type of gastric carcinoma among various epithelial neoplasms. *J Med Virol* 2001; **64**: 513-518

26 **Yuan FP,** Huang PS, Wang Y, Gong HS. Relationship between EBV infection in fujian HCC and HBV and P53 protein expression. *Shijie Huaren Xiaohua Zazhi* 1999; **7**: 491-493

Edited by Xia HHX and Zhu LH **Proofread by** Xu FM

PO Box 2345, Beijing 100023, China
Fax: +86-10-85381893
E-mail: wjg@wjgnet.com www.wjgnet.com

World J Gastroenterol 2004;10(23):3414-3418
World Journal of Gastroenterology
Copyright © 2004 by The WJG Press ISSN 1007-9327

• LIVER CANCER •

Expressions of cysteine-rich61, connective tissue growth factor and Nov genes in hepatocellular carcinoma and their clinical significance

Zhi-Jun Zeng, Lian-Yue Yang, Xiang Ding, Wei Wang

Zhi-Jun Zeng, Lian-Yue Yang, Xiang Ding, Wei Wang, Liver Cancer Laboratory, Department of Surgery, Xiangya Hospital, Central South University, Changsha 410008, Hunan Province, China
Supported by the National Key Technologies R and D Program, No. 2001BA703BO4 and the National Natural Science Foundation of China, No.30371595
Correspondence to: Lian-Yue Yang, Liver Cancer Laboratory, Department of Surgery, Xiangya Hospital, Central South University, Changsha 410008, Hunan Province, China. lianyueyang@hotmail.com
Telephone: +86-731-4327326 **Fax:** +86-731-4327332
Received: 2004-02-28 **Accepted**: 2004-03-04

Abstract

AIM: To investigate the expression of cysteine-rich61 (Cyr61), connective tissue growth factor (CTGF) and nephroblastoma overexpressed gene (Nov) in hepatocellular carcinoma (HCC), and to evaluate the relationship between Cyr61, CTGF and Nov genes expression with invasion and metastasis of HCC.

METHODS: Thirty-one HCC specimens were divided into small hepatocellular carcinoma (SHCC), nodular hepatocellular carcinoma (NHCC), solitary large hepatocellular carcinoma (SLHCC) according to their diameter and number of nodes. Reverse transcription polymerse chain reaction (RT-PCR) was used to detect the mRNA expression levels of Cyr61, CTGF and Nov genes in 31 resected specimens of hepatocellular carcinoma and para-cancerous normal liver tissues semi-quantitatively and the relation between their expression levels and clinical pathological parameters were compared.

RESULTS: The expressions of Cyr61 and CTGF mRNA in carcinoma tissues were significantly higher than those in para-cancerous normal liver tissues ($P<0.01$). The expressions of Cyr61 and CTGF mRNA in HCC with venous invasion were higher than those in HCC without venous invasion. CTGF expression in HCC Edmondson's grade III-IV was significantly higher than that in HCC Edmondson's grade I-II ($P = 0.022$). There was no obvious correlation between Nov mRNA and clinical-pathological features. Compared to NHCC, SLHCC had better cell differentiation, easier capsule formation, less microscopic venous invasion, milder liver cirrhosis. The expressions of Cyr61 and CTGF mRNA in NHCC were significantly higher than those in SLHCC and SHCC.

CONCLUSION: Cyr61 and CTGF genes may play an important role in hepatocellular carcinogenesis and correlate with recurrence and metastasis of hepatocellular carcinoma. SLHCC has better biological behaviors than NHCC.

Zeng ZJ, Yang LY, Ding X, Wang W. Expressions of cysteine-rich61, connective tissue growth factor and Nov genes in hepatocellular carcinoma and their clinical significance. *World J Gastroenterol* 2004; 10(23): 3414-3418
http://www.wjgnet.com/1007-9327/10/3414.asp

INTRODUCTION

Hepatocellular carcinoma (HCC) is one of the most common malignant cancers in the world, and the fourth most common cause of death from cancer, the second-leading cause of cancer death in China, which alone accounts for 53% of all liver cancer deaths worldwide. Although HCC resection plays an important role in improving HCC prognosis, it has been generally accepted that the high incidence of recurrence and metastasis is the most crucial prognostic factor in patients with HCC[1]. The high recurrent rate in the liver with mainly intrahepatic metastatic spread remains a major obstacle to further improvement in the long-term survival after curative HCC resection[2]. The mechanism of recurrence and metastasis of hepatocellular carcinoma is very complicated, and includes cell adhesion, matrix degradation, cell migration and angiogenesis[3-7].

CCN gene family is a group of growth factor-inducible immediate-early genes, including cysteine-rich61 (Cyr61), connective tissue growth factor (CTGF), nephroblastoma overexpressed gene (Nov), Wnt-1 induced secreted protein 1 (WISP-1), WISP-2, WISP-3[8,9]. CCN proteins are secreted extracellular matrix (ECM)-associated proteins that regulate cellular processes, such as adhesion, migration, mitogenesis, differentiation and survival[10]. They also regulate more complex biological processes such as angiogenesis, chondrogenesis, tumorigenesis, fibrotic and vascular diseases[11-13]. Cyr61 gene was originally identified as an immediately-early gene of mouse 3T3 fibroblasts, and was also found to be expressed in developing mouse cartilaginous elements and placental tissues[14]. CTGF was originally identified in the conditioned culture medium of human umbilical vein endothelial cells, and revealed to be induced by transforming growth factor in human skin fibroblasts. Nov gene was identified as an aberrantly expressed gene in avian nephroblastomas induced by myeloblastosis-associated viruses. The overexpression of Nov gene was reported relative to human Wilsm's tumors.

Taking cues from clinical observations and results of our laboratory researches, we have hypothesized that solitary large hepatocellular carcinoma (SLHCC) possesses relatively better biological behaviors[15]. Furthermore, we have preliminarily proved our hypothesis by a series of researches[16]. The clinical pathological features of SLHCC were better than nodular hepatocellular carcinoma (NHCC) and the molecular biological study also suggested that SLHCC possessed better molecular pathological features.

Cyr61, CTGF and Nov gene may overexpress in HCCs. In this report, we studied the expressions of Cyr61, CTGF and Nov genes in HCCs and para-cancerous normal liver tissues, to clarify whether these genes might play an important role in the recurrence and metastasis of HCCs. Furthermore, we examined the expressions of Cyr61, CTGF and Nov genes in SLHCC, NHCC and SHCC and compared their differences.

MATERIALS AND METHODS

Patients and tissue preparation

Thirty-one fresh HCC specimens and corresponding para-cancerous liver tissues were obtained by surgical resection at

Xiangya Hospital between March 2002 and March 2003. The patients with HCC consisted of 26 men and 5 women and the age of them ranged from 21 to 69 years (mean, 48 years). The patients were classified as SHCC (tumor largest diameter ≤ 5 cm for a single tumor nodule or the sum of diameters ≤ 5 cm for two tumor nodules), SLHCC (a single tumor nodule and tumor largest diameter >5 cm), NHCC (the nodules of tumor ≥ 2, only two tumor nodules and the sum of diameters ≤ 5 cm were excluded). Furthermore, we divided 31 specimens into six groups: tumors <5 cm diameter and ≥ 5 cm, grade I-II and grade III-IV, liver cirrhosis and no liver cirrhosis, capsule formation and no capsule formation, microscopic portal vein tumor thrombosis and no microscopic portal vein tumor thrombosis. All specimens were examined under a microscope after haematoxylin and eosin (HE) staining.

RNA extraction and RT-PCR

Total RNA was isolated using Trizol reagent (GIBCO BRL, USA) and cDNA was synthesized from RNA by M-MLV reverse transcriptase (Promega, USA) with oligo-dT primers (Sango Technology, China). The primer sequences of Cyr61, CTGF and Nov genes were as follows: Cyr61, upstream: 5'-ACTTCATGGTCCCAGTGCGC-3', downstream: 5'-AAATCCGGGTTTCTTTCACA-3'; CTGF, upstream: 5'-GCAGGCTAGAGAAGCAGAGC-3', downstream: 5'-ATGTCTTCATGCTGGTGCAG-3'; Nov, upstream: 5'-AGCATGCAGAGTGTGCAGAG-3', downstream: 5'-GGTGTGCCACTTACCTGTCC-3'; β-actin, upstream: 5'-CTGCAATCCGAAAGAAGCTG-3', downstream: 5'-ATCTTCAAACCTCCATGATG-3'. The conditions of PCR were as follows: after an initial denaturation at 94 ℃ for 2 min, 30 cycles of denaturation at 94 ℃ for 30 s, annealing at 54 ℃ for 1 min and extension at 72 ℃ for 1 min. The bands representing amplified products were analyzed by Stratagene Eagle-eye scanner. Expressions of Cyr61, CTGF and Nov genes were presented by the relative yield of the PCR products of the target sequence to that of the β-actin gene.

Statistical analysis

The results of RT-PCR were statistically analyzed using the Student's *t* test. Fisher's exact test was used to determine the relationship between the expressions of Cyr61, CTGF and Nov genes and clinicopathological characteristics of HCCs. SPSS11.0 software was used. $P<0.05$ was considered statistically significant.

RESULTS

Expression of Cyr61, CTGF and Nov mRNA in HCC and para-cancerous liver tissues

The expressions of Cyr61 and CTGF mRNA in HCC tissues were significantly higher than those in para-cancerous normal liver tissues. The expression of Nov gene was higher than that in para-cancerous normal liver tissues (Table 1). The difference in Nov gene expression between these two groups did not reach statistical significance. The expressions of Cyr61, CTGF and Nov genes are shown in Figure 1.

Table 1 Expression of Cyr61, CTGF and Nov mRNA in HCC and para-cancerous liver tissues (mean±SD)

	n	Cyr61	CTGF	Nov
HCC	31	2.34±0.46[b]	2.21±0.34[b]	1.56±0.21
Para-cancerous	31	0.48±0.29	0.65±0.33	0.89±0.64

[b]$P<0.01$ *vs* para-cancerous tissues.

Between the groups with different pathological characteristics, the expressions of Cyr61, CTGF and Nov genes were significantly different. Especially, the differences between the two groups with and without microscopic portal vein tumor thrombosis were of great significance. Moreover, CTGF expression was significantly different between Edmondson's grades I-II and III-IV. The relationship between the expression of Cyr61, CTGF, Nov mRNA and clinicopathological features of HCC patients is shown in Table 2.

Clinical and pathological features of three types of HCC

Thirty-one HCC specimens were divided into SLHCC, SHCC and NHCC according to their diameter and number of nodules. Liver cirrhosis, microvascular invasion, capsule formation, Edmondson's classification of HCC were studied in each group. NHCC group had a higher incidence of microvascular invasion compared with SLHCC and SHCC ($P<0.05$). Only 8.3% of NHCCs were classified as Edmondson's grade I-II, while 62.5% of SLHCC and 63.6% of SHCC were classified as Edmondson's grade I-II. The differentiation of NHCC was significantly poorer than that of SLHCC and SHCC ($P<0.05$). The other three pathological features of SLHCC and SHCC were also better than NHCC but did not reach statistical significance. No statistical difference in the five pathological features was observed between SLHCC and SHCC (Table 3).

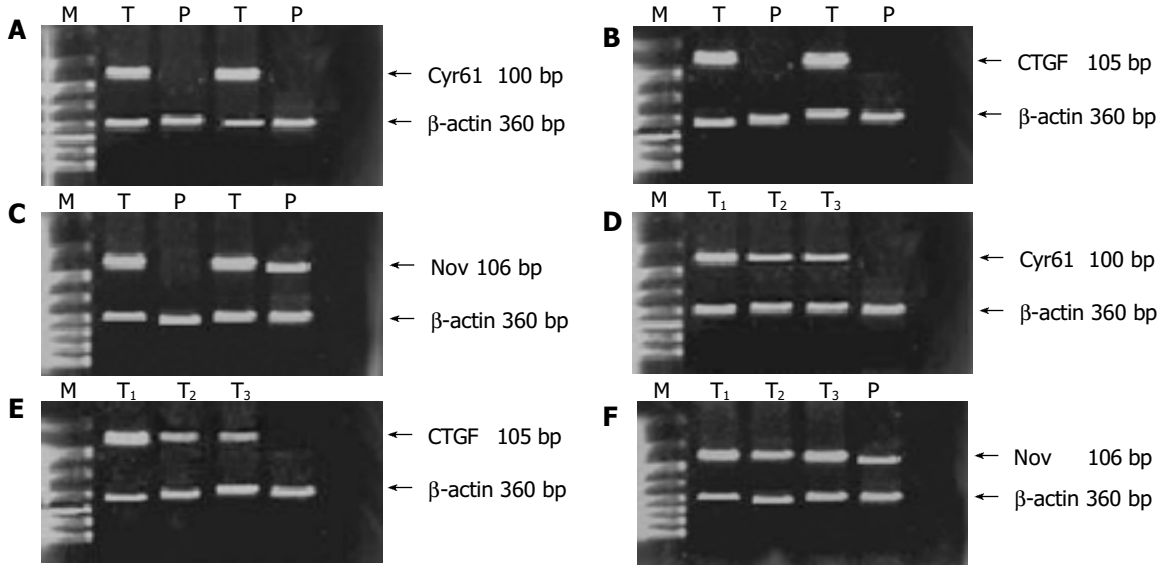

Figure 1 Expressions of Cyr61, CTGF and Nov mRNA in hepatocellular carcinoma A and D : Cyr61 mRNA expression, product size 100 bp; B and E : CTGF mRNA expression, product size 105 bp; C and F: Nov mRNA expression, product size106 bp; M, DNA marker; T, tumor; P, para-cancerous normal liver tissues; T_1, NHCC; T_2, SLHCC; T_3, SHCC. PCR product of β-actin was 360 bp.

Table 2 Relationship between Cyr61, CTGF and Nov mRNA expressions and clinicopathological features (mean±SD)

	n	Cyr61	*P*	CTGF	*P*	Nov	*P*
PV thrombosis							
Present	16	2.59±0.41	0.024	2.41±0.39	0.031	1.45±0.56	0.147
Absent	15	2.08±0.65		2.10±0.58		1.56±0.45	
AFP level							
≤20 ng/mL	19	2.26±0.48	0.068	2.21±0.20	0.063	1.38±0.43	0.241
>20 ng/mL	12	2.36±0.71		2.23±0.84		1.66±0.71	
Tumor size (cm)							
≤ 5 cm	20	2.35±0.86	0.124	2.26±0.79	0.071	1.59±0.58	0.251
> 5 cm	11	2.32±0.41		2.09±0.53		1.55±0.31	
Capsule formation							
Positive	18	2.35±0.34	0.136	2.31±0.34	0.132	1.87±0.65	0.135
Negative	13	2.33±0.67		2.15±0.87		1.36±0.81	
Histological grade							
I-II	13	2.21±0.39	0.052	1.89±0.54	0.022	1.35±0.47	0.132
III-IV	18	2.51±0.41		2.51±0.61		1.58±0.68	

PV: portal vein.

Table 3 Pathological features of three types of HCC

Pathological features	*n*	SHCC (*n*=11)	NHCC (*n*=12)	SLHCC (*n*=8)
Microvascular invasion				
Present	16	3	10	3[a]
Absent	15	8	2	5
Capsule formation				
Present	18	8	4	6
Absent	13	3	8	2
Edmondson's classification				
I-II	13	7	1	5[a]
III-IV	18	4	11	3
Liver cirrhosis				
Present	9	4	9	2
Absent	22	7	3	6
AFP consentration				
≤20 ng/mL	19	6	9	4
>20 ng/mL	12	5	3	4

[a]$P<0.05$ *vs* NHCC.

Expression of Cyr61, CTGF and Nov mRNA in three types of HCCs

The expression of Cyr61 mRNA in NHCC was significantly higher than that in SLHCC and SHCC ($P = 0.024$ and $P = 0.031$, respectively). The expression of CTGF mRNA in nodular HCC was also significantly higher than that in SLHCC and SHCC ($P = 0.016$ and $P = 0.027$, respectively). No statistical difference in the expression of Nov gene among NHCC, SLHCC and SHCC was observed (Table 4).

DISCUSSION

All members of the CCN gene family possess a secretory signal peptide at the N terminus, indicating that they are secreted proteins. Several lines of evidence supported a role of CCN molecules in tumorigenesis[8].

Cyr61 is a secreted, 40-kDa, cysteine-rich and heparin-binding protein coded by a growth factor-inducible immediate early gene[14]. Recently, it has been reported as an angiogenic inducer that can promote tumor growth and vascularization[17]. A mechanistic framework for the biological properties of Cyr61 has been provided by the finding that Cyr61 binds to integrin $\alpha_v\beta_3$, which represents the first molecularly defined receptor for any member of the CCN family[18]. Interaction of $\alpha_v\beta_3$ with Cyr61 may account for its promotion of chemotaxis and growth factor-mediated DNA synthesis as well as cell adhesion since integrins have been known to modulate cell migration and growth factor signaling in other systems[16,17]. In a direct interaction between the two molecules, Cyr61-mediated adhesion and migration of cultured endothelial cells were specifically inhibited by the peptide RGDS and/or antiintegrin $\alpha_v\beta_3$[19-23]. In addition to its intergrin-binding property, Cyr61 appears to be localized to its site of synthesis by associating with the ECM, possibly by binding to heparin-like molecules. This interaction could limit the extent of Cyr61 diffusion so that its site of action is in close proximity of its site of synthesis[24]. In our study, the expression of Cyr61 gene in HCC tissue was markedly higher than that in para-cancerous normal liver tissues, indicating that Cyr61 may play an important role in hepatocellular carcinogenesis.

CTGF is a cysteine-rich mitogenic peptide that was originally identified as a growth factor secreted by vascular endothelial cells[25]. It was selectively induced in fibroblasts after activation with TGF[26]. A previous study demonstrated the coordinate expression of TGF1 and CTGF in granulation beds during wound

Table 4 Cyr61, CTGF and Nov mRNA expressions in three types of HCCs

HCC	*n*	Cyr61	*P*	CTGF	*P*	Nov	*P*
SLHCC	8	2.22±0.36		2.09±0.44		1.52±0.41	
NHCC	12	2.51±0.53	0.037[a]	2.38±0.29	0.043[a]	1.58±0.36	0.287
SHCC	11	2.18±0.42		2.03±0.31		1.46±0.19	

[a]$P<0.05$ *vs* SLHCC.

repair, and found that dermal fibroblasts in scleroderma lesions overexpressed CTGF[27]. In addition to contributing to TGF-β-mediated AIG, CTGF could interact synergistically with EGF, PDGF, IGF-I, or bFGF, suggesting that it activates the receptors and/or signaling pathways used by other growth factors[28,29]. Consistent with its profibrotic properties, CTGF has been found to be overexpressed in pancreatic cancers, mammary tumors, and melanomas[30-32]. In our study, the expression of CTGF gene in HCC tissue was obviously higher than that in para-cancerous normal liver tissues, indicating that CTGF might play an important role in hepatocellular carcinogenesis.

Nov gene was first recognized as an overexpressed gene in nephroblastomas induced by myeloblastosis-associated virus type 1[33]. Unlike the other members of this family, Nov gene expression was associated with quiescence and transcriptionally downregulated upon expression of p60 v-src in RSV-infected CEF[34]. It has been reported that overexpression of normal Nov gene in CEF has an inhibitory effect on cell growth, whereas expression of an amino-terminal truncated form of Nov gene was able to induce morphological transformation[35,36]. Therefore, Nov is a negative regulator of cell growth, the amino-truncation of which would result in oncogenic activiation[37,38]. Also, Koliopanos *et al*.[42] reported that Nov was a ligand of integrins $\alpha_v\beta_3$ and $\alpha_5\beta_1$, and acted directly upon endothelial cells to stimulate pro-angiogenic activities, thus inducing angiogenesis *in vivo*. While, in our study, the expression of Nov gene in HCC and para-cancerous normal liver tissues had no difference. The diagnostic significance of Nov gene expression in HCC needs to be further investigated with more samples.

Metastasis and invasion of HCC is a multistep process, the molecular and cellular mechanisms of which have not been fully understood[39]. They may involve matrix degradation, cell motility, angiogenesis, *etc*. CCN proteins could regulate biological processes such as angiogenesis, chondrogenesis, tumorigenesis, fibrotic and vascular diseases[4-6,40]. Numerous *in vitro* studies indicated that Cyr61 protein was related to angiogenesis[41]. Overexpressions of Cyr61, CTGF and Nov genes have been found in metastatic lesions of esophageal cancer, breast cancer, colon tumors, lung cancer and osteosarcoma[42-45]. In the present study, we statistically analyzed the clinical and pathological parameters. No significant correlation was found among the parameters of age, sex, cause of liver diseases. Cyr61 and CTGF mRNA levels in patients with portal vein tumor thrombosis were significantly higher compared to those in patients without portal vein invasion. Moreover, CTGF mRNA level in Edmondson's grade III-IV was significantly higher than that in Edmondson's grade I-II. These results indicated that Cyr61 and CTGF had a close relationship with invasion and metastasis of HCC.

Previous studies have shown that SLHCC is different from other types of HCC in pathological features and invasiveness[16]. Coordinated with this, the relatively better pathological features of SHCC were found in this study. The differentiation of SLHCC was much better than that of NHCC, and microvascular invasion was observed more frequently in NHCC compared with SLHCC. No statistical difference in pathological features was observed between SHCC and SLHCC. In addition, the transcription level of Cyr61 and CTGF in NHCC was much higher than that in SLHCC and SHCC, while no statistical difference was observed between SLHCC and SHCC. The lower transcription of Cyr61 and CTGF mRNA in SLHCC was probably due to the relatively better molecular pathological features of SLHCC.

Our findings indicate that Cyr61 and CTGF genes are related to tumorigenesis of HCC, and may enhance the invasion and metastasis of HCC. Its molecular basis remains to be elucidated. What are the most important factors regulating the expression level of CCN family and how does CCN gene family regulate effector protein will be the subjects of our future studies. When the upstream and downstream signaling pathways are understood, those findings will provide new potential tools for the prognosis or prevention of invasion and metastasis of HCC.

REFERENCES

1 **Zhou XD.** Recurrence and metastasis of hepatocellular carcinoma: progress and prospects. *Hepatobiliary Pancreat Dis Int* 2002; **1**: 35-41

2 **Nakashima Y,** Nakashima O, Tanaka M, Okuda K, Nakashima M, Kojiro M. Portal vein invasion and intrahepatic micrometastasis in small hepatocellular carcinoma by gross type. *Hepatol Res* 2003; **26**: 142-147

3 **Shiratori Y,** Yoshida H, Omata M. Management of hepatocellular carcinoma: advances in diagnosis, treatment and prevention. *Expert Rev Anticancer Ther* 2001; **1**: 277-290

4 **Ariizumi S,** Takasaki K, Yamamoto M, Ohtsubo T, Katsuragawa H, Katagiri S. Histopathologic differentiation of the main nodule determines outcome after hepatic resection for synchronous multicentric hepatocellular carcinomas. *Hepatogastroenterology* 2004; **51**: 500-504

5 **McGlynn KA,** Edmonson MN, Michielli RA, London WT, Lin WY, Chen GC, Shen FM, Buetow KH. A phylogenetic analysis identifies heterogeneity among hepatocellular carcinomas. *Hepatology* 2002; **36**: 1341-1348

6 **Murawaki Y,** Ikuta Y, Okamoto K, Mimura K, Koda M, Kawasaki H. Plasma matrix metalloproteinase-9 (gelatinase B) in patients with hepatocellular carcinoma. *Res Commun Mol Pathol Pharmacol* 2000; **108**: 351-357

7 **Mukai M,** Nakamura H, Tatsuta M, Iwasaki T, Togawa A, Imamura F, Akedo H. Hepatoma cell migration through a mesothelial cell monolayer is inhibited by cyclic AMP-elevating agents via a Rho-dependent pathway. *FEBS Lett* 2000; **484**: 69-73

8 **Bork P.** The modular architecture of a new family of growth regulators related to connective tissue growth factor. *FEBS Lett* 1993; **327**: 125-130

9 **Brigstock DR,** Goldschmeding R, Katsube KI, Lam SC, Lau LF, Lyons K, Naus C, Perbal B, Riser B, Takigawa M, Yeger H. Proposal for a unified CCN nomenclature. *Mol Pathol* 2003; **56**: 127-128

10 **Kireeva ML,** MO FE, Yang GP, Lau LF. Cyr61, a product of a growth factor-inducible immediate-early gene, promotes cell proliferation, migration, and adhesion. *Mol Cell Biol* 1996; **16**: 1326-1334

11 **Hadjiargyrou M,** Ahrens W, Rubin CT. Temporal expression of the chondrogenic and angiogenic growth factor CYR61 during fracture repair. *J Bone Miner Res* 2000; **15**: 1014-1023

12 **Brigstock DR,** Steffen CL, Kim GY, Vegunta RK, Diehl JR, Harding PA. Purification and characterization of novel heparin-binding growth factors in uterine secretory fluids. Identification as heparin-regulated M_r 10000 forms of connective tissue growth factor. *J Biol Chem* 1997; **272**: 20275-20282

13 **Lake AC,** Bialik A, Walsh K, Castellot JJ Jr. CCN5 is a growth arrest-specific gene that regulates smooth muscle cell proliferation and motility. *Am J Pathol* 2003; **162**: 219-231

14 **O'Brien TP,** Lau LF. Expression of the growth factor-inducible immediate early gene cyr61 correlates with chondrogenesis during mouse embryonic development. *Cell Growth Differ* 1992; **3**: 645-654

15 **Yang LY,** Huang GW. Surgical strategy of large hepatocellular carcinoma. *Linchuang Waike Zazhi* 2001; **9**: 4-5

16 **Liu HL,** Yang LY, Huang GW, Yang JQ. The effect of integrin α_v subunit on the angiogenesis, invasiveness and metastasis of hepatocellular carcinoma. *Zhonghua Putong Waike Zazhi* 2002; **9**: 542-543

17 **Inoki I,** Shiomi T, Hashimoto G, Enomoto H, Nakamura H, Makino K, Ikeda E, Takata S, Kobayashi K, Okada Y. Connective tissue growth factor binds vascular endothelial growth factor (VEGF) and inhibits VEGF-induced angiogenesis. *FASEB J* 2002; **16**: 219-221

18 **Leng E,** Malcolm T, Tai G, Estable M, Sadowski I. Organization and expression of the Cyr61 gene in normal human fibroblasts. *J Biomed Sci* 2002; **9**: 59-67

19 **Grzeszkiewicz TM,** Kirschling DJ, Chen N, Lau LF. CYR61

stimulates human skin fibroblast migration through Integrin alpha vbeta 5 and enhances mitogenesis through integrin alpha vbeta 3, independent of its carboxyl-terminal domain. *J Biol Chem* 2001; **276**: 21943-21950

20 **Fataccioli V,** Abergel V, Wingertsmann L, Neuville P, Spitz E, Adnot S, Calenda V, Teiger E. Stimulation of angiogenesis by Cyr61 gene: a new therapeutic candidate. *Hum Gene Ther* 2002; **13**: 1461-1470

21 **Hilfiker A,** Hilfiker-Kleiner D, Fuchs M, Kaminski K, Lichtenberg A, Rothkotter HJ, Schieffer B, Drexler H. Expression of CYR61, an angiogenic immediate early gene, in arteriosclerosis and its regulation by angiotensin II. *Circulation* 2002; **106**: 254-260

22 **Kothapalli D,** Grotendorst GR. CTGF modulates cell cycle progression in cAMP-arrested NRK fibroblasts. *J Cell Physiol* 2000; **182**: 119-126

23 **Schober JM,** Chen N, Grzeszkiewicz TM, Jovanovic I, Emeson EE, Ugarova TP, Ye RD, Lau LF, Lam SC. Identification of integrin alpha (M) beta (2) as an adhesion receptor on peripheral blood monocytes for Cyr61 (CCN1) and connective tissue growth factor (CCN2): immediate-early gene products expressed in atherosclerotic lesions. *Blood* 2002; **99**: 4457-4465

24 **Tamura I,** Rosenbloom J, Macarak E, Chaqour B. Regulation of Cyr61 gene expression by mechanical stretch through multiple signaling pathways. *Am J Physiol Cell Physiol* 2001; **281**: C1524-1532

25 **Surveyor GA,** Wilson AK, Brigstock DR. Localization of connective tissue growth factor during the period of embryo implantation in the mouse. *Biol Reprod* 1998; **59**: 1207-1213

26 **Wang JF,** Olson ME, Reno CR, Wright JB, Hart DA. The pig as a model for excisional skin wound healing: characterization of the molecular and cellular biology, and bacteriology of the healing process. *Comp Med* 2001; **51**: 341-348

27 **Maquart FX,** Chastang F, Simeon A, Birembaut P, Gillery P, Wegrowski Y. Triterpenes from Centella asiatica stimulate extracellular matrix accumulation in rat experimental wounds. *Eur J Dermatol* 1999; **9**: 289-296

28 **Denton CP,** Abraham DJ. Transforming growth factor-beta and connective tissue growth factor: key cytokines in scleroderma pathogenesis. *Curr Opin Rheumatol* 2001; **13**: 505-511

29 **Ehrchen J,** Heuer H, Sigmund R, Schafer MK, Bauer K. Expression and regulation of osteopontin and connective tissue growth factor transcripts in rat anterior pituitary. *J Endocrinol* 2001; **169**: 87-96

30 **Wenger C,** Ellenrieder V, Alber B, Lacher U, Menke A, Hameister H, Wilda M, Iwamura T, Beger HG, Adler G, Gress TM. Expression and differential regulation of connective tissue growth factor in pancreatic cancer cells. *Oncogene* 1999; **18**: 1073-1080

31 **Frazier KS,** Grotendorst GR. Expression of connective tissue growth factor mRNA in the fibrous stroma of mammary tumors. *Int J Biochem Cell Biol* 1997; **29**: 153-161

32 **Kubo M,** Kikuchi K, Nashiro K, Kakinuma T, Hayashi N, Nanko H, Tamaki K. Expression of fibrogenic cytokines in desmoplastic malignant melanoma. *Br J Dermatol* 1998; **139**: 192-197

33 **Perbal B.** NOV (nephroblastoma overexpressed) and the CCN family of genes: structural and functional issues. *Mol Pathol* 2001; **54**: 57-79

34 **Babic AM,** Kireeva ML, Kolesnikova TV, Lau LF. CYR61, a product of a growth factor-inducible immediate early gene, promotes angiogenesis and tumor growth. *Proc Natl Acad Sci U S A* 1998; **95**: 6355-6360

35 **Xie D,** Nakachi K, Wang H, Elashoff R, Koeffler HP. Elevated levels of connective tissue growth factor, WISP-1, and CYR61 in primary breast cancers associated with more advanced features. *Cancer Res* 2001; **61**: 8917-8923

36 **Sakamoto K,** Yamaguchi S, Ando R, Miyawaki A, Kabasawa Y, Takagi M, Li CL, Perbal B, Katsube K. The nephroblastoma overexpressed gene (NOV/ccn3) protein associates with Notch1 extracellular domain and inhibits myoblast differentiation via Notch signaling pathway. *J Biol Chem* 2002; **277**: 29399-29405

37 **Kocialkowski S,** Yeger H, Kingdom J, Perbal B, Schofield PN. Expression of the human NOV gene in first trimester fetal tissues. *Anat Embryol* 2001; **203**: 417-427

38 **Lin CG,** Leu SJ, Chen N, Tebeau CM, Lin SX, Yeung CY, Lau LF. CCN3 (NOV) is a novel angiogenic regulator of the CCN protein family. *J Biol Chem* 2003; **278**: 24200-24208

39 **Zhao ZC,** Zheng SS, Wan YL, Jia CK, Xie HY. The molecular mechanism underlying angiogenesis in hepatocellular carcinoma: the imbalance activation of signaling pathways. *Hepatobiliary Pancreat Dis Int* 2003; **2**: 529-536

40 **Chaqour B,** Whitbeck C, Han JS, Macarak E, Horan P, Chichester P, Levin R. Cyr61 and CTGF are molecular markers of bladder wall remodeling after outlet obstruction. *Am J Physiol Endocrinol Metab* 2002; **283**: E765-774

41 **Wenger C,** Ellenrieder V, Alber B, Lacher U, Menke A, Hameister H, Wilda M, Iwamura T, Beger HG, Adler G, Gress TM. Expression and differential regulation of connective tissue growth factor in pancreatic cancer cells. *Oncogene* 1999; **18**: 1073-1080

42 **Koliopanos A,** Friess H, di Mola FF, Tang WH, Kubulus D, Brigstock D, Zimmermann A, Buchler MW. Connective tissue growth factor gene expression alters tumor progression in esophageal cancer. *World J Surg* 2002; **26**: 420-427

43 **Pennica D,** Swanson TA, Welsh JW, Roy MA, Lawrence DA, Lee J, Brush J, Taneyhill LA, Deuel B, Lew M, Watanabe C, Cohen RL, Melhem MF, Finley GG, Quirke P, Goddard AD, Hillan KJ, Gurney AL, Botstein D, Levine AJ. WISP genes are members of the connective tissue growth factor family that are up-regulated in wnt-1- transformed cells and aberrantly expressed in human colon tumors. *Proc Natl Acad Sci U S A* 1998; **95**: 14717-14722

44 **Astolfi A,** De Giovanni C, Landuzzi L, Nicoletti G, Ricci C, Croci S, Scopece L, Nanni P, Lollini PL. Identification of new genes related to the myogenic differentiation arrest of human rhabdomyosarcoma cells. *Gene* 2001; **274**: 139-149

45 **Sampath D,** Winneker RC, Zhang Z. Cyr61, a member of the CCN family, is required for MCF-7 cell proliferation: regulation by 17beta-estradiol and overexpression in human breast cancer. *Endocrinology* 2001; **142**: 2540-2548

Edited by Kumar M and Wang XL **Proofread by** Zhu LH and Xu FM

PO Box 2345, Beijing 100023, China
Fax: +86-10-85381893
E-mail: wjg@wjgnet.com www.wjgnet.com

World J Gastroenterol 2004;10(23):3419-3423
World Journal of Gastroenterology
Copyright © 2004 by The WJG Press ISSN 1007-9327

• LIVER CANCER •

Peroxisome proliferator-activated receptor γ ligands suppress liver carcinogenesis induced by diethylnitrosamine in rats

Yan-Tong Guo, Xi-Sheng Leng, Tao Li, Jing-Ming Zhao, Xi-Hou Lin

Yan-Tong Guo, Jing-Ming Zhao, Xi-Hou Lin, Department of General Surgery, Beijing Jishuitan Hospital, the Forth Clinical Medical College of Peking University, Beijing 100035, China
Xi-Sheng Leng, Tao Li, Department of General Surgery, People Hospital of Peking University, Beijing 100044, China
Supported by the National Natural Science Foundation of China, No. 30371387
Correspondence to: Yan-Tong Guo, PhD and M.D., Department of General Surgery, Beijing Jishuitan Hospital, the Forth Clinical Medical College of Peking University, Beijing 100035, China. guoyantong2002@sohu.com
Telephone: +86-10-86995076
Received: 2004-03-11 **Accepted:** 2004-04-13

Abstract

AIM: Peroxisome proliferator-activated receptor γ (PPARγ) is known to regulate growth arrest and terminal differentiation of adipocytes and is used clinically as a new class of antidiabetic drugs. Recently, several studies have reported that treatment of cancer cells with PPARγ ligands could induce cell differentiation and apoptosis, suggesting a potential application as chemopreventive agents against carcinogenesis. In the present study, 3 different kinds of PPARγ ligands were subjected to the experiments to confirm their suppressive effects on liver carcinogenesis.

METHODS: Three PPARγ ligands, pioglitazone (Pio) (200 ppm), rosiglitazone (Rosi) (200 ppm), and troglitazone (Tro) (1 000 ppm) were investigated on the induction of the placental form of rat glutathione S-transferase (rGST P) positive foci, a precancerous lesion of the liver,and liver cancer formation using a diethylnitrosamine-induced liver cancer model in Wistar rats, and dose dependency of a PPARγ ligand was also examined.

RESULTS: PPARγ ligands reduced the formation of rGST P-positive foci by diethylnitrosamine and induction of liver cancers was also markedly suppressed by a continuous feeding of Pio at 200 ppm.

CONCLUSION: PPARγ ligands are potential chemopreventive agents for liver carcinogenesis.

Guo YT, Leng XS, Li T, Zhao JM, Lin XH. Peroxisome proliferator-activated receptor γ ligands suppress liver carcinogenesis induced by diethylnitrosamine in rats. *World J Gastroenterol* 2004; 10(23): 3419-3423
http://www.wjgnet.com/1007-9327/10/3419.asp

INTRODUCTION

Carcinogenesis is a complex process that has been divided into three stages: initiation, promotion and progression[1]. These three stages of tumor formation have been characterized in many mammalian tissues, particularly in the liver[2,3]. According to the concept of multistage carcinogenesis, clones of cells arise with increasing autonomy from normal growth regulation at each stage of development, and from these selected populations of cells, neoplasms ultimately develop[4]. The placental form of rat glutathione S-transferase (rGST P) positive foci is thought to be preneoplastic lesions of the liver[5-12].

Peroxisome proliferators-activated receptor γ (PPARγ), a nuclear hormone receptor, provides a strong link between lipid metabolism and regulation of gene transcription. PPARγ is known to regulate growth arrest and terminal differentiation of adipocytes, and a group of PPARγ activators are now widely prescribed and form a new class of antidiabetic drugs. Several specific ligands have been identified, such as the thiazolidinedione groups, including pioglitazone (Pio), rosiglitazone (Rosi), and troglitazone (Tro), 15-deoxy-prostaglandin J2, and certain polyunsaturated fatty acids[13]. PPARγ is expressed in various organs including adipose tissue, breast epithelium, small intestine, lungs, and liver[13]. Several studies have reported that treatment of cancer cells with PPARγ ligands could induce cell differentiation and apoptosis, suggesting a potential application as chemopreventive agents against carcinogenesis[14].

In present study, 3 different kinds of PPARγ ligands were subjected to the experiments to confirm their suppressive effects on liver carcinogenesis in the rat model. In experiment 1, we investigated the effects of 3 PPARγ ligands, Pio, Rosi, and Tro, on the development of rGST P-positive foci that were induced by diethylnitrosamine (DEN)[6]. Dose dependency of the PPARγ ligand was also examined. In experiment 2, a long-term carcinogenesis study of DEN was conducted[15]. Our findings indicate that PPARγ ligands are potential chemopreventive agents for liver carcinogenesis.

MATERIALS AND METHODS

Chemicals and animals

DEN was purchased from Beijing Chemical Reagents Company (Beijing, China). Three different PPARγ ligands, Pio, Rosi, and Tro, were kindly provided by GlaxoSmithKline (BN, United Kingdom). To prepare experimental diets, each PPARγ ligand was mixed with a powdered basal diet and stored at 4 ℃ until use. Fresh diets were provided to the rats once a week, and the dietary intake and body mass (bm) for each group of rats were measured every week. Concentrations of PPARγ in experimental diets were 200 and 1 000 ppm for Pio and Tro, respectively. For Rosi, various concentrations in the diet, ranging from 0.88 to 500 ppm, were used to evaluate the dose-response effect of PPARγ ligands on the formation of rGST P-positive foci. Fifteen-week-old male Wistar rats were purchased from Peking University Health Science Center (Beijing, China) and housed in a ventilated, temperature-controlled room (23±1 ℃) with a 12-h light/dark cycle. After a period of 1-week acclimatization to the housing environment and the basal diet, groups of rats were fed either the basal diet or the experimental diet containing one of the PPARγ ligands, from sixteen weeks of age until termination.

Induction of rGST P-positive foci (Experiment 1)

Rats were divided into 8 experimental groups, 4 DEN treated and

4 vehicle-treated. In DEN -treated cases (groups 1-4, Figure 1A), groups of 10 rats were fed diets without ligands (basal diet, group 1) or with a PPARγ ligand (experimental diet, groups 2-4), beginning 1 wk prior to the subcutaneous injection of DEN as described below and continued until the end of the experiment. Starting at sixteen weeks of age (experimental wk 1), rats in each group were administered DEN subcutaneously twice, at 1-week intervals at a dose of 20 mg/kg bm in saline. In the vehicle-treated groups (groups 5-8, Figure 1A), groups of 5 rats were fed the basal diet (group 5) or experimental diet (groups 6-8) and given subcutaneous injections of an equal volume of saline without DEN. Four weeks after the first administration of DEN or saline, all rats were killed at experimental week 5. In a separate experiment, dose-dependent effect of Rosi, within the range of 0.67-500 ppm in diet, on formation of rGST P-positive foci was also examined. The entire liver was removed, and fixed in 40 g/L neutralized formaldehyde overnight at 4 ℃. Then the liver sections were embedded in paraffin. Immunohistochemical staining was performed on sections by the peroxidase-antiperoxidase method, using the antibody against the rGST P. Sections were counterstained with haematoxylin. The number of rGST P-positive foci (consisting of single to several GST P positive cells, indicating preneoplastic lesions) was expressed as per cm^2 of liver sections[16].

Induction of liver tumors (Experiment 2)

As in Experiment 1, rats were fed either the experimental diet or the basal diet, starting 1 wk prior to the injection of DEN or vehicle. A total of 80 rats were divided into 4 experimental groups, 2 DEN treated and 2 vehicle treated. For the former, groups of 30 rats were fed diets without ligands (basal diet) or with PPARγ ligands (basal diet + pioglitazone 200 ppm), beginning 1 wk prior to the subcutaneous injection of DEN as described below and continued until the end of the experiment (Figure 1B). Starting at 16 wk of age (experimental week 1), rats in each group were administered DEN subcutaneously 6 times at 1-wk intervals at a dose of 20 mg/kg bm in saline. In the vehicle-treated groups, groups of 10 rats were fed the basal diet or experimental diet (basal diet + pioglitazone 200 ppm) and given subcutaneous injections of an equal volume of saline without DEN (Figure 1B). All surviving animals were killed 60 wk after the first injection of DEN. Livers were removed and fixed in 10% neutralized formalin as described above. The number, size, and location of liver tumors dectected macroscopically or by stereomicroscopic observation were determined. Diameters were measured in 3 dimensions, and tumor size was calculated by (height + width + length)/3.

Histologic analysis of liver slices

Liver slices were embedded in paraffin blocks according to the standard procedures. In the case of liver tumors, lesions were resected, fixed in neutralized 40 g/L formaldehyde overnight at 4 ℃, and embedded in paraffin blocks according to the standard procedures. Some of the tumors were bisected, and a half was frozen in liquid nitrogen and stocked at -80 ℃ until used for the frozen section preparation and RNA extraction. The other half was embedded in paraffin blocks as described above. Paraffin sections were prepared at 3.0-μm thickness, stained with H & E, and subjected to histologic analysis.

Immunohistochemical analysis of liver tumors

Paraffin-embedded sections were deparaffinized and subjected to immunohistochemical staining using rabbit alpha fetoprotein polyclonal antibody (Novus Biologicals, Inc.) and rabbit PPARγ polyclonal antibody (Santa Cruz Biotechnology, Inc.) following the manufacturer's instructions. The primary alpha fetoprotein (AFP) antibody was diluted at 1:200 and the PPARγ antibody

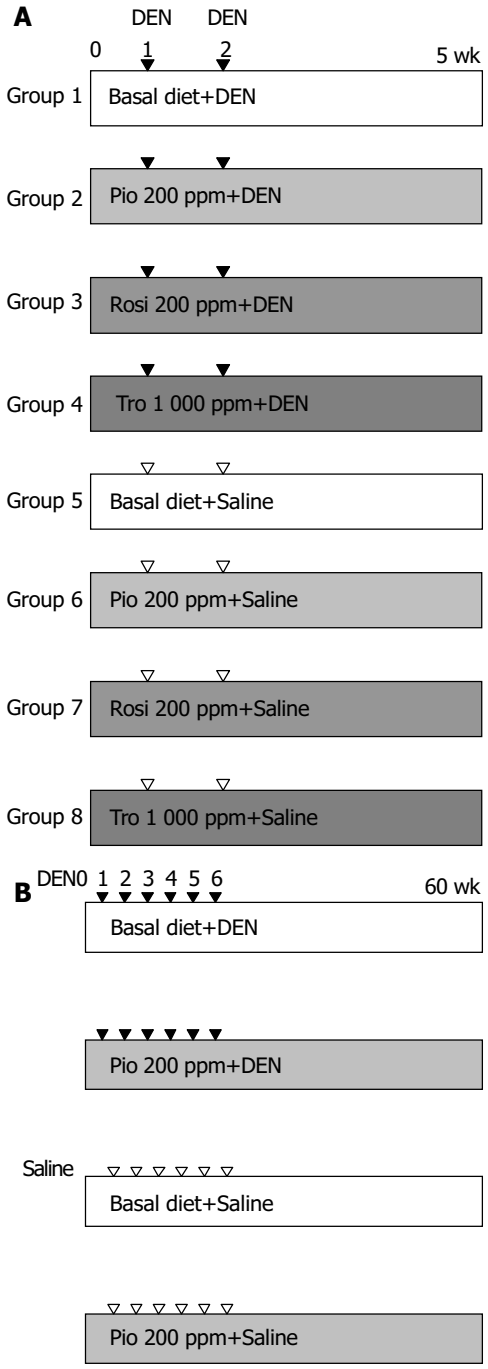

Figure 1 Experimental design for evaluation of chemoprevention efficacy of PPARγ ligands against liver carcinogenesis.A: In the short-term study of rGST P-positive foci, groups of male Wistar rats were fed experimental diets containing 0 or 200 or 1 000 ppm of PPARγ ligands from 1 wk prior to exposure to DEN at 20 mg/kg bm until the termination. B: For liver tumor study, groups of animals were given the basal diet or experimental diet containing 200-ppm Pio continuously from 1 wk prior to exposure of animals to DEN, IP, at 1to 6 experimental weeks at 20 mg/kg bm until the termination.

to 1:400. To confirm the specificity of PPARγ staining, addition of an excess amount of the N-terminal peptide of PPARγ, used for immunization, was also carried out.

RT-PCR analysis for PPARγ and β-actin expressions

RNA extraction from liver tumors and surrounding normal liver tissues was carried out as follows. Serial sections were prepared at 7-μm thickness from frozen tissues, lesions were microdissected by scraping with a razor blade under microscopic observation,

and RNA was extracted using TRI reagent (Sigma). Extracted RNA was transcribed to cDNA using Oligo(dT)12-18 primer and SuperScript II RT (Invitrogen, Carlsbad, CA) and subjected to semiquantitative reverse-transcriptase (RT)-PCR analysis to quantify messenger RNA (mRNA) expression levels of the PPARγ gene. PCR primers designed to amplify the 299-bp fragment of the PPARγ gene were 5'-AGGATTCATGAC-CAGGGAGTT-3' (forward) and 5'-TCTGCCTGAGGTCT-GTCATCT-3' (reverse). For the internal control, expression of the β-actin gene for each sample was also quantified as above by amplifying the 138-bp fragment using a primer set: 5'-AGACTTCGAGCAGGAGATGGC-3' (forward) and 5'-AAGAAGGAAGGCTGGAAAAGA-3' (reverse). PCR amplification was carried out at 94 ℃ for 30 s, at 59 ℃ for 30 s, and at 72 ℃ for 45 s using MasterMix kit (tw-biotech, China) under the reaction conditions recommended by the manufacturer, and PCR cycles were set at 30 and 25 cycles for PPARγ and β-actin, respectively. PCR products were run on 20 g/L agarose gels and visualized by ethidium bromide staining. In addition, the amount of PCR products was also quantified in real-time PCR using Taq RT-PCR kit (Ambion Inc.) and Smart cycler system (Cepheid, Sunny Vale, CA). Experiments were repeated at least twice, which gave similar results.

Statistical analysis

Statistical analysis for rGST P-positive foci and liver tumor multiplicity were conducted using the *t*-test (SPSS 10.0 for Windows). Other statistical analyses for liver tumor incidences and the distribution of tumor sizes were performed using the χ^2-test (SPSS 10.0 for Windows). Differences were considered significant when *P* values were <0.05.

RESULTS

Effect of PPARg ligands on formation of rGST P-positive foci

One animal in the DEN+ 200-ppm Rosi-treated group and 4 in the DEN+1000-ppm Tro-treated group died within a few days after the injection of DEN, which were not included in the effective number of rats. Based on the diet consumption, the daily intake of PPARγ ligands was estimated to be approximately 25 mg/kg bm (200 ppm in diet) for Pio and Rosi and 125 mg/kg bm (1 000 ppm in diet) for Tro. The mean body weight of rats given DEN was slightly decreased but stayed within 10% of the control value (data not shown). Administration of PPARγ ligands alone did not significantly alter the body mass within the observation period of 5 wk (data not shown). After the administration of DEN, rats fed with the basal diet without a PPARγ ligand developed 7.5±3.1 rGST P-positive foci per cm^2 of liver sections by experimental wk 5. Treatment with 200-ppm Pio, 200-ppm Rosi, and 1000-ppm Tro significantly reduced that to 2.5±1.2, 1.7±1.1, and 5.6±2.3, respectively (Table 1). This suppressive effect was observed in a dose-dependent manner within the range of 0.88 to 500 ppm of Rosi (Figure 2). Histologic analysis of a total of 40 liver sections of rGST P-positive foci (10 liver sections of rGST P-positive foci each from groups 1, 2, 3, and 4) revealed no significant histologic change. No rGST P-positive foci were induced by feeding experimental diet or basal diet alone without DEN administration.

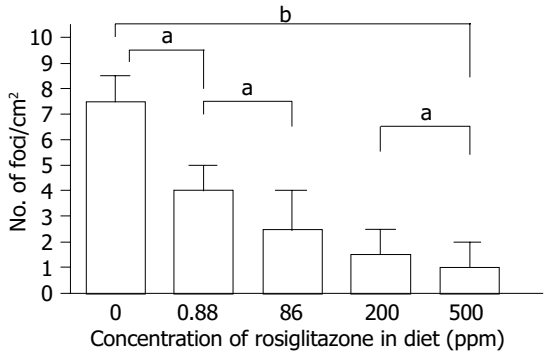

Figure 2 Dose-dependent suppression of the formation of rGST P-positive foci by rosiglitazone. As clearly demonstrated, Rosi suppressed the formation of rGST P-positive foci in a dose-dependent manner within the range of 0.88-500 ppm in diet (^aP<0.05, ^bP<0.01).

Effects of PPARγ ligands on induction of liver tumors

Five animals treated with DEN+200 ppm Pio died before the termination without tumor development, which were not included in the effective number. With administration of DEN, body weight gradually dereased to approximately 90% of the vehicle-treated group by experimental wk 18, but the difference stayed within 10% of the control mass throughout the experimental period. Data for incidences, multiplicities (average numbers of tumors per animal), histologic features of liver tumors, and size distribution of tumors are summarized in Table 2. Administration of 200-ppm Pio almost halved the incidence of liver tumors, and the multiplicity was also significantly reduced by Pio treatment. As to the size, only 38% (3 of 8) of tumors observed in the Pio-treated group were more than 2 mm in diameter, and 38% (3 of 8) were less than 1 mm. In contrast, 76% (19 of 25) of those in rats without Pio treatment were more than 2 mm in diameter, and only 8% (2 of 25) were less than 1 mm (*P*<0.05). All of the lesions developed in both Pio-treated and untreated groups were diagnosed as hepatocellular carcinoma. No liver tumors were observed in the rats fed with the basal diet alone or diet with 200-ppm Pio (data not shown).

Table 1 Effect of PPARγ ligands on the multiplicity of DEN-induced rGST P-positive foci in male Wistar rats (mean±SD)

Experimental group	DEN	Diet	No. of rats	No. of rGST P-positive foci/cm^2 of liver sections
Group 1	+	Basal diet alone	10	7.5±3.1
Group 2	+	Basal diet+pioglitazone 200 ppm	10	2.5±1.2[a]
Group 3	+	Basal diet+rosiglitazone 200 ppm	9	1.7±1.1[a]
Group 4	+	Basal diet+troglitazone 1000 ppm	6	5.6±2.3[a]
Group 5	-	Basal diet alone	5	0
Group 6	-	Basal diet+pioglitazone 200 ppm	5	0
Group 7	-	Basal diet+rosiglitazone 200 ppm	5	0
Group 8	-	Basal diet+troglitazone 1000 ppm	5	0

[a]*P*<0.05 *vs* group 1.

Table 2 Effect of PPARγ ligands on the incidence, multiplicity, and size of DEN-induced liver tumors in male Wistar rats (mean±SD)

Experimental group	Incidence(%)[1]	Histology		Tumor size(mm)[1]		
		Hepatocarcinoma	Multiplicity	0-1	1-2	>2
DEN+basal diet	13/30 (43)	25	0.83±1.22	2	4	19
DEN+pioglitazone 200 ppm	5/25 (20)[a]	8	0.32±0.75[a]	3	2	3[a]

[1]Statistical analysis was conducted using χ^2 test. [a]$P<0.05$ *vs* DEN+basal diet group.

Histologic findings and immunohistochemical staining of liver tumors

Liver tumors in both Pio-treated and untreated rats demonstrated no appreciable histologic differences on H & E staining or AFP immunostaining. Furthermore, no variation was observed in PPARγ expression levels in tumors developed in Pio-treated and untreated rats. Addition of an excessive antigenic PPARγ N-terminal peptide used for immunization before incubation of the sections with the antibody blocked the staining completely (data not shown).

Expression of PPARγ mRNA in liver tumors

RNA samples from 2 liver tumors and 1 normal liver sample from both Pio-treated and untreated groups were subjected to semiquantitative RT-PCR analysis. No products were amplified without reverse transcriptase (data not shown). Liver tumors and normal tissue from both Pio-treated and untreated animals expressed PPARγ mRNA as shown in Figure 3, and the relative amounts, normalized to β-actin mRNA, were almost equivalent in liver tumors as compared with normal liver tissue in both groups. Real-time PCR analysis also gave similar results (data not shown).

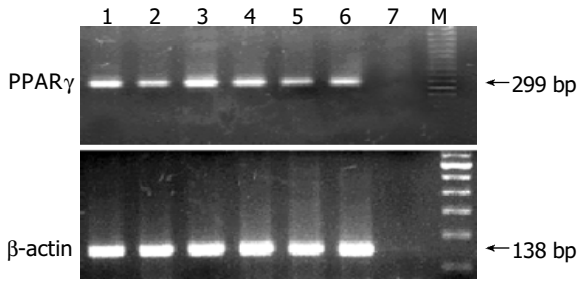

Figure 3 Expression of PPARγ mRNA in liver tumors. Lanes 1 and 4: normal liver tissues; lanes 2, 3, 5, and 6: liver tumor tissues; lane 7: water.

DISCUSSION

In the present study of short- and long-term effects, clear evidence was obtained for preventive influence of the 3 different PPARγ ligands, Pio, Rosi, and Tro, on rat liver carcinogenesis induced by DEN. In the short-term experiment, all 3 significantly suppressed the formation of rGST P-positive foci, the effect of the former 2 was particularly strong. Because this suppression was proved to be dose dependent, we considered the inhibitory effect of PPARγ ligands on the formation of rGST P-positive foci to be due to pharmacologic actions rather than nonspecific toxicity. There were no significant differences in histopathologic features of rGST P-positive foci. In this context, the fact that the compounds reduced the formation of rGST P-positive foci without otherwise affecting their pathology is important. In the long-term carcinogenic experiment, the single PPARγ ligand investigated also significantly suppressed the induction of liver tumors.

Our results are in good agreement with those from Rumi *et al*.[17], which demonstrated an inhibitory effect of PPARγ on cell growth through PPARγ activation. Our study has an advantage of the suppressive effect of rGST P-positive foci and liver tumors using 3 PPARγ ligands in the rat model, including the dose-dependent experiments. In addition, PPARγ could play roles in apoptosis, cell-cycle control through regulating p21$^{waf/cipl}$[18]. Antiinflammatory activity of PPARγ could also be involved in its suppression of liver carcinogenesis[19]. However, the results of Hosokawa *et al*.[20] and Kim *et al*.[21], showing clofibrate, a peroxisome proliferator, enhanced liver carcinogenesis in their rat model in which GST-P-positive cells induced by DEN were changed to GST-P-negative cells on subsequent treatment with peroxisome proliferator, need to be taken into account. Now we have no reasonable explanation for the discrepancy.

In conclusion, PPARγ ligands have substantial suppressive effects on liver carcinogenesis without affecting the histologic features of preneoplastic lesions or tumors. Although the molecular mechanisms underlying the inhibitory influence still remain largely unsolved, PPARγ ligands may be potential chemopreventive agents against liver carcinogenesis.

REFERENCES

1 **Dragan YP**, Pitot HC. The role of the stages of initiation and promotion in phenotypic diversity during hepatocarcinogenesis in the rat. *Carcinogenesis* 1992; **13**: 739-750

2 **Farber E**, Solt D, Cameron R, Laishes B, Ogawa K, Medline A. Newer insights into the pathogenesis of liver cancer. *Am J Pathol* 1977; **89**: 477-482

3 **Pitot HC**, Barsness L, Goldsworthy T, Kitagawa T. Biochemical characterization of stages of hepatocarcinogenesis after a single dose of diethylnitrosamine. *Nature* 1978; **271**: 456-458

4 **Pitot HC**, Dragan Y, Sargent L, Xu YT. Biochemical markers associated with the stages of promotion and progression during hepatocarcinogenesis in the rat. *Environ Health Perspect* 1991; **93**: 181-189

5 **Satoh K,** Kitahara A, Soma Y, Inaba Y, Hatayama I, Sato K. Purification, induction, and distribution of placental glutathione transferase: anew marker enzyme for preneoplastic cells in the rat chemical hepatocarcinogenesis. *Proc Natl Acad Sci U S A* 1985; **82**: 3964-3968

6 **Ito N**, Tatematsu M, Hasegawa R, Tsuda H. Medium-term bioassay system for detection of carcinogens and modifiers of hepatocarcinogenesis utilizing the GST-P positive liver cell focus as an endpoint marker. *Toxicol Pathol* 1989; **17**(4 Pt 1): 630-641

7 **Reddy TV**, Daniel FB, Lin EL, Stober JA, Olson GR. Chloroform inhibits the development of diethylnitrosamine-initiated, phenobarbital-promoted gamma-glutamyltranspeptidase and placental form glutathione S-transferase-positive foci in rat liver. *Carcinogenesis* 1992; **13**: 1325-1330

8 **Zhu HZ**, Zhang XL, Chen YS. Expression of glutathione S-transferase placental mRNA in hepatic preneoplastic lesions in rats. *World J Gastroenterol* 1998; **4**: 38-40

9 **Denda A,** Kitayama W, Konishi Y, Yan Y, Fukamachi Y, Miura M, Gotoh S, Ikemura K, Abe T, Higashi T, Higashi K. Genetic properties for the suppression of development of putative preneoplastic glutathione S-transferase placental form-positive foci in the liver of carcinogen-resistant DRH strain rats.

Cancer Lett 1999; **140**: 59-67
10 **Sporn MB**, Suh N. Chemoprevention of cancer. *Carcinogenesis* 2000; **21**: 525-530
11 **Nishikawa T**, Wanibuchi H, Ogawa M, Kinoshita A, Morimura K, Hiroi T, Funae Y, Kishida H, Nakae D, Fukushima S. Promoting effects of monomethylarsonic acid, dimethylarsinic acid and trimethylarsine oxide on induction of rat liver preneoplastic glutathione S-transferase placental form positive foci: a possible reactive oxygen species mechanism. *Int J Cancer* 2002; **100**: 136-139
12 **Suzuki S**, Asamoto M, Tsujimura K, Shirai T. Specific differences in gene expression profile revealed by cDNA microarray analysis of glutathione S-transferase placental form (GST-P) immunohistochemically positive rat liver foci and surrounding tissue. *Carcinogenesis* 2004; **25**: 439-443
13 **Lambe KG**, Tugwood JD. A human peroxisome-proliferator-activated receptor-gamma is activated by inducers of adipogenesis, including thiazolidinedione drugs. *Eur J Biochem* 1996; **239**: 1-7
14 **Chang TH**, Szabo E. Induction of differentiation and apoptosis by ligands of peroxisome proliferator-activated receptor γ in non small cell lung cancer. *Cancer Res* 2000; **60**: 1129-1138
15 **Dragan YP**, Hully J, Baker K, Crow R, Mass MJ, Pitot HC. Comparison of experimental and theoretical parameters of the Moolgavkar-Venzon-Knudson incidence function for the stages of initiation and promotion in rat hepatocarcinogenesis. *Toxicology* 1995; **102**: 161-175
16 **Carter JH**, Richmond RE, Carter HW, Potter CL, Daniel FB, DeAngelo AB. Quantitative image cytometry of hepatocytes expressing gamma-glutamyl transpeptidase and glutathione S-transferase in diethylnitrosamine-initiated rats treated with Phenobarbital and/or phthalate esters. *J Histochem Cytochem* 1992; **40**: 1105-1115
17 **Rumi MA**, SatoH, Ishihara S, Kawashima K, Hamamoto S, Kazumori H, Okuyama T, Fukuda R, Nagasue N, Kinoshita Y. Peroxisome proliferator-activated receptor gamma ligand-induced growth inhibition of human hepatocellular carcinoma. *Br J Cancer* 2001; **84**: 1640-1647
18 **Kaga H**, Sakisaka S, Harada M, Takagi T, Hanada S, Taniguchi E, Kawaguchi T, Sasatomi K, Kimura R, Hashimoto O, Ueno T, Yano H, Kojiro M, Sata M. Involvement of p21(waf/cipl), p21 (kipl), and p18(INK4C) in troglitazone-induced cell-cycle arrest in human hepatoma cell lines. *Hepatology* 2001; **33**: 1087-1097
19 **Chawla A**, Barak Y, Nagy L, Liao D, Tontonoz P, Evans RM. PPAR-γ dependent and independent effects on macrophage-gene expression in lipid metabolism and inflammation. *Nat Med* 2001; **7**: 48-52
20 **Hosokawa S**, Tatematsu M, Aoki T, Nakanowatari J, Igarashi T, Ito N. Modulation of diethylnitrosamine-initiated placental glutathione S-transferase positive preneoplastic and neoplastic lesions by clofibrate, a hepatic peroxisome proliferator. *Carcinogenesis* 1989; **10**: 2237-2241
21 **Kim DJ**, Lee KK, Hong JT. Differential effects of nongenotoxic and genotoxic carcinogens on the preneoplastic lesions in the rat liver. *Arch Pharm Res* 1998; **21**: 363-369

Edited by Zhang JZ and Wang XL **Proofread by** Xu FM

PO Box 2345, Beijing 100023, China
Fax: +86-10-85381893
E-mail: wjg@wjgnet.com www.wjgnet.com

World J Gastroenterol 2004;10(23):3424-3427
World Journal of Gastroenterology
Copyright © 2004 by The WJG Press ISSN 1007-9327

• LIVER CANCER •

Preparation of human hepatocellular carcinoma-targeted liposome microbubbles and their immunological properties

Ai-Na Bian, Yun-Hua Gao, Kai-Bin Tan, Ping Liu, Gong-Jun Zeng, Xin Zhang, Zheng Liu

Ai-Na Bian, Yun-Hua Gao, Kai-Bin Tan, Ping Liu, Gong-Jun Zeng, Xin Zhang, Zheng Liu, Department of Ultrasonic Diagnosis, Xinqiao Hospital the Third Military Medical University, Chongqing 400037, China
Supported by the National Natural Science Foundation of China, No. 30270384
Correspondence to: Professor. Yun-Hua Gao, Director of Department of Ultrasonic Diagnosis, Xinqiao Hospital, the Third Military Medical University, Chongqing 400037, China. gyhxq@sina.com
Telephone: +86-23-68755631 **Fax:** +86-23-68755631
Received: 2003-12-23 **Accepted:** 2004-01-15

Abstract

AIM: To prepare the human hepatocellular carcinoma.(HCC)-targeted liposome microbubbles and to investigate their immunological properties.

METHODS: Human hepatocarcinoma specific monoclonal antibody HAb18 was attached to the surface of home-made liposome microbubbles by static attraction to prepare the targeted liposome microbubbles. The combination of HAb18 with liposome microbubbles was confirmed by the slide agglutination test and immunofluorescent assay. Their immunological activity was measured by ELISA. Rosette formation test, rosette formation blocking test and immunofluorescent assay were used to identify the specific binding of targeted liposome microbubbles to SMMC-7721 hepatoma cells, and cytotoxicity assay was used to detect their effect on human hepatocytes.

RESULTS: The targeted liposome microbubbles were positive in the slide agglutination test and immunofluorescent assay. ELISA indicated that the immunological activity of HAb18 on the liposome microbubbles was similar to that of free HAb18. SMMC-7721 cells were surrounded by the targeting liposome microbubbles to form rosettes, while the control SGC-7901 gastric cancer cells were not. Proliferation of SMMC-7721 cells and normal human hepatocytes was not influenced by the targeted liposome microbubbles.

CONCLUSION: The targeted liposome microbubbles with a high specific biological activity have been successfully prepared, which specifically bind to human hepatocarcinoma cells, and are non-cytotoxic to hepatocytes. These results indicate that the liposome microbubbles can be used as a HCC-targeted ultrasound contrast agent that may enhance ultrasound images and thus improve the diagnosis of HCC, especially at the early stage.

Bian AN, Gao YH, Tan KB, Liu P, Zeng GJ, Zhang X, Liu Z. Preparation of human hepatocellular carcinoma-targeted liposome microbubbles and their immunological properties. *World J Gastroenterol* 2004; 10(23): 3424-3427
http://www.wjgnet.com/1007-9327/10/3424.asp

INTRODUCTION

Targeted ultrasound imaging is a promising method of imaging diagnosis[1]. This technique can significantly improve the sensitivity and specificity of ultrasonic diagnosis. At present, several targeted ultrasound contrast agents that can enhance imaging of specific tissues, such as thrombus-specific and inflammatory tissue-specific targeted ultrasound contrast agent, have successfully been developed abroad[2-15], while study on hepatocellular carcinoma-targeted ultrasound contrast agent has not been reported.

In this study, liposome microbubbles containing fluorocarbon gases were prepared in our laboratory. Then human hepatocarcinoma specific monoclonal antibody HAb18 was attached to the surface of home-made liposome microbubbles to prepare targeted liposome microbubbles. Finally the immunological properties of targeted liposome microbubbles were investigated.

MATERIALS AND METHODS

Materials

Human hepatocarcinoma specific monoclonal antibody HAb18 was kindly provided by Research Centre of Cell Engineering, the Fourth Military Medical University. Rabbit anti-mouse serum was purchased from Beijing Zhongshan Biotechnology Co.,Ltd,China. FITC conjugated sheep anti-mouse IgG and HRP conjugated sheep anti-mouse IgG were purchased from Huamei Bioengineering Company,China. MTT was purchased from Sigma. Human hepatoma cell line SMMC-7721 and human gastric carcinoma cell line SGC-7901 were maintained in our laboratory. Primary cultures of normal human hepatocytes were established from human liver tissue collected from person who died in accident.

Preparation of liposome microbubbles

The lipid film prepared previously in our laboratory and some mediators were mixed in proportion[16]. Then the resulting mixture was sonicated, into which perfluoropropane gas was injected. The concentration and size of the microbubbles were measured under microscope. Zeta potential of the microbubbles was determined by the Chongqing Comed Nanopharma Co., Ltd, China.

Preparation of targeted liposome microbubbles

Human hepatocarcinoma specific monoclonal antibody HAb18 was added to the liposome microbubble suspension in proportion and mixed for 2 h at pH4.0, 4 ℃[17]. After the mixture was separated into 2 distinct layers, the lower layer was discarded and the upper layer was washed three times with phosphate-buffered saline (PBS) to elute the free HAb18.

Identification of targeted liposome microbubbles

Slide agglutination test A drop of rabbit anti-mouse serum or normal saline was mixed with a drop of targeted liposome microbubbles or liposome microbubbles respectively for about 5 min. The results were observed under a ×100 field of microscope.

Immunofluorescent assay A 100 μL of FITC conjugated sheep anti-mouse IgG was put into 200 μL of targeted liposome microbubbles and mixed for 30 min at 4 ℃. After the mixture was separated into 2 distinct layers, the lower layer was discarded and the upper layer was washed three times with PBS to elute the free FITC conjugated sheep anti-mouse IgG. Then the microbubbles were observed under fluorescence microscope.

Assessment of immunological activity of targeted liposome microbubbles

SMMC-7721 cells (1×10^5) were placed in each well of a 96-well ELISA plate and cultured overnight. The cells were fixed in 0.25 g/L glutaraldehyde for 20 min. A 30 g/L of defatted milk powder was added and incubated for 1 h at 37 ℃. Different concentrations of targeted liposome microbubbles or free HAb18 were added and incubated for 1.5 h at 37 ℃. HRP conjugated sheep anti-mouse IgG was added and incubated for 1.5 h at 37 ℃. O-phenylenediamine (OPD) and H_2O_2 were added and incubated for 10 min at 25 ℃. A 2 mmol/L of H_2SO_4 was added to terminate the reaction. The optical absorbance (*A*) value at 490 nm was detected with ELISA.

Specific binding of targeted liposome microbubbles to SMMC-7721 cells

Rosette formation test[18] Log phase SMMC-7721 cells and SGC-7901 cells were digested with 2.5 g/L trypsin. The isolated cells were adjusted to a concentration of 2×10^5/mL in PBS respectively. One hundred μL of targeted liposome microbubbles or liposome microbubbles was added to 200 μL of SMMC-7721 or SGC-7901 cell suspension and mixed for 30 min at 25 ℃. The resulting mixture was observed under microscope and the cells that formed rosette were counted.

Rosette formation blocking test SMMC-7721 cells were mixed with different concentrations of HAb18 for 30 min at 25 ℃. The mixture was centrifuged and washed with PBS to elute free HAb18. Then targeted liposome microbubbles were added to cell suspension and mixed for 30 min at 25 ℃. Cells forming rosette were counted under microscope.

Immunofluorescent assay one hundred μL of targeted liposome microbubbles combined with FITC conjugated sheep anti-mouse IgG and 200 μL of SMMC-7721 cells or SGC-7901 cells were mixed for 30 min at 25 ℃. The suspension was observed under fluorescence microscope.

Cytotoxicity assay of targeted liposome microbubbles

SMMC-7721 cells or human hepatocytes (1×10^5 per well) were added into a 96-well culture plate. About three hours later different concentrations of targeted liposome microbubbles were added, while PBS was used as control. Three wells were used for each concentration. They were cultured in a CO_2 incubator at 37 ℃ for 48 h, then MTT (2 g/L, 50 μL/well) was added and incubated at 37 ℃ for 6 h. The medium was discarded, and 100 μL/well DMSO was added. The culture plate was shaken for 10 min and the optical absorbance (*A*) value at 570 nm was detected with ELISA.

RESULTS

Preparation of liposome microbubbles

The average diameter of liposome microbubbles ranged from 2 to 5 μm, the concentration was 7×10^9 bubbles/mL (Figure 1). The mean zeta potential was -71.2 mV. Animal experiment demonstrated that the microbubbles could significantly enhance the ultrasound images of several tissues.

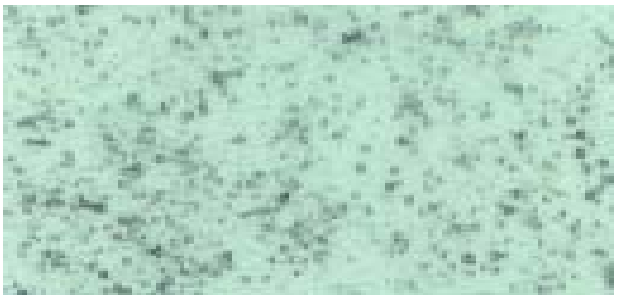

Figure 1 Light micrograph of liposome microbubbles under a ×200 field of microscope.

Preparation and identification of targeted liposome microbubbles

The average diameter of targeted liposome microbubbles was similar to that of liposome microbubbles. HAb18 did not affect the size of microbubbles. The concentration was 5×10^8 bubbles/mL.

After rabbit anti-mouse serum was added, targeted liposome microbubbles agglutinated (Figure 2), but liposome microbubbles did not. While normal saline (NS) did not lead to agglutination of two kinds of microbubbles.

The surfaces of targeted liposome microbubbles gave out bright yellow-green fluorescence after they were stained with fluorescent agents (Figure 3), whereas liposome microbubbles did not give out any fluorescence.

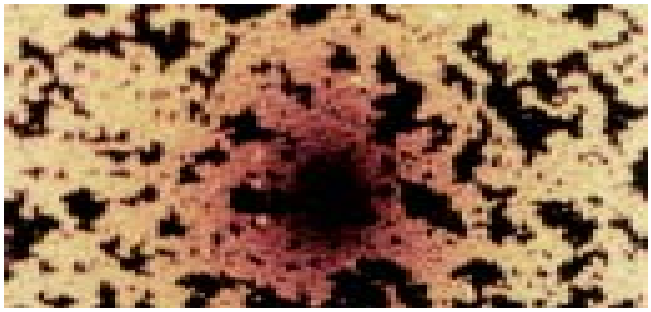

Figure 2 Direct agglutination of targeted liposome microbubbles in the presence of rabbit anti-mouse serum.

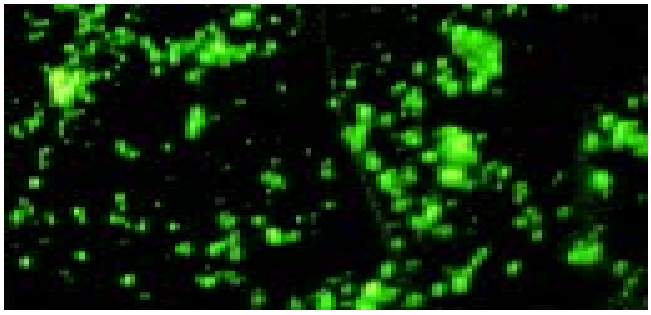

Figure 3 Immunofluoresce staining of targeted liposome microbubbles with FITC conjugated sheep anti-mouse IgG. Targeted liposome microbubbles were stained in yellow-green under a ×400 field of fluorescence microscope.

Assessment of immunological activity of targeted liposome microbubbles

ELISA indicated that the immunological activity of HAb18 on liposome microbubbles was similar to that of free HAb18. There were no significant differences in optical absorbance (*A*) value between free HAb18 ground and conjugated HAb18 ground (Figure 4).

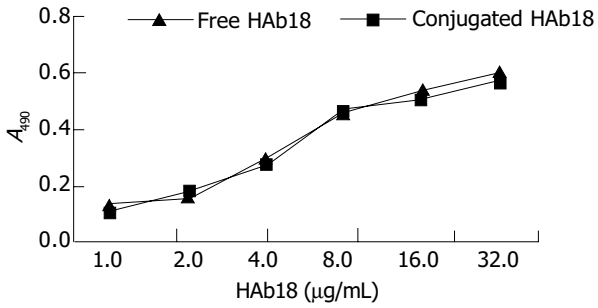

Figure 4 Activity assay of free HAb18 and conjugated HAb18 on microbubbles by ELISA.

Specific binding of targeted liposome microbubbles to SMMC-7721 cells

After targeted liposome microbubbles and SMMC-7721 cells or SGC-7901 cells were mixed for 30 min, SMMC-7721 cells were surrounded by targeted liposome microbubbles to form rosettes and the rate of rosettes reached 90% (Figure 5), while SGC-7901 cells were negative. Rosettes were not observed in the mixture of liposome microbubbles and SMMC-7721 cells under microscope. After SMMC-7721 cells were pretreated with different concentrations of HAb18, the rate of rosettes declined significantly, even dropped to 0. Immunofluorescent assay indicated that SMMC-7721 cells were surrounded by the microbubbles and gave out bright yellow-green fluorescence to form rosettes (Figure 6), whereas control cells were negative.

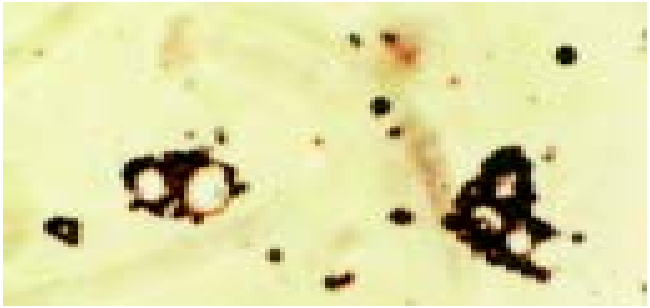

Figure 5 Light micrograph of the binding of targeted liposome microbubbles to SMMC-7721 cells under a ×400 field of microscope. SMMC-7721 cells were surrounded by targeted liposome microbubbles to form rosettes.

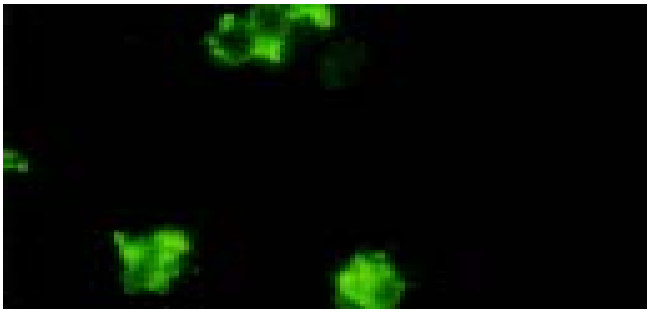

Figure 6 Immunofluorescent assay for identification of the binding of targeted liposome microbubbles to SMMC-7721 cells. SMMC-7721 cells were surrounded by the microbubbles and gave out bright yellow-green fluorescence.

Cytotoxicity assay of targeted liposome microbubbles

The result of MTT assay showed that the proliferation of human hepatocytes and SMMC-7721 cells were not influenced by targeted liposome microbubbles. There were no significant differences in average optical absorbance (A) value between experiment group and control group (Figure 7).

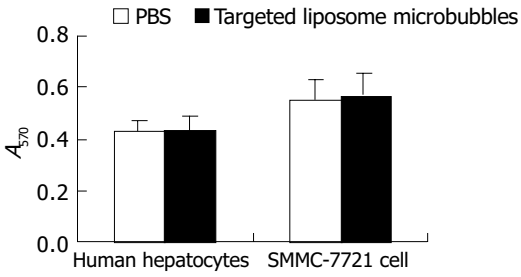

Figure 7 Effect of targeted liposome microbubbles on the proliferation of human hepatocytes and SMMC-7721 cells.

DISCUSSION

It has been nearly thirty years since the conception of ultrasound contrast imaging was suggested. Especially in recent years it has been developed rapidly and a number of ultrasound contrast agents have been described, but most of these are nontargeted. Now several targeted contrast agents that can bind to a specific acceptor have been developed[2-15,19], and it has been demonstrated that such agents can enhance ultrasound images of chosen target tissues. Skyba *et al.*[17,20-25] observed that ultrasound could induce intravascular microbubble destruction and bioeffects, and found that the application of ultrasound to thin-shelled microbubbles flowing through small microvessels (<7 μm in diameter) could produce vessel wall ruptures and the microspheres in vessel could go out through the ruptured walls. Thus antibody-loaded ultrasound contrast microbubbles could also cross the ruptured microvessels and bind specifically to the target tissues.

At present, hepatocellular carcinoma (HCC) is one of the most common malignant tumors with a high incidence and mortality in the world[26]. This cancer severely threatens our health and needs to be diagnosed as early as possible, but differential diagnosis of HCC at its early stage is still difficult. So it is important to find a specific and sensitive diadynamic method for it. Studies[27] have demonstrated that human hepatocarcinoma specific monoclonal antibody HAb18 could specifically bind to hepatocellular carcinoma cells and can be used for site targeting. If the antibody was used as a target carrier to prepare targeted ultrasound contrast agent, the contrast agent could assemble in a higher concentration of hepatoma tissues and the aim of target imaging could be achieved.

In this study, we prepared and identified targeted liposome microbubbles and investigated their immunological properties. The results indicated that human hepatocarcinoma specific monoclonal antibody HAb18 was firmly attached to the surfaces of liposome microbubbles by static attraction and the immunological activity of HAb18 on liposome microbubbles was similar to that of free HAb18. These demonstrate that it is feasible to prepare targeted liposome microbubbles by static attraction. This method is simple and inexpensive. Moreover, the activity of the antibody can be retained completely. Besides, in order to investigate the properties of targeted liposome microbubbles bound specifically to target cells, rosette formation test and rosette formation blocking test as well as immunofluorescent assay were performed. These tests indicated that targeted liposome microbubbles could bind to human hepatocarcinoma cells specifically and effectively, and the binding was mediated by HAb18.

In order to evaluate the safety of targeted liposome microbubbles, we performed cytotoxicity assay. The result indicated the microbubbles did not influence the proliferation of human hepatocytes and SMMC-7721 cells. These results lay a good foundation for further study.

REFERENCES

1 **Bian AN,** Gao YH. Research progress of targeted ultrasound contrast. *Zhonghua Chaosheng Yingxiangxue Zazhi* 2003; **12**: 558-559

2 **Unger E,** Metzger P 3rd, Krupinski E, Baker M, Hulett R, Gabaeff D, Mills J, Ihnat D, McCreery T. The use of a thrombus-specific ultrasound contrast agent to detect thrombus in arteriovenous fistulae. *Invest Radiol* 2000; **35**: 86-89

3 **Unger EC,** Matsunaga TO, McCreery TP, Sweitzer RH. Biomedical implications of a thrombus-specific US contrast agent. *Acad Radiol* 2002; **9**(Suppl 1): S56-57

4 **Hamilton A,** Huang SL, Warnick D, Stein A, Rabbat M, Madhav T, Kane B, Nagaraj A, Klegerman M, MacDonald R, McPherson D. Left ventricular thrombus enhancement after intravenous injection of echogenic immunoliposomes: studies in a new experimental model. *Circulation* 2002; **105**: 2772-2778

5 **Schumann PA,** Christiansen JP, Quigley RM, McCreery TP, Sweitzer RH, Unger EC, Lindner JR, Matsunaga TO. Targeted-microbubble binding selectively to GPIIb IIIa receptors of platelet thrombi. *Invest Radiol* 2002; **37**: 587-593

6 **Demos SM,** Onyuksel H, Gilbert J, Roth SI, Kane B, Jungblut P, Pinto JV, McPherson DD, Klegerman ME. *In vitro* targeting of antibody-conjugated echogenic liposomes for site-specific ultrasonic image enhancement. *J Pharm Sci* 1997; **86**: 167-171

7 **Unger EC,** McCreery TP, Sweitzer RH, Shen D, Wu G. *In vitro* studies of a new thrombus-specific ultrasound contrast agent. *Am J Cardiol* 1998; **81**: 58G-61G

8 **Takeuchi M,** Ogunyankin K, Pandian NG, McCreery TP, Sweitzer RH, Caldwell VE, Unger EC, Avelar E, Sheahan M, Connolly R. Enhanced visualization of intravascular and left atrial appendage thrombus with the use of a thrombus-targeting ultrasonographic contrast agent (MRX-408A1): *In vivo* experimental echocardiographic studies. *J Am Soc Echocardiogr* 1999; **12**: 1015-1021

9 **Demos SM,** Alkan-Onyuksel H, Kane BJ, Ramani K, Nagaraj A, Greene R, Klegerman M, McPherson DD. *In vivo* targeting of acoustically reflective liposomes for intravascular and transvascular ultrasonic enhancement. *J Am Coll Cardiol* 1999; **33**: 867-875

10 **Christiansen JP,** Leong-Poi H, Klibanov AL, Kaul S, Linder JR. Noninvasive imaging of myocardial reperfusion injury using leukocyte-targeted contrast echocardiography. *Circulation* 2002; **105**: 1764-1767

11 **Lindner JR,** Song J, Xu F, Klibanov AL, Singbartl K, Ley K, Kaul S. Noninvasive ultrasound imaging of inflammation using microbubbles targeted to activated leukocytes. *Circulation* 2000; **102**: 2745-2750

12 **Lindner JR,** Song J, Christiansen J, Klibanov AL, Xu F, Ley K. Ultrasound assessment of inflammation and renal tissue injury with microbubbles targeted to P-selectin. *Circulation* 2001; **104**: 2107-2112

13 **Klibanov AL,** Hughes MS, Villanueva FS, Jankowski RJ, Wagner WR, Wojdyla JK, Wible JH, Brandenburger GH. Targeting and ultrasound imaging of microbubble-based contrast agents. *MAGMA* 1999; **8**: 177-184

14 **Dayton PA,** Ferrara KW. Targeted imaging using ultrasound. *J Magn Reson Imaging* 2002; **16**: 362-377

15 **Hamilton A,** Rabbat M, Jain P, Belkind N, Huang SL, Nagaraj A, Klegerman M, Macdonald R, McPherson DD. A physiologic flow chamber model to define intravascular ultrasound enhancement of fibrin using echogenic liposomes. *Invest Radiol* 2002; **37**: 215-221

16 **Liu P,** Gao YH, Tan KB, Zuo S, Liu Z. Enhanced imaging of the rabbit liver using the self-made Liposome contrast agent: an earlier experimental study. *Zhongguo Chaosheng Yixue Zazhi* 2003; **19**: 4-6

17 **Shohet RV,** Chen S, Zhou YT, Wang Z, Meidell RS, Unger RH, Grayburn PA. Echocardiographic destruction of albumin microbubbles directs gene delivery to the myocardium. *Circulation* 2000; **101**: 2554-2556

18 **Kang JC,** Samten BK, Xie SS, Wei SL. Separation of human bladder cancer cells from bone marrow with a kind of immunomagnetic microspheres. *Yaoxue Xuebao* 1998; **33**: 52-56

19 **Leong-Poi H,** Christiansen J, Klibanov AL, Kaul S, Lindner JR. Noninvasive assessment of angiogenesis by ultrasound and microbubbles targeted to alpha (v) -integrins. *Circulation* 2003; **107**: 455-460

20 **Skyba DM,** Price RJ, Linka AZ, Skalak TC, Kaul S. Direct *in vivo* visualization of intravascular destruction of microbubbles by ultrasound and its local effects on tissue. *Circulation* 1998; **98**: 290-293

21 **Price RJ,** Skyba DM, Kaul S, Skalak TC. Delivery of colloidal particles and red blood cells to tissue through microvessel ruptures created by targeted microbubble destruction with ultrasound. *Circulation* 1998; **98**: 1264-1267

22 **Mukherjee D,** Wong J, Griffin B, Ellis SG, Porter T, Sen S, Thomas JD. Ten-fold augmentation of endothelial uptake of vascular endothelial growth factor with ultrasound after systemic administration. *J Am Coll Cardiol* 2000; **35**: 1678-1686

23 **Lawrie A,** Brisken AF, Francis SE, Cumberland DC, Crossman DC, Newman CM. Microbubble-enhanced ultrasound for vascular gene delivery. *Gene Ther* 2000; **7**: 2023-2027

24 **Price RJ,** Kaul S. Contrast ultrasound targeted drug and gene delivery: an update on a new therapeutic modality. *J Cardiovasc Pharmacol Ther* 2002; **7**: 171-180

25 **Zhang DZ,** Ren H, Wang ZG, Leng ZY, Ran HT, Zhang DF. Ultrasound enhancing the infection efficiency of adenoviral vector into the intact hepaocyte. *Linchuang Chaosheng Yixue Zazhi* 2002; **4**: 321-323

26 **Qian J,** Truebenbach J, Graepler F, Pereira P, Huppert P, Eul T, Wiemann G, Claussen C. Application of poly-lactide-co-glycolide-microspheres in the transarterial chemoembolization in an animal model of hepatocellular carcinoma. *World J Gastroenterol* 2003; **9**: 94-98

27 **Bian HJ,** Chen ZN, Lou C, Mi L, Wang J, Deng JL, Yu XL. ^{188}Re-labeled HAb18 F $(ab')_2$ for hepatoma radio-immunoimaging. *Zhongliu* 2000; **20**: 181-184

Edited by Zhang JZ and Wang XL **Proofread by** Xu FM

PO Box 2345, Beijing 100023, China
Fax: +86-10-85381893
E-mail: wjg@wjgnet.com www.wjgnet.com

World J Gastroenterol 2004;10(23):3428-3432
World Journal of Gastroenterology
Copyright © 2004 by The WJG Press ISSN 1007-9327

• LIVER CANCER •

Effect of hepatoma H22 on lymphatic endothelium *in vitro*

Hua Yu, Hong-Zhi Zhou, Chun-Mei Wang, Xiao-Ming Gu, Bo-Rong Pan

Hua Yu, Chun-Mei Wang, Electron Microscopy Center, School of Basic Medicine, Fourth Military Medical University, Xi'an 710032, Shaanxi Province, China
Hong-Zhi Zhou, Xiao-Ming Gu, College of Stomatology, Fourth Military Medical University, Xi'an 710032, Shaanxi Province, China
Bo-Rong Pan, Department of Oncology, Xijing Hospital, Fourth Military Medical University, Xi'an 710032, Shaanxi Province, China
Co-first-authors: Hua Yu and Hong-Zhi Zhou
Correspondence to: Chun-Mei Wang, Electron Microscopy Center, School of Basic Medicine, Fourth Military Medical University, Xi'an 710032, Shaanxi Province, China. wangcm@fmmu.edu.cn
Telephone: +86-29-83374569 **Fax:** +86-29-83374467
Received: 2004-04-14 **Accepted:** 2004-05-09

Abstract

AIM: To determine the effect of metastatic hepatoma cells on lymphangioma-derived endothelium, and to establish *in vitro* model systems for assessing metastasis-related response of lymphatic endothelium.

METHODS: Benign lymphangioma, induced by intraperitoneal injection of the incomplete Freund's adjuvant in BALB/c mice, was embedded in fibrin gel or digested and then cultured in the conditioned medium derived from hepatoma H22. Light and electron microscopy, and the transwell migration assay were used to determine the effect of H22 on tissue or cell culture. Expressions of Flt-4, c-Fos, proliferating cell nuclear antigen (PCNA), and inducible nitric oxide synthase (iNOS) in cultured cells, and content of nitric oxide in culture medium were also examined.

RESULTS: The embedded lymphangioma pieces gave rise to array of capillaries, while separated cells from lymphangioma grew to a cobblestone-like monolayer. H22 activated growth and migration of the capillaries and cells, induced expressions of Flt-4, c-Fos, PCNA and iNOS in cultured cells, and significantly increased the content of NO in the culture medium.

CONCLUSION: Lymphangioma-derived cells keep the differentiated phenotypes of lymphatic endothelium, and the models established in this study are feasible for *in vitro* study of metastasis-related response of lymphatic endothelium.

Yu H, Zhou HZ, Wang CM, Gu XM, Pan BR. Effect of hepatoma H22 on lymphatic endothelium *in vitro*. *World J Gastroenterol* 2004; 10(23): 3428-3432
http://www.wjgnet.com/1007-9327/10/3428.asp

INTRODUCTION

Metastasis of most cancers occurs primarily through the lymphatic system, and is responsible for the majority of cancer deaths. But tumor-associated lymphatic system has been overshadowed by the greater emphasis placed on the blood vascular system[1]. This scenario is changing rapidly after the identification of lymphangiogenic vascular endothelial growth factor C[2]. The traditional view that lymphatic capillaries are passive participants in metastasis is currently being challenged, and recent studies indicate the importance of lymphatic vessel activation in tumor dissemination[3-5].

Better understanding of the lymphatic endothelial properties and their alteration in cancer may develop a new way to therapeutic intervention[6,7]. *In vitro* experiments have been proven to be valuable, expeditious and easy of quantification in providing initial information on angiogenesis, a potentially important oncotherapy target[8]. However such *in vitro* models have not been well established for revealing metastasis-related response of lymphatic endothelium. Therefore, the aim of our study was to determine the effect of metastatic hepatoma cells on lymphangioma-derived endothelium, and to establish *in vitro* model systems for assessing metastasis-related response of lymphatic endothelium.

MATERIALS AND METHODS

Animals and reagents

BALB/c mice of either gender, 2 mo old and weighing 22-25 g, were provided by Laboratory Animal Research Center, Fourth Military Medical University (FMMU, Xi'an, China). A mouse ascitic hepatoma cell line, H22, was obtained from Institute of Digestive Diseases, FMMU. Reagents for *in vitro* culture of lymphatic endothelium included incomplete Freund's adjuvant, Hanks' balanced salt solution (HBSS), M199 medium and fetal calf serum (FCS), which were purchased from Gibco Company (Carlsbad, California, USA), bovine fibrinogen, thrombin, gelatin, endothelial cell growth supplement (ECGS), heparin, collagenases I and II, which were products of Sigma Company (Saint Louis, Missouri, USA). The sABC and sABC-AP kits for immunohistochemical staining were purchased from Boster Company (Wuhan, China). Polyclonal anti-Flt-4 antibodies, monoclonal anti-iNOS antibody, anti-c-Fos antibody, and anti-PCNA antibody were products of Santa Cruz Company (Santa Cruz, California, USA). Nitric oxide (NO) detection kit was purchased from Nanjing Jiancheng Bioengineering Institute (Nanjing, China). Millicell culture plate inserts (12.0 μm) for transwell cell migration test were purchased from Millipore Corporation (Billerica, Massachusetts, USA).

Preparation of conditioned medium of H22

Hepatoma H22 cells were inoculated into abdominal cavity of 5 BALB/c mice for passage. To verify the capability of spontaneous lymphatic metastasis of H22, the generated carcinomatous ascites was transplanted into hindlimb claw pad of 10 healthy BALB/c mice and the lymph nodes in groin were harvested 10 d later for pathological examination. The conditioned medium of H22 (H22 CM) was prepared as a mixture of sterile ultra-filtrate of H22 ascites and M199 medium at the ratio of 1:5, supplemented with 150 mL/L FCS. The control medium was M199 medium supplemented with 150 mL/L FCS.

Induction of lymphangioma

Twenty healthy animals of BALB/c strain were intraperitoneally injected twice, with a 15-d interval, with 200 μL of the emulsified (1:1 with HBSS) incomplete Freund's adjuvant and killed one month later. Multicentric and clearly delimited white neoplasm on the abdominal surface of the diaphragm, varying in size from 3 to 15 mm^2, was collected for the following experiments. Histopathological examination of the tumors in our preparative experiment and other previous studies[9] confirmed that this

neoplasm was benign lymphangioma.

Tri-dimensional lymphangioma culture

The lymphangioma masses were washed by HBSS, and cut into 1-mm^2 pieces. HBSS containing 3 g/L bovine fibrinogen was added into 48-well culture plates (0.5 mL/well), and fibrin gel clotting was induced by addition of 10 μL 50 kU/Lthrombin. A piece of lymphangioma was then placed on gel surface, and additional 0.5 mL fibrinogen solution and 10 μL thrombin were added to embed the tissue. H22 CM was then added into 24 wells (as an experimental group), and the control medium into another 24 wells (as a control group). The gels were incubated, with culture medium changed every other day, at 37 ℃ with 50 mL/L CO_2 in air, and examined daily under an inverted microscope. To perform a quantitative analysis, images were taken every second day under same conditions (in brightness, contrast, and magnification), and measured by a computer-assisted image analysis system of Quantimet 570. For electron microscopy, six gels from each group were fixed two weeks later with 10 g/L glutaraldehyde in 0.1 mol/L sodium phosphate buffer, post-fixed with 10 g/L OsO_4 in s-collidine buffer, dehydrated in graded ethanol, and embedded in Epon. Ultrathin sections were cut and stained with lead citrate and examined with a JEM-200EX transmission electron microscope.

Primary cell culture

Lymphangioma masses were mechanically broken, and washed in M199 medium, supplemented with 100 kU/L penicillin. The tissues were then incubated for 30 min at 37 ℃ in HBSS containing 0.5 g/L collagenases (1:1 mixture of type I and II), and washed with a medium containing 150 mL/L FCS to stop digestion. Cells were centrifuged at 700 r/min, resuspended in M199 medium supplemented with 150 mL/L FCS, and equally seeded on 10 g/L gelatin-coated cover slips in a 24-well plate. To allow cell attachment, the plates were put still for one hour in an incubator at 37 ℃ with 50 mL/L CO_2 in air. Then the wells were gently washed to remove floating cells, and refilled with 2 mL H22 CM (24 wells) or 2 mL control medium (24 wells). Attached cells were cultured routinely, and examined daily under a phase-contrast microscope.

Immunocytochemical testing

Six days after primary cell seeding, the cover slips were fixed with 40 g/L formaldehyde in PBS for 20 min, with 2 g/L Triton X-100 in PBS, and incubated with 200 mL/L normal goat serum. Polyclonal anti-Flt-4 antibodies, monoclonal anti-iNOS antibody, anti-PCNA antibody and anti-c-Fos antibody were used as primary antibodies, and biotin-labeled goat anti-rabbit IgG antibodies as second antibodies. Streptavidin and biotinylated horseradish peroxidase complex (sABC) and DAB were used for anti-Flt-4 and anti-iNOS antibodies, and sABC-AP (alkaline phosphatase) and BCIP/NBT for anti-PCNA and anti-c-Fos antibodies.

Nitric oxide detection

The content of NO in fresh H22 CM and control medium was indicated by determining the total concentration of nitrite/nitrate by using the colorimetric method, according to the instructions provided with the NO detection kit. After primary cells were equally seeded and cultured with 2 mL H22 CM or control M199 medium for 48 h, the levels of NO in the two media were detected again. For an empty control, the two media were added into an empty plate, which was then incubated at 37 ℃ for 48 h before NO detection.

Transwell migration assay

Primary cells from lymphangioma were cultured to a confluent monolayer with a complete endothelium growth medium (M199 supplemented with 100 mg/L heparin, 30 mg/L ECGS and 150 mL/L FCS), subjected to serum starvation for 4 h by switching the culture medium to M199 medium without growth factors or serum, trypsinized and suspended (1×10^8 cells/L) in serum-free M199 medium. Transwell migration assays were performed in Millicell inserts, with 1 g/L gelatin-coated 12 μm filter membrane, in a 24-well culture plate. H22 CM and the control medium were added, respectively, into 12 wells of the plate, and 0.5 mL of suspended cells was placed in chambers of the inserts. After 4-h incubation at 37 ℃, the medium in the insert chamber was aspirated, and cells on the upper surface of the filter membrane were removed with a cotton swab. Cells on the lower surface were fixed, stained with hematoxylin and counted in 5 high-power fields per chamber under light microscope.

RESULTS

Basic feasibility of the assay

Spontaneous lymphatic metastasis of transplant H22 tumor was found in all 10 animals as demonstrated by pathological examination of the groin lymph nodes (Figure 1). H22 CM could be easily prepared, and stored for the entire experiments to ensure the continuity of the different parts of the assay. The induction of lymphangioma was also confirmed to be a simple and well duplicable procedure, and could provide adequate original tissues for the following experiments.

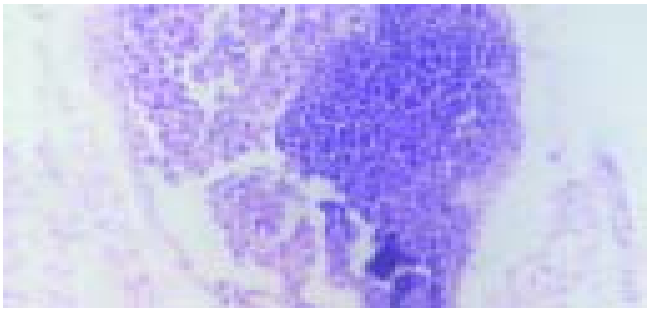

Figure 1 Metastatic H22 tumor in the groin lymph node (×100).

Effect of H22 CM on lymphangioma culture

Lymphangioma embedded in the fibrin gels gave rise to capillaries when cultured 3-4 d in both H22 CM and control M199 media. Neo-branches of the micro-vessels with obvious lumina were generated every day. Under the effect of H22 CM, rather straight capillaries stretching out to the fringe of the gel were generated, and the number of branching in micro-vessels increased more rapidly (Figure 2). Transmission electron microscopy revealed that the ultrastructure of the capillaries was plasmalemma invagination of a single cell, or formed by cytoplasmic flaps joined by overlapping contacts and specialized tight junction complexes (Figure 3). End-to-end intercellular contacts were rare. No typical Weibel-Palade body was distinguished in the cytoplasm.

Effect of H22 CM on primary cell activation

Primary cell culture was successfully established on gelatin-coated cover slips. When cultivated in H22 CM, the cells proliferated, albeit at a low rate with a doubling time of about 36-60 h, and reached sub-confluence in 6 d. At this stage, the lymphangioma cells showed appearance like cobblestone, the classical morphology of endothelial cells. In contrast, when cultured in the control M199 medium, the cells showed no obvious proliferation after attachment. Correspondingly, immunocytochemical staining for Flt-4, PCNA, and c-Fos were positive in cells cultured in H22 CM (Figure 4), but negative in cells cultured in the control medium.

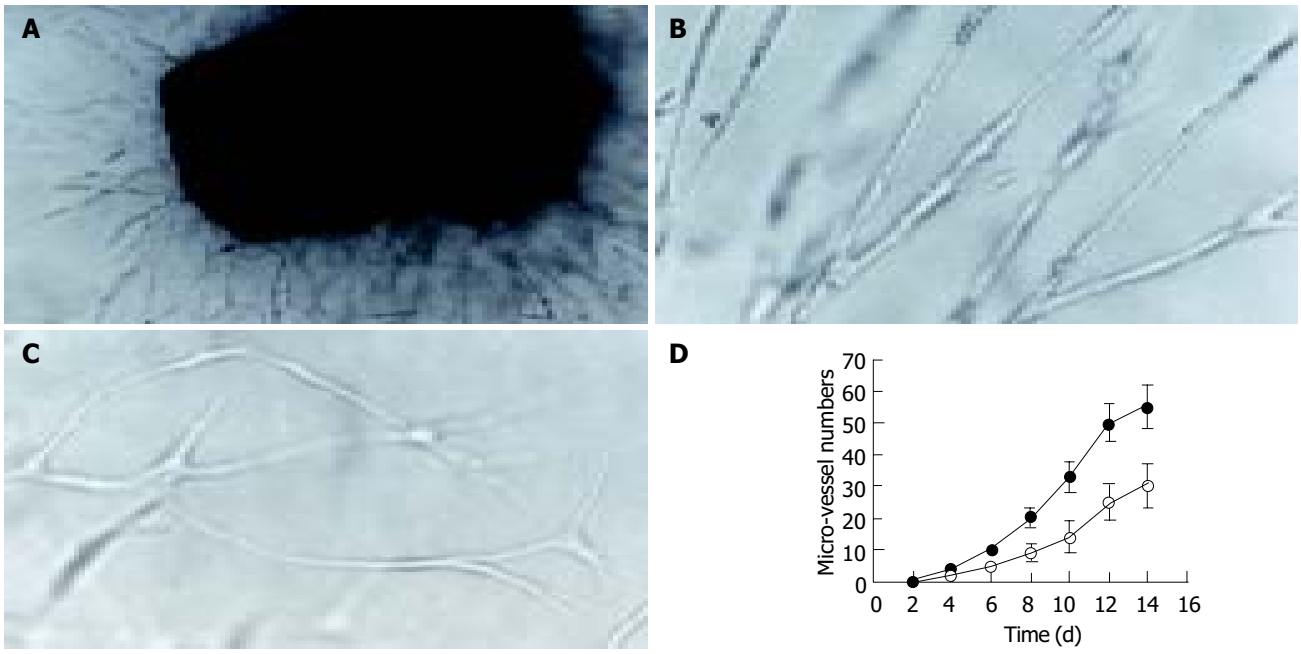

Figure 2 Tri-dimensional culture of lymphangioma. A: Microphotograph of the capillary network in the fibrin gel (×100); B: Straight micro-vessels in H22 CM (×200); C: Tortuous micro-vessels in the control medium (×200); D: Growth curves of micro-vessels in H22 CM (●) and the control medium (○). Data are expressed as means of 24 samples, and error bars represent SE.

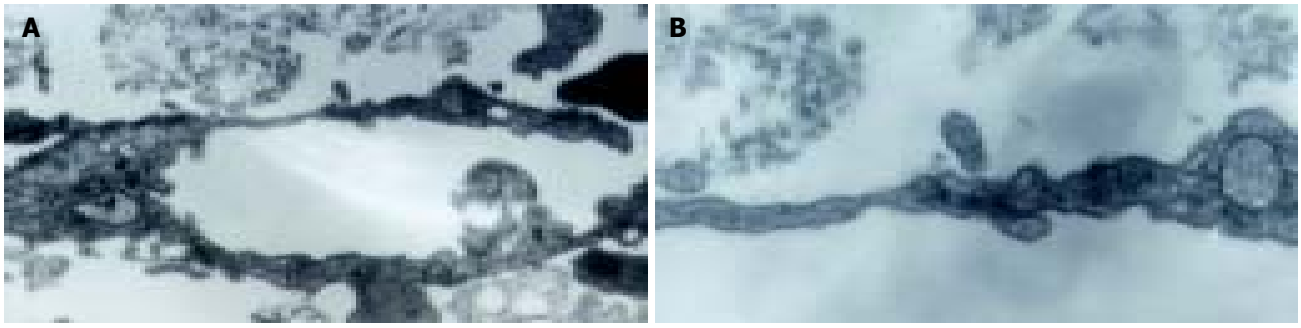

Figure 3 Electron transmission micrographs of the micro-vessel in fibrin gel. A: Lumen formed by cytoplasmic flaps joined by overlapping contacts (×2 000); B: Tight junction complexes between overlapping contacts (×10 000).

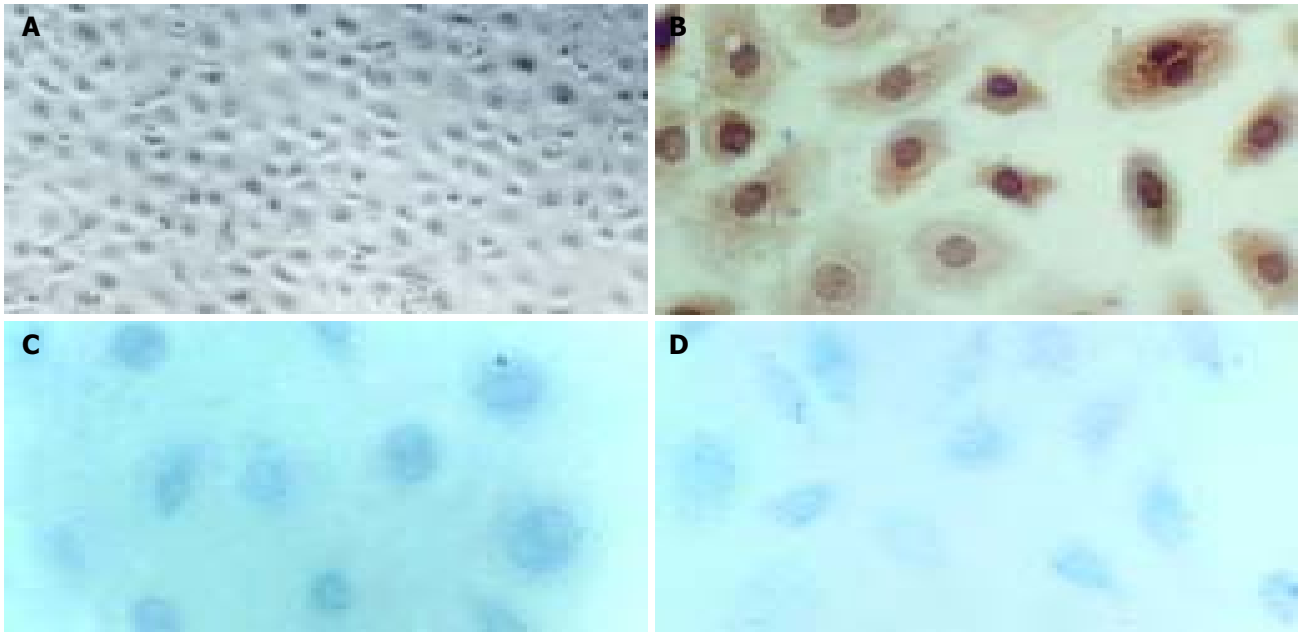

Figure 4 Primary cell culture with H22 CM and immunocytochemical staining. A: Microphotograph of the confluent cell monolayer (×100); B: Positive staining of Flt-4 (nucleus counterstained with hematoxylin, ×300); C: Positive staining of PCNA (×400); D: Positive staining of c-Fos (×400).

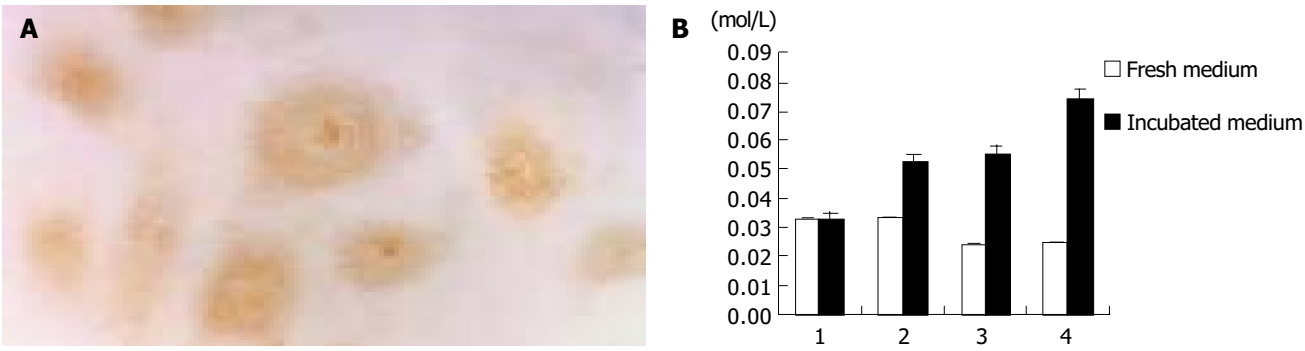

Figure 5 Expression of iNOS in lymphangioma cells and changes of NO level of the media after incubation. A: Positive staining of iNOS in cells cultured with H22 CM (×400); B: Changes of NO level of the control medium in empty plate (1) or primary culture plate (2), and H22 CM in empty plate (3) or primary culture plate (4).

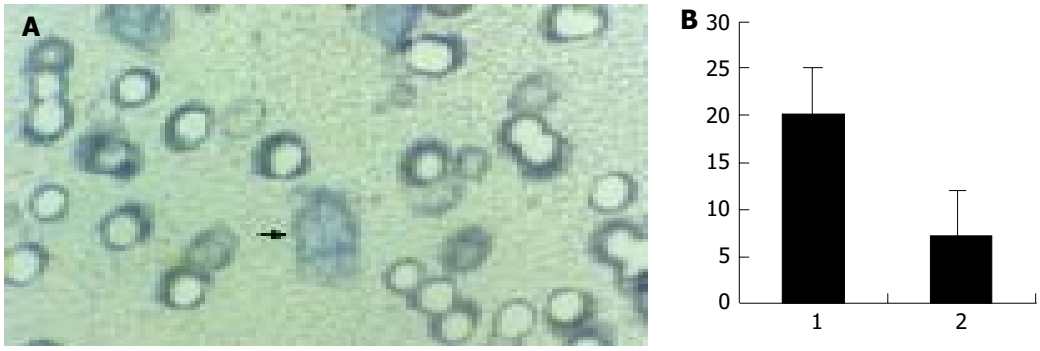

Figure 6 Transwell migration assay. A: Cells on lower surface of the filter membrane of the Millicell insert (×400); B: Migration cell number in H22 CM (1) and the control medium (2).

Effect of H22 CM on NO production

Immunostaining showed the expression of iNOS in lymphangioma cells after culture in H22 CM, and significantly increased content of NO in the culture medium (Figure 5). In contrast, cells cultured in the control M199 medium did not express iNOS, and the level of NO was rather low in the control medium.

Effect of H22 CM on cell migration

When cultured in the complete medium, the lymphangioma cells grew to a confluent monolayer in 8-10 d, and showed specialized cobblestone morphology, which further confirmed the nature of the cells. In transwell migration assay, the number of the cells on the lower surface of the filter membrane in H22 CM was significantly greater than in control medium (Figure 6).

DISCUSSION

The ascitic hepatoma H22 is a cell line with high potential of spontaneous lymphatic metastasis[10], which was also verified in our experiments, and has been generally used in various experimental studies in oncology[11-14]. It is proven to be a convenient and feasible tumor model for *in vitro* assessment on metastasis-related response of lymphatic endothelium.

The difficulty in isolation of lymphatic endothelium, especially from the animals commonly used in oncological experiments such as mice and rats, has limited studies on its reactions in tumorous environments. We used induced lymphangioma to solve this problem. When cultured in the fibrin gel, lymphangioma sprouts capillaries with ultrastructure similar to that of lymphatic vessels[4,15]. Moreover, gelatin-anchorage dependent primary cell culture, and cobblestone morphology of confluent or subconfluent monolayer, are also specialized phenotype of lymphatic endothelium[16,17]. Finally, positive expression of Flt-4 (also known as VEGFR-3), a marker of lymphatic endothelium in proliferation[18,19], confirmed the nature of the endothelium. These findings prove that lymphangioma is a proper original tissue for *in vitro* assay on lymphatic endothelium or lymphangiogenesis.

Despite the possible lymphangiogenic effect of fibrin[20], H22 CM induced a faster formation of capillary network from lymphangioma in fibrin gels. Moreover, in primary cell culture, H22 CM showed similar capability to the complete growth medium in activating proliferation of lymphatic endothelial cells. Immunostaining for the common proliferating nuclear marker, PCNA[21], and early-response gene signaling factor, c-Fos[22], further confirmed the microscopic findings. Our results accord with the opinion on lymphatic vessel activation in cancer.

Endogenous NO is one of the key factors in the control of dilation of the lymphatic micro-vessels[23,24]. The expression of iNOS in cancers is related to lymph node metastasis[25,26]. iNOS is also evenly distributed throughout the cytoplasm of lymphatic endothelial cells[27-29]. Our study demonstrates sustained expression of iNOS in cultured lymphatic endothelium and marked increase of NO levels in the culture medium under the effect of H22 CM, suggesting that dilation of lymphatics may be important for cancer invasion and metastasis.

There have been rare assays on lymphatic endothelial cell migration, which is an important event that initiates and coordinates lymphangiogenesis[30]. Results from our study suggest that some soluble factors in H22 CM activate migration of lymphatic endothelial cells and tropistic lymphangiogenesis. The coadjutant models established in our experiment are useful for further studies on migration inhibitors.

To our knowledge, this study is the first of its kind that bridges the gap between *in vivo* and *in vitro* studies on lymphatic endothelium and lymphangiogenesis. Both the culture medium and gel matrix in the experiment can be manipulated pharmacologically, which allows us to evaluate the activity of either soluble or solid-phase lymphangiogenesis inhibitors. Moreover, this spontaneous lymphatic metastasis

model of transplant H22 tumor will be helpful to determine whether inhibition of lymphangiogenesis is a realistic therapeutic strategy for inhibiting tumor dissemination and metastasis.

REFERENCES

1 **Pepper MS**. Lymphangiogenesis and tumor metastasis: myth or reality? *Clin Cancer Res* 2001; **7**: 462-468

2 **Joukov V**, Pajusola K, Kaipainen A, Chilov D, Lahtinen I, Kukk E, Saksela O, Kalkkinen N, Alitalo K. A novel vascular endothelial growth factor, VEGF-C, is a ligand for the Flt4 (VEGFR-3) and KDR (VEGFR-2) receptor tyrosine kinases. *EMBO J* 1996; **15**: 290-298

3 **Nathanson SD**. Insights into the mechanisms of lymph node metastasis. *Cancer* 2003; **98**: 413-423

4 **Pepper MS**, Skobe M. Lymphatic endothelium: morphological, molecular and functional properties. *J Cell Biol* 2003; **163**: 209-213

5 **Cassella M**, Skobe M. Lymphatic vessel activation in cancer. *Ann N Y Acad Sci* 2002; **979**: 120-130

6 **Stacker SA**, Hughes RA, Achen MG. Molecular targeting of lymphatics for therapy. *Curr Pharm Des* 2004; **10**: 65-74

7 **Mou JH**, Yan XC, Wang D, Wu XH, Li ZP, Xiang DB. Relationship between VEGF-C expression and lymph node metastasis and prognosis in large intestinal carcinoma. *Shijie Huaren Xiaohua Zazhi* 2004; **12**: 1061-1064

8 **Auerbach R**, Lewis R, Shinners B, Kubai L, Akhtar N. Angiogenesis assays: a critical overview. *Clin Chem* 2003; **49**: 32-40

9 **Mancardi S**, Stanta G, Dusetti N, Bestagno M, Jussila L, Zweyer M, Lunazzi G, Dumont D, Alitalo K, Burrone OR. Lymphatic endothelial tumors induced by intraperitoneal injection of incomplete Freund's adjuvant. *Exp Cell Res* 1999; **246**: 368-375

10 **Jiang XP**, Tang ZY, Liu KD, Zhou XD, Lin ZY, Ling MY, Wu XF. mRNA levels of nm23 in murine ascites hepatoma (H22) clones with different lymphatic metastatic potential. *J Cancer Res Clin Oncol* 1996; **122**: 55-58

11 **Zhang J**, Zhang JK, Zhuo SH. A vaccine prepared by fusion of H_{22} cells with the spleen-drived dendritic cells. *Shijie Huaren Xiaohua Zazhi* 2004; **12**: 276-279

12 **Yuan SF**, Wang L, Li KZ, Yan Z, Han W, Zhang YQ. Inhibitory effect of MUC1 gene immunization on H22 hepatocellular carcinoma growth. *Shijie Huaren Xiaohua Zazhi* 2003; **11**: 1322-1325

13 **Liang J**, Sun JY, Xie YH, Li Y, Yan L, Wang SW. Effect of monoclonal antibody 3A5 coupled with Chinese medicine compound Andi in targeted treatment of hepatocellular carcinoma. *Shijie Huaren Xiaohua Zazhi* 2003; **11**: 404-407

14 **Li ZS**, Zhu ZG, Yin HR, Chen SS, Lin YZ. Diversity of telomerase activity in human and murine tumor cells transfected with cytokine genes. *Shijie Huaren Xiaohua Zazhi* 1999; **7**: 194-196

15 **Azzali G**. The lymphatic vessels and the so-called "lymphatic stomata" of the diaphragm: a morphologic ultrastructural and three-dimensional study. *Microvasc Res* 1999; **57**: 30-43

16 **Mizuno R**, Yokoyama Y, Ono N, Ikomi F, Ohhashi T. Establishment of rat lymphatic endothelial cell line. *Microcirculation* 2003; **10**: 127-131

17 **Leak LV**, Jones M. Lymphatic endothelium isolation, characterization and long-term culture. *Anat Rec* 1993; **236**: 641-652

18 **Kaipainen A**, Korhonen J, Mustonen T, van Hinsbergh VW, Fang GH, Dumont D, Breitman M, Alitalo K. Expression of the fms-like tyrosine kinase 4 gene becomes restricted to lymphatic endothelium during development. *Proc Natl Acad Sci U S A* 1995; **92**: 3566-3570

19 **Karkkainen MJ**, Makinen T, Alitalo K. Lymphatic endothelium: a new frontier of metastasis research. *Nat Cell Biol* 2002; **4**: E2-5

20 **Palumbo JS**, Potter JM, Kaplan LS, Talmage K, Jackson DG, Degen JL. Spontaneous hematogenous and lymphatic metastasis, but not primary tumor growth or angiogenesis, is diminished in fibrinogen-deficient mice. *Cancer Res* 2002; **62**: 6966-6972

21 **Enholm B**, Karpanen T, Jeltsch M, Kubo H, Stenback F, Prevo R, Jackson DG, Yla-Herttuala S, Alitalo K. Adenoviral expression of vascular endothelial growth factor-C induces lymphangiogenesis in the skin. *Circ Res* 2001; **88**: 623-629

22 **Deed R**, Rooney P, Kumar P, Norton JD, Smith J, Freemont AJ, Kumar S. Early-response gene signalling is induced by angiogenic oligosaccharides of hyaluronan in endothelial cells. Inhibition by non-angiogenic, high-molecular-weight hyaluronan. *Int J Cancer* 1997; **71**: 251-256

23 **Nakaya K**, Mizuno R, Ohhashi T. B16-BL6 melanoma cells release inhibitory factor(s) of active pump activity in isolated lymph vessels. *Am J Physiol Cell Physiol* 2001; **281**: C1812-1818

24 **Mizuno R**, Koller A, Kaley G. Regulation of the vasomotor activity of lymph microvessels by nitric oxide and prostaglandins. *Am J Physiol* 1998; **274**(3pt 2): R790-796

25 **Niu XJ**, Wang ZR, Wu SL, Geng ZM, Zhang YF, Qing XL. Relationship between inducible nitric oxide synthase expression and angiogenesis in primary gallbladder carcinoma tissue. *World J Gastroenterol* 2004; **10**: 725-728

26 **Song ZJ**, Gong P, Wu YE. Relationship between the expression of iNOS, VEGF, tumor angiogenesis and gastric cancer. *World J Gastroenterol* 2002; **8**: 591-595

27 **Ji RC**, Kato S. Histochemical analysis of lymphatic endothelial cells in lymphostasis. *Microsc Res Tech* 2001; **55**: 70-80

28 **Marchetti C**, Casasco A, Di Nucci A, Reguzzoni M, Rosso S, Piovella F, Calligaro A, Polak JM. Endothelin and nitric oxide synthase in lymphatic endothelial cells: immunolocalization *in vivo* and *in vitro*. *Anat Rec* 1997; **248**: 490-497

29 **Marchetti C**, Casasco A, Di Nucci A, Cornaglia AI, Reguzzoni M, Rosso S, Piovella F, Calligaro A, Polak JM. Immunolocalization of endothelin and nitric oxide-synthase in lymphatic vessels and cultured lymphatic endothelial cells. *Microvasc Res* 1997; **53**: 282-285

30 **Boardman KC**, Swartz MA. Interstitial flow as a guide for lymphangiogenesis. *Circ Res* 2003; **92**: 801-808

Edited by Xia HHX **Proofread by** Zhu LH and Xu FM

PO Box 2345, Beijing 100023, China
Fax: +86-10-85381893
E-mail: wjg@wjgnet.com www.wjgnet.com

World J Gastroenterol 2004;10(23):3433-3440
World Journal of Gastroenterology
Copyright © 2004 by The WJG Press ISSN 1007-9327

• LIVER CANCER •

Methylation profile of the promoter CpG islands of 14 "drug-resistance" genes in hepatocellular carcinoma

Sheng Ding, Bang-Dong Gong, Jian Yu, Jun Gu, Hong-Yu Zhang, Zu-Bin Shang, Qi Fei, Peng Wang, Jing-De Zhu

Sheng Ding, Bang-Dong Gong, Jian Yu, Jun Gu, Hong-Yu Zhang, Zu-Bin Shang, Qi Fei, Peng Wang, Jing-De Zhu, The State-Key Laboratory for Oncogenes and Related Genes, Shanghai Cancer Institute, Shanghai Jiaotong University, Shanghai 200032, China
Supported by the National High Technology Research and Development Program of China (863 program), No. 2002AA2Z3353 and the Science Foundation of Shanghai Municipal Government, No. 02DJ14056
Co-first-authors: Sheng Ding, Bang-Dong Gong and Jian Yu
Correspondence to: Dr. Jing-De Zhu, The State-key Laboratory for Oncogenes and Related Genes, Shanghai Cancer Institute, Shanghai Jiaotong University, LN 2200/25, Xie-Tu Road, Shanghai 200032, China. zhujingde@yahoo.com
Telephone: +86-21-64224285 **Fax:** +86-21-64224285
Received: 2003-04-14 **Accepted:** 2003-05-09

Abstract

AIM: To establish the DNA methylation patterns of the promoter CpG islands of 14 "drug-resistance" genes in hepatocellular carcinoma (HCC).

METHODS: The methylation specific polymerase chain reaction in conjunction with sequencing verification was used to establish the methylation patterns of the 14 genes in the liver tissues of four healthy liver donors, as well as tumor and the paired non-cancerous tissues of 30 HCC patients.

RESULTS: While 11 genes (ATP-binding cassette, sub-family G (WHITE), member 2(*ABCG2*), activating transcription factor (*ATF2*), beta-2-microglobulin (*B2M*), deoxycytidine kinase (*DCK*), occludin (*OCLN*), v-raf-1 murine leukemia viral oncogene homolog (*RAF1*), ralA binding protein 1 (*RALBP1*), splicing factor (45 kD) (*SPF45*), S-phase kinase-associated protein 2 (p45) (*SKP2*), tumor protein p53 (Li-Fraumeni syndrome) (*TP53*) and topoisomerase (DNA) II beta (*TOP2B*)) maintained the unmethylated patterns, three genes displayed to various extents the hypermethylation state in tumor tissues in comparison with the normal counterparts. The catalase (*CAT*) was hypermethylated in tumor and the neighboring non-cancerous tissue of one case (3.3%). Both glutathione S-transferase pi (*GSTpi*) (80%, 24/30 in tumor and 56.7%, 17/30 in the paired non-cancerous tissues) and cystic fibrosis transmembrane conductance regulator, ATP-binding cassette (sub-family C, member 7) (*CFTR*) (77%, 23/30 in tumor and 50%, 15/30 in the paired non-cancerous tissues) genes were prevalently hypermethylated in HCC as well as their neighboring non-cancerous tissues. No significant difference in the hypermethylation occurrence was observed between the HCC and its neighboring non-cancerous tissues.

CONCLUSION: Hypermethylation of promoter CpG islands of both *CFTR* and *GSTpi* genes occurs prevalently in HCC, which may correlate with the low expression of these two genes at the mRNA level and has the profound etiological and clinical implications. It is likely to be specific to the early phase of HCC carcinogenesis.

Ding S, Gong BD, Yu J, Gu J, Zhang HY, Shang ZB, Fei Q, Wang P, Zhu JD. Methylation profile of the promoter CpG islands of 14 "drug-resistance" genes in hepatocellular carcinoma. *World J Gastroenterol* 2004; 10(23): 3433-3440 http://www.wjgnet.com/1007-9327/10/3433.asp

INTRODUCTION

Hepatocellular carcinoma (HCC) is one of the most threatening malignancies, occurring prevalently in China[1]. Its poor prognostic prospects have not only been attributed to the rapid advancing nature as well as the notorious metastasizing potential of the primary lesions, but also resulted from its refractoriness to the conventional chemotherapeutic practices[2-4]. Altered expression of the crucial genes, even prior to the relevant treatment, is common in cancer cells, including HCC. The intrinsic drug resistance, reflected by the changes in the expression profile of the key genes in relevant pathways, including apoptosis, cell cycle progression, DNA repairs, *etc*., is common in cancer cells, which certainly contributes to the more rapid growth ability of cancerous cells than the normal counterparts, in the adverse environments in particular. Furthermore, cancer cells can also acquire resistance to chemotherapeutic remedies during treatment. It has been regarded as the key mechanism for the post-remission return of the full-blew cancer of same origin. Therefore, a long-standing challenge in cancer field is the underlying mechanisms of the drug resistance nature of tumors. The genetic defects leading to the intrinsic drug resistance have been well-established, but the mechanisms at the epigenetic levels, DNA methylation in particular resulting in the changes in expression, have only gained the justified recognition recently[5].

Over 50% of the protein coding genes are marked with the CpG rich segment at their 5' end, the methylation status of which profoundly affects the transcription status of the genes[6]. Biochemically, the methylated CpG affects the sequence-specific DNA-protein interactions by eliminating the otherwise binding of the transcription factors to their cognate cis-elements, while unfolding the cascade of reactions leading to chromatin condensation initiated by the binding to the methylated CpG by members of the methyl CpG binding protein family (MBD). Hypermethylation of the promoter CpGs has been linked to the long-term transcription-silencing status of DNA segments, including genes as well as the transposon-like-repetitive sequences in cells[7,8]. The genome-wide hypomethylation has been regarded contributive to activation of transcription of the otherwise silenced transposon like repetitive sequences (such as the Alu and LINE repeats in mammals) and instrumental to the transposition mediated loss of the genome stability during cell transformation[9-11]. The CpG islands of several tumor suppressor genes, which are hypomethylated and express in normal cells, became frequently hypermethylated in almost all the cancers investigated, contributing to the loss of function of the tumor suppressor genes in cancer. On the other hand, the reverse processes, such as hypomethylation of CpG islands may also result in transcription activation of the otherwise inert genes[12].

In our previous studies on HCC[13], we have assessed a number of genes in the category of "drug-resistance" genes, including the O-6-methylguanine-DNA methyltransferase (*MGMT*) gene encoding an enzyme responsible for the cell's resistance to the alkylating type of chemotherapeutic drugs, and mutL homolog 1, colon cancer, nonpolyposis type 2 (*hMLH1*), a mismatch repairing gene[14]. The former is frequently methylated while the later maintains the unmethylated status in HCC tissues in comparison with the normal liver tissues. In this study, we extended our profiling efforts in the same group of HCC patients to other 14 "drug-resistance" genes, 13 of which were touched for the first time. This specifically oriented survey to "drug-resistance" should provide valuable insights into our understanding of the underlying mechanisms for the development of intrinsic resistance of HCC to chemotherapeutic drugs, and have important etiological implications to carcinogenesis of HCC.

MATERIALS AND METHODS

Tissue samples and DNA preparation

With the informed consent of all patients and approval of the ethics committee, the samples of tumors were collected from HCC patients (n = 30) during operation. The pathological classification of tumor tissues was carried out, and the stage of each case was graded according to the WHO classification[15]. Total genomic DNA was extracted from frozen tissue specimens (50-100 mg) according to a standard protocol with some modifications[16,17]. Frozen pulverized powders of the specimens were re-suspended with 2 mL lysis buffer containing 50 mmol/L Tris-HCl pH 8.0, 50 mmol/L EDTA, 10 g/L SDS, 10 mmol/L NaCl plus 100 μg/mL boiling-treated RNase A (Sigma, USA). Following 1-h incubation at 37 ℃, proteinase K (Roche, USA) was added to the cellular lysates for a final concentration of 100 μg/mL, and the digestion was carried out at 55 ℃ for 2 h. Organic extractions with a half volume of phenol/chloroform/isoamyl alcohol (1:1:0.04) were repeatedly carried out until no visible interphase remained after centrifugation. DNA was precipitated from the aqueous phase in the presence of 0.3 mol/L NaOAc (pH 7.0) and two and a half volumes of ethanol, washed once in 700 mL/L ethanol, dissolved at 65 ℃ for 30 min with 0.2-0.4 mL TE (10 mmol/L Tris-HCl pH 7.4 and 1 mmol/L EDTA) and stored at 4 ℃ until use. The DNA concentrations were calculated according to the $A_{260\,nm}$ readings.

Bioinformatics search for "drug-resistance" genes

We used "drug resistance" as the key word to search from the NCBI LocusLink database (http://www.ncbi.nlm.nih.gov/LocusLink/list.cgi). The sequence of the coding region (63 targets) plus 5 kb segments at each ends were downloaded, and subjected to search for the existence of the CpG island. The parameters were set as OBS/EXP (the minimum average observed to expected ratio of C plus G to CpG) = 0.6, MINPC (the minimum average percentage of G plus C) = 50, and LENGTH (the minimum length that a CpG island has to be) = 200 bp (http://www.ebi.ac.uk/emboss/cpgplot/). Thirty six genes were found containing the promoter CpG island (Table 1). Among this list 14 genes were selected for the methylation profiling, as they represent in different categories for the functions and properties (Table 2). The primer pairs (Table 3) for methylation specific polymerase chain reaction (MSP) in this report were designed according to the same principle with assistance of the web server for identification of the CpG islands (http://www.ebi.ac.uk/emboss/cpgplot/index.html) and the primer design software (http://micro-gen.ouhsc.edu/cgi-bin/primer3_www.cgi) (Table 3).

Table 1 The "drug-resistance" genes containing the promoter CpG island

Genes	Location relative to transcription start site	Genes	Location relative to transcription start site
ABCC4	-487 to +466	GSTP1	-391 to +91
ABCC1	-356 to +406	hMLH1	-72 to +393
ABCC13	+138 to +386	KIAA1337	-553 to +413
ABCC3	-96 to +358	MAPK14	-371 to +319
ABCB11	+1 255 to +1 565	OCLN	-9 to +967
ABCC5	-219 to +87	POLB	-209 to +34
ABCC6	-229 to +89	RAF1	-466 to +399
ABCC8	-185 to +531	RALBP1	-901 to +325
ABCG2	-741 to -17	RRM2	-718 to +426
ATF2	-418 to +545	SKP2	-663 to +182
B2M	-170 to +83	SLC19A1	-719 to +268
BCAR3	-328 to +126	SLC22A1L	-265 to +158
BCL2	-7 to +573	SPF45	-547 to +92
BIRC4	-527 to -235	SRI	-251 to +257
CAT	+35 to +395	SSA2	-195 to +152
CFTR	-515 to -55	TOP2A	-123 to +506
DCK	-267 to +155	TOP2B	-805 to +393
ERBB2	+173 to +534	TP53	+130 to +337

Bisulfite treatment of DNA and MSP

The methylation status of the promoter CpG islands of the 14 genes in all sample DNAs were analyzed by MSP on the sodium-bisulfite converted DNA[16,17]. The primer pairs for MSP and the genes' genome access on GenBank are detailed in Table 3. In detail, 2 μg DNA in 50 μL TE was incubated with 5.5 μL of 3 mol/L NaOH at 37 ℃ for 10 min, followed by a 16 h treatment at 50 ℃ after adding 30 μL of fresh-prepared 10 mmol/L hydroquinone and 520 μL of freshly prepared 3.6 mol/L sodium-bisulfite at pH 5.0. The DNA was desalted using a home-made dialysis system with 10 g/L agarose. Then, the DNA (approximately 100 μL) was denatured at 37 ℃ for 15 min with 5.5 μL of 3 mol/L NaOH, followed by ethanol precipitation with 33 μL 10 mol/L NH_4OAc and 300 μL ethanol. After washing with 700 mL/L ethanol, the gently dried DNA pellet was dissolved with 30 μL TE at 65 ℃ for 10 min. The DNA sample was finally stored at -20 ℃ until further use. PCR reaction was carried out in a volume of 15 μL with 50 ng or less template DNA with JumpStart Taq polymerase (Sigma, USA). An initial denaturation step at 94 ℃ for 4 min was followed by 35 cycles of reaction at 94 ℃ for 20 s, variable annealing temperature (Table 3) for 20 s and 72 ℃ for 25 s, and a final extension at 72 ℃ for 5 min. The PCR products were separated by 12 g/L ethidium bromide containing agarose gel electrophoresis with 1×Tris Acetate EDTA (TAE) buffer and visualized under UV illumination. To verify the PCR results, representative bands from each target were gel-purified and cloned into T-vector (Buocai, Shanghai, China), followed by automatic DNA sequencing provided by Buocai. Only verified results are presented in this report.

The M. Sss I treated DNA from the normal liver tissue was used in the MSP procedure as the control template. The DNA from the liver tissue of the healthy liver donor[14,16] was batch cleaved with *Eco*RI, followed by M. Sss I treatment overnight according to the manufacturer's instruction (New England Biol., Boston, USA). The purified DNA was bisulphate treated as usual, and subjected to MSP with the primer pairs for 11 genes where no methylated alleles were detected in both cell lines and HCC tissues.

Cell culture and semi-quantitative reverse transcription[18]

The established cell lines, BEL-7402 (human hepatocellular carcinoma cell line, No. TCHu68, Cell Bank in Shanghai),

Table 2 The "drug resistance" genes in this study

Resistance mechanism	Genes and ref.	Function
Plasma membrane transporters / pump decrease or increase to concentration	ABCG2	Belongs to the abc transporter family, appears to play a major role in the multidrug resistance phenotype of MCF-7 breast cancer cell line. When over-expressed, the transfected cells become resistant to mitoxantrone, daunorubicin and doxorubicin, display diminished intracellular accumulation reduce intracellular drug of daunorubicin, and manifest an ATP-dependent increase in the efflux of rhodamine
	CFTR	Belongs to the abc transporter family. MRP subfamily, involved in the transport of chloride ions
	RALBP1	Activates specifically hydrolysis of GTP bound to RAC1 and CDC42. Mediates ATP-dependent transport of S-(2,4-dinitrophenyl)-glutathione (DNP-SG) and doxorubicin(DOX) and is the major ATP-dependent transporter of glutathione conjugates of electrophiles (GS-E) and DOX in erythrocytes. Can catalyze transport of glutathione conjugates and xenobiotics, and may contribute to the multidrug resistance phenomenon
Transcription factor and / or tumor suppressor	ATF2	Belongs to the bZIP family, ATF subfamily, binding the cAMP response element (CRE) (consensus sequence: 5'GTGACGT(A / C)(A / G)-3') as a transcription activator
	TP53	Acts as a tumor suppressor in many tumor types, involved in cell cycle regulation as a transcription activator that acts to negatively regulate cell division by controlling a set of genes required for this process
The enzymes involved in drug activation or inactivation metabolism abnormality	CAT	Belonging to the catalase family ,serves to protect cells from the toxic effects of hydrogen peroxide
	GSTP1	Belongs to the GST superfamily. Pi family; Conjugation of reduced glutathione to a wide number of exogenous and endogenous hydrophobic electrophiles
	TOP2B	Control of topological states of DNA by ATP-dependent breakage, passage and rejoining of double-stranded DNA
	DCK	Required for the phosphorylation of several deoxyribonucleosides and certain nucleoside analogs widely employed as antiviral and chemotherapeutic agents
Cell signaling alteration and cell cycle checkpoints alteration	RAF1	Belongs to the Ser / Thr family of protein kinases. RAF subfamily. Involved in the transduction of mitogenic signals from the cell membrane to the nucleus as a part of the Ras-dependent signaling pathway from receptors to the nucleus
	SKP2	Involved in regulation of G1 / S transition as substrate recognition component of the SCF (SKP1-CUL1-F- box protein) E3 ubiquitin ligase complex which mediates the ubiquitination and subsequent proteasomal degradation of target proteins involved in cell cycle progression, signal transduction and transcription
Unclear mechanisms	B2M	Beta-2-microglobulin is the beta-chain of major histocompatibility complex class I molecules, Containing 1 immunoglobulin-like domain
	OCLN	May play a role in the formation and regulation of the tight junction (TJ) paracellular permeability barrier
	SPF45	Involved in nuclear mRNA splicing, via spliceosome

Note: All the information in this table was obtained from the web site of the OMIM section of the locus link (http://www.ncbi.nlm.nih.gov/LocusLink/) and GeneCards(http://bioinfo.weizmann.ac.il/cards/).

SMMC-7721 (human hepatocellular carcinoma cell line, No. TCHu13, Cell Bank in Shanghai), Hep3B (human hepatocellular carcinoma cell line, ATCC Number: HB-8064), HepG2 (human hepatocellular carcinoma cell line, ATCC Number: HB-8065), HCCLM3 (human hepatocellular carcinoma cell line, Cell Bank in Zhongshan Hospital, Shanghai), and L02 (immortalized normal liver cell line, No GNHu6, Cell Bank in Shanghai) were cultured in DEME medium plus 100 mL/L new born calf serum at 37 ℃ in a 50 mL/L CO_2 atmosphere.

Total RNA from various HCC cell lines was extracted using the TriPure isolation reagent kit (Roche, USA). Reverse transcription was subsequently carried out using the superscript II RNase H-reverse transcriptase kit. β-actin was used as an internal control in separate reaction. The *GSTpi* cDNA primers (sense: 5'-GGAGACCTCACCCTGTACCA-3'; anti-sense: 5'-GGGCAGTGCCTTCACATAGT-3') were the same as in a previously published paper[19]. The primer sequences and reaction conditions are listed in Table 4. RT-PCR products were visualized under UV illumination after electrophoresis in 1.2% agarose, followed by the densitometric quantification.

Statistics

The methylation data were dichotomized as 1 for the co-existence of the methylated and unmethylated alleles; 2, for methylated allele only; and 0 for the unmethylated for both alleles to facilitate statistical analysis using contingency tables. The statistic analyses for the association between the methylation profile of the gene and each of the clinical-pathological parameters were carried out with the statistics package (http://www.R-project.org/). Both Pearson's Chi-square test with Upton's adjustment and Fisher's exact test (http://www.R-project.org/) were used to deal with the sample cells with the low expected values. The relative frequency with a 95% confidence interval (P<0.05) for a binomial distribution was calculated for the tumors and the paired non-cancerous tissues.

RESULTS

Our previous efforts[14,16] provided an HCC specific altered pattern in DNA methylation of 11 among 44 genes by MSP in conjunction with sequencing verification. Among that list, there were several genes that might be classified as the drug resistance related genes, i.e., the *hMLH1* and *MGMT* genes. The former maintained the unmethylated status and the later displayed hypermethylation in liver cancer. Although the impart of the tumor specific changes in methylation pattern of the *MGMT* gene has not been fully evaluated experimentally, it remains desirable to establish the methylation profile of more genes in the category of "drug resistance". Such efforts should provide new insights into the underlying mechanisms as well

Table 3 The primers for MSP analysis

GenBank No.	Gene symbol		Sense 5'-3'	Antisense 5'-3'	Position	Size(bp)
NT_016354	ABCG2	m	TGTCGCGTTGAGTCGTTA	AACGTCCCCGATACTTCG	-698 to -464	235
		U	TGTGTTTTGTTGTGTTGAGTTGT	TCACTCTAATTCATTCCATTCAATC	-591 to -457	135
NT_005403	ATF2	m	GGGTCGGAATAACGAACG	ATCACCTCGAATACTCCTAACG	230 to 375	146
		U	GGAGGGGTTGGAATAATGAAT	CCCATTTCCCATCACCTCAA	220 to 379	160
NT_010194	B2M	m	ATTTGGTATTGCGTCGTTG	ACGAAACGAAACATCTCGAC	-128 to 23	151
		U	TTTTTAATTTGGTATTGTGTTGTTG	AACTCACACTAAATAACCTCCAAAC	-134 to 83	217
NT_009237	CAT	m	AGTAGCGGGTCGCGTAG	AACCACCCGAACCTATCG	118 to 372	255
		U	GGAAGGAGTAGTGGGTTGTGT	AACCACCCAAACCTATCACA	112 to 372	261
NT_007933	CFTR	m	AGAGGTCGCGATTGTCGTT	CGACTTTCTCCACCCACTACG	-316 to -114	203
		U	TTAAAGAGAGGTTGTGATTGTTGTT	TCCTTCACTCCCTCACCA	-322 to -174	149
NT_006216	DCK	m	TATACGCGCGGTTTCGT	CGCCGACGAATATCGAA	-168 to 27	195
		U	TTTTTTGTTATATGTGTGGTTTTGT	TACCCCTCAACCCTCACC	-176 to -75	102
NT_078018	OCLN	m	TGCGTTCGTTAGGTGAGC	CGAATCCCAACTCGAAAACG	538 to 753	216
		U	GTTAGGTGTGTTTGTTAGGTGAGT	CACACCTCTCTAATTCCCACA	532 to 772	241
NT_022517	RAF1	m	TCGGTCGTTTTGGAAGTC	CCCTAAAACGCGAAACG	-72 to 180	252
		U	GGTTTGGTTGTTTTGGAAGTT	CACCAAATATAACCACCTCCCACT	-2 to 183	185
NT_010859	RALBP1	m	GGGTAAGTCGTTCGTTTTCG	CCTCTCCGCTCAAACGACT	-495 to -215	281
		U	GTTAGTATTATATTGGGGTAAGTTGTTTG	CCCTTCATCCCCAAACTCA	-510 to -371	140
NT_006576	SKP2	m	GTCGTAGCGTCGTTCGTT	CTACAACCCGCTCTACTTCG	-198 to 10	208
		U	TTTTTTAGTTAGTTGTAGTGTTGTTTGTT	ACCCACTCTACTTCACAACCAC	-209 to 5	214
NT_077569	SPF45	m	AGTGTCGTTCGGTTTCGTT	CCTCGAAAACTCCGACTACG	-216 to -6	211
		U	GTGGAGTGTTGTTTGGTTTTGT	AACTTACATCTAACACCTCCCAAA	-220 to -67	154
NT_022517	TOP2B	m	TGGGTTTCGTCGTTTCGT	CCGCGCTAAACCCGAAC	-241 to -66	176
		U	GGTTGTTGGGTTTTGTTGTTTT	TTCTCCTCAACCACCACACTAA	-254 to -60	195
NT_010718	TP53	m	CGGAGTCGAGAGTTCGTG	CCGAAAACACTTTACGTTCG	157 to 279	123
		U	GTTGAAAATATATGGAGTTGAGAGTTT	CTTTCCACAACAATAACACACTTC	190 to 291	102
NT_033903	GSTP1	m	GCGATTTCGGGGATTTTA	ACGACGACGAAACTCCAA	-183 to 16	199
		U	GTTGGGGATTTGGGAAAG	TATAAAAATAATCCCACCCCACT	-230 to -28	203

as the capability of predicting HCC patient's intrinsic profile of drug resistance, based upon the changes in DNA methylation pattern of the genes involved.

Bioinformatics search for the "drug-resistance" genes

Sixty three genes were revealed from NCBI LocusLink database from the searching with "drug-resistance" as the key words (http://www.ncbi.nlm.nih.gov/LocusLink/list.cgi). To identify the genes falling into the category of CpG island containing genes, the sequence of the coding region plus 5 kb each upstream and downstream was downloaded and subjected to the analysis with CpG island identification software (http://www.ebi.ac.uk/emboss/cpgplot/). Forty four genes were found containing one or more CpG islands, but only 36 genes really had the promoter embedded in a CpG island (Table 1). Hence, transcription of these 36 genes is likely to be subjected to the control of the DNA methylation status. From these genes, 14 genes representing different functions and mechanisms in "drug-resistance" (Table 2) were selected for methylation profiling; three genes encoding the various membrane transporters: *ABCG2*, *CFTR*, and *RALBP*1, two encoding the transcription factors, *ATF2*, and *TP53*, four encoding the enzymes mediating the drug activation or inactivation: *CAT*, *GSTpi*, *TOP2B* and *DCK*, two encoding the proteins involved in signaling or cell-cycle progression: *RAF1* and *SKP2*, and three with unknown underlying mechanisms: *B2M*, *OCLN* and *SPF45*.

Technological consideration

MSP is the most popular method for methylation profiling of any given targets in human cancers for both its easiness and sensitiveness. Based upon the distinguished difference in sensitivity of the methyl-cytosine from the cytosine to be converted to uridine by bisulphate treatment: the later is amenable, but the former is resistant, the methylation status of the target fragments can be determined by parallel PCR reactions with one pair of the primers in which the CG in the wide-type sequence is maintained for detection of methylated allele, and the other in which the CG is replaced with TG for the unmethylated allele. However, inherent with the PCR-type assays, there are compelling reasons to eliminate both false positive and negative PCR reactions. As 13 genes in this list except for the *GSTpi* gene had not been subjected to MSP previously, we carried out optimization of the PCR reaction with a panel of five established cell lines. For those targets, only the unmethylated allele was detected, MSP with the DNA from the normal liver tissue was carried out, showing that all 14 genes were unmethylated. To ensure that failure to detect the methylated allele was not false negative artifact in PCR reaction, we *in vitro* methylated the DNA from the normal liver with M. Sss I methyl-transferase that was capable of transferring methyl to the fifth carbon atom of the cytosine in the CpG dinucleotides, followed by methylation profiling. As shown in Figure 1, while no methylated allele was detected with the methylation targeted primers with the liver DNA, the M. Sss I treated DNA led to the positive PCR reaction, indicating that the PCR condition used for the tumor samples was capable of detecting the methylated targets, including *ABCG2*, *ATF2*, *B2M*, *DCK*, *RAF1*, *RALBP1*, *SPF45*, *SKP2*, *TP53*, and *TOP2B* genes (panels 1-10, respectively). As the rest four genes were heterozygously methylated in some of liver cancer cell lines, it indicated that the PCR reactions specific to the methylated allele was acceptable (for instance, lane 11 for *OCLN*, Figure 1), the *in vitro* methylation by M. Sss I testing was exempted. To eliminate the false negative results, the representative PCR bands were subjected to T-cloning

and sequencing verification. Only the data, the bands of which had the correct identity in sequence, were regarded informative.

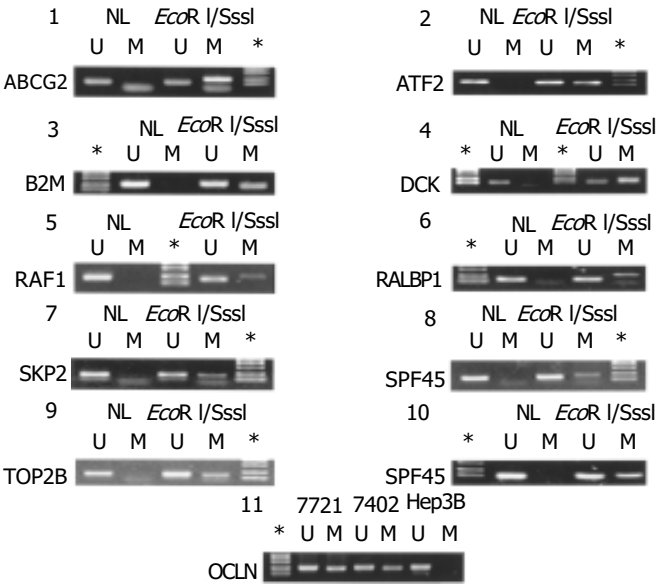

Figure 1 MSP testing with the M. Sss I treated normal liver tissue DNA. The *in vitro* methylated DNA from the normal liver tissue was used for MSP along with the untreated. Panels: 1, *ABCG2*; 2, *ATF2*; 3, *B2M*; 4, *DCK*; 5, *RAF1*; 6, *RALBP1*; 7, *SKP2*; 8, *SPF45*; 9, *TOP2b*; and 10, *TP53*. The PCR conditions for *OCLN* gene were assessed by PCR in three liver cancer cell lines, 7721, 7402, and Hep3B (panel 11). U, unmethylated allele; M, methylated allele, NL, normal liver tissue; *the DNA size marker: DL-2000.

The methylation profiles of 14 genes in HCC

By MSP analysis, 13 genes displayed a uniform unmethylated status in the liver tissues from all four healthy donors, while the *RAF1* gene was heterozygous in one case, but fully unmethylated in the rest three cases. In all 30 cases of HCC, the following 11 genes: *ABCG2, ATF2, B2M, DCK, RAF1, RALBP1, SPF45, SKP2, TOP2B, OCLN* and *TP53* maintained the same unmethylated status in both HCC tissues and the paired non-cancerous tissues (Figure 2), indicating no DNA methylation mediated changes in the control of the expression of these 11 genes in HCC. The remaining three genes displayed in varying degree hypermethylation in HCC tissues (Figure 2 and Table 4). Since hypermethylation of the *CAT* gene rarely occurred (3.3%) (Figure 2), its impacts on the HCC pathology might be rather trivial. Both *GSTpi* and *CFTR* genes were prevalently hypermethylated in HCC and their neighboring non-cancerous tissues (80% and 56.7%, and 77% and 50%, respectively, Table 4), highlighting the possibility that inactivation of transcription of these two genes may indeed occur in HCC, and have certain etiological significance.

It has been well recognized that the so-called non-cancerous cells pathologically defined may have already suffered from certain genetic lesions as the corresponding cancerous tissues. Inclusion of the neighboring non-cancerous tissues in this study made it possible to analyze our results from the stage-specific perspective of carcinogenesis. As shown in Table 5, no significant difference was detected in the occurrence of hypermethylated *GSTpi* and *CFTR* genes between HCC and the paired non-cancerous tissues (P>0.05) (Table 4). If the neighboring non-cancerous tissues have indeed suffered from the early stage genetic and/or epigenetic lesions, the methylation changes of these two genes might occur at the early stage of HCC carcinogenesis.

To correlate the hypermethylated status with the transcription silencing of *GSTpi* gene, we carried out MSP analysis of this gene and semi-quantitative RT-PCR for its expression in five established liver cancer cell lines. As shown in Figure 3, three liver cancer cell lines (i.e. HepG2, Hep3B and L-02) were fully methylated, and did not express *GSTpi*, while SMMC-7721 and HCCLM3 cell lines were heterozygously methylated, and expressed a detectable level of *GSTpi* mRNA. Therefore, the general notion stands correct in this case, that the hypermethylated status of the promoter CpG island is inversely correlated with the long-term transcription silencing state of the gene.

Glutathione-S-transferases (GSTs) are a family of phase II detoxification enzymes that catalyze the conjugation of glutathione to a wide variety of endogenous and exogenous electrophilic compounds, including subclasses of carcinogens and cytotoxic therapeutic drugs[20,21], so that the cells are protected from DNA damages[22]. Furthermore, the *GSTpi* isoform also regulates the mitogen-activated protein (MAP) kinase pathway that participates in cellular survival and death signals via protein: protein interactions with c-Jun N-terminal kinase 1 (JNK1) and apoptosis signal-regulating kinase (ASK1)[23]. Therefore, GSTs serve two distinct roles in the development of drug resistance to both substrate-type and other types of chemotherapeutic drugs via direct detoxification as well as acting as inhibitors of the MAP kinase pathway[24].

The cystic fibrosis trans-membrane conductance regulator (CFTR) belongs to the ABC transporter superfamily, and regulates the chloride permeability mainly in epithelial cells. Its defects may contribute to cystic fibrosis, a common autosomal recessive disorder among the Caucasian population, which affects multiple organs, including lung, pancreas, liver, sweat gland, reproductive system and intestine. *CFTR* gene has high expression level of transcripts in epithelial cells in pancreas and nasal polyps; low in lung, liver, and kidney; and undetectable in brain and fibroblasts[25]. It functions as a cAMP-regulated chloride channel, a conductance regulator by an autocrine mechanism involving ATP and/or chloride efflux, and an inhibitor of epithelial Na+ channels when chlorides are released[26]. The involvement of *CFTR* gene in drug resistance is implicated by observation that the forced over-expression of *CFTR* gene confers the multiple drug resistance to NIH 3T3 cells[27], a similar behavior to the founding member of this family, multiple drug resistance 1 (MDR1), which was identified three decades ago, for its etiological role in the cellular resistance to the multiple chemotherapeutic drugs. The unmethylated status of *CFTR* gene in the normal liver tissues suggested that its expression may be necessary for the physiological activities of hepatocytes. Although whether this gene is expressed in HCC has not been tested, the possibility does remain for the functional loss of this gene in HCC, indicated by the prevalent hypermethylation of its promoter CpG islands.

Therefore, lacking of expression of these two genes, implicated by the hypermethylated state of the promoter CpG islands, may make the cells more susceptible to the carcinogenic insults, a feature associated with the proneness to the malignant state of cells. Hypermethylation of the promoter CpG islands may reflect the long-term silencing state of transcription of both *GSTpi* and *CFTR* genes in HCC, which may offer growth advantages of the malignant cells over their normal counterparts *in vivo*. Indeed, the hypermethylation of both genes was an early phase event, as no statistically significant difference in the hypermethylation frequency between the paired neighboring non-cancerous and HCC tissues was observed (Table 5). Nevertheless, the hypermethylated status of these two genes may not be all bad, as the HCC with the hypermethylated alleles of these two genes (if either or both genes did not express) may be more sensitive to the relevant chemotherapeutic drugs than their unmethylated counterparts. Indeed, in a recent report, a better response to chemotherapy was achieved in breast cancer patients lacking *GSTpi* expression than the expressing counterparts[28].

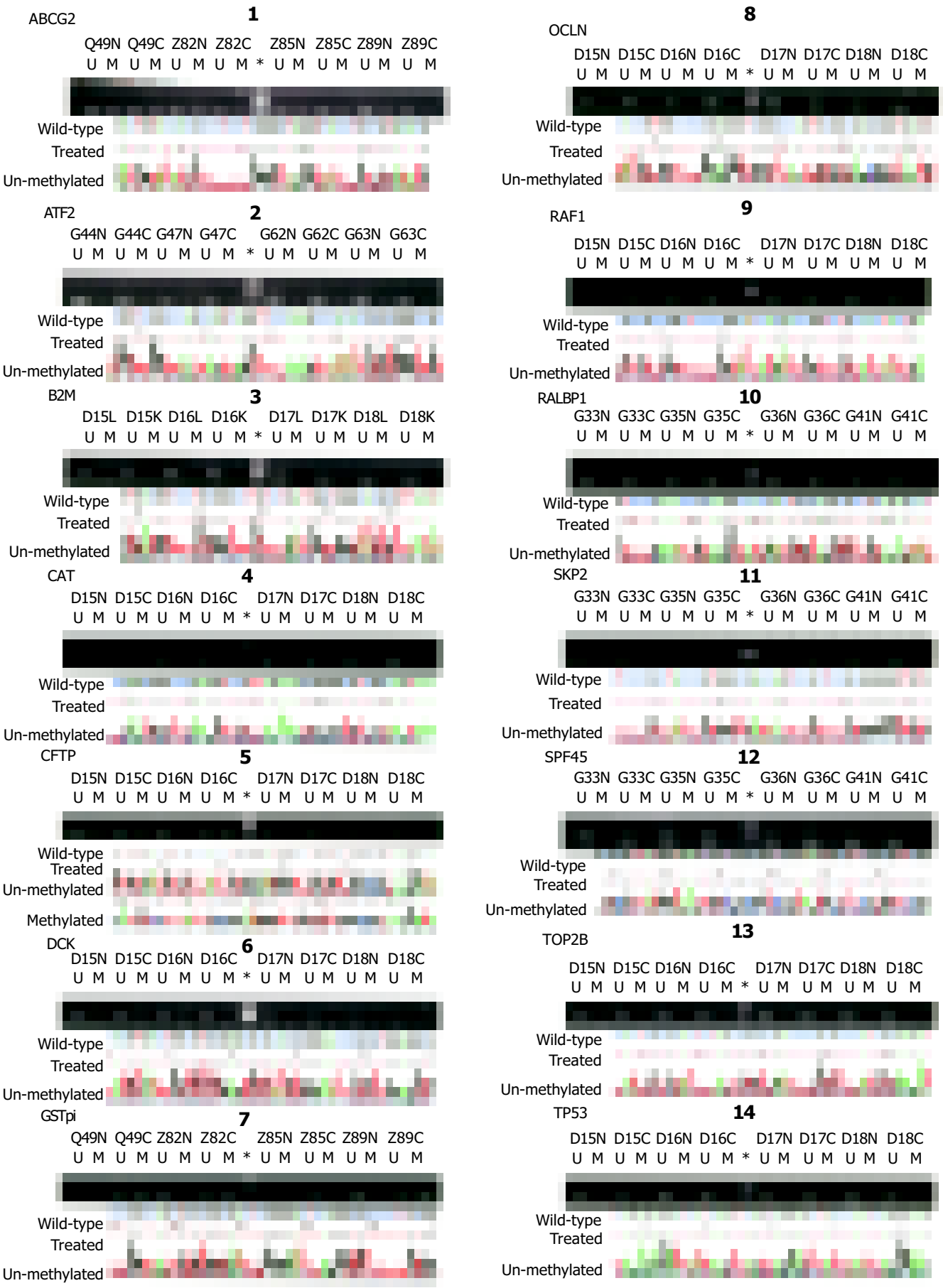

Figure 2 Methylation profiles of the promoter CpG islands of 24 genes in HCC. Both electrophoretic patterns of the representative PCR products of each of 14 targets and the sequencing verification of one representative PCR product were presented. To indicate the methylation status, the sequenced data are aligned with the wild-type sequence. *, size markers, the bands of 250 bp and 100 bp were shown. U, unmethylated; and M, the hypermethylated. Panels: 1, *ABCG2*; 2, *ATF2*; 3, *B2M*; 4, *CAT*; 5, *CFTR*; 6, *DCK*; 7,*GSTpi*; 8, *OCLN*; 9, *RAF1*; 10,*RALBP1*; 11, *SKP2*; 12, *SPF45*; 13, *TOP2B*; and 14, *TP53*.

Table 4 The hypermethylation for each gene in each of HCC patient samples

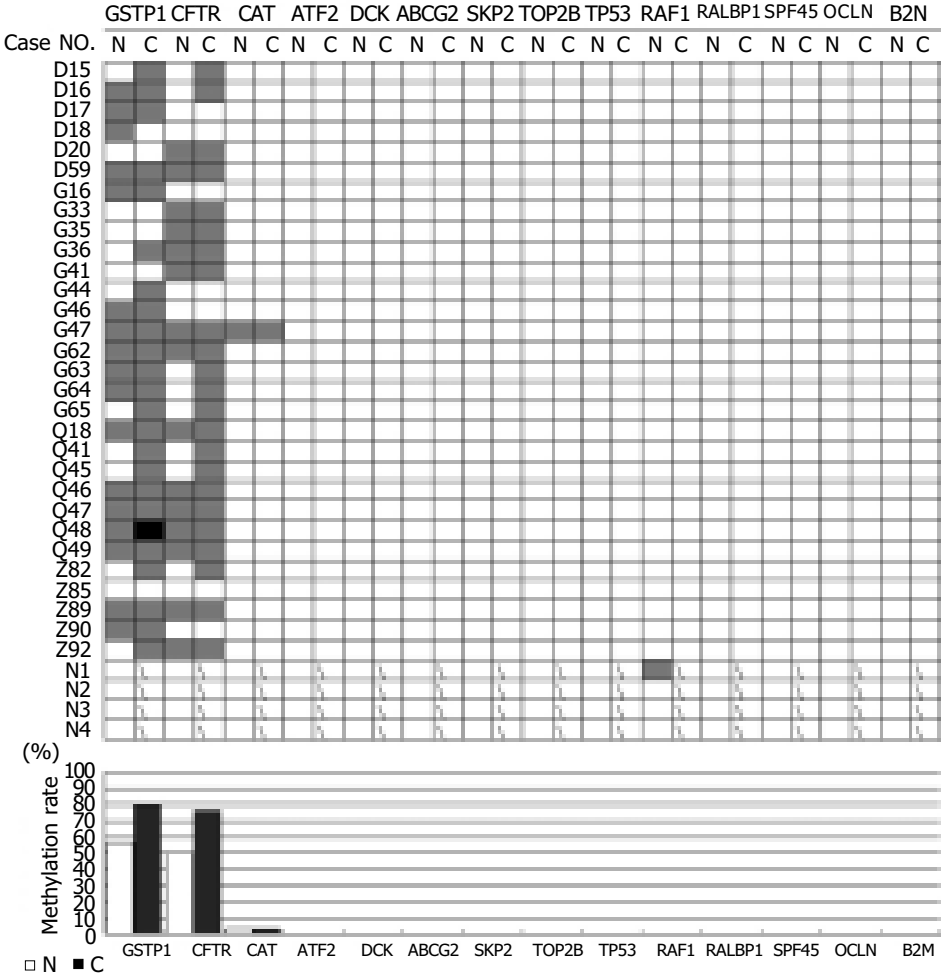

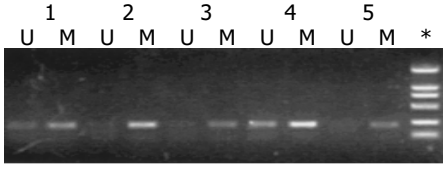

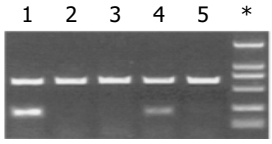

Lanes	1	2	3	4	5
Cell lines	SMMC-7721	Hep3B	HepG2	HCCLM3	L-02
Target gene	103.9	0	0	24.1	0
β-actin	100	98.4	101.6	79.8	98.4
Methy status	u/m	m	m	u/m	m
Ratio	1.04	0.00	0.00	0.30	0.00

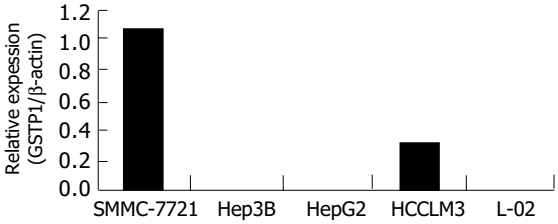

Figure 3 Methylation status of the promoter CpG Island correlated the expression state of the GSTpi gene in liver cancer cell lines. Both methylation status (panel 1) and mRNA level (panel 2) of the GSTpi gene in SMMC-7721 (lane 1), Hep3B (lane 2), HepG2 (Lane 3), HCCLM3 (lane 4) are determined and presented. *, size markers, the bands of 250 bp and 100 bp are shown. U, unmethylated; and M, the hypermethylated. The density of the bands (indicated in panel 3) for the intemal control β-actin and the GSTpi gene were densitometrically recorded, where the density of the β-actin in SMMC-7721 cells was arbitrarily taken as 100%. The band-ratio of the GSTpi over the β-actin genes were calculated and summarized in the table and plot (panel 3).

Table 5 The early stage-specific change in methylation

Gene	C / M	N / M	*P*
GSTpi	24 / 30	17 / 30	0.052
CFTR	23 / 30	16 / 30	0.058

DISCUSSION

Drug resistance of cancers represents a formidable challenge in cancer management, and the underlying mechanisms of its formation remain poorly defined. Both genetic and epigenetic defects can result in changes in expression of the "drug-resistance" genes in tumors. DNA methylation state of the promoter CpG islands has been demonstrated as a useful indicator for the transcriptional silencing state of the relevant genes. In this study, we determined the methylation profile of the genes at the focal point, classified as the drug-resistance type in DNA database in HCC, one of most devastating human cancers in Far East Asia, including China.

To identify suitable targets for such a study, we carried out

the search with key word "drug resistance" from the LocusLink part of the human genome database. Among 63 entries (http://www.ncbi.nlm.nih.gov/LocusLink/list.cgi), 44 (approximately 70%) fall into the category "the CpG island containing genes", of which, 36 genes have their promoter embedded in the CpG island (Tables 2, 3). Hence, the DNA methylation mediated mechanism likely exerts the important control of over expression of this type of genes, the key function of which is somehow linked to the drug-resistance of cancer cells. Finally, 14 genes were selected for the methylation profiling in HCC. Although 11 genes maintained the unmethylated state in all the tissue samples tested, including four cases of the liver tissues from the healthy liver donors, 30 HCC tissues and their neighboring non-cancerous tissues, three genes, *CAT*, *GSTpi* and *CFTR*, exhibited to various degrees the hypermethylation status in HCC. *CAT* was only hypermethylated in one (3.3%) case. Both *GSTpi* and *CFTR* genes were prevalently hypermethylated (Figure 2 and Table 4) in both HCC and the paired non-cancerous tissues. There was no significant difference in occurrence of the hypermethylated status between the HCC and the paired non-cancerous tissues, indicating that the hypermethylation of these two genes is likely to be the early rather than the late phase events behind the same rationale described previously[14]. This observation would strengthen the notion that the DNA methylation mediated transcription silencing of these two genes may promote carcinogenesis of HCC, by failing to protect the cells from both intracellular and extracellular genotoxic insults. On the other hand, this may offer certain advantages from the angle of the chemotherapeutic treatment of HCC. It is probably true that the HCC with hypermethylated *GSTpi* and *CFTR* genes may respond to the relevant chemotherapies better than the unmethylated counterparts. To further evaluate this hypothesis, both retrospective and prospective clinical studies specifically addressing the association between the chemotherapeutic responses of the HCC and the methylation state of the promoter CpG islands of the drug resistance genes, including *GSTpi*, *CFTR* and *MGMT*[14] genes with a larger cohort of HCC patients are underway.

ACKNOWLEDGEMENTS

Thanks are due to Jian-Guo Chen from Qidong Liver Cancer Institute, China, Li-Sheng Zhang from Guangxi Cancer Institute, Guangxi, China, Meng-Chao Wu from Eastern Hepatobiliary Surgery Hospital, Shanghai, China and Su-Shen Zhen, The First Affiliated Hospital, College of Medicine, Zhejiang University, Zhejiang, China for providing the patients' samples.

REFERENCES

1 **Parkin DM,** Pisani P, Ferlay J. Global cancer statistics. *CA Cancer J Clin* 1999; **49**: 33-64
2 **Bosch F.** Global epidemiology of hepatocellular carcinoma. *New York: Churchill Livingstone* 1997: 13-28
3 Aflatoxins. *IARC Monogr Eval Carcinog Risks Hum* 1993; **56**: 245-395
4 **Parkin DM,** Pisani P, Ferlay J. Estimates of the worldwide incidence of eighteen major cancers in 1985. *Int J Cancer* 1993; **54**: 594-606
5 **Kruh GD**. Introduction to resistance to anticancer agents. *Oncogene* 2003; **22**: 7262-7264
6 **Jaenisch R,** Bird A. Epigenetic regulation of gene expression: how the genome integrates intrinsic and environmental signals. *Nat Genet* 2003; **33**(Suppl): 245-254
7 **Jones PA**. Epigenetics in carcinogenesis and cancer prevention. *Ann N Y Acad Sci* 2003; **983**: 213-219
8 **Feninberg A**. Cancer epigenetics takes center stage. *Proc Natl Acad Sci U S A* 2001; **98**: 392-394
9 **Eden A,** Gaudet F, Waghmare A, Jaenisch R. Chromosomal instability and tumors promoted by DNA hypomethylation. *Science* 2003; **300**: 455
10 **Gaudet F,** Hodgson JG, Eden A, Jackson-Grusby L, Dausman J, Gray JW, Leonhardt H, Jaenisch R. Induction of tumors in mice by genomic hypomethylation. *Science* 2003; **300**: 489-492
11 **Chen RZ,** Pettersson U, Beard C, Jackson-Grusby L, Jaenisch R. DNA hypomethylation leads to elevated mutation rates. *Nature* 1998; **395**: 89-93
12 **Cho B,** Lee H, Jeong S, Bang YJ, Lee HJ, Hwang KS, Kim HY, Lee YS, Kang GH, Jeoung DI. Promoter hypomethylation of a novel cancer/testis antigen gene CAGE is correlated with its aberrant expression and is seen in premalignant stage of gastric carcinoma. *Biochem Biophys Res Commun* 2003; **307**: 52-63
13 **Cao L,** Owsianik G, Jaspers M, Janssens A, Cuppens H, Cassiman JJ, Nilius B. Functional analysis of CFTR chloride channel activity in cells with elevated MDR1 expression. *Biochem Biophys Res Commun* 2003; **304**: 248-252
14 **Yu J,** Zhang HY, Ma ZZ, Lu W, Wang YF, Zhu JD. Methylation profiling of twenty four genes and the concordant methylation behaviours of nineteen genes that may contribute to hepatocellular carcinogenesis. *Cell Res* 2003; **13**: 319-333
15 **Burger P,** Scheithauer B, Paulus W, Giannini C, Kleihues P. Astrocytic Tumours. In Pathology and Genetics of Tumours of the Nervous. *Lyon*: *IARC Press* 2000: 9-54
16 **Yu J,** Ni M, Xu J, Zhang H, Gao B, Gu J, Chen J, Zhang L, Wu M, Zhen S, Zhu J. Methylation profiling of twenty promoter-CpG islands of genes which may contribute to hepatocellular carcinogenesis. *BMC Cancer* 2002; **2**: 29
17 **Clark SJ,** Harrison J, Paul CL, Frommer M. High sensitivity mapping of methylated cytosines. *Nucleic Acids Res* 1994; **22**: 2990-2997
18 **Cai L,** Zhu JD. The tumor-selective over-expression of the human Hsp70 gene is attributed to the aberrant controls at both initiation and elongation levels of transcription. *Cell Res* 2003; **13**: 93-109
19 **Bakker J,** Lin X, Nelson WG. Methyl-CpG binding domain protein 2 represses transcription from hypermethylated pi-class glutathione S-transferase gene promoters in hepatocellular carcinoma cells. *J Biol Chem* 2002; **277**: 22573-22580
20 **Henderson CJ,** McLaren AW, Moffat GJ, Bacon EJ, Wolf CR. Pi-class glutathione S-transferase: regulation and function. *Chem Biol Interact* 1998; **111**: 69-82
21 **Zimniak P,** Nanduri B, Pikula S, Bandorowicz-Pikula J, Singhal SS, Srivastava SK, Awasthi S, Awasthi YC. Naturally occurring human glutathione S-transferase GSTP1-1 isoforms with isoleucine and valine in position 104 differ in enzymic properties. *Eur J Biochem* 1994; **224**: 893-899
22 **Ryberg D,** Skaug V, Hewer A, Phillips DH, Harries LW, Wolf CR, Ogreid D, Ulvik A, Vu P, Haugen A. Genotypes of glutathione transferase M1 and P1 and their significance for lung DNA adduct levels and cancer risk. *Carcinogenesis* 1997; **18**: 1285-1289
23 **Townsend DM,** Tew KD. The role of glutathione-S-transferase in anti-cancer drug resistance. *Oncogene* 2003; **22**: 7369-7375
24 **Tew KD**. Glutathione-associated enzymes in anticancer drug resistance. *Cancer Res* 1994; **54**: 4313-4320
25 **Bannykh SI,** Bannykh GI, Fish KN, Moyer BD, Riordan JR, Balch WE. Traffic pattern of cystic fibrosis transmembrane regulator through the early exocytic pathway. *Traffic* 2000; **1**: 852-870
26 **Morales MM,** Capella MA, Lopes AG. Structure and function of the cystic fibrosis transmembrane conductance regulator. *Braz J Med Biol Res* 1999; **32**: 1021-1028
27 **Wei LY,** Stutts MJ, Hoffman MM, Roepe PD. Overexpression of the cystic fibrosis transmembrane conductance regulator in NIH 3T3 cells lowers membrane potential and intracellular pH and confers a multidrug resistance phenotype. *Biophys J* 1995; **69**: 883-895
28 **Su F,** Hu X, Jia W, Gong C, Song E, Hamar P. Glutathion S transferase pi indicates chemotherapy resistance in breast cancer. *J Surg Res* 2003; **113**: 102-108

Edited by Xia HHX **Proofread by** Zhu LH and Xu FM

PO Box 2345, Beijing 100023, China
Fax: +86-10-85381893
E-mail: wjg@wjgnet.com www.wjgnet.com

World J Gastroenterol 2004;10(23):3441-3454
World Journal of Gastroenterology
Copyright © 2004 by The WJG Press ISSN 1007-9327

• COLORECTAL CANCER •

Methylation profile of the promoter CpG islands of 31 genes that may contribute to colorectal carcinogenesis

Xiao-Li Xu, Jian Yu, Hong-Yu Zhang, Meng-Hong Sun, Jun Gu, Xiang Du, Da-Ren Shi, Peng Wang, Zhen-Hua Yang, Jing-De Zhu

Xiao-Li Xu, Meng-Hong Sun, Xiang Du, Da-Ren Shi, Department of Pathology, Cancer Hospital, Fudan University, Shanghai 200032, China
Jian Yu, Hong-Yu Zhang, Jun Gu, Peng Wang, Jing-De Zhu, The State-Key Laboratory for Oncogenes and Related Genes, Cancer Institute of Shanghai Jiaotong University, Shanghai 200032, China
Zhen-Hua Yang, Institute of Respiratory Disease, Zhong Shan Hospital, Fudan University, Shanghai 200032, China
Supported by the National High Technology Research and Development Program of China (863 Program), No. 2002AA2Z3352, the Science Foundation of Shanghai Municipal Government, No. 02DJ14056, and the Special Fund set up by the State-Key Laboratory for Oncogenes and Related Genes, Shanghai Cancer Institute, Shanghai Jiaotong University, This work was also supported by the Science Foundation of Shanghai Municipal Government to Xiang Du, No. 024119010
Co-first-authors: Xiao-Li Xu, Jian Yu, Hong-Yu Zhang
Correspondence to: Jing-De Zhu, The State-Key Laboratory for Oncogenes and Related Genes, Cancer Institute of Shanghai Jiaotong University, LN2200/25, Xietu Road, Shanghai 200032, China. zhujingde@yahoo.com
Telephone: +86-21-64224285 **Fax:** +86-21-64224285
Received: 2004-04-22 **Accepted:** 2004-05-09

Abstract

AIM: To establish the methylation profile of the promoter CpG islands of 31 genes that might play etiological roles in colon carcinogenesis.

METHODS: The methylation specific PCR in conjunction of sequencing verification was used to establish the methylation-profile of the promoter CpG islands of 31 genes in colorectal cancer (n = 65), the neighboring non-cancerous tissues (n = 5), colorectal adenoma (n = 8), and normal mucosa (n = 1). Immunohistochemically, expression of 10 genes was assessed on the home-made tissue microarrays of tissues from 58 patients. The correlation of tumor specific changes with each of clinical-pathologic features was scrutinized with relevant statistic tools.

RESULTS: In comparison with the normal mucosa of the non-cancer patients, the following 14 genes displayed no tumor associated changes: breast cancer 1, early onset (*BRCA1*), cadherin 1, type 1, E-cadherin (epithelial) (*CDH1*), death-associated protein kinase 1 (*DAPK1*), DNA (cytosine-5-)-methyltransferase 1 (*DNMT1*), melanoma antigen, family A, 1 (directs expression of antigen MZ2-E) (*MAGEA1*), tumor suppressor candidate 3 (*N33*), cyclin-dependent kinase inhibitor 1A (p21, Cip1) ($p21^{WAF1}$), cyclin-dependent kinase inhibitor 1B (p27, Kip1) ($p27^{KIP1}$), phosphatase and tensin homolog (mutated in multiple advanced cancers 1) (*PTEN*), retinoic acid receptor, beta (*RAR-* , Ras association (RalGDS/AF-6) domain family 1 C (*RASSF1C*), secreted frizzled-related protein 1 (*SFRP1*), tissue inhibitor of metalloproteinase 3 (Sorsby fundus dystrophy, pseudoinflammatory) (*TIMP3*), and von Hippel-Lindau syndrome (*VHL*). The rest 17 targets exhibited to various extents the tumor associated changes. As changes in methylation of the following genes occurred marginally, their impact on the formation of colorectal cancer were trivial: adenomatous polyposis coli (*APC*) (8%, 5/65), Ras association (RalGDS/AF-6) domain family 1A (*RASSF1A*) (3%, 2/65) and cyclin-dependent kinase inhibitor 2A, alternated reading frame ($p14^{ARF}$) (6%, 4/65). The following genes exhibited moderate changes in methylation: O-6-methylguanine-DNA methyltransferase (*MGMT*) (20%, 13/65), mutL homolog 1, colon cancer, nonpolyposis type 2 (E. coli) (*hMLH1*) (18%, 12/65), cyclin-dependent kinase inhibitor 2A (melanoma, p16, inhibits CDK4) ($p16^{INK4a}$) (10%, 10/65), methylated in tumor 1 (*MINT1*) (15%, 10/65), methylated in tumor 31 (*MINT31*) (11%, 7/65). The rest changed greatly in the methylation pattern in colorectal cancer (CRC): cyclin A1 (*cyclin a*1) (100%, 65/65), caudal type homeobox transcription factor 1 (*CDX1*) (100%, 65/65), *RAR-* (85%, 55/65), myogenic factor 3 (*MYOD1*) (69%, 45/65), cyclin-dependent kinase inhibitor 2B (p15, inhibits CDK4) ($p15^{INK4b}$) (68%, 44/65), prostaglandin-endoperoxide synthase 2 (prostaglandin G/H synthase and cyclooxygenase) (*COX2*) (72%, 47/65), cadherin 13, H-cadherin (heart) (*CDH13*) (65%, 42/65), CAAX box 1 (*CXX1*) (58%, 38/65), tumor protein p73 (*p73*) (63%, 41/65) and Wilms tumor 1 (*WT1*) (58%, 38/65). However, no significant correlation of changes in methylation with any given clinical-pathological features was detected. Furthermore, the frequent changes in methylation appeared to be an early phase event of colon carcinogenesis. The *in situ* expression of 10 genes was assessed by the immunohistochemical approach at the protein level: *CDH1*, *CDH13*, *COX2*, *cyclin A1*, *hMLH1*, *MGMT*, $p14^{ARF}$, *p73*, *RAR-* , *and TIMP3* genes in the context of the methylation status in colorectal cancer. No clear correlation between the hypermethylation of the promoter CpG islands and the negative expression of the genes was established.

CONCLUSION: The methylation profile of 31 genes was established in patients with colon cancer and colorectal adenomas, which provides new insights into the DNA methylation mediated mechanisms underlying the carcinogenesis of colorectal cancer and may be of prognostic values for colorectal cancer.

Xu XL, Yu J, Zhang HY, Sun MH, Gu J, Du X, Shi DR, Wang P, Yang ZH, Zhu JD. Methylation profile of the promoter CpG islands of 31 genes that may contribute to colorectal carcinogenesis. *World J Gastroenterol* 2004; 10(23): 3441-3454
http://www.wjgnet.com/1007-9327/10/3441.asp

INTRODUCTION

Colorectal carcinoma (CRC) is the third most common malignancy in the developed countries, with an annual incidence approximately 35-50/100 000[1,2]. The risk factors of CRC include Western diet (low fiber, high fat diet), family history, smoking, obesity and inflammatory colorectal diseases. As a whole, China falls into the low incidence country in the world, with the relative incidence of CRC rates being the 4th-6th of the total malignances and the 2nd-3rd of those in the digestive system in China. However, CRC

occurrence exhibits an increasing trend, with an average 4.2% increase per year in the last two decades[3]. CRC is the 3rd common malignancy in Shanghai and occurs more frequently in China (http://www.caca.org.cn/zlyy/shanghai/index.asp). Clinically and pathologically, CRC has been grouped as the sporadic (approximately 80% cases) and hereditary types of diseases (roughly 20% in the total).

Both activation of proto-oncogenes (e.g. the *CDH13 gene*) and inactivation of tumor suppressor genes (e.g. the *APC*, *p53* and genes responsible for the mismatch repaired activity in cells) attributed to genetic defects have been proved instrumental to carcinogenesis of colorectal cancer. The well-known adenoma-carcinoma sequence of the genetic defects by Volgestein has gained both experimental supports and general recognition. However, the predicted accumulation of genetic events has not been substantiated in sporadic colorectal adenocarcinomas, and the expected increase in the number of genetic events in aging tissues has not materialized[4]. Both observations are indeed at odds with the exponential increase in the incidence of colorectal cancer with age. Therefore, alternative mechanisms must be accounted for such a shortfall, which is associated with DNA methylation mediated control of the expression of critical genes overseeing cell growth, apoptosis, as well as cell cycle progression.

Addition of the methyl group at the fifth carbon of cytosine of CpGs is the only covalent DNA modification in vertebrate[5]. Such epigenetic signatures in parental cells are passed to the daughter cells at high fidelity, by a similar semi-conserved mechanism during duplication of the genetic information. The hypermethylated status of CpGs can affect the DNA-protein interaction by eliminating the otherwise occurring DNA-protein interactions involved with the methylation-sensitive transcription factors, while unfolding a cascade of reactions toward the condensed chromatin that is initiated with binding to the methylated CpG by members of the methylated CpG binding protein family[6]. Cancer specific changes in methylation occur widely in all the cancers tested[7]. The global demethylation of DNA has been linked to the increased genome instability as the otherwise transcription-/ transposition-silenced repetitive sequences in normal cells are reactivated by DNA demethylation[8,9]. Paradoxically, local hypermethylation (at the promoter CpG island) has been well established for inactivation of tumor suppressor genes and caught great attention. However, the local demethylation in human tumors has also been recently reported to be associated with transcription reactivation of the silenced genes in normal tissues, such as the *MAGEA1* gene in hepatocellular carcinoma[10]. In view of the fact that the majority of the promoter CpG island containing genes (50% of the protein-coding genes fall into this category) have not been properly looked in the context of the tumor biology, methylation profiling remains valuable for new insights into the etiological mechanism.

CRC is one of the first few types of cancers for methylation profiling[11,12]. Learnt from the rather extensive survey with more than 30 targets, a so called "CpG island methylation (CIM)" phenomenon has been reported, i.e., a clustering occurrence of multiple hypermethylated targets including upto a dozen of tumor suppressor genes[11]. In this study, we recruited 65 CRC tissues, eight colorectal adenomatous tissues, five neighboring non-cancerous tissues and one normal mucosa tissue from Shanghai Cancer Hospital for a middle scale methylation profiling with the promoter CpG islands of 31 genes, aiming, to establish the methylation profile of CRC patients in China, and to assess the association between the methylation status and expression profile of the genes *in situ*. Our results presented in this report should provide some new insights into the role of the epigenetic mechanism in CRC carcinogenesis.

MATERIALS AND METHODS

Clinical-pathological profiles of CRC patients

With the informed consent of all patients and approval of the ethics committee, tumor tissues were obtained during surgery from 65 CRC patients at the Cancer Hospital of Fudan University in 1996-2003. They were 39 patients with sporadic colorectal cancer (SCRC), 10 with hereditary non-polyposis colorectal cancer (HNPCC) fulfilling Amsterdam criteria of IGC and Japanese criteria, and 16 in the category of Bethesda CRC. In addition, tissues were taken from the neighboring non-cancerous mucosa (at least 5-10 cm away from the tumorous lesions) of five patients. A cecum sample was obtained from a 68-year old female patient with inflammatory pseudotumor. In addition, Bethesda CRC concomitant adenomatous samples from six patients and sporadic colon adenomatous samples (one was cancer concomitant) from two patients were taken.

All samples were freshly obtained and cut into two parts. One was buried into an optimal cutting temperature compound (OCT, Miles Inc, USA), and put into fluid nitrogen for storage. The rest was fixed in formalin, embedded in paraffin and then cut into 4-5 μm sections for routine pathological diagnosis.

Clinical-pathological features including the age and gender of patients, the tumor site histological type, Duke's stages, differentiation grades (only moderate and poor differentiation), lymph node metastasis status, and more than 3 years follow-up results (36 cases) are shown in Table 1. The clinical-pathologic data of the eight adenomas are shown in Table 2.

Table 1 Clinical-pathologic profiles of the CRC cases in this study

Clinical-pathologic features		Number of cases
Gender	Male	37
	Female	28
Age (yr)	Median	60
	Range	28-85
Tumor site	Left colon and rectum	43
	Right colon	22
Histological types	Adenocarcinoma	51
	Mucinousi carcinoma	5
	Other types combined[1]	9
Differentiation	Moderate	51
	Poor	14
Follow-up (3 yr)	Survival	27
	Deceased	9
Duke's stage	A	6
	B	15
	C	30
	D	14

[1]Other types combined included the mixed squamous cell carcinoma, carcinoid carcinoma, *etc.*

Table 2 Clinical-pathologic profiles of adenomas and neighboring tumor-free mucosae

Clinical-pathologic features		Adenoma	Mucosa
Gender	Male	4	2
	Female	4	4
Age (yr)	Median	60	68
	Range	34-83	47-76
Tumor site	Left colon	6	4
	Right colon	2	2
Histological type	Tubular	3	
	Tubulovillous	5	
Dysplasia	Light-moderate	8	

Table 3 Target CpG islands and the primers for MSP

Gene	GenBank No.	Primer		Location to transcription start	Size (bp)
		Sense (5'-3')	Anti-sense (5'-3')		
APC	U02509	(U) GTGTTTTATTGTGGAGTGTGGGTT	CCAATCAACAAACTCCCAACAA	-17 147 to -17 050	108
		(M) TATTGCGGAGTGCGGGTC	TCGACGAACTCCCGACGA	-17 153 to -17 046	97
BRCA1	L78833	(U) GGTTAATTTAGAGTTTTGAGAGATG	TCAACAAACTCACACCACACAATCA	-320 to -138	182
		(M) GGTTAATTTAGAGTTTCGAGAGACG	TCAACGAACTCACGCCGCGCAATCG	-320 to -138	182
CDH1	NM_004938	(U) GGTGGGTGGGTTGTTAGTTTTGT	AACTCACAAATCTTTACAATTCCAAC	-266 to -93	172
		(M) GTGGGCGGGTCGTTAGTTTC	CTCACAAATACTTTACAATTCCGACG	-265 to -93	172
CDH13	AB001090	(U) TTGTGGGGTTTGTTTTTTGT	AACTTTTCATTCATACACACA	-267 to -24	243
		(M) TCGCGGGGTTCGTTTTTCGC	GACGTTTTCATTCATACACGCG	-267 to -24	243
CDX1	NT_029289	(U) TGATTGGGTTGTTGTTTATGG	TACCACCACCACCTCCAA	+290 to +522	233
		(M) CGATTGGGTCGTCGTTTA	CCGCATCCACTCGTAAAA	+290 to +491	202
COX2	NT_004487	(U) TTGTTTGTTGTTGTGATGTTTG	TCCAAACTCTTTCCCAAATC	-119 to -324	206
		(M) GTTCGTCGTTGCGATGTT	CCAAACTCTTTCCCAAATCA	-121 to -323	203
CXX1	NT_011786	(U) TTAGGTTGGTTTTTGTGGATATG	CACCCAACCATCCATCAC	-24 to +92	117
		(M) AGGTCGGTTTTCGTGGAT	GATCGATATCGCCGTCAA	-22 to +192	215
Cyclina1	AF124143	(U) GGGTAGTTTTGTTGTGTTTTAGTTG	AACCACTAACAACCCCCTCT	-762 to -565	199
		(M) TCGTCGCGTTTTAGTCGT	ACCCGTTCTCCCAACAAC	-755 to -550	206
DAPK1	NM_004938	(U) GGATAGTTGGATTGAGTTAATGTC	CAAATCCCTCCCAAACACCAA	-332 to -229	103
		(M) GGATAGTCGGATCGAGTTAACGTC	CCCTCCCAAACGCCGA	-332 to -234	98
DNMT1	NT_011176	(U) GGGTGGTAGATGTTGTTTTTGT	CACCCTACCTATCCCCCTAA	-359 to -130	230
		(M) CGTCGTTTTCGTTTATCGTT	ATACCTACCGCCTACGAACA	-320 to -140	181
hMLH1	AB017806	(U) TTTTGATGTAGATGTTTTATTAGGGTTGT	ACCACCTCATCATAACTACCCACA	-526 to -654	118
		(M) ACGTAGACGTTTTATTAGGGTCGC	CCTCATCGTAACTACCCGCG	-531 to -655	124
MAGEA1	U82670	(U) GTTTGGTTGAAGGAATTTGA	ACCCACAACCCTCCCTCTTA	+24 to +347	324
		(M) GTTCGGTCGAAGGAATTTGA	CCACAACCCTCCCTCTTAAA	+24 to +345	322
MGMT	AL355531	(U) TTTGTGTTTTGATGTTTGTAGGTTTTTGT	AACTCCACACTCTTCCAAAAACAAAACA	-451 to -266	209
		(M) TTTCGACGTTCGTAGGTTTTCGC	GCACTCTTCCGAAAACGAAACG	-469 to –261	186
MINT1	AF135501	(U) TATTTTTGAAGTGTTTGTTTGGTGT	TCCCTCTCCCCTCTAAACTTC		202
		(M) TTCGAAGCGTTTGTTTGG	CGCCTAACCTAACGCACA	*	160
MINT31	AF135531	(U) GGGTGGGAATTGAGATGATT	CATCACCACCCCTCACTTTA		131
		(M) GCGGGAATTGAGACGATT	ACGCTTACGCCACTACGA	*	176
MYOD1	NT_009307	(U) ATTTGATGGTTTTTGATGGTTT	CACACACATACTCATCCTCACA	+206 to +418	213
		(M) GACGGTTTTCGACGGTTT	GCCCGAAACCGAATACAC	+210 to +393	184
N33	NT_030737	(U) TTTGGTGAATTGGATGTTTTG	CACCCAACTCCTACCACACAC	+20 to +169	150
		(M) TTTTCGGTGAATCGGATG	TACGCGCCCAACTCCTA	+18 to +173	156
p14^{ARF}	L41934	(U) TGAGTTTGGTTTTGGAGGTGG	AACCACAACAACAAACACCCCT	+97 to +262	165
		(M) GTCGAGTTCGGTTTTGGAGG	AAAACCACAACGACGAACG	+95 to +255	160
p15^{INK4b}	NM_004936	(U) TGTGATGTGTTTGTATTTTGTGGTT	CCATACAATAACCAAACAACCAA	-318 to -164	154
		(M) GCGTTCGTATTTTGCGGTT	CGTACAATAACCGAACGACCGA	-312 to -165	147
p16^{INK4a}	NM_000077	(U) TTATTAGAGGGTGGGGTGGATTGT	CAACCCCAAACCACAACCATAA	-80 to +71	151
		(M) TTATTAGAGGGTGGGGCGGATCGC	ACCCCGAACCGCGACCGTAA	-80 to +69	149
p21^{WAF1}	NT_007592	(U) TTTTTGTAGTATGTGAGGTTTTGG	AACACAACTCAACACAACCCTA	-200 to -1	200
		(M) TGTAGTACGCGAGGTTTCG	TCAACTAACGCAACTCAACG	-196 to +5	202
p27^{KIP1}	AB003688	(U) TGTGATTTTGATGTTGGTAAGGT	CAAACCACAACCCAAACTCT	-363 to -141	223
		(M) CGACGTCGGTAAGGTTTG	AAACGCGCAAAAACTACG	-355 to -163	193
p73	AB031234	(U) TGGGTGTTTGGTTTGTAGGT	CCAACTCTCAACTCCCAAAA	-1 725 to -1 505	221
		(M) GCGTTCGGTTCGTAGGTT	CTCAACTCCCAAAACCCAA	-1 722 to -1 511	212
PTEN	NM_000314	(U) TGGTTTTTTGAGGTGTTTG	TTCCATCATAACTACAACTTCCA	-979 to -812	167
		(M) GGTTTTTCGAGGCGTTCG	CGCCTCACAACGACTCAACT	-978 to -786	192
RAR-β	NM_016152	(U) TTGAGAATGTGAGTGATTTGA	AACCAATCCAACCAAAACAA	-343 to -197	146
		(M) TCGAGAACGCGAGCGATTCG	GACCAATCCAACCGAAACGA	-343 to -197	146
RASSF1A	NT_022517	(U) TTTGGTTGGAGTGTGTTAATGTG	CAAACCCCACAAACTAAAAACAA	+70 to +178	108
		(M) GTGTTAACGCGTTGCGTATC	AACCCCGCGAACTAAAAACGA	+82 to +176	94
RASSF1C	NT_022517	(U) GGAGTTTGGATTGTTGGTTTTG	CACCCCCAAAAATAACCTCAT	-370 to -137	187
		(M) AGTTTGGATTGTCGGTTTCG	TCACAAACCCCACCTACCAC	-370 to -137	187
SFRP1	NT_008251	(U) GTTTTGTGGTTGTAAGTTGTTGTT	AAACCCCACACACTCCAA	-180 to +19	199
		(M) TCGCGGTCGTAAGTTGTT	CGCACTCCAACCCTACAA	-177 to +11	188
TIMP3	NM_000362	(U) TTTTGTTTTGTTATTTTTTGTTTTTGGTTTT	CCCCCAAAAACCCCACCTCA	-454 to -335	119
		(M) CGTTTCGTTATTTTTTGTTTTCGGTTTC	CCGAAAACCCCGCCTCG	-451 to -335	116
VHL	AF010238	(U) GTTGGAGGATTTTTTTGTGTATGT	CCCAAACCAAACACCACAAA	-185 to -20	165
		(M) TGGAGGATTTTTTTGCGTACGC	GAACCGAACGCCGCGAA	-183 to -25	158
WT1	X74840	(U) TGGGATTTGGGTGGTATTTG	CACCAACACCCACTACACCA	+295 to +510	216
		(M) GTTAGGCGTCGTCGAGGTTA	AAAACGCAAAATCCAACACC	+321 to +526	206

DNA preparation and methylation specific PCR analysis

Genomic DNA was extracted from frozen tissues by the protein precipitation method[13]. Frozen tissue block was cut into 10-20 μm sections, put into a 1.5 mL Eppendorf tube, and then incubated at 37 ℃ in the cellular lysis buffer with proteinase K (SABC, Shanghai) for a final concentration of 100 μg/mL. The digestion was carried out at 55 ℃ for at least 2 h. After centrifuged, the upper liquid was collected and the protein precipitation mix was added. After centrifuged, 1:1 isopropanol was added. The deposition was washed with 750 mL/L ethanol, and naturally dried. The DNA pellet was washed once with 700 mL/L ethanol and dissolved with TE (10 mmmol/L Tris HCl, pH 7.4 and 1 mmol/L EDTA), and stored at a concentration of 1 mg/mL at 4 ℃.

The primers for methylation specific PCR (MSP) (Table 3) were adopted as the previously published works[10,14] or designed with the assistance of the web server for the CpG islands identification (http://www.ebi.ac.uk/emboss/cpgplot/index.html) and the primer design software (http://micro-gen.ouhsc.edu/cgi-bin/primer3_www.cgi). DNA treatment and PCR reaction were carried out by the previously described method[10,14,15]. In detail, 10 μg DNA in 50 μL TE was incubated with 5.5 μL of 3 mol/L NaOH at 37 ℃ for 10 min, followed by a 16 h treatment at 50 ℃ after 30 μL of freshly prepared 10 mmol/L hydroquinone and 520 μL of freshly prepared 3.6 mol/L sodium-bisulfite at pH 5.0 were added. The DNA was desalted using a home dialysis system with 10 g/L agarose. The DNA in the desalted sample (approximately 100 μL in volume) was denatured at 37 ℃ for 15 min with 5.5 μL of 3 mol/L NaOH followed by ethanol precipitation with 33 μL 10 mol-L NH4OAc and 300 μL ethanol. After washed with 700 mL/L ethanol, the gently dried DNA pellet was dissolved with 30 μL TE at 65 ℃ for 10 min. DNA samples were finally stored at -20 ℃ until further use. The sample of 50 ng of DNA was reserved for PCR reaction. PCR reaction was carried out in a volume of 15 μL with 50 ng or less template DNA with FastStart Taq polymerase (Roche, Germany) as follows. After an initial denaturing step for 3 min at 94 ℃, 35 cycles at 94 ℃ for 30 s, at varying temperatures with primer pairs for 30 s and at 72 ℃ for 30 s, were carried out. The PCR products were separated by 12 g/L ethidium bromide containing agarose gel electrophoresis with 1×TAE and visualized under UV illumination. To verify the PCR results, representative bands from each target were gel-purified. Then the PCR products were sequenced directly or cloned into T-vector (Promega, USA) followed by automatic DNA sequencing provided by Bioasia (Shanghai, China). Only verified results were presented in this report.

Immunohistochemistry analysis on a home made tissue microarray

The paraffin embedded tissues from 58 cancer cases were made into the tissue microarray paraffin blocks, followed by sectioning. For each sample, the H&E stained sections were first reviewed and marked for the picked point. At least 4 points of cancer tissue and 1 point of normal mucosa tissue were taken from the different positions on the paraffin block. The diameter of our tissue microarray punch was 1 mm. We put about 40-80 tissue dots in one array. To identify the tissue put into the array, all the made tissue microarray sections were stained with H&E and reviewed by two pathologists independently.

The immunostaining was performed with each of 10 commercially available antibodies (Table 4) using DAKO Envision system/3,3-diaminoben-aidine (DAB) staining. The result was scored by conjunction with both staining intensity and the percentage of positive staining cells. Each sample was given an intensity score (0-3) and a percentage of cell positive score (0 = less than 5%, 1 = 5-25%, 2 = 25-50%, 3 = 50-75%, 4 = more than 75%). An overall immunohistochemistry score was calculated by multiplying the intensity and percentage of cell positive scores. Scores of 1-4 were recorded as +, 6-8 as ++, and 9-12 as +++.

Table 4 Antibodies for immunohistochemical analysis

Antibody name	Expression location	Company	Catalogue No.
CDH1	Membrane/Cytoplasm	Antibody Diagnostica INC.	M-0536
CDH13	Cytoplasm	Santa Cruz	sc-7940
COX2	Cytoplasm	Santa Cruz	sc-1746
Cyclin a1	Nuclear	Novocastra Lab.	NCL-CYCLINA
hMLH1	Nuclear	PharMingen	G168-15
MGMT	Cytoplasm	DAKO	M3610
$p14^{ARF}$	Nulear/Cytoplasm	Santa Cruz	sc-8340
p73	Cytoplasm	Santa Cruz	sc-17823
RAR	Nuclear/ Cytoplasm	Santa Cruz	sc-552
TIMP3	Cytoplasm	Oncogene	IM43T

Statistical analysis

A comparison of the proportion was performed using Pearson ^{2} test or the Fisher's exact method. Analysis of methylation status *vs* protein expression was performed using the contingency coefficient.

RESULTS

Among the 65 CRC patients, there were 39 SCRCs, 10 HNPCCs and 16 colorectal carcinoma in Bethesda category. In addition, eight colorectal adenomas, five non-cancerous mucosa tissues and one normal mucosa sample were also recruited for this study.

Twenty four genes among the 31 targets studied in this study were previously analyzed in liver cancer[10] and astrocytoma (unpublished data) in this and other laboratories. They were *APC*, *BRCA1*, *CDH1*, *CDH13*, *DAPK1*, *hMLH1*, $p14^{ARF}$, $p15^{INK4b}$, $p16^{INK4a}$, $p27^{KIP1}$, *p73*, *PTEN*, *RAR-b*, *RASSF1A*, *RASSF1C*, *VHL* and *WT1*. The *CDX1*, *COX2*, *CXX1*, *MINT1*, *MINT31* and *TIMP3* genes have also been studied in colon cancer, the methylation pattern of which was found altered in CRC[16] so that the relevant inter-study comparison of the methylation behaviors should be possible. In this list, there were genes with the proven roles in as well as those lacking any obvious association with the carcinogenesis of human tumors. For the later group, hypermethylation of the myogenetic lineage-specific transcription factor: MYOD1, occurs more frequently in aging tissues than its younger counterparts[17]. In the category of cancer associated genes, the tumor suppressor genes made up the major part. There were proteins operating in the RB1/$p16^{INK4a}$ pathway: $p14^{ARF}$, $p15^{INK4b}$ and $p16^{INK4a}$, as well as the three cyclin-dependent kinase inhibitors: $p21^{WAF1}$, $p27^{KIP1}$[18] and $p57^{KIP2}$[19]. The rest in this subset were the p53 analogue, p73[18,20], the two alternative forms of a tumor suppressors in the Ras mediated signal transduction pathway: RASSF1A and RASSF1C[21], VHL[22], APC[23], PTEN[6], N33 as well as the Wilms tumor 1 gene, WT1[24]. Also included were the genes encoding the cell membrane proteins or nuclear receptors acting actively in intercellular interactions: *e.g.* melanoma specific antigen A1 (MAGEA1)[25], and cadherins, CDH1[26]and CDH13[26]. One gene implicated in signal transduction was *cyclin A1*[27]. The gene encoding O-6-methylguanine-DNA methyltransferase, *MGMT*[28] was also included, which plays a key role in the cellular responses to alkalyting agents and heavy metal stresses. The genes acting in DNA repair process were *hMLH1*[29] and *BRCA1*[30] as well as the gene acting in apoptosis, *DAPK1*[31].

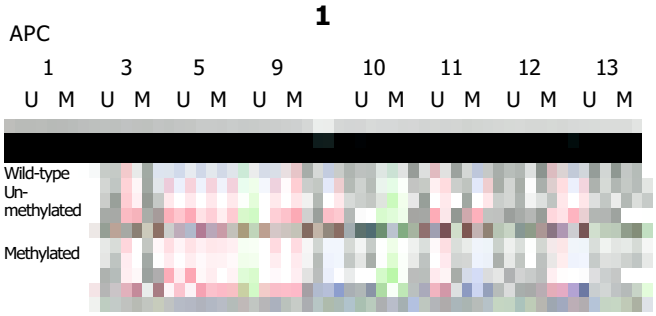
1
APC
1 3 5 9 10 11 12 13
U M U M U M U M U M U M U M U M
Wild-type
Un-methylated
Methylated

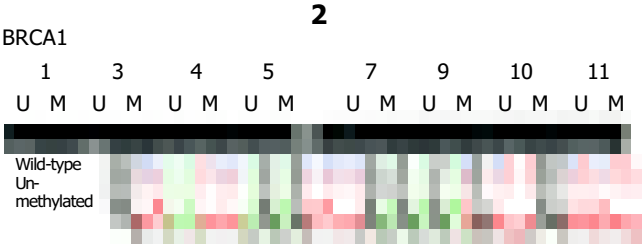
2
BRCA1
1 3 4 5 7 9 10 11
U M U M U M U M U M U M U M U M
Wild-type
Un-methylated

3
CDH1
1 3 4 5 7 9 10 11
U M U M U M U M U M U M U M U M
Wild-type
Un-methylated

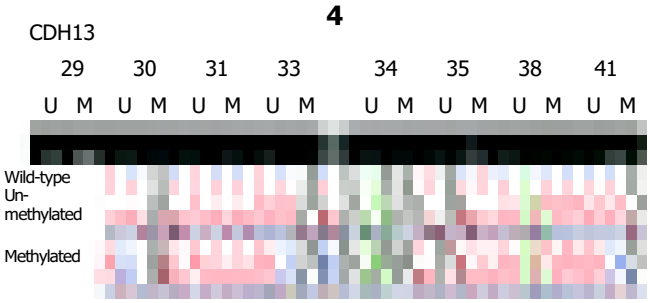
4
CDH13
29 30 31 33 34 35 38 41
U M U M U M U M U M U M U M U M
Wild-type
Un-methylated
Methylated

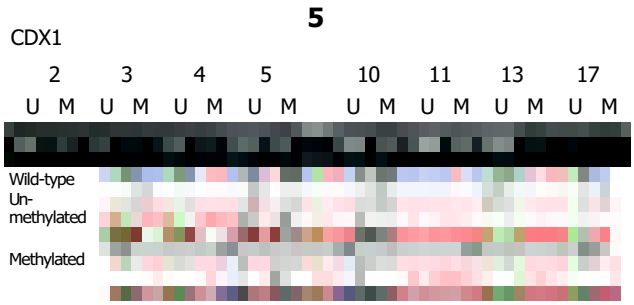
5
CDX1
2 3 4 5 10 11 13 17
U M U M U M U M U M U M U M U M
Wild-type
Un-methylated
Methylated

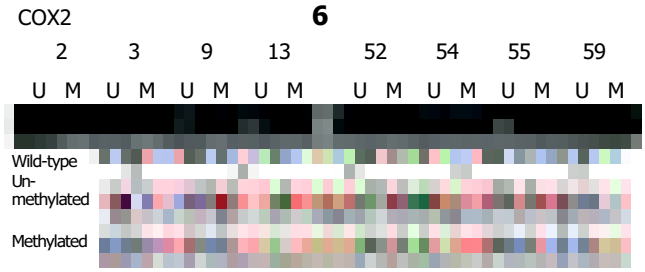
6
COX2
2 3 9 13 52 54 55 59
U M U M U M U M U M U M U M U M
Wild-type
Un-methylated
Methylated

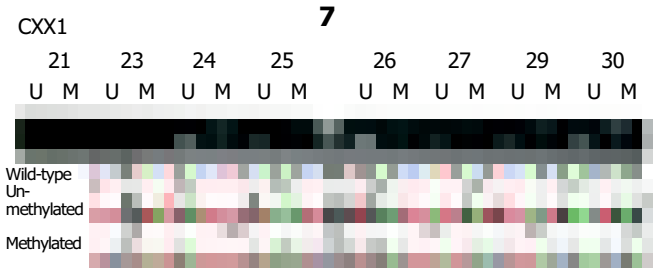
7
CXX1
21 23 24 25 26 27 29 30
U M U M U M U M U M U M U M U M
Wild-type
Un-methylated
Methylated

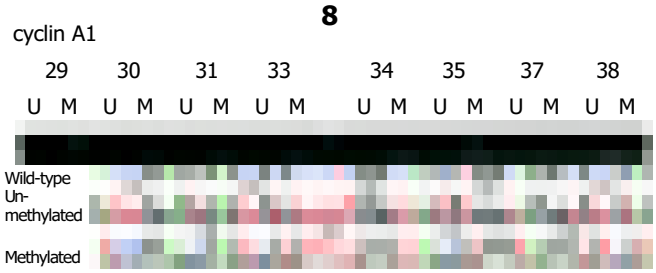
8
cyclin A1
29 30 31 33 34 35 37 38
U M U M U M U M U M U M U M U M
Wild-type
Un-methylated
Methylated

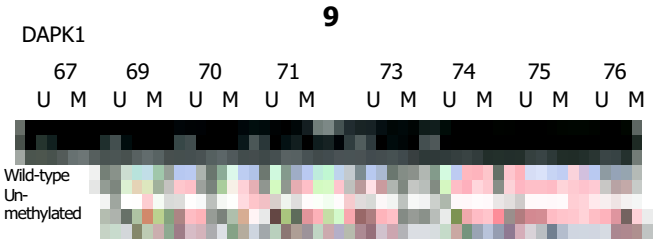
9
DAPK1
67 69 70 71 73 74 75 76
U M U M U M U M U M U M U M U M
Wild-type
Un-methylated

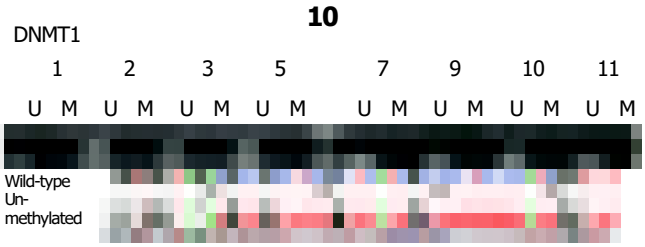
10
DNMT1
1 2 3 5 7 9 10 11
U M U M U M U M U M U M U M U M
Wild-type
Un-methylated

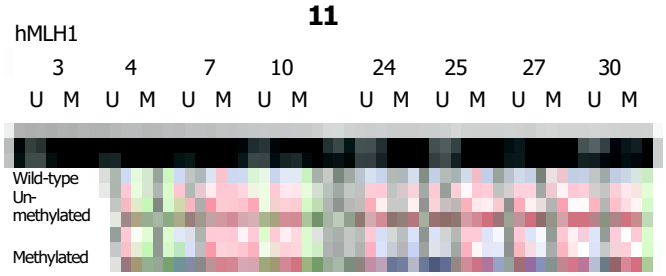
11
hMLH1
3 4 7 10 24 25 27 30
U M U M U M U M U M U M U M U M
Wild-type
Un-methylated
Methylated

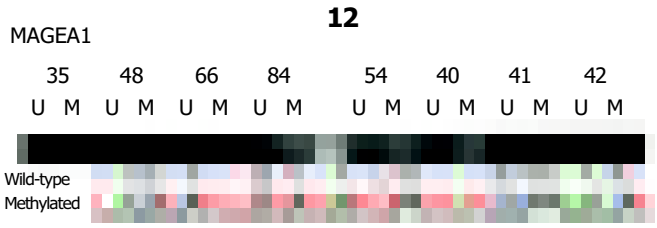
12
MAGEA1
35 48 66 84 54 40 41 42
U M U M U M U M U M U M U M U M
Wild-type
Methylated

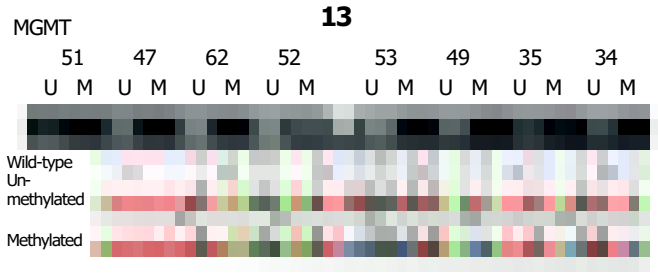
MGMT
13
51 47 62 52 53 49 35 34
U M U M U M U M U M U M U M U M
Wild-type
Un-methylated
Methylated

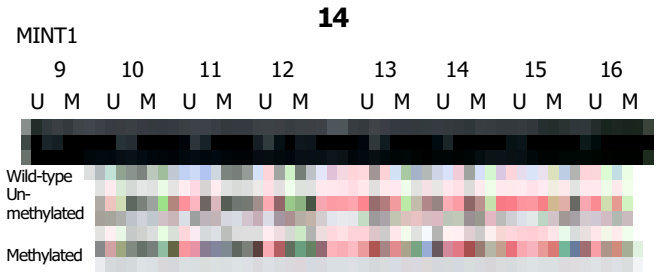
MINT1
14
9 10 11 12 13 14 15 16
U M U M U M U M U M U M U M U M
Wild-type
Un-methylated
Methylated

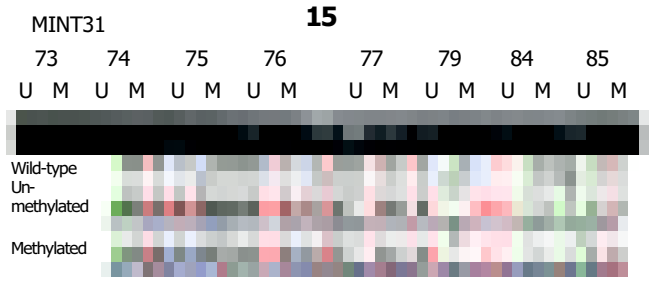
MINT31
15
73 74 75 76 77 79 84 85
U M U M U M U M U M U M U M U M
Wild-type
Un-methylated
Methylated

MYOD1
16
1 3 4 5 7 9 10 11
U M U M U M U M U M U M U M U M
Wild-type
Un-methylated
Methylated

N33
17
1 3 4 5 7 9 10 11
U M U M U M U M U M U M U M U M
Wild-type
Un-methylated
Methylated

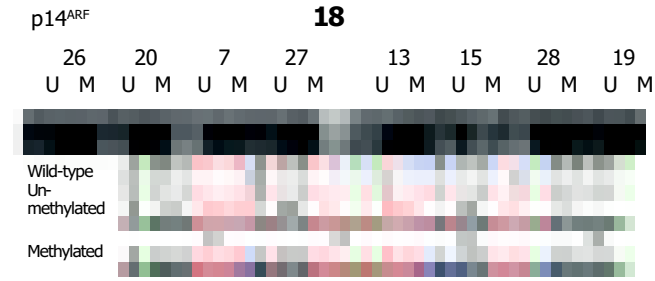
p14ARF
18
26 20 7 27 13 15 28 19
U M U M U M U M U M U M U M U M
Wild-type
Un-methylated
Methylated

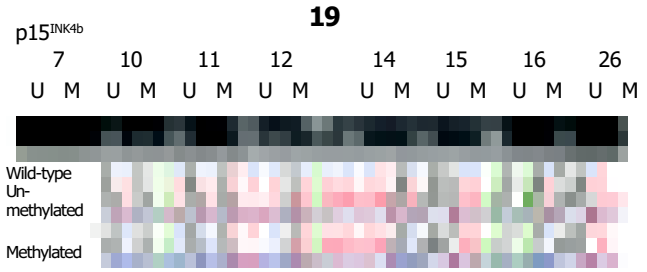
p15INK4b
19
7 10 11 12 14 15 16 26
U M U M U M U M U M U M U M U M
Wild-type
Un-methylated
Methylated

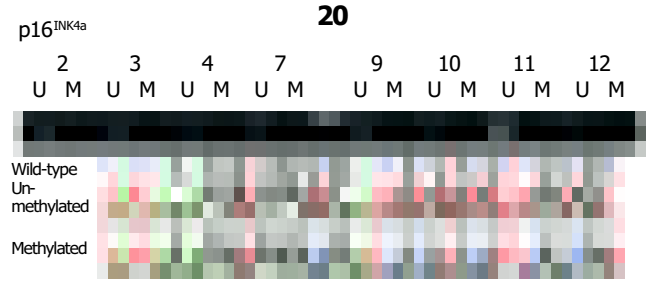
p16INK4a
20
2 3 4 7 9 10 11 12
U M U M U M U M U M U M U M U M
Wild-type
Un-methylated
Methylated

p21WAF1
21
41 42 43 45 52 53 54 55
U M U M U M U M U M U M U M U M
Wild-type
Un-methylated

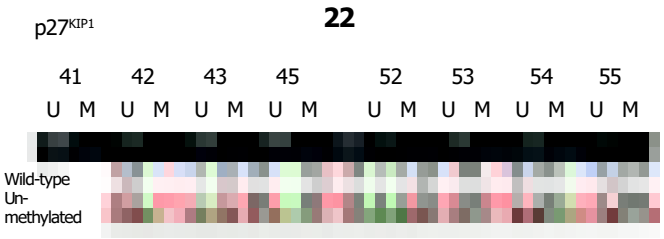
p27KIP1
22
41 42 43 45 52 53 54 55
U M U M U M U M U M U M U M U M
Wild-type
Un-methylated

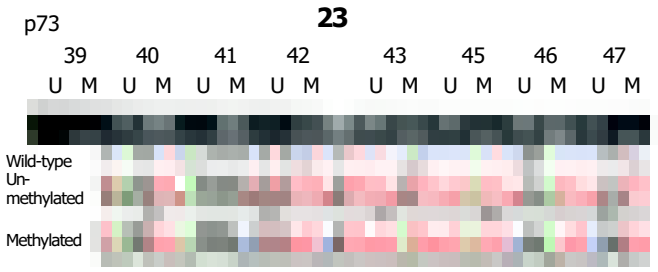
p73
23
39 40 41 42 43 45 46 47
U M U M U M U M U M U M U M U M
Wild-type
Un-methylated
Methylated

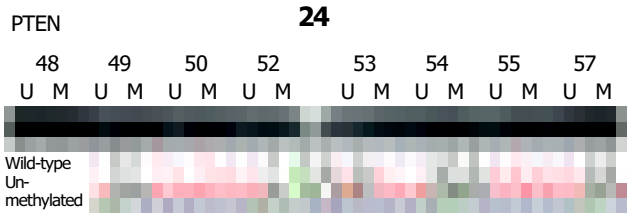
PTEN
24
48 49 50 52 53 54 55 57
U M U M U M U M U M U M U M U M
Wild-type
Un-methylated

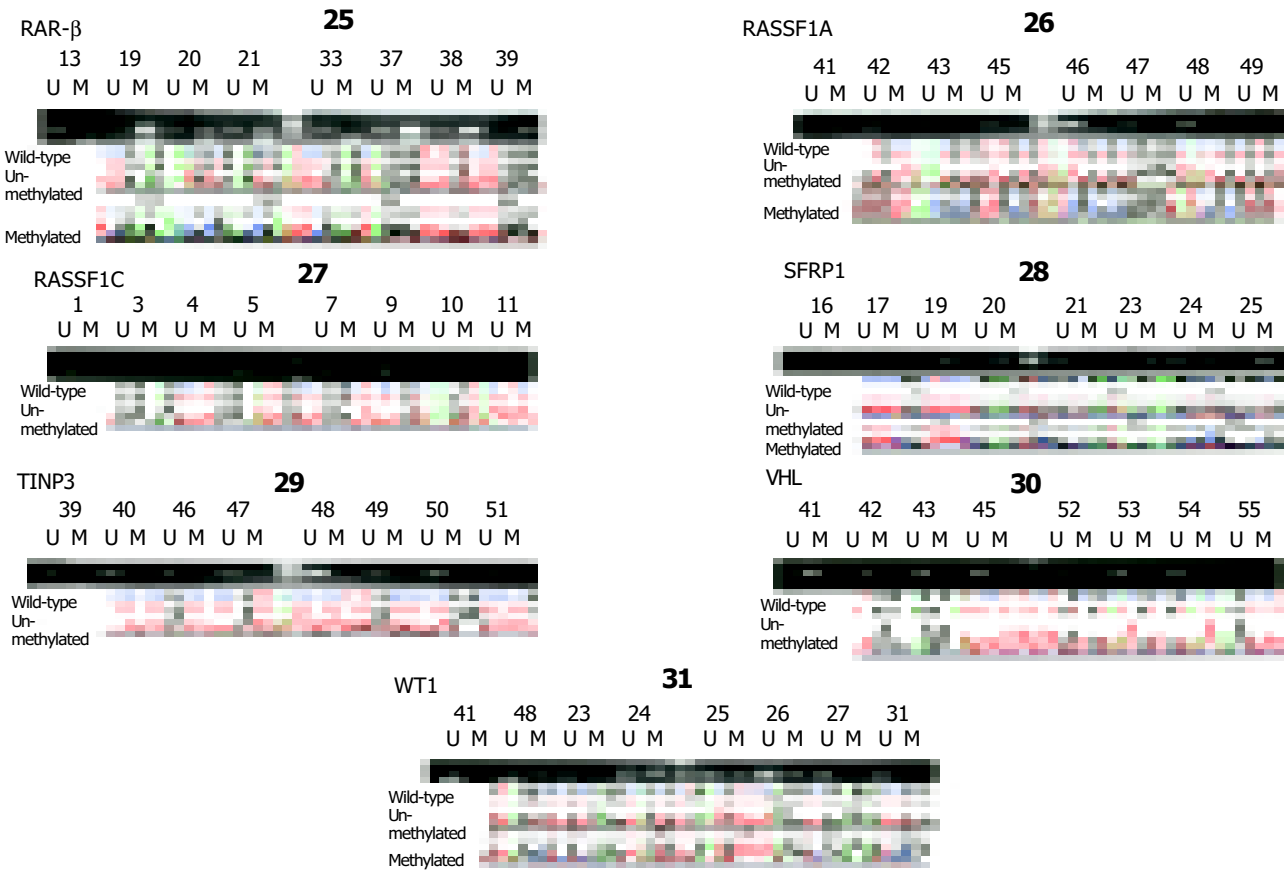

Figure 1 Methylation profiles of the promoter CpG islands of 31 genes in CRC. Both electrophoretic patterns of the representative PCR products of each of 31 targets (indicated respectively, at the top of figures) and the sequencing verification of the one representative PCR product are presented. To indicate the methylation status, the sequenced data are aligned with the wild-type sequence. [1]Size markers, the bands of 250 bp and 100 bp are shown. U, the unmethylated; M, hypermethylated. Panels: 1, *APC*, 2, *BRCA1*, 3, *CDH1*, 4, *CDH13*, 5, *CDX1*, 6, *COX2*, 7,*CXX1*, 8, *cyclin A1*, 9, *DPAK1*, 10, *DNMT1*, 11, *hMLH1*, 12, *MAGEA1*, 13, *MGMT*, 14, *MINT1*, 15, *MINT31*, 16, *MYOD1*, 17, *N33*, 18, $p14^{ARF}$, 19, $p15^{INK4b}$, 20, $p16^{INK4a}$ 21, $p21^{WAF1}$, 22, $p27^{KIP1}$, 23, *p73*, 24, *PTEN*, 25, *RAR-b*, 26, *RASSF1A*, 27, *RASSF1C*, 28, *SFRP1*, 29, *TIMP3*, 30, *VHL*, and 31, *WT1*.

Genes displayed no changes in methylation profile in tumor samples

As shown in Figure 1 and summarized in Figure 2, by comparing with the normal mucosa of non-cancerous samples, the following 14 genes did not display any tumor associated changes: *BRCA1* (panel 2), *CDH1* (panel 3), *DAPK1*(panel 9), *DNMT1*(panel 10), *MAGEA1*(panel 12), *N33*(panel 17), $p21^{WAF1}$ (panel 21), $p27^{KIP1}$ (panel 22), *PTEN* (panel 24), *RAR-* (panel 25), *RASSF1C* (panel 27), *SFRP1* (panel 28), *TIMP3* (panel 29) and *VHL* genes (panel 30). The *MAGEA1* gene was the only target that tends to be demethylated and transcription-activated in tumors, as we previously demonstrated in hepatocellular carcinoma (HCC)[10]. But the hypermethylated state of its promoter CpG islands maintained in all the samples tested. The likely explanations for such no-change-type-observations were the following: no changes in expression of this set of genes occurred in CRC, and the changes in expression indeed occured, but the DNA methylation mediated mechanisms was not involved.

It should be pointed out that our no change conclusion as to both *N33* and *TIMP3* genes was at odds with the previous report where both genes were hypermethylated rather frequently in CRC[32]. Whether it was attributed to the inherent difference between patient groups in different studies remains to be clarified.

Genes displayed changes in methylation profile in tumor samples

To score the changes in each CRC case, the methylated status in the mucosa tissue of the non-cancerous patients was taken as the reference, any deviation from which was scored as positive (increasing methylation extent) or negative (decrease in methylation extent).

Seventeen genes in this list displayed to various extents the tumor associated changes. As shown in Figures 1, 2, the changes of the following genes occurred marginally, and their impact on CRC looked trivial: *APC* (panel 1) (8%, 5/65), *RASSF1A* (3%, 2/65) (panel 26) and $p14^{ARF}$ (6%, 4/65) (panel 18). It was surprising to see that the extremely low frequency in hypermethylation of the *RASSF1A* gene in CRC, which was hypermethylated in a wide range of the human tumors, including hepatocellular carcinoma[10,14], astrocytoma (unpublished results) and other tumors[33,34].

The following genes displayed significant alterations in methylation pattern deviated from that of the mucosa of the non-cancer tissues, including those with the moderate levels of changes: *MGMT* (20%, 13/65, panel 13), *hMLH1* (18%, 12/65, panel 11), $p16^{INK4a}$(10%, 10/65, panel 20), *MINT1* (15.4%, 10/65, panel 14), *MINT31* (11%, 7/65, panel 15); and with a great level of changes: *COX2* (72%, 47/65, (panel 6), *cyclin A1* (100%, 65/65, panel 8) and *CDX1* (100%, 65/65, panel 5), *RAR-* (85%, 55/65, panel 25), *MYOD1* (69%, 45/65, panel 16), $p15^{INK4b}$(68%, 44/65, panel 19), *CDH13* (66%, 43/65, panel 4), *CXX1* (58%, 38/65, panel 7), *p73* (63%, 41/65, panel 23) and *WT1* (58%, 38/65, panel 31, Figure 1). In this list, while changes in methylation pattern of the majority of targets, were compatible with the previously reported frequencies in CRC patients in the Western countries[7,11,35,36], there was a noticeable difference. For instance, we have found the $p15^{INK4b}$ was significantly methylated in CRC (68%, 44/65), while this gene was not methylated at all in a similar study in USA[35].

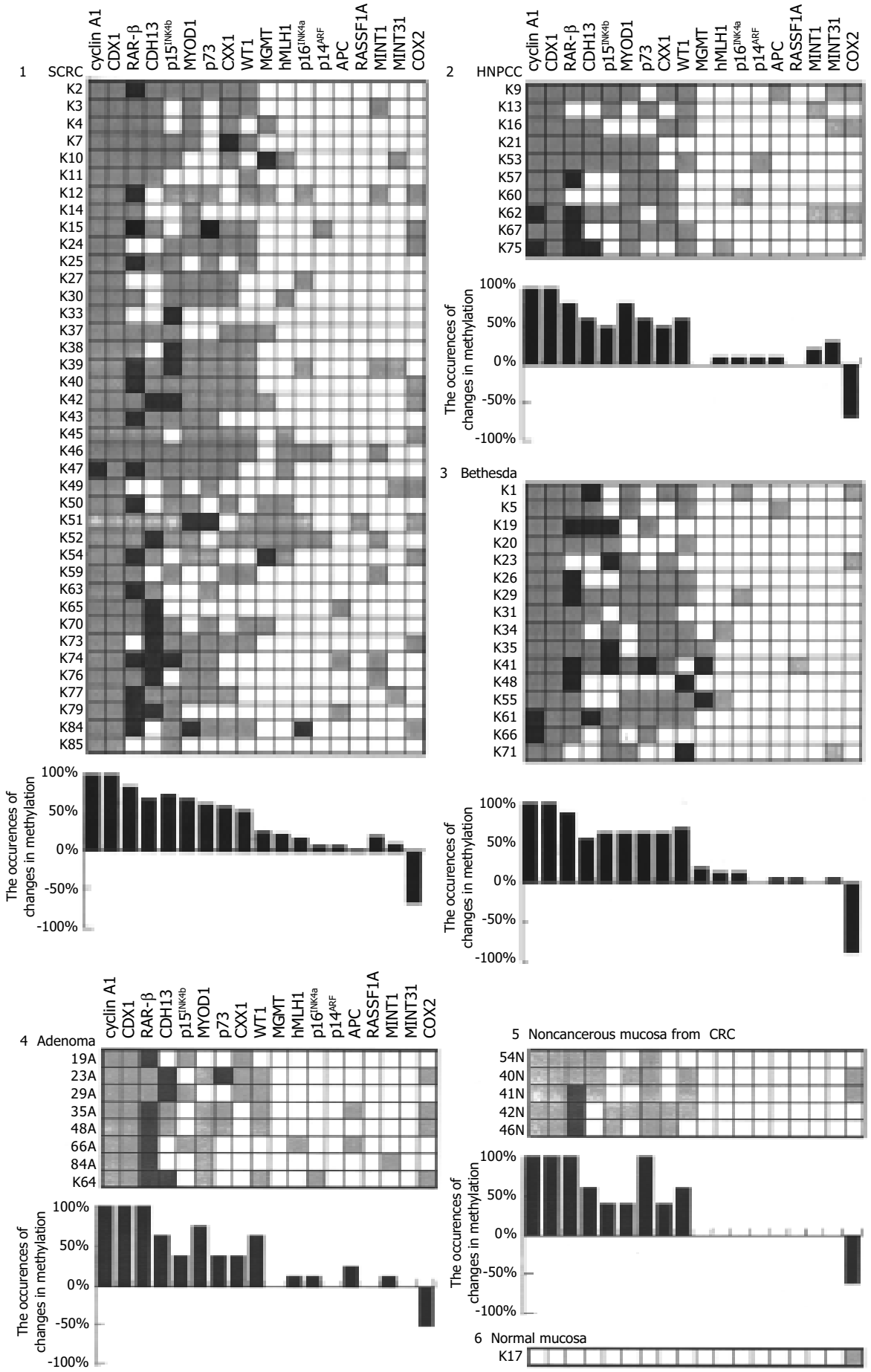

Figure 2 Changes in methylation pattern of genes in CRC and other relevant tissues. The frequency (%) of the hypermethylated targets among the total cases was calculated, and the frequency of the changes in the methylation pattern is presented in the plot as well as in the attached table. Panels: 1, SCRC, 2, HNPCC, 3, Bethesda, 4, Adenoma, 5, Non-cancerous mucosa from CRC patients and 6, the normal mucosa from a non-cancerous patient.

It was also our intention to correlate the methylation pattern with the clinical-pathological features of CRC patients. Subjected to the stringent statistic analysis (P<5%), none of the comparisons displayed any significant correlation. For instance, there was no statistic significance between the methylation changes of any given genes among different subgroups of CRC: SCRC and HNPCC as well as against other cohorts of tissues, such as colorectal adenoma and adjacent mucosa. This was likely to attribute to the small sample size. Although there was a decent number for SCRC (n = 39), the sample sizes for other subgroups were rather small: 10 HNPCCs, 16 Bethesda CRCs, eight adenomas, five non-cancerous mucosae and one normal mucosa.

It has been well recognized that the so-called non-cancerous cells pathologically defined may have already suffered some genetic lesions as the corresponding cancerous tissues, the outcome of the earlier events of carcinogenesis. The scenario of the genetic events from the normal mucosa to the full-blown CRC within the context of the well defined clinical and pathological parameters has been well characterized[37]. In this study, we included samples of non-cancerous mucosa from five CRC patients, adenomatous samples from eight patients and tumorous tissues from 65 CRC cases including 39 SCRCs, 10HNPCCs and 16 Bethesda CRCs, which enabled us to determine whether the changes in methylation pattern in CRC were specific to the early or late phases of carcinogenesis. Judged by the no difference in methylation pattern between the non-cancerous mucosa and adenoma and /or CRC (Figures 1, 2) (the same rationale used in our previous work on the hepatocellular carcinoma[10]), we suggested that the high frequent changes in methylation pattern of the genes might be the early rather than the late phase events during carcinogenesis of CRC.

CRC was among the first few types of human cancers subjected to the rather intensive DNA methylation profiling, where changes in methylation in tumor samples were classified as the aging related as well as the cancer specific[17,38,39]. For instance, the *MYOD1* was found also hypermethylated more frequently in the aged healthy epithelia tissues than their younger counterparts[17]. Also from the studies of CRC, the concordant methylation profile of multiple genes was firstly reported, called "CpG island methylation phenotype (CIMP)", short for CpG island methylator phenotype[11]. It implies that the unknown genetic mechanism (s) operating in CRC may contribute to the clustering profile of the DNA methylation of the multiple genes together. Among the 65 CRC cases, the distribution in occurrence of changes in the multiple genes was as following, 1, 3, 5, 7, 12, 11, 11, 7, 4, 1, and 3 cases, for assuming the methylation change of from 2, progressing step by step to 12 genes, respectively (Figure 3), with the 7 gene group as the peak.

In situ expression profile of 10 genes in CRC

Hypermethylation of the promoter CpG islands could reflect the transcriptional silencing status of the gene. However, exceptions also were reported, suggesting the involvement of other mechanisms in the control of the gene transcription. To verify this notion, we immunostained 10 target proteins *in situ* on the home-made tumor tissue arrays, where the tissue blocks from 58 CRC samples along with several controls of the non-cancerous mucosa from the cancer patients were present. The results were scored from the negative (-), to positive: ranging from + to +++. With the expression level in the non-cancerous mucosa as reference, the relative level of expression of each protein in the context of the methylation state of the promoter CpG islands of the genes was assessed. As shown in Figure 4 and summarized in Table 5, the unmethylated states of the promoter CpG islands of the following genes were indeed positively correlated with the expression levels of the genes. Among the cases of the fully unmethylated targets, expression of each protein ⩾ one + level occurred very frequently: for the *CDH13*, 73% (16/22); *RAR-b*, 100% (8/8); COX2, 80% (35/44); *p73*, 60% (12/20); *hMLH1*, 75% (35/47); $p14^{ARF}$, 100% (51/51); *TIMP3*, 80% (46/58) and *CDH1*, 98% (57/58). The only exception was *MGMT*, only 25% (2/8) of the unmethylated cases expressed this protein, suggesting the mechanisms other than DNA hypermethylation being involved. For the CRC cases with the heterozygous methylated status (u/m), expression of each proteins was: *CDH13*, 50% (14/28); *cyclin A1*, 70% (37/53); *RAR-* , 79% (22/28); *COX2*, 100% (14/14); *p73*, 54% (19/35); *MGMT*, 24% (11/46); *hMLH1*, 36% (4/11) and $p14^{ARF}$, 100% (2/2), respectively. For the CRC cases with the fully methylated targets, the expression profile of the genes was as the following: *CDH13*, 38% (33/58), *cyclin A1*, 80% (4/5), *RAR-* , 85% (17/20) and *MGMT*, 50% (2/4). Except for the *CDH13*, which expressed less frequently in the methylated than the unmethylated containing cases, the expression frequency was not significantly less prevalently in the methylated cases, even higher as far as the *MGMT* was concerned. Therefore, the correlation between the methylation status and level of expression of these 10 genes was not in a good agreement with the conventional notion.

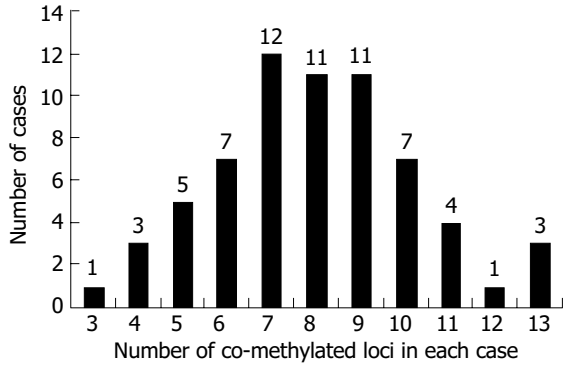

Figure 3 Concordant behavior of the multiple methylated loci in CRC.

Table 5 Expression profile of the genes in the context of DNA methylation status

Methylation status	Positive rate % (Positive cases / the total cases)									
	CDH13	Cyclin a1	RAR-	COX2	P73	MGMT	hMLH1	p14ARF	TIMP3	CDH1
U	73 (16/22)	/	100 (8/8)	81 (35/43)	60 (12/20)	24 (11/46)	74 (35/47)	100 (51/51)	80 (46/58)	98 (57/58)
U/M	50 (14/28)	70 (37/53)	79 (22/28)	93 (14/15)	54 (19/35)	25 (2/8)	36 (4/11)	100 (2/2)	/	/
M	38 (3/8)	80 (4/5)	85 (17/20)	/	/	50 (2/4)	/	/	/	/
Total	57 (33/58)	71 (41/58)	84 (47/56)	84 (49/58)	53 (31/58)	26 (15/58)	67 (39/58)	100 (53/53)	79 (46/58)	98 (57/58)
Non-cancerous mucosa	+	/	++	/	+	+	++	+	+	++

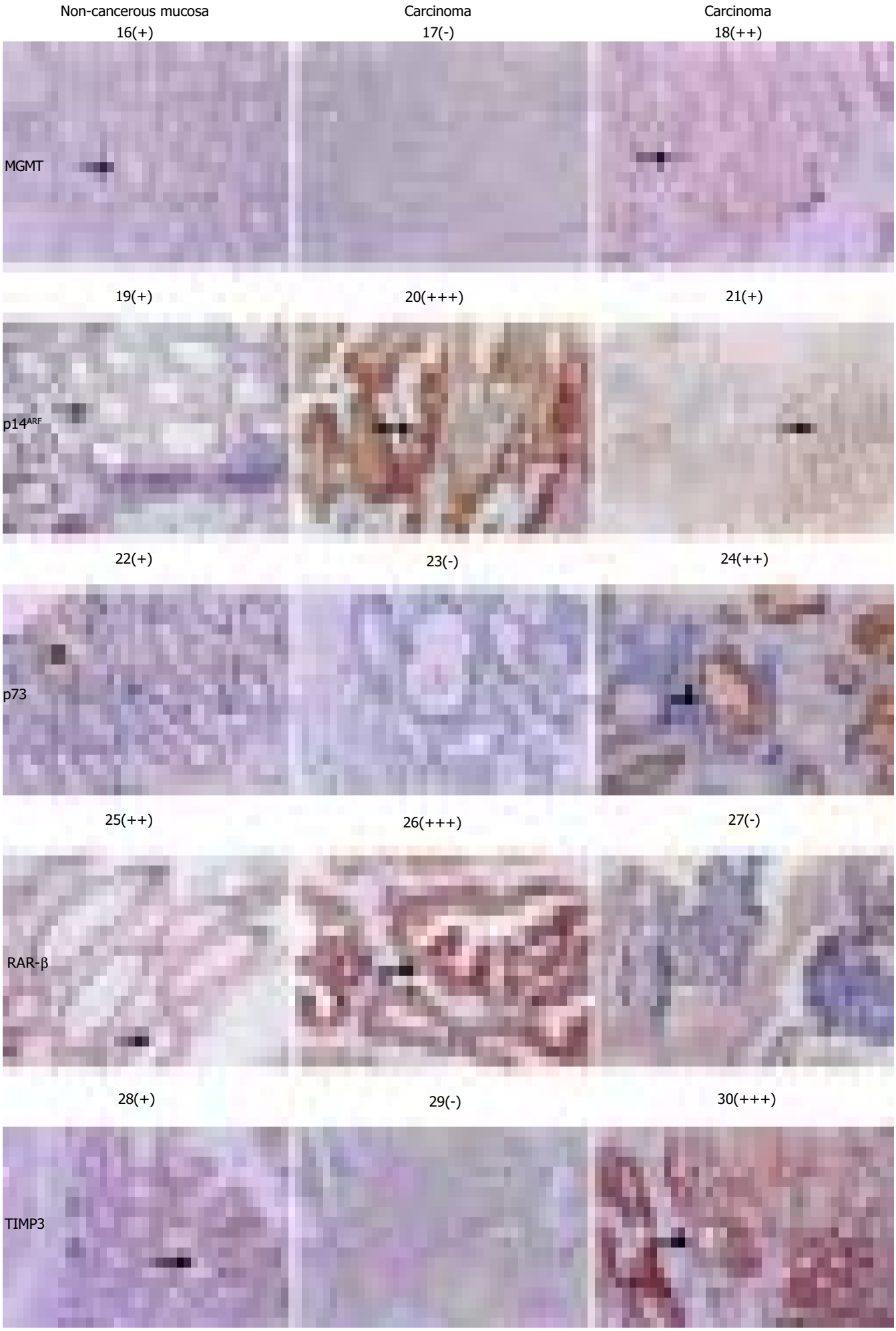
Non-cancerous mucosa
Carcinoma
Carcinoma
16(+)
17(-)
18(++)
MGMT
19(+)
20(+++)
21(+)
p14ARF
22(+)
23(-)
24(++)
p73
25(++)
26(+++)
27(-)
RAR-β
28(+)
29(-)
30(+++)
TIMP3

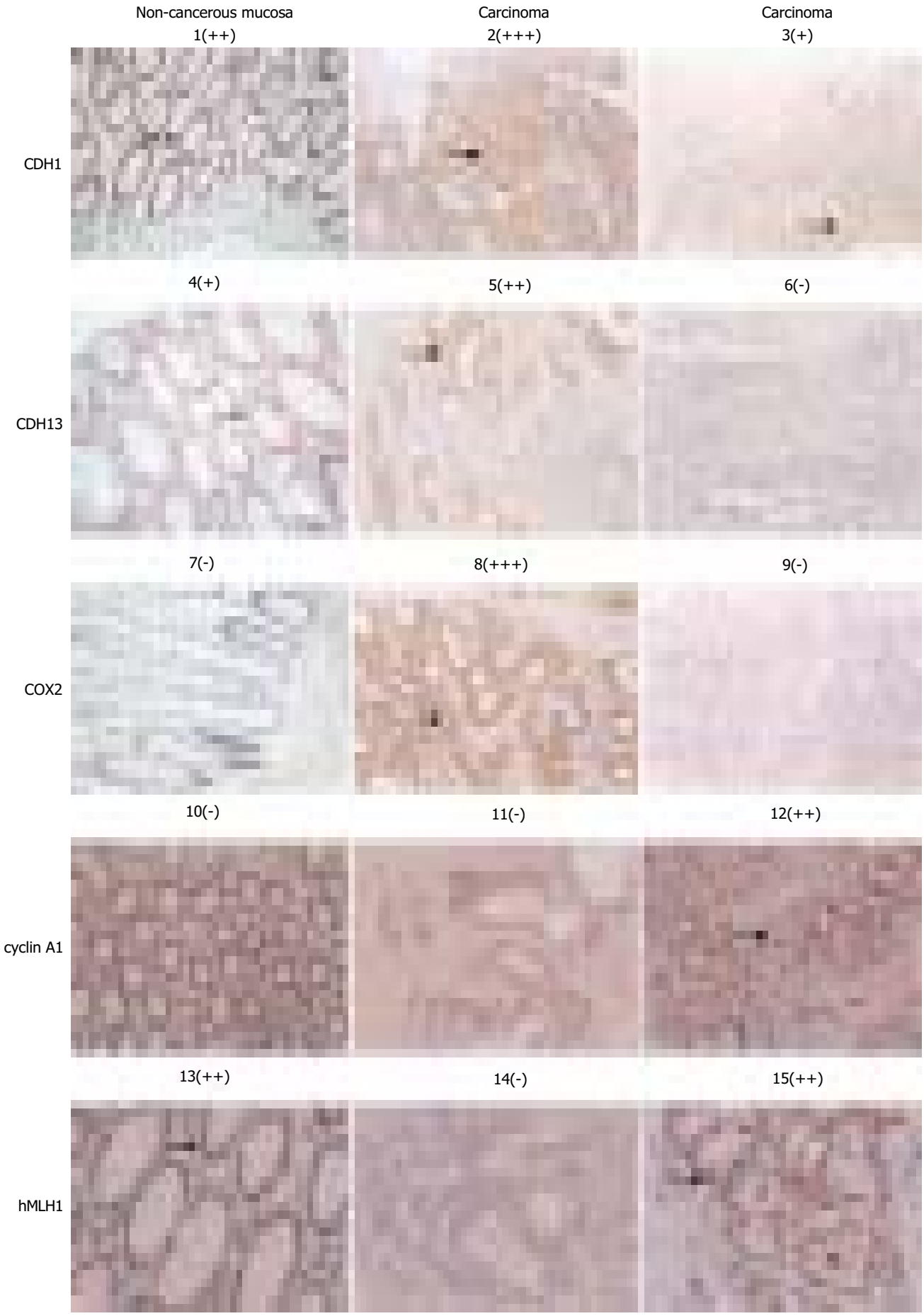

Figure 4 Immunochemical assessment of the expression level of each of 10 target genes. Both the protein targets (left site to) and sample identities (top down) of the immuno-chemical stained picture are indicated. The signs: -, +, ++, and +++ in bracket are used to provide the quantitative reference in pictures below. The areas pointed by the arrows are the regions showing the immunostaining data quantified.

DISCUSSION

In this study, 31 targets were selected to be studied, 65 cases of CRC, 8 cases of adenoma, five cases of non-cancerous mucosa from the cancer patients and one case mucosa from the non-cancerous patient. As far as the number of genes was concerned, this study is rather extensive, and it is the first of such a kind with CRC patients in China, and in Shanghai in particular.

Changes in methylation pattern of the promoter CpG islands are very common in CRC

By taking the methylation profile of the mucosa from the non-cancerous patient as the reference, CRC associated changes in methylation pattern were a very extensive event, 17 among of 31 targets assumed the altered patterns, the following 14 changed in more than 20% of CRC cases as a whole: *MGMT* (20%, 13/65), *hMLH1* (18%, 12/65), $p16^{INK4a}$ (10%, 10/65), *MINT1* (15.4%, 10/65), *MINT31* (11%, 7/65), *COX2* (72%, 47/65), *cyclin A1* (100%, 65/65), *CDX1* (100%, 65/65), *RAR-* (85%, 55/65), *MYOD1* (69%, 45/65), $p15^{INK4b}$ (68%, 44/65), *CDH13* (66%, 43/65), *CXX1* (58%, 38/65), *p73* (63%, 41/65) and *WT1* (58%, 38/65) genes. Furthermore, there was only one case assuming the methylation changes with three genes (Figure 3), no less than 76.3 % of cases assumed changes in methylation more than seven targets (49/65), 86% more than six targets (56/65), 93.8% more than five targets (61/65). This observation indeed supports the concept, "CpG island methylator phenotype", for that changes in methylation pattern in CRC indeed tend to be clustered. As a similar survey with the astrocytoma showed that less 26.4% patients assumed no more than two gene (among 31 targets being surveyed), and the occurrence of changes in methylation pattern for at least five, six and seven targets was 41.51%, 20.75 and 9.43% in a cohort of 56 astrocytoma patients (unpublished data). The high incidence of changes in CRC may be partly attributed to the fact that colorectal epithelial cells were much amenable to the environmental challenges.

Except for the genes that have been proved in the category of tumor associated genes, such as $p16^{INK4a}$, $p15^{CDKN4b}$, $p14^{ARF}$, $p27^{KIP1}$, *WT1*, *VHL*, *RB*, *p73*, *APC*, *N33*, *PTEN* and *BRCA1*, the *MAGEA1* and *RAR-* genes have not been studied in CRC. While the *MAGEA1* gene displayed the homozygously methylated state in all samples tested, the *RAR-* gene indeed changes its methylated state from the unmethylated in the normal mucosa toward the hypermethylated state at a significantly higher frequency in CRC, over 85% (55/65). The retinoic acid receptor (RAR) gene is a putative tumor suppressor gene on chromosome 3p24, where a high incidence of loss of heterozygosity (LOH) is detected in many types of tumors. Retinoic acid suppresses cancer cell growth through binding to RARs, especially RAR-, indicating a critical role in mediating anticancer effects. Selective loss or down-regulation of the *RAR* mRNA and protein has been reported in prostate cancers. The DNA methylation mediated silencing of this gene has been suggested as an etiological factor for carcinogenesis of prostate cancer[40]. This result indicates that the *RAR-* hypermethylation may be the mechanism of expression silencing in these tumor cells[41]. However, its etiological significance in carcinogenesis of CRC remains to be clarified.

The following genes: *CXX1*, *CDX1*, *SFRP1*, *MINT1 and MINT31* were initially identified as the CRC associated hypomethylated genes by an approach at the genome level[16]. Except for the *SERP1* gene that was not methylated with all the samples being tested, the rest targets were indeed hypermethylated to varying extents in CRC (Figures 1, 2). Tumor suppressor gene *RASSF1A* was inactivated predominantly by promoter methylation and rarely by somatic mutations. wagner *et al.*[34] investigated RASSF1A promoter methylation in colorectal cancer and detected RASSF1A methylation in 80% (4/5) colorectal cancer cell lines and 45% (13/29) primary colorectal cancers. But we found that the frequency of *RASSF1A* methylation was extremely low in CRC although we previously found this gene was hypermethylated (100%) in HCC[14].

Does the methylation profile of the promoter CpG islands of the genes correlate with the expression of the genes?

Although it has been generally accepted that the hypermethylated status of the promoter CpG islands represents the long-term transcription silencing state of the genes, its credential has not been thoroughly checked in clinical samples, due to various limiting factors, including availability and inherent diversity of the cell types in the actual samples. In this study, we immunostained the genes with antibodies to assess the expression of 10 genes in a home-made tissue array. For both homozygously and heterozygously unmethylated samples, nine of 10 targets (except for *MGMT*) expressed at a detectable level of more than 60% cases. It was generally fit with the expectation. For the fully methylated CRC, only four targets were involved, among which the profile of the *CDH13* gene met the expected profile. The expression frequency (38%, 3/8) in methylated samples was significantly lower than heterozygously methylated (50%, 14/28), and homozygously unmethylated (73%, 16/22). The profiles of the other three targets did not comply with the role at all. Both *cyclin A1* and *RAR-* genes expressed equally well as the CRC samples of m/u type. Furthermore, it was paradoxically found that the *MGMT* gene expressed more prevalently in the methylated CRC cases (50%, 2/4) than its counterparts (u/m: 25%, 2/8 and u: 25%, 11/46). As we have previously shown in astrocytoma cell lines, the methylated status of the promoter CpG islands inversely correlated with the expression of the *MGMT* gene (unpublished data), this rather unexpected observation should be looked into further. In conclusion, despite the general roles that have been followed as to the inverse correlation between the methylation state of the promoter CpG islands and expression, the exception is also distinguishingly noticeable. Therefore, it should be very cautious in correlating the methylated status with the expression profile of the genes.

Demethylation of the COX2 gene correlates with the increased frequency in its expression

Cyclo-oxygenase 2 (COX2), an inducible isoform of prostaglandin H synthase, which mediates prostaglandin synthesis during inflammation, and is selectively over-expressed in colon tumors, is thought to play an important role in colorectal carcinogenesis[42]. Its expression in the normal epithelial cells is low, but can be induced by a variety of stressing agents, including tumor promoters and inflammatory cytokines. In the list of the genes displaying changes in methylation, it was noticed that the *COX2* gene was the only target that displayed CRC associated demethylation, i.e., from the heterozygous methylated state to fully demethylated in 47 among 65 cases being studies (72%) (Figures 1, 2). The *COX2* gene did not express in the control non-cancerous tissues, indicating that it seems less likely to have the physiological role in normal colon epithelial cells. Although there was no increase in the frequency of expression in CRC from the heterozygously to the fully unmethylated CRC cases (Figure 2), the fact that over 82% CRC cases expressed this gene was indeed supportive.

Tumor type specificity of the methylation profile

It has been well established that the methylation profile as an inheritable epigenetic signature in any given cells reflects both history of cell differentiation and the chronicle of aging, in addition to those closely associated with the biological profiles

of tumors[6,43,44]. It is desirable to identify the changes, specific to one type of tumor from the others, otherwise our efforts to use the DNA methylation pattern, as the biomarkers for tumor diagnosis would be severely constrained. Therefore, we compared the methylation patterns in HCC[10,14] with those in CRC. As shown in Figure 5, there were methylation changes common to both HCC and CRC i.e., the *p73* gene: 73% in HCC *vs* 62.5% in CRC and the *MYOD1* gene: 57.8% in HCC *vs* 69.23% in CRC. The following changes were more prevalent in CRC than in HCC: the *cyclin A1* gene: 100% in CRC *vs* 53.85% in HCC; the *WT1* gene: 58.46% in CRC *vs* 30.77% in HCC; and the *CDH13* gene: 64.62% in CRC *vs* 23.08% in HCC. The following two genes were more frequently hypermethylated in HCC than in CRC: the *RASSF1A* gene: 100% in HCC *vs* 2.08% in CRC; and the *p16^{INK4a}* gene: 53.85% in HCC *vs* 15.38% in CRC. Although little is known about the mechanisms underlying the tumor specific methylation profiles of CRC *vs* those of HCC, the distinct profiles of CRC *vs* HCC should have the profound implication in the future diagnostic tools to differentiate these two common human cancers.

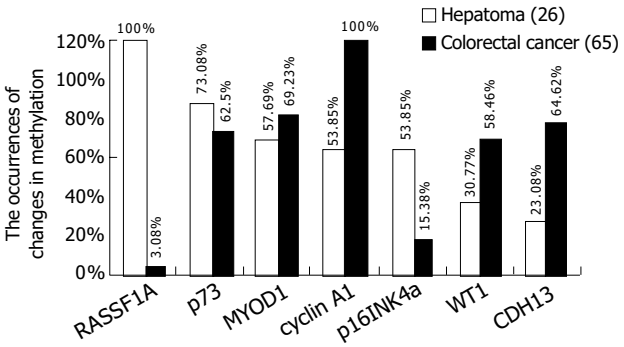

Figure 5 Tumor specific methylation pattern: CRC verse HCC.

In conclusion, the altered promoter CpG island methylation patterns of 17 genes are the common and distinguished hallmarks specific to the early phase of colon carcinogenesis, although no significant correlation has been detected between the changes in the methylation patterns with any given clinical-pathological features. The correlation between the methylated state of the promoter CpG islands and the expression of the corresponding genes has not been proved as close as previously suggested. Our observations from this rather extensive methylation-profiling maneuver would provide new insights into the role of the DNA methylation mediated control in the colon carcinogenesis as well as the clues for the development of robust diagnostic and prognostic tools for colorectal cancer.

REFERENCES

1 **Du BR**. COX-2 in large bowel cancer: a one-sided story. *Gut* 1999; **45**: 636-637

2 **Kinzler KW**, Vogelstein B. Landscaping the cancer terrain. *Science* 1998; **280**: 1036-1037

3 **Parkin DM**, Pisani P, Ferlay J. Global cancer statistics. *CA Cancer J Clin* 1999; **49**: 33-64

4 **DePinho RA**. The age of cancer. *Nature* 2000; **408**: 248-254

5 **Bird AP**. CpG-rich islands and the function of DNA methylation. *Nature* 1986; **321**: 209-213

6 **Jaenisch R**, Bird A. Epigenetic regulation of gene expression: how the genome integrates intrinsic and environmental signals. *Nat Genet* 2003; **33**(Suppl): 245-254

7 **Feinberg AP**. Cancer epigenetics takes center stage. *Proc Natl Acad Sci U S A* 2001; **98**: 392-394

8 **Chen RZ**, Pettersson U, Beard C, Jackson-Grusby L, Jaenisch R. DNA hypomethylation leads to elevated mutation rates. *Nature* 1998; **395**: 89-93

9 **Gaudet F**, Hodgson JG, Eden A, Jackson-Grusby L, Dausman J, Gray JW, Leonhardt H, Jaenisch R. Induction of tumors in mice by genomic hypomethylation. *Science* 2003; **300**: 489-492

10 **Yu J**, Zhang HY, Ma ZZ, Lu W, Wang YF, Zhu JD. Methylation profiling of twenty four genes and the concordant methylation behaviours of nineteen genes that may contribute to hepatocellular carcinogenesis. *Cell Res* 2003; **13**: 319-333

11 **Toyota M**, Ahuja N, Ohe-Toyota M, Herman JG, Baylin SB, Issa JP. CpG island methylator phenotype in colorectal cancer. *Proc Natl Acad Sci U S A* 1999; **96**: 8681-8686

12 **van Rijnsoever M**, Grieu F, Elsaleh H, Joseph D, Iacopetta B. Characterisation of colorectal cancers showing hypermethylation at multiple CpG islands. *Gut* 2002; **51**: 797-802

13 **Cai Q**, Molecular genetics research of HNPCC in China, Departmetn of Pathology, Cancer Hosptital of Fudan University, Fudan University, Shanghai 2002

14 **Yu J**, Ni M, Xu J, Zhang H, Gao B, Gu J, Chen J, Zhang L, Wu M, Zhen S, Zhu J. Methylation profiling of twenty promoter-CpG islands of genes which may contribute to hepatocellular carcinogenesis. *BMC Cancer* 2002; **2**: 29

15 **Herman JG**, Graff JR, Myohanen S, Nelkin BD, Baylin SB. Methylation-specific PCR: a novel PCR assay for methylation status of CpG islands. *Proc Natl Acad Sci U S A* 1996; **93**: 9821-9826

16 **Suzuki H**, Gabrielson E, Chen W, Anbazhagan R, van Engeland M, Weijenberg MP, Herman JG, Baylin SB. A genomic screen for genes upregulated by demethylation and histone deacetylase inhibition in human colorectal cancer. *Nat Genet* 2002; **31**: 141-149

17 **Ahuja N**, Li Q, Mohan AL, Baylin SB, Issa JP. Aging and DNA methylation in colorectal mucosa and cancer. *Cancer Res* 1998; **58**: 5489-5494

18 **Kibel AS**, Christopher M, Faith DA, Bova GS, Goodfellow PJ, Isaacs WB. Methylation and mutational analysis of p27(kip1) in prostate carcinoma. *Prostate* 2001; **48**: 248-253

19 **Li Y**, Nagai H, Ohno T, Yuge M, Hatano S, Ito E, Mori N, Saito H, Kinoshita T. Aberrant DNA methylation of p57(KIP2) gene in the promoter region in lymphoid malignancies of B-cell phenotype. *Blood* 2002; **100**: 2572-2577

20 **Watanabe T**, Huang H, Nakamura M, Wischhusen J, Weller M, Kleihues P, Ohgaki H. Methylation of the p73 gene in gliomas. *Acta Neuropathol* 2002; **104**: 357-362

21 **Agathanggelou A**, Honorio S, Macartney DP, Martinez A, Dallol A, Rader J, Fullwood P, Chauhan A, Walker R, Shaw JA, Hosoe S, Lerman MI, Minna JD, Maher ER, Latif F. Methylation associated inactivation of RASSF1A from region 3p21.3 in lung, breast and ovarian tumours. *Oncogene* 2001; **20**: 1509-1518

22 **Linehan WM**, Lerman MI, Zbar B. Identification of the von Hippel-Lindau (VHL) gene. Its role in renal cancer. *Jama* 1995; **273**: 564-570

23 **Neibergs HL**, Hein DW, Spratt JS. Genetic profiling of colon cancer. *J Surg Oncol* 2002; **80**: 204-213

24 **Laux DE**, Curran EM, Welshons WV, Lubahn DB, Huang TH. Hypermethylation of the Wilms' tumor suppressor gene CpG island in human breast carcinomas. *Breast Cancer Res Treat* 1999; **56**: 35-43

25 **De Smet C**, De Backer O, Faraoni I, Lurquin C, Brasseur F, Boon T. The activation of human gene MAGE-1 in tumor cells is correlated with genome-wide demethylation. *Proc Natl Acad Sci U S A* 1996; **93**: 7149-7153

26 **Toyooka S**, Toyooka KO, Harada K, Miyajima K, Makarla P, Sathyanarayana UG, Yin J, Sato F, Shivapurkar N, Meltzer SJ, Gazdar AF. Aberrant methylation of the CDH13 (H-cadherin) promoter region in colorectal cancers and adenomas. *Cancer Res* 2002; **62**: 3382-3386

27 **Muller C**, Readhead C, Diederichs S, Idos G, Yang R, Tidow N, Serve H, Berdel WE, Koeffler HP. Methylation of the cyclin A1 promoter correlates with gene silencing in somatic cell lines, while tissue-specific expression of cyclin A1 is methylation independent. *Mol Cell Biol* 2000; **20**: 3316-3329

28 **Esteller M**, Corn PG, Baylin SB, Herman JG. A gene hypermethylation profile of human cancer. *Cancer Res* 2001; **61**: 3225-3229

29 **Viswanathan M**, Tsuchida N, Shanmugam G. Promoter hypermethylation profile of tumor-associated genes p16, p15, hMLH1, MGMT and E-cadherin in oral squamous cell carcinoma. *Int J Cancer* 2003; **105**: 41-46

30 **Fearon ER**. BRCA1 and E-cadherin promoter hypermethylation and gene inactivation in cancer-association or mechanism? *J Natl Cancer Inst* 2000; **92**: 515-517
31 **Zochbauer Muller S**, Fong KM, Virmani AK, Geradts J, Gazdar AF, Minna JD. Aberrant promoter methylation of multiple genes in non-small cell lung cancers. *Cancer Res* 2001; **61**: 249-255
32 **Issa J**. Genes Affected by Promoter CpG Island Methylation in Aging and/or Cancer, http://www.mdanderson.org/departments/methylation/dIndex.cfm?pn = D02B3250-57D7-4F61-88358636A8073A08 2001
33 **Maruyama R**, Toyooka S, Toyooka KO, Harada K, Virmani AK, Zochbauer-Muller S, Farinas AJ, Vakar-Lopez F, Minna JD, Sagalowsky A, Czerniak B, Gazdar AF. Aberrant promoter methylation profile of bladder cancer and its relationship to clinicopathological features. *Cancer Res* 2001; **61**: 8659-8663
34 **Wagner KJ**, Cooper WN, Grundy RG, Caldwell G, Jones C, Wadey RB, Morton D, Schofield PN, Reik W, Latif F, Maher ER. Frequent RASSF1A tumour suppressor gene promoter methylation in Wilms' tumour and colorectal cancer. *Oncogene* 2002; **21**: 7277-7282
35 **Esteller M**, Fraga MF, Guo M, Garcia-Foncillas J, Hedenfalk I, Godwin AK, Trojan J, Vaurs-Barriere C, Bignon YJ, Ramus S, Benitez J, Caldes T, Akiyama Y, Yuasa Y, Launonen V, Canal MJ, Rodriguez R, Capella G, Peinado MA, Borg A, Aaltonen LA, Ponder BA, Baylin SB, Herman JG. DNA methylation patterns in hereditary human cancers mimic sporadic tumorigenesis. *Hum Mol Genet* 2001; **10**: 3001-3007
36 **Suh ER**, Ha CS, Rankin EB, Toyota M, Traber PG. DNA methylation down-regulates CDX1 gene expression in colorectal cancer cell lines. *J Biol Chem* 2002; **277**: 35795-35800
37 **Kinzler KW**, Vogelstein B. Lessons from hereditary colorectal cancer. *Cell* 1996; **87**: 159-170
38 **Jubb AM**, Bell SM, Quirke P. Methylation and colorectal cancer. *J Pathol* 2001; **195**: 111-134
39 **Rashid A**, Shen L, Morris JS, Issa JP, Hamilton SR. CpG island methylation in colorectal adenomas. *Am J Pathol* 2001; **159**: 1129-1135
40 **Nakayama T**, Watanabe M, Yamanaka M, Hirokawa Y, Suzuki H, Ito H, Yatani R, Shiraishi T. The role of epigenetic modifications in retinoic acid receptor beta2 gene expression in human prostate cancers. *Lab Invest* 2001; **81**: 1049-1057
41 **Cote S**, Momparler RL. Activation of the retinoic acid receptor beta gene by 5-aza-2'-deoxycytidine in human DLD-1 colon carcinoma cells. *Anticancer Drugs* 1997; **8**: 56-61
42 **Plummer SM**, Holloway KA, Manson MM, Munks RJ, Kaptein A, Farrow S, Howells L. Inhibition of cyclo-oxygenase 2 expression in colon cells by the chemopreventive agent curcumin involves inhibition of NF-kappaB activation via the NIK/IKK signalling complex. *Oncogene* 1999; **18**: 6013-6020
43 **Jones PA**. Epigenetics in carcinogenesis and cancer prevention. *Ann N Y Acad Sci* 2003; **983**: 213-219
44 **Jubb AM**, Quirke P, Oates AJ. DNA methylation, a biomarker for colorectal cancer: implications for screening and pathological utility. *Ann N Y Acad Sci* 2003; **983**: 251-267

Edited by Xia HHX and Wang XL **Proofread by** Xu FM

PO Box 2345, Beijing 100023, China
Fax: +86-10-85381893
E-mail: wjg@wjgnet.com www.wjgnet.com

World J Gastroenterol 2004;10(23):3455-3458
World Journal of Gastroenterology
Copyright © 2004 by The WJG Press ISSN 1007-9327

• COLORECTAL CANCER •

Effects of phosphorothioate anti-sense oligodeoxynucleotides on colorectal cancer cell growth and telomerase activity

Xi-Shan Wang, Kuan Wang, Xue Li, Song-Bin Fu

Xi-Shan Wang, Kuan Wang, Department of Abdominal Surgery, Tumour Hospital of Harbin Medical University, Harbin 150040, Heilongjiang Province, China
Xue Li, Song-Bin Fu, Department of Genetics, Harbin Medical University, Harbin 150086, Heilongjiang Province, China
Supported by the Youth Science Foundation of Heilongjiang Province, China, No.QC01C08, and Heilongjiang Provincial Technology Council Foundations, China, No.GC03C605-6
Correspondence to: Dr. Xi-Shan Wang, Department of Abdominal Surgery, Tumour Hospital of Harbin Medical University, Harbin 150040, Heilongjiang Province, China. 1966120808@sina.com
Telephone: +86-451-86677583 Ext. 2146 **Fax:** +86-451-86663760
Received: 2004-02-14 **Accepted:** 2004-02-24

Abstract

AIM: To investigate the inhibitory effect of phosphorothioate anti-sense oligodeoxynucleotides (PASODN) on colorectal cancer LS-174T cells *in vitro* and the mechanism of inhibition of telomerase activity in these cells.

METHODS: PASODN were used to infect LS-174T cells and block human telomerase RNA (hTR) through anti-sense technology. The inhibitory effect of PASODN was evaluated by colony-forming inhibition assay and growth curve. Changes of telomerase activity in LS-174T cells were detected by polymerase chain reaction-enzyme-linked immunosorbent assay (PCR-ELISA), and the level of apoptosis was analyzed by flow cytometry (FCM) assay.

RESULTS: PASODN showed a dose and time-dependent inhibition of cell proliferation. The optimal dosage of PASODN was 10 μmol/L. The colony-forming efficiency was 10.3% in PASODN group after 10 d, whereas that in phosphorothioate mis-sense oligodeoxynucleotides (PMSODN) group with the same concentration and in PBS group (blank control) was 49.1% and 50.7%, respectively. PCR-ELISA results indicated that telomerase activity in the PASODN group was obviously inhibited in comparison with in the control groups (P<0.01, t = 3.317 and 3.241, $t_{0.01\,(20)}$ = 2.845). Meanwhile, before the number of cells was decreased, the morphological changes were observed in the cells of PASODN group. The cells in PASODN group showed the apoptotic peak at 72 h after infection, whereas the control group did not show.

CONCLUSION: Specific sequence oligonucleotides can inhibit telomerase activity and lead to cell apoptosis, suggesting a novel treatment strategy for malignant tumors induced by telomerase.

Wang XS, Wang K, Li X, Fu SB. Effects of phosphorothioate anti-sense oligodeoxynucleotides on colorectal cancer cell growth and telomerase activity. *World J Gastroenterol* 2004; 10(23): 3455-3458
http://www.wjgnet.com/1007-9327/10/3455.asp

INTRODUCTION

Telomerase, a ribonucleic acid-protein complex, adds hexameric repeats of 5'-TTAGGG-3' to the ends of telomeres to compensate for the progressive loss in malignant tumor cells[1,2]. Because of its preferential expression in malignant tumors and lack of expression in normal tissues[3-5], the idea that telomerase is a potential target of cancer therapy has been widely accepted[6,7]. From the theoretical point of view, telomerase-associated therapeutic approach to telomerase-positive tumors is the anti-telomerase cancer therapy that directly inhibits telomerase activity, resulting in apoptotic cell death or growth arrest. Two major components of the telomerase holoenzyme complex: human telomerase RNA (hTR) and catalytic subunit (human telomerase reverse transcriptase, hTERT), are considered as the therapeutic targets[8]. Since the growth of majority, or even parts of malignant tumors depends on telomerase, the strategy of anti-telomrease cancer therapy is necessary and important. In this study, we investigated the inhibitory effect of PASODN on colorectal cancer cells.

MATERIALS AND METHODS

Human colorectal cancer cell line LS-174T was obtained from Shanghai Institute of Cell Biology (Shanghai, China). Oligonucleotides were synthesized in Shenggong Company (Shanghai, China). The sequences of oligonucleotides were as follows: PASODN: 5'-TTAGGG-3', and PMSODN: 5'-TGTGAG-3'. Telomerase PCR-ELISA kit (No. 1854666) was purchased from Roche Company.

Cell culture

Colorectal cancer LS-174T cells were cultured in RPMI 1640 (GIBCO, UK) supplemented with 100 mL/L charcoal-stripped FCS (GIBCO, UK), 500 units/mL penicillin and 0.1 μg/mL streptomycin (SIGMA, USA) at 37 ℃ with a humidified atmosphere containing 50 mL/L CO_2. The medium was changed every 48 h. Cell cycle was 12 h approximately. Cells in logarithmic phase were used in all experiments.

Selection of optimal concentration of PASODN

The LS-174T cells (100 cells/mL in each well) were transferred to 24-well plates and cultured in 500 μL of RPMI 1640. Wells were divided into six groups with different final concentrations of PASODN: 0,1,2.5,5,10 and 20 μmol/L, respectively, the first one acted as a control. The medium was changed every other day. Ten days later, the cells in each well were stained with Giemsa and the colony-forming units were counted (consisting of more than 50 cells) under a phase contrast microscope. The optimal concentration of PASODN was screened according to the relative rate of inhibition of colony forming according to the formula: the relative rate of inhibition of colony-forming (%) = (1-numer of clone in experiment group/ number of clones in control group)×100%.

Inhibition of colony formation

Logarithmic phase cells were digested, suspended and calculated, and then suspension was transferred to 6-well plates. Cell concentration was 400 cells/mL in each well. Wells were divided into: PASODN group, PMSODN group, and PBS group. The

later two groups acted as controls. Twenty hours after the cells were adhered, RPMI 1640 was removed and wells were washed with 2.5×PBS. Cells were incubated with 2 mL of RPMI 1640 culture medium containing 10 μmol/L PASODN, 10 μmol/L PMSODN and PBS (same volume). Medium was changed every other day. The incubation was terminated 10 d later. The colony-forming units were stained by Giemsa dye and counted. Colony-forming efficiency = (unit number /cell number)×100%.

Inhibition of cell proliferation

LS-174T cells (10×10^3 cells/mL in each well) were transferred to 24-well plates. Wells were divided into three groups and the cells were treated as mentioned above in 1 mL of RPMI1640 culture medium. Medium was changed every other day. The number of cells in each group was counted every day, and morphological changes were observed. The growth curve of the cells was obtained 13 d later.

Variation of telomerase activity detected by PCR-ELISA and silver staining assay

PCR-ELISA was performed following the manufacturer's instructions. All solutions were provided by the kit from Roche.

Briefly, the cells were digested, collected and centrifuged at 800 r/min for 10 min seven days after treatment with the reagents mentioned above. The supernatant was discarded. A total volume of 200 mL of the refrigerated lysis medium was added into a tube and placed on ice for 30 min. The cells were centrifuged at at 16 000 *g* for 20 min at 4 ℃. Then 100 mL of the supernatant was removed into a new tube. The telomere sequence was amplified in a 50 mL PCR system containing 25 mL of reaction solution, 2 mL of supernatant, 23 mL of triple-distilled water. PCR amplification was performed in the 9600 thermal cycler (PEPKIN ELMER): one cycle of primer extension at 25 ℃ for 30 min, 2 cycles of the inactivation at 94 ℃ for 5 min, 3-32 cycles of amplification at 94 ℃ for 30 s, at 50 ℃ for 30 s, at 72 for 90 s. The amplification products were stored at 4 ℃.

The hybridization and ELISA were carried out as described below.

Denaturation solution and PCR products were incubated at room temperature for 10 min, 225 mL of hybridization solution was added and mixed thoroughly. Then 100 mL of the mixture was put in a 96-wells plate (provided by the kit), and the plate was vibrated (300 r/min) while it was incubated at 37 ℃ for 2 h. All the mixture was removed and the plate was rinsed 3 times. One hundred mL of anti-DIG peroxidase was added to each well, vibrated (300 r/min) and incubated at room temperature for 30 min. The solution was completely removed and each well was rinsed 5 times, 100 mL of substrate solution was added and incubated at room temperature for 15 min. Then the substrate solution was reserved, 100 mL stop solution was added into each well to terminate the discoloration development. The absorbance of the samples was measured (ΔSA value) at 450 nm and at 690 nm within 30 min after termination of the reaction. If the value of ΔSA of the sample was higher than '0.2ΔSA450 nm-ΔSA690nm', then the telomerase in the sample was regarded as positive. The final value was expressed as mean±SD, a statistical treatment was performed by using *t* test.

FCM analysis

Cells in logarithmic phase were incubated with 10 μmol/L PASODN for 72 h and subsequently harvested by trypsinization, beated upon with PRMI 1640 culture containing serum, and centrifuged at 1 000 r/min for 10 min. The supernatant was removed. The cells were fixed with 700 mL/L cold ethanol. FCM analysis of the DNA content was performed on a flow cytometer (FACS Calibur™ B.D USA).

Statistical analysis

The data were expressed as mean±SD. Analysis of data was performed using student's *t* test. $P<0.01$ was considered as statistically significant.

RESULTS

Optimal concentration of PASODN

Although colony formation in LS-174T cells was inhibited by PASODN at the lower concentrations (1, 2.5, 5 μmol/L) in a dose-dependent manner, 10 μmol/L seemed the best concentration and the relative rate of inhibition was 82.8% (slightly lower than that in 20 μmol/L group) (Table 1).

Table 1 Selection of optimal concentration of PASODN

Clones	Concentration of PASODN (μmol/L)					
	0	1	2.5	5	10	20
Mean	64.7	51.5	41.0	24.7	11.1	8.4
Inhibitive rate (%)	0	20.4	36.6	61.8	82.8	87.0

Effect of PASODN on colony formation

The colony-forming efficiency of cells treated with PASODN was 10.3%, which was significantly lower than that in PMSODN group ($P<0.01$, $t=3.174$) and PBS group ($P<0.01$, $t=3.263$). No significant difference was observed between PMSODN group and PBS group (Table 2).

Table 2 Colony-forming efficiency in each group (mean±SD)

	PASODN (10 μmol/L)	PMSODN (10 μmol/L)	PBS (same volume)
Mean±SD	41.2±5.5	196.3±13.5	202.8±8.5
Efficiency (%)	10.3	49.1	50.7
vs PASODN		$P<0.01$	$P<0.01$

Effect of PASODN on growth and morphology of LS-174T cells

No significant effect was observed during the initial 5 d, but a time-dependent effect was observed during the subsequent days (Table 3 and Figure 1). The growth inhibition was observed obviously from the 7th d, which reached the peak from the 11th to 13th d. But PMSODN had no evident effect on cell growth. Under microscopy, obvious morphological changes were observed in the cells of experiment group as follow. Cells turned round, cell membrances shrank, and nuclei were concentrated at the karyothecae. The number of cells was very small and cells did not compact with each other. On the other hand, cells in other groups grew bloomy and tightly (Figure 2).

Table 3 Variation of telomerase activity (mean±SD)

Group	*SA*	*P*
PASODN	0.18±0.12	
PMSODN	1.89±0.24	<0.01
PBS	1.98±0.25	<0.01

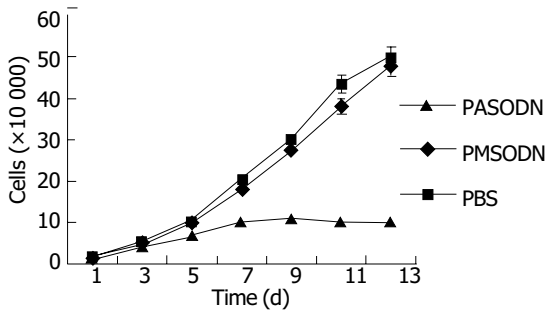

Figure 1 Curve of cell growth with time.

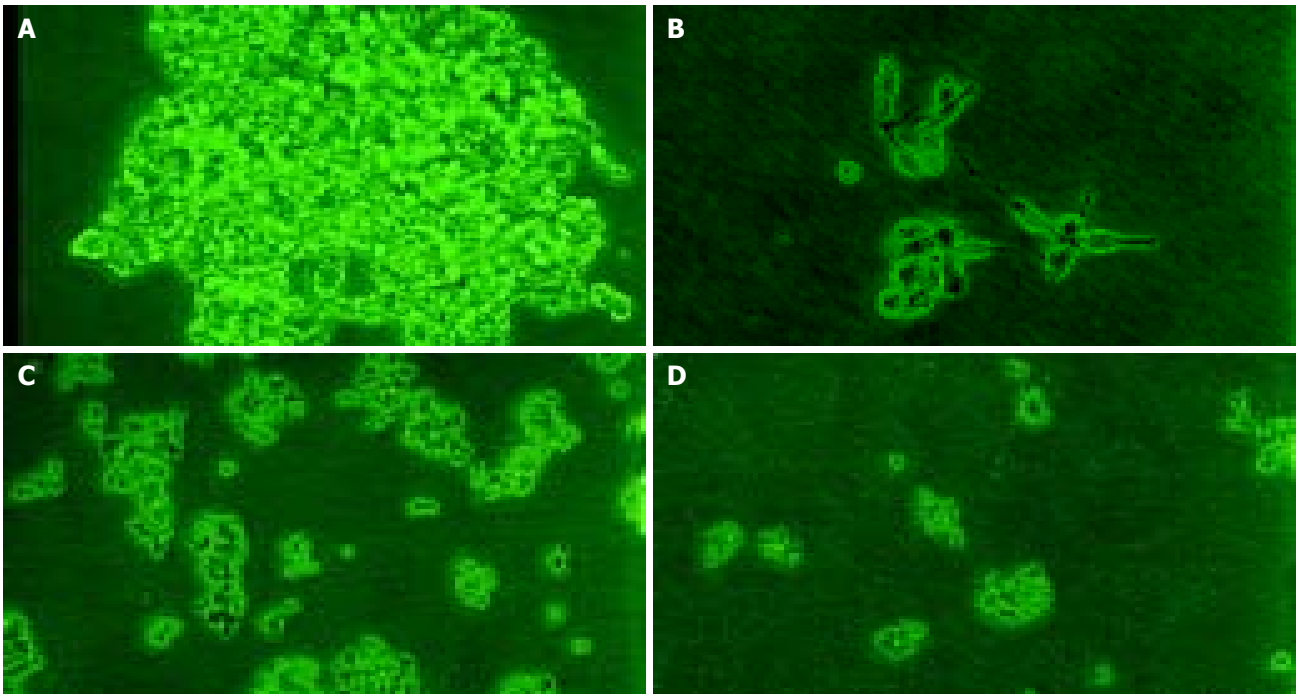

Figure 2 Changes in cell morphology and distribution. A: PMSODN group (10×40); B: PASODN group (10×40); C: PMSODN group (10×10); D: PASODN group (10×10).

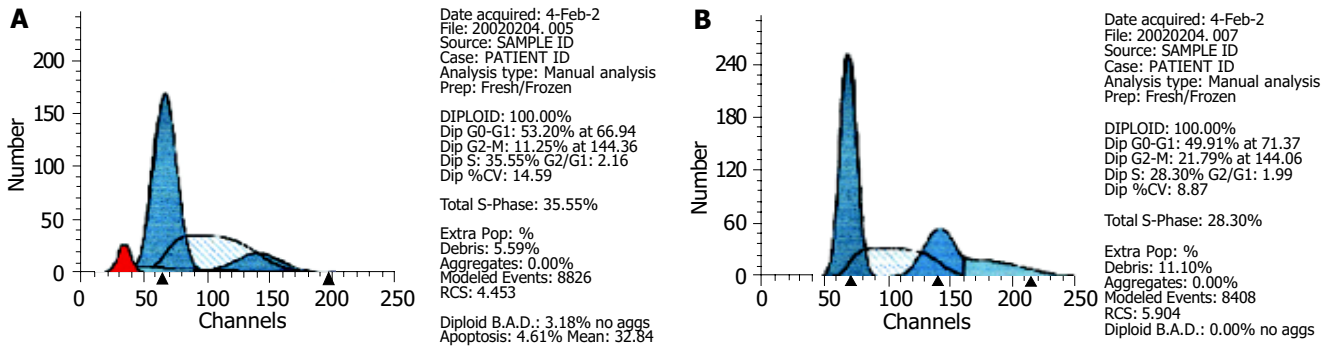

Figure 3 Cell cycle after 72 h of treatment with PASODN(A) and PMSODN(B) detected by FCM.

Variation of telomerase activity

Telomerase activity in PASODN group had no change. The ΔSA value of telomerase activity in PASODN group was significantly different from that in the other two control groups ($P<0.01$, $t = 3.317$ and 3.241, $t_{0.01\,(20)} = 2.845$) (Table 3).

Results of FCM

FCM analysis showed that the proportion of cells in G_0/G_1 and S phases increased appreciably 72 h after 10 μmol/L PASODN treatment, but no difference was observed between experiment and control groups (Table 4). A hypo diploid apex representing the apoptotic cells, was found before the apex of G_0/G_1 in the experiment group (Figure 3A), but not in control group (Figure 3B).

Table 4 Effect of PASODN on LS-174T cell cycle

Groups	G_0/G_1	G_2/M	S
Control	49.91	21.79	28.30
PASODN	53.20	11.25	35.55

DISCUSSION

With the development of living conditions, the incidence of colorectal cancer has been going up year by year. Colorectal cancer is not sensitive to traditional chemotherapy[9]. So, it seems important to exploit potent and nontoxic drugs in this field. Telomerase activity has been reported to express in cancer but not in most normal somatic cells, suggesting that telomerase might be an important target for chemotherapy. Telomerase consists of an RNA component (hTR) that binds to telomere and a protein component (hTERT) that acts as a reverse transcriptase. In our opinion, targeting the template region of hTR with anti-sense reagents (such as oligonucleotides) may offer more advantages than targeting hTERT gene. It has been reported that the expression of telomerase activity depends on Watson-Crick base pair between hTR gene and telomere[10]. This accessibility and indispensability make hTR an ideal and convincible target for oligonucleotides.

PASODN exerted its inhibitory effect on LS-174T cells both at the cellular and molecular levels, whereas no such effects were observed in the control groups. Moreover, the inhibitory effect was time and dose-dependent. The inhibitory effect of PASODN on the cells had a certain latent phase. The growth curve showed that the inhibitory effect of PASODN on the growth of LS-174T cells was obvious on the seventh day, and reached the greatest value from the 11th to 13th d. Besides, the growth curve combined with the result of telomerase activity showed that after telomerase activity turned negative (on the 7th d), the cells could still continue to cleavage a certain number

of times, and the phenomenon might be the "retarded effect" of telomerase inhibitor treatment.

In conclusion, specific oligonucleotide sequences can inhibit telomerase activity and lead to apoptotic cell death. The intrinsic existence of hTR in malignant tumors makes telomerase an ideal target for anti-sense reagent attack. But, we must pay attention to the fact that hTR also exists in normal somatic cells[11,12]. How to improve the tumor-affinity to oligonucleotids is still a problem. The lag phase[13] indicated that anti-telomerae inhibitors were unlikely to produce acute anti-proliferative effects. However, with researches going on in the field of telomerase and the advanced experiences of oligonucleotides in other molecular fields[14-16], the trial in animals and humans will be taken in near future.

REFERENCES

1 **Morin GB.** The human telomere terminal transferase enzyme is a ribonucleoprotin that synthesizes TTAGGG repeats. *Cell* 1989; **59**: 521-529

2 **Meyerson M**, Counter CM, Eaton EN, Ellisen LW, Steiner P, Caddle SD, Ziaugra L,Beijersbergen RL, Davidoff MJ, Liu Q, Bacchetti S, Haber DA, Weinberg RA. hEST2, the putative human telomerase catalytic subunit gene, is up-regulated in tumor cells and during immortalization. *Cell* 1997; **90**: 785-795

3 **Kim NW**. Clinical implications of telomerase in cancer. *Eur J Cancer* 1997; **33**: 781-786

4 **Wang XS,** Wang K, Zhang QF, Chen F, Zhang DZ, Fu SB. Clinical significance of determination of telomerase activity in gastric cancer. *Zhongguo Zhongliu Linchuang Zazhi* 2001; **28**: 450-453

5 **Shong SH,** Dong XS, Wang XS, Gao DQ, Fu SB, Li Y. Study on telomerase activity in human colorectal carcinoma and metastatic lymph nodes. *Haerbin Yike Daxue Xuebao* 2002; **36**: 29-31

6 **Kim NW**, Piatyszek MA, Prowse KR, Harley CB, West MD, Ho PL, Coviello GM, Wright WE, Weinrich SL, Shay JW. Specific association of human telomerase activity with immortal cells and cancer. *Science* 1994; **266**: 2011-2015

7 **Zhang FX**, Zhang XY, Fan DM, Deng ZY, Yan Y, Wu HP, Fan JJ. Antisense telomerase RNA induced human gastric cancer cell apoptosis. *World J Gastroenterol* 2000; **6**: 430-432

8 **Kyo S**, Inoue M. Complex regulatory mechanisms of telomerase activity in normal and cancer cells: how can we apply them for cancer therapy? *Oncogene* 2002; **21**: 688-697

9 **Bearss DJ**, Subler MA, Hundley JE, Troyer DA, Salinas RA, Windle JJ. Genetic determinants of response to chemotherapy in transgenic mouse mammary and salivary tumors. *Oncogene* 2000; **19**: 1114-1122

10 **Egholm M,** Buchardt O, Christensen L, Behrens C, Freier SM, Driver DA, Berg RH, Kim SK, Norden B, Nielsen PE. PNA hybridizes to omplementary oligonucleotides obeying the Watson-Crick hydrogen- bonding rules. *Nature* 1993; **365**: 566-568

11 **Hiyama E,** Hiyama K. Clinical utility of telomerase in cancer. *Oncogene* 2002; **21:** 643-649

12 **Nakamura TM**, Morin GB, Chapman KB, Weinrich SL, Andrews WH, Lingner J, Harley CB, Cech TR. Telomerase catalytic subunit homologs from fission yeast and human. *Science* 1997; **277**: 955-959

13 **Corey DR.** Telomerase inhibition, oligonucleotides, and clinical trials. *Oncogene* 2002; **21**: 631-637

14 **Crooke ST.** Potential roles of antisense technology in cancer chemotherapy. *Oncogene* 2000; **19**: 6651-6659

15 **Lebedeva I**, Stein CA. Antisense oligonucleotides: promise and reality. *Annu Rev Pharmacol Toxicol* 2001; **41**: 403-419

16 **Grillone LR**, Lanz R. Fomivirsen. *Drugs Today* 2001; **37**: 245-255

Edited by Wang XL and Kumar M **Proofread by** Xu FM

PO Box 2345, Beijing 100023, China
Fax: +86-10-85381893
E-mail: wjg@wjgnet.com www.wjgnet.com

World J Gastroenterol 2004;10(23):3459-3463
World Journal of Gastroenterology
Copyright © 2004 by The WJG Press ISSN 1007-9327

• COLORECTAL CANCER •

Honokiol: A potent chemotherapy candidate for human colorectal carcinoma

Fei Chen, Tao Wang, Yi-Feng Wu, Ying Gu, Xiao-Li Xu, Shu Zheng, Xun Hu

Fei Chen, Tao Wang, Ying Gu, Xiao-Li Xu, Shu Zheng, Xun Hu, Cancer Institute, Second Affiliated Hospital of Zhejiang University, Hangzhou 310009, Zhejiang Province, China
Yi-Feng Wu, Life Science College, Zhejiang University, Hangzhou 310027, Zhejiang Province, China
Supported by Cheung Kong Scholars Programme of National Ministry of Education, China, and Li Ka Shing Foundation, Hong Kong
Co-first-authors: Fei Chen and Tao Wang
Correspondence to: Professor Xun Hu, Cancer Institute, Second Affiliated Hospital of Zhejiang University, Hangzhou 310009, Zhejiang province, China. huxun@zju.edu.cn
Telephone: +86-571-87783868 **Fax:** +86-571-87214404
Received: 2004-02-14 **Accepted:** 2004-02-24

Abstract

AIM: To investigate the anticancer activity of Honokiol on RKO, a human colorectal carcinoma cell line *in vitro* and *in vivo*, and to evaluate its possible use in clinic.

METHODS: *In vitro* anticancer activity of honokiol was demonstrated by its induction of apoptosis in tumor cells. We analyzed cell proliferation with MTT assay, cell cycle with flow cytosmeter, DNA fragment with electrophoresis on agarose gels. To test the mechanism of honokiol-induced apoptosis, Western blotting was used to investigate the factors involved in this process. The pharmacokinetics study of honokiol was tested by high phase liquid chromatography. In *in vivo* study, Balb/c nude mice were incubated with RKO cells. Honokiol was injected intraperitoneally every other day into tumor bearing Balb/c nude mice.

RESULTS: Our results showed that honokiol induced apoptosis of RKO cells in a time- and dose-dependent manner. At 5-10 ug/mL for 48 h, honokiol induced apoptosis through activating Caspase cascades. Pharmacokinetics study demonstrated that, honokiol could be absorbed quickly by intraperitoneal injection, and maintained in plasma for more than 10 h. In nude mice bearing RKO-incubated tumor, honokiol displayed anticancer activity by inhibiting tumor growth and prolonging the lifespan of tumor bearing mice.

CONCLUSION: With its few toxicity to normal cells and potent anticancer activity *in vitro* and *in vivo*, honokiol might be a potential chemotherapy candidate in treating human colorectal carcinoma.

Chen F, Wang T, Wu YF, Gu Y, Xu XL, Zheng S, Hu X. Honokiol: A potent chemotherapy candidate for human colorectal carcinoma. *World J Gastroenterol* 2004; 10(23): 3459-3463
http://www.wjgnet.com/1007-9327/10/3459.asp

INTRODUCTION

In traditional Chinese medicine, Houpu (*Magnolia officinalis*) has long been one of the important herbs. It is widely used by Chinese people in treating thrombotic stroke, typhoid fever, anxiety and nervous disturbance[1] when used in combination with other herbs. With its major active constituent extracted from the bark of Houpu, honokiol has been found having a variety of pharmacological effects, such as anti-inflammatory[2], antithrombotic[3], anti-arrhythmic[4], antioxidative[5] and anxiolytic effects[6]. Recently, honokiol has been reported to exhibit a potent cytotoxicity by inducing cell apoptosis in rat and human leukemia cells[7,8], human fibrosarcoma cells[9], human squamous lung cancer CH27 cells[10] and human SVR angiosarcoma cells[11], yet there has been no report on honokiol in the treatment of human colorectal carcinoma.

Previous studies have shown that honokiol can induce apoptosis with characteristic morphological changes and DNA fragments, involvement of Caspase family and Bcl-2 family[10]. It could reduce tumor volume of SVR angiosarcoma in nude mice[11]. However, it is still unclear whether honokiol can be used as a monomer in clinic. In this study, we chose colorectal carcinoma cells to investigate its possible application in clinical practice.

MATERIALS AND METHODS

Cell line and reagents

Human colorectal cell line RKO was provided by the Cancer Institute of Zhejiang University. Cells were maintained in RPMI-1640 medium (Gibco BRL) supplemented with 100 mL/L heat-inactivated fetal bovine serum (Si-Ji-Qing Biotechnology Co, Hangzhou, China), 100 U/mL penicillin and 100 μg/mL streptomycin at 37 ℃ in a 50 mL/L CO_2 atmosphere. Antibodies used in this study including Caspases-3, -9 and pan-actin were purchased from NeoMarkers, Fremont, CA, USA. Honokiol was obtained from the National Institute for Pharmaceutical and Biological Products, Beijing, China. The drug was dissolved in dimethyl sulfoxide (DMSO) at the stock concentration of 10 g/L. It was further diluted in culture medium at the final DMSO concentration <1%. 3-(4, 5-dimethylthiazol-2-yl)-2, 5-diphenyltetrazolium bromide (MTT) was purchased from Sigma Chemical Corporation, USA. Six weeks old female Balb/c mice and female BALB/c nude mice (weighing 20±2 g each) were provided by the Experimental Animal Center of Zhejiang University.

Cell proliferation assay

Cells (1×10^4 in 100 μL) were seeded on 96-well plates in triplicate. Following a 24-h- culture at 37 ℃, the medium was replaced with fresh medium at various concentrations of honokiol in a final volume of 200 μL. Cells were incubated at 37 ℃ for 68 h[12,13]. Then 50 μL of MTT (2 mg/mL in PBS) was added to each well, incubated for an additional 4 h, the plate was centrifuged at 1 000 r/min for 10 min, then the medium was removed. MTT formazan precipitate was dissolved in 100 μL of DMSO, shaken mechanically for 10 min and then read immediately at 570 nm in a plate reader (Opsys MR, Denex Technology, USA).

Morphological changes and detection of DNA fragmentation

RKO cells were exposed to a variety of concentrations of honokiol for 24 h, then examined under reverse microscope

(Olympus) and imaged with a digital camera. To detect DNA fragments, the cells were collected and lysed with lysis buffer containing 50 mmol/L Tris-HCL (pH 7.5), 20 mmol/L EDTA, and 10 g/L NP-40. Then 10 g/L SDS and RNase (5 μg/mL) were added to the supernatants, and incubated at 56 ℃ for 2 h, followed by incubation with proteinase K (2.5 μg/mL) at 37 ℃ for 2 h. After the DNA was precipitated by addition of both ammonium acetate (3.3 mol/L) and ethanol (99.5 %), it was dissolved in a loading buffer. DNA fragmentation was detected by electrophoresis on 15 g/L agarose gels and was visualized with ethidium bromide staining.

Cell cycle analysis by FCM

Honokiol-treated RKO cells and vehicles were fixed with 700 mL/L alcohol for 15 min at 4 ℃, then stained with 1.0 μg/mL propidium dodide (PI, Sigma, USA). The red fluorescence of DNA-bound PI in individual cells was measured at 488 nm with a FACSCalibur (Becton Dickinson, USA) and the results were analyzed using ModFit 3.0 software. Ten thousand events were analyzed for each sample.

Western blot assay

RKO cells (5×10^6) were lysed by 4 g/L trypsin containing 0.2 g/L EDTA, then collected after washed twice with phosphate-buffered saline (PBS, pH 7.4). Total protein extracts from the cells were prepared using cell lysis buffer [150 mmol/L NaCl, 0.5 mol/L Tris-HCL (pH 7.2), 0.25 mol/L EDTA (pH 8.0), 10 g/L Triton X-100, 50 mL/L glycerol, 12.5 g/L SDS]. The extract (30 μg) was electrophoresed on 120 g/L SDS-PAGE gel and electroblotted onto polyvinydene difluoride membrane (PVDF, Millipore Corp., Bedford, MA) for 2 h in a buffer containing 25 mmol/L Tris-HCL (pH 8.3), 192 mmol/L glycine and 200 mL/L methanol. The blots were blocked with 50 g/L nonfat milk in TBST washing buffer for 2 h at room temperature and then incubated at 4 ℃ overnight with anti-caspase-3 and -9 antibodies (NeoMarkers), all of which were diluted 1:400 in TBST. After washed at room temperature with washing buffer, they were labeled with peroxidase-conjugated secondary antibodies.

Cell toxicity on primary cells

Primary human fibroblast cells were derived from fresh skin[13]. Human monocytes were isolated from umbilical blood by Ficoll-Hyaque separation method while seeded in 96-well microplates at the concentration of 5 μg/mL phytohemagglutinin (PHA)[14]. HUVECs isolated from fresh human umbilical cords were inoculated into 96-well microplates at 5 000 cells/well[15]. Following treatment with the concentrations of 5, 10, 20, 40 μg/mL of honokiol for 24 h, cell viability was estimated by trypan blue exclusion. Three wells were measured at each time point/concentration. Six wells were measured for each concentration of test compound. All toxicity experiments were at least repeated three times.

Pharmacokinetics study

For intraperitoneal (ip) pharmacokinetics study, honokiol was mixed with PEG400/dextrose by 7:3 in volume at a concentration of 20 g/L. Thirty Balb/c mice received honokiol by i.p. at a dose of 250 mg/kg. Blood samples were collected as described[16]. The plasma concentrations were tested by the total fluorescence intensity at 290 nm with high phase liquid chromatograph (HPLC, HEWLETT PACKARD)[17]. Chromatography was carried out using a Hypersil C18 column (5 mm×100 mm×2.1 mm) with a flow rate of 0.2 mL/min. Pharmacokinetic parameters were estimated by Modkine programs (Biosoft, UK).

In vivo efficacy evaluation

Effect of honokiol on ascites formation in Balb/c nude mice

Five Balb/c nude mice in each group were transplanted with 1×10^7 RKO cells by ip. Honokiol was dissolved in PEG400/Tween 20 (9:1 by volume). Honokiol-treated group was intragastrically administered 2 mg of honokiol per mice on d 0, 2, 4, 6, 8 and 10 after inoculation of RKO cells. While the control group was given the same volume of PEG400/Tween20. Animals were regularly monitored for the appearance of peritoneal bulge and body weight.

Effect of honokiol on solid tumor growth in Balb/c nude mice

RKO cells (5×10^6) were injected subcutaneously at the axilla of Balb/c nude mice. When tumors became visible about one week after implant, the animals were randomized into four groups: Adriamycin-treated, honokiol-treated, vehicle and control. All mice received ip injection on days 8-11, 14-17, 21-24 and 28-31. Each mouse of honokiol-treated group received 80 mg/(kg/d) of honokiol suspended in PEG400/dextrose (7:3 by volume) intraperitoneally, while vehicle given equivalent solvent of PEG400/dextrose. Adriamycin dissolved in saline was injected ip at a dose of 2 mg/kg. Mice of control group were given the same volume of saline. Tumor growth was monitored with calipers every other day, and tumor volume was calculated using the modified ellipsoid formula: $A/6\times A\times B^2$, where A is the longer axis and B is the axis perpendicular to A (Figure 1)[18].

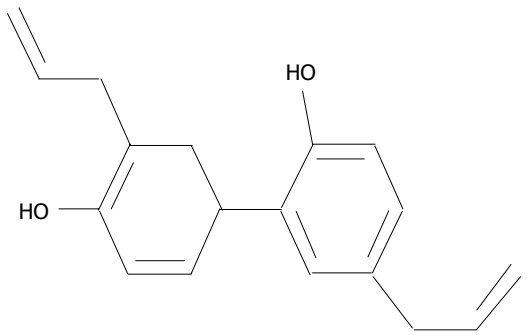

Figure 1 Chemical structure of honokiol ($C_{18}H_{18}O_2$, MW = 266.33).

Statistitical analysis

Values were given as mean±SD. Statistical comparisons were made by Student's *t*-test, and $P<0.05$ was taken as significant.

RESULTS

Inhibition of RKO cell proliferation

Cells treated with honokiol resulted in a dose- and time- dependent cytotoxicity in RKO cells. As shown in Figure 2A, honokiol-mediated cytotoxicity occurred at the concentration of 5 μg/mL and above. A significant decrease in cell number was seen at 10 μg/mL. The concentration leading to a 50% decrease in cell number (IC50) was about 12.47 μg/mL. Moreover, treatment of RKO cells with 5 μg/mL or 10 μg/mL of honokiol resulted in a significant growth inhibition at various time points (Figure 2B).

Morphological changes and DNA fragmentation detection in RKO cells

According to MTT results, we chose 5, 10, 15 μg/mL of honokiol to detect molecular changes. Under an inverted phase contrast microscope, honokiol-treated cells exhibited morphological features of apoptosis (Data not shown): rounded and granulated morphology, some vacuoles coming from cytoplasm, cell shrinkage and eventually detached from culture plates. In honokiol-treated cells, a degradation of chromosomal DNA into small internucleosomal fragments was evidenced by the formation of 180-200 bp DNA ladders on agarose gels (Figure 3), hallmark of cells undergoing apoptosis. No DNA ladders were detected in the samples isolated from control cultures. These results indicated that honokiol induced an apoptotic cell death in RKO cells.

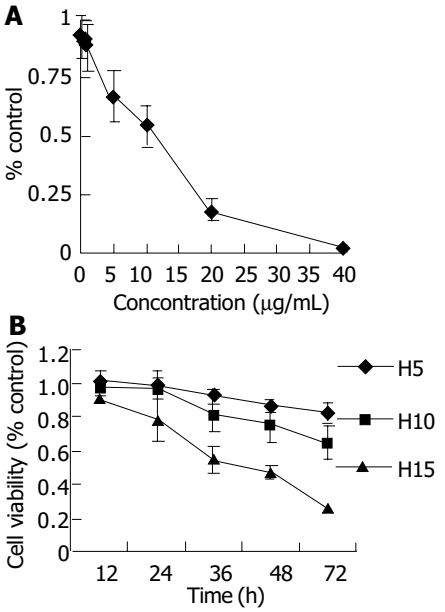

Figure 2 Concentration- and time-dependent inhibition of RKO cells exposed to honokiol shown by MTT assay. (A) RKO cells were plated in quadruplicate in 96-well plates and treated with increasing concentrations of honokiol for 68 h. (B) RKO cells treated with 5, 10 and 15 μg/mL of honokiol were tested at different time points.

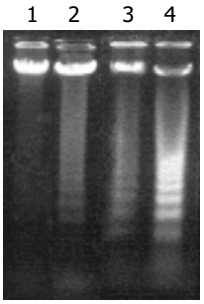

Figure 3 Differences in vehicle or honokiol induced apoptotic DNA laddering of RKO cells. lane 1: control; lane 2: 5 μg/mL; lane 3: 10 μg/mL; lane 4: 15 μg/mL.

Effect of honokiol on cell cycle analysis of RKO cells

RKO cells were exposed to increasing concentrations of honokiol (5-15 μg/mL) for 48 h, and the growth of cells was analyzed with flow cytometry. In the absence of honokiol, the cell populations were at G1, S, and G2/M phases (Figure 4), accompanied with increased concentrations of honokiol by a concomitant increase of the G1 phase (Table 1). From Figure 4, the peak areas of subdiploid were enlarged with increased concentrations of honokiol. This observation led to a suggestion of G1 arrest. DNA fragmentation was seen when the cells were exposed to honokiol at 10 μg/mL and above (14.10% and 20.31%, respectively).

Table 1 Effect of honokiol on cell cycle distribution and apoptosis of RKO cells

Groups	Cell cycle distribution (%)			Apoptosis (%)
	G0/G1	S	G2/M	
ControL	44.45	45.10	10.14	0.27
5 μg/mL	48.03	42.37	9.60	4.51
10 μg/mL	54.04	40.30	5.66	14.10[a]
15 μg/mL	58.94	39.36	1.70	20.31[b]

[a]$P<0.05$, [b]$P<0.01$ *vs* corresponding control group. Cell cycle distribution was determined after 48 h of treatment in each group. The tabulated percentages were an average calculated on the results of three separate experiments. The results were represented by mean±SD (n = 3).

Caspase -3 and -9 expression by Western blot

Since Caspases are the main factors in the apoptotic pathway, we investigated whether Caspases were involved in inducing apoptosis of RKO cells treated with honokiol. Cells induced for 48 h were analyzed for protein expression by Western blot. The results showed that Caspase-3 and -9 were up-regulated in a dose-dependent manner (Figure 5).

Effects of honokiol on primary cultured cells

As shown in Figure 6, honokiol had little cytocidal effect on primary human fibroblast cells and human lymphocytes even up to 40 μg/mL. HUVEC cells after honokiol treatment resulted in a sharply dose-dependent cytotoxicity. These

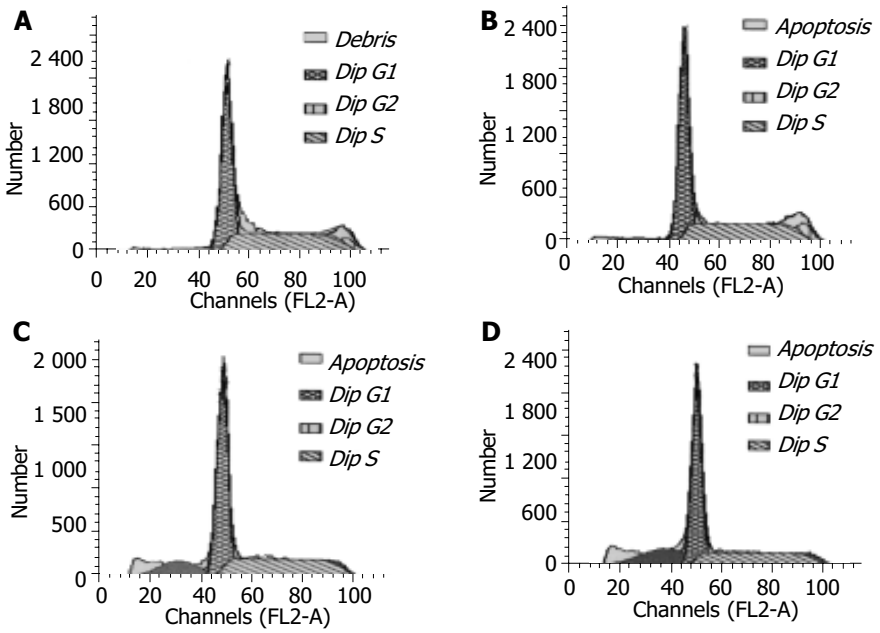

Figure 4 Apoptosis of RKO cells detected by FCM. (A) control; (B) 5 μg/mL; (C) 10 μg/mL; (D) 15 μg/mL.

results demonstrated that human fibroblast cells and lymphocytes were more resistant to the honokiol-mediated cytotoxicity than HUVECs.

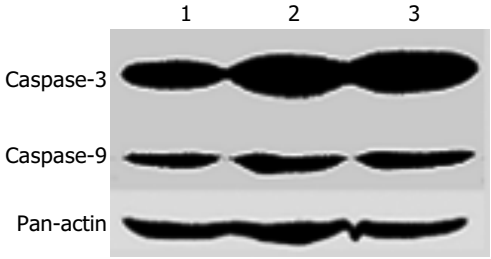

Figure 5 Western blot analysis for the expression of Caspase-3 and -9 in human colorectal carcinoma cell line RKO cells. Lane 1: vehicle; lane 2: 5 μg / mL; lane 3: 10 μg / mL.

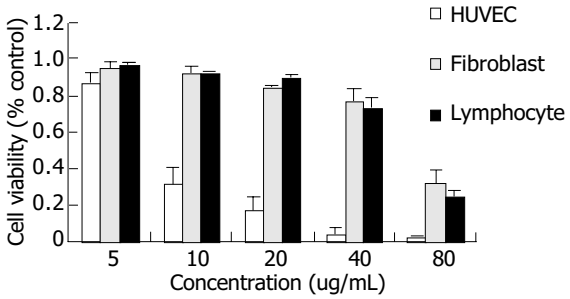

Figure 6 Cytocidal effect of honokiol on the growth of primary cultured human umbilical vein endothelial cells, primary human fibroblast cells and human lymphocytes.

Pharmacokinetics studies

The pharmacokinetics of honokiol was evaluated after intraperitoneal injection of 250 mg/kg to BALB/c mice. The maximum plasma concentration of honokiol was observed at 27.179±6.252 min after administration (Figure 7). The plasma disappearance curve could best be described by a first-order absorption one-compartment model, with an absorption half-life of 10.121±2.761 min, and an elimination half-life of 5.218±0.461 h (Figure 7).

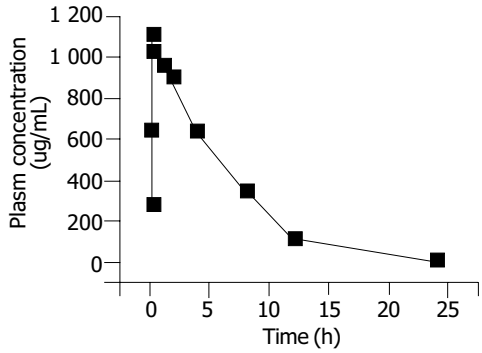

Figure 7 Honokiol concentration in plasma of BALB / c mice.

Inhibition of tumor growth in nude mice implanted with RKO cells

We studied the effect of honokiol on the growth of RKO tumor. There was significant inhibition of tumor growth by honokiol (Table 2). All the control mice developed peritoneal bulge and died by d 12. However, no peritoneal bulge was observed in 80% of the honokiol-treated animals and the mice survived for up to 30 d. These observations indicated the anti-tumor activity of honokiol *in vivo* (Table 2).

Table 2 Effect of honokiol on ascites growth of tumor in Babl / c nude mice

Group	Ascites	MST (d)	Dead (D)	Living (L)	Survival percentage (L / (D+L)×100%)
Control	5	10.7	5	0	0%
Honokiol	1	34.3	1	4	80%

MST: Mean survival time. RKO cells were transplanted intraperitoneally. Honokiol was administered 2 mg per mice on d 0, 2, 4, 6, 8, and 10 after tumor transplantation. The mice were monitored for peritoneal bulge and survived for up to 30 d. Control mice died by d 12 of RKO inoculation.

Inhibition of solid tumor growth in nude mice bearing RKO cells

From Figure 8, animals in control and vehicle groups showed a progressive increase in tumor volume, with a growth rate of 1627.6% and 1408.2% respectively on d 28. While in treated groups, tumor growth rate was increased to 968.9% in adriamycin group and 709.9% in honokiol-treated group. There was a significant difference between honokiol-treated group and its control (treated with PEG400/dextrose) (P<0.05). Similar results were found between adriamycin-treated group and its control (P<0.05). These data further confirmed that honokiol had an effective anticancer activity *in vivo*.

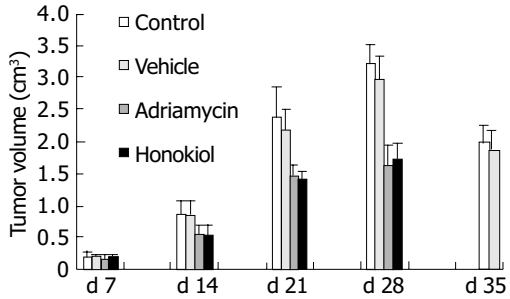

Figure 8 Effect of honokiol on the growth of xenografted RKO in Balb / c nude mice. The Y-axis represents tumor volume, X-axis represents time (day) after RKO cell inoculation.

Prolongation of life-span in nude mice bearing RKO solid tumor

The lifespan of mice in honokiol-treated group (80 mg/kg) was monitored and compared to the vehicle and adriamycin-treated group (Table 3). The mean survival time was 50.9 d in honokiol-treated group, with a significant prolongation compared to vehicle group (29.7 d, P<0.05). The survival rate in honokiol-treated group was 176.7%, much higher than that in vehicle group (P<0.01). There was no significant difference between control and vehicle groups and between adriamycin-treated and honokiol-treated groups. The results demonstrated that honokiol had a similar effect to adriamycin in prolongation of lifespan of tumor-bearing nude mice.

Table 3 Effect of honokiol on MST and T / C% in Balb / c nude mice bearing RKO-incubated tumor

Group	Number of mice	MST (d)	T / c (%)
Control	7	28.8	100
Vehicle	6	29.7	104.5
Adriamycin	7	46.2[a]	160.4[b]
Honokiol	7	50.9[a]	176.7[b]

MST, mean survival time. The survival rate (T / C%) was calculated according to the following equation: T / C (%) = [average survival period in the test group / average survival period in the control group]×100. [a]P<0.05; [b]P<0.01 *vs* vehicle or control.

DISCUSSION

Many anticancer drugs kill tumor cells by inducing apoptosis. Previous studies suggest that growth inhibition by honokiol resulted from the induction of apoptosis in several cell lines[7-11]. A further study reported that in human squamous lung cancer cells, honokiol induced apoptosis by down-regulating Bcl-X_L and sequentially activating Caspase cascade[10]. Our results confirmed this honokiol-mediated apoptotic progression in cultured RKO cells.

A variety of compounds with potent anticancer activity *in vitro* could not be used in clinic, one probable reason was due to their strong toxicities to normal cells[17,18]. Therefore, we first investigated honokiol's effects on the toxicity of primary cultured human cells. Our data demonstrated that the IC50s were much higher in human fibroblasts and lymphocytes than in RKO cells, with the exception that HUVECs were more sensitive to honokiol. The safe doses for fibroblasts and lymphocytes could be up to 40 μg/mL (Figure 6), much greater than that for RKO and other tumor cells (data not shown). The phenomenon that primary cultured endothelial cells were more sensitive to honokiol might be related to the finding that honokiol had antiangiogenesis activity by inhibiting VEGF and its receptor 2 *in vitro*[11]. In chemotherapy, antiangiogenesis is another important target besides apoptosis induction in tumor cells. Based on the fewer toxicity to normal fibroblasts and lymphocytes, we thus proposed that honokiol could be a safe and potent candidate of chemotherapy for colorectal cancer *in vivo*.

Another major obstacle was that many potent agents were poorly absorbed and quickly cleared *in vivo*, such as curcumin. Curcumin was difficult to absorb in the gastrointestinal tract and, even when systemically administered, it was rapidly cleared by hepatic metabolism[11].

We then established two *in vivo* models with Babl/c nude mice bearing RKO cells, the ascitic tumor model and the solid tumor model. In RKO ascitic tumor model, honokiol exhibited a strong efficiency in prolonging the lifespan of ascitic tumor bearing mice and was highly effective on inhibiting intraperitoneal ascites in Balb/c nude mice. In our another model, honokiol also exhibited a potent efficiency in inhibiting solid tumor growth. In RKO incubated tumor bearing mice, honokiol at 80 mg/kg significantly inhibited the tumor growth and prolonged the lifespan compared to the vehicle ($P<0.05$). The antitumor efficiency of honokiol was similar to that of the commonly used chemotherapy drug, adriamycin.

The results of the present study are encouraging because honokiol has shown significant inhibition of tumor growth *in vitro* and *in vivo*, as well as prolongation of lifespan in tumor-bearing mice *in vivo*. Together with its safety to human, honokiol might be a promising chemotherapy candidate in treating colorectal carcinoma or other cancers in clinic.

REFERENCES

1 **Squires RF,** Ai J, Witt MR, Kahnberg P, Saederup E, Sterner O, Nielsen M. Honokiol and magnolol increase the number of [3H] muscimol binding sites three-fold in rat forebrain membranes in vitro using a filtration assay, by allosterically increasing the affinities of low-affinity sites. *Neurochem Res* 1999; **24:** 1593-1602

2 **Liou KT,** Shen YC, Chen CF, Tsao CM, Tsai SK. The anti-inflammatory effect of honokiol on neutrophils: mechanisms in the inhibition of reactive oxygen species production. *Eur J Pharmacol* 2003; **475**: 19-27

3 **Teng CM,** Chen CC, Ko FN, Lee LG, Huang TF, Chen YP, Hsu HY. Two antiplatelet agents from Magnolia officinalis. *Thromb Res* 1988; **50**: 757-765

4 **Liou KT,** Lin SM, Huang SS, Chih CL, Tsai SK. Honokiol ameliorates cerebral infarction from ischemia-reperfusion injury in rats. *Planta Med* 2003; **69**: 130-134

5 **Lo YC,** Teng CM, Chen CF, Chen CC, Hong CY. Magnolol and honokiol isolated from Magnolia officinalis protect rat heart mitochondria against lipid peroxidation. *Biochem Pharmacol* 1994; **47**: 549-553

6 **Kuribara H,** Kishi E, Hattori N, Yuzurihara M, Maruyama Y. Application of the elevated plus-maze test in mice for evaluation of the content of honokiol in water extracts of magnolia. *Phytother Res* 1999; **13**: 593-596

7 **Hirano T,** Gotoh M, Oka K. Natural flavonoids and lignans are potent cytostatic agents against human leukemic HL-60 cells. *Life Sci* 1994; **55**: 1061-1069

8 **Hibasami H,** Achiwa Y, Katsuzaki H, Imai K, Yoshioka K, Nakanishi K, Ishii Y, Hasegawa M, Komiya T. Honokiol induces apoptosis in human lymphoid leukemia Molt 4B cells. *Int J Mol Med* 1998; **2**: 671-673

9 **Nagase H,** Ikeda K, Sakai Y. Inhibitory effect of magnolol and honokiol from Magnolia obovata on human fibrosarcoma HT-1080. Invasiveness *in vitro*. *Planta Med* 2001; **67**: 705-708

10 **Yang SE,** Hsieh MT, Tsai TH, Hsu SL. Down-modulation of Bcl-Xl, release of cytochrome c and sequential activation of caspases during honokiol-induced apoptosis in human squamous lung cancer CH27 cells. *Biochem Pharmacol* 2002; **63**: 1641-1651

11 **Bai X,** Cerimele F, Ushio-Fukai M, Waqas M, Campbell PM, Govindarajan B, Der CJ, Battle T, Frank DA, Ye K, Murad E, Dubiel W, Soff G, Arbiser JL. Honokiol, a small molecular weight natural product, inhibits angiogenesis *in vitro* and tumor growth *in vivo*. *J Biol Chem* 2003; **278**: 35501-35507

12 **Arbiser JL,** Panigrathy D, Klauber N, Rupnick M, Flynn E, Udagawa T, D'Amato RJ. The antiangiogenic agents TNP-470 and 2-methoxyestradiol inhibit the growth of angiosarcoma in mice. *J Am Acad Dermatol* 1999; **40**(6pt 1): 925-929

13 **LaMontagne KR Jr,** Moses MA, Wiederschain D, Mahajan S, Holden J, Ghazizadeh H, Frank DA, Arbiser JL. Inhibition of MAP kinase kinase causes morphological reversion and dissociation between soft agar growth and *in vivo* tumorigenesis in angiosarcoma cells. *Am J Pathol* 2000; **157**: 1937-1945

14 **Beddy D,** Watson RW, Fitzpatrick JM, O'Connell PR. Increased vascular endothelial growth factor production in fibroblasts isolated from strictures in patients with Crohn's disease. *Br J Surg* 2004; **91**: 72-77

15 **Goldrosen MH,** Gannon PJ, Lutz M, Hloyoke ED. Isolation of human peripheral blood lymphocytes: modification of a double discontinuous density gradient of Ficoll-Hypaque. *J Immunol Methods* 1977; **14**: 15-17

16 **Agrawal S,** Jiang Z, Zhao Q, Shaw D, Cai Q, Roskey A, Channavajjala L, Saxinger C, Zhang R. Mixed-backbone oligonucleotides as second generation antisense oligonucleotides: *in vitro* and *in vivo* studies. *Proc Natl Acad Sci U S A* 1997; **94**: 2620-2625

17 **Tsai TH,** Chou CJ, Cheng FC, Chen CF. Pharmacokinetics of honokiol after intravenous administration in rats assessed using high-performance liquid chromatography. *J Chromatogr B Biomed Appl* 1994; **655**: 41-45

18 **Eikesdal** HP**,** Bjerkvig R, Dahl O. Vinblastine and hyperthermia target the neovasculature in BT (4) AN rat gliomas: therapeutic implications of the vascular phenotype. *Int J Radiat Oncol Biol Phys* 2001; **51**: 535-544

Edited by Wang XL **Proofread by** Zhu LH and Xu FM

PO Box 2345, Beijing 100023, China
Fax: +86-10-85381893
E-mail: wjg@wjgnet.com www.wjgnet.com

World J Gastroenterol 2004;10(23):3464-3469
World Journal of Gastroenterology
Copyright © 2004 by The WJG Press ISSN 1007-9327

• *H pylori* •

Diagnosis of *Helicobacter pylori* infection and diseases associated with *Helicobacter pylori* by *Helicobacter pylori* outer membrane proteins

Zheng Jiang, Ai-Long Huang, Xiao-Hong Tao, Pi-Long Wang

Zheng Jiang, Xiao-Hong Tao, Pi-Long Wang, Department of Gastroenterology, the First Affiliated Hospital, Chongqing University of Medical Sciences, Chongqing 400016, China
Ai-Long Huang, Institute of Viral Hepatitis, Chongqing University of Medical Sciences, Chongqing 400010, China
Supported by the Basic Research Fund of Science and Technology Committee of Chongqing, [2002] 18-86; National Natural Science Foundation of China, No.30371318
Correspondence to: Dr. Zheng Jiang, Department of Gastroenterology, the First Affiliated Hospital, Chongqing University of Medical Sciences, Chongqing 400016, China. jianggooddoctor@mail.china.com
Telephone: +86-23-68891218
Received: 2003-10-15 **Accepted:** 2003-12-06

Abstract

AIM: To examine the serological response of patients with upper gastrointestinal diseases and *Helicobocter pylori* (*H pylori*) infection to two *H pylori* outer membrane proteins (OMPs) (M_r18 000 and M_r26 000) acquired by gene recombinant technique, and to determine the diagnostic significance of serological tests derived from these OMPs.

METHODS: Recombinant vectors encoding the two *H pylori* OMPs were used to transform and express in BL21 (DE3) *E.coli*. After purification with Ni^{2+}-NTA agarose resin, colloid gold kits were prepared with purified recombinant proteins to detect *H pylori* infection and *H pylori*-associated diseases by the immunity-marker technology. We selected 150 patients with *H pylori* infection and digestive symptoms without previous treatment, including chronic gastritis (n = 60), duodenal ulcer (n = 30), gastric ulcer (n = 30), and gastric cancer (n = 30). As controls, 33 *H pylori*-negative healthy volunteers were also recruited. Serum samples were collected from all subjects, and the antibodies to specific proteins of *H pylori* were tested with the colloid gold test kits. The sensitivity, specificity and accuracy of the colloid gold tests were evaluated, by using the combination of standard diagnostic methods (^{13}C urea breath test and bacteria culture) and classic enzyme-linked immunosorbent assay (ELISA) as reference.

RESULTS: After purification with Ni^{2+}-NTA agarose resin, the purity of recombinant fusion proteins was about 95%. The recombinant fusion proteins were recognized by the specific monoclonal antibodies against the two *H pylori* OMPs, as demonstrated by the ELISA. Of the 150 serum samples from patients infected with *H pylori* 141 (94.0%) responded positively to the recombinant protein with M_r26 000, while the seropositive rates were 95.0%, 96.7%, 96.7% and 90.0% for patients with *H pylori*-associated chronic gastritis, duodenal ulcer, gastric ulcer, and gastric cancer respectively. The sensitivity, specificity, and accuracy of the colloid gold kit with M_r26 000 protein were 94.0%, 97.0%, and 94.5%, respectively. Compared with the classic ELISA, bacteria culture and ^{13}C urea breath test results in detecting *H pylori*-infection, there was no significant difference (P>0.05). For the colloid gold kit with M_r18 000, the seropositive rates were 52.0%, 40.0%, 40.0%, 53.3% and 86.7%, respectively, in *H pylori*-infected patients, and those with *H pylori*-associated chronic gastritis, duodenal ulcer, gastric ulcer, and gastric cancer. There was a significant difference (P<0.05) in seropositivity between patient with gastric cancer (86.7%) and those with other diseases (43.3%).

CONCLUSION: The two colloid gold kits derived from the recombinant OMPs are useful tools either for detecting *H pylori* infection, or for, predicting *H pylori*-associated gastric malignancy.

Jiang Z, Huang AL, Tao XH, Wang PL. Diagnosis of *Helicobacter pylori* infection and diseases associated with *Helicobacter pylori* by *Helicobacter pylori* outer membrane proteins. *World J Gastroenterol* 2004; 10(23): 3464-3469
http://www.wjgnet.com/1007-9327/10/3464.asp

INTRODUCTION

Since the initial report of an unidentified curved bacillus located on the gastric epithelium of patients with chronic active gastritis, the discovery of *Helicobocter pylori* (*H pylori*) and its association with a number of gastrointestinal diseases has revolutionized gastroenterology. It has attracted the interest of scholars in gastroenterology and microbiology. Infection of gastric mucosa with *H pylori* could be found in approximately 50% of the world population[1], its association with peptic ulcer disease, chronic gastritis, mucosa-associated lymphoid tissue lymphoma, and gastric adenocarcinoma has been well documented over the past two decades[2-19]. Moreover it was also found in some extradigestive diseases[20-36]. The direct evidence of carcinogenesis was recently demonstrated in an animal model[37,38], so this organism has been recently categorized as a class I carcinogenetic factor by the World Health Organization. It is obviously important to detect and eradicate *H pylori* infection.

The routine detecting methods including invasive and non-invasive tests have differences in sensitivity and specificity, each with their indication and characteristics in clinical practice[39-48]. Because of great quantity of serum samples especially in epidemiological studies, enzyme linked immunosorbent assay (ELISA) is the widely used test[49-52]. Antigens used in ELISA are divided into three kinds. The first is the total cell of microbacteria sonicated by ultrasonic wave, which is easy to be confused with *Helicobacter*, campylobacter, or a diverse range of other bacteria and incur to intercourse response with each other in detecting *H pylori* infection. The second is the partly purified antigens, with greatly increased specificity and decreased intercourse response, but *H pylori* could not be cultured in great quantity without special apparatus and conditions. The last is the recombinant purified antigen by gene recombinant technique. To date, many genes of OMP of *H pylori* have been amplified by scholars with polymerase chain

reaction from *H pylori* chromosomes and inserted into the compatible sites of expression vectors by using T_4 DNA ligase. Moreover recombinant vectors could be expressed in *E.coli*[53-62], but a few reports are available on lower-molecular-mass OMP application to the detection of *H pylori* infection and diagnose *H pylori*-associated diseases. In order to acquire a great amount of purified 18 000, 26 000 OMP of *H pylori*, we constructed recombinant vectors containing genes encoding with M_r18 000, 26 000 OMP of *H pylori* expressed in *E.coli* respectively and identified the antigenicity of expressed products[63]. So we prepared the colloid gold kits with purified recombinant proteins by antigen-antibody reaction and gold-marked technique to determine whether they were capable of detecting *H pylori* infection and *H pylori*-associated diseases.

MATERIALS AND METHODS

Material

Well-characterized strains of BL21/pET32a (+) /Omp_{26}, BL21/pET32a (+) /Omp_{18} were constructed, expressed and identified by the Department of Microbiology. The expression fusion proteins were recognized by the corresponding monoclonal antibody with M_r18 000, 26 000 OMP of *H pylori* and the animal's serum immunized with recombinant fusion proteins respectively. After purification using Ni^{2+}-NTA agarose resin columniation, the purity of recombinant fusion proteins was about 95%. ^{13}C urea breath test was purchased from Headway Company, Ni^{2+}-NTA agarose resin columniation was obtained from QIAGEN Company, ultrasonic liquid (50 mmol/L NaH_2PO_4, 300 mmol/L NaCl, PH 7.0), abluent (50 mmol/L phosphate, 300 mmol/L NaCl, 20 mmol/L imidazole, pH 7.80) and lavation (50 mmol/L phosphate, 300 mmol/L NaCl, 250 mmol/L imidazole, pH 7.80) were provided by the Institute of Viral Hepatitis of Chongqing University of Medical Sciences.

Sample collection

Sera were collected from 150 patients with gastrointestinal symptoms and *H pylori* infection in the Outpatient Clinic of the Gastroenterology Department of the University Hospital during Jan. 2002 to Dec. 2002 including 60 cases of gastritis, 30 cases of gastric ulcer, 30 cases of duodenal ulcer and 30 cases of gastric cancer diagnosed by gastroscopy. Sera from 31 healthy volunteers without *H pylori* infection were collected as control. All testee were forbidden to take H_2-antagonists, corticosteriods, proton pump inhibitors and antibiotics within 4 wk.

Expression of recombinant plasmid

Single bacterial colonies (BL21/pET32a (+) /Omp_{18}, BL21/pET32a (+) /Omp_{26}) were picked and cultured respectively in 2 mL LB broth containing 100 mg/L of ampicillin, at 300 r/min at 37 ℃ overnight. On the next day, BL21 *E.coli* strains containing recombinant plasmids were grown until mid-log phase (Absorbence at 600 nm = 0.5 to 1.0), and then induced to express recombinant fusion proteins in 100 mL LB by adding 1 mmol/L IPTG for 4 h. Following induction, bacteria were harvested by centrifugation at 12 000 r/min for 15 min, and stored at -20 ℃ for SDS-PAGE analysis.

Immunoblot analysis of recombinant fusion protein

Due to C end of recombinant fusion antigens with six histidines, recombinant fusion antigens were purified with Ni^{2+}-NTA agarose resin. Briefly, 500 mL of cultivated bacteria suspension was prepared, centrifuged, resuspended with the buffer liquid (50 mmol/L phosphate, 300 mmol/L NaCl, pH 7.0), and sonicated by ultrasonic wave with the energy of 600 W×35% for 40 min, and ultracentrifuged for 15 min at 10 000 *g* at 4 ℃. The sonicated recombinant fusion antigens were purified using Ni^{2+}-NTA agarose resin with abluent (50 mmol/L phosphate, 300 mmol/L NaCl, 20 mmol/L imidazole, pH 7.80) and lavation (50 mmol/L phosphate, 300 mmol/L NaCl, 250 mmol/L imidazole, pH 7.80), and quantified. The antigenicities of expressed recombinant fusion proteins were determined by immunoblotting. Following electrophoretic transfer of SDS-PAGE-separated (150 g/L acrylamide) recombinant fusion proteins to 0.45 μm pore size PVDF membrane, and after a 30-min wash in tris-saline blotting buffer, antigen-impregnated PVDF strips were incubated with the sera from patients infected with *H pylori* and anti-Omp_{18} or anti-Omp_{26} antibody for 2 h at RT. After washed, the proteins were detected by incubating the strips in alkaline phosphatase-conjugated goat anti-man IgG and alkaline phosphatase-conjugated goat anti-mice IgG antibody for 1 h at RT.

Colloid gold test of H pylori OMP

With gold marker and special antigen-antibody reaction technique, *H pylori* infection could be detected using the antigen-antibody-antigen method. The recombinant fusion proteins were impregnated in nitrocellulose membrane (NC) as a detecting strip, the recombinant fusion proteins were marked with gold as a colored reagent by which the special antibody of patient serum to *H pylori* could be detected in seconds. The criteria of the test were as follows: Negative (-): antigen-impregnated NC membrane was not recognized by patient serum, non-special antibody to *H pylori* in patient serum, so there was only an aubergine strip in mass-control district, and not in detecting district simultaneously. Positive (+): antigen-impregnated NC membrane was recognized by patient serum, special antibody to *H pylori* in patient serum. In mass-control and detecting district, there were aubergine strips. If there was no aubergine strip in mass-control district, errors might occur in experiment course. The colloid gold test paper is shown in Figure 1.

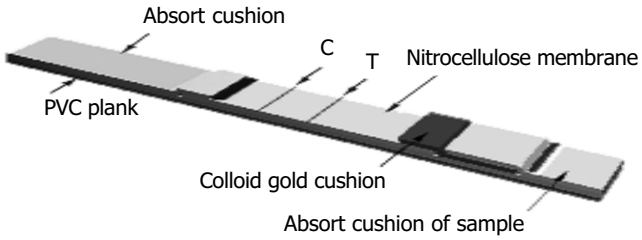

Figure 1 Colloid gold test paper.

Diagnostic criteria of the test

The sensitivity, specificity and accuracy of the colloid gold kits were evaluated on the basis of the serum ELISA results taken as reference with combined of standard diagnostic methods (^{13}C urea breath test, bacteria culture as the gold standard). Patients were defined as *H pylori* infection if one out of two validated tests of ^{13}C urea breath test and culture was positive, and as non-*H pylori* infection if two tests were negative. Patients infected with *H pylori* were determined as false negative if the colloid gold kits were negative; patients without *H pylori* infection were determined as false positive if the colloid gold kits were positive. Based on the above results, the applied value of the colloid gold kit in clinical practice was evaluated.

RESULTS

Analysis of recombinant fusion protein

After pET32a (+) /Omp_{18} and pET32a (+) /Omp_{26} were transfected into BL21 *E.coli* strains, the strains with high expressions of fusion proteins were selected and grown respectively until mid-log phase (Absorbence at 600 nm = 0.4 to 0.6), and then

induced to express recombinant fusion proteins by adding of 1 mmol/L IPTG for 4 h. Following induction, bacteria were harvested by centrifugation at 12 000 *g* for 5 min, resuspended in protein-buffer and seethed for 5 min. Their molecular mass was M_r38 000 and 46 000 respectively by 150 g/L SDS-PAGE gel analysis. After the recombinant bacteria were sonicated by ultrasonic wave and ultracentrifuged (10 000 *g*, 15 min, 4 ℃), the levels of soluble fusion proteins in the supernatant were about 18.96% and 26.38% of total cellular protein respectively. After purification by Ni^{2+}-NTA agarose resin columniation, the purity was about 95%. Recombinant fusion proteins were all recognized by the corresponding monoclonal antibody with M_r18 000, 26 000 OMP of *H pylori* and the animal's serum immunized with recombinant fusion proteins respectively. The results showed recombinant fusion proteins could provide excellent antigenicity.

Detection of H pylori infection by colloid gold kit

Sera from 150 patients with gastrointestinal symptoms and *H pylori* infection including 60 cases of gastritis, 30 cases of gastric ulcer, 30 cases of duodenal ulcer and 30 cases of gastric cancer examined by gastroscopies, and sera from 33 healthy volunteers without *H pylori* infection were assayed using the colloid gold kits with M_r18 000, 26 000 respectively (Table 1, Figure 2). The results were as follows. Ninety-four percent of patients infected with *H pylori* showed response to recombinant protein with M_r26 000, while 95%, 96.7%, 96.7% and 90.0% of patients with *H pylori*-infected chronic gastritis, gastric ulcer, duodenal ulcer, and gastric cancer showed responses (Table 2). There was no significant difference between the conventional examined methods and the colloid gold kits (P>0.05), indicating that the prevalence of infection diagnosed by both methods was similar. To specific recombinant protein with M_r18 000, 52.0% of patients showed response, while 40.0%, 40.0%, 53.3% and 86.7% of patients with *H pylori*-infected chronic gastritis, gastric ulcer, duodenal ulcer, and gastric cancer respectively showed responses (Table 3). Moreover there was a significant difference (P<0.05) in the detecting rates of *H pylori* infection between patients with gastric cancer (86.7 %) and those with other diseases (43.3%). Based on the classic ELISA, bacteria culture and ^{13}C urea breath test results, the sensitivity, specificity, and accuracy of the colloid gold kit with M_r26 000 protein were 94.0%, 97.0%, and 94.5%, respectively.

Table 1 Detecting results of *H pylori* infection using colloid gold kit with M_r18 000, 26 000 OMP

Methods	Testee	Positive	Negative	False positive	False negative
Routine methods	183	144	32	1	6
M_r26 000 protein	183	141	32	1	9
M_r18 000 protein	183	78	33	0	72

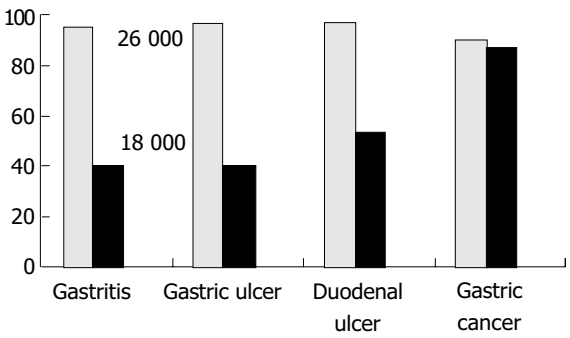

Figure 2 Detecting results of diseases infected with *H pylori* using colloid gold test kits with M_r26 000, 18 000 OMP.

Table 2 Detecting results of diseases infected with *H pylori* using colloid gold kit with M_r26 000 OMP

Disease	Patients	yr	Positive	Negative
Gastritis	60	50.3±15.9	57	3
Gastric ulcer	30	57.3±13.2	29	1
Duodenal ulcer	30	46.5±14.2	29	1
Gastric cancer	30	64.7±17.4	27	3

Table 3 Detecting results of diseases infected with *H pylori* using colloid gold kit with M_r18 000 OMP

Disease	Patients	yr	Positive	Negative
Gastritis	60	50.3±15.9	24	36
Gastric ulcer	30	57.3±13.2	12	18
Duodenal ulcer	30	46.5±14.2	16	14
Gastric cancer	30	64.7±17.4	26	4

DISCUSSION

M_r18 000, 26 000 OMP of *H pylori* are commonly expressed in all *H pylori* strains examined so far. Furthermore, no cross-reaction has been shown when antibodies (polyclonal and monoclonal) to low-molecular outer membrane proteins were used to screen closely related species of *Helicobacteria*, campylobacteria, or a diverse range of other bacteria[64]. In our study, *H pylori* 18 000, 26 000 OMP were successfully expressed in *E.coli* with good antigenicity. With marked gold and special antigen-antibody reaction technique, *H pylori* infection could be detected by the antigen-antibody-antigen method. Recombinant fusion proteins were impregnated in NC membrane as a detecting strip, and marked with gold as a colored reagent by which the special antibody to *H pylori* could be determined in seconds. At first the recombinant proteins were prepared in large quantities, purified and regulated. Due to the diameter size of grained gold would affect directly the result of test, the diameter of grained gold was adjusted to 40-60 nm, at the same time the concentration of antibody was adjusted in order to acquire steady and reliable products marked with gold. A test detecting IgG antibodies to *H pylori* was thus constructed.

Sera were collected from 150 patients with gastrointestinal symptoms and *H pylori* infection and from 33 healthy volunteers without *H pylori* infection used as controls during one year. The detecting results using colloid gold kit were as follows. Ninety-four percent of patients infected with *H pylori* showed response to recombinant protein with M_r26 000, 95.0%, 96.7%, 96.7% and 90.0% of patients with *H pylori*-infected chronic gastritis, gastric ulcer, duodenal ulcer, and gastric cancer, showed responses to specific proteins with M_r26 000 respectively, There was no significant difference between the routine examined methods and colloid gold kits (P>0.05). 52.0% of patients infected with *H pylori* showed response to recombinant protein with M_r18 000, while 40.0%, 40.0%, 53.3% and 86.7% of patients with *H pylori*-infected chronic gastritis, gastric ulcer, duodenal ulcer, and gastric cancer respectively, showed responses to specific proteins with M_r18 000, moreover there was a significant difference (P<0.05) in the detecting rates of *H pylori* infection between gastric cancer (86.7 %) and other diseases (43.3%). The results showed that colloid gold kits with M_r26 000 proteins of *H pylori* could be used as a conventional examination method. Based on the classic ELISA, bacteria culture and ^{13}C urea breath test results, the sensitivity, specificity, and accuracy of the rapid test kit with M_r26 000 protein were 94.0%, 97.0%, and 94.5%, respectively, and a significant association was found between the serologic response to M_r18 000 OMP antigen and malignant outcome of *H pylori* infection. The two colloid gold kits with

M_r26 000, 18 000 proteins of *H pylori*, could be used to detect *H pylori* infection and *H pylori*-associated diseases, and to predict the risk of peptic ulcer or malignancy. The results mentioned above were consistent with those reported[65-67].

All strains of *H pylori* could express low-molecular-mass OMP, which stimulates the body to produce corresponding antibodies, moreover the antibodies produced are related to the corresponding molecular size of antigens and immuno-status of the body. Decrease of the antibodies was associated with the corresponding molecular size of the antibodies. So the results showed that the responses of patients infected with *H pylori* to recombinant proteins with M_r26 000 were stronger (94.0%) than that (52.0%) to recombinant proteins with M_r18 000, while the growth of gastric cancer was associated with much more factors and stages. All pathogenic factors may act on the pre-carcinoma stage alone or together with each other in the model of chronic gastritis-atrophic gastritis-intestinal metaplasia-atypical hyperplasia-gastric cancer. Chua *et al*.[68] compared the seroprevalence of antibodies with various *H pylori* antigens in Singaporeans with gastric adenocarcinoma and the normal Singaporean population using both conventional immunoglobulin (Ig) G ELISA and Western blot immunoassay, and found that strains of *H pylori* including antigens with M_r19 500 and seronegative antigens with M_r35 000 could provide their potential for carcinogenesis. Immunoreactive species-specific M_r19 500 OMP of *H pylori* is actually Lpp20, while its actual molecular mass is 18 000 OMP. So *H pylori* strains based on carcinogenic potential could provide a basis for selective surveillance and eradication therapy. Low-molecular-mass OMP could lead to the 12th gene mutation of C-Ha-ras, and amplify p^{21} protein expressed by ras gene and c-met protein could also be overexpressed. Therefore the detecting rate of low-molecular-weight OMP of *H pylori* in gastric cancer is higher than other OMP. In our study, the detecting rate of M_r26 000 OMP of *H pylori* in gastric cancer was similar to that of M_r18 000 OMP. The results showed low-molecular-weight OMP could be used, not only in vaccine target candidates, but also in detection of gastric cancer in highly risk patients with *H pylori* infection. In a nutshell, the colloid gold kit constructed with M_r18 000, 26 000 OMP of *H pylori* could detect anti-*H pylori* IgG-antibody. Compared with other methods, this method not only provides a rapid, simple and painless test, but also gives a reliable specificity, especially in diagnosis of gastrointestinal tumors. The colloid gold kit based on marked gold and special antigen-antibody reaction technique is a rapid diagnostic kit, only a few minutes are required to complete an assay, and no special instruments are needed. Compared with other immunoassay techniques, the colloid gold kit has following advantages. It is based on the antigen-antibody reaction on membranes, its detecting time is much shorter than ELISA, at the same time colloid gold is red in color, so there is no need to add other colored reagents, moreover, the products marked with gold are more stable than those marked with enzyme. The colloid gold kit evaluated in our study enables a simple, rapid, noninvasive, and accurate diagnosis of *H pylori* infection, and is an ideal test method for screening patients with gastrointestinal tumors.

REFERENCES

1 **Michetti P,** Kreiss C, Kotloff KL, Porta N, Blanco JL, Bachmann D, Herranz M, Saldinger PF, Corthesy-Theulaz I, Losonsky G, Nichols R, Simon J, Stolte M, Ackerman S, Monath TP, Blum AL. Oral immunization with urease and escherichia coli heat-labile enterotoxin is safe and immunogenic in *Helicobacter pylori*-infected adults. *Gastroenterology* 1999; **116**: 804-812

2 **Hiyama T,** Haruma K, Kitadai Y, Masuda H, Miyamoto M, Ito M, Kamada T, Tanaka S, Uemura N, Yoshihara M, Sumii K, Shimamoto F, Chayama K. Clinicopathological features of gastric mucosa-associated lymphoid tissue lymphoma: a comparison with diffuse large B-cell lymphoma without a mucosa-associated lymphoid tissue lymphoma component. *J Gastroenterol Hepatol* 2001; **16**: 734-739

3 **Nakamura S,** Matsumoto T, Suekane H, Takeshita M, Hizawa K, Kawasaki M, Yao T, Tsuneyoshi M, Iida M, Fujishima M. Predictive value of endoscopic ultrasonography for regression of gastric low grade and high grade MALT lymphomas after eradication of *Helicobacter pylori*. *Gut* 2001; **48**: 454-460

4 **Uemura N,** Okamoto S, Yamamoto S, Matsumura N, Yamaguchi S, Yamakido M, Taniyama K, Sasaki N, Schlemper RJ. *Helicobacter pylori* infection and the development of gastric cancer. *N Engl J Med* 2001; **345**: 784-789

5 **Kate V,** Ananthakrishnan N, Badrinath S. Effect of *Helicobacter pylori* eradication on the ulcer recurrence rate after simple closure of perforated duodenal ulcer: retrospective and prospective randomized controlled studies. *Br J Surg* 2001; **88**: 1054-1058

6 **Xue FB,** Xu YY, Wan Y, Pan BR, Ren J, Fan DM. Association of *H pylori* infection with gastric carcinoma: a Meta analysis. *World J Gastroenterol* 2001; **7**: 801-804

7 **Peng ZS**, Liang ZC, Liu MC, Ouang NT. Studies on gastric epithelial cell proliferation and apoptosis in *Hp* associated gastric ulcer. *Shijie Huaren Xiaohua Zazhi* 1999; **7**: 218-219

8 **Xiao SD,** Liu WZ. Current statue in treatment of *Hp* infection. *Shijie Huaren Xiaohua Zazhi* 1999; **7**: 3-4

9 **Meyer JM,** Silliman NP, Dixon CA, Siepman NY, Sugg JE, Hopkins RJ. *Helicobacter pylori* and early duodenal ulcer status post-treatment: a review. *Helicobacter* 2001; **6**: 84-92

10 **Casella G,** Buda CA, Maisano R, Schiavo M, Perego D, Baldini V. Complete regression of primary gastric MALT-lymphoma after double eradication *Helicobacter pylori* therapy: role and importance of endoscopic ultrasonography. *Anticancer Res* 2001; **21**: 1499-1502

11 **Hurenkamp GJ,** Grundmeijer HG, Van Der Ende A, Tytgat GN, Assendelft WJ, Van Der Hulst RW. Arrest of chronic acid suppressant drug use after successful *Helicobacter pylori* eradication in patients with peptic ulcer disease: a six-month follow-up study. *Aliment Pharmacol Ther* 2001; **15**: 1047-1054

12 **Guo CQ,** Wang YP, Liu GY, Ma SW, Ding GY, Li LC. Study on *Helicobacter pylori* infection and p53, *c-erbB*-2 gene expression in carcinogenesis of gastric mucosa. *Shijie Huaren Xiaohua Zazhi* 1999; **7**: 313-315

13 **Hiyama T,** Haruma K, Kitadai Y, Masuda H, Miyamoto M, Ito M, Kamada T, Tanaka S, Uemura N, Yoshihara M, Sumii K, Shimamoto F, Chayama K. Clinicopathological features of gastric mucosa-associated lymphoid tissue lymphoma: a comparison with diffuse large B-cell lymphoma without a mucosa-associated lymphoid tissue lymphoma component. *J Gastroenterol Hepatol* 2001; **16**: 734-739

14 **Hu PJ.** *Hp* and gastric cancer: challenge in the research. *Shijie Huaren Xiaohua Zazhi* 1999; **7**: 1-2

15 **Quan J,** Fan XG. Progress in experimental research of *Helicobacter pylori* infection and gastric cancinoma. *Shijie Huaren Xiaohua Zazhi* 1999; **7**: 1068-1069

16 **Delchier JC,** Lamarque D, Levy M, Tkoub EM, Copie-Bergman C, Deforges L, Chaumette MT, Haioun C. *Helicobacter pylori* and gastric lymphoma: high seroprevalence of CagA in diffuse large B-cell lymphoma but not in low-grade lymphoma of mucosa-associated lymphoid tissue type. *Am J Gastroenterol* 2001; **96**: 2324-2328

17 **Morgner A,** Miehlke S, Fischbach W, Schmitt W, Muller-Hermelink H, Greiner A, Thiede C, Schetelig J, Neubauer A, Stolte M, Ehninger G, Bayerdorffer E. Complete remission of primary high-grade B-cell gastric lymphoma after cure of *Helicobacter pylori* infection. *J Clin Oncol* 2001; **19**: 2041-2048

18 **Zhang XQ,** Lin SR. Progress in research on the relationship between *Hp* and stomach cancer. *Shijie Huaren Xiaohua Zazhi* 2000; **8**: 206-207

19 **Hua JS.** Effect of *Hp*: cell proliferation and apoptosis on stomach cancer. *Shijie Huaren Xiaohua Zazhi* 1999; **9**: 647-648

20 **Armitage GC.** Periodontal infections and cardiovascular disease-how strong is the association? *Oral Dis* 2000; **6**: 335-350

21 **Tsai CJ,** Huang TY. Relation of *Helicobacter pylori* infection and angiographically demonstrated coronary artery disease. *Dig Dis Sci* 2000; **45**: 1227-1232

22 **Gocyk W,** Niklinski T, Olechnowicz H, Duda A, Bielanski W,

Konturek PC, Konturek SJ. *Helicobacter pylori*, gastrin and cyclooxygenase-2 in lung cancer. *Med Sci Monit* 2000; **6**: 1085-1092

23 **Baysoy G,** Ertem D, Ademoglu E, Kotiloglu E, Keskin S, Pehlivanoglu E. Gastric *Histopathology*, Iron status and iron deficiency anemia in children with *Helicobacter pylori* infection. *J Pediatric Gastroenterol Nutr* 2004; **38**: 146-151

24 **Caselli M,** Zaffoni E, Ruina M, Sartori S, Trevisani L, Ciaccia A, Alvisi V, Fabbri L, Papi A. *Helicobacter pylori* and chronic bronchitis. *Scand J Gastroenterol* 1999; **34**: 828-830

25 **Dauden E,** Jimenez Alonso I, Garcia Diez A. *Helicobacter pylori* and idiopathic chronic urticaria. *Int J Dermatol* 2000; **39**: 446-452

26 **Ojetti V,** Armuzzi A, De-Luca A, Nucera E, Franceschi F, Candelli M, Zannoni GF, Danese S, Di-Caro S, Vastola M, Schiavino D, Gasbarrini G, Patriarca G, Pola P, Gasbarrini A. *Helicobacter pylori* infection affects eosinophilic cationic protein in the gastric juice of patients with idiopathic chronic urticaria. *Int Arch Allergy Immunol* 2001; **125**: 66-72

27 **Vainio E,** Huovinen S, Liutu M, Uksila J, Leino R. Peptic ulcer and *Helicobacter pylori* in patients with lichen planus. *Acta Derm Venereol* 2000; **80**: 427-429

28 **Szlachcic A,** Sliwowski Z, Karczewska E, Bielanski W, Pytko-Polonczyk J, Konturek SJ. *Helicobacter pylori* and its eradication in rosacea. *J Physiol Pharmacol* 1999; **50**: 777-786

29 **Avci O,** Ellidokuz E, Simsek I, Buyukgebiz B, Gunes AT. *Helicobacter pylori* and Behcet's disease. *Dermatology* 1999; **199**: 140-143

30 **Yazawa N,** Fujimoto M, Kikuchi K, Kubo M, Ihn H, Sato S, Tamaki T, Tamaki K. High seroprevalence of *Helicobacter pylori* infection in patients with systemic sclerosis: association with esophageal involvement. *J Rheumatol* 1998; **25**: 650-653

31 **Emilia G,** Longo G, Luppi M, Gandini G, Morselli M, Ferrara L, Amarri S, Cagossi K, Torelli G. *Helicobacter pylori* eradication can induce platelet recovery in idiopathic thrombocytopenic purpura. *Blood* 2001; **97**: 812-814

32 **Parkinson AJ,** Gold BD, Bulkow L, Wainwright RB, Swaminathan B, Khanna B, Petersen KM, Fitzgerald MA. High prevalence of *Helicobacter pylori* in the Alaska native population and association with low serum ferritin levels in young adults. *Clin Diagn Lab Immunol* 2000; **7**: 885-888

33 **Konno M,** Muraoka S, Takahashi M, Imai T. Iron-deficiency anemia associated with *Helicobacter pylori* gastritis. *J Pediatr Gastroenterol Nutr* 2000; **31**: 52-56

34 **Annibale B,** Lahner E, Bordi C, Martino G, Caruana P, Grossi C, Negrini R, Delle-Fave G. Role of *Helicobacter pylori* infection in pernicious anaemia. *Dig Liver Dis* 2000; **32**: 756-762

35 **Choe YH,** Kwon YS, Jung MK, Kang SK, Hwang TS, Hong YC. *Helicobacter pylori*-associated iron-deficiency anemia in adolescent female athletes. *J Pediatr* 2001; **139**: 100-104

36 **Kaptan K,** Beyan C, Ural AU, Cetin T, Avcu F, Gulsen M, Finci R, Yalcin A. *Helicobacter pylori*-is it a novel causative agent in Vitamin B12 deficiency? *Arch Intern Med* 2000; **160**: 1349-1353

37 **Nozaki K,** Shimizu N, Inada K, Tsukamoto T, Inoue M, Kumagai T, Sugiyama A, Mizoshita T, Kaminishi M, Tatematsu M. Synergistic promoting effects of *Helicobacter pylori* infection and high-salt diet on gastric carcinogenesis in mongolian gerbils. *Jpn J Cancer Res* 2002; **93**: 1083-1089

38 **Crabtree JE,** Court M, Aboshkiwa MA, Jeremy AH, Dixon MF, Robinson PA. Gastric mucosal cytokine and epithelial cell responses to *Helicobacter pylori* infection in mongolian gerbils. *J Pathol* 2004; **202**: 197-207

39 **Chua TS,** Fock KM, Teo EK, Ng TM. Validation of 13C-urea breathtest for the diagnosis of *Helicobacter pylori* infection in the singapore population. *Singapore Med J* 2002; **43**: 408-411

40 **Kawai T,** Kawakami K, Kudo T, Ogiahara S, Handa Y, Moriyasu F. A new serum antibody test kit (E plate) for evaluation of *Helicobacter pylori* eradication. *Intern Med* 2002; **41**: 780-783

41 **Day AS,** Sherman PM. Accuracy of office-based immunoassays for the diagnosis of *Helicobacter pylori* infection in children. *Helicobacter* 2002; **7**: 205-209

42 **Oyedeji KS,** Smith SI, Arigbabu AO, Coker AO, Ndububa DA, Agbakwuru EA, Atoyebi OA. Use of direct Gram stain of stomach biopsy as a rapid screening method for detection of *Helicobacter pylori* from peptic ulcer and gastritis patients. *J Basic Microbiol* 2002; **42**: 121-125

43 **Wong WM,** Wong BC, Tang VS, Lai KC, Yuen ST, Leung SY, Hu WH, Lam SK. An evaluation of the pyloriTek test for the diagnosis of *Helicobacter pylori* infection in Chinese patients before and after eradication therapy. *J Gastroenterol Hepatol* 2001; **16**: 976-980

44 **Kakinoki K,** Takemori Y, Noda Y. Efficacy of the urine antibody test for detection of *Helicobacter pylori*: comparison with serum antibody tests. *Nippon Shokakibyo Gakkai Zasshi* 2001; **98**: 935-941

45 **Fujisawa T,** Kaneko T, Kumagai T, Akamatsu T, Katsuyama T, Kiyosawa K, Tachikawa T, Kosaka O, Machikawa F. Evaluation of urinary rapid test for *Helicobacter pylori* in general practice. *J Clin Lab Anal* 2001; **15**: 154-159

46 **Miwa H,** Akamatsu S, Tachikawa T, Sogabe T, Ohtaka K, Nagahara A, Sugiyama Y, Sato N. On-site diagnosis of *H pylori* infection by urine. *Diagn Microbiol Infect Dis* 2001; **39**: 95-97

47 **Yamamoto S,** Uemura N, Okamoto S, Yamaguchi S, Mashiba H, Tachikawa T. A new rapid test for detecting anti-*Helicobacter pylori* antibody excreted into urine. *Helicobacter* 2000; **5**: 160-164

48 **Ladas SD,** Malamou H, Giota G, Varzakakos I, Kitsanta P, Georgopoulos S, Spiliadi C, Raptis SA. Prospective evaluation of a whole-blood antibody test (FlexPack HP) for in-office diagnosis of *Helicobacter pylori* infection in untreated patients. *Eur J Gastroenterol Hepatol* 2000; **12**: 727-731

49 **Gisbert JP,** Cruzado AI, Cabrera MM, Carpio D, Benito LM, Perez Poveda JJ, Valbuena M, Cantero J, Pajares JM. "Rapid" serology for the diagnosis of *Helicobacter pylori* infection. Evaluation of its accuracy compared with a gold-standard and its concordance with "classic" serology. *Gastroenterol Hepatol* 2000; **23**: 159-164

50 **Xia HH,** Kalantar JS, Wyatt JM, Adams S, Cheung K, Eslick GD, Talley NJ. High sensitivity and specificity of a laboratory-based serological test, pylori DTect ELISA, for detection of *Helicobacter pylori* infection. *Diagn Microbiol Infect Dis* 2000; **36**: 69-74

51 **Miwa H,** Hirose M, Kikuchi S, Terai T, Iwazaki R, Kobayashi O, Takei Y, Ogihara T, Sato N. How useful is the detection kit for antibody to *Helicobacter pylori* in urine (URINELISA) in clinical practice? *Am J Gastroenterol* 1999; **94**: 3460-3463

52 **Garcia Diaz E,** Castro Fernandez M, Romero Gomez M, Vargas-Romero J. The effectiveness of (IgG-ELISA) serology as an alternative diagnostic method for detecting *Helicobacter pylori* infection in patients with gastro-intestinal bleeding due to gastro-duodenal ulcer. *Rev Esp Enferm Dig* 2002; **94**: 725-736

53 **Liang SH,** Mao YF, Yan J. Cloning, expression and identification of flaB gene from a clinical isolate of *Helicobacter pylori*. *Zhejiang Daxue Xuebao Yixueban* 2003; **32**: 13-16

54 **Mao YF,** Yan J, Li LW. Cloning, expression and identification of hpaA gene from a clinical isolate of *Helicobacter pylori*. *Zhejiang Daxue Xuebao Yixueban* 2003; **32**: 9-12

55 **Liu X,** Hu J, Zhang X, Fan D. Oral immunization of mice with attenuated Salmonella typhimurium expressing *Helicobacter pylori* urease B subunit. *Chin Med J* 2002; **115**: 1513-1516

56 **Londono Arcila P,** Freeman D, Kleanthous H, O'Dowd AM, Lewis S, Turner AK, Rees EL, Tibbitts TJ, Greenwood J, Monath TP, Darsley MJ. Attenuated salmonella enterica serovar typhi expressing urease effectively immunizes mice against *Helicobacter pylori* challenge as part of a heterologous mucosal priming-parenteral boosting vaccination regimen. *Infect Immun* 2002; **70**: 5096-5106

57 **Reiche N,** Jung A, Brabletz T, Vater T, Kirchner T, Faller G. Generation and characterization of human monoclonal scFv antibodies against *Helicobacter pylori* antigens. *Infect Immun* 2002; **70**: 4158-4164

58 **Miyashita M,** Joh T, Watanabe K, Todoroki I, Seno K, Ohara H, Nomura T, Miyata M, Kasugai K, Tochikubo K, Itoh M, Nitta M. Immune responses in mice to intranasal and intracutaneous administration of a DNA vaccine encoding *Helicobacter pylori*-catalase. *Vaccine* 2002; **20**: 2336-2342

59 **Liao W,** Chen M, Zhu S. Construction of attenuated salmonella typhimurium vaccine strain expressing *Helicobacter pylori*

catalase and observation on its protective immunity. *Natl Med J China* 2001; **81**: 613-616

60 **Koesling J,** Lucas B, Develioglou L, Aebischer T, Meyer TF. Vaccination of mice with live recombinant salmonella typhimurium aroA against *H pylori*: parameters associated with prophylactic and therapeutic vaccine efficacy. *Vaccine* 2001; **20**: 413-420

61 **Jiang Z,** Pu D, Huang AL, Tao XH, Wang PL. Construction, expression and antigenic study of bivalent vaccine candidate with 26000 OMP and hspA of human *H pylori*. *Zhonghua Yixue Zazhi* 2003; **83**: 862-867

62 **Bumann D,** Metzger WG, Mansouri E, Palme O, Wendland M, Hurwitz R, Haas G, Aebischer T, von Specht BU, Meyer TF. Safety and immunogenicity of live recombinant salmonella enterica serovar typhi Ty21a expressing urease A and B from *Helicobacter pylori* in human volunteers. *Vaccine* 2001; **20**: 845-852

63 **Jiang Z,** Huang A, Wang P. Gene cloning and expression of outer membrane protein of *Helicobacter pylori*. *Zhonghua Yixue Zazhi* 2001; **81**: 1416-1419

64 **Keenan J,** Oliaro J, Domigan N, Potter H, Aitken G, Allardyce K, Roake J. Immune response to an 18-kilodalton outer membrane antigen identifies lipoprotien 20 as a *Helicobacter pylori* vaccine candidate. *Infect Immun* 2000; **68**: 3337-3343

65 **Raymond J,** Sauvestre C, Kalach N, Bergeret M, Dupont C. Immunoblotting and serology for diagnosis of *Helicobacter pylori* infection in children. *Pediatr Infect Dis J* 2000; **19**: 118-121

66 **Todoroki I,** Joh T, Watanabe K, Miyashita M, Seno K, Nomura T, Ohara H, Yokoyama Y, Tochikubo K, Itoh M. Suppressive effects of DNA vaccines encoding heat shock protein on *Helicobacter pylori*-induced gastritis in mice. *Biochem Biophys Res Commun* 2000; **277**: 159-163

67 **Shiesh SC,** Sheu BS, Yang HB, Tsao HJ, Lin XZ. Serologic response to lower-molecular-weight proteins of *Helicobacter pylori* is related to, clinical outcome of *Helicobacter pylori* infection in Taiwan. *Dig Dis Sci* 2000; **45**: 781-788

68 **Chua TS,** Fock KM, Chan YH, Dhamodaran S, Sim CS, Ng TM, Teo EK. Seroreactivity to 19.5-kDa antigens in combination with absence of seroreactivity to 35-kDa antigens is associated with an increased risk of gastric adenocarcinoma. *Helicobacter* 2002; **7**: 257-264

Edited by Wang XL and Xu JY **Proofread by** Xu FM

PO Box 2345, Beijing 100023, China
Fax: +86-10-85381893
E-mail: wjg@wjgnet.com www.wjgnet.com

World J Gastroenterol 2004;10(23):3470-3474
World Journal of Gastroenterology
Copyright © 2004 by The WJG Press ISSN 1007-9327

• BASIC RESEARCH •

Ethanol inhibits the motility of rabbit sphincter of Oddi *in vitro*

Réka Sári, Attila Pálvölgyi, Zoltán Rakonczay Jr, Tamás Takács, János Lonovics, László Czakó, Zoltán Szilvássy, Péter Hegyi

Réka Sári, Attila Pálvölgyi, Zoltán Rakonczay Jr, Tamás Takács, János Lonovics, László Czakó, Peter Hegyi, First Department of Medicine, Faculty of Medicine, University of Szeged H-6720, Koranyi fasor 10, Hungary
Zoltán Szilvássy, Department of Pharmacology, Medical University of Debrecen H-4032, Nagyerdei krt, 98, Hungary
Supported by The Wellcome Trust (Grant No. 022618), and by the Hungarian Scientific Research Fund (D42188, T43066 and T042589)
Correspondence to: Péter Hegyi, M.D., Ph.D., First Department of Medicine, University of Szeged, H-6701, PO Box 469, Hungary. hep@in1st.szote.u-szeged.hu
Telephone: +36-62-545200 **Fax:** +36-62-545185
Received: 2004-04-10 **Accepted:** 2004-05-25

Abstract

AIM: The role of the sphincter of Oddi (SO) in ethanol (ETOH)-induced pancreatitis is controversial. Our aim was to characterise the effect of ETOH on basal and stimulated SO motility.

METHODS: SOs removed from white rabbits were placed in an organ bath (Krebs solution, pH7.4, 37 ℃). The effects of 2 mL/L, 4 mL/L, 6 mL/L and 8 mL/L of ETOH on the contractile responses of the sphincter were determined. SOs were stimulated with either 0.1 μmol/L carbachol, 1 μmol/L erythromycin or 0.1 μmol/L cholecystokinin (CCK).

RESULTS: ETOH at a dose of 4 mL/L significantly decreased the baseline contractile amplitude from 11.98±0.05 mN to 11.19±0.07 mN. However, no significant changes in the contractile frequency were observed. ETOH (0.6%) significantly decreased both the baseline amplitude and the frequency compared to the control group (10.50±0.01 mN, 12.13±0.10 mN and 3.53±0.13 c/min, 5.5±0.13 cycles(c)/min, respectively). Moreover, 0.8% of ETOH resulted in complete relaxation of the SO. Carbachol (0.1 μmol/L) or erythromycin (1 μmol/L) stimulated the baseline amplitudes (by 82% and 75%, respectively) and the contractile frequencies (by 150% and 106%, respectively). In the carbachol or erythromycin-stimulated groups 2-6 mL/L of ETOH significantly inhibited both the amplitude and the frequency. Interestingly, a 4-5 min administration of 6 mL/L ETOH suddenly and completely relaxed the SO. CCK (0.1 μmol/L) stimulated the baseline amplitude from 12.37±0.05 mN to 27.40±1.82 mN within 1.60±0.24 min. After this peak, the amplitude decreased to 17.17±0.22 mN and remained constant during the experiment. The frequency peaked at 12.8±0.2 c/min, after which the constant frequency was 9.43±0.24 c/min throughout the rest of the experiment. ETOH at a dose of 4 mL/L significantly decreased the amplitude from 16.13±0.23 mN to 14.93±0.19 mN. However, no significant changes in the contractile frequency were observed. ETOH at a dose of 6 mL/L inhibited both the amplitudes and the frequencies in the CCK-stimulated group, while 8 mL/L of ETOH completely relaxed the SO.

CONCLUSION: ETOH strongly inhibits the basal, carbachol, erythromycin, and CCK-stimulated rabbit SO motility. Therefore, it is possible that during alcohol-intake the relaxed SO opens the way for pancreatic fluid to flow out into the duodenum in rabbits. This relaxation of the SO may protect the pancreas against alcohol-induced damage.

Sári R, Pálvölgyi A, Rakonczay Z Jr, Takács T, Lonovics J, Czakó L, Szilvássy Z, Hegyi P. Ethanol inhibits the motility of rabbit sphincter of Oddi *in vitro*. *World J Gastroenterol* 2004; 10(23): 3470-3474
http://www.wjgnet.com/1007-9327/10/3470.asp

INTRODUCTION

It is well documented that ethanol (ETOH) can cause acute pancreatitis[1,2], but the mechanisms by which alcohol causes this severe pancreatic injury are not clear. Two main hypotheses have been put forward to explain the role of the sphincter of Oddi (SO) in ETOH induced pancreatitis. One is the obstruction-hypersecretion theory which holds that ETOH induces spasm of the SO and can increase the pressure in the pancreatic ductal system, which may lead to the disruption of small pancreatic ducts. Therefore, pancreatic juice can enter the parenchyma evoking acute pancreatitis[3,4]. The other is the duodenopancreatic reflux theory which believes that ETOH reduces the SO motility, thus, the reflux of bile, activated enzymes, or other substances into the pancreatic ducts may cause pancreatitis after alcohol ingestion[5,6]. Despite these contradictory theories, no data are available concerning the effect of alcohol on physiologically (postprandial)-stimulated SO motility.

Cholecystokinin (CCK) is generally regarded as the major hormone regulating postprandial SO motility. This regulatory effect of CCK is rather complex. CCK could directly stimulate SO motility in guinea pigs[7], opossum[8], rabbits[9-11] and dogs[12]. On the other hand, CCK could induce acetylcholine (Ach) and vasoactive intestinal peptide release from pre- and postjunctional sites in the enteric nervous system via CCK_A and CCK_B receptors in the canine gastrointestinal tract, which suggests an indirect effect of CCK[13]. Others have also demonstrated that the contractile response of the guinea pig SO to CCK consists of a direct effect and an indirect effect mediated by Ach release from postganglionic parasympathetic neurons[7,14].

Motilin is also a key peptide regulating phasic contractile activity of the stomach, duodenum, SO, and gallbladder[15]. This regulation is mediated by the migrating myoelectric complex of the gastrointestinal tract[16]. Motilin provoked an increase of the SO spike activity in a dose-dependent manner in rabbits[17]. Erythromycin, a motilin agonist, has been found to stimulate interdigestive motility of the duodenum and SO in dogs[18], Australian opossum[19] and also in humans[20]. However, there are no available data concerning the effect of erythromycin on rabbit SO motility.

The parasympathetic nervous system plays an important role in the stimulation of gastrointestinal motility after a meal. The parasympathetic neurotransmitter Ach and its analogues have been shown to stimulate SO motility in different species[21]. Furthermore, Ach can be released from postganglionic parasympathetic neurons after hormonal stimuli, as described above.

In this study our aim was to characterise the effects of ETOH on the basal and differently stimulated SO motility in rabbits.

MATERIALS AND METHODS

Ethics

The present experiments conformed to the European Guiding Principles for Care and Use of Experimental Animals. In addition, the experimental protocol applied was approved by the local ethical boards of the Universities of Szeged and Debrecen, Hungary.

Isometric tension measurements

Isometric tension measurements were described in detail previously[22]. Biliary SO muscle rings of approximately 6 mm long from adult male New Zealand white rabbits weighing 2-2.5 kg were prepared. The papilla Vateri was eliminated and the ampullary part of the muscle rings of approximately 3 mm long were mounted horizontally on two small L-shaped glass hooks, of which one was connected to a force transducer (SG-O2, Experimetria, Budapest, Hungary) attached to a six channel polygraph (R61 6CH, Mikromed, Budapest, Hungary) for measurement and recording of isometric tension as described[22]. One muscle ring was prepared from one animal. The experiments were carried out in an organ bath (5 mL) containing Krebs bicarbonate buffer (in mmol/L: NaCl 118.1, KCl 4.7, $MgSO_4$ 1.0, KH_2PO_4 1.0, $CaCl_2$ 2.5, $NaHCO_3$ 25.0, glucose 11.1) which was maintained at 37 ℃ and aerated continuously with carbogen (50 mL/L CO_2/950 mL/L O_2).

Experimental protocol

The muscle rings underwent brief experimental protocols as follows. Phasic activity of SO: contractile frequencies and their amplitudes were measured over 50 min in each experiment. The initial tension was set at 10 milliNewtons (mN) and the rings were allowed to equilibrate for over 30 min. After that amplitudes and frequencies were recorded for 60 min. In the first 10 min, baseline phasic activity was measured. From the second 10 min, phasic activities were stimulated with 0.1 μmol/L carbachol, 1 μmol/L erythromycin or 0.1 μmol/L CCK. During the last 40 min, ETOH was administered at the doses of 2 mL/L, 4 mL/L, 6 mL/L and 8 mL/L for equal periods (4 times, 10 min). The control SOs received no treatments.

Drugs and chemicals

All laboratory chemicals (including ions, carbachol, erythromycin, CCK and ETOH) were obtained from Sigma Chemical Company (Budapest, Hungary). CCK and carbachol were dissolved in Krebs solution, while erythromycin was dissolved in dimethyl sulfoxide.

Data and statistical analysis

Parameters producing the data for evaluation were as follows. The *amplitude of contractions* (mN) was referred to as the difference between peak contractions and relaxations. The average of the amplitudes was calculated every minute (results were expressed as mean±SE, n = number of frequencies in a minute). The *frequencies of contractions* (c/min) were calculated every minute. Statistical analysis was performed for 10 min of each of the experiments using either Student's t-test (when the data consisted of two groups) or ANOVA (when three or more data groups were compared). Results were expressed as mean±SE, $n = 5$, $P<0.05$ was considered statistically significant.

RESULTS

Effect of ETOH on basal SO motility

The amplitudes and frequencies of the basal SO motility were stable during the control experiments (11.98±0.04 mN and 5.37±0.07 c/min, respectively). ETOH (2 mL/L) had no effects on the baseline amplitudes and frequencies. When ETOH was administered at a dose of 4 mL/L, the baseline amplitude was significantly decreased *vs* the control (11.19±0.07 mN and 11.98±0.05 mN, respectively) (Figure 1A, B). However, no significant changes in the contractile frequency were observed *vs* the control (Figure 1C,D). ETOH (6 mL/L) significantly decreased both the baseline amplitude and frequency *vs* control (10.50±0.01 mN, 12.13±0.10 mN and 3.53±0.13 c/min, 5.50±0.17 c/min, respectively). ETOH (8 mL/L) completely relaxed the SO within 10 s. Therefore, neither the frequencies nor the amplitudes could be detected during the last 10 min of the experiments.

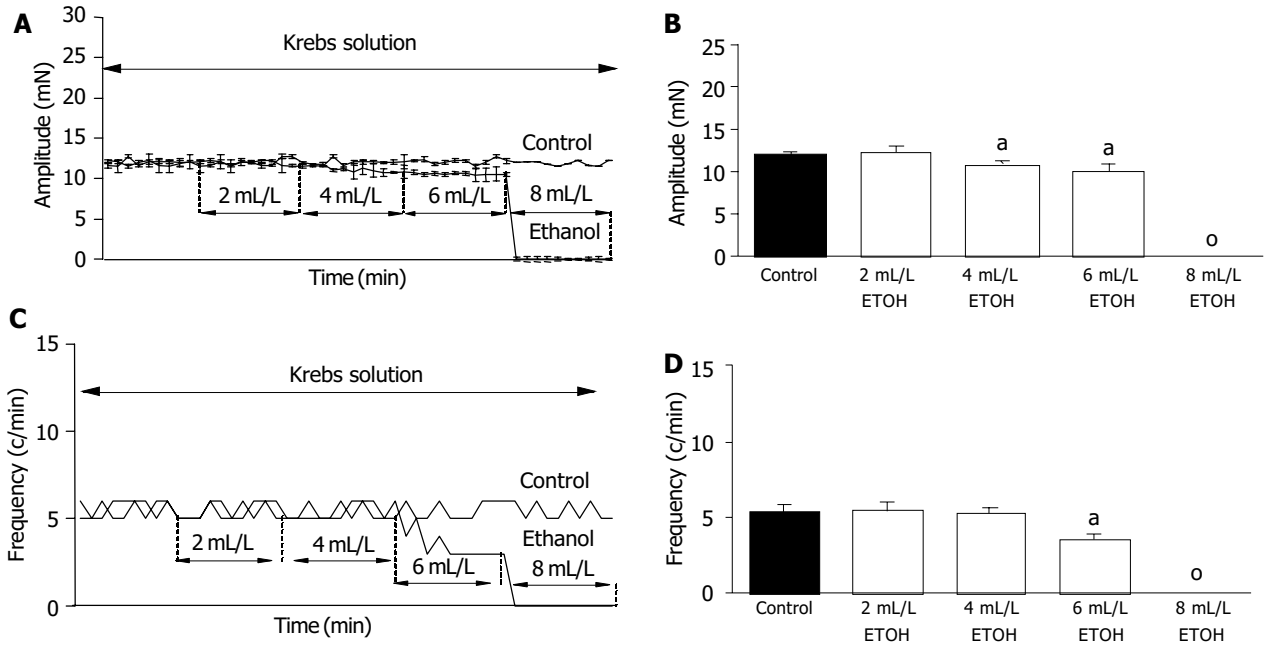

Figure 1 Basal SO motility inhibited by ETOH. Sphincter of Oddi (SO) was exposed to increasing doses of ethanol (ETOH; 2 mL/L, 4 mL/L, 6 mL/L and 8 mL/L). Each concentration of ETOH was administered for 10 min. A: Effect of ETOH on the baseline amplitude. Representative experiments of the control and the ETOH-treated groups are shown. B: Summary of the effect of ETOH on the baseline amplitude. mean±SE, $n = 5$, $^aP<0.05$ *vs* the control; o: no contractile activity. C: Effect of ETOH on the contractile frequency. Representative experiments of the control and the ETOH-treated groups are shown. D: Summary of the effect of ETOH on the contractile frequency. mean±SE, $n = 5$, $^aP<0.05$ *vs* the control; o: no contractile activity.

Effect of ETOH on carbachol-stimulated SO motility

Carbachol (0.1 μmol/L) stimulated the baseline amplitude by 82% and the contractile frequency by 150%. This carbachol-stimulated SO motility was stable during the experiment (Figure 2A-C). ETOH (2 mL/L) significantly inhibited both the amplitude and frequency *vs* the carbachol-stimulated group (19.42±1.16 mN, 20.81±0.49 mN and 12.32±0.16 c/min, 12.91±0.10 c/min, respectively) (Figure 2A-D). ETOH (4 mL/L) further reduced the amplitude (13.92±0.49 mN) and the frequency (9.24±0.21 c/min) of the SO motility. ETOH (6 mL/L) decreased the contractile frequency of the SO by 50% (4.61±0.46 c/min). However, it did not modify the amplitude frequency (12.23±0.22 mN). Interestingly, a 4.20±1.47 min administration of 6 mL/L ETOH suddenly and completely relaxed the SO.

Effect of ETOH on erythromycin-stimulated SO motility

Erythromycin (1 μmol/L) stimulated the baseline amplitude by 75% and the contractile frequency by 106%. This erythromycin-stimulated SO motility was constant over the experiment. ETOH (2 mL/L) significantly inhibited both the amplitude and the frequency *vs* the carbachol-stimulated group (19.10±0.25 mN, 19.65±0.45 mN and 9.66±0.29 c/min, 10.45±0.20 c/min, respectively). ETOH (4 mL/L) significantly decreased both the amplitude (16.27±0.33 mN) and the frequency (8.32±0.22 c/min), (Figure 2E-H). Administration of 6 mL/L ETOH caused a further decrease in the amplitude and frequency (11.85±0.41 mN and 4.10±0.37 c/min, respectively). Similar to that seen in the carbachol-stimulated group, a 4.10±0.55 min administration of 6 mL/L ETOH suddenly and completely relaxed the SO.

Effect of ETOH on CCK-stimulated SO motility

CCK (0.1 μmol/L) stimulated the baseline amplitude from 12.37±0.05 mN to 27.4±1.82 mN within 1.60±0.24 min. After this peak, the amplitude decreased to 17.17±0.22 mN and was constant during the experiment. The frequency peaked at 12.8±0.2 c/min, after which the constant frequency was 9.43±0.24 c/min throughout the rest of the experiment. ETOH (2 mL/L) mildly decreased the amplitude frequency (16.13±0.23 mN and 17.05±0.14 mN), but had no effect on the contractile frequency of the SO (9.32±0.15 mN and 9.50±0.31 mN). ETOH (4 mL/L) further decreased the amplitude frequency from 16.13±0.23 mN to 14.93±0.19 mN, but still had no effect on the contractile frequency of the SO (9.82±0.23 c/min). ETOH (6 mL/L) further decreased the amplitude and frequency of the SO to 12.13±0.11 mN and 7.26±0.27 c/min, respectively. ETOH (8 mL/L) resulted in complete relaxation of the SO within 10 s (Figure 2 I-L). After this time neither frequencies nor amplitudes could be detected during the remaining part of the experiments.

DISCUSSION

It has been widely known for a long time that ETOH may evoke acute pancreatitis[23]. The role of SO in the pathogenesis of alcohol-induced acute pancreatitis has also been suggested[3,6]. However, the effect of ETOH on SO is controversial. On the one hand, it has been demonstrated that ETOH reduces the SO pressure[3,6]. On the other hand, alcohol was found to induce spasm of the SO[24,25]. These contradictory results indicate that much more information is needed to clarify the effect of ETOH on SO motility.

To investigate these issues, we tested the effect of four different concentrations of ETOH on the resting SO motility. ETOH (2 mL/L) had no effect on the basal SO motility. This result is in accordance with the findings of Cullen *et al*.[26]. They reported that ETOH at a dose of 2 mL/L had no significant effect on the baseline amplitude and the contractile frequency of SO in opossum. ETOH (4 mL/L) mildly decreased the baseline amplitude of the spontaneously contracting SO, but had no effect on the contractile frequency. When ETOH concentration was elevated to 6 mL/L, both the baseline SO contractile amplitude and the frequency were decreased (13%, 34% respectively), while 8 mL/L of ETOH completely relaxed the SO.

Next we tested the effect of different doses of ETOH on physiologically stimulated SO motility (carbachol, erythromycin and CCK). We tested 3 different stimuli at the ED_{50} doses. Carbachol was used to mimic the activity of parasympathetic nervous system, while CCK and a motilin receptor agonist erythromycin were administered to mimic neurohumoral stimuli.

Carbachol (0.1 μmol/L) stimulated the frequency (150%) and the amplitude (82%) of SO contractions. ETOH (2 mL/L) decreased the baseline amplitude and frequency of the carbachol-stimulated SO by the same rate (12%). ETOH (4 mL/L) decreased the amplitude of SO motility to the basal level, but the frequency still remained elevated. A 4-5 min administration of 6 mL/L ETOH completely relaxed the SO. These results demonstrate that ETOH may inhibit the activity of SO motility stimulated by the parasympathetic nervous system in a dose-dependent manner. Moreover, we can conclude that ETOH has a stronger effect on the contractile amplitude than on the frequency of SO.

The effect of ETOH was almost the same on erythromycin-stimulated as on carbachol-stimulated SO. ETOH (2 mL/L) mildly decreased the baseline amplitude and frequency by 10%. ETOH (4 mL/L) decreased both the amplitude and the frequency of erythromycin-stimulated SO. A 4-5 min administration of 6 mL/L ETOH completely relaxed the SO, as it was found during carbachol-stimulation.

Finally, the effect of ETOH was tested on CCK-stimulated SO motility. CCK stimulated the baseline amplitude and the contractile frequency of SO by 39 % and 74%, respectively. ETOH (2 mL/L) mildly decreased the baseline amplitude (6 mL/L), but had no effect on the frequency of the SO. ETOH (4 mL/L) further decreased the baseline amplitude. Interestingly, 4 mL/L ETOH still had no effect on the contractile frequency. When the concentration of ETOH was increased to 6 mL/L, both the baseline amplitude and the contractile frequency of SO were decreased (29% and 23% respectively). ETOH (8 mL/L) immediately and completely relaxed the SO as it was seen during the study of unstimulated SO.

Taken together, ETOH inhibited the basal and neurally (carbachol), hurmorally (erythromycin, a motilin agonist) and neurohumorally (CCK) stimulated SO motility in a dose-dependent manner. Viceconte *et al*.[6] suggested that alcohol might cause a hormone-mediated relaxation, but they could not exclude a nervous or direct mechanism. Cullen *et al*.[26] demonstrated that 2 mL/L ETOH could decrease the frequency of H_2O_2-stimulated SO motility. These findings suggest that the main effect of alcohol is direct, independent of a specific neural and/or humoral pathway. Interestingly, we have to note that the inhibitory effect of ETOH was more pronounced during carbachol or erythromycin stimulation than during CCK stimulation. Therefore, we could not totally exclude a marginal specific effect of ETOH. There is no data available concerning the effect of low doses of ETOH on the SO in human. However, gastric absorption accounted for 30% of ETOH administered with food[27], therefore, during a low alcohol-concentrated-fluid (2-5%) intake, small doses of alcohol may be found around the SO. These findings need further investigation.

The inhibitory effect of ETOH on SO motility may have an important pathophysiological role. ETOH has been found to increase basal pancreatic flow rate and protein output[28,29], thus, elevating the intraluminal pressure in the pancreatic ductal system. The relaxation of SO opens the way for pancreatic fluid to flow out into the duodenum, thus, preventing the pancreas from the damage by the elevated intraluminal pressure during acute ETOH administration. It is hard to believe, that a duodeno-pancreatic reflux against the high pancreatic-juice-flow could play a decisive role in the pathogenesis of alcohol-induced

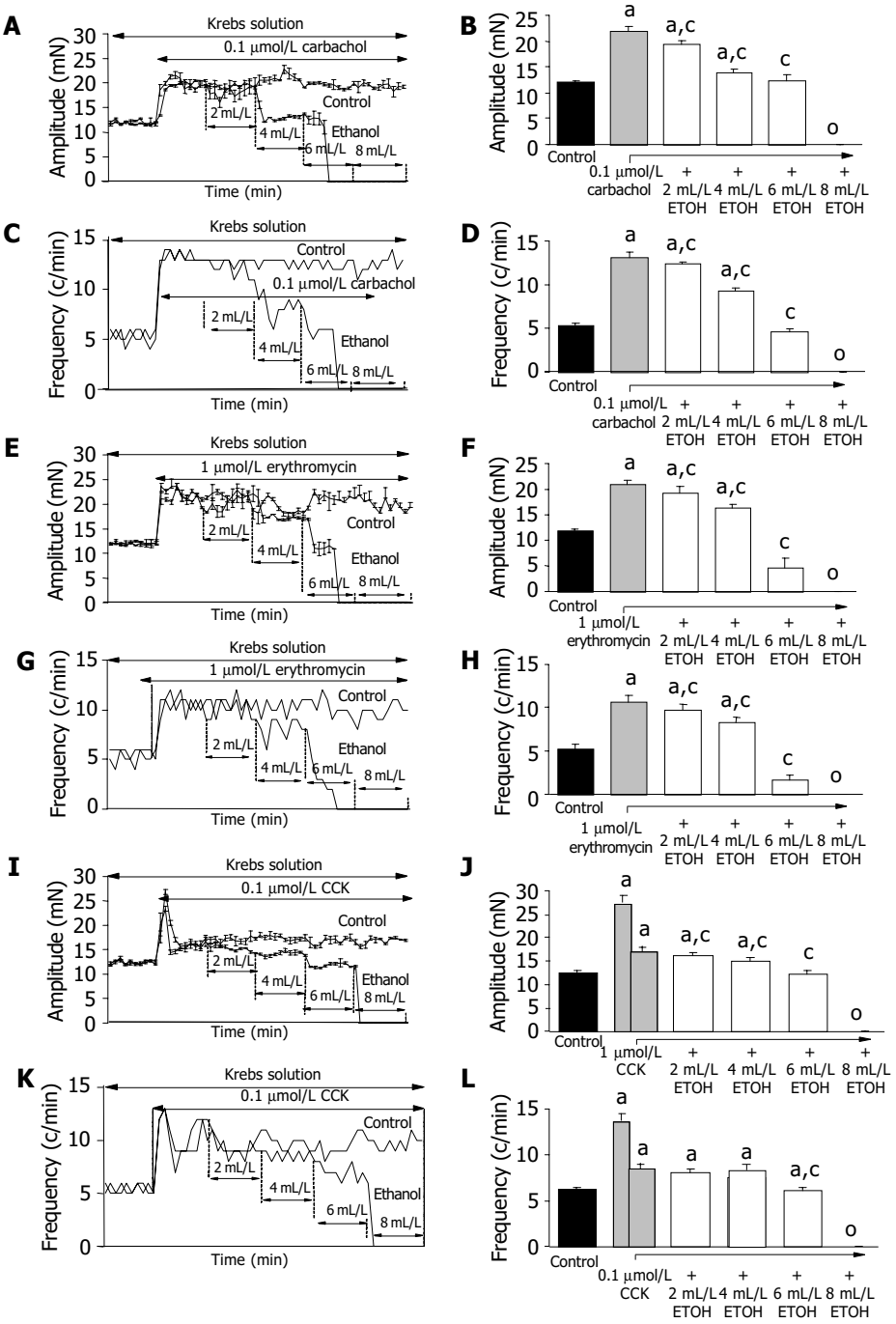

Figure 2 Effect of ETOH on carbachol, erythromycin, CCK stimulated SO motility. All of the SOs were stimulated by 0.1 μmol/L carbachol for 40 min. Different concentrations of ETOH were administered as described in Figure 1. A: Effect of ETOH on the carbachol-stimulated baseline amplitude. Representative experiments of the control (carbachol-treated) and the ETOH-carbachol-treated groups are shown. B: Summary of the effect of ETOH on the carbachol-stimulated baseline amplitude. mean±SE, n = 5, ^aP<0.05 *vs* control, ^cP<0.05 *vs* the carbachol-stimulated group, o: no contractile activity. C: Effect of ETOH on the contractile frequency. Representative experiments of the (carbachol-treated) and the ETOH-carbachol-treated groups are shown. D: Summary of the effect of ETOH on the carbachol-stimulated contractile frequency. mean±SE, n = 5, ^aP<0.05 *vs* control, ^cP<0.05 *vs* the carbachol-stimulated group, o: no contractile activity. E: Effect of ETOH on the erythromycin-stimulated baseline amplitude. Representative experiments of the control (erythromycin-treated) and the ETOH-erythromycin-treated groups are shown. F: Summary of the effect of ETOH on the erythromycin-stimulated baseline amplitude. mean±SE, n = 5, ^aP<0.05 *vs* the control, ^cP<0.05 *vs* the erythromycin-stimulated group, o: no contractile activity. G: Effect of ETOH on the contractile frequency. Representative experiments of the control (erythromycin-treated) and the ETOH-erythromycin-treated groups are shown. H: Summary of the effect of ETOH on the erythromycin-stimulated contractile frequency. mean±SE, n = 5, ^aP<0.05 *vs* the control, ^cP<0.05 *vs* the erythromycin-stimulated group, o: no contractile activity. I: Effect of ETOH on the carbachol-stimulated baseline amplitude. Representative experiments of the control (CCK-treated) and the ETOH-CCK-treated groups are shown. J: Summary of the effect of ETOH on the CCK-stimulated baseline amplitude. mean±SE, n = 5, ^aP<0.05 *vs* the control; o: no contractile activity. In the 0.1 μmol/L CCK-treated group, the first column represents the peak amplitude of contractile frequencies. The second column represents the constant amplitudes after the peak. ^aP<0.05 *vs* the constant amplitude of the CCK-treated group. K: Effect of ETOH on the contractile frequency. Representative experiments of the (CCK-treated) and ETOH-CCK-treated groups are shown. L: Summary of the effect of ETOH on the CCK-stimulated contractile frequency. mean±SE, n = 5, ^aP<0.05 *vs* the control; o: no contractile activity. In the 0.1 μmol/L CCK-treated group, the first column represents the peak of frequencies. The second column represents the constant frequencies after the peak. ^cP<0.05 *vs* the constant frequency of the CCK-treated group.

acute pancreatitis. Furthermore, it is also well documented that SO relaxants[30-32] and endoscopic sphincterotomy[33,34] have benefical effects during acute pancreatitis, which argue against the duodeno-pancreatic reflux theory. All in all, we think that the response of SO motility to ETOH administration is protective against pancreatic injury rather than harmful to the pancreas.

In conclusion, ETOH can strongly inhibit the basal, carbachol, erythromycin, and CCK stimulated SO motility in rabbits, and it is possible that SO opens the way for the pancreatic fluid to flow out into the duodenum. This relaxation of the SO may prevent the pancreas against alcohol-induced damage.

REFERENCES

1 **Schneider A**, Whitcomb DC, Singer MV. Animal models in alcoholic pancreatitis-what can we learn? *Pancreatology* 2002; **2:** 189-203

2 **Dubagunta S**, Still CD, Komar MJ. Acute pancreatitis. *J Am Osteopath Assoc* 2001; **101**(4 Suppl Pt 1): S6-9

3 **Yamasaki K**, Okazaki K, Sakamoto Y, Yamamoto Y, Yamamoto Y, Okada T. Effects of ethanol on the motility of papillary sphincter and exocrine pancreas in the monkey. *Am J Gastroenterol* 1993; **88:** 2078-2083

4 **Becker JM**, Sharp SW. Effect of alcohol on cyclical myoelectric activity of the opossum sphincter of Oddi. *J Surg Res* 1985; **38:** 343-349

5 **Goff JS.** The effect of ethanol on the pancreatic duct sphincter of Oddi. *Am J Gastroenterol* 1993; **88:** 656-660

6 **Viceconte G.** Effects of ethanol on the sphincter of Oddi: an endoscopic manometric study. *Gut* 1983; **24:** 20-25

7 **Harada T**, Katsuragi T, Furukawa T. Release of acetylcholine mediated by cholecystokinin receptor from the guinea pig sphincter of Oddi. *J Pharmacol Exp Ther* 1986; **239:** 554-558

8 **Becker JM**, Moody FG. The dose/response effects of gastrointestinal hormones ont he opossum biliary sphincter. *Curr Surg* 1980; **37:** 60-62

9 **Sarles JC**, Delecourt P, Castello H, Gaeta L, Nacchiero M, Amoros JP, Devaux MA, Awad R. Action of gastrointestinal hormones on the myoelectric activity of the sphincter of Oddi in living rabbit. *Regul Pept* 1981; **2:** 113-124

10 **Chiu JH**, Kuo YL, Lui WY, Wu CW, Hong CY. Somatic electrical nerve stimulation regulates the motility of sphincter of Oddi in rabbits and cats: evidence for a somatovisceral reflex mediated by cholecystokinin. *Dig Dis Sci* 1999; **44:** 1759-1767

11 **Elbrond H**, Ostergaard L, Huniche B, Larsen LS, Andersen MB. Rabbit sphincter of Oddi and duodenal pressure and slow-wave activity. Effects of cholecystokinin. *Scand J Gastroenterol* 1994; **29:** 537-544

12 **Muller EL**, Lewinski MA, Pitt HA. Action of cholecystokinin on sphincter of Oddi phasic wave activity in the prairie dog. *Curr Surg* 1985; **42:** 128-130

13 **Vergara P**, Woskowska Z, Cipris S, Fox-Threlkeld JE, Daniel EE. Mechanisms of action of cholecystokinin in the canine gastrointestinal tract: role of vasoactive intestinal peptide and nitric oxide. *J Pharmacol Exp Ther* 1996; **279:** 306-316

14 **Pozo MJ**, Salido GM, Madrid JA. Action of cholecystokinin on the dog sphincter of Oddi: influence of anti-cholinergic agents. *Arch Int Physiol Biochim* 1990; **98:** 353-360

15 **Chaussade S**, Michopoulos S, Sogni P, Guerre J, Couturier D. Motilin agonist erythromycin increases human lower esophageal sphincter pressure by stimulation of cholinergic nerves. *Dig Dis Sci* 1994; **39:** 381-384

16 **Bormans V**, Peeters TL, Janssens J, Pearce D, Vandeweerd M, Vantrappen G. In man, only activity fronts that originate in the stomach correlate with motilin peaks. *Scand J Gastroenterol* 1987; **22:** 781-784

17 **Sarles JC**, Delecourt P, Devaux MA, Amoros JP, Guicheney JC, Wunsch E. *In vivo* effect of 13 Leu motilin on the electric activity of the rabbit sphincter of Oddi. *Horm Metab Res* 1981; **13:** 340-342

18 **Kaufman HS**, Ahrendt SA, Pitt HA, Lillemoe KD. The effect of erythromycin on motility of the duodenum, sphincter of Oddi, and gallbladder in the prairie dog. *Surgery* 1993; **114:** 543-548

19 **Saccone GT**, Liu YF, Thune A, Harvey JR, Baker RA, Toouli J. Erythromycin and motilin stimulate sphincter of Oddi motility and inhibit trans-sphincteric flow in the Australian possum. *Naunyn Schmiedebergs Arch Pharmacol* 1992; **346:** 701-706

20 **Wehrmann T**, Pfeltzer C, Caspary WF. Effect of erythromycin on human biliary motility. *Aliment Pharmacol Ther* 1996; **10:** 421-426

21 **Konomi H**, Simula ME, Meedeniya AC, Toouli J, Saccone GT. Induction of duodenal motility activates the sphincter of Oddi (SO)-duodenal reflex in the Australian possum *in vitro*. *Auton Autacoid Pharmacol* 2002; **22:** 109-117

22 **Lonovics J**, Jakab I, Szilvassy J, Szilvassy Z. Regional differences in nitric oxide-mediated relaxation of the rabbit sphincter of Oddi. *Eur J Pharmacol* 1994; **255:** 117-122

23 **Sarles H**, Lebreuil G, Tasso F, Figarella C, Clemente F, Devaux MA, Fagonde B, Payan H. A comparison of alcoholic pancreatitis in rat and man. *Gut* 1971; **12:** 377-388

24 **Sarles JC**, Midejean A, Devaux MA. Electromyography of the sphincter of Oddi. Technic and experimental results in the rabbit: effect of certain drugs. *Am J Gastroenterol* 1975; **63:** 221-231

25 **Guelrud M**, Mendoza S, Rossiter G, Gelrud D, Rossiter A, Souney PF. Effect of local instillation of alcohol on sphincter of Oddi motor activity: combined ERCP and manometry study. *Gastrointest Endosc* 1991; **37:** 428-432

26 **Cullen JJ**, Ledlow A, Murray JA, Conklin JL. Effect of hydroxyl radical (OH.) on sphincter of Oddi motility. *Digestion* 1997; **58:** 452-457

27 **Levitt MD**, Li R, DeMaster EG, Elson M, Furne J, Levitt DG. Use of measurements of ethanol absorption from stomach and intestine to assess human ethanol metabolism. *Am J Physiol* 1997; **273**(Pt 1)**:** G951-957

28 **Alonso RM**, Alvarez MC, San Roman JI, Garcia LJ, Calvo JJ, Lopez MA. Effects of acute intravenous ethanol on basal exocrine pancreatic secretion in rat: cholinergic involvement. *Rev Esp Fisiol* 1994; **50:** 81-87

29 **Nakamura T**, Okabayashi Y, Fujii M, Tani S, Fujisawa T, Otsuki M. Effect of ethanol on pancreatic exocrine secretion in rats. *Pancreas* 1991; **6:** 571-577

30 **Lai KH**. Sphincter of Oddi and acute pancreatitis: a new treatment option. *JOP* 2002; **3:** 83-85

31 **Lai KH**, Lo GH, Cheng JS, Fu MT, Wang EM, Chan HH, Wang YY, Hsu PI, Lin CK. Effect of somatostatin on the sphincter of Oddi in patients with acute non-biliary pancreatitis. *Gut* 2001; **49:** 843-846

32 **Velosy B**, Madacsy L, Szepes A, Pavics L, Csernay L, Lonovics J. The effects of somatostatin and octreotide on the human sphincter of Oddi. *Eur J Gastroenterol Hepatol* 1999; **11:** 897-901

33 **Zhou MQ**, Li NP, Lu RD. Duodenoscopy in treatment of acute gallstone pancreatitis. *Hepatobiliary Pancreat Dis Int* 2002; **1:** 608-610

34 **Park SH**, Watkins JL, Fogel EL, Sherman S, Lazzell L, Bucksot L, Lehman GA. Long-term outcome of endoscopic dual pancreatobiliary sphincterotomy in patients with manometry-documented sphincter of Oddi dysfunction and normal pancreatogram. *Gastrointest Endosc* 2003; **57:** 483-491

Edited by Wang XL **Proofread by** Zhu LH and Xu FM

PO Box 2345, Beijing 100023, China
Fax: +86-10-85381893
E-mail: wjg@wjgnet.com www.wjgnet.com

World J Gastroenterol 2004;10(23):3475-3479
World Journal of Gastroenterology
Copyright © 2004 by The WJG Press ISSN 1007-9327

• BASIC RESEARCH •

DNA ploidy and *c-Kit* mutation in gastrointestinal stromal tumors

Ju Han Lee, Xianglan Zhang, Woon Yong Jung, Yang Seok Chae, Jong-Jae Park, Insun Kim

Ju Han Lee, Xianglan Zhang, Woon Yong Jung, Yang Seok Chae, Insun Kim, Department of Pathology, Medical College, Korea University, Seoul, Korea
Jong-Jae Park, Department of Internal Medicine, Medical College, Korea University, Seoul, Korea
Correspondence to: Dr. Insun Kim, Department of Pathology, Guro Hospital, 80, Guro-dong, Guro-Ku, Seoul, Korea
Telephone: +822-818-6233 **Fax:** +822-818-6239
Received: 2003-12-28 **Accepted:** 2004-01-30

Abstract

AIM: To investigate the prognostic significance of *c-Kit* gene mutation and DNA ploidy in gastointestinal stromal tumors (GISTs).

METHODS: A total of 55 cases of GISTs were studied for the expression of *c-Kit* by immunohistochemistry, and the *c-Kit* gene mutations in exons 9, 11, 13, and 17 were detected by polymerase chain reaction-single strand confirmation polymarphism (PCR-SSCP) and denaturing high performance liquid chromatography (D-HPLC) techniques. DNA ploidy was determined by flow cytometry.

RESULTS: Of the 55 cases of GISTs, 53 cases (96.4%) expressed *c-Kit* protein. The *c-Kit* gene mutations of exons 11 and 9 were found in 30 (54.5%) and 7 cases (12.7%), respectively. No mutations were found in exons 13 and 17. DNA aneuploidy was seen in 10 cases (18.2%). The *c-Kit* mutation positive GISTs were larger in size than the negative GISTs. The aneuploidy tumors were statistically associated with large size, high mitotic counts, high risk groups, high cellularity and severe nuclear atypia, and epithelioid type. There was a tendency that *c-Kit* mutations were more frequently found in aneuploidy GISTs.

CONCLUSION: DNA aneuploidy and *c-Kit* mutations can be considered as prognostic factors in GISTs.

Lee JH, Zhang X, Jung WY, Chae YS, Park JJ, Kim I. DNA ploidy and *c-Kit* mutation in gastrointestinal stromal tumors. *World J Gastroenterol* 2004; 10(23): 3475-3479
http://www.wjgnet.com/1007-9327/10/3475.asp

INTRODUCTION

Gastrointestinal stromal tumors (GISTs) are the most common mesenchymal neoplasms of the gastrointestinal tract. The term, GIST, was first introduced in the 1980s to include a group of nonlymphomatous, nonepithelial tumors of the gut[1]. With the advent of immunohistochemistry, CD117 (c-Kit) negative tumors, such as schawannomas, leiomyomas, and leiomyosarcomas, were excluded from the noncommittal term of "gastrointestinal stromal tumors". Recently, based on immunophenotypic and ultrastructural similarities, it is widely accepted that the precursor cells in GISTs are the interstitial cells of Cajal (ICCs)[2]. Immunohistochemically, GISTs are typically positive for *c-Kit* and CD34, but negative for S-100 protein, desmin, and may express smooth muscle actin in 20% to 40% of cases[3].

Yet despite their recognition as a distinct pathologic entity, because GISTs are widely diverse in terms of clinical presentation, morphology, and biologic behavior, the prediction of malignancy on the basis of pathologic features is often difficult. Many studies have analyzed the prognostic relevance of a variety of parameters such as anatomical location, mucosal invasion, tumor necrosis, and high cellularity, rather often leading to conflicting conclusions[1,4-6]. However, two morphologic features have emerged as fairly reliable predictors of outcome: mitotic rate and tumor size[4,7-12]. A consensus conference held at National Institutes of Health in April 2001 provided both an evidence-based definition and a practical scheme for assessing the risk (very low risk, low risk, intermediate risk, and high risk) of aggressive clinical behavior[13]. Recently, a prognostic significance of *c-Kit* mutations was suggested by several clinicopathologic studies[14-17]. The largest series has shown that *c-Kit* mutation in exon 11 was more common in large tumors, and that the presence of this mutation was an adverse prognostic factor[14].

The conceptual evolution of GISTs and *c-Kit* mutation has been the subject of numerous previous articles. However, DNA ploidy studies in relation to *c-Kit* mutation are not well established. The purpose of this study was to examine the *c-Kit* mutations and DNA ploidy in GISTs to evaluate them as the prognostic factors.

MATERIALS AND METHODS

Histological review

The cases included in this study were retrieved from patients who were diagnosed as GISTs and treated at Korea University Hospitals between January 1997 and August 2003. The clinical history and postoperative courses were obtained from the review of clinical records. The tumor size in greatest dimension and the location were taken from the pathology reports. Histological slides were reviewed by two of the authors (Kim, I and Lee, JH) in all of the cases. The tumor cell type was determined by light microscopic study. The spindle cell type had a predominant fusiform morphology. Both cytoplasm and nuclei were elongated and aligned within the microscopic field. The epithelioid cell type had a predominantly spherical morphology. The nuclei were round and tended to be centrally placed within tumor cells. The number of mitosis was determined by counting the mitotic activity in 50 adjacent high-power fields (HPF) at a magnification of ×400. The cytologic atypia of the tumor cells was determined to be mild, moderate, or severe. The cytologic atypia was assessed within the most proliferative area. Mild atypia indicated that the tumor cells were histologically benign or mildly atypical. Moderate atypia indicated that the tumor cells had moderately enlarged hyperchromatic or vesicular nuclei with or without prominent nucleoli and some nuclear irregularity. Severe atypia indicated that the tumor cells had enlarged irregular, hyperchromatic, or vesicular pleomorphic nuclei with prominent nucleoli. The cellularity was scored as low if the cell count was below 1 000/mm^2, intermediate for a range from 1 000 to 2 000 cells per mm^2, and high if exceeding 2 000 cells/mm^2. Tumor necrosis was determined to be present or absent. Tumor hemorrhage was determined to be present or absent. The growth pattern was determined to be expansive or invasive. GISTs were reclassified as very low, low, intermediate, and high risk groups for their estimated potential for aggressive clinical behavior as suggested by NIH consensus[13].

Immunohistochemistry

Representative sections from each lesion were subjected to immunohistochemical staining by using the avidin-biotin-peroxidase complex (ABC) method. The target differentiation antigens visualized by the monoclonal and polyclonal antibodies were *c-Kit* (1:400; Dako, Glostrup, Denmark), CD34 (1:200; Neomarker, CA, USA), smooth muscle actin (SMA, 1:200; Dako, Glostrup, Denmark), and S-100 protein (1:400; Neomarker, CA, USA). The tumors were designated as positive when more than 10% of the tumor cells showed a positive reaction for CD34, SMA and S-100 protein. Positive reactions were classified by using the following criteria for *c-Kit*: (-) negative, if <10% cells were stained; (+), if 10-50% cells were immunoreactive; (++), if 51-100% cells were immunoreactive. The tumors which showed positive reaction for CD34 and/or *c-Kit* protein with or without SMA and S-100 protein were included in GISTs.

DNA extraction

DNA was extracted from the formaldehyde-fixed, paraffin-embedded tissue sections by using standard methods with proteinase K digestion and phenol/chloroform purification.

Polymerase - chain reaction - single strand confirmation polymorphism (PCR-SSCP)

PCR primers were designated to amplify exons 9, 11, 13, and 17 (Table 1). PCR was carried out with the following conditions: 50 μL total reaction volume, with 5 μL template, 5 μL of each oligonucleotide primer, 10 μL dNTP, 10 μL ddH_2O, 2 μL Taq polymerase, 8 μL Mg^{2+} and 5 μL 10× PCR buffer. Cycling conditions were as follows: an initial penetration at 95 ℃ for 4 min, 38 cycles each at 94 ℃ for 1 min, at 56 ℃ for 1 min, at 72 ℃ for 1 min, followed by one cycle at 72 ℃ for 10 min. PCR products were visualized by gel electrophoresis in 1.7 g/L agarose. Then the PCR products were subjected to 80 g/L non-denaturation polyacrylamide gel electrophoresis with 50 g/L glycerin and silver nitrate staining.

Table 1 Primer sequence for *c-Kit* exons 9, 11, 13, and 17 and the corresponding annealing temperature (T_A) and the size of expected PCR size products

c-Kit exon No.	Primers	Primer sequence 5'->3'	T_A (℃)	Product size (bp)
9	hEx9-F	TTCCTAGAGTAAGCCAGGG	53	298
	hEx9-R	AATCATGACTGATATGGT		
11	hEx11-F	CAGGTAACCATTTATTTGT	53	326
	hEx11-R	TCATTGTTTCAGGTGGAAC		
13	hEx13-F	ATCAGTTTGCCAGTTGTGCT	53	250
	hEx13-R	TTTATAATCTAGCATTGCC		
17	hEx17-F	GTTTTCACTCTTTACAAGT	53	277
	hEx17-R	TTACATTATGAAAGTCACAGGAAAC		

Denaturing high performance liquid chromatography (D-HPLC)

To enhance heteroduplex formation, the untreated PCR products (5-7 μL) were denaturated at 95 ℃ for 5 min followed by gradual reannealing to room temperature for over 30 min. Samples were analyzed in WAVE DHPLC. The gradient was formed by mixing buffer A (0.1 mmol/L TEAA) and buffer B (0.1 mol/L TEAA, 250 g/L acetonitrile). The analysis was carried out at a flow rate of 0.9 mL/min and buffer B gradient increase of 20 g/L per minute for 4 min. Oven temperature for optimal heteroduplex separation under partial DNA denaturation was determined for each amplified fragment by using WAVE Marker software. The most important criteria for assigning the presence of a sequence alteration in each DHPLC fragment were the numbers and the shape of elution peaks in comparison with a wild-type subject elution profile used as reference. To allow the detection of heteroduplex DNA molecules in homozygous patients, those amplicons were pre-mixed with sequence-confirmed wild-type PCR controls. The mixed samples were then denatured at 94 ℃ for 5 min and cooled for over 45 min at room temperature, before D-HPLC analysis.

DNA ploidy

Nuclear suspensions from the selected tissue blocks, previously used in the immunohistochemical study, were prepared in each case. Three 50-μm thick sections from the tissue block were dewaxed in xylene and rehydrated in a sequence of decreasing concentrations of alcohol. After being washed in Dulbecco's phosphate buffered saline (DPBS), the tissue was incubated in 2 g/L pepsin (Sigma Chemical Company, St. Louis, USA) at 37 ℃ water bath for 2.5 h. Then, the samples were neutralized by citrate buffer and treated with trypsin at 37 ℃ water bath for 10 min. After RNase treatment at 37 ℃ water bath for 30 min, the samples were stained with propidium iodide at 4 ℃ for 30 min. By using a FACS analyzer, the DNA histograms were obtained.

Statistical analysis

The data were analyzed with Chi-square and *t* tests by using SPSS 10.0 program.

RESULTS

Clinicopathologic charateristics

There were 25 males and 30 females. The mean age of the patients at the time of diagnosis was 60 (range: 29-80) years. The locations of tumors were as follows: one in the esophagus, 43 in the stomach, 10 in the small intestine (including duodenum), and one in the mesentery. The symptoms of patients were as follows: 24 cases of abdominal pain, 11 cases of gastrointestinal bleeding, 4 cases of palpable mass and 12 cases of nonspecific. The mean diameter of tumors was 5.29 (range: 0.4-17.0) cm. Three patients showed liver metastasis at the time of surgery. Two patients received re-operation due to recurrence. One patient had a local gastric recurrence after 17 mo and the other had a local duodenal recurrence after 33 mo.

Patients included in this study were diagnosed to have a GIST by a variety of histologic criteria. Spindle cell lesions occurred with or without an epithelioid component, the most common tumor lesions showed interlacing fascicles of spindle cells. Some lesions showed a palisaded morphology resembling peripheral neurilemmomas, but storiform, fascicular, or mixed growth patterns were seen. Some of them were composed of round and epithelioid cells appearing with perinuclear shrinkage of cytoplasm. In some tumors or parts of tumors, there was a mixture of epithelioid cells and spindle cells. Fifteen (27.3%) tumors were epithelioid cell type, whereas the remaining 40 (72.7%) were spindle cell type (Figure 1). The mitotic index ranged from 0 to 100 (mean: 11.4). The degree of cytologic atypia was mild in 27 (49.1%) patients, moderate in 21 (38.2%), and severe in 7 (12.7%). The degree of cellularity was low in 11 (20.0%) patients, intermediate in 37 (67.3%), and high in 7 (12.7%). Necrosis was present in 11 (20.0%), and hemorrhage was present in 17 (30.9%) tumors. Expansive growth was found in 30 (54.5%), and invasive growth in 25 (45.5%) tumors.

Correlation of risk groups and clinicopatholgic parameters

Tumors were divided into very low (10/55, 18.2 %), low (26/55, 47.3 %), intermediate (4/55, 7.3%) and high risk (15/55, 27.3%) groups by NIH consensus[13]. Correlation of risk groups and other clinicopthologic parameters is shown in Table 2. Higher risk (intermediate and high risk) groups showed more frequent necrosis, more severe nuclear atypia and higher cellularity than lower risk (very low and low risk) groups which were statistically significant. The epithelioid cell type was more frequent in higher risk group.

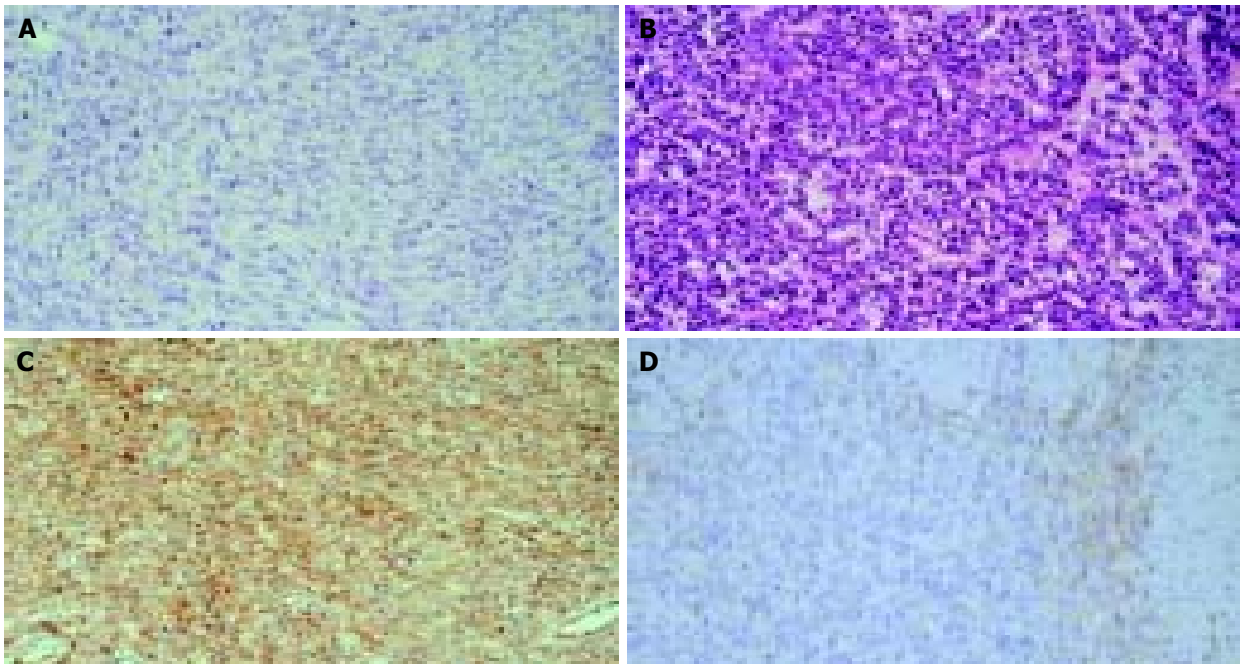

Figure 1 Histological features of various cell types of gastrointestinal stromal tumors and immunohistochemical staining for *c-Kit*. ×200. A: Spindle cell type; B: Epithelioid type; C: >50% tumor cells are positive for *c-Kit*; D: 10-50% tumor cells are positive for *c-Kit*.

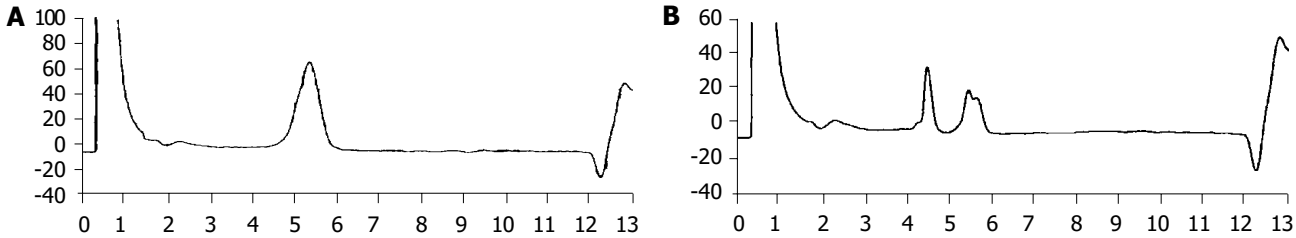

Figure 2 *c-Kit* mutations in exon 11 by denaturing high performance liquid chromatography. A: Normal; B: mutation.

Table 2 Comparison of clinicopathologic parameters according to the risk groups of gastrointestinal stromal tumors

Parameter\Risk group		Very low and low (n = 36)	Intermediate and high (n = 19)	P
Cellularity	Low	11	0	
	Intermediate	22	15	0.019
	High	3	4	
Nuclear atypia	Mild	22	5	
	Moderate	12	9	0.019
	Severe	2	5	
Necrosis	Absent	34	10	0.000
	Present	2	9	
Hemorrhage	Absent	28	10	0.055
	Present	8	9	
Infiltrative	Absent	22	8	0.178
Growth pattern	Present	14	11	
Tumor cell type	Spindle	29	11	0.001
Epithelioid		7	8	

Results of immunohistochemistry

A positive reaction for *c-Kit* protein was obtained in 53 (96.4%), CD 34 in 53 (96.4%), SMA in 17 (30.9%), and S-100 protein in 3 (5.5%). Among 53 *c-Kit* positive cases, 10 cases (18.9%) were (+) and 43 cases (81.1%) were (++) (Figure 1).

Correlation of c-kit mutation with clinicopatholgic parameters

Thirty cases (54.5%) showed mutations of *c-Kit* in exon 11 (Figure 2). Among 30 cases, 16 cases showed mutations by both PCR-SSCP and D-HPLC methods, 9 cases by PCR-SSCP, and 5 cases by D-HPLC method. Seven cases (12.7%) showed mutations of *c-Kit* in exon 9. Among them, 3 cases showed mutations by both PCR-SSCP and D-HPLC methods, 3 cases by PCR-SSCP, and 1 case by D-HPLC method. Two cases showed mutations of both exons 9 and 11. No mutations were found in exons 13 and 17. The mutation-positive GISTs belonged to the large tumors (Table 3), but the association with the other parameters was not significant.

Table 3 Comparison of clinicopathologic parameters according to *c-Kit* mutations

Parameter		Mutations		P
		Negative (n = 20)	Positive (n = 35)	
Sex (M:F)		11:9	14:21	0.283
Age (mean, yr)		58.2	61.0	0.360
Mean tumor size (cm)		3.8	6.2	0.020
Mean mitoses counts		7.8	13.4	0.360
Risk group: Very low/low		14	22	0.592
Intermediate/high		6	13	
Cellularity: Low		5	6	0.741
Intermediate		13	24	
High		2	5	
Nuclear atypia	Mild	10	17	0.898
	Moderate	7	14	
	Severe	3	4	
Necrosis	Absent	18	26	0.161
	Present	2	9	
Hemorrhage	Absent	17	21	0.054
	Present	3	14	
Infiltrative growth	Absent	12	18	0.539
	Present	8	17	
Tumor cell type	Spindle	13	27	0.330
	Epithelioid	7	8	

Correlation of c-kit mutation with c-kit expression

Among 10 *c-Kit* (+) cases, 6 cases showed mutations of *c-Kit* in exon 9 or 11. Among 43 *c-Kit* (++) cases, 31 cases showed mutations of *c-Kit* in exon 9 or 11. The rate of *c-Kit* mutations was higher in *c-Kit* (++) group than that in c-Kit (+) group ($P = 0.05$).

Correlation of DNA aneuploidy with clinicopatholgic parameters

Ten cases (18.2%) were DNA aneuploidy (Figure 3). The tumors with aneuploidy were associated with the larger tumor size, high mitotic counts, higher risk groups, high cellularity, and severe nuclear atypia, and epithelioid cell type (Table 4).

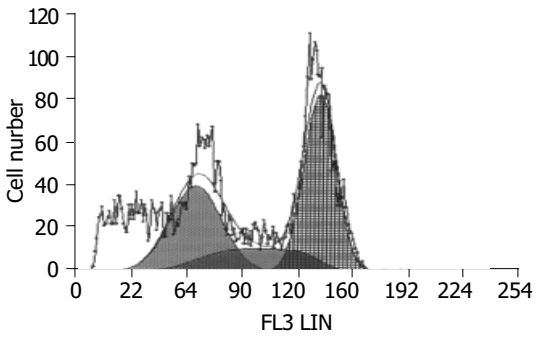

Figure 3 DNA aneuploidy in gastrointestinal stromal tumors.

Table 4 Comparison of clinicopathologic parameters according to DNA ploidy

Parameter		Diploid (n = 45)	Aneuploid (n = 10)	P
Sex (M:F)		21:24	4:6	0.702
Age(mean, yr)		60.8	56.1	0.225
Mean tumor size (cm)		4.1	10.5	0.007
Mean mitoses counts		5.0	40.0	0.022
Risk group:	Very low / low	34	2	0.001
	Intermediate / high	11	8	
Cellularity	Low	11	0	0.008
	Intermediate	31	6	
	High	3	4	
Nuclear atypia	Mild	24	3	0.016
	Moderate	18	3	
	Severe	3	4	
Necrosis	Absent	38	6	0.080
	Present	7	4	
Hemorrhage	Absent	33	5	0.149
	Present	12	5	
Infiltrative growth	Absent	27	3	0.085
	Present	18	7	
Tumor cell type	Spindle	36	4	0.010
	Epithelioid	9	6	

Correlations of c-kit mutation and DNA aneuploidy with metastasis or recurrence

Three metastatic GISTs showed *c-Kit* mutation. Among them, two cases showed mutations in exon 11, and the other one showed mutation in exon 9. Two of these 3 tumors had DNA aneuploidy. Among two recurrent GISTs, only one case showed mutation in exon 11, and the two cases were DNA diploidy.

Correlation of c-kit mutation with DNA aneuploidy

Correlation of *c-Kit* mutation with DNA ploidy state was analyzed (Table 5). There was a tendency that *c-Kit* mutations were more frequent in aneuploid tumors than in diploid ones, but not statistically significant ($P = 0.063$).

Table 5 Correlation of *c-Kit* mutation and DNA ploidy

DNA ploidy[1]	*c-Kit* mutation	
	Negative	Positive
Diploid	19	26
Aneuploid	1	9

[1]$P = 0.063$.

DISCUSSION

It has been reported that GISTs are strongly and nearly consistent *c-Kit* positive, and associated with the mutations of the *c-Kit* gene. Approximately 40% to 50 % of GISTs, mostly the malignant variants, had mutations in the juxtamembrane domain (exon 11) of the *c-Kit* gene[14-16], although some studies found mutations in only 15%[18] or the others in as many as 80%[19] of the analyzed cases. Lack of mutations in exon 11 in a significant portion of GISTs may suggest that mutations may occur in other domains of the *c-Kit* gene. However, no mutations were found in exon 17 (kinase domain) in a large group of GISTs studied[14], which was the area where *c-Kit* mutations occur in mastocytoma[20] and seminoma[21]. Recently, new mutational hotspots were identified as a result of comprehensive sequencing of *c-Kit* cDNA obtained from 13 GISTs, which were negative for exon 11 mutations. Mutations in exon 9 and exon 13 were detected in 6 (46%) and 2 (15%) of them, suggesting that such mutations may be relatively common in GISTs[19].

In this study, we analyzed 55 GISTs. Thirty cases (54.5%) showed mutations of *c-Kit* in exon 11 and 7 cases (12.7%) showed mutations in exon 9. No mutations were found in exon 13 and exon 17. The *c-Kit* mutation positive GISTs were large in size, and all three metastatic GISTs showed mutations, but the association with other clinicopathologic factors was not evident. The rate of *c-Kit* mutations was higher in *c-Kit* (++) group rather than in *c-Kit* (+) group.

The factors related to the tumor biology might usefully complement the clinical and morphological data. Thus, DNA aneuploidy has been claimed to allow a sensitive and specific discrimination between benign and malignant tumors of the gastrointestinal tract and to correlate with their prognosis[22-28]. However, in other reports, aneuploidy could not be used as a diagnostic criterion of malignancy, but was associated with a mere tendency to an adverse outcome[29,30]. In our study, 10 cases (18.2%) showed DNA aneuploidy. The aneuploid GISTs were associated with large tumor size, high mitotic counts, higher risk groups, high cellularity, severe nuclear atypia and epithelioid type. These results suggest that DNA aneuploidy represents high risk groups of GISTs suggested by NIH consensus[13].

In conclusion, there is a tendency that *c-Kit* mutations are more frequent in aneuploid GISTs. Therefore, DNA ploidy and *c-Kit* mutations might be closely related.

REFERENCES

1 **Appelman HD.** Smooth muscle tumors of the gastrointestinal tract. What we know now that Stout didn't know. *Am J Surg Pathol* 1986; **10**: 83-99

2 **Kindblom LG,** Remotti HE, Aldenborg F, Meis-Kindblom JM. Gastrointestinal pacemaker cell tumor (GIPACT): gastrointestinal stromal tumors show phenotypic characteristics of the interstitial cells of Cajal. *Am J Pathol* 1998; **152**: 1259-1269

3 **Miettinen M,** Sarlomo-Rikala M, Lasota J. Gastrointestinal stromal tumors – recent advances in understanding of their biology. *Hum Pathol* 1999; **30**: 1213-1220

4 **Appelman HD.** Mesenchymal tumors of the gut: historical perspectives, new approaches, new results and dose it make any difference? *Monogr Pathol* 1990; **31**: 220-246

5 **Emory TS,** Sobin LH, Lukes L, Lee DH, O'Leary TJ. Prognosis of gastrointestinal smooth muscle (stromal) tumors. Dependence on anatomic site. *Am J Surg Pathol* 1999; **23**: 82-87
6 **Miettinen M,** Sarlomo-Rikala M, Sobin LH, Lasota J. Esophageal stromal tumors. A clinicopathologic, immunohistochemical and molecular genetic study of 17 cases and comparison with esophageal leiomyomas and leiomyosarcomas. *Am J Surg Pathol* 2000; **24**: 211-222
7 **Dematteo RP,** Lewis JJ, Leung D, Mudan SS, Woodruff JM, Brennam MF. Two hundred gastrointestinal stromal tumors. Recurrence patterns and prognostic factors for survival. *Ann Surg* 2000; **231**: 51-58
8 **Evans HL.** Smooth muscle tumors of the gastrointestinal tract. A study of 56 cases followed for a minimum of 10 years. *Cancer* 1985; **56**: 2242-2250
9 **Franquemont DW.** Differentiation and risk assessment of gastrointestinal stromal tumors. *Am J Clin Pathol* 1995; **103**: 41-47
10 **Miettinen M,** Lasota J. Gastrointestinal stromal tumors: definition, clinical, histological, immunohistochemical and molecular genetic features and differential diagnosis. *Virchows Arch* 2001; **438**: 1-12
11 **Ranchod M,** Kempson RL. Smooth muscle tumors of the gastrointestinal tract and retroperitoneum. A pathologic analysis of 100 cases. *Cancer* 1977; **39**: 255-262
12 **Reith JD,** Goldblum JR, Lytes RH, Weiss SW. Extra-gastrointestinal (soft tissue) stromal tumors: an analysis of 48 cases with emphasis on histological predictors of outcome. *Mod Pathol* 2000; **13**: 577-585
13 **Fletcher CDM,** Berman JJ, Corless C, Gorstein F, Lasota J, Longley BJ, Miettinen M, O'Leary TJ, Remotti H, Rubin BP, Shmookler B, Sobin LH, Weiss SW. Diagnosis of gastrointestinal stromal tumors: a consensus approach. *Hum Pathol* 2002; **33**: 459-465
14 **Taniguchi M,** Nishida T, Hirota S, Isozaki K, Ito T, Nomura T, Matsuda H, Kitamura Y. Effect of *c-kit* mutation on prognosis of gastrointestinal stromal tumors. *Cancer Res* 1999; **59**: 4297-4300
15 **Ernst SI,** Hubbs AE, Przygodzki RM, Emory TS, Sobin LH, O'Leary TJ. KIT mutation portends poor prognosis in gastrointestinal stromal/smooth muscle tumors. *Lab Invest* 1998; **78**: 1633-1636
16 **Lasota J,** Jasinski M, Sarlomo-Rikala M, Miettinen M. Mutations in exon 11 of *c-kit* occur preferentially in malignant versus benign gastrointestinal stromal tumors and do not occur in leiomyomas or leiomyosarcomas. *Am J Pathol* 1999; **154**: 53-60
17 **Lasota J,** Wozniak A, Sarlomo-Rikala M, Rys J, Kordek R, Nassar A, Sobin LH, Miettinen M. Mutations in exons 9 and 13 of KIT gene are rare events in gastrointestinal stromal tumors. A study of 200 cases. *Am J Pathol* 2000; **157**: 1091-1095
18 **Moskaluk CA,** Tian Q, Marshall CR, Rumpel CA, Franquemont DW, Frierson HF Jr. Mutations of c-kit JM domain are found in a minority of human gastrointestinal stromal tumors. *Oncogene* 1999; **18**: 1897-1902
19 **Lux ML,** Rubin BP, Biase TL, Chen CJ, Maclure T, Demetri G, Xiao S, Singer S, Fletcher CDM, Fletcher JA. KIT extracellular and kinase domain mutations in gastrointestinal stromal tumors. *Am J Pathol* 2000; **156**: 791-795
20 **Nagata H,** Worobec AS, Oh CK, Chowdhury BA, Tannenbaum S, Suzuki Y, Metcalfe DD. Identification of a point mutation in the catalytic domain of the protooncogene *c-kit* in peripheral blood mononuclear cells of patients who have mastocytosis with an associated hematologic disorder. *Proc Natl Acad Sci U S A* 1995; **92**: 10560-10564
21 **Tian Q,** Frierson HF, Krystal GW, Moskaluk CA. Activating c-kit mutations in human germ cell tumors. *Am J Pathol* 1999; **154**: 1643-1647
22 **Federspiel BH,** Sobin LH, Helwig EB, Mikel UV, Bahr GF. Morphometry and cytophotometric assessment of DNA in smooth- muscle tumors (leiomyomas and leiomyosarcomas) of the gastrointestinal tract. *Anal Quant Cytol Histol* 1987; **9**: 105-114
23 **Cooper PN,** Quirke P, Hardy GJ, Dixon MF. A flow cytometric, clinical and histological study of stromal neoplasm of the gastrointestinal tract. *Am J Surg Pathol* 1992; **16**: 163-170
23 **Carrillo R,** Candia A, Rodriquez-Peralto JL, Caz V. Prognostic significance of DNA ploidy and proliferative index (MIB-1 index) in gastrointestinal stromal tumors. *Hum Pathol* 1997; **28**: 160-165
24 **Kiyabu MT,** Bishop PC, Parker JW, Turner RR, Fitzgibbons PL. Smooth muscle tumors of the gastrointestinal tract: flow cytometric quantitation of DNA and nuclear antigen content and correlation with histologic grade. *Ann J Surg Pathol* 1988; **12**: 954-960
25 **Suzuki H,** Sugihira N. Prognostic value of DNA ploidy in primary gastric leiomyosarcoma. *Br J Surg* 1993; **80**: 1549-1550
26 **Shimamoto T,** Haruma K, Sumii K, Kajiyama G, Tahara E. Flow cytometric DNA analysis of gastric smooth muscle tumors. *Cancer* 1992; **70**: 2031-2034
27 **Cunningham RE,** Federspiel BH, McCarthy WF, Sobin LH, O'Leary TJ. Predicting prognosis of gastrointestinal smooth muscle tumors: role of clinical and histologic evaluation, flow cytometry, and image cytometry. *Am J Surg Pathol* 1993; **17**: 588-594
28 **Tsushima K,** Rainwater LM, Goellner JR, van Heerden JA, Lieber MM. Leiomyosarcomas and benign smooth muscle tumors of the stomach: Nuclear DNA patterns studied by flow cytometry. *Mayo Clin Proc* 1987; **62**: 275-280
29 **Lerma E,** Oliva E, Tugues D, Prat J. Stromal tumors of the gastrointestinal tract: a clinicopathologic and ploidy analysis of 33 cases. *Virchows Arch* 1994; **424**: 19-24
30 **Lerma E,** Lee SJ, Tugues D, Oliva E, Gich I, Prat J. Ploidy of 36 stromal tumors of the gastrointestinal tract: a comparative study with flow cytometry and image analysis. *Anal Quant Cyto Histol* 1994; **16**: 435-440

Edited by Wang XL and Xu CT **Proofread by** Pan BR and Xu FM

PO Box 2345, Beijing 100023, China
Fax: +86-10-85381893
E-mail: wjg@wjgnet.com www.wjgnet.com

World J Gastroenterol 2004;10(23):3480-3484
World Journal of Gastroenterology
Copyright © 2004 by The WJG Press ISSN 1007-9327

• BASIC RESEARCH •

Genomic determination of CR1 CD35 density polymorphism on erythrocytes of patients with gallbladder carcinoma

Xing-Yuan Jiao, Ming-De Lü, Jie-Fu Huang, Li-Jian Liang, Jing-Sen Shi

Xing-Yuan Jiao, Ming-De Lü, Jie-Fu Huang, Li-Jian Liang, Department of Hepatobiliary Surgery, First Affiliated Hospital, Sun Yat-Sen University, Guangzhou 510080, Guangdong Province, China
Jing-Sen Shi, Hepatobiliary Research Laboratory, First Affiliated Hospital, Xi' an Jiaotong University, Xi' an 710061, Shaanxi Province, China
Supported by National Postdoctor Natural Science Foundation of China, No. 2001-14
Correspondence to: Xing-Yuan Jiao, Department of Hepatobiliary Surgery, First Affiliated Hospital, Sun Yat-Sen University, Guangzhou 510080, Guangdong Province, China. jiaoxingyuan@hotmail.com.cn
Telephone: +86-20-34152243 **Fax:** +86-20-34152456
Received: 2004-01-09 **Accepted:** 2004-03-16

Abstract

AIM: To study the changes of quantitative expression, adhering activity and genomic density polymorphism of complement types in erythrocytes (CR1) of patients with gallbladder carcinoma and the related clinical significance.

METHODS: Polymerase chain reaction (PCR), *Hind* III restriction enzyme digestion, quantitative assay of CR1 and adhering activity assay of CR1 in erythrocytes were used.

RESULTS: The number and adhering activity of CR1 in patients with gallbladder carcinoma (0.738±0.23, 45.9±5.7) were significantly lower than those in chronic cholecystitis and cholecystolithiasis (1.078±0.21, 55.1±5.9) and healthy controls (1.252±0.31, 64.2±7.4) (P<0.01). The number and adhering activity of CR1 in patients with chronic cholecystitis and cholecystolithiasis (1.078±0.21, 55.1±5.9) were significantly lower than those in healthy controls (1.252±0.31, 64.2±7.4) (P<0.05). There was a positive correlation between quantitative expression and adhering activity of CR1 (r = 0.79, P<0.01). Compared with those on preoperative day (0.738±0.23, 45.4±4.9), the number and adhering activity of CR1 in patients with gallbladder carcinoma decreased greatly on the third postoperative day (0.310±0.25, 31.8±5.1) (P<0.01), and on the first postoperative week (0.480±0.25, 38.9±5.2) (P<0.01), but they were increased slightly than those on the preoperative day (P>0.05). The number and adhering activity of CR1 recovered in the second postoperative week (0.740±0.24, 46.8±5.9) (P<0.01) and increased greatly in the third postoperative week (0.858±0.35, 52.7±5.8) (P<0.01) in comparison with those on the preoperative day and in the first postoperative week. The number and adhering activity of CR1 of gallbladder carcinoma patients with infiltrating, adjacent lymphogenous and distant organ metastases were significantly lower than those of gallbladder carcinoma patients without them (P<0.01). No difference was observed between the patients with gallbladder carcinoma and healthy individuals in the spot mutation rate of CR1 density gene (χ^2 = 0.521, P>0.05). The distribution of expression was 67.8% in high expression genomic type, 24.8% in moderate expression genomic type, and 7.4% in low expression genomic type. The number and adhering activity of CR1 high expression genomic type gallbladder carcinomas (0.749±0.22, 42.1±6.2) were significantly lower than those of healthy individuals(1.240±0. 29, 63.9±7.2), and were also significantly lower than those of healthy individuals (0.921±0.23, 54.8±7.1), but no difference was observed between the number and adhering activity of CR1 lower expression genomic type gallbladder carcinomas (0.582±0.18, 44.3±5.5) and those of healthy individuals (0.610±0.20, 45.8±5.7) (P>0.05).

CONCLUSION: Defective expression of CR1 in gallbladder carcinoma is mostly acquired through central peripheral mechanisms. The changes in CR1 quantitative expression and adhering activity are consanguineously related to the development and metastasis in gallbladder carcinoma.

Jiao XY, Lü MD, Huang JF, Liang LJ, Shi JS. Genomic determination of CR1 CD35 density polymorphism on erythrocytes of patients with gallbladder carcinoma. *World J Gastroenterol* 2004; 10 (23): 3480-3484
http://www.wjgnet.com/1007-9327/10/3480.asp

INTRODUCTION

Carcinoma of the gallbladder is the most common neoplasm in biliary tract, and its incidence has been rising in recent years[1-4]. The C3b receptors (CR1, Cd35) on erythrocytes serve as the primary transport system for immune complexes from peripheral blood of the liver[5-8], and CR1 plays an important role in this system, the rate of clearance of immune complexes from the circulation is directly related to the number of CR1 molecules expressed on erythrocytes[9-11]. However, there are few reports on the changes of genomic density polymorphism of complement types in erythrocytes of patients with gallbladder carcinoma. We previously demonstrated the altered levels of cellular immunity and humoral immunity in patients with gallbladder carcinoma, and the effects of radical cholecystectomy on nutritional and immune status in patients with gallbladder carcinoma[12-15]. In this study, we reported the changes in quantitative expression, adhering activity and genomic density polymorphism of complement types in erythrocytes (CR1) of patients with gallbladder carcinoma.

MATERIALS AND METHODS

Patients

A total of 33 patients with gallbladder carcinoma were admitted to the First Affiliated Hospital of Sun Yat-Sen University from August 2000 to August 2002.Those were 16 men and 17 women aged from 50 to 70 years (median, 52.7 years). Nineteen patients were preoperatively diagnosed as polypois, cholecystolithiasis and chronic cholecystitis, and diagnosed as gallbladder carcinoma by frozen sections after surgery. Fourteen patients were diagnosed as gallbladder carcinoma preoperatively, of them, 4 patients had radical cholecystectomy, 7 patients had U-tube drainage operation, 3 patients cholecystectomy. Direct invasion or distant metastasis was found in 10 patients during operation, simple gallbladder carcinoma in 15 patients, both gallbladder carcinoma and cholecystolithiasis in 18 patients. The patients with gallbladder

carcinoma were grouped according to the staging system of Nevin[16], the number of cases on stages I, II, III, IV and V was 7, 11, 5, 7 and 11, respectively. Tumor size ranged from 1.8 cm to 6 cm in diameter (median, 2 cm), 23 patients had tumors smaller than 2 cm in diameter, 10 patients had tumors larger 2 cm in diameter.

No therapy was administered to patients preoperatively. Meanwhile, 90 patients with cholecystits or cholecystolithiasis had cholecystectomy, including 44 patients with cholecystitis and 46 patients with choleithiasis. No severe systemic diseases were found, such as, myocardial infarction, cerebral vascular accidents, uncontrollable diabetes mellitus, Hypertension. Their disease was stable in a period of one month. All the surgical specimens were examined histologically, and classified into hyperplasia, atypical hyperplasia (mild, moderate and severe) according to Gong *et al*.[17]. A total of 59 patients exhibited epithelial hyperplasia, 10 patients had mild dysplasia, 10 patients moderate dysplasia, 11 patients severe dysplasia. Normal controls were 30 healthy individuals (18 men and 12 women) aged from 56 years to 72 years (median 61.7 years).

Methods

Quantitative expression, adhering activity and genomic density polymorphism of complement types in erythrocytes (CR1) patients with gallbladder carcinoma were assessed preoperatively (1 wk before surgery), and on d 3, 7, 14 and 21 postoperatively.

Genomic determination of CR1 (Cd35) density polymorphism on erythrocytes[18]

DNA samples DNA was extracted using the following simplified protocol. Following lysis of erythrocytes, nucleated cells from 10 mL of blood were incubated in 3.5 mL of 10 mmol/L Tris, 2 mmol/L EDTA buffer pH7.5, containing 0.4 mol/L NaCL, 7 g/L sodium dodecylsulfate and proteinase K (30 mg/L) for 16 h at 37 ℃, 1 mL of 6 mol/L NaCL was added. After vortexed and ethanol-precipitated, the pellets were washed three times in 700 mL/L ethanol and solubilized in 10 mmol/L Tris, 1 mmol/L EDTA buffer pH7.5.

Sequencing

A construct in pUC-18 containing *Hin*d III-kpn fragments from the introns located within the first and second exons of the short consensus repeat d2 from the long homologous repeat D of CR1 was sequenced. Sequencing was performed using the modified Sanger method with a commercial T_7 DNA polymerase kit.

Primers

Primers were designed based on the analysis of internal homologies within the CR1 gene and homologies with other human sequences obtained from the EMBL databank using the Bisance software. The 5' primer was from base 4 415 to base 4 435 from the CR1 cDNA sequence. The 3' primer was 75 to 55 from the *Hin*d III monomorphic restriction site in the introns. The latter primer was chosen due to the presence of five mismatches between the CR1 intron sequence and the consensus *Hin*d III 1.9 ku repetitive sequence. Primers were synthesized on a 380 Applied Biosystem apparatus. Twenty base oligonucleotides were recovered from the solid phase by rinsing the column with 250 g/L ammonium. After incubation at 55 ℃ for 16 h, ammonium was expelled through evaporation using a Speed-Vac apparatus. Primers were used without further purification.

Amplification and agarose gel electrophoresis

PCR was performed using a Techne PHC-I apparatus with the Taq polymerse.

Amplified DNA was precipitated and then digested using the *Hin*d III restriction enzyme, and separated by electrophoresis in 20 g/L agarose gels. Gels were analyzed under UV illumination. The genomic density polymorphism of complement type 1 (CR1) in erythrocytes was classified into three types: high expression genomic type (1.8 Kb1), moderate expression type (1.8 kb, 1.3 Kb and 1.5 Kb) and low expression genomic type (1.3 Kb, 0.5 Kb).

Quantitative expression of CR1 in erythrocytes of patients with gallbladder carcinoma

EBC enzyme-linked immunosorbent assay This assay was based on the method of Cornillet *et al*.[18]. All RBCs in the assay were routinely glutaraldchyde-fixed. Finally, 20 μL of S/BSA were added to each well, followed by 20 μL of substrate. The plates were incubated at 37 ℃ for 90 min with gentle agitation every 15-20 min to ensure the maximum contact of RBC with substrate. Subsequently, 100 μL of S/BSA was added to each well, the plate was centrifuged at 1 800 r/min for 90 s and 100 μL of supernatant was transferred to a clean microtitre plate for readings in a plate reader at 405 nm (Dynatech MR5000; DynatchmBillingshurst, Suaaex, UK). In each case, a mean of the readings obtained for the RBC without first antibody (the blank controls) was subtracted from the other readings obtained, in order to correct nonspecific phoshatase-like activity within RBC membranes. Duplicate values were obtained for each RBC sample with each antibody. Black control values were obtained for both the antimouse conjuates and for the anti-rabbit conjuates.

Adhering activity of CR1 in erythrocytes of patients with gallbladder carcinoma

A 50 μL of 1×10^8/mL RBC suspensions was added to each well, then added and 50 μL of plasma itself and 100 μL of 1×10^6/mL tumor cells, mixed completely, stained. Fields were examined (×640), 5 RBC combined each tumor cell were labeled as a flower, tumor cell flowers were assessed.

Statistical analysis

For each variable, mupltiple analysis of variance for repeated measurements was used to compare the values measured before operation with those measured at four subsequent time points. The results were presented as mean±SE based on the mixed model of repeated measurement analysis. Statistical analysis was performed with SAS software. $P<0.05$ was considered statistically significant.

RESULTS

The number and adhering activity of CR1 in patients with gallbladder carcinoma, chronic cholecystitis and cholecystolithiasis and healthy individuals

As shown in Table 1, the number and adhering activity of CR1 in patients with gallbladder carcinoma (0.738±0.23, 45.9±5.7) were significantly lower than those in patients chronic cholecystitis and cholecystolithiasis (1.078±0.21, 55.1±5.9) and healthy individuals controls (1.252±0.31, 64.2±7.4) ($P<0.01$). In Table 2 the number and adhering activity of CR1 in patients with chronic cholecystitis and cholecystolithiasis were significantly lower than those in healthy controls ($P<0.05$). There was a positive correlation between quantitative expression and adhering activity of CR1($r = 0.79$, $P<0.01$).

In the series of epithelial pathologic changes including hyperplasia, atypical hyperplasia, carcinoma *in situ* or invasive carcinoma, the number and adhering activity of CR1 decreased gradually (Table 3), and there was a positive correlation between quantitative expression and adhering activity of CR1 ($r = 0.77$, $P<0.01$). In Table 4 compared with those on the preoperative day (0.738±0.23, 45.4±4.9), the number and adhering activity of CR1 in patients with gallbladder carcinoma decreased greatly on the third postoperative day (0.310±0.25, 31.8±5.1) ($P<0.01$) and in the first postoperative week (0.480±0.25, 38.9±5.2) ($P<0.01$), but they were increased slightly than those on the preoperative

day (P>0.05). In comparison with those on the preoperative day and in the first postoperative week, the number and adhering activity of CR1 recovered in the second postoperative week (0.740±0.24, 46.8±5.9) (P<0.01), and increased greatly in the third postoperative week (0.858±0.35, 52.7±5.8) (P<0.01).

The number and adhering activity of CR1 in gallbladder carcinoma patients with infiltrating, adjacent lymph node and distant organ metastases were significantly lower than those in gallbladder carcinoma patients without metastasis (Table 5, P<0.01).

Table 1 The number and adhering activity of CR1 in different groups before operation (mean±SE)

Group	Cases	CR1 (A_{405})	Adhering activity (%)
Healthy individuals	30	1.252±0.31	64.2±7.4
Chronic cholecystitis	90	1.078±0.21[a]	55.1±5.9[a]
Cholecystolithiasis			
Gallbladder carcinoma	33	0.738±0.23[bc]	45.9±5.7[bd]

[a]P<0.05, [b]P<0.01 *vs* normal control; [c]P<0.05, [d]P<0.01 *vs* chronic cholecystitis and cholecystolithiasis.

Table 2 The number and adhering activity of CR1 in different groups before operation (mean±SE)

Group	Cases	CR1(A_{405})	Adhering activity(%)
Healthy individuals	30	1.252±0.31	64.2±7.4
cholecystolithiasis	46	1.027±0.27[a]	54.4±5.9[a]
Gallbladder carcinoma with cholecystolithiasis	18	0.731±0.26[bc]	45.1±6.1[bd]
Simple gallbladder carcinoma	15	0.728±0.23[bc]	44.8±6.4[bd]

[a]P<0.05, [b]P<0.01 *vs* normal control; [c]P<0.05, [d]P<0.01 *vs* chronic cholecystitis.

Table 3 The number and adhering activity of CR1 in different groups before operation (mean±SE)

Type	Cases	CR1(A_{405})	Adhering activity(%)
Simple hyperplasia	59	1.175±0.22	61.1±6.2
Atypical hyperplasia	21	0.906±0.24[b]	50.8±5.7[b]
Gallbladder carcinoma (I-III stage)	23	0.761±0.23[b]	41.6±6.1[b]
Gallbladder carcinoma (IV-V stage)	10	0.602±0.31[b]	30.4±6.5[b]
F		6.4	11.5
P		<0.01	<0.01

[b]P<0.01 *vs* each group.

Changes of genomic density polymorphism of CR1 in patients with gallbladder carcinoma

The distribution of genomic density polymorphism of CR1 in patients was 67.8% in high expression genomic type, 24.8% in moderate expression genomic type, 7.4% in low expression genomic type. Compared with healthy controls, no difference was observed between the patients with gallbladder carcinoma and healthy in the spot mutation rate of CR1 density gene (χ^2 = 0.521, P>0.05). The number and adhering activity of CR1high expression genomic type gallbladder carcinomas (0.749±0.22, 42.1±6.2) were significantly lower than those in healthy individuals (1.240±0.29, 63.9±7.2). The number and adhering activity of CR1 moderate expression genomic type gallbladder carcinomas (0.641±0.19, 34.2±5.1) were also significantly lower than those in healthy individuals (0.921±0.23, 54.8±7.1), but no difference was observed between the number and adhering activity of CR1 lower expression genomic type gallbladder carcinomas (0.582±0.18, 44.3±5.5) and those of healthy individuals (0.610±0.20, 45.8±5.7) (P>0.05).

DISCUSSION

The immune functions of erythrocytes have been studied at gene levels[5-8]. RBCs are the major cellular component of the peripheral blood and occupy 50% of the total blood volume[9]. Normal RBC cytosol contains the majority of natural killer enhancing factors and other factors, such as PIF. Damaged RBC could produce tumor necrosis factor inducing factor. RBCs appear to have an important regulating role in immune function, and RBC activity involves in regulating multiple cytokines such as IL-2, IL-3, CSF, IL-6, TNF-r, TNF. CD44 and CD58 expressed by RBC could serve as the center in controlling immune status, which can directly affect the development and progression of tumors[8-11]. The changes of CR1 quantitative expression and adhering activity are consanguineously related to the development and metastasis of liver carcinoma.

In our study, the number and adhering activity of CR1 high expression genomic type gallbladder carcinomas were significantly lower than those in healthy individuals, indicating that defective expression of CR1 in gallbladder carcinoma is mostly acquired through central peripheral mechanisms.

Gallbladder carcinoma is often associated with cholecystolithiasis and cholecystitis in 40-100% of cases[19-28]. Although no carcinogenic substance has so far been isolated from the bile or the stones in patients with cholecystolithiasis and cholecystitis, many scholars suggested that gallstone might play a role as a chronic injury factor to induce a series of epithelial pathologic changes[29-38]. Gong *et al.*[17] reported that in 150 consecutive cholecystectomy specimens for detection of cholelithiasis or cholecystitis, 76.68% exhibited epithelial hyperplasia, 16.89%

Table 4 The number and adhering activity of CR1 on preoperative and postoperative day (mean±SE)

Group	Preoperative	3rd d	1st wk	2nd wk	3rd wk
CR1 (A_{405})	0.738±0.23	0.310±0.25[b]	0.480±0.25[b]	0.740±0.24	0.85±0.32[a]
Adhering activity (%)	45.4±4.9	31.8±5.1[b]	38.9±5.2[b]	46.8±5.9	52.7±5.8[a]

[a]P<0.05, [b]P<0.01 *vs* normal control.

Table 5 The number and adhering activity of CR1 in gallbladder carcinoma with adjacent lymph nodes and metastasis (mean±SE)

Group	Healthy individu als	Infiltrating (-)	Infiltrating (+)	Adjacent lymph node (-)	Adjacent lymph node (+)	Metastasis (-)	Metastasis (+)
Cases	30	15	18	18	15	23	10
CR1 (A_{405})	1.252±0.31	0.95±0.22[a]	0.81±0.29[ab]	0.88±0.27[a]	0.73±0.25[ab]	0.78±0.26[a]	0.44±0.29[ad]
Adhering activity (%)	64.2±7.4	52.8±6.7[a]	48.1±7.2[ab]	47.6±7.0[a]	41.1±7.1[ab]	46.1±6.1[a]	38.9±6.2[ad]

[b]P<0.01 *vs* normal control; [a]P<0.05, [d]P<0.01 *vs* negative.

atypical hyperplasia, 1.32% carcinoma *in situ* and 2.11% invasive carcinoma. Simple epithelial hyperplasia was found in the mucus adjacent to invasive carcinoma.With the passage of time, a significant number of atypical hyperplasiae presumably would progress to a higher grade lesion, becoming carcinoma. Toyonaga *et al*.[39] reported that in 200 consecutive cholecystectomy specimens for detection of cholelithiasis or cholecystitis, 83% simple epithelial hyperplasiae, 13.5% atypical hyperplasiae and 3.5% carcinomas *in situ*. In general, a significant number of atypical hyperplasiae presumably would progress to a higher grade lesion, 80% atypical hyperplasiae could become precancer lesions. Albores-Saavedra *et al*.[11] results showed that cholelithiasis or cholecystitis produced a series of epithelial pathologic changes, such as simple epithelial hyperplasia, atypical hyperplasia and carcinoma *in situ*, which represented the precancer lesion of gallbladder carcinoma. The probable sequence of events appear to be as follows. Hyperplasia has been found to have atypical hyperplasia which in turn may progress to neoplasia. With the passage of time, a significant number of atypical hyperplasiae presumably would progress to carcinoma *in situ* and invasive carcinoma[24]. So almost all scholars have suggested that a small number of hyperplasiae of the gallbladder would evolve toward *in situ* carcinoma which finally becomes invasive carcinoma[40]. In our study, the number and adhering activity of CR1 in patients with gallbladder carcinoma were significantly lower than those in patients with chronic cholecystitis and cholelithiasis and healthy individuals ($P<0.01$). The number and adhering activity of CR1 in patients with chronic cholecystitis and cholelithiasis were significantly lower than those in healthy individuals. There was a positive linear correlation between quantitative expression and the adhering activity of ECR1 ($r = 0.79$, $P<0.01$). Compared with data the on preoperative day, the number and adhering activity of CR1 in patients with gallbladder carcinoma decreased greatly on the third postoperative day and in the first postoperative week, indicting that surgery plays an injurious role in the disorder of RBC and cytokine functions[12,41,42]. The number and adhering activity of CR1 recovered in the second postoperative week, and increased greatly in the third postoperative week.

The number and the adhering activity of CR1 in gallbladder carcinoma patients with infiltrating, adjacent lymph node and distant organ metastases were significantly lower than those in patients without metastasis. This study demonstrates CR1 can be used as an immune therapy for gallbladder carcinoma.

REFERENCES

1 **Jiao XY,** Lü MD, Huang JF. Current advances in the risk factors for gallbladder carcinoma. *Zhonghua Putong Waike Zazhi* 2002; **17**: 117-119

2 **Lü MD,** Jiao XY. Current status of research on tumor markers of biliary tumors. *Zhongguo Shiyong Waike Zazhi* 2001; **9**: 522-523

3 **Jiao XY,** Li DM, Lü MD, Huang JF, Liang LJ. Significance of nucleolar organizers regions associated proteins of T lymphocytes in diagnosis and monitoring of gallbladder carcinoma. *Zhonghua Putong Waike Zazhi* 2002; **117**: 313-314

4 **Zou SQ**, Zhang L. Relative risk factors analysis of 3922 cases of gallbladder cancer. *Zhonghua Waike Zazhi* 2000; **38**: 800-805

5 **Birmingham DJ,** Chen W, Liang G, Schmitt HC, Gavit K, Nagaraja HN. A CR1 polymorphism associated with constitutive erythrocyte CR1 levels affects binding to C4b but not C3b. *Immunology* 2003; **108**: 531-538

6 **Rowe JA,** Raza A, Diallo DA, Baby M, Poudiougo B, Coulibaly D, Cockburn IA, Middleton J, Lyke KE, Plowe CV, Doumbo OK, Moulds JM. Erythrocyte CR1 expression level does not correlate with a Hind III restriction fragment length polymorphism in africans; implications for studies on malaria susceptibility. *Genes Immun* 2002; **3**: 497-500

7 **Zorzetto M,** Bombieri C, Ferrarotti I, Medaglia S, Agostini C, Tinelli C, Malerba G, Carrabino N, Beretta A, Casali L, Pozzi E, Pignatti PF, Semenzato G, Cuccia MC, Luisetti M. Complement receptor 1 gene polymorphisms in sarcoidosis. *Am J Respir Cell Mol Biol* 2002; **27**: 17-23

8 **Nagayasu E,** Ito M, Akaki M, Nakano Y, Kimura M, Looareesuwan S, Aikawa M. CR1 density polymorphism on erythrocytes of falciparum malaria patients in Thailand. *Am J Trop Med Hyg* 2001; **64**: 1-5

9 **Moulds JM,** Zimmerman PA, Doumbo OK, Kassambara L, Sagara I, Diallo DA, Atkinson JP, Krych-Goldberg M, Hauhart RE, Hourcade DE, McNamara DT**,** Birmingham DJ, Rowe JA, Moulds JJ, Miller LH. Molecular identification of knops blood group polymorphisms found in long homologous region D of complement receptor 1. *Blood* 2001; **97**: 2879-2885

10 **Wang HB,** Qian BH, Niu F, Jiang AQ. Changes of genomic density polymorphism and quantitative expression of complement receptor type 1 in patients with liver diseases. *Zhonghua Ganzangbing Zazhi* 2000; **8**: 335-337

11 **Wang HB,** Zhao XP, Guo F. Changes of quantitative expression, adhering activity and genomic density polymorphism of complement type1 in erythocytes (CR1) of patients with liver cancer. *Zhonghua Jianyan Yixue Zazhi* 20001; **24**: 31-33

12 **Jiao XY,** Shi JS, Wang JS, Yang JY, He P. Effects of radical cholecystectomy on nutritional and immune status in patients with gallbladder carcinoma. *World J Gastroenterol* 2000; **6**: 445-447

13 **Jiao XY,** Shi JS, Gao JS, Zhou LS. Determination of levels of cellular immunity and humoral immunity in patients with gallbladder carcinoma. *Zhongguo Puwai Jichu Yu Linchuang Zazhi* 1999; **4**: 227-229

14 **Jiao XY,** Shi JS, Gao JS, Zhou LS, Han WS, Liu G, Lu Y. Study on the serum IL-2, SIL-2r and CEA levels in patients with gallbladder carcinoma. *Zhonghua Gandan Waike Zazhi* 1999; **5**: 342

15 **Shi JS,** Wang JS, Liu G, Yu YL, Lu Y, Jiao XY, Yang YJ, Li GC, Han Y. Early diagnosis of primary gallbladder carcinoma. *Hepatobiliary Pancreat Dis Int* 2002; **1**: 273-275

16 **Nevin JE,** Moran TJ, Kay S, King R. Carcinoma of the gallbladder: staging, treatment, and prognosis. *Cancer* 1976; **37**: 141-148

17 **Gong FQ,** Gao ZY, Wang JB, Liu SG, Liu JQ. Pathologic study of precancerous lesion of the gallbladder. *Zhonghua Zhongliu Zazhi* 1989; **11**: 127-129

18 **Cornillet P,** Philbert F, Kazatchkine MD, Cohen JHM. Genomic determination of the CR1 (CD35) density polymorphism on erythrocytes using polymerase chain reaction amplification and *Hind* III restriction enzyme digestion. *J Immunol Methods* 1991; **136**: 193-197

19 **Noshiro H,** Chijiiwa K, Yamaguchi K, Shimizu S, Sugitani A, Tanaka M. Factors affecting surgical outcome for gallbladder-carcinoma. *Hepatogastroenterology* 2003; **50**: 939-544

20 **Wakai T,** Shirai Y, Yokoyama N, Ajioka Y, Watanabe H, Hatakeyama K. Depth of subserosal invasion predicts long-term survival after resection in patients with T2 gallbladder carcinoma. *Ann Surg Oncol* 2003; **10**: 447-454

21 **Ishikawa T,** Horimi T, Shima Y, Okabayashi T, Nishioka Y, Hamada M, Ichikawa J, Tsuji A, Takamatsu M, Morita S. Evaluation of aggressive surgical treatment for advanced carcinoma of the gallbladder. *J Hepatobiliary Pancreat Surg* 2003; **10**: 233-238

22 **Nakakubo Y,** Miyamoto M, Cho Y, Hida Y, Oshikiri T, Suzuoki M, Hiraoka K, Itoh T, Kondo S, Katoh H. Clinical significance of immune cell infiltration within gallbladder cancer. *Br J Cancer* 2003; **89**: 1736-1742

23 **Enomoto T,** Todoroki T, Koike N, Kawamoto T, Matsumoto H. Xanthogranulomatous cholecystitis mimicking stage IV gallbladder cancer. *Hepatogastroenterology* 2003; **50**: 1255-1258

24 **Jarnagin WR,** Ruo L, Little SA, Klimstra D, D'Angelica M, DeMatteo RP, Wagman R, Blumgart LH, Fong Y. Patterns of initial disease recurrence after resection of gallbladder carcinoma and hilar cholangiocarcinoma: implications for adjuvant therapeutic strategies. *Cancer* 2003; **98**: 1689-1700

25 **Yanagisawa N,** Mikami T, Yamashita K, Okayasu I. Microsatellite instability in chronic cholecystitis is indicative of an early stage in gallbladder carcinogenesis. *Am J Clin Pathol* 2003; **120**: 413-417

26 **Shukla VK,** Adukia TK, Singh SP, Mishra CP, Mishra RN. Micronutrients, antioxidants, and carcinoma of the gallbladder. *J Surg Oncol* 2003; **84**: 31-35

27 **Kokudo N,** Makuuchi M, Natori T, Sakamoto Y, Yamamoto J,

Seki M, Noie T, Sugawara Y, Imamura H, Asahara S, Ikari T. Strategies for surgical treatment of gallbladder carcinoma based on information available before resection. *Arch Surg* 2003; **138**: 741-750

28 **Bani-Hani KE,** Yaghan RJ, Matalka II, Shatnawi NJ. Gallbladder cancer in northern Jordan. *J Gastroenterol Hepatol* 2003; **18**: 954-959

29 **Malik IA.** Clinicopathological features and management of gallbladder cancer in pakistan: A prospective study of 233 cases. *J Gastroenterol Hepatol* 2003; **18**: 950-953

30 **Andrea C,** Francesco C. Squamous-cell and non-squamous-cell carcinomas of the gallbladder have different risk factors. *Lancet Oncol* 2003; **4**: 393-394

31 **Hemminki K,** Li X. Familial liver and gall bladder cancer: a nationwide epidemiological study from Sweden. *Gut* 2003; **52**: 592-596

32 **Kondo S,** Nimura Y, Kamiya J, Nagino M, Kanai M, Uesaka K, Yuasa N, Sano T, Hayakawa N. Factors influencing postoperative hospital mortality and long-term survival after radical resection for stage IV gallbladder carcinoma. *World J Surg* 2003; **27**: 272-277

33 **Haratake J,** Kasai T, Makino H. Diffuse mucosal carcinoma of intrahepatic and extrahepatic bile ducts including gallbladder. *Pathol Int* 2002; **52**: 784-788

34 **Pandey M.** Risk factors for gallbladder cancer: a reappraisal. *Eur J Cancer Prev* 2003; **12**: 15-24

35 **Shi JS,** Zhou LS, Jiao XY, Lu Y, Hao XY, Han WS, Liu G. Clinical significance of detecting tumor necrosis factor and its receptor in serum and bile in patients with gallbladder cancer and gallstone. *Zhonghua Gandan Waike Zazhi* 2001; **7**: 82-83

36 **Misra S,** Chaturvedi A, Misra NC, Sharma ID. Carcinoma of the gallbladder. *Lancet Oncol* 2003; **4**: 167-176

37 **Parwani AV,** Geradts J, Caspers E, Offerhaus GJ, Yeo CJ, Cameron JL, Klimstra DS, Maitra A, Hruban RH, Argani P. Immunohistochemical and genetic analysis of non-small cell and small cell gallbladder carcinoma and their precursor lesions. *Mod Pathol* 2003; **16**: 299-308

38 **Rashid A.** Cellular and molecular biology of biliary tract cancers. *Surg Oncol Clin N Am* 2002; **11**: 995-1009

39 **Toyonaga T,** Chijiiwa K, Nakano K, Noshiro H, Yamaguchi K, Sada M, Terasaka R, Konomi K, Nishikata F, Tanaka M. Completion radical surgery after cholecystectomy for accidentally undiagnosed gallbladder carcinoma. *World J Surg* 2003; **27**: 266-271

40 **Henson DE,** Albores-Saavedra J, Corle D. Carcinoma of the gallbladder carcinoma, histologic types, stage of disease, grade, and survival rates. *Cancer* 1992; **70**: 1493-1497

41 **Albores-Saavedra J,** Alcantra-Vazquez A, Cruz-Ortiz H, Herrera-Goepfert R. The precursor lesions, of invasive gallbladder carcinoma, hyperplasia, atypical hyperplasia and carcinoma *in situ*. *Cancer* 1980; **45**: 919-927

42 **Fan YZ,** Zhang JT, Yang HC, Yang YQ. Expression of MMP-2, TIMP-2 protein and the ratio of MMP-2/TIMP-2 in gallbladder carcinoma and their significance. *World J Gastroenterol* 2002; **8**: 1138-1143

Edited by Wang XL and Ren SY **Proofread by** Xu FM

PO Box 2345, Beijing 100023, China
Fax: +86-10-85381893
E-mail: wjg@wjgnet.com www.wjgnet.com

World J Gastroenterol 2004;10(23):3485-3489
World Journal of Gastroenterology
Copyright © 2004 by The WJG Press ISSN 1007-9327

• BASIC RESEARCH •

Effects of dermatan sulfate derivatives on platelet surface P-selectin expression and protein C activity in blood of inflammatory bowel disease patients

Sheng-Li Ji, Hai-Yan Du, Yan-Qing Chi, Hui-Fei Cui, Ji-Chao Cao, Mei-Yu Geng, Hua-Shi Guan

Sheng-Li Ji, Mei-Yu Geng, Hua-Shi Guan, Key Laboratory of Marine Drugs, Marine Drug and Food Institute, Ocean University of China, Qingdao 266003, Shandong Province, China
Sheng-Li Ji, Hai-Yan Du, Hui-Fei Cui, Ji-Chao Cao, Institute of Biochemical and Biotech Drugs, School of Pharmacy, Shandong University, Jinan 250012, Shandong Province, China
Yan-Qing Chi, Department of Pharmacy, Shandong Provincial Hospital, Jinan 250021, Shandong Province, China
Supported by the National Natural Science Foundation of China, No. 30370613, and the Major State Basic Research Development Program of China, No. 2001CCA01600, and the Shandong Provincial Natural Science Foundation, No. Y2000C22
Co-correspondents: Hua-Shi Guan
Correspondence to: Sheng-Li Ji, Institute of Biochemical and Biotech drugs, School of Pharmacy, Shandong University, Jinan 250012, Shandong Province, China. shengliji@sdu.edu.cn
Telephone: +86-531-8380288 **Fax:** +86-531-2929312
Received: 2004-03-31 **Accepted:** 2004-05-13

Abstract

AIM: To investigate the effect of dermatan sulfate (DS) derivatives on platelet surface P-selectin expression and blood activated protein C (APC) activity in patients with inflammatory bowel disease (IBD), and to clarity the anti-inflammatory mechanism of DS derivatives.

METHODS: Dermatan sulfate (DS) was sulfated with chlorosulfonic acid to prepare polysulfated dermatan sulfate (PSDS). The major disaccharides of DS and PSDS were determined by ^{1}H nuclear magnetic resonance spectroscopy (^{1}H-NMR) and ^{13}C-NMR. Both DS and PSDS were depolymerized with hydrogen peroxide. The fragments were separated by gel filtration chromatography. The effects of DS derivatives on P-selectin expression were assayed by ELISA method, and blood APC activity was assayed by the synthetic chromogenic substrate method.

RESULTS: The major disaccharides of DS and PSDS were IdoA-1→3-GalNAc-4-SO_3 and IdoA-2SO_3-1→3-GalNAc4, 6-diSO_3, respectively. Compared with the adenosine diphosphate stimulated group and IBD control group, DS and its derivatives all had significant inhibitory effects on P-selectin expression (P<0.01), but there was no difference between DS-derived oligosaccharides (DSOSs) and PSDS-derived oligosaccharides (PSDSOSs). The experiments on APC activity showed that DS and its derivatives all enhanced APC activity. The most active DSOS was the one with a relative molecular weight (M_r) of 4 825, which enhanced the APC activity from 106.5±11.5% to 181.8±22.3% (P<0.01). With the decrease of M_r, the activity of DSOSs decreased gradually. The effect of PSDS on APC activity enhancement was more significant than that of DS, and the APC activity was raised to 205.2±22.1% (P<0.01). All the PSDSOSs were more active than DSOSs on the basis of comparable M_r. With the decrease of M_r, the activity of PSDSOSs increased gradually, and the most active PSDSOS was PSDSOS$_3$ with M_r of 2 749, which enhanced the APC activity to 331.2±27.8% (P<0.01), then the activity of PSDSOSs decreased gradually.

CONCLUSION: DS and its derivatives can significantly inhibit P-selectin expression on platelet surface, but the effect has no correlation with DS molecular mass and sulfation. The effect of DS or its derivatives on APC activity at molecular level involves complex mechanisms that depend on the molecular mass, the degree of sulfation, and the heterogeneous composition of DS. On the same molecular size, the higher the degree of DS sulfation, the more significant the effect on enhancing APC activity.

Ji SL, Du HY, Chi YQ, Cui HF, Cao JC, Geng MY, Guan HS. Effects of dermatan sulfate derivatives on platelet surface P-selectin expression and protein C activity in blood of inflammatory bowel disease patients. *World J Gastroenterol* 2004; 10(23): 3485-3489
http://www.wjgnet.com/1007-9327/10/3485.asp

INTRODUCTION

Inflammatory bowel disease (IBD) is a chronic non-specific intestinal inflammation. Recent researches have revealed a number of links between inflammation and coagulation, patients with IBD may be at increased risk of having venous thromboembolism[1-9]. Abnormal platelet activity has been reported in patients with ulcerative colitis (UC) and Crohn's disease (CD), and plays an important role in inflammation aggravation[10-12]. P-selectin, a membrane glycoprotein expressed on activated platelets and endothelial cells, plays a crucial role in thrombosis and inflammatory response[13]. P-selectin antagonism could decrease thrombosis and inflammation in animal models of venous thrombosis prophylaxis[14]. The protein C anticoagulant pathway appeares to be the major pathway involved in the cross link between inflammation and coagulation. Activated protein C (APC) contributes to systemic anticoagulant and anti-inflammatory activities[15], and may reduce organ damage by inhibiting thrombin generation and leukocyte activation[16]. To inhibit the release of P-selectin and enhance APC activities are helpful for the treatment of IBD and related thrombosis[17].

Dermatan sulfate (DS) is a member of the family of structurally complex, sulfated and linear polysaccharides called glycosaminoglycans (GAGs). It is mainly composed of [4-α-L-IdoA-1→3-β-D-GalNAc-1]$_n$ and [4-α-L-GlcA-1→3-β-D-GalNAc-1]$_n$ and their derivatives with sulfate groups at C-2 of L-IdoA, C-4 or/and C-6 of D-GalNAc (IdoA, iduronic acid, GalNAc, *N*-acetylgalactosamine, GlcA, glucuronic acid). The relative molecular weight (M_r) of natural DS is within 15 ku to 45 ku[18]. Polysulfated DS is the sulfated product of DS reacting with chlorosulfonic acids. DS-derived oligosaccharides (DS-Oligs) are the oligosaccharides from depolymerizing DS and PSDS. DS is an important glycosaminoglycan found in a wide variety of tissues

in animals. Recently, growing evidence has suggested that DS, like the better studied heparin and heparan sulfate, is an important cofactor in a variety of cell behaviors[18]. Many of the biological activities of DS proteoglycans are associated with their glycosaminoglycan structure[19]. In addition to its anticoagulant and antithrombotic activities[20,21], DS has also been reported possessing anti-inflammatory activities[22-24]. The mechanisms of anti-inflammation of DS are unknown. To the author's knowledge, the relationships between the molecular structure of DS-Oligs and their effects on P-selectin and APC activity have not been studied. The present study was designed to observe the effects of DS-Oligs with different M_r and structure on platelet surface P-selectin expression and blood APC activities in patients with IBD, and to clarify the anti-inflammatory mechanisms of DS in the treatment of IBD.

MATERIALS AND METHODS

Materials

Dermatan sulfate was donated by Dongying Tiandong Biochemical Industrial Co. Ltd and 300 mL/L hydrogen peroxide (H_2O_2) was purchased from Laiyang Fine Chemical Reagent Co. Ltd. Adenosine diphosphate (ADP) was purchased from Sigma Co., USA. Superdex-30 was purchased from Amersham Biosciences. Human P-selectin ELISA kit (96 tests) and protein C CSA were purchased from Shanghai Sun Diagnostics, China.

Preparation of DS-Oligs

PSDS was prepared by the reaction of DS with chlorosulfonic acids. DS and PSDS were degraded by oxidative depolymerization with hydrogen peroxide[25] respectively. All DS-Oligs were obtained from the products separated by gel filtration chromatography with Superdex 30 column (26 mm×1 200 mm), and the DS-Oligs were eluted with 0.25 mol/L ammonium bicarbonate and dried with lyophilization.

Determination of the relative molecular weight of DS-Oligs

The relative molecular weight (M_r) of the Oligs was determined by high performance liquid chromatography (HPLC)[26].

^{1}H-NMR and ^{13}C-NMR analysis of DS and PSDS

^{1}H-NMR and ^{13}C-NMR spectra of DS and PSDS were assayed using a 600 MHz instrument as previously described[27].

Patients and controls

Ten healthy blood-donors served as a control group and blood samples from 10 IBD patients, including five patients with UC and five patients with CD were used for experiments.

Collection of blood samples

Blood used to prepare platelets was collected in silicone-coated tubes containing 32 g/L sodium citrate as anticoagulant just before preparation and analysis.

Preparation of isolated platelets (IP)

Nine milliliter of blood with sodium citrate as anticoagulant blood was centrifuged at 500 r/min for 20 min at room temperature to obtain platelet rich plasma (PRP). The upper PRP was taken out, and the remaining plasma was centrifuged at 3 000 r/min for 15 min again and the platelet poor plasma (PPP) was obtained. The PRP was diluted with PPP to the platelet density of 3.0×10^8 cells/mL for P-selectin test.

Preparation of P-selectin standard calibration curve

Standard *P*-selectin was diluted to 80, 40, 20, 10, 5 and 2.5 ng/mL with assay buffer, and then added to the standard wells. The standard curve was tested according to the test kit manufacturer's instructions.

Measurement of P-selectin in IP by ELISA

A total of 225 μL of afore-mentioned PRP was added to tubes, 30 μL of saline was added to the control group and adenosine diphosphate (ADP) control tubes, and then 30 μL of 2.50 mg/mL DS, PSDS and DS-Oligs saline solution were added to the sample tubes. All the tubes were incubated for 10 min at 37 ℃. Then 25 μL of 4.68 μmol/L ADP solution was added to the ADP and sample tubes and an equal volume of saline was added to the blank control tubes. Then all the tubes were incubated for 5 min at 37 ℃, followed by centrifugation for 15 min at 3 000 r/min, and finally the P-selectin in the upper solution was tested by ELISA according to the test kit manufacturer's instructions.

Specimen collection and preparation for APC test

Five milliliter of venous blood, containing 32 g/L sodium citrate as an anticoagulant, was collected from ten patients with IBD and the sample was centrifuged immediately. The plasma was collected and stored at 2-8 ℃ until use.

Preparation of protein C activity standard calibration curve

Normal plasma was dissolved in 200 μL of buffer and the APC activity was defined as 200%. The solution was diluted three times to make the activities 100%, 50% and 25%, respectively. The activity of buffer was 0% criterion. Twenty five microliters of the four standards was added to the standard wells of the test plate, then 50 μL of activator at the concentration of 0.1 mg/mL was added to activate protein C. These points were determined according to the manufacturer's instructions at 405 nm. The absorbance (A_{405nm}) was plotted versus the known percentage of standard APC activity to give a standard curve.

Detection of APC activity

APC activity in the plasma pre-incubated with DS and its derivatives was determined according to test kit manufacturer's instructions with minor modifications. Fifty microliters of DS and its derivatives solution at the concentration of 0.20 g/L was used to produce 50 μL of activator. The APC enhancement by 50 μL of DS at the concentration of 0.20 g/L was defined as 100%. Fifty microliters of buffer served as a blank control without any activator. The APC activities of the DS-Oligs were calculated according to the calibration curve.

Statistical analysis

Data were expressed as mean±SD. Student's *t* test and one-way analysis of variance were used for statistical analysis according to the data obtained. *P* values less than 0.05 were considered statistically significant.

RESULTS

Analysis of ^{1}H-NMR and ^{13}C-NMR spectra of DS and PSDS

The ^{1}H-NMR and ^{13}C-NMR spectra of DS and PSDS and the main disaccharides in their structure are shown in Figure 1. The major disaccharide sequence in DS was IdoA-1→3-GalNAc-4-SO_3. In the ^{1}H-NMR spectra of PSDS (Figures 1B, D), the chemical shift of all the protons was shifted downfield in PSDS with respect to the DS. Similar effects could also be seen in the ^{13}C-NMR spectra (Figures 1 A, C). The chemical shift of C-6 in GalNAc was shifted downfield (from 63.89 ppm to 68.60 ppm), while that of C-5 in GalNAc was shifted upfield (from 74.63 ppm to 69.98 ppm). The same phenomenon occurred in IdoA. The spectra showed that the hydroxyl group of C-6 in GalNAc and C-2 in IdoA of PSDS was sulfated, and the major disaccharide sequence was IdoA-2SO_3-1→3-GalNAc4, 6-diSO_3.

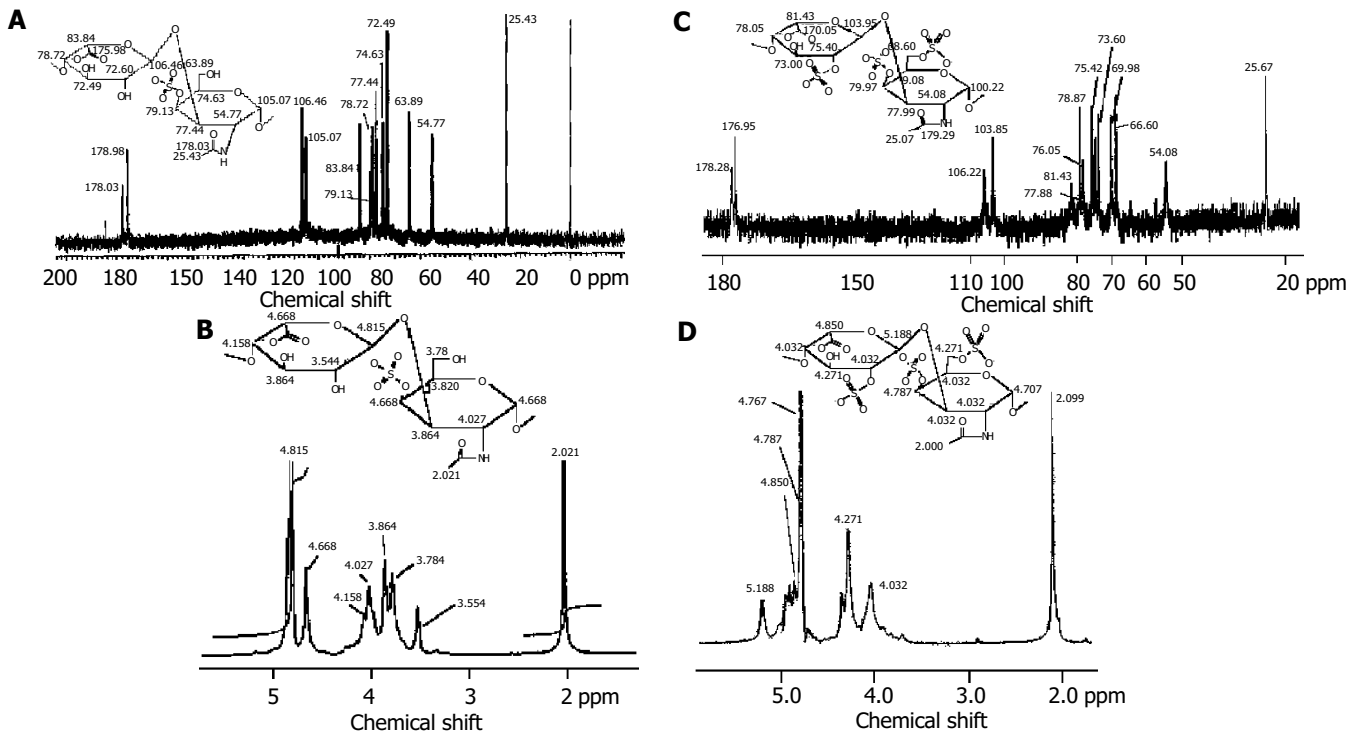

Figure 1 ^{1}H-NMR and ^{13}C-MNR spectra of DS and PSDS. A and B: ^{13}C-MNR and ^{1}H-NMR spectra of DS and the chemical shift of major disaccharides in DS; C and D: ^{13}C-MNR and ^{1}H-NMR spectra of PSDS and the chemical shift of the major disaccharides in PSDS.

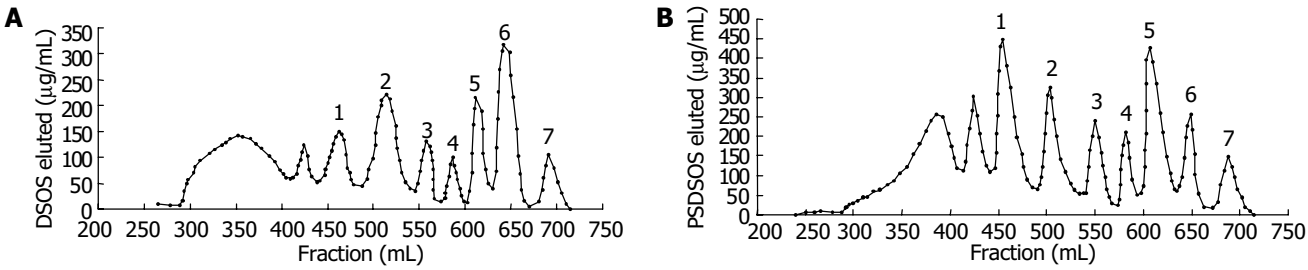

Figure 2 Fragment size separation of DS-Oligs. The products were separated on a Superdex 30 size exclusion column (26 mm×1 200 mm) at a flow rate of 0.5 mL/min in 0.25 mol/L ammonium bicarbonate. Elution profiles were monitored by carbazole assay. A and B: depolymerized products of DS and PSDS.

Fractionation of DS-Oligs

The DS-Oligs prepared from DS and PSDS degradation and separated by gel filtration chromatography are shown in Figure 2. The peaks numbered were DS-Oligs collected for the experiments on P-selectin and APC, and their M_r are listed in Table 1.

Table 1 M_r of DS-Oligs

DS oligosaccharides	M_r	PSDS oligosaccharides	M_r
$DSOS_1$	4 825	$PSDSOS_1$	4 959
$DSOS_2$	3 926	$PSDSOS_2$	4 280
$DSOS_3$	2 254	$PSDSOS_3$	2 749
$DSOS_4$	1 696	$PSDSOS_4$	2 107
$DSOS_5$	1 309	$PSDSOS_5$	1 594
$DSOS_6$	1 038	$PSDSOS_6$	1 021
$DSOS_7$	709	$PSDSOS_7$	785

Effects of DS derivatives on the expression of platelet surface P-selectin

Expression of platelet surface P-selectin on IP of IBD control group was significantly increased from 13.92±1.69 ng/mL (control group) to 23.95±2.51 ng/mL, and the ADP group showed a significant increase in P-selectin expression after stimulation with ADP (P<0.01). All DS and its derivative groups showed a significant decrease in P-selectin expression compared with the ADP-stimulated group and IBD control group (P<0.01), but no significant differences could be seen as compared with the control group, and between DSOS and PSDSOS groups (Figure 3).

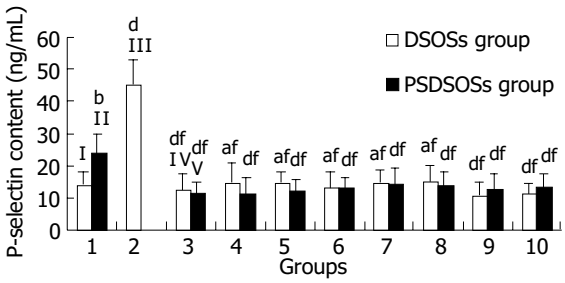

Figure 3 Effects of DS derivatives on expression of P-selectin on IP surface. Bars I, II, III, IV and V represent control group, IBD control group, ADP group, DS group and PSDS group, respectively. Groups 4 to 10 represent DS-Oligs from 1 to 7 listed in Table 1. ^{b}P<0.01 *vs* control group; ^{a}P<0.05, ^{d}P<0.01 *vs* IBD control group; ^{f}P<0.01 *vs* ADP group (n = 10 for each group).

Effects of DS derivatives on APC activity

The experimental results showed that all DS and its derivatives enhanced APC activity. The most active DSOS was $DSOS_1$ with M_r of 4 825, which enhanced the APC activity from 106.5±11.5% (DS group) to 181.8±22.3% (P<0.01). With the decrease of M_r, the activity of DSOSs decreased gradually. PSDS was more active than DS, which enhanced the APC activity from 106.5±11.5% (DS group) to 205.2±22.1% (P<0.01). On the same molecular size basis, PSDSOSs were more active than DSOSs. With the decrease of M_r, the activity of PSDSOSs increased, and the most active one was $PSDSOS_3$ with M_r of 2 749, which enhanced the APC activity to 331.2±27.8%, then decreased gradually (Figure 4).

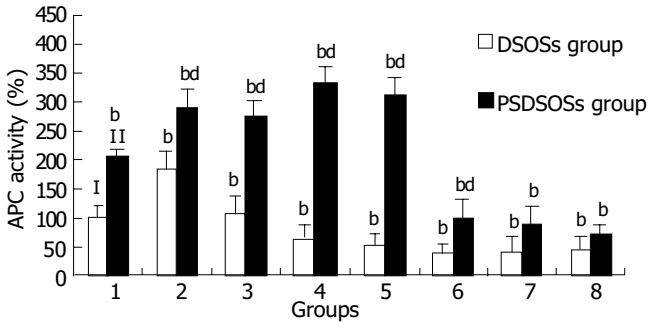

Figure 4 Effects of DS and its derivatives on APC activity. Bars I and II represent DS group and PSDS group, respectively. Groups 2 to 8 represent DS-Oligs from 1 to 7 listed in Table 1. ^bP<0.01 *vs* DS group, ^dP<0.01 *vs* PSDS group (n = 10 for each group).

DISCUSSION

IBD is a gastrointestinal disorder of unknown aetiology. Current research has paid attention to platelet dysfunction as a possible contributor to the disease, and the prevalence of IBD seems to be lower among patients with coagulation disorders[28]. Platelets play a crucial role in hemostasis and inflammatory response. Normally, platelets circulate in a quiescent state, but after stimulation with agonists, such as thrombin, ADP and epinephrine, platelets begin to express P-selectin and release inflammatory mediators and factors, thereby promoting hemostasis[29]. P-selectin acts as a cell-adhesion molecule in activated platelets and endothelial cells, and its main actions are to adhere to neutrophils and monocytes[30] and to facilitate diapedesis. It has been reported that DS acts as a ligand to bind to P-selectin, and the sulfation plays an important role in the interactions between L- or P-selectin and DS[31,32]. Our results showed that DS, PSDS and their derivatives significantly inhibited the P-selectin expression on IP surface, but there was no difference between DS and PSDS, and the effect seemed to be independent of molecular weight.

The increased risk of thrombosis in IBD patients has been attributed to a hypercoagulable state[33-37]. Investigations of the hypercoagulation state and clinical risk factors in patients with IBD are of interest because thromboembolism is a significant and serious complication in IBD patients, with a high morbidity and mortality. The incidence of arterial and venous thromboembolic disease in patients with UC and CD is between 1% and 8%, and was 39% in some postmortem studies[38]. Deficiencies and functional abnormalities of protein C, antithrombin III and protein S are the well-recognized causes of thrombotic disease[8,39]. Blood coagulation is carefully controlled *in vivo* by several anticoagulant systems. Protein C pathway is one of these natural anticoagulant systems. It could regulate the coagulation process through proteolytic cleavage and inactivation of the two cofactors in the coagulation cascade, the activated forms of factor V and VIII[40-42]. The response of UC to heparin therapy[43] and the low risk of IBD in patients with hemophilia and von Willebrand's disease[29] also suggested that thrombosis and vascular occlusion might be important in the pathogenesis of IBD.

DS has been widely used as an antithrombotic drug. Its anticoagulant activity may involve multiple mechanisms. One of the mechanisms is that DS could promote the inhibition of thrombin activity by heparin cofactor II[44]. The present experiments were designed to investigate the relationships between the APC activity enhancement and structures of DS or its derivatives *in vitro*. The results showed that DS and its derivatives all enhanced APC activity. Furthermore, a variety of experiments based on enhancement of APC activity compared the activity of various DS derivatives and defined the influences of DS molecular size and degree of sulfation on this activity. Two important variables of DS derivatives are the relative molecular weight and the degree of sulfation of the molecules. To assess the influence of molecular size, we studied different DS and PSDS fragments with M_r ranging from 0.7 ku to 5.0 ku. A clear correlation between the molecular size of DS and PSDS fragments and the degree of APC activity enhancement was observed by the synthetic chromogenic substrate method. With the decrease of molecular weight, the activity of DS-Oligs increased, and then decreased gradually. DSOS with M_r of 4 825, containing 16 to 24 monosaccharide residues, had more significant activity than undegraded DS. The same tendency was observed on PSDSOSs. But the most active PSDSOS was $PSDSOS_3$ with M_r of 2 749 containing about 8 to 10 monosaccharide residues.

To study the influence of the sulfate groups in DS molecules on APC enhancement, a chemically modified DS with a high degree of sulfation was prepared and compared with its parent DS. PSDSOSs were also compared with DSOSs with comparable M_r. The APC activity enhancement of PSDSOSs was much higher than that of DSOSs.

In conclution interactions between APC and DS-Oligs at the molecular level involve complex mechanisms that depend on the M_r, the degree of sulfation, and the heterogeneous composition of DS, and are of great importance in the development of new anti-thrombotic DS-derived drugs.

REFERENCES

1 **Xia B,** Han H, Zhang KJ, Li J, Guo GS, Gong LL, Zeng XC, Liu JY. Effects of low molecular weight heparin on platelet surface P-selectin expression and serum interleukin-8 production in rats with trinitrobenzene sulphonic acid-induced colitis. *World J Gastroenterol* 2004; **10:** 729-732

2 **Fichera A,** Cicchiello LA, Mendelson DS, Greenstein AJ, Heimann TM. Superior mesenteric vein thrombosis after colectomy for inflammatory bowel disease: a not uncommon cause of postoperative acute abdominal pain. *Dis Colon Rectum* 2003; **46:** 643-648

3 **Saibeni S,** Cattaneo M, Vecchi M, Zighetti ML, Lecchi A, Lombardi R, Meucci G, Spina L, de Franchis R. Low vitamin B (6) plasma levels, a risk factor for thrombosis, in inflammatory bowel disease: role of inflammation and correlation with acute phase reactants. *Am J Gastroenterol* 2003; **98:** 112-117

4 **Guedon C,** Le Cam-Duchez V, Lalaude O, Menard JF, Lerebours E, Borg JY. Prothrombotic inherited abnormalities other than factor V Leiden mutation do not play a role in venous thrombosis in inflammatory bowel disease. *Am J Gastroenterol* 2001; **96:** 1448-1454

5 **Bernstein CN,** Blanchard JF, Houston DS, Wajda A. The incidence of deep venous thrombosis and pulmonary embolism among patients with inflammatory bowel disease: a population-based cohort study. *Thromb Haemost* 2001; **85:** 430-434

6 **Grip O,** Svensson PJ, Lindgren S. Inflammatory bowel disease promotes venous thrombosis earlier in life. *Scand J Gastroenterol* 2000; **35:** 619-623

7 **Jackson LM,** O'Gorman PJ, O'Connell J, Cronin CC, Cotter KP, Shanahan F. Thrombosis in inflammatory bowel disease: clinical setting, procoagulant profile and factor V Leiden. *QJM* 1997; **90:** 183-188

8 **Jorens PG,** Hermans CR, Haber I, Kockx MM, Vermylen J, Parizel GA. Acquired protein C and S deficiency, inflammatory bowel disease and cerebral arterial thrombosis. *Blut* 1990; **61:** 307-310

9 **Ghosh S,** Mackie MJ, McVerry BA, Galloway M, Ellis A, McKay J. Chronic inflammatory bowel disease, deep-venous thrombosis and antithrombin activity. *Acta Haematol* 1983; **70:** 50-53

10 **Mannaioni PF,** Di Bello MG, Masini E. Platelets and inflammation: role of platelet-derived growth factor, adhesion molecules and histamine. *Inflamm Res* 1997; **46:** 4-18

11 **Schaufelberger HD,** Uhr MR, McGuckin C, Logan RP, Misiewicz JJ, Gordon-Smith EC, Beglinger C. Platelets in ulcerative colitis and Crohn's disease express functional interleukin-1 and interleukin-8 receptors. *Eur J Clin Invest* 1994; **24:** 656-663

12 **Collins CE,** Rampton DS. Review article: platelets in inflammatory bowel disease-pathogenetic role and therapeutic implications. *Aliment Pharmacol Ther* 1997; **11:** 237-247

13 **Blann AD,** Noteboom WM, Rosendaal FR. Increased soluble P-selectin levels following deep venous thrombosis: cause or effect? *Br J Haematol* 2000; **108:** 191-193

14 **Myers D,** Wrobleski S, Londy F, Fex B, Hawley A, Schaub R, Greenfield L, Wakefield T. New and effective treatment of experimentally induced venous thrombosis with anti-inflammatory rPSGL-Ig. *Thromb Haemost* 2002; **87:** 374-382

15 **Esmon CT.** The anticoagulant and anti-inflammatory roles of the protein C anticoagulant pathway. *J Autoimmun* 2000; **15:** 113-116

16 **Shibata M,** Kumar SR, Amar A, Fernandez JA, Hofman F, Griffin JH, Zlokovic BV. Anti-inflammatory, antithrombotic, and neuroprotective effects of activated protein C in a murine model of focal ischemic stroke. *Circulation* 2001; **103:** 1799-1805

17 **Fagerstam JP,** Whiss PA, Strom M, Andersson RG. Expression of platelet P-selectin and detection of soluble P-selectin, NPY and RANTES in patients with inflammatory bowel disease. *Inflamm Res* 2000; **49:** 466-472

18 **Linhardt RJ,** Hileman RE. Dermatan sulfate as a potential therapeutic agent. *Gen Pharmacol* 1995; **26:** 443-451

19 **Whinna HC,** Choi HU, Rosenberg LC, Church FC. Interaction of heparin cofactor II with biglycan and decorin. *J Biol Chem* 1993; **268:** 3920-3924

20 **Linhardt RJ,** al-Hakim A, Liu JA, Hoppensteadt D, Mascellani G, Bianchini P, Fareed J. Structural features of dermatan sulfates and their relationship to anticoagulant and antithrombotic activities. *Biochem Pharmacol* 1991; **42:** 1609-1619

21 **Andrew M,** Mitchell L, Berry L, Paes B, Delorme M, Ofosu F, Burrows R, Khambalia B. An anticoagulant dermatan sulfate proteoglycan circulates in the pregnant woman and her fetus. *J Clin Invest* 1992; **89:** 321-326

22 **Kuschert GS,** Coulin F, Power CA, Proudfoot AE, Hubbard RE, Hoogewerf AJ, Wells TN. Glycosaminoglycans interact selectively with chemokines and modulate receptor binding and cellular responses. *Biochemistry* 1999; **38:** 12959-12968

23 **Kuwaba K,** Kobayashi M, Nomura Y, Irie S, Koyama Y. Elongated dermatan sulphate in post-inflammatory healing skin distributes among collagen fibrils separated by enlarged interfibrillar gaps. *Biochem J* 2001; **358:** 157-163

24 **Gozzo AJ,** Nunes VA, Carmona AK, Nader HB, von Dietrich CP, Silveira VL, Shimamoto K, Ura N, Sampaio MU, Sampaio CA, Araujo MS. Glycosaminoglycans affect the action of human plasma kallikrein on kininogen hydrolysis and inflammation. *Int Immunopharmacol* 2002; **2:** 1861-1865

25 **Fussi F,** inventors; Hepar Industries Inc., Assignee. Process for obtaining low molecular weight heparins endowed with elevated pharmacological properties, and product so obtained. US patent 4, 281, 108, 1981 July 28

26 **Kristensen HI,** Tromborg EM, Nielsen JR, Nielsen JI, Johansen KB, Ostergaard PB. Development and validation of a size exclusion chromatography method for determination of molecular masses and molecular mass distribution in low molecular weight heparin. *Thromb Res* 1991; **64:** 131-141

27 **Mascellani G,** Liverani L, Bianchini P, Parma B, Torri G, Bisio A, Guerrini M, Casu B. Structure and contribution to the heparin cofactor II-mediated inhibition of thrombin of naturally oversulphated sequences of dermatan sulphate. *Biochem J* 1993; **296:** 639-648

28 **Collins CE,** Rampton DS, Rogers J, Williams NS. Platelet aggregation and neutrophil sequestration in the mesenteric circulation in inflammatory bowel disease. *Eur J Gastroenterol Hepatol* 1997; **9:** 1213-1217

29 **Thompson NP,** Wakefield AJ, Pounder RE. Inherited disorders of coagulation appear to protect against inflammatory bowel disease. *Gastroenterology* 1995; **108:** 1011-1015

30 **de Bruijne-Admiraal LG,** Modderman PW, Von dem Borne AE, Sonnenberg A. P-selectin mediates Ca (2+)-dependent adhesion of activated platelets to many different types of leukocytes: detection by flow cytometry. *Blood* 1992; **80:** 134-142

31 **Kawashima H,** Hirose M, Hirose J, Nagakubo D, Plaas AH, Miyasaka M. Binding of a large chondroitin sulfate/dermatan sulfate proteoglycan, versican, to L-selectin, P-selectin, and CD44. *J Biol Chem* 2000; **275:** 35448-35456

32 **Kawashima H,** Atarashi K, Hirose M, Hirose J, Yamada S, Sugahara K, Miyasaka M. Oversulfated chondroitin/dermatan sulfates containing GlcAβ1/IdoAα1-3GalNAc (4, 6-O-disulfate) interact with L- and P-selectin and chemokines. *J Biol Chem* 2002; **277:** 12921-12930

33 **Talbot RW,** Heppell J, Dozois RR, Beart RW Jr. Vascular complications of inflammatory bowel disease. *Mayo Clin Proc* 1986; **61:** 140-145

34 **Webberley MJ,** Hart MT, Melikian V. Thromboembolism in inflammatory bowel disease: role of platelets. *Gut* 1993; **34:** 247-251

35 **Lam A,** Borda IT, Inwood MJ, Thomson S. Coagulation studies in ulcerative colitis and Crohn's disease. *Gastroenterology* 1975; **68:** 245-251

36 **Hudson M,** Hutton RA, Wakefield AJ, Sawyerr AM, Pounder RE. Evidence for activation of coagulation in Crohn's disease. *Blood Coagul Fibrinolysis* 1992; **3:** 773-778

37 **Hudson M,** Chitolie A, Hutton RA, Smith MS, Pounder RE, Wakefield AJ. Thrombotic vascular risk factors in inflammatory bowel disease. *Gut* 1996; **38:** 733-737

38 **Koutroubakis IE,** Sfiridaki A, Mouzas IA, Maladaki A, Kapsoritakis A, Roussomoustakaki M, Kouroumalis EA, Manousos ON. Resistance to activated protein C and low levels of free protein S in Greek patients with inflammatory bowel disease. *Am J Gastroenterol* 2000; **95:** 190-194

39 **Aadland E,** Odegaard OR, Roseth A, Try K. Free protein S deficiency in patients with chronic inflammatory bowel disease. *Scand J Gastroenterol* 1992; **27:** 957-960

40 **Heneghan MA,** Cleary B, Murray M, O'Gorman TA, McCarthy CF. Activated protein C resistance, thrombophilia, and inflammatory bowel disease. *Dig Dis Sci* 1998; **43:** 1356-1361

41 **Griffin JH,** Evatt B, Wideman C, Fernandez JA. Anticoagulant protein C pathway defective in majority of thrombophilic patients. *Blood* 1993; **82:** 1989-1993

42 **Bertina RM,** Koeleman BP, Koster T, Rosendaal FR, Dirven RJ, de Ronde H, van der Velden PA, Reitsma PH. Mutation in blood coagulation factor V associated with resistance to activated protein C. *Nature* 1994; **369:** 64-67

43 **Gaffney PR,** Doyle CT, Gaffney A, Hogan J, Hayes DP, Annis P. Paradoxical response to heparin in 10 patients with ulcerative colitis. *Am J Gastroenterol* 1995; **90:** 220-223

44 **Maimone MM,** Tollefsen DM. Structure of a dermatan sulfate hexasaccharide that binds to heparin cofactor II with high affinity. *J Biol Chem* 1990; **265:** 18263-18271

Edited by Kumar M and Wang XL **Proofread by** Xu FM

PO Box 2345, Beijing 100023, China
Fax: +86-10-85381893
E-mail: wjg@wjgnet.com www.wjgnet.com

World J Gastroenterol 2004;10(23):3490-3494
World Journal of Gastroenterology
Copyright © 2004 by The WJG Press ISSN 1007-9327

• BASIC RESEARCH •

Inhibitory effect of heparin-derived oligosaccharides on secretion of interleukin-4 and interleukin-5 from human peripheral blood T lymphocytes

Sheng-Li Ji, Hui-Fei Cui, Feng Shi, Yan-Qing Chi, Ji-Chao Cao, Mei-Yu Geng, Hua-Shi Guan

Sheng-Li Ji, Mei-Yu Geng, Hua-Shi Guan, Key Laboratory of Marine Drugs, Marine Drug and Food Institute, Ocean University of China, Qingdao 266003, Shandong Province, China
Sheng-Li Ji, Hui-Fei Cui, Feng Shi, Ji-Chao Cao, Institute of Biochemical and Biotech drugs, School of Pharmacy, Shandong University, Jinan 250012, Shandong Province, China
Yan-Qing Chi, Department of Pharmacy, Shandong Provincial Hospital, Jinan 250021, Shandong Province, China
Supported by the National Natural Science Foundation of China, No. 30370613 and the Major state Basic Research Development Program of China, 2001CCA01600
Correspondence to: Sheng-Li Ji, Institute of Biochemical and Biotech Drugs, School of Pharmacy, Shandong University, Jinan 250012, Shandong Province, China. shengliji@sdu.edu.cn
Telephone: +86-531-8380288 **Fax:** +86-531-2929312
Received: 2004-03-19 **Accepted:** 2004-04-07

Abstract

AIM: To investigate the inhibitory effect of heparin-derived oligosaccharides (Oligs) on secretion of interleukin-4 (IL-4) and interleukin-5 (IL-5) from human peripheral blood T lymphocytes (PBTLs).

METHODS: Oligs were prepared by three different heparin depolymerization methods and separated by gel filtration chromatography. PBTLs from ten adult patients with allergic eosinophilic gastroenteritis were treated with phytahematoagglutinin (PHA) and Oligs. The supernatants from the cell culture of PBTLs were harvested and subjected to the determination of IL-4 and IL-5 contents by ELISA method.

RESULTS: At the concentration of 5 μg/mL, Oligs with different M_r had different effects on the secretion of IL-4 and IL-5. The tetrasaccharide with M_r of 1 142, produced by depolymerizing heparin with hydrogen peroxide, had the strongest inhibitory effect on the secretion of IL-4. It decreased the IL-4 content from 375.6±39.2 ng/L (PHA group) to 12.5±5.7 ng/L (P<0.01). The hexasaccharide with M_r of 1 806, produced by depolymerizing heparin with β-elimination method, had the strongest inhibitory effect on the secretion of IL-5. It decreased the IL-5 content from 289.2±33.4 ng/L (PHA group) to 22.0±5.2 ng/L (P<0.01).

CONCLUSION: The inhibitory activity of Oligs on the secretion of IL-4 and IL-5 from human PBTLs closely depends on their molecular structure, and there may be an essential structure to act as an inhibitor. The most effective inhibitors of IL-4 and IL-5 secretion are tetrasaccharides and hexasaccharides, respectively.

Ji SL, Cui HF, Shi F, Chi YQ, Cao JC, Geng MY, Guan HS. Inhibitory effect of heparin-derived oligosaccharides on secretion of interleukin-4 and interleukin-5 from human peripheral blood T lymphocytes. *World J Gastroenterol* 2004; 10(23): 3490-3494
http://www.wjgnet.com/1007-9327/10/3490.asp

INTRODUCTION

Heparin is a highly sulfated, polyanionic glycosaminoglycan. It is composed of the trisulfated disaccharide unit [- *L*-iduronic acid-2-sulfate (IdoA2S) (1→4)-α-*D*- glucosamine-*N*,6 -disulfate (GlcNS6S)-], interrupted by irregular sequences containing undersulfated (or oversulfated) uronic acids and amino sugar residues, with an average relative molecular mass (M_r) of 12 000-15 000[1]. In addition to its anticoagulatory effect, heparin has anti-inflammatory property, which has been used for treatment of ulcerative colitis and other inflammatory bowel diseases (IBD)[2-15]. Although many studies have reported heparin's anti-inflammatory activities, there is little information available in literature about the specific oligosaccharide structures in heparin that inhibits the secretion of IL-4 and IL-5. IL-4 and IL-5 abnormalities have been reported to be consistent with the elevated IgE and eosinophilia in allergic eosinophilic gastroenteritis, suggesting that strategies targeting T lymphocytes may be efficacious in treatment of this kind of diseases[16-19]. Here, we examined whether there was a relationship between the molecular weight of heparin-derived Oligs and their inhibitory effect on IL-4 and IL-5 secretion from PBTLs in allergic eosinophilic gastroenteritis.

MATERIALS AND METHODS

Drugs and reagents

Heparin sodium was donated by Dongying Tiandong Biochemical Industrial Co. Ltd, and 300 mL/L hydrogen peroxide (H_2O_2) was purchased from Laiyang Fine Chemical Regent Co, Ltd. Benzethonium chloride and (4-chloro)-benzyl chloride were purchased from Sigma Co., USA. Sodium nitrite was purchased from Jinan Chemical Reagents Co., Ltd. Superdex-30 was purchased from Amersham Biosciences. Human IL-4 and IL-5 ELISA kits (96 tests) were purchased from Bender Medsystems, USA. Phytahematoagglutinin (PHA) was purchased from Shanghai Yihua Medical Science and Technology Co., Ltd. RPMI 1640 culture medium was purchased from Gibco, Paisley, UK.

Preparation of Oligs

Heparin was degraded by oxidative depolymerization with hydrogen peroxide[20], deaminative cleavages with nitrous acid[21] and β-eliminative cleavages with alkaline[22], respectively. All Oligs were obtained from the products separated by gel filtration chromatography with Superdex-30 column (26 mm×1200 mm), and the oligosaccharides were eluted with 0.25 mol/L ammonium bicarbonate and dried with lyophilization.

Determination of the relative molecular weight of Oligs

The M_r of Oligs was determined by high performance size exclusion chromatography (HPSEC) on two Ultrahydrogel 250 (7.8 mm×300 mm) columns in series. The calibration was based on low molecular mass heparin for calibration CRS (Batch No 1A, European Pharmacopoeia) standards with number average molecular mass (M_n) of 3 700. A refractometer (RI) detector connected in series to an ultraviolet (UV) spectrophotometer

set at 234 nm was used for detection, and 28.4 g/L solution of sodium sulphate (pH 5.0) was used as the mobile phase at a flow rate of 0.5 mL/min[23].

T cell separation and culture

Twenty-five milliliters of edetic acid anticoagulant peripheral blood was taken from ten adult patients with allergic eosinophilic gastroenteritis, and then mixed with 25 mL of PBS (pH 7.4, containing 50 mL/L fetal bovine serum). The diluted peripheral blood was then laid on 50 mL of lymphocyte separating solution carefully and centrifuged for 20 min at 2 000 r/min at room temperature. The peripheral blood lymphocytes (PBL) were collected and washed two times with PBS and suspended in RPMI 1640 solution (containing 200 mL/L fetal bovine serum). One millilitre of PBL suspending solution was added to the column of Nylon cotton (5 mm×16 mm). Then 0.2 mL of RPMI 1640 (containing 200 mL/L fetal bovine serum) was added on the Nylon cotton surface to close the column. The column was incubated for 30 min at 37 ℃ in an incubator. After that, PBTLs were eluted with RPMI 1640 (containing 200 mL/L fetal bovine serum) solution and then centrifuged for 10 min at 2 000 r/min. PBTLs were diluted to the cell density of 1.0×10^6 cells/mL, and 0.2 mL of the diluted cell suspending solution was added to a well of 96-well plate as a blank control. Another well was added into 0.2 mL of diluted cell suspending solution containing 20 μg of PHA as PHA control group. Other wells were added into 0.2 mL of diluted cell suspending solution containing 20 μg of PHA and 1 μL of 1.0 mg/mL heparin and Oligs. The cells were incubated for 48 h at 37 ℃ in a humidified atmosphere containing 50 mL/L CO_2 in air.

Detection of cytokines

The cells were harvested and centrifuged for 10 min at 1 000 r/min at room temperature. IL-4 and IL-5 in the cell culture solution were assayed by ELISA according to the manufacturer's instructions.

Statistical analysis

Data were expressed as mean±SD. Student's *t* test and one-way analysis of variance were used for statistical analysis. *P* values less than 0.05 were considered statistically significant.

RESULTS

Figure 1 shows the Oligs prepared from heparin degradation and separated by gel filtration chromatography. The peaks numbered were Oligs collected for inhibiting IL-4 and IL-5 experiments, and their M_r is listed in Table 1.

Table 1 Oligs obtained from chromatography eluted solution and their M_r

Oligs produced by H_2O_2 oxidation		Oligs produced by β-elimination		Oligs produced by degradation with HNO_2	
Samples	M_r	Samples	M_r	Samples	M_r
Olig H1	6 032	Olig B1	6 621	Olig N1	6 680
Olig H2	3 206	Olig B2	3 375	Olig N2	3 150
Olig H3	2 381	Olig B3	2 447	Olig N3	2 334
Olig H4	1 786	Olig B4	1 804	Olig N4	1 747
Olig H5	1 142	Olig B5	1 344	Olig N5	1 047
Olig H6	632	Olig B6	702	Olig N6	609

The effect of Oligs on secretion of IL-4 showed that all the Oligs had inhibitory activities and Oligs prepared from different methods or with different M_r had different effects. First, the Olig prepared from H_2O_2 depolymerizing method, was Olig H5 with M_r of 1 142 (tetrasaccharides), which had the strongest inhibitory effect and decreased the IL-4 content from 375.6±39.2 ng/L (PHA group) to 12.5±5.7 ng/L ($P<0.01$). Second, among the Oligs from β-eliminative cleavage heparin, Olig B5 with M_r of 1 344 (tetrasaccharides) had the strongest inhibitory activity and decreased the IL-4 content to 54.4±6.3 ng/L ($P<0.01$). Third, the Olig from nitrous acid deaminative cleavage heparin, was Olig N5 with M_r of 1 107 (tetrasaccharides), which had the strongest inhibitory activity and decreased the IL-4 content to 47.4±5.8 ng/L ($P<0.01$). Although all these Oligs were tetrasaccharides, they had different M_r, because the amount of sulfate groups in their structure was different. The IL-4 content in the heparin group was 152.4±17.9 ng/L, and the difference in inhibitory activities between Oligs and heparin group was significant ($P<0.01$, Figures 2A, 3A).

The inhibitory effect of Oligs on secretion of IL-5 and IL-4 was similar. But there were some differences. Firstly, the Oligs prepared from H_2O_2 oxidation method, were Olig H4 with M_r of 1 786 and Olig H5 with M_r of 1 142, which had strongest inhibitory activities. They decreased the IL-5 content from 289.2±33.4 ng/L (PHA group) to 31.7±5.6 ng/L and 35.5±4.4 ng/L, respectively ($P<0.01$). Secondly, among the Oligs from β-eliminative cleavage heparin, Olig B4 with M_r of 1 804 (hexasaccharides) had the strongest inhibitory activity and decreased the IL-5 content to 22.0±5.2 ng/L ($P<0.01$). Thirdly, among the Oligs from nitrous acid deaminative cleavage heparin, Olig N4 with M_r of 1 747 (hexasaccharides) had the strongest inhibitory activity and decreased the IL-5 content to 69.2±6.3 ng/L ($P<0.01$). The inhibitory activities of these Oligs were stronger than those of unfractioned heparin ($P<0.01$, Figure 2B). The strongest inhibitor was Olig B4 (Figure 3B).

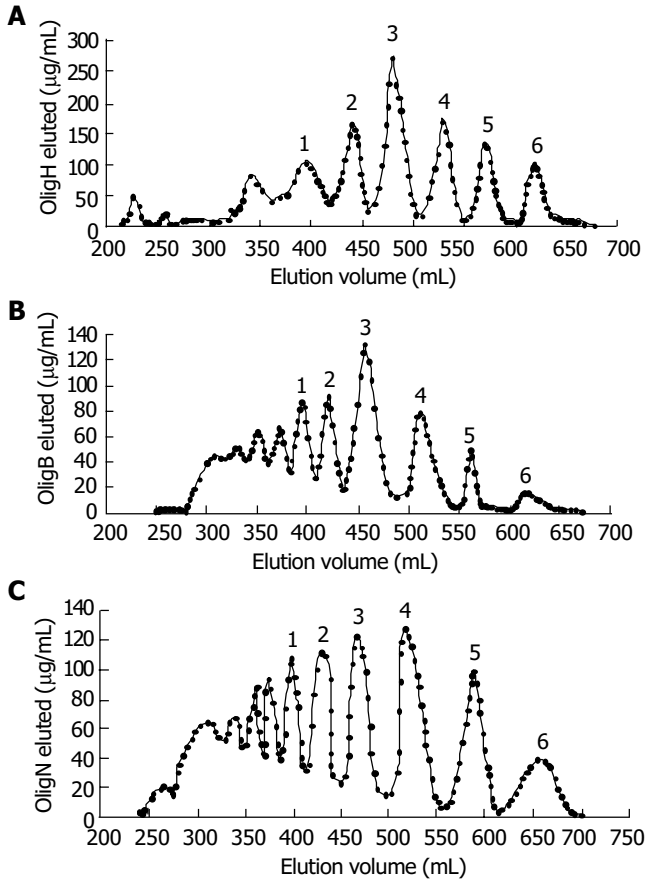

Figure 1 Size separation of heparin oligosaccharides. A: heparin degraded with hydrogen peroxide; B: heparin degraded with β-eliminative cleavage; C: heparin degraded with nitrous acids. The reaction products were separated on a Superdex 30 size exclusion column (26 mm×1 200 mm) at a flow rate of 0.5 mL/min in 0.25 mol/L ammonium bicarbonate. Elution profiles were monitored by carbazole assay.

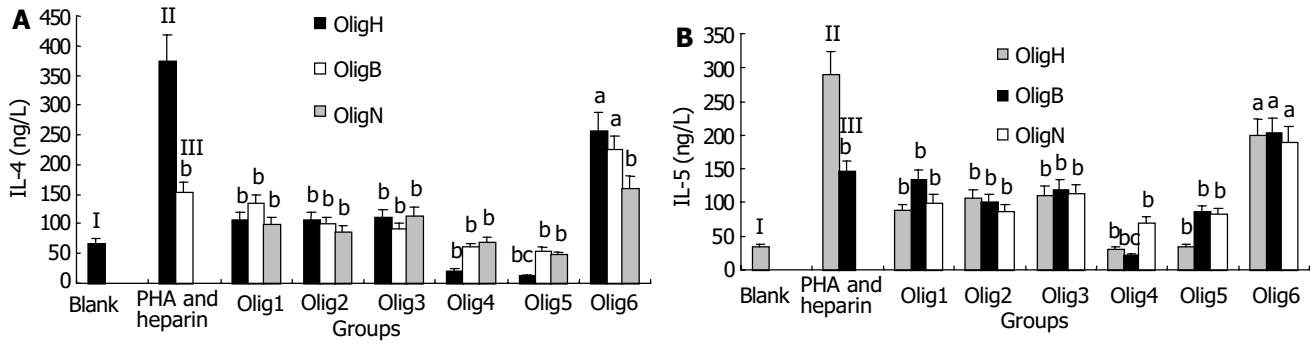

Figure 2 Content of IL-4 (A) and IL-5 (B) in PBTL culture solution of different groups. I, II and III represent blank control group, PHA control group and heparin group respectively. Olig1 to Olig 6 represent corresponding oligasaccharide samples described in Table 1 (from 1 to 6), respectively. $^{a}P<0.05$, $^{b}P<0.01$ *vs* PHA group; $^{c}P<0.05$ *vs* Olig H4 group. (n = 10 for each group).

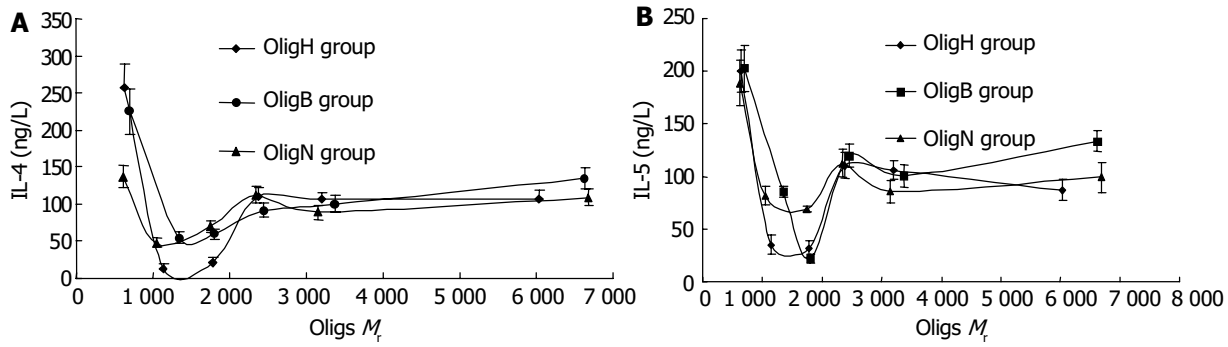

Figure 3 Relationship between M_r of Oligs and their activity on inhibiting IL-4 (A) and IL-5 (B) secretion. $^{a}P<0.05$ *vs* Olig H4 group.

DISCUSSION

Allergic eosinophilic gastroenteritis is characterized by elevated total immunoglobulin E (IgE). IgE plays a significant role in allergic IBD by mediating the cross-linking of high-affinity Fc receptors (FcεRI) on mast cells, thus resulting in the release of a vast array of pro-inflammatory mediators including histamine, leukotrienes, and cytokines[24] (Figure 4). In clinical studies, increased secretion of IL-4 and IL-5 by peripheral blood T cells has been reported in patients with eosinophilic gastroenteritis[17]. Furthermore, T cells derived from the duodenum of patients with eosinophilic gastrointestinal disorder could preferentially secrete helper T cell 2 (Th2) cytokines that pre-dominantly include IL-4 and IL-5 when stimulated with milk proteins[17]. IL-4 might play a critical role in mediating IgE-dependent allergic reactions, and regulation of IL-4 production or action might be useful for the prevention or therapy of immediate hypersensitivity disorders[25-27]. IL-5, on the other hand, is most specific to the eosinophil lineage and responsible for the selective expansion of eosinophils and their release from bone marrow. Eosinophil granules contain a crystalloid core composed of major basic proteins (MBP) and a matrix composed of eosinophil cationic protein (ECP)[28] (Figure 4). These cationic proteins share certain pro-inflammatory properties but differ in other aspects. MBP also triggers degranulation of mast cells and basophils. Triggering of eosinophils through engagement of receptors for cytokines could lead to the generation of a wide range of inflammatory cytokines, including IL-1, IL-3, IL-4, IL-5, IL-13, granulocyte-macrophage colony stimulating factor (GM-CSF), transforming growth factors (TGF), TNF-α, RANTES, macrophage inflammatory protein 1α, vascular endothelial cell growth factor, and eotaxin 1, indicating that they have the potential to modulate multiple aspects of the immune response[29]. These findings imply that regulation of IL-5 production or action may also be useful for the prevention or therapy of allergy symptoms and inflammation.

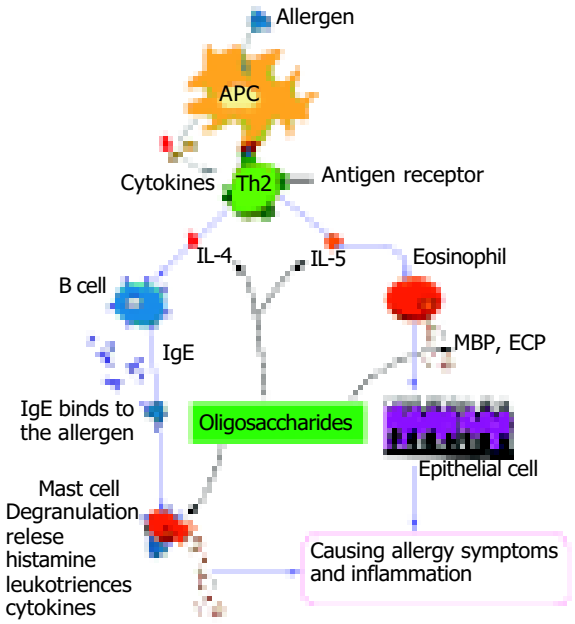

Figure 4 Interactions among inflammatory cells in pathogenesis of allergic eosinophilic gastroenteritis. Broken arrows denote the inhibitory effect of heparin-derived oligosaccharides on the various targets shown. MBP: major basic protein; and ECP: eosinophil cationic protein.

Heparin is a kind of polyanionic polysaccharides. In addition to its anticoagulant activity, heparin has a wide range of biological activities, including inhibition of complement activation[30], regulation of cell proliferation[31], inhibition of angiogenesis and tumor growth[32,33], and antiviral activity[34,35]. Over the last decade, heparin and low molecular mass heparin have been used to treat IBD in clinical practice[36-50]. The mechanisms by

which heparin is able to treat IBD include its ability to inhibit the recruitment of neutrophils, reduce production of pro-inflammatory cytokines[51] and restore the high-affinity receptor binding to antiulcerogenic growth factor[12,13]. The ability of heparin to inhibit neutrophil activation, adhesion, and chemotaxis was also found in a mouse model of IBD[14], suggesting that balanced interactions between mast cells and neutrophils might be important for the development of IBD. Furthermore, unfractioned heparin has potent immunomodulatory effects[52-57]. Administration of unfractioned heparin may therefore be rational in patients with ulcerative colitis or Crohn's disease resistant to conventional forms of treatment[39,40]. The anti-inflammatory effects of heparin can be most probably attributed to its physical binding to a variety of heparin-binding proteins such as TNF-α, IL-4, IL-5, RANTES, secretory leukocyte protease inhibitor, neutrophil-derived elastase and cathepsin G, eosinophil-derived major basic protein, and L- and P-selectins[58-61]. Alternatively, heparin has been shown to specifically inhibit the inositol 1,4, 5-triphosphate signal transduction pathway, which is important for a vast array of inflammatory cellular responses[62,63].

If heparin is to be used as an anti-inflammatory drug, the risk of inducing bleeding must be abrogated. It has been reported that the anti-inflammatory effects of heparin were independent of its anticoagulant activity[64-67], especially when it was used for treatment of allergic inflammation. Partial chemical modifications of heparin, such as depolymerization or partial desulfation, are the aim to develop heparin-derived anti-inflammatory drugs. We degraded heparin and separated the fragments by gel filtration chromatography. The oligosaccharides obtained were used as anti-inflammatory reagents and the results were promising. The hypothetic mechanisms for anti-inflammatory effects, such as inhibiting secretion of IL-4 and IL-5, were studied. Our results showed that Oligs with different M_r had different activities on inhibiting the secretion of IL-4 and IL-5. The Oligs, which had the strongest inhibitory activities on IL-4 secretion, were tetrasaccharides, but they had different M_r corresponding to the production methods. That was because different methods caused different desulfation during the process of degradation. The same phenomenon occured in inhibiting the secretion of IL-5, but the strongest inhibitors were hexasaccharides other than tetrasaccharides. The mechanism needs further studies.

REFERENCES

1 **Casu B**. Heparin structure. *Haemostasis* 1990; **20**(Suppl 1): 62-73

2 **Gaffney PR,** Doyle CT, Gaffney A, Hogan J, Hayes DP, Annis P. Paradoxical response to heparin in 10 patients with ulcerative colitis. *Am J Gastroenterol* 1995; **90:** 220-223

3 **Evans RC,** Wong VS, Morris AI, Rhodes JM. Treatment of corticosteroid-resistant ulcerative colitis with heparin-a report of 16 cases. *Aliment Pharmacol Ther* 1997; **11:** 1037-1040

4 **Yoshikane H,** Sakakibara A, Ayakawa T, Taki N, Kawashima H, Arakawa D, Hidano H. Disseminated intravascular coagulation in an ulcerative colitis case not associated with surgery. *Hepatogastroenterology* 2000; **47:** 1608-1610

5 **Cui HF,** Jiang XL. Treatment of corticosteroid-resistant ulcerative colitis with oral low molecular weight heparin. *World J Gastroenterol* 1999; **5:** 448-450

6 **Ang YS,** Mahmud N, White B, Byrne M, Kelly A, Lawler M, McDonald GS, Smith OP, Keeling PW. Randomized comparison of unfractionated heparin with corticosteroids in severe active inflammatory bowel disease. *Aliment Pharmacol Ther* 2000; **14:** 1015-1022

7 **Folwaczny C,** Wiebecke B, Loeschke K. Unfractioned heparin in the therapy of patients with highly active inflammatory bowel disease. *Am J Gastroenterol* 1999; **94:** 1551-1555

8 **Dotan I,** Hallak A, Arber N, Santo M, Alexandrowitz A, Knaani Y, Hershkoviz R, Brazowski E, Halpern Z. Low-dose low-molecular weight heparin (enoxaparin) is effective as adjuvant treatment in active ulcerative colitis: an open trial. *Dig Dis Sci* 2001; **46:** 2239-2244

9 **Vrij AA**, Jansen JM, Schoon EJ, de Bruine A, Hemker HC, Stockbrugger RW. Low molecular weight heparin treatment in steroid refractory ulcerative colitis: clinical outcome and influence on mucosal capillary thrombi. *Scand J Gastroenterol Suppl* 2001; **234:** 41-47

10 **Torkvist L,** Thorlacius H, Sjoqvist U, Bohman L, Lapidus A, Flood L, Agren B, Raud J, Lofberg R. Low molecular weight heparin as adjuvant therapy in active ulcerative colitis. *Aliment Pharmacol Ther* 1999; **13:** 1323-1328

11 **Papa A,** Danese S, Gasbarrini A, Gasbarrini G. Review article: potential therapeutic applications and mechanisms of action of heparin in inflammatory bowel disease. *Aliment Pharmacol Ther* 2000; **14:** 1403-1409

12 **Michell NP,** Lalor P, Langman MJ. Heparin therapy for ulcerative colitis? Effects and mechanisms. *Eur J Gastroenterol Hepatol* 2001; **13:** 449-456

13 **Day R,** Forbes A. Heparin, cell adhesion, and pathogenesis of inflammatory bowel disease. *Lancet* 1999; **354:** 62-65

14 **Wan MX,** Liu Q, Wang Y, Thorlacius H. Protective effect of low molecular weight heparin on experimental colitis: role of neutrophil recruitment and TNF-alpha production. *Inflamm Res* 2002; **51:** 182-187

15 **Fries W,** Pagiaro E, Canova E, Carraro P, Gasparini G, Pomerri F, Martin A, Carlotto C, Mazzon E, Sturniolo GC, Longo G. The effect of heparin on trinitrobenzene sulphonic acid-induced colitis in the rat. *Aliment Pharmacol Ther* 1998; **12:** 229-236

16 **Lalani T,** Simmons RK, Ahmed AR. Biology of IL-5 in health and disease. *Ann Allergy Asthma Immunol* 1999; **82:** 317-333

17 **Jaffe JS,** James SP, Mullins GE, Braun-Elwert L, Lubensky I, Metcalfe DD. Evidence for an abnormal profile of interleukin-4 (IL-4), IL-5, and gamma-interferon (gamma-IFN) in peripheral blood T cells from patients with allergic eosinophilic gastroenteritis. *J Clin Immunol* 1994; **14:** 299-309

18 **Lorentz A,** Schwengberg S, Mierke C, Manns MP, Bischoff SC. Human intestinal mast cells produce IL-5 *in vitro* upon IgE receptor cross-linking and *in vivo* in the course of intestinal inflammatory disease. *Eur J Immunol* 1999; **29:** 1496-1503

19 **Madden KB,** Whitman L, Sullivan C, Gause WC, Urban JF Jr, Katona IM, Finkelman FD, Shea-Donohue T. Role of STAT6 and mast cells in IL-4- and IL-13-induced alterations in murine intestinal epithelial cell function. *J Immunol* 2002; **169:** 4417-4422

20 **Fussi F.** Process for obtaining low molecular weight heparins endowed with elevated pharmacological properties, and product so obtained. *United States Patent* 1981; **4:** 108-281

21 **Lormeau JC,** Petitou M, Choay J, Choay SA. Oligosaccharides having anti-Xa activity and pharmaceutical compositions containing them. *United States Patent* 1998; **35:** 770

22 **Uzan A,** Rhone-Poulenc Rorer SA. Sulfated polysaccharides obtained from heparin, preparation process, pharmaceutical composition and use thereof. *United States Patent* 1998; **5:** 721-849

23 **Kristensen HI,** Tromborg EM, Nielsen JR, Nielsen JI, Johansen KB, Ostergaard PB. Development and validation of a size exclusion chromatography method for determination of molecular masses and molecular mass distribution in low molecular weight heparin. *Thromb Res* 1991; **64**: 131-141

24 **Yamaguchi M,** Sayama K, Yano K, Lantz CS, Noben-Trauth N, Ra C, Costa JJ, Galli SJ. IgE enhances Fc epsilon receptor I expression and IgE-dependent release of histamine and lipid mediators from human umbilical cord blood-derived mast cells: synergistic effect of IL-4 and IgE on human mast cell Fc epsilon receptor I expression and mediator release. *J Immunol* 1999; **162:** 5455-5465

25 **Madden KB,** Urban JF Jr, Ziltener HJ, Schrader JW, Finkelman FD, Katona IM. Antibodies to IL-3 and IL-4 suppress helminth-induced intestinal mastocytosis. *J Immunol* 1991; **147:** 1387-1391

26 **Schreiber S,** Heinig T, Panzer U, Reinking R, Bouchard A, Stahl PD, Raedler A. Impaired response of activated mononuclear phagocytes to interleukin 4 in inflammatory bowel disease. *Gastroenterology* 1995; **108:** 21-33

27 **West GA,** Matsuura T, Levine AD, Klein JS, Fiocchi C. Interleukin 4 in inflammatory bowel disease and mucosal immune reactivity. *Gastroenterology* 1996; **110:** 1683-1695

28 **Gleich GJ**. Mechanisms of eosinophil-associated inflammation. *J Allergy Clin Immunol* 2000; **105:** 651-663

29 **Gharaee-Kermani M,** Phan SH. The role of eosinophils in pulmonary fibrosis (Review). *Int J Mol Med* 1998; **1:** 43-53

30 **Sharath MD,** Merchant ZM, Kim YS, Rice KG, Linhardt RJ, Weiler JM. Small heparin fragments regulate the amplification pathway of complement. *Immunopharmacology* 1985; **9:** 73-80

31 **Wright TC Jr,** Castellot JJ Jr, Petitou M, Lormeau JC, Choay J, Karnovsky MJ. Structural determinants of heparin's growth inhibitory activity. Interdependence of oligosaccharide size and charge. *J Biol Chem* 1989; **264:** 1534-1542

32 **Folkman J,** Langer R, Linhardt RJ, Haudenschild C, Taylor S. Angiogenesis inhibition and tumor regression caused by heparin or a heparin fragment in the presence of cortisone. *Science* 1983; **221:** 719-725

33 **Crum R,** Szabo S, Folkman J. A new class of steroids inhibits angiogenesis in the presence of heparin or a heparin fragment. *Science* 1985; **230:** 1375-1378

34 **Holodniy M,** Kim S, Katzenstein D, Konrad M, Groves E, Merigan TC. Inhibition of human immunodeficiency virus gene amplification by heparin. *J Clin Microbiol* 1991; **29:** 676-679

35 **Shieh MT,** Spear PG. Herpesvirus-induced cell fusion that is dependent on cell surface heparan sulfate or soluble heparin. *J Virol* 1994; **68:** 1224-1228

36 **Head KA,** Jurenka JS. Inflammatory bowel disease Part 1: ulcerative colitis-pathophysiology and conventional and alternative treatment options. *Altern Med Rev* 2003; **8:** 247-283

37 **Aiikhan R,** Cohen AT, Combe S, Samama MM, Desjardins L, Eldor A, Janbon C, Leizorovicz A, Olsson CG, Turpie AG. Prevention of venous thromboembolism in medical patients with enoxaparin: a subgroup analysis of the MEDENOX study. *Blood Coagul Fibrinolysis* 2003; **14:** 341-346

38 **Jani N,** Regueiro MD. Medical therapy for ulcerative colitis. *Gastroenterol Clin North Am* 2002; **31:** 147-166

39 **Prajapati DN,** Newcomer JR, Emmons J, Abu-Hajir M, Binion DG. Successful treatment of an acute flare of steroid-resistant Crohn's colitis during pregnancy with unfractionated heparin. *Inflamm Bowel Dis* 2002; **8:** 192-195

40 **Papa A,** Danese S, Gasbarrini A, Gasbarrini G. Review article: potential therapeutic applications and mechanisms of action of heparin in inflammatory bowel disease. *Aliment Pharmacol Ther* 2000; **14:** 1403-1409

41 **Kassis J,** Fugere F, Dube S. The safe use of epidural anesthesia after subcutaneous injection of low-dose heparin in general abdominal surgery. *Can J Surg* 2000; **43:** 289-294

42 **Ang YS,** Mahmud N, White B, Byrne M, Kelly A, Lawler M, McDonald GS, Smith OP, Keeling PW. Randomized comparison of unfractionated heparin with corticosteroids in severe active inflammatory bowel disease. *Aliment Pharmacol Ther* 2000; **14:** 1015-1022

43 **Katz S.** Update in medical therapy in inflammatory bowel disease: a clinician's view. *Dig Dis* 1999; **17:** 163-171

44 **Koutroubakis IE,** Sfiridaki A, Mouzas IA, Maladaki A, Kapsoritakis A, Roussomoustakaki M, Kouroumalis EA, Manousos ON. Resistance to activated protein C and low levels of free protein S in Greek patients with inflammatory bowel disease. *Am J Gastroenterol* 2000; **95:** 190-194

45 **Day R,** Ilyas M, Daszak P, Talbot I, Forbes A. Expression of syndecan-1 in inflammatory bowel disease and a possible mechanism of heparin therapy. *Dig Dis Sci* 1999; **44**: 2508-2515

46 **Haslam N,** Standen GR, Probert CS. An investigation of the association of the factor V Leiden mutation and inflammatory bowel disease. *Eur J Gastroenterol Hepatol* 1999; **11:** 1289-1291

47 **Torkvist L,** Thorlacius H, Sjoqvist U, Bohman L, Lapidus A, Flood L, Agren B, Raud J, Lofberg R. Low molecular weight heparin as adjuvant therapy in active ulcerative colitis. *Aliment Pharmacol Ther* 1999; **13:** 1323-1328

48 **Day R,** Forbes A. Heparin, cell adhesion, and pathogenesis of inflammatory bowel disease. *Lancet* 1999; **354:** 62-65

49 **McCarty MF.** Vascular heparan sulfates may limit the ability of leukocytes to penetrate the endothelial barrier-implications for use of glucosamine in inflammatory disorders. *Med Hypotheses* 1998; **51:** 11-15

50 **Korzenik JR,** Hsu A, Robert ME. Effect of heparin on dextran sulfate sodium-induced colitis. *Dig Dis Sci* 1998; **43:** 1800-1805

51 **Papa A,** Danese S, Gasbarrini A, Gasbarrini G. Review article: potential therapeutic applications and mechanisms of action of heparin in inflammatory bowel disease. *Aliment Pharmacol Ther* 2000; **14:** 1403-1409

52 **Ahmed T,** Abraham WM, D'Brot J. Effects of inhaled heparin on immunologic and nonimmunologic bronchoconstrictor responses in sheep. *Am Rev Respir Dis* 1992; **145:** 566-570

53 **Bowler SD,** Smith SM, Lavercombe PS. Heparin inhibits the immediate response to antigen in the skin and lungs of allergic subjects. *Am Rev Respir Dis* 1993; **147:** 160-163

54 **Chang NS,** Intrieri C, Mattison J, Armand G. Synthetic posu78-8Ifatd hyaluronic acid is a potent inhibitor for tumor necrosis factor production. *J Leukoc Biol* 1994; **55:** 74

55 **Lantz M,** Thysell H, Nilsson E, Olsson I. On the binding of tumor necrosis factor (TNF) to heparin and the release *in vivo* of the TNF-binding protein I by heparin. *J Clin Invest* 1991; **88:** 2026-2031

56 **Nelson RM,** Cecconi O, Roberts WG, Aruffo A, Linhardt RJ, Bevilacqua MP. Heparin oligosaccharides bind L- and P-selectin and inhibit acute inflammation. *Blood* 1993; **82:** 3253-3258

57 **Teixeira MM,** Hellewell PG. Suppression by intradermal administration of heparin of eosinophil accumulation but not oedema formation in inflammatory reactions in guinea-pig skin. *Br J Pharmacol* 1993; **110:** 1496-1500

58 **Lider O,** Mekori YA, Miller T, Bar-Tana R, Vlodavsky I, Baharav E, Cohen IR, Naparstek Y. Inhibition of T lymphocyte heparanase by heparin prevents T cell migration and T cell-mediated immunity. *Eur J Immunol* 1990; **20:** 493-499

59 **Fath MA,** Wu X, Hileman RE, Linhardt RJ, Kashem MA, Nelson RM, Wright CD, Abraham WM. Interaction of secretory leukocyte protease inhibitor with heparin inhibits proteases involved in asthma. *J Biol Chem* 1998; **273:** 13563-13569

60 **Tyrell DJ,** Kilfeather S, Page CP. Therapeutic uses of heparin beyond its traditional role as an anticoagulant. *Trends Pharmacol Sci* 1995; **16:** 198-204

61 **Jones CA,** Williams KA, Finlay-Jones JJ, Hart PH. Interleukin 4 production by human amnion epithelial cells and regulation of its activity by glycosaminoglycan binding. *Biol Reprod* 1995; **52:** 839-847

62 **Ghosh TK,** Eis PS, Mullaney JM, Ebert CL, Gill DL. Competitive, reversible, and potent antagonism of inositol 1,4,5-trisphosphate-activated calcium release by heparin. *J Biol Chem* 1988; **263:** 11075-11079

63 **Ahmed T,** Syriste T, Mendelssohn R, Sorace D, Mansour E, Lansing M, Abraham WM, Robinson MJ. Heparin prevents antigen-induced airway hyperresponsiveness: interference with IP3-mediated mast cell degranulation? *J Appl Physiol* 1994; **76:** 893-901

64 **Sy MS,** Schneeberger E, McCluskey R, Greene MI, Rosenberg RD, Benacerraf B. Inhibition of delayed-type hypersensitivity by heparin depleted of anticoagulant activity. *Cell Immunol* 1983; **82:** 23-32

65 **Xie X,** Rivier AS, Zakrzewicz A, Bernimoulin M, Zeng XL, Wessel HP, Schapira M, Spertini O. Inhibition of selectin-mediated cell adhesion and prevention of acute inflammation by nonanticoagulant sulfated saccharides. Studies with carboxyl-reduced and sulfated heparin and with trestatin a sulfate. *J Biol Chem* 2000; **275:** 34818-34825

66 **Fryer A,** Huang YC, Rao G, Jacoby D, Mancilla E, Whorton R, Piantadosi CA, Kennedy T, Hoidal J. Selective O-desulfation produces nonanticoagulant heparin that retains pharmacological activity in the lung. *J Pharmacol Exp Ther* 1997; **282:** 208-219

67 **Kariya Y,** Kyogashima M, Suzuki K, Isomura T, Sakamoto T, Horie K, Ishihara M, Takano R, Kamei K, Hara S. Preparation of completely 6-O-desulfated heparin and its ability to enhance activity of basic fibroblast growth factor. *J Biol Chem* 2000; **275:** 25949-25958

Edited by Kumar M and Wang XL **Proofread by** Xu FM

PO Box 2345, Beijing 100023, China
Fax: +86-10-85381893
E-mail: wjg@wjgnet.com www.wjgnet.com

World J Gastroenterol 2004;10(23):3495-3499
World Journal of Gastroenterology
Copyright © 2004 by The WJG Press ISSN 1007-9327

• CLINICAL RESEARCH •

Selection criteria for preoperative endoscopic retrograde cholangiopancreatography before laparoscopic cholecystectomy and endoscopic treatment of bile duct stones: Results of a retrospective, single center study between 1996-2002

Laszlo Lakatos, Gabor Mester, Gyorgy Reti, Attila Nagy, Peter Laszlo Lakatos

Laszlo Lakatos, Gabor Mester, 1st Department of Medicine, Csolnoky F, Province Hospital, Veszprem, H-8200 Hungary
Gyorgy Reti, Attila Nagy, Department of Surgery, Csolnoky F, Province Hospital, Veszprem, H-8200 Hungary
Peter Laszlo Lakatos, 1st Department of Medicine, Semmelweis University, Budapest, H-8200 Hungary
Correspondence to: Laszlo Lakatos, M.D., PhD, 1st Department of Medicine, Csolnoky F, Province Hospital, Korhaz u.1, Veszprem, H-8200 Hungary. laklaci@hotmail.com
Telephone: +36-20-9119339 **Fax:** +36-1-3130250
Received: 2004-04-04 **Accepted:** 2004-05-25

Abstract

AIM: The optimal treatment for bile duct stones (in terms of cost, complications and accuracy) is unclear. The aim of our study was to determine the predictive factors for preoperative endoscopic retrograde cholangiopancreatography (ERCP).

METHODS: Patients undergoing preoperative ERCP (⩽90 d before laparoscopic cholecystectomy) were evaluated in this retrospective study from the 1st of January 1996 to the 31st of December 2002. The indications for ERCP were elevated serum bilirubin, elevated liver function tests (LFT), dilated bile duct (⩾8 mm) and/or stone at US examination, coexisting acute pancreatitis and/or acute pancreatitis or jaundice in patient's history. Suspected prognostic factors and the combination of factors were compared to the result of ERCP.

RESULTS: Two hundred and six preoperative ERCPs were performed during the observed period. The rate of successful cannulation for ERC was (97.1%). Bile duct stones were detected in 81 patients (39.3%), and successfully removed in 79 (97.5%). The number of prognostic factors correlated with the presence of bile duct stones. The positive predictive value for one prognostic factor was 1.2%, for two 43%, for three 72.5%, for four or more 91.4%.

CONCLUSION: Based on our data preoperative ERCP is highly recommended in patients with three or more positive factors (high risk patients). In contrast, ERCP is not indicated in patients with zero or one factor (low risk patients). Preoperative ERCP should be offered to patients with two positive factors (moderate risk patients), however the practice should also be based on the local conditions (*e.g.* skill of the endoscopist, other diagnostic tools).

Lakatos L, Mester G, Reti G, Nagy A, Lakatos PL. Selection criteria for preoperative endoscopic retrograde cholangiopancreatography before laparoscopic cholecystectomy and endoscopic treatment of bile duct stones: Results of a retrospective, single center study between 1996-2002. *World J Gastroenterol* 2004; 10 (23): 3495-3499
http://www.wjgnet.com/1007-9327/10/3495.asp

INTRODUCTION

The rate of coexisting common bile duct stones (CBDS) in patients undergoing cholecystectomy for cholelithiasis is approximately 7-20%[1-3]. The dramatic shift from conventional to laparoscopic cholecystectomy (LC) in the last 15 years has opened a large debate over the optimal management of patients with CBDS undergoing cholecystectomy[4,5]. It is generally accepted that bile duct stones should be removed (even if asymptomatic), because they may be associated with severe complications such as pancreatitis and cholangitis. The management of coexisting CBDS may be surgical or endoscopic followed by surgery. Gallbladder preservation has also been suggested, however it has not become universal[6]. A group of surgeons have recommended laparoscopic management of coexisting CBDS by intraoperative cholangiography or intraoperative ERCP and surgical removal of the stones[7-9]. However, manipulation of the bile duct during LC is not popular among laparoscopic surgeons. Recent studies suggest that it can be done safely and does not prolong hospitalisation[10,11], but minimal invasiveness and cost-effectivity remain questionable[12].

ERCP is the most popular peri-LC bile duct imaging method. It is readily available, safe, highly accurate and has therapeutic potential, even in old patients[13]. Furthermore ERCP offers the possibility to study bile duct anatomy, identify abnormalities of the bile ducts as well as being useful in the differential diagnosis of questionable lesions (*e.g.* malignancy). The role of new, less invasive imaging techniques (*e.g.* endoscopic ultrasound - EUS, magnetic resonance cholangiopancreatography - MRCP) is less well characterized[14-16].

Routine preoperative ERCP may not be recommended, due to the low percentage of coexisting cholecysto-choledocholithiasis, a large number of negative investigations, and a small but significant risk of associated morbidity and high additional costs. Postoperative ERCP could reduce the number of unnecessary interventions and the majority of retained stones and postoperative leakages can be treated, although a second operation is required in case of failure. The development of more reliable predictors of CBD stones, based on the patient's clinical, biochemical and ultrasound (US) presentations, could allow a more appropriate use of preoperative ERCP (or EUS, MRCP). However, there is still no consensus as to which particular indicator, or set of indicators should be used, or as to the threshold values of various indicators[3,17-22].

The aim of this study was to determine a precise and easily applicable clinical, biochemical and US (selection) criteria for patients who should undergo further investigation (preoperative ERCP) prior to LC/surgery.

MATERIALS AND METHODS

Patients who underwent preoperative ERCP from the 1st January 1996 to the 1st January 2003 (⩽90 d before laparoscopic cholecystectomy) were evaluated in this retrospective study.

The indications for ERCP were one or more of the following: elevated serum bilirubin (⩾2× upper limit of normal - ULN) concentration, elevated liver function tests [LFT, ⩾1.5× ULN: either aspartate-aminotransferase (AST), alanine-aminotransferase (ALT), alkaline phosphatase (ALP) or γ-glutamyl transpeptidase (GGT) activities], dilated bile duct (⩾8 mm) and/or stones at US examination, coexisting acute pancreatitis and/or acute pancreatitis or jaundice in patient's history. The predictive values of age, sex and colic were also investigated. The majority of the ERCPs were performed by two expert endoscopists. Suspected prognostic factors and combination of factors were compared to the results of the ERCP.

Serum bilirubin concentration, AST, ALT, ALP and GGT activities were measured by Olympus AU600 (Olympus Co. Ltd, Shizuoka, Japan) autoanalyser at 37 ℃. The enzyme activities were expressed in U/L and serum bilirubin concentration was given in μmol/L.

Statistical analysis

Sensitivity, specificity, positive and negative predictive values were calculated for individual factors (compared to all other cases) and for combination of factors. Student *t*-test with separate variance estimates was performed to test the demographic differences. χ^2 test and Fisher exact test were performed to compare between patients with a different number of suggested factors. $P<0.05$ was considered statistically significant. For the statistical analysis Statistica 6.1 (Statsoft Inc, OK, USA) was used.

RESULTS

A total of 2985 ERCPs and 1248 LCs were performed in the Csolnoky F. Province Hospital between 1st January 1996 and the 31st December 2002. Using our selection criteria (a minimum of one positive factor) preoperative ERCP was performed in 206 patients (16.5%, Table 1). Seventy-seven percent of the patients were women and 23% men. The mean age of women was significantly lower ($P = 0.02$, Table 2). The mean waiting time between ERCP and LC was 17.3 d. Thirty-nine percent of the patients were operated within 3 d, almost 60% within one week.

Table 1 Number of ERCP and/or LC cases per year in the Csolnoky Ferenc Hospital, Veszprém, Hungary

Year	ERCP	LC	ERCP-LC
1996	373	99	15
1997	393	164	28
1998	375	140	27
1999	490	189	33
2000	558	183	36
2001	378	246	42
2002	391	227	25
Total	2 258	1 248	206
Average	423/yr	178	29/yr

Table 2 Preoperative ERCP, age and gender of patients (*n*=206)

Gender	*n* (%)	Mean age
Male	48 (23)	57.4
Female	158 (77)	51.0
Total	206 (100)	52.5

A successful cannulation was done in 200 patients (97.1%, Table 3). CBD stones were found in 81 patients (39.3%), the stone/stones were removed endoscopically in 79 cases (97.5%). There was a tendency of increased frequency of CBD stones in men (24/48 = 50.0%) compared to women (57/158 = 36.1%, $P = 0.06$ by Fisher exact test), but CBD stones were equally common in elder (⩾60 years) and younger (<60 years) patients (50/128 = 39.1% *vs* 31/78 = 39.7%).

The results for each individual criterion are shown in Tables 4, 5. With the exception of jaundice or pancreatitis in the patient's history the positive predictive value of each criterion was high (58-72%). Sensitivity and specificity were compared to patients lacking the specific factor.

Table 3 Results of preoperative ERCPs performed prior to LC (*n* = 206)

ERCP finding	*n*	%
Common bile duct (CBD) stone	81	39.3
Negative	119	57.8
CBD not filled	6	2.9
Successful EST and duct clearance	79/81	97.5
Complication	3	1.5
-bleeding	1	0.5
-pancreatitis	1	0.5
-stone impaction	1	0.5

Table 4 Common bile duct stones in cases of different positive prognostic factors (PPF)

Factor	Number	Stone	Negative	Unsuccessful	%
Hyperbilirubinaemia (>2)	61	44	16	1	72
Elevated ASAT/ALAT (>50%)	116	74	39	3	64
Elevated GGT/ALP (>50%)	134	79	52	3	59
Acute pancreatitis (AP)	26	18	7	1	69
AP in the anamnesis	20	4	16	0	20
Jaundice in the anamnesis	29	1	26	2	3
US: CBD ⩾8 mm	53	38	14	1	71
US: bile duct stone	7	4	3	0	57
Biliary colic	106	62	42	2	58

Table 5 Total predictive value of different positive predictive factors (PPF) for common bile duct stone

Factor	PPV %	NPV %	Sensitivity %	Specificity %
Hyperbilirubinaemia	73.3	73.6	54.3	86.6
Elevated ASAT/ALAT	65.4	91.9	91.3	67.2
Elevated GGT/ALP	60.3	97.1	97.5	56.3
Acute pancreatitis (AP)	72.0	73.5	22.2	96.2
AP in the anamnesis	20.0	57.2	4.9	86.5
Jaundice in the anamnesis	3.7	53.7	1.2	78.2
US: CBD ⩾8 mm	73.1	70.9	46.9	88.2
US: bile duct stone	57.1	60.1	4.9	97.5

A more realistic approach was to compare the predictive value in association with other factors. Table 6 demonstrates that the positive predictive value of the investigated factor was high in cases with (at least) two concurrently positive factors. The positive predictive value of two positive markers was 41-55%, again with the exception of pancreatitis or jaundice in the anamnesis.

Table 6 Predictive value of positive predictive factors (PPF) for CBD stones and effect of associated other factors, *n* (%)

Factor	Alone	One further factor	Two or more further factors
Hyperbilirubinaemia	0/3	1/5 (20)	43/53 (81)
Elevated ASAT/ALAT	1/11 (9)	13/32 (41)	60/73 (82)
Elevated GGT/ALP	1/24 (4)	16/35 (46)	62/75 (83)
Acute pancreatitis (AP)	-	0/3	18/23 (78)
AP in the anamnesis	1/12 (8)	0/3	3/5 (60)
Jaundice in the anamnesis	0/27	1/2 (50)	-
US: CBD ⩾8 mm	0/7	6/11 (55)	32/35 (91)
US: bile duct stone	0/1	-	4/6 (67)

The association between the number of positive factors and the presence of CBD stones is shown in Tables 7, 8. One factor alone was associated with a very low risk of CBD stone (1.2%). In patients with two, three and four or more positive factors, CBD stones were detected in 43.1%, 72.5% and 91.4% respectively. If we omitted history of jaundice and pancreatitis from the factors the corresponding data were 2.7% (1/41), 1.9% (1/54), 45.6% (23/48) and 82.3% (56/69) for patients with zero, one, two and three or more positive factors.

Table 7 Association between the number of positive predictive factors and ERCP findings (n = 206)

Number of positive factors	Number	Stone	Negative	Unsuccessful	%
1	84	1	80	3	1.2
2	46	19	25	2	43.1
3	40	29	11	0	72.5
⩾4	36	32	3	1	91.4

P<0.00001 for the whole group, P<0.00001, between group 1 and groups 2, 3, 4, group 2 and group 4, P = 0.008, between groups 2 and 3, P = 0.035, between groups 3 and 4.

Table 8 Predictive value of predictive factors according to the number of positive factors

Number of positive factors	Number	PPV %	NPV %	Sensitivity %	Specificity %
1	84	1.2	-	-	-
2	46	43.1	98.7	95.2	76.1
3	40	72.5	84.0	59.1	90.5
⩾4	36	91.4	72.0	40.2	98.4

P<0.00001 for the whole group, P<0.00001, between group 1 and groups 2, 3, 4 and group 2 and group 4, P = 0.008, between groups 2 and 3, P = 0.035, between groups 3 and 4.

DISCUSSION

Although laparoscopic cholecystectomy has become the treatment of choice for cholelithiasis, the treatment of coexisting cholecysto-choledocho-lithiasis is still controversial[1,3,8,10,15,17]. The surgical management of CBD stones requires a skilled laparoscopic surgeon and the options of management include conversion to open CBD exploration, intraoperative or postoperative ERC. In contrast, no single non-invasive method is sensitive and/or specific enough to predict the presence of CBD stones. Individual findings are less important than the overall clinical presentation.

A number of methods have been used for the diagnosis of CBDS, including new and improved radiological techniques. However some of them are invasive, more expensive and require special equipment. A major advantage of ERCP is that it could also offer a therapeutic possibility. Approximately 90-95% of CBDS could be managed endoscopically[1,23], but it is expensive, technically demanding and is associated with small but significant morbidity.

The question is whether preoperative ERCP should be routinely indicated or whether it should be kept for selected cases only. Most of the studies concluded that routine preoperative ERCP was not indicated[1,20,24]. One of the earliest studies is the well-known study from Neuhaus *et al.*[24]. They performed routine preoperative ERCP in 288 prospective patients prior to LC. The rate of successful cannulation was 91.7%, and normal anatomy was found in 86%. CBDS were proved in 29 patients (11%), the stone was asymptomatic in 9 patients. Endoscopic sphincterotomy was performed in all cases and the stones were extracted in all but three patients. One additional patient was operated due to complications. In concordance with the reported rate of 6-13.2% in other studies[1,14,20], coexisting cholecysto-choledocho-lithiasis was found in 6.5% of our LC patients (81 cases by preoperative ERCP).

The aim of this and previous studies was to determine a precise and easily applicable selection of clinical, biochemical and US criteria, which would enable the identification of patients with low risk of CBD stones (without the necessity for invasive procedures), and with higher risk of CBD stones who should undergo further preoperative investigation. The selection of patients was difficult. CBD stones were more common in patients with symptoms (e.g. jaundice, cholangitis, pancreatitis) and laboratory alterations including elevated serum bilirubin and liver function test. However, 8-10% of gallstone patients might have asymptomatic ductal stones[3,25,26].

The positive predictive value of laboratory data for CBD stones was found to be 60-87% in various studies[26,27]. In our study it was 57.1-73.3% in univariate analysis. However in most of the cases they were not individual parameters. In concordance with previous studies we could not identify jaundice and pancreatitis in the anamnesis as a predictor variable.

Traditional abdominal US is a valuable diagnostic tool. Although it is less sensitive (20-30%) in the detection of ductal gallstones, it provides important additional information about the degree of dilation of the bile ducts. The sensitivity of iv. cholangiography is also relatively low, moreover, it is associated with a severe risk of side effects. However, due to new non-ionic radiocontrast agents and radiological techniques, more and more research groups have started to routinely apply this technique again with improving results[3]. Laparoscopic intraoperative cholangiography is a useful and reliable method, although its indication remains debated[10,28]. The sensitivity of traditional CT is similar to that of US, but 3D helical techniques could offer an accuracy comparable to that of MRCP[29]. MRCP and endoscopic US could approach the diagnostic value of ERCP[14,15,30].

None of the aforementioned and analyzed factors is fit for the prediction of bile duct stones with sufficient certainty by itself. A combination of the prognostic factors is routinely applied. Several authors have constructed complicated scoring systems[16,23,27]. However, most of these systems require highly specific and sophisticated softwares, and no universally accepted system exists. More practical is the use of suggested clinical scores based on routine clinical data (jaundice, pancreatitis, liver function tests, ductal dilation and/or stones in the choledochus on US) in everyday practice[17,20]. Some authors also included the presence of small gallstones, old age and gender.

In concordance with our study, in the different studies based on large patient populations, CBDS/ductal stones or other pathologic deviations were found in 40-60% of ERCP cases performed on selected/restricted indications[1,16,18,20]. Based on the prognostic factors, patients were usually divided into low,

medium and high-risk CBD stone groups.

Peter Cotton[31] has presented his guidelines in the American Journal of Surgery. In his opinion the main constituents of the indications of preoperative ERCP were the following: positive predictive factors for CBD stones, the expertise of the endoscopist, and the pressure for laparoscopic intervention as opposed to open surgery. In concordance with our suggestion, he identified low, medium and high-risk patients for CBD stones based on the anamnesis, liver function tests, and ductal dilation on US. According to his conclusions, preoperative ERCP was not indicated for low-risk patients, while it must absolutely be performed in the high-risk group. As for the medium risk group, seemingly paradoxically, preoperative ERCP was only indicated, if the local endoscopist was mediocre. With an experienced endoscopist, preoperative intervention should be avoided, ERCP is to be performed only after the surgery, if the need arises.

Rieger *et al*.[26] found CBD stones in 56 patients (53%) of the 106 ERCP performed in combination with 1140 LC. More than two-fold elevation in any liver function test, multiple abnormal laboratory tests, stones in the biliary tract on US, a more than 7 mm, dilated ductus choledochus were taken as positive predicting factors for preoperative ERCP. The multi-center study of Welbourn *et al*.[32] in England also aimed to identify the exact indications of selective preoperative ERCP. The retrospective analysis of 306 preoperative ERC and 1396 LC showed that the predictive value of jaundice was 75%, that of pancreatitis 56%, while the predictive value of pathologic US or liver function tests was 48 %. In a prospective study of Sarli *et al*.[3], 74 symptom-free, CBD stone patient data were evaluated. Positive US, biliary colic, elevated serum aminotransferase and alkaline phosphatase levels and the presence of multiple, smaller stones were associated with a higher risk, while acute cholecystitis and non-specific upper gastrointestinal complaints were associated with a lower risk. In our study jaundice, elevated LFTs and dilated choledochus or stones in the bile duct on US examination gave a similarly high positive predictive value in univariate analysis for bile duct stones.

In our opinion, the major shortcoming of the above studies is that they analyzed the effects of different predictive factors separately, which in accordance with our own findings, could easily result in misleading conclusions. Santucci *et al*.[33] and Geron *et al*.[7] came to the same conclusion, emphasizing the importance of the co-existence of several pathologic markers at the same time. Furthermore, the American Society for Gastrointestinal Endoscopy (ASGE) in its guideline[29] favors the establishment of the aforementioned risk categories based on "simple clinical" data, such as clinical picture, laboratory findings and US. Interestingly, it recommends intraoperative (during the laparoscopic cholecystectomy) cholangiography to be performed even in low-risk/negative patients, followed by laparoscopic or endoscopic postoperative intervention, if required. In the medium-risk group endosonography or MRCP is recommended as the method of choice or, if these are not available, ERCP. According to the guideline, ERCP should be the first (therapeutic) intervention for high-risk patients.

In Hungary, ERCP is performed on a relatively high level and is generally available. Among the new imaging techniques, the availability of MRCP and endosonography is still limited. At the same time, due to financing reasons, ERCP turns out to be more cost-effective. The accessibility of intraoperative laparoscopic imaging techniques is also limited.

In summary, based on the literature and our own results, the following duideline can be established about the indications of preoperative ERCP.

The possibility of CBD stones should be considered after the evaluation of clinical, laboratory and US findings. Zero or one positive predictive factor indicates low risk, while the risk is high if three or more factors are present. Two positive predictive factors suggest medium risk. In the low risk group preoperative ERCP is not recommended, LC is advisable without restrictions. In the high risk group the indication of preoperative ERCP is unambiguous. In the medium-risk population, preoperative ERCP is generally indicated. If available, MRCP can be a good alternative. In case of a highly qualified endoscopist, ERCP should be postponed until the surgery can be considered.

REFERENCES

1 **Sarli L,** Iusco DR, Roncoroni L. Preoperative endoscopic sphincterotomy and laparoscopic cholecystectomy for the management of cholecystocholedocholithiasis: 10-year experience. *World J Surg* 2003; **27**: 180-186

2 **Miller RE,** Kimmelstiel FM, Winkler WP. Mamagement of common bile stones in the era of laparoscopic cholecystectomy. *Am J Surg* 1995; **169**: 272-276

3 **Sarli L,** Costi R, Gobbi S, Sansebastiani G, Roncoroni L. Asymptomatic bile duct stones: selection criteria for intravenous cholangiography and / or endoscopic retrograde cholangiography prior to laparoscopic cholecystectomy. *Eur J Gastroenterol Hepatol* 2000; **12**: 1175-1180

4 **McEntee G,** Grace PA, Bouchier-Hayes D. Laparoscopic cholecystectomy and the common bile duct. *Br J Surg* 1991; **78**: 385-386

5 **Sahai AV,** Mauldin PD, Marsi V, Hawes RH, Hoffman BJ. Bile duct stones and laparoscopic cholecystectomy: a decision analysis to assess the roles of intraoperative cholangiography, EUS, and ERCP. *Gastrointest Endosc* 1999; **49**: 334-343

6 **Tian MG,** Shi WJ, Wen XY, Yu HW, Huo JS, Zhou DF. Outcome of gallbladder preservation in surgical management of primary bile duct stones. *World J Gastroenterol* 2003; **9**: 1871-1873

7 **Geron N,** Reshef R, Shiller M. The role of endoscopic retrograde cholangiopancreatography in the laparoscopic era. *Surg Endosc* 1999; **13**: 452-456

8 **Cuschieri A,** Lezoche E, Morino M, Croce E, Lacy A, Toouli J, Faggioni A, Ribeiro VM, Jakimowicz J, Visa J, Hanna GB. E.A. E.S. multicenter prospective randomized trial comparing two-stage vs single-stage management of patients with gallstone disease and ductal calculi. *Surg Endosc* 1999; **13**: 952-957

9 **Rhodes M,** Sussman L, Cohen L, Lewis MP. Randomised trial of laparoscopic exploration of common bile duct versus postoperative endoscopic retrograde cholangiography for common bile duct stones. *Lancet* 1998; **351**: 159-161

10 **Patel AP,** Lokey JS, Harris JB, Sticca RP, McGill ES, Arrillaga A, Miller RS, Kopelman TR. Current management of common bile duct stones in a teaching community hospital. *Am Surg* 2003; **69**: 555-560

11 **Enochsson L,** Lindberg B, Swahn F, Arnelo U. Intraoperative endoscopic retrograde cholangiopancreatography (ERCP) to remove common bile duct stones during routine laparoscopic cholecystectomy does not prolong hospitalization: a 2-year experience. *Surg Endosc* 2004; **17**: 2

12 **Urbach DR,** Khajanchee YS, Jobe BA, Standage BA, Hansen PD, Swanstrom LL. Cost-effective management of common bile stones. *Surg Endosc* 2001; **15**: 4-13

13 **Rodriguez-Gonzalez FJ,** Naranjo-Rodriguez A, Mata-Tapia I, Chicano-Gallardo M, Puente-Gutierrez JJ, Lopez-Vallejos P, Hervas-Molina AJ, de Dios-Vega JF. ERCP in patients 90 years of age and older. *Gastrointest Endosc* 2003; **58**: 220-225

14 **Napoleon B,** Dumortier J, Keriven-Souquet O, Pujol B, Ponchon T, Souquet JC. Do normal findings at biliary endoscopic ultrasonography obviate the need for endoscopic retrograde cholangiography in patients with suspicion of common bile duct stone? A prospective follow-up study of 238 patients. *Endoscopy* 2003; **35**: 411-415

15 **Kohut M,** Nowak A, Nowakowska-Dulawa E, Marek T, Kaczor R. Endosonography with linear array instead of endoscopic retrograde cholangiography as the diagnostic tool in patients with moderate suspicion of common bile duct stones. *World J Gastroenterol* 2003; **9**: 612-614

16 **Sharma SK,** Larson KA, Adler Z, Goldfarb MA. Role of endo-

scopic retrograde cholangiopancreatography in the management of suspected choledocholithiasis. *Surg Endosc* 2003; **17**: 868-871

17 **Rijna H,** Kemps WG, Eijsbouts Q, Meuwissen SG, Cuesta MA. Preoperative ERCP approach to common bile duct stones: results of a selective policy. *Dig Surg* 2000; **17**: 229-233

18 **Masci E,** Fanti L, Mariani A, Guerini S, Zuliani W, Baccari P, Giacomelli M, Tittobello A. Selection criteria for pre-operative endoscopic retrograde cholangiography and endoscopic-laparoscopic treatment of biliary stones. *Eur J Gastroenterol Hepatol* 1999; **11**: 781-784

19 **Hamy A,** Hennekinne S, Pessaux P, Lada P, Randriamananjo S, Lermite E, Boyer J, Arnaud JP. Endoscopic sphincterotomy prior to laparoscopic cholecystectomy for the treatment of cholelithiasis. *Surg Endosc* 2003; **17**: 872-875

20 **Charfare H,** Cheslyn-Curtis S. Selective cholangiography in 600 patients undergoing cholecystectomy with 5-year follow-up for residual bile duct stones. *Ann R Coll Surg Engl* 2003; **85**: 167-173

21 **Tanaka M,** Sada M, Eguchi T, Konomi H, Naritomi G, Takeda T, Ogawa Y, Chijiiwa K, Deenitchin GP. Comparison of routine and selective endoscopic retrograd cholangiography before laparoscopic cholecystectomy. *World J Surg* 1996; **20**: 267-271

22 **Abboud PA,** Malet PF, Berlin JA, Staroscik R, Cabana MD, Clarke JR, Shea JA, Schwartz JS, Williams SV. Predictors of common bile stones prior to cholecystectomy: a meta-analysis. *Gastrointest Endosc* 1996; **44**: 450-459

23 **Sahai AV,** Mauldin PD, Marsi V, Hawes RH, Hoffman BJ. Bile duct stones and laparoscopic cholecystectomy: a decision analysis to assess the roles of intraoperative cholangiography, EUS, and ERCP. *Gastrointest Endosc* 1999; **49**: 334-343

24 **Neuhaus H,** Feussner H, Ungeheuer A, Hoffmann W, Siewert JR, Classen M. Prospective evaluation of the use of endoscopic retrograde cholangiography prior to laparoscopic cholecystectomy. *Endoscopy* 1992; **24**: 745-749

25 **Fussi F**, inventors; Hepar Industries Inc., Assignee. Process for obtaining low molecular weight heparins endowed with elevated pharmacological properties, and product so obtained. *United States Patent* 1981; **281**: 108

26 **Rieger R,** Sulzbacher H, Woisetschlager R, Schrenk P, Wayand W. Selective use of ERCP in patients undergoing laparoscopic cholecystectomy. *World J Surg* 1994; **18**: 900-905

27 **Onken JE,** Brazer SR, Eisen GM, Williams DM, Bouras EP, DeLong ER, Long TT 3rd, Pancotto FS, Rhodes DL, Cotton PB. Predicting the presence of choledocholithiasis in patients with symptomatic cholelithiasis. *Am J Gastroenterol* 1996; **91**: 762-767

28 **van der Hul RL,** Plaisier PW, Hamming JF, Bruining HA. Detection and management of common bile duct stones in the era of laparoscopic cholecystectomy. *Scand J Gastroenterol* 1993; **28**: 929-933

29 **Eisen GM,** Dominitz JA, Faigel DO, Goldstein JL, Kalloo AN, Petersen BT, Raddawi HM, Ryan ME, Vargo JJ 3rd, Young HS, Fanelli RD, Hyman NH, Wheeler-Harbaugh J. American Society for Gastrointestinal Endoscopy. Standards of Practice Committee. An annotated algorithm for the evaluation of choledocholithiasis. *Gastrointest Endosc* 2001; **53**: 864-866

30 **Hintze RE,** Adler A, Veltzke W, Abou-Rebyeh H, Hammerstingl R, Vogl T, Felix R. Clinical significance of magnetic resonance cholangiopancreatography (MRCP) compared to endoscopic retrograde cholangiopancreatography (ERCP). *Endoscopy* 1997; **29**: 182-187

31 **Cotton PB.** Endoscopic retrograde cholangiopancreatography and laparoscopic cholecystectomy. *Am J Surg* 1993; **165**: 474-478

32 **Welbourn CR,** Mehta D, Armstrong CP, Gear MW, Eyre-Brook IA. Selective preoperative endoscopic retrograde cholangiography with sphincterotomy avoids bile duct exploration during laparoscopic cholecystectomy. *Gut* 1995; **37**: 576-579

33 **Santucci L,** Natalini G, Sarpi L, Fiorucci S, Solinas A, Morelli A. Selective endoscopic retrograde cholangiography and preoperative bile duct removal in patients scheduled for laparoscopic cholecystectomy: a prospective study. *Am J Gastroenterol* 1996; **91**: 1326-1330

Edited by Wang XL **Proofread by** Zhu LH and Xu FM

PO Box 2345, Beijing 100023, China
Fax: +86-10-85381893
E-mail: wjg@wjgnet.com www.wjgnet.com

World J Gastroenterol 2004;10(23):3500-3505
World Journal of Gastroenterology
Copyright © 2004 by The WJG Press ISSN 1007-9327

• CLINICAL RESEARCH •

Effect of integrated traditional Chinese and Western medicine on SARS: A review of clinical evidence

Ming-Ming Zhang, Xue-Mei Liu, Lin He

Ming-Ming Zhang, Chinese Evidence-Based Medicine Center, West China Hospital, Sichuan University, Chengdu 610041, Sichuan Province, China
Xue-Mei Liu, Editorial Department, Chinese Journal of Evidence-Based Medicine, Chinese Evidence-Based Medicine Center, West China Hospital, Sichuan University, Chengdu 610041, Sichuan Province, China
Lin He, Library of West China Hospital, Sichuan University, Chengdu 610041, Sichuan Province, China
Correspondence to: Mrs. Xue-Mei Liu, Editorial Department, Chinese Journal of Evidence-Based Medicine, Chinese Evidence-Based Medicine Center, West China Hospital, Sichuan University, Chengdu 610041, Sichuan Province, China. cochrane@mail.sc.cninfo.net
Telephone: +86-28-85422079 **Fax:** +86-28-85422253
Received: 2003-12-23 **Accepted:** 2004-02-08

Abstract

AIM: To assess the possible effect of integrated traditional Chinese and Western medicine on severe acute respiratory syndromes.

METHODS: The current available randomized controlled trials of integrated traditional Chinese and Western medicine on SARS were identified through systematically searching literature in any languages or any types of publications. Additional studies of gray literature were also collected. The quality of studies was evaluated by two investigators independently based largely on the quality criteria specified CONSORT. Statistical analysis of the results was performed using RevMan 4.2.0 software developed by the Cochrane Collaboration.

RESULTS: Six studies (n = 366) fulfilling the inclusion criteria were found, of which the quality of one study was graded as B, the remaining five were graded as C. Two studies were performed with meta-analysis, the other four studies existed some heterogeneity for which meta-analysis could not be performed, a significant effect on lung infiltrate absorption was found in the treatment groups of these two studies [RR 6.68, 95% CI (2.93, 15.24), P<0.01], there was no significant differences between the mortality [RR 0.86, 95% CI (0.22, 3.29), P = 0.82] and the average dosage of corticosteroid [WMD -39.65, 95% CI (-116.84, 37.54), P = 0.31]. The other three studies also showed significant differences in infiltrate absorption, including national drug No. 2. 3. 4 in combination with Western medicine [RR 5.45, 95% CI (1.54, 19.26)], compound formulas NO. 1 combined with Western medicine [WMD 0.24, 95% CI (0.02, 0.46)], compound formulas combined with Western medicine [RR 8.06, 95% CI (0.40, 163.21)]. Kangfeidian No.4 in combination with Western medicine had no significant effect on symptom improvement such as loss of dyspnea and cough [RR 1.50, 95%CI (0.41, 5.43)] and [RR 1.29, 95%CI (0.30, 5.43)].

CONCLUSION: Integrated traditional Chinese and Western medicines has some positive effects on lung infiltrate absorption in SARS patients, and is recommended as an adjunct treatment for SARS. However, its effect on SARS requires further careful study due to limited available randomized control trials.

Zhang MM, Liu XM, He L. Effect of integrated traditional Chinese and Western medicine on SARS: A review of clinical evidence. *World J Gastroenterol* 2004; 10(23): 3500-3505 http://www.wjgnet.com/1007-9327/10/3500.asp

INTRODUCTION

Severe acute respiratory syndromes (SARS) is a readily transmissible new disease emerged in the 21st century that imposes a threat to international health[1-3]. SARS is caused by a novel coronavirus, first identified in Hong Kong, United States of American and Germany. It is due to an infection with SARS associated coronavirus (SARS-CoV). The genome of SARS-CoV is 29 727 nucleotides in length and has 11 open reading frames, and its genome organization is similar to that of other coronaviruses[4-7], SARS is an acute respiratory illness with typical symptoms of fever, cough and difficult breathing. Besides, it may be associated with other symptoms, such as headache, muscular stiffness, myalgia, loss of appetite, malaise, chills, confusion, dizziness, rash, night sweat, nausea and diarrhea. SARS can be divided into 5 types and 4 stages. The 5 types are common type (typical type), mild type, severe type and more severe type. The four stages are potential stage (2-10 d), initial stage (1-7 d), developing stage (8-14 d), and recovery stage (1-14 d), which are classified based on the developing process of SARS patient conditions by the criteria of Western medicine. SARS can also be divided as initial stage (1-5 d), acute stage (3-10 d), critical stage (7-14 d) and recovery stage (10-18 d) based on the theory of traditional Chinese medicine[8-11].

SARS demonstrates dramatically the global havoc that its epidemic had broken out worldwide including mainland China, Taiwan, Hong Kong, Vietnam, Singapore, Macao, North American and Europe when the first case was found in Foshan city, Guangdong Province, China on November 16, 2002. Airborne droplets from SARS patients are the main transmission routes. Based on the data from WHO. SARS epidemic appears to have peaked and is on the wane [12,13]. A total of 916 SARS patients died in 8 422 cases and the mortality was about 11%. A total of 5 327 SARS patients occurred in mainland China and 349 of them died, the mortality was about 7%. A total of 1 755 SARS patients occurred in Hong Kong Special Administrative Region, China and 300 of them died, the mortality was about 17%. A total of 655 SARS patients occurred in Taiwan, China and 180 of them died, the mortality was 27%. The case fatality ratio was estimated to be less than 1% in persons aged 24 years or younger, 6% in persons aged 25 to 44 years, 15% in persons aged 45 to 64 years, and greater than 50% in persons aged 65 years and older[14,15].

Western medicine for SARS

The treatment of SARS involves multiple disciplines, and current recommendations are mainly based on the methods of Western medicine including aliment therapy, respiratory

auxiliary ventilation, anti-infection and glucocorticoid therapy. The effectiveness for SARS was limited especially in the first and recovery stages. For example, in severe cases, corticosteriods and ribavirin (antiviral medication) were used, however there was no evidence to support their general or routine use at this stage and to confirm the risks and benefits of Western medicine in the treatment of SARS. Selective therapies included the use of antiviral agents, immunopotentiators and Chinese herbs[8,9,11,15]

Chinese herbs in combination with western medicine for SARS

Traditional Chinese medicine (TCM) is a useful model for scientific therapies and has been practiced worldwide. Among the components of TCM, herbal agents possess complex biological activities. In the theory of TCM, herbs preparations might resolve toxin, eliminate pathological dampness, disperse the lung, invigorate the blood circulation and resolve the blood stasis, benefit Qi and nourish Yin[16,17]. Based on this principle, Chinese practitioners suspected that SARS was caused by pestilential toxin, one of the important characteristics of SARS. Nine traditional Chinese patent medicines are optimized for controlling different symptoms of SARS. Compared with the simple treatment of Western medicine, Chinese medicine in combination with Western medicine for SARS may have better effects in that it may reduce the adverse events induced by anti-biotic and anti-virus treatments and other complications, shorten fever period and hospital stay, promote lung infiltrate absorption and decrease damage to the lung[18-20]. The 5 kinds of herbs are Kangfeidian No.1,2,3[29,34], compound formula No.1[32], national drugs No.2,3,4[31], compound herbs[30], Kangfeidian No.4[33]. Unfortunately, no strong evidence is available to demonstrate the benefits and risks of Chinese herbs in combination with Western medicine for SARS.

This review evaluated the possible effect of Chinese herbs in combination with Western medicine for SARS, summarized randomized controlled trials (RCT) and methods of integrated traditional Chinese and Western medicine for SARS, as well as a recommendation for future research.

MATERIALS AND METHODS

Data collection

A comprehensive searching strategy was used to identify all current relevant RCTs regardless of languages or types of publication (published, unpublished, in press, and in progress). We searched MEDLINE for relevant trials (1966 to 2003), EMBASE (1980 to 2003), CBM (Chinese Biomedical Database, 1981 to 2003), Chinese Cochrane Centre Controlled Trial Register (up to 2003), Cochrane Controlled Trial Register in Cochrane Library (issues 1 to 4, 2003), Current Controlled Trials and The National Research Register. The search terms were: “severe acute respiratory syndrome”, “acute respiratory syndrome”, “randomized-controlled-trial”, “random allocation” “double blind method”, “single blind method”, placebo”, “herbs”, “Chinese medicinal” .

The references of relevant trials and reviews were identified and RCTs in the Database of Chinese Evidence-Based Medicine Center and in journals not included in this Database were manually searched. We also checked the citations of existing reviews and all studies identified by the above methods. The authors of identified literature and relevant specialists were contacted for additional information.

Types of studies and participants

Only randomized controlled trials of Chinese herbs in combination with Western medicine for SARS were included regardless of blinding, follow up, language or publication status. The followings were excluded such as clinical controlled trials of SARS patients that failed to allocate into either trial, control group, case study or animal experiments.

Only randomized controlled trials of Chinese herbs in combination with Western medicine for the diagnosis of SARS patients with standard criteria of WHO in 2003 were included. Moreover, those SARS patients complicated with other diseases such as diabetes, cardiovascular disease, hypertension, or cancers were also included. The suspected SARS patients and misdiagnosed patients were excluded.

Quality assessment

We screened the titles, abstracts, and keywords of every document retrieved to determine the quality of the papers. We retrieved the full articles for further assessment if the information given suggested that the study included diagnosed SARS patients; compared Chinese herbs in combination with Western medicine with placebo, Chinese herbs, Western medicine or any other active intervention; used random allocation to the comparison groups. Where differences in opinion existed, we would solve them through discussion. If we were unable to solve the disagreement through discussion, we would contact the authors for clarification.

The quality of each trial was assessed based largely on the quality criteria specified CONSORT[21]. In particular, the following factors were assessed[22,23] such as minimization of selection bias, minimization of performance bias, minimization of attrition bias, and minimization of detection bias. Based on these criteria, studies were subdivided into the following three categories[23]: low risk of bias which met all quality criteria graded as A. moderate risk of bias which met one or more of the quality criteria graded as B, high risk of bias which did not meet one or more criteria graded as C.

Statistical analysis

Data were extracted independently by two investigators with a standardized form and analyzed using RevMan 4.2.0 software developed by the Cochrane Collaboration[23,24]. Heterogeneity was tested using the *Z score* and *the Chi square*. Statistical significance was set at $P<0.05$. We performed a meta-analysis for the data. The dichotomous data expressed as relative risk (RR). The continuous data expressed as weighted mean difference (WMD). We calculated the overall results based on the random effect model.

Hypothesis

When data were pooled, we hypothesized that all Western medicine interventions used in control and trial groups had the same effect on all the outcome measures indexed in this review.

RESULTS

Studies identified

The initial searching using the electronic search strategy listed above and manual searching yielded 650 studies. After scanned, 48 studies of Chinese herbs in combination with Western medicine for SARS were identified to meet the inclusion criteria. Most of the studies were published in Chinese. Of the 48 studies, one study of clinical report on the suspected SARS patients was excluded upon further scrutiny and the other 28 case reports and 9 case control studies were identified. There were 10 RCT studies identified. Because of some reasons, we did not obtain the complete report of studies. Further exclusion included one study identified as randomized sample, but not randomization allocation[25], one study which compared Western medicine versus Western medicine for SARS[26] and the other two studies which were duplicate publication[27,28]. Finally, 6 RCT studies of Chinese herbs in combination with Western medicine fulfilling the inclusion criteria were identified[29-34].

Six studies (n = 366) were included[29-34]. The details of the designs of these studies are shown in Table 2. All six studies

were conducted in China. The median time of treatment was 17 d. Four studies reported the number of patients in common type and severe type[29-31,34]; two studies performed a meta-analysis, the data were sufficient in quality, and similar[29,34]. One study was Western medicine plus compound herbs[32]; the other three studies were about Western medicine plus national drugs 2,3,4[30-32] and Kangfeidian No.4[33]. The constituents and dosage of Chinese herbs varied. Most of the studies with the heterogeneity of intervention prevented us from doing a meta-analysis and a meaningful subgroup analysis on Chinese herbs.

Study methodology

Most of the included studies had poor quality ('C')[29-31,33,34] one study was graded as B[32] (Table 1).

All of the studies claimed as randomization, but none of them described the method of randomization in details, and none of the studies referred allocation concealment. Of the six studies, one described its design in detailed randomization process and the baseline data were reported adequately[32]. Two studies were described as stratified randomization[31,33] and the other three studies only mentioned 'randomization'[29,30,34]. Withdrawals and loss of follow-up were not reported in six studies and none of the studies reported intention-to-treat analysis.

No adverse events of Chinese herbs were observed in the included studies. Only one study reported the quality of life as result index[32]. The effect of integrated traditional Chinese medicine and Western medicine for SARS see Table 2.

Mortality

The mortality[29-31,34] was reported in 4 studies.

National drugs No. 2. 3. 4 in combination with Western medicine did not show a significant difference on mortality compared to simple Western medicine (RR 0 .41, 95% CI 0.04, 4.78).

Kangfeidian No. 1.2. 3 in combination with Western medicine was tested in two studies[29,34] which used the same dosage and treatment time and had the same outcome. Compared to simple Western medicine, there was no significant effect on mortality [RR 0.86, 95% CI (0.22, 3.29), $P = 0.82$, Table 3].

Table 1 Design of the RCTs of traditional Chinese medicine in combination with Western medicine for SARS

Study ID	Grade of method	Participants (case)				Trial interventions	Control interventions	Duration	Follow up	Main results
		Common type		Severe type						
Zhao CH 2003	C	51		26		Western medicine plus compound herbs of kangfeidian No.1,2,3.	Western medicine	14-21d	No	Mortality, lung infiltrate absorption, symptom improvement, dosage of glucocorticosteroids.
Wang BE 2003	C	Trial 13	Control 17	Trial 18	Control 12	Western medicine plus compound herbs.	Western medicine	10-20 d	No	Mortality, lung infiltrate absorption, Secondary infections, dosage of methypred nisolone, SO_2,
Wang RB 2003	C	Trial 5	Control 7	Trial 30	Control 23	Western medicine plus national drug No.2,3,4.	Western medicine	14 d	No	Mortality, lung infiltrate absorption, Secondary infections, symptom improvement
Jiang ZY 2003	B	40				Western medicine plus compound herbs No.1,2,3.	Western medicine	21 d or so	Yes	Lung infiltrate absorption, symptom improvement, quality of life
Zhang SN 2003	C	63				Western medicine plus kangfeidian No.4	Western medicine	7 d	No	Dose of glucocorticoid, lung infiltrate absorption, symptom improvement
Zhang XM 2003	C	Trial 7	Control 9	Trial 24	Control 23	Western medicine plus compound herbs of kangfeidian No.1,2,3.	Western medicine	21 d	No	Mortality, lung infiltrate absorption, symptom improvement, dose of glucocorticoid, length of fever

Table 2 Results of meta-analysis of integrated traditional Chinese and Western medicine for SARS at the end of treatment

Comparison or outcomes	Study	Participants			Statistical method	Effect estimate
		Total	Trial	Control		
National drugs No.2.3.4 combined with Western medicine versus Western medicine						
Mortality	Wang RB 2003	65	1/35	2/30	RR (fixed) 95%	0.41 (0.04, 4.78)
Lung infiltrate absorption		53	25/30	11/23		5.45 (1.54, 19.26)
The secondary infection		65	4/35	7/30		0.42 (0.11, 1.62)
Compound formulas No.1 combined with Western medicine versus Western medicine						
Symptom improvement integral	Jiang ZY 2003	40	7.90 (5.81)	6.50 (3.83)	WMD (fixed) 95%	1.40 (-1.65, 4.45)
Lung infiltrate absorption		40	0.65 (0.35)	0.38 (0.37)		0.24 (0.02, 0.46)
Quality of life integral		40	19.93 (3.69)	22.10 (4.90)		-2.17 (-4.86, 0.52)
Compound formulas combined with Western medicine versus Western medicine						
Lung infiltrate absorption	Wang BN 2003	59	30/30	26/29	RR (fixed) 95%	8.06 (0.40, 163.21)
Kangfeidian No.4 combined with Western medicine versus Western medicine						
Loss of dyspnea	Zhang SN 2003	38	12/20	9/18	RR (fixed) 95%	1.50 (0.41, 5.43)
Loss of cough		30	9/16	7/14		1.29 (0.30, 5.43)

Table 3 Effect of Kangfeidian No.1,2, 3 with Western medicine in SARS patients

Outcome measure		Kangfeidian No.1, 2, 3 combined with Western medicine	Western medicine alone	Relative risk (95% CI)	*P*	Reference
Mortality		(n/N)				
		4/31	4/32	1.04 (0.24, 4.57)		Zhang XM *et al.*
		0/37	1/39	0.34 (0.01, 8.67)		(2003)
	Overall	4/68	5/71	0.86 (0.22, 3.29)	0.82	
Lung infiltrate		27/31	18/32	5.25 (1.49, 18.53)		Zhao CH *et al.*
Absorbing		22/37	6/39	8.07 (2.71, 23.98)		(2003)
	Overall	49/68	24/71	6.68 (2.93, 15.24)	<0.00001	Zhao CH *et al.*
The average		N (mean±SD)		WMD(95% CI)		(2003)
Dosage of						
Glucocrticosteroids		31 (304.13±143.42)	32 (347.40±173.10)	-43.2 7(-121.67, 35.13)		Zhang XM *et al.*
		15 (1 400.00±685.00)	20 (1 325.00±623.00)	75.00 (-366.27, 516.27)		(2003)
						Zhao CH *et al.*
						(2003)
	Overall	46	52	-39.65 (-116.84, 37.54)	0.31	

Lung infiltrate absorption

Six studies reported the effect of Chinese herbs in combination with Western medicine on the lung infiltrate absorption[29,34]. Of the six studies, three reported that Chinese herbs in combination with Western medicine had a better effect than simple Western medicine[29,31,34].

National drugs No. 2. 3. 4 in combination with Western medicine[31] showed a significant difference in lung infiltrate absorption [RR 5.45, 95% CI (1.54, 19.26)]. Kangfeidian No. 1. 2. 3 in combination with Western medicine[29,34] showed a better positive effect on lung infiltrate absorption [RR 6.68, 95% CI (2.93, 15.24), $P<0.01$] (Table 3). In the original study[34], $n = 31$ in treatment group, $n = 32$ in control group, 21 d after treatment with Kangfeidian No. 1. 2. 3 in combination with Western medicine, symptoms were improved by 87% in treatment group, and 56% in control group. In the original study, $n = 77$[29], it was reported that the lung infiltrate absorption was less two days in treatment group. In treatment group $n = 22$, the basic absorption time (16±8.8 d) and in control group $n = 6$, the basic absorption time (18.4±8.2 d).

Compound formulas No 1. in combination with Western medicine[32] showed no significant difference in lung infiltrate absorption between treatment group and control group [WMD 0.24, 95% CI (0.02, 0.46)]. Compound formulas in combination with Western medicine[31] showed a positive effect on lung infiltrate absorption [RR 8.06, 95% CI (0.40, 163.21)].

Dosage of glucocorticosteroids

Kangfeidian No. 1. 2. 3 in combination with Western medicine versus Western medicine[29,34] for SARS showed no significant effect on the treatment group [WMD -39.65, 95% CI (-116.84, 37.54) $P = 0.31$] (Table 3).

Additional results

Kangfeidian No 4 combined with Western medicine versus Western medicine[33] showed no significant effects on loss of dyspnea [RR 1.50, 95% CI (0.41, 5.43)] and loss of cough [RR 1.29, 95% CI (0.30, 5.43)] (Table 3).

DISCUSSION

Standard treatment and outcome index

To assess accurately any potential benefits and risks in the treatment of SARS, treatment of Chinese herbs must be scientifically evaluated. Standard treatment and outcome index need to be developed, based on the principles used by the Chinese herb practitioners. For example, criteria for the dosage and components of compound herbs, duration of treatment, withdrawal and follow up, treatment protocols should be adjusted according to the conditions of patients[35,36]. In the six

studies, none of them were standardized and one study described not any details on the dosage and components of compound herbs[33]. Principal criteria for outcome index are another important issue to be taken into account, such as mortality, symptom improvement, lung infiltrate absorption, quality of life and adverse events. The six studies varied in outcome index.

Treatments to be tested should be selected and standardized so that potentially effective and important treatments are evaluated first. The best evidence should be systematically reviewed, summarized, and disseminated, which in turn would lead to evidence-based decision making in traditional Chinese medicine.

Long term studies

Most of the current studies had a short duration, ranging from 7 to 21 d and a small sample size. All studies did not report data on compliance and follow up. As a new kind of respiratory disease many unknown factors remain to be solved. SARS is likely to require a longer period of follow-up. Based on the current investigation, Chinese herbs may also be considered as an adjuvant treatment to improve the quality of life. Meanwhile, whether herbs have any toxic effects should also be considered and attention should be paid to their long-term adverse events. For example, adverse events should be monitored by a standardized effective reporting system in clinical trials and some severe adverse events should also be studied or observed by epidemiological studies.

Adequate randomization method

SARS is a sudden outbreak disease. It is somewhat difficulty for us to conduct RCT, particularly in acute or critical stage. The current six RCTs conducted suggest that it is a promising work. However, a well designed RCT requires a thorough understanding of randomization so that better research results could be achieved.

Randomization includes 3 important steps: namely sequence generation, allocation concealment and randomization implementation[37]. Sequence generation is a method used to generate the random allocation sequence, including details of any restriction. Allocation concealment is to implement the random allocation sequence. Randomization implementation is to generate the allocation sequence. Well designed RCTs are required to evaluate Chinese herbs combined with Western medicine versus Western medicine.

REFERENCES

1 WHO. Severe acute respiratory syndrome (SARS): Status of the outbreak and lessons for the immediate future. *Geneva World Health Organization* 20 May 2003. Available from: URL: http://www.who.int/csr/media/en/sars_wha.pdf

2 **Chan-Yeung M,** Ooi GC, Hui DS, Ho PL, Tsang KW. Severe acute respiratory syndrome. *Int J Tuberc Lung Dis* 2003; **7**: 1117-1130

3 **Marra MA,** Jones SJ, Astell CR, Holt RA, Brooks-Wilson A, Butterfield YS, Khattra J, Asano JK, Barber SA, Chan SY, Cloutier A, Coughlin SM, Freeman D, Girn N, Griffith OL, Leach SR, Mayo M, McDonald H, Montgomery SB, Pandoh PK, Petrescu AS, Robertson AG, Schein JE, Siddiqui A, Smailus DE, Stott JM, Yang GS, Plummer F, Andonov A, Artsob H, Bastien N, Bernard K, Booth TF, Bowness D, Czub M, Drebot M, Fernando L, Flick R, Garbutt M, Gray M, Grolla A, Jones S, Feldmann H, Meyers A, Kabani A, Li Y, Normand S, Stroher U, Tipples GA, Tyler S, Vogrig R, Ward D, Watson B, Brunham RC, Krajden M, Petric M, Skowronski DM, Upton C, Roper RL. The Genome sequence of the SARS-associated coronavirus. *Science* 2003; **300**: 1399-1404

4 **Rota PA,** Oberste MS, Monroe SS, Nix WA, Campagnoli R, Icenogle JP, Penaranda S, Bankamp B, Maher K, Chen MH, Tong S, Tamin A, Lowe L, Frace M, DeRisi JL, Chen Q, Wang D, Erdman DD, Peret TC, Burns C, Ksiazek TG, Rollin PE, Sanchez A, Liffick S, Holloway B, Limor J, McCaustland K, Olsen-Rasmussen M, Fouchier R, Gunther S, Osterhaus AD, Drosten C, Pallansch MA, Anderson LJ, Bellini WJ. Characterization of a novel coronavirus associated with severe acute respiratory syndrome. *Science* 2003; **300**: 1394-1399

5 **Peiris JS,** Lai ST, Poon LL, Guan Y, Yam LY, Lim W, Nicholls J, Yee WK, Yan WW, Cheung MT, Cheng VC, Chan KH, Tsang DN, Yung RW, Ng TK, Yuen KY. Coronavirus as a possible cause of severe acute respiratory syndrome. *Lancet* 2003; **361**: 1319-1325

6 **Drosten C,** Gunther S, Preiser W, van der Werf S, Brodt HR, Becker S, Rabenau H, Panning M, Kolesnikova L, Fouchier RA, Berger A, Burguiere AM, Cinatl J, Eickmann M, Escriou N, Grywna K, Kramme S, Manuguerra JC, Muller S, Rickerts V, Sturmer M, Vieth S, Klenk HD, Osterhaus AD, Schmitz H, Doerr HW. Identification of a novel coronavirus in patients with severe acute respiratory syndrome. *N Engl J Med* 2003; **348**: 1967-1976

7 **Huang GH,** Feng YL. SARS diagnosis and therapy. *Zhongguo Huxi Yu Weizhong Jianhu Zazhi* 2003; **2**: 153-158

8 **Xu XY,** Wang GF, Lu HY, Li HC, Huo N, Wang J, Nie LG, Que XL. The stage of SARS and the experience of SARS. *Beijing Daxue Xuebao* 2003; **5**(Suppl): 5-6

9 SARS preventive and treatment protocol by TCM. *Tianjin Zhongyiyao Feidian Zhuanji* 2003; **20**: 106-107

10 **Zhong LS.** Diagnosis and treatment protocol for SARS. *Zhonghua Yixue Zazhi* 2003; **83**: 1731-1752

11 **Nie HQ,** Luo XD, Zhang JZ, Su Q. Current status of severe acute respirator syndrome in China. *World l Gastroenterol* 2003; **9**: 1635-1645

12 **Drazen JM.** SARS-looking back over the first 100 days. *N Engl J Med* 2003; **349**: 319-320

13 WHO. Summary table of SARS cases by country, 1 November 2002-7August 2003. Available from:URL:http://www.who.int/csr/sars/country/en/country2003_08_15.pdf.

14 WHO. Cumulative number of reported probable cases of SARS. Available from: URL: http://www.who.int/csr/sars/country/2003_06_25/en/

15 **Liu P,** Cao Y, Qiao X. Clinical study on shenmai injection in promoting postoperative recovery in patients of breast cancer. *Zhongguo Zhongxiyi Jiehe Zazhi* 2000; **20**: 328-329

16 **Cohen I,** Tagliaferri M, Tripathy D. Traditional Chinese medicine in the treatment of breast cancer. *Semin Oncol* 2002; **29**: 563-574

17 **Li XH,** Zhang K, Hu JH, Guo XH, Hu ZJ, Yang Y, Liang LC. Clinical evaluation of the integrated traditional Chinese medicine with western medicine on treatment of severe acute respiratory syndrome (SARS). *Proceedings International Science Symposium SARS* 2003: 125-130

18 **Hai X.** Clinical experience of treating SARS in Guangdong hospital of TCM. *Tianjin Zhongyiyao Feidian Zhuanji* 2003; **20**: 24-25

19 **Xiao PG,** Wang YY, Cheng HS. Some research clues on Chinese herbal medicine for SARS prevention and treatment. *Zhongguo Zhongyao Zazhi* 2003; **28**: 481-483

20 **Xiao XH,** Wang JB, He CS. On the rational exertion for the prescriptions and drugs of TCM in prevention and treating SARS. *Zhongguo Zhongyao Zazhi* 2003; **28**: 664-668

21 **Moher D,** Schulz KF, Altman D. The CONSORT statement: revised recommendations for improving the quality of reports of parallel-group randomized trials. *JAMA* 2001; **285**: 1987-1991

22 **Schulz KF,** Chalmers I, Hayes RJ, Altman DG. Empirical evidence of bias. Dimensions of methodological quality associated with estimates of treatment effects in controlled trials. *JAMA* 1995; **273**: 408-412

23 **Clarke M,** Oxman AD, editors, Cochrane Reviewers' Handbook 4.2 In: Review Manager (RevMan) [Computer program]. Version 4.2. Oxford, England: *The Cochrane Collaboration*, updated June 2000

24 **Egger M,** Davey Smith G, Schneider M, Minder C. Bias in meta-analysis detected by a simple graphical test. *BMJ* 1997; **315**: 629-634

25 **Kang J.** The experience of treatment and preventing SARS by traditional Chinese integrated western medicine. Symposium on treating SARS by integrated traditional Chinese and western medicine from five provinces in north China and Guangdong

province. Hosted by Chinese association for science & technology, Held by Chinese association of the integration of traditional and western medicine. *Beijing China* 2003: 39-41

26 **Zhao ZW,** Zhang FC, Xu M, Huang K, Zhong WL, Cai WP, Yin ZB, Huang SD, Deng ZB, Wei M. Clinical analysis of 190 cases of outbreak with atypical pneumonia in Guangzhou in spring 2003. *Zhonghua Yixue Zazhi* 2003; **83**: 713-719

27 **Wang RB,** Liu JM, Jian YY, Wu YZ, Wang XJ, Xu DZ. Traditional Chinese medicine treatment of 11 SARS cases. *Beijing Zhongyiyao Zazhi* 2003; **22**: 8-9

28 **Wang RB,** Liu JM, Wu YZ, Jiang YY, Wang XJ, Chi PP, Sun FX. Therapeutic effects of integrative traditional Chinese medicine and western medicine for SARS. *Proceedings international Sciences Symposium SARS* 2003: 293-297

29 **Zhao CH,** Li XH, Zhang K, Jing RH, Gou CY, Hu ZJ, Ye J, Yang Y, Guo XH, Liang LC, Hu JH, Li XM, Wu JS. Randomized control study of integrative traditional Chinese and western medicine in the treatment of 77 patients. *Zhongguo Zhongxiyi Jiehe Jijou Zazhi* 2003; **10**: 197-200

30 **Wang BE,** Zhang SW, Ren AM. Integrated traditional Chinese and western medicine for SARS. Symposium on treating SARS by integrated traditional Chinese and western medicine from five provinces in north China and Guangdong province. Hosted by Chinese association for science & technology, Held by Chinese association of the integration of traditional and western medicine. *Beijing China:* 2003: 50-52

31 **Wang RB,** Liu JM, Jiang YY, Wu YZ, Wang XJ, Chi PP, Sun FX. Preliminary study on clinical efficacy of integrative Chinese and western medicine in treating severe acute respiratory syndrome. *Zhongguo Zhongxiyi Jiehe Zazhi* 2003; **23**: 492-493

32 **Jiang ZY,** Tang XD, Qi WS, Bian YJ, Song QQ, Zhang ZZ, Li CX, Fu YL, Wang YH, Xiang XP, Wang RB, Chen YF, Liu BY, Xie YM. Clinical efficacy evaluation of TCM for convalescent patients with SARS Symposium on treating SARS by integrated traditional Chinese and western medicine from five provinces in north China and Guangdong province. Beijing China: Chinese association for science & technology, Chinese association of the integration of traditional and western medicine, June 2003: 41-54

33 **Zhang SL.** The clinical effect and character of traditional Chinese medicine integrated western medicine for lung fibrosis induced by SARS. *Chinese General Practice* 2003; **6**: 576-577

34 **Zhang XM,** Zhang YL, Yang ZF, Jin YW, Tang XH, Zhang Y, Feng GL, Ma YM, Yang YK, Wang MY, He YH, Zhang Y, Liu XS, Wang YL, Jin ZA, Lin Q, Liu WN. Clinical effective of serial SARS formula for SARS. *Zhongguo Yiyao Xuebao* 2003; **18**: 323-325

35 **Lin L,** Han Y, Yang ZM. Clinical observation on 103 patients of severe acute respiratory syndrome treated by integrative traditional Chinese and Western Medicine. *Zhongguo Zhongxiyi Jiehe Zazhi* 2003; **23**: 409-413

36 Integrative Chinese medicine and western medicine for SARS. *Zhongguo Zhongxiyi Jiehe Zazhi* 2003; **23**: 484-485

37 **Zheng SP.** Principle and method of clinical research design In: Wang JL. Clinical epidemiology-clinical research design and review. 2nd ed. Shanghai: *Shanghai Science Press* 2001: 47-59

Edited by Wang XL and Ren SY **Proofread by** Xu FM

PO Box 2345, Beijing 100023, China
Fax: +86-10-85381893
E-mail: wjg@wjgnet.com www.wjgnet.com

World J Gastroenterol 2004;10(23):3506-3510
World Journal of Gastroenterology
Copyright © 2004 by The WJG Press ISSN 1007-9327

• CLINICAL RESEARCH •

HDR-^{192}Ir intraluminal brachytherapy in treatment of malignant obstructive jaundice

Yi Chen, Xiao-Lin Wang, Zhi-Ping Yan, Jie-Min Cheng, Jian-Hua Wang, Gao-Quan Gong, Sheng Qian, Jian-Jun Luo, Qing-Xin Liu

Yi Chen, Xiao-Lin Wang, Zhi-Ping Yan, Jie-Min Cheng, Jian-Hua Wang, Gao-Quan Gong, Sheng Qian, Jian-Jun Luo, Qing-Xin Liu, Department of Radiology, Affiliated Zhongshan Hospital, Medical Center of Fudan University, Shanghai 200032, China
Correspondence to: Dr. Yi Chen, Department of Radiology, Affiliated Zhongshan Hospital, Medical Center of Fudan University, 180 Fenglin Road, Shanghai 200032, China
Telephone: +86-21-64041990 Ext. 2533
Received: 2004-01-10 **Accepted:** 2004-03-24

Abstract

AIM: To determine the feasibility and safety of intraluminal brachytherapy in treatment of malignant obstructive jaundice (MOJ) and to evaluate the clinical effect of intraluminal brachytherapy on stent patency and patient survival.

METHODS: Thirty-four patients with MOJ were included in this study. Having biliary stent placed, all patients were classified into intraluminal brachytherapy group (group A, n = 14) and control group (group B, n = 20) according to their own choice. Intraluminal brachytherapy regimen included: HDR-^{192}Ir was used in the therapy, fractional doses of 4-7 Gy were given every 3-6 d for 3-4 times, and standard points were established at 0.5-1.0 cm. Some patients of both groups received transcatheter arterial chemoembolization (TACE) after stent placement.

RESULTS: In group A, the success rate of intraluminal brachytherapy was 98.0%, RTOG grade 1 acute radiation morbidity occurred in 3 patients, RTOG/EORTC grade 1 late radiation morbidity occurred in 1 patient. Mean stent patency of group A (12.6 mo) was significantly longer than that of group B (8.3 mo) (P<0.05). There was no significant difference in the mean survival (9.4 mo *vs* 6.0 mo) between the two groups.

CONCLUSION: HDR-^{192}Ir intraluminal brachytherapy is a safe palliative therapy in treating MOJ, and it may prolong stent patency and has the potentiality of extending survival of patients with MOJ.

Chen Y, Wang XL, Yan ZP, Cheng JM, Wang JH, Gong GQ, Qian S, Luo JJ, Liu QX. HDR-^{192}Ir intraluminal brachytherapy in treatment of malignant obstructive jaundice. *World J Gastroenterol* 2004; 10(23): 3506-3510
http://www.wjgnet.com/1007-9327/10/3506.asp

INTRODUCTION

Self-expanding metal stent, due to its minimal invasion, low risk of migration and efficient bile drainage, has been widely used for management of malignant obstructive jaundice (MOJ)[1-11]. Although self-expanding metal stent seems to be the first choice in the palliation of MOJ, high rates of stent occlusion, which were mainly caused by tumor ingrowth or overgrowth, usually lead to jaundice recurrence[12,13]. Therefore, treating underlying malignancy is critical to extend stent patency and patient survival. Intraluminal brachytherapy is characterized by superiority in treatment of ductal or periductal tumor, thus preventing tumor from invading or compressing the duct. We designed a prospective study to evaluate the feasibility, safety of intraluminal brachytherapy in the treatment of MOJ and the clinical effect of intraluminal brachytherapy on stent patency and survival of patients.

MATERIALS AND METHODS

Study design

Patients were selected among those admitted to our department between November 2001 and September 2002 with the diagnosis of MOJ. Patients who had percutaneous transhepatic cholangiography and drainage (PTCD) followed by stent placement were included. Exclusion criteria were: (1) patients who were in end-stage MOJ; (2) serum total bilirubin concentration decreased to less than 100 μmol/L or 50% of that before PTCD. After the nature of intraluminal brachytherapy was fully explained, patients were classified into two groups: group A with intraluminal brachytherapy and group B without intraluminal brachytherapy as control group, according to their own choice whether to receive the therapy. The study was performed with the approval of the institutional ethics committees. Written informed consent was obtained from all patients before treatment.

Methods of treatment

Venous blood samples were taken 1-3 d before PTCD for biochemical test. Intraluminal brachytherapy was routinely performed in group A within 1-3 wk after stent placement. Patients in group B did not receive the therapy. Some patients in both groups underwent transcatheter arterial chemoembolization (TACE).

Intraluminal brachytherapy: After stent placement, a 10 F external-internal drainage catheter or a 7 F long vascular sheath was placed, with its distal tip across the stricture. The applicator and sham source were placed through the drainage catheter or the sheath as a whole under fluoroscopic guidance. Irradiated volume was customized to extend 1 cm proximal and distal to the maximum length of the stricture as determined by cholangiography. Dwell positions were recorded, and therapy planning system (TPS) was connected to the remote afterloading microSelectron (Nuclectron. Holland). After the sham source was manually removed, HDR-^{192}Ir (111-370 GBq) was driven by the remote afterloading system to the programmed locations (Figure 1). Fractional dose of 4-7 Gy was prescribed 0.5-1 cm from the source axis. The procedure was performed 3-4 times with an interval of 3-6 d. The drainage catheter or sheath was removed 1 wk later in case there were no complications related to the procedure.

Follow-up

The acute morbidity scoring criteria by Radiation Therapy Oncology Group (RTOG) and the late morbidity scoring criteria by Radiation Therapy Oncology Group/European Organization for Research and Treatment of Cancer (RTOG/EORTC) were used to evaluate the radiation toxicity[14]. Follow-up of each patient was based on outpatient examinations, telephone interviews, and questionnaires.

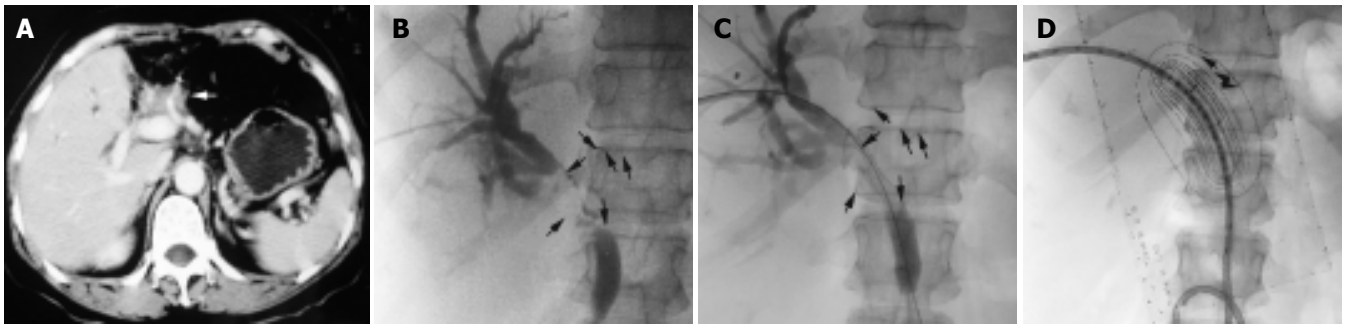

Figure 1 HDR-^{192}Ir (111-370 GBq) driven to the programmed locations. A: In the patient who had undergone left-lobe resection due to cholangiocarcinoma, hilar recurrence with bile duct dilation was shown by portal-phase CT scan (arrow). B: The stricture of bile duct was clearly shown by cholangiography during PTCD (arrow). C: An 8 mm×60 mm SMART stent was deployed across the stricture. D: The applicator and sham source were inserted though a 10 F internal-external drainage catheter. The dose distribution curves were obtained from the TPS (arrow).

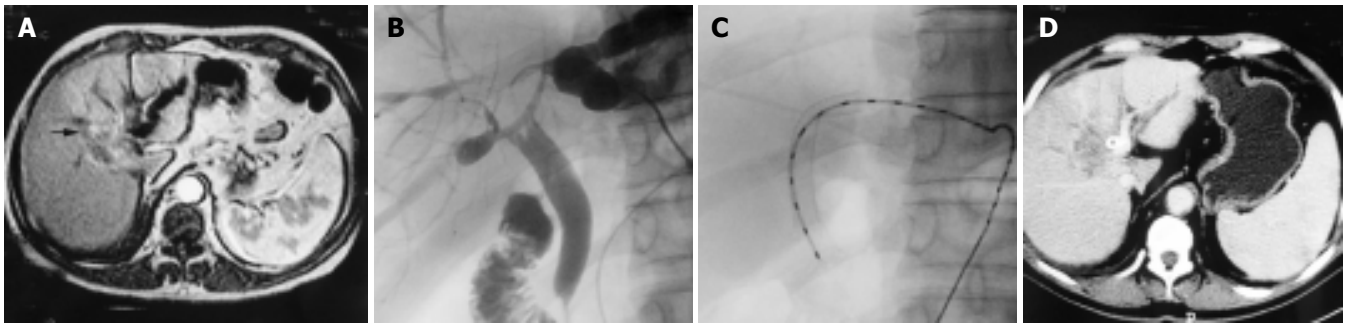

Figure 2 Cholangiography, CT, or US before and after intraluminal brachytherapy. A: Bile duct dilation of left lobe caused by cholangiocarcinoma was shown by CT (arrow). B: Cholangiography showed hilar stricture (arrow). C: Intraluminal brachytherapy (fractional dose 7 Gy, total dose 21 Gy) was performed after an 8 mm×60 mm SMART stent insertion. D: CT follow-up 11 mo after intraluminal brachytherapy showed no progress of the tumor and no redilation of the bile duct (arrow).

In this study, stent patency period was defined as the interval between stent placement and obstructive jaundice recurrence. If occlusion did not occur during a patient's life time, the patency period was considered equal to the survival period but censored. Jaundice recurrence was defined as the symptom of jaundice recurred after it had subsided and met one of the followings: (1) cholangiography, CT or US demonstrated redilation of bile duct, (2) combined serum bilirubin concentration/total serum bilirubin concentration $\geqslant$35% (Figure 2).

Statistical analysis

Comparisons between the two groups were performed with paired-samples *t* tests for metric data and χ^2 tests for frequencies. Stent patency and survival were evaluated according to the Kaplan-Meier method and compared with the log rank test. For all tests, a *P* value less than 0.05 was considered statistically significant.

RESULTS

Baseline data of patients

A total of 34 patients were enrolled in this study (18 male and 16 female; age range, 41-87 years; mean age, 62.0 years). Thirty-seven SMART stents (Cordis. Johnson & Johnson. USA) were placed and 28 TACE procedures were performed in these patients, 14 patients underwent intraluminal brachytherapy. In group A (n = 14), the causes of obstruction were cholangiocarcinoma (n = 7), gallbladder carcinoma (n = 2) and metastatic lymphadenopathy (n = 5, from stomach, colorectum or breast). In group B (n = 20), the causes of obstruction were cholangiocarcinoma (n = 9), gallbladder carcinoma (n = 2) and metastatic lymphadenopathy (n = 9, from stomach, colorectum or breast). The diagnosis was based on clinical, radiological findings or histology. There were no differences between the two groups according to gender, mean age, preoperative serum bilirubin, alanine aminotransferase, alkaline phosphatase, albumin, hemoglobin concentration, obstructive duration, obstructive level, and times of TACE performed (Table 1).

Table 1 Baseline clinical characteristics of patients

Factor	Group A (n = 14)	Group B (n = 20)	*P*
Mean age (yr)	57.9±9.2	63.3±11.4	0.356
Gender			
Male	8	10	0.681
Female	6	10	
Mean total serum bilirubin concentration (μmol/L)	318±94	314±115	0.913
Mean alanine aminotransferase concentration (U/L)	71±52	106±107	0.261
Mean albumin concentration (g/L)	33.6±4.3	33.5±3.4	0.914
Mean alkaline phosphatase (U/L)	443±334	543±400	0.449
Mean hemoglobin concentration (g/L)	111±12	105±16	0.275
Mean obstructive duration (wk)	3.7±0.9	4.0±1.4	0.512
Obstructive level			
Hilar	8	12	0.868
Common bile duct	6	8	
TACE			
Performed	9	10	0.409
Not performed	5	10	

Intraluminal brachytherapy

A total of 52 procedures were programmed and 51 procedures were successfully performed, achieving the technical success rate of 98.0%. In 1 patient, a drainage catheter kink, which was caused by an acute angle on the drainage passage, resulted in the failure of driving HDR-^{192}Ir to scheduled position in the third procedure. The total dose of these 14 patients was 14-21 Gy. One patient developed nausea, one complained of abdominal upset, one developed diarrhea. One patient, who had undergone bilobectomy 4 mo before stent placement, developed hemobilia for a period of 4 d (Figure 3). The bleeding stopped soon after hemostatic was prescribed without transfusions. According to RTOG acute morbidity scoring criteria, 3 patients were classified into RTOG grade 1 acute morbidity, the others RTOG grade 0 acute morbidity. According to RTOG/EORTC late morbidity scoring criteria, 1 patient was classified into RTOG/EORTC grade 1 late morbidity, the others grade 0 late morbidity.

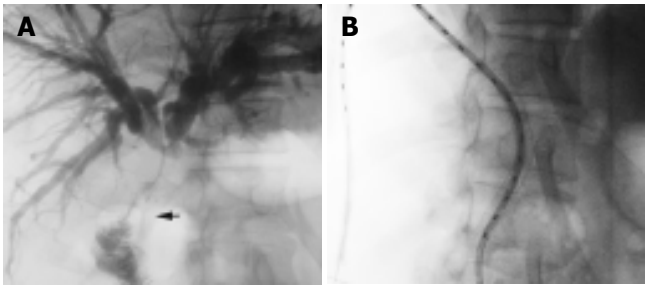

Figure 3 One patient undergoing bilienterostomy and ostomy, which was shown in irradiation region in intraluminal brachy therapy. A: Cholangiography indicated that jejunum was invaded by the malignancy (arrow). B: Jejunum and ostomy were in the irradiation region.

Stent patency and patient survival

The median follow-up time was 6.0 mo (range, 1-17 mo). In group B, 1 patient died 1 mo after stent placement of uncontrolled bleeding caused by tumor rupture, another one died 5 mo after stent placement due to cerebrovascular accident. The mean stent patency was 12.6 mo (median, 10.0 mo) with stent occlusion of 21.4% (3 of 14 patients) in group A, whereas the mean stent patency was 8.3 mo (median, 6.0 mo) with stent occlusion of 45.0% (9 of 20 patients) in group B. The stent patency of group A was significantly longer than that of group B (P<0.05, Figure 4). The mean survival was 9.6 mo (median 7.0 mo) in group A and 6.4 mo (median 6.0 mo) in group B, showing no significant difference.

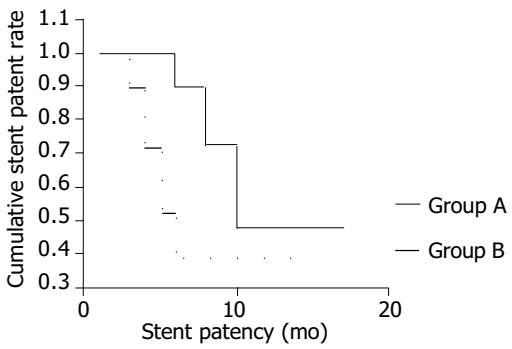

Figure 4 Stent patency of the two groups.

DISCUSSION

As a part of brachytherapies, intraluminal brachytherapy is defined as performing brachytherapy by inserting an applicator and radioactive source into a lumen (or cavity) such as nasopharyngeal cavity, uterine cavity, esophagus, rectum and bile duct[15]. The properties of this radiotherapeutic technique include[16]: (1) Small source size enables itself to be very close to or contact with the target tissue. (2) The effective therapeutic range is 0.5-2.0 cm, which has little effect on normal tissue. (3) The absorbed dose is in inverse proportion to the square of the distance from radioactive source. With its irradiation extent confined to ductal wall and tissue adjacent to duct, intraluminal brachytherapy is a proper therapy for malignancy arising from a duct or adjacent to a duct. Because the absorbed dose falls off rapidly with increasing distance from the sources, intraluminal brachytherapy can deal with the malignancy without significantly affecting the adjacent normal tissues. To date, intraluminal brachytherapy not only has been the major therapeutics in treating the carcinoma of nasopharyngeal, uterine cervix, vagina, and endometrium[17-20], but complementary to the treatment of carcinoma of esophagus, lung, and rectum[21-23].

A number of isotopes were available for brachytherapy, including ^{226}Ra, ^{60}Co, ^{137}Cs, ^{192}Ir and ^{90}Sr. With advantages of highly specific activity, relatively short half-life, easy to be shielded, and technical flexibility, ^{192}Ir is the most widely used brachytherapy source in clinical practice[24]. According to the dose delivered per hour, brachytherapy can be classified into low dose rate (LDR, 0.4-2 Gy/h), median dose rate (MDR, 2-12 Gy/h) and high dose rate (HDR, >12 Gy/h). Among them, LDR and HDR are more frequently used. By comparison with LDR, HDR represents a technologic advance that offers the following advantages[25]: (1) Improved physical dose delivery due to the short treatment time and negligible organ motion. (2) Improved radiation safety and protection with decreased exposure to personnel. (3) Reduced possibility of human error through computerized remote afterloading. (4) Increased efficiency because more patients can be treated with HDR per unit time. Additionally, while treating patients with MOJ by LDR, the applicator and radioactive source must be kept in the drainage catheter for several hours to several days, which may influence bile drainage and increase the risk of infection. The course of HDR therapy only needs several minutes, thus having no effect on bile drainage[26]. For all the reasons mentioned above, we used HDR-^{192}Ir as the radioactive source in our study.

Intraluminal brachytherapy takes use of the drainage passage established during PTCD, making the procedure uncomplicated and inducing less damage. We only failed to complete the therapy in 1 patient in his third procedure. In this case we found an acute angle on the drainage passage. The narrow applicator lumen caused by the kink on the drainage catheter resulted in failure in radioactive source transmission. In patients who are scheduled to receive intraluminal brachytherapy, an acute angle should be avoided on the drainage passage during PTCD. Dose distribution of intraluminal brachytherapy is characterized by "inverse-square law" as we discussed before. In our study it was technically impossible to use instrument such as balloon-catheter to centralize the radioactive source in the bile duct, that is to say, the radioactive source usually located eccentrically in the lumen. The absorbed dose of bile duct wall close to the radioactive source is too high to be calculated by the "inverse-square law". Brambs[27] investigated the bile duct tolerance in intraluminal brachytherapy in a swine model, and demonstrated that fractional dose of 7.5 Gy only caused slight fibrosis in the bile duct. Because the radiation damage in human is similar to that in swine, fractional dose of 7.5 Gy is deemed to be safe in clinical practice. As to other structures adjacent to bile duct such as hepatic artery, portal vein, duodenum, and pancreas, the distance between radioactive source and those structures makes the "inverse-square law" calculation possible. A tumor causing obstructive jaundice is thought to be at the advanced stage of the disease, the aim of the therapy is palliation rather than cure. Palliative

radiation therapy generally follows the regimen[28]: the total dose of 20-30 Gy and the fractional dose of 5-10 Gy, with an intention to alleviate pain, maintain patency, stop bleeding, and reduce morbidity. In consideration of the poor clinical status of patients due to hyperbilirubinemia in our study, we prescribed fractional dose of 4-7 Gy with a total dose of 14-21 Gy, which was certainly tolerable. In this study, only 3 patients developed RTOG grade 1 acute morbidity, and 1 patient developed RTOG/EORTC grade 1 morbidity. One patient developed hemobilia for a period of 4 d without the need for transfusions. This patient had undergone bilienterostomy and the ostomy, which was shown to be invaded by the malignancy, was in irradiation region in intraluminal brachytherapy. One of the reasons for hemobilia is tumor necrosis. On condition that block of tumor tissue necroses before the supplying arteriole could occlude, tumor bleeding will occur. The other one is ostomy hemorrhage. Jejunum and ostomy are dose-limiting tissues susceptible to irradiation.

MOJ is usually caused by cholangiocarcinoma, gallbladder carcinoma, metastatic lymphadenopathy (from stomach, colorectum, or breast), and pancreatic carcinoma. TACE has limited effect on these malignancies in most cases because of their character of relative avascularity[29]. Cholangiocarcinoma, gallbladder carcinoma, and pancreatic carcinoma have the tendency of invading bile duct, so the rate of stent occlusion due to tumor ingrowth or overgrowth is inevitably high[30-32]. There is an increasing demand for efficient therapy to palliate these malignancies, so to prolong stent patency and patient survival. External-beam irradiation has been used to treat abdominal tumors for nearly a hundred years. Major deterrents to improved results with MOJ are the limited tolerance of the structures (liver, duodenum, stomach, and kidney) around the lesion, lack of clear definition of the lesion's location, poor clinical status of the patients, and respiration interfering with the irradiation field[33]. Fortunately, intraluminal brachytherapy, with special dosimetric characteristics and accurate location, overcome all the above shortcomings. Intraluminal brachytherapy in MOJ can efficiently palliate the underlying malignancies with fewer morbidities. Dvorak[34,35] and cooperators reported their experiences of HDR-^{192}Ir intraluminal brachytherapy in treatment of 2 groups of patients with MOJ after bile drainage. The causes of MOJ were cholangiocarcinoma and gallbladder carcinoma in one group, cholangiocarcinoma and pancreas carcinoma in the other. The mean survival of both groups was 9 mo. After stent placement and subsequent jaundice subsidence, the underlying malignancy could be controlled by intraluminal brachytherapy, and invasion and compression of the bile duct avoided. Bruha *et al.*[36] reported that patients with MOJ treated with intraluminal brachytherapy using HDR-^{192}Ir, the mean stent patency in patients with cholangiocarcinoma and gallbladder carcinoma were 418 and 220 d, respectively. The result of our study showed that the mean stent patency of intraluminal brachytherapy group (12.6 mo) was significantly longer than the control group (8.3 mo). We attribute the effect on prolonging stent patency to the followings: (1) Prohibit tumor from growing through the mesh of the stent (ingrowth) (2) Prohibit tumor from growing over the edge of the stent (overgrowth) (3) In cases with hilar obstruction, intraluminal brachytherapy in ipsilateral duct can prevent tumor tissue from invading contralateral duct. Although not statistically significant, it appeared that the mean survival in group A (9.6 mo) was longer than in group B (6.4 mo). We speculated that the advantage of intraluminal brachytherapy in extending survival be more prominent on condition that the cases were expanded or the follow-up was prolonged.

In conclusion, because the special dosimetric characteristics of HDR-^{192}Ir and the high dose tolerance of bile duct, HDR-^{192}Ir intraluminal brachytherapy is a safe and feasible method in the treatment of MOJ. HDR-^{192}Ir intraluminal brachytherapy may prolong stent patency and has the potentiality of extending survival of patients with MOJ.

REFERENCES

1 **Freeman ML**, Overby C. Selective MRCP and CT-targeted drainage of malignant hilar biliary obstruction with self-expanding metallic stents. *Gastrointest Endosc* 2003; **58**: 41-49

2 **Mao AW**, Gao ZD, Xu JY, Yang RJ, Xiao XS, Jiang TH, Jiang WJ. Treatment of malignant digestive tract obstruction by combined intraluminal stent installation and intra-arterial drug infusion. *World J Gastroenterol* 2001; **7**: 587-592

3 **Inal M**, Akgul E, Aksungur E, Seydaoglu G. Percutaneous placement of biliary metallic stents in patients with malignant hilar obstruction: unilobar versus bilobar drainage. *J Vasc Interv Radiol* 2003; **14**: 1409-1416

4 **Inal M**, Aksungur E, Akgul E, Oguz M, Seydaoglu G. Percutaneous placement of metallic stents in malignant biliary obstruction: one-stage or two-stage procedure? Pre-dilate or not? *Cardiovasc Intervent Radiol* 2003; **26**: 40-45

5 **Shah RJ**, Howell DA, Desilets DJ, Sheth SG, Parsons WG, Okolo P 3rd, Lehman GA, Sherman S, Baillie J, Branch MS, Pleskow D, Chuttani R, Bosco JJ. Multicenter randomized trial of the spiral Z-stent compared with the Wallstent for malignant biliary obstruction. *Gastrointest Endosc* 2003; **57**: 830-836

6 **Pinol V**, Castells A, Bordas JM, Real MI, Llach J, Montana X, Feu F, Navarro S. Percutaneous self-expanding metal stents versus endoscopic polyethylene endoprostheses for treating malignant biliary obstruction: randomized clinical trial. *Radiology* 2002; 225: 27-34

7 **Ahmad J**, Siqueira E, Martin J, Slivka A. Effectiveness of the Ultraflex Diamond stent for the palliation of malignant biliary obstruction. *Endoscopy* 2002; **34**: 793-796

8 **Nakamura T**, Hirai R, Kitagawa M, Takehira Y, Yamada M, Tamakoshi K, Kobayashi Y, Nakamura H, Kanamori M. Treatment of common bile duct obstruction by pancreatic cancer using various stents: single-center experience. *Cardiovasc Intervent Radiol* 2002; **25**: 373-380

9 **Hatzidakis AA**, Tsetis D, Chrysou E, Sanidas E, Petrakis J, Gourtsoyiannis NC. Nitinol stents for palliative treatment of malignant obstructive jaundice: should we stent the sphincter of Oddi in every case? *Cardiovasc Intervent Radiol* 2001; **24**: 245-248

10 **Ferlitsch A**, Oesterreicher C, Dumonceau JM, Deviere J, Leban T, Born P, Rosch T, Suter W, Binek J, Meyenberger C, Mullner M, Schneider B, Schofl R. Diamond stents for palliation of malignant bile duct obstruction: a prospective multicenter evaluation. *Endoscopy* 2001; **33**: 645-650

11 **Caldicott DG**, Ziprin P, Morgan R. Transhepatic insertion of a metallic stent for the relief of malignant afferent loop obstruction. *Cardiovasc Intervent Radiol* 2000; **23**: 138-140

12 **Kim HS**, Lee DK, Kim HG, Park JJ, Park SH, Kim JH, Yoo BM, Roe IH, Moon YS, Myung SJ. Features of malignant biliary obstruction affecting the patency of metallic stents: a multicenter study. *Gastrointest Endosc* 2002; **55**: 359-365

13 **Eschelman DJ**, Shapiro MJ, Bonn J, Sullivan KL, Alden ME, Hovsepian DM, Gardiner GA Jr. Malignant biliary duct obstruction: long-term experience with Gianturco stents and combined-modality radiation therapy. *Radiology* 1996; **200**: 717-724

14 **Cox JD**, Stetz J, Pajak TF. Toxicity criteria of the radiation therapy oncology group (RTOG) and the european organization for research and treatment of cancer (EORTC). *Int J Radiat Oncol Biol Phys* 1995; **31**: 1341-1346

15 **Liu TF**. Xiandai Fangshe Zhongliuxue. 1sted. Shanghai: *Fudan University Pub* 2001: 105-153

16 **Perez CA**, Brady LW. Principles and practice of radiation oncology. 3rded. Philadelphia: *Lippincott Raven Pub* 1997: 405-467

17 **Hareyama M**, Sakata K, Oouchi A, Nagakura H, Shido M, Someya M, Koito K. High-dose-rate versus low-dose-rate intracavitary therapy for carcinoma of the uterine cervix: a randomized trial. *Cancer* 2002; **94**: 117-124

18 **Alektiar KM**, McKee A, Venkatraman E, McKee B, Zelefsky MJ, Mychalczak BR, Hoskins WJ, Barakat RR. Intravaginal high-dose-rate brachytherapy for Stage IB (FIGO Grade 1, 2) endometrial cancer. *Int J Radiat Oncol Biol Phys* 2002; **53**: 707-713
19 **Kong W**, Sun J. Outcome with intracavitary high-dose-rate brachytherapy for primary vaginal cancer. *Zhonghua Fuchanke Zazhi* 2002; **37**: 94-96
20 **Syed AM**, Puthawala AA, Damore SJ, Cherlow JM, Austin PA, Sposto R, Ramsinghani NS. Brachytherapy for primary and recurrent nasopharyngeal carcinoma: 20 years' experience at Long Beach Memorial. *Int J Radiat Oncol Biol Phys* 2000; **47**: 1311-1321
21 **Sharma V**, Mahantshetty U, Dinshaw KA, Deshpande R, Sharma S. Palliation of advanced/recurrent esophageal carcinoma with high-dose-rate brachytherapy. *Int J Radiat Oncol Biol Phys* 2002; **52**: 310-315
22 **Aumock A**, Birnbaum EH, Fleshman JW, Fry RD, Gambacorta MA, Kodner IJ, Malyapa RS, Read TE, Walz BJ, Myerson RJ. Treatment of rectal adenocarcinoma with endocavitary and external beam radiotherapy: results for 199 patients with localized tumors. *Int J Radiat Oncol Biol Phys* 2001; **51**: 363-370
23 **Jain SK**, Dupuy DE, Cardarelli GA, Zheng Z, DiPetrillo TA. Percutaneous radiofrequency ablation of pulmonary malignancies: combined treatment with brachytherapy. *Am J Roentgenol* 2003; **181**: 711-715
24 **Hu YM**, Liu Z, She F, Xue WL. 1st ed. Beijing: *Atomic Energy Publishing House* 1999: 101-102
25 **Manning MA**, Arthur DW, Schmidt-Ullrich RK, Arnfield MR, Amir C, Zwicker RD. Interstitial high-dose-rate brachytherapy boost: the feasibility and cosmetic outcome of a fractionated outpatient delivery scheme. *Int J Radiat Oncol Biol Phys* 2000; **48**: 1301-1306
26 **Mohan DS**, Nori D. Intraluminal brachytherapy in the treatment of pancreas and bile ductcarcinoma: regarding Montemaggi *et al*., IJROBP 32:437; 1995. *Int J Radiat Oncol Biol Phys* 1995; **33**: 773-774
27 **Brambs HJ**, Freund U, Bruggmoser G, Laaff H, Kluger UW, Roth R, Wannenmacher M. Radiation sensitivity of the normal bile duct during high dose rate afterloading irradiation with Iridium 192. Experimental studies in pigs. *Strahlenther Onkol* 1993; **169**: 721-728
28 **Xu BY**, Yu SC, Zeng DW, Chen GX. Modern Tumor Radiotherapy. 1st ed Beijing: *People's Malitary Publishing House* 2000: 190-199, 23-34
29 **Kawahara N**, Ono M, Taguchi K, Okamoto M, Shimada M, Takenaka K, Hayashi K, Mosher DF, Sugimachi K, Tsuneyoshi M, Kuwano M. Enhanced expression of thrombospondin-1 and hypovascularity in human cholangiocarcinoma. *Hepatology* 1998; **28**: 1512-1517
30 **Shirabe K**, Shimada M, Harimoto N, Sugimachi K, Yamashita Y, Tsujita E, Aishima S. Intrahepatic cholangiocarcinoma: its mode of spreading and therapeutic modalities. *Surgery* 2002; **131**(1 Suppl): S159-164
31 **Kim JH**, Kim TK, Eun HW, Kim BS, Lee MG, Kim PN, Ha HK. Preoperative evaluation of gallbladder carcinoma: efficacy of combined use of MR imaging, MR cholangiography, and contrast-enhanced dual-phase three-dimensional MR angiography. *J Magn Reson Imaging* 2002; **16**: 676-684
32 **Rieber A**, Brambs HJ. Metallic stents in malignant biliary obstruction. *Cardiovasc Intervent Radiol* 1997; **20**: 43-49
33 **Hayes JK Jr**, Sapozink MD, Miller FJ. Definitive radiation therapy in bile duct carcinoma. *Int J Radiat Oncol Biol Phys* 1988; **15**: 735-744
34 **Dvorak J**, Petera J, Papik Z, Melichar B, Vanasek T, Hulek P, Jandik P, Mergancova J, Zoul Z, Vacek Z. Transduodenal intraluminal high dose rate brachytherapy in the treatment of carcinomas of the subhepatic region. *Hepatogastroenterology* 2002; **49**: 1045-1047
35 **Dvorak J**, Jandik P, Melichar B, Jon B, Mergancova J, Zoul Z, Vacek Z, Petera J. Intraluminal high dose rate brachytherapy in the treatment of bile duct and gallbladder carcinomas. *Hepatogastroenterology* 2002; **49**: 916-917
36 **Bruha R**, Petrtyl J, Kubecova M, Marecek Z, Dufek V, Urbanek P, Kodadova J, Chodounsky Z. Intraluminal brachytherapy and selfexpandable stents in nonresectable biliary malignancies-the question of long-term palliation. *Hepatogastroenterology* 2001; **48**: 631-637

Edited by Chen WW and Zhu LH **Proofread by** Xu FM

PO Box 2345, Beijing 100023, China
Fax: +86-10-85381893
E-mail: wjg@wjgnet.com www.wjgnet.com

World J Gastroenterol 2004;10(23):3511-3513
World Journal of Gastroenterology
Copyright © 2004 by The WJG Press ISSN 1007-9327

• BRIEF REPORTS •

Cloning and sequencing of cagA gene fragment of *Helicobacter pylori* with coccoid form

Ke-Xia Wang, Xue-Feng Wang

Ke-Xia Wang, Xue-Feng Wang, School of Medicine, Anhui University of Science &Technology Huainan 232001, Anhui Province, China
Supported by Natural Science Foundation of the Education Department of Anhui Province, China No.2003kj111
Correspondence to: Dr. Ke-Xia Wang, Department of Etiology and Immunology, School of Medicine, Anhui University of Science & Technology, Huainan 232001, Anhui Province, China. kexiawang2003@yahoo.com.cn
Telephone: +86-554-6658770 **Fax:** +86-554-6662469
Received: 2003-10-20 **Accepted:** 2003-12-08

Abstract

AIM: To clone and sequence the cagA gene fragment of *Helicobacter pylori* (*H pylori*) with coccoid form.

METHODS: *H pylori* strain NCTC11637 were transformed to coccoid form by exposure to antibiotics in subinhibitory concentrations. The coccoid *H pylori* was collected. cagA gene of the coccoid *H pylori* strain was amplified by PCR. After purified, the target fragment was cloned into plasmid pMD-18T. The recombinant plasmid pMD-18T-cagA was transformed into *E.coli* JM109. Positive clones were screened and identified by PCR and digestion with restriction endonucleases. The sequence of inserted fragment was then analysed.

RESULTS: cagA gene of 3 444 bp was obtained from the coccoid *H pylori* genome DNA. The recombinant plasmid pMD-18T-cagA was constructed, then it was digested by *Bam*H I+*Sac* I, and the product of digestion was identical with the predicted one. Sequence analysis showed that the homology of coccoid and the reported original sequence *H pylori* was 99.7%.

CONCLUSION: The recombinant plasmid containing cagA gene from coccoid *H pylori* has been constructed successfully. The coccoid *H pylori* contain completed cagA gene, which may be related to pathogenicity of them.

Wang KX, Wang XF. Cloning and sequencing of cagA gene fragment of *Helicobacter pylori* with coccoid form. *World J Gastroenterol* 2004; 10(23): 3511-3513
http://www.wjgnet.com/1007-9327/10/3511.asp

INTRODUCTION

Helicobacter pylori (*H pylori*) is one of the common bacteria causing chronic infection, which infects more than 50% of the human population, causes chronic gastritis and plays an important role in the pathogenesis of gastroduodenal ulceration. *H pylori* has also been suggested to be involved in the genesis of adenocarcinoma and MALT lymphoma of the stomach.[1-5] *H pylori* cells growing actively *in vitro* are curved rods, which evolve into metabolically active but nonculturable coccoid cells after prolonged incubation[6-8]. In the stomach mostly spiral-shaped bacteria are found, but coccoid cells have been observed in the more severely damaged regions of the gastric mucosa[9,10]. Many scholars believed that coccoid *H pylori* might lead to difficult recovery, easy relapse and epidemical transmission[11]. But the pathogenicity of coccoid *H pylori* is unclear at present. The cytotoxin-associated protein encoded by *cagA* (cytotoxin-associated gene A) is important virulence determinated by *H pylori*. *cagA*$^+$ *H pylori* strains have been linked to more severe gastric inflammation, peptic ulcer disease, and gastric cancer in adults[12-15]. CagA gene is a mono-replicon and locates 3' region of cag-PAI (cag pathogenity island), whose length varies from 3 400 bp to 4 000 bp. In order to probe into possible pathogenesis of coccoid *H pylori*, the recombinant plasmid encoding cagA gene of coccoid *H pylori* was constructed and detected for the sequence in this study.

MATERIALS AND METHODS

Materials

The strain NCTC11637 of *H pylori* was afforded by Chinese center for disease control and prevention. JM109 *E.coli* strains were preserved by our laboratory, pMD-18T (T-Vector), restriction endonuclease enzymes (*Bam*H I, *Sac* I), T_4 DNA ligase, LA Taq DNA polymerase, DNA Extraction Kit and DNA purification reagent kit were provided by TaKaRa Company.

Bacterial culture and induction of coccoid forms *H pylori* strains were grown on Columbia agar with 50 m/L frozen-melting sheep blood, 100 mL/L fetal bovine serum, and Skirrow's antibiotic supplement in a microaerophilic atmosphere for 3 d at 37 ℃, then the bacteria were suspended in brucella broth and supplemented with 0.02 mg/L of amphotericin, still were incubated at 37 ℃ for 3, 5, 7, and 10 d. Baterial morphology was determined by light microscopy after Gram staining. The coccoid forms were collected and stored at -20 ℃.

Extraction of genomic DNA *H pylori* of coccoid form were added to a 1.5 mL microcentrifuge tube, rinsed once with phosphate-buffered saline (PH 7.2), and pelleted by centrifugation at 11 000 *g*. Genomic DNA was extracted by TaKaRa MiniBEST Bacterial Genomic DNA Extraction Kit, the DNA pellet was suspended in TE (10 mmol/L Tris-HCL, 1 mmol/L PH 8.0 EDTA), and stored at -20 ℃.

Synthetic primers A single primer pair was used to amplify coccoid *H pylori* cagA gene based on GenBank. The primers had a *Bam*H I site incorporated into the 5' end and a *Sac* I site at the 3' end and their sequences as follows (5'-3'): AAGGATCC ACTAACGAAACCATTGACCA (forward) and AAGAGCTCA GATTTTTGGAAACCACCTT (reverse). The 5' region initiator and 3' end stop codon were banned.

PCR amplification PCR was performed in a 100 μL reaction mixture in 0.6-mL tube in an automatic thermal cycler (TP3000; TaKaRa BIO INC). The PCR mixture contained 10 μL of 10×PCR buffer, 1 μL of sample DNA, 10 μL of 2.5 mmol/L deoxynucleoside triphoshpate, 4 μL of 10 μmol/L oligonucleotide primers, 0.5 μL of LA Taq polymerase, 74.5 μL of molecular-biology-grade distilled water. The mixtures were incubated for 1 min at 94 ℃ for initial denaturation of the target DNA and then subjected to 30 cycles of denaturation at 98 ℃ for 10 s, annealing at 55 ℃ for 30 s, and extension at 72 ℃ for 210 s. The amplified products (5 μL) were analyzed by electrophoresis on 10 g/L agarose gel

containing 0.1 μg of ethidium bromide per ml in TBE buffer. The PCR product was visualized under UV light and photographed.

Construction of recombinant plamids The PCR product was purified by TaKaRa PCR Fragment Recovery Kit. The purified product was cloned into the compatible sites of the T-vector pMD-18T by using T_4 DNA ligase at a molar ratio of 6:1 at 16 ℃ for 3 h. After the above product was transformed into *E.coli* JM109, pMD-18T/cagA was selected and identified by PCR and enzyme digestion.

Extraction of recombinant plasmid The single bacterial colony (JM109/pMD-18T/cagA) was picked, and cultivated in 3 mL LB broth containing 100 mg/L of ampicillin, at 300 r/min at 37 ℃ overnight, then recombinant plasmids were extracted according to manufacturer's instructions (TaKaRa MiniBest DNA Purification Kit), in the meantime, identified by PCR and restriction endomuclease enzyme digestion.

Sequence determination and homology analysis The sequence determination of cagA gene of recombinant plasmid was carried out by Takara Company, in the meantime, the sequence of gene and amino acid were analyzed by software sequence 3.0, and compared the homology based on the GenBank.

RESULTS

PCR amplification of coccoid H pylori cagA gene

H pylori with coccoid form cagA was amplified by PCR from the above primers and The PCR product was electrophoresed and visualized by 10 g/L agarose gel (Figure 1). It revealed that the size of cagA DNA fragment amplified by PCR was 3 444 bp, and was compatible with the expectant size.

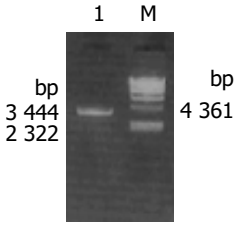

Figure 1 10 g/L agarose gel electrophoresis of cagA DNA fragment amplified by PCR from coccoidal *H pylori*. Lane 1. PCR products, Lane M: λ-*Hin*d III DNA marker.

Identification of recombinant vector by PCR

The plasmid was extracted from recombinant bacteria and conducted as template to amplify by PCR under the condition mentioned above. The PCR products were visualized by 10 g/L agarose gel electrophoresis (Figure 2). It indicated that recombinant plasmid contained the objective gene. At the same time, it was successful in transforming recombinant plasmid into JM109 *E.coli*.

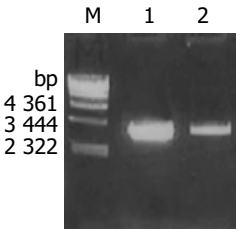

Figure 2 Identification of recombinant vector by PCR. Lane m: λ-*Hin*d III DNA marker; Lane 1: amplification cagA gene from recombinant pMD-18T-cagA plasmid by PCR; Lane 2: Amplification cagA gene from coccoid *H pylori* genome DNA by PCR.

pMD-18T/cagA identification by restriction enzyme digestion

Recombinant plasmid pMD-18T/cagA was digested by bi-enzyme digestion with *Bam*H I and *Sac* I, then digestive product was visualized on 10 g/L agarose gel (Figure 3). It demonstrated that recombinant plasmid was digested to 3 444 bp and 2 692 bp DNA fragment, which contained the objective gene.

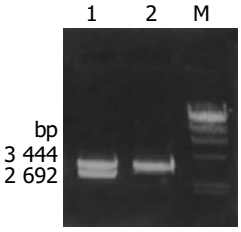

Figure 3 The identification of the pMD-18T-cagA by digestion with restriction endonucleases Lane1: Recombinant pMD-18T-cagA digested by *Bam*H I puls *Sac* I; Lane 2: Amplification cagA gene from coccoid *H pylori* genome DNA by PCR; m: λ-*Hin*d III DNA marker.

Sequence analysis of cloned cagA gene of coccoid

H pylori Sequence of inserted DNA was analyzed with BcaBEST Primer M13-47/BcaBEST Primer RV-M using automatic sequence analyzer by Sanger dideoxy chain termination method. The result of analysis showed that the size of inserted DNA was about 3 444 bp and 99.7% affinity in comparison with DNA sequence published on GenBank (locus: AB015416). The sequence of partial vacA gene was showed in Figure 4.

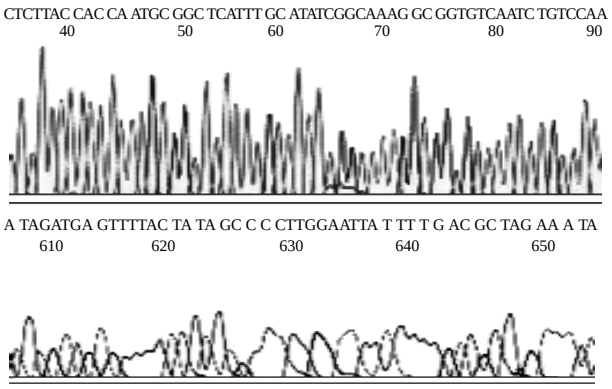

Figure 4 sequencing result of partial cagA gene.

DISCUSSION

Morphological conversion from spiral *H pylori* to coccoid forms has been described under several suboptinal conditions. These conditions include aerobiosis, alkaline pH, high temperature, extended incubation, or treatment with proton pump inhibitor or antibiontics[16-18]. This coccoid form conversion phenomenon, which has been thought to result in a viable but nonculturable form of the bacterium, is not exclusive to *H pylori*, as it is common for other enteric pathogens. Controversy remains about the pathogenicity of coccoid *H pylori*. Many investigators have suggested that the coccoid form of *H pylori* represents a degenerative form with no infectious capability, but others believed that the coccoid form retains a weak metabolic activety, important structural components, and patogenicity[19-21]. Recently, successful infection with coccoid forms of *H pylori* in animal models has been reported[22-24]. These findings have highlighted the possible role of the coccoid forms in transmission of infection and morphological conversion of coccoids to the spiral form. It is well known that cagA is an important virulence factor of *H pylori* and related to severe gastrointestinal diseases. However, the research of cagA gene of coccoidal *H pylori* is few at present. In order to observe cagA and vacA expression

during conversion to the coccoid form, Sisto *et al*.[25] analyzed the expression of ureA, cagA, vacA genes after prolonged incubation in a liquid medium in 2000, the results showed that although the coccoid forms had decreased DNA and RNA levels after 31 d, they were not degraded and still expressed the urease, cytotoxic island and vacuolating toxin genes. So in conclusion, coccoid forms are therefore viable and may act as a transmissible agent that plays a crucial role in disease relapses after antibiotic therapy. She *et al*. explored the virulence and the potential pathogenicity of coccoid *H pylori* transformed from spiral form by exposure to antibiotic in 2001, and found that the content of the protein with the molecular weight over M_r 74 000 decreased, but vacA, cagA, urea, ureB, hpaA gene remained to be preserved, so they concluded that the virulence and the proteins with molecular weight over M_r 74 000 in coccoid *H pylori* decrease, but no deletion exists in amplification fragments from ureA, ureB, hpaA, vacA and cagA genes, and suggested that coccoid *H pylori* may have potential pathogenicity. Furthermore, Monstein *et al*.[26] confirmed that the transcription and translation of cagA and vacA gene might actively take place in coccoid *H pylori* cells.

In order to research the cagA gene existence, and explore the possible mechanism of pathogenicity in coccoid *H pylori*, we designed the specific primers based on cagA gene sequence reported in GenBank, and successfully amplified the cagA gene of coccoid *H pylori* by PCR, then inserted into pMD-18T vector. The recombinant plasmids were successfully identified containing cagA gene fragment by PCR and enzyme digestion, and sequence determination confirmed that cagA gene existed in coccoid *H pylori*, though existence of 0.3% difference with the reported sequence in GenBank. The reason for the discrepancy might be as follows: (1) the mutant base could come from the process of PCR amplification and sequencing, (2) *H pylori* provided have the transformation ability, which could lead to *H pylori* variation and genome reset. Our results also support the assumption that virulence-gene expression is differently regulated among *H pylori* strains[26].

In this study, the NCTC11637 strain with amphotericin for 3 d generated a high proportion of coccoid forms. Forms obtained after removal of bacterial clumps and amorphous debris by centrifugation at 600 r/min for 5 min were nearly 100% coccoid. Due to similar to the condition *in vivo* by antibiotic induction, the collected coccoid *H pylori* still remained complete celluar structure, and their genome DNA lost was less, so some important virulent gene, such as vacA, cagA and so on, could exist in their cells. Once coccoid *H pylori* live in suitable condition, they can recover their virulence and lead to the occurrence of diseases. Or coccoid *H pylori* may revert helical form, and result in the transmission and/or relapse of diseases with the complete cagA gene.

REFERENCES

1 **Nguyen TN,** Barkun AN, Fallone CA. Host determinants of *Helicobacter pylori* infection and its clinical outcome. *Helicobacter* 1999; **4**: 185-197

2 **Vandenplas Y.** *Helicobacter pylori* infection. *World J Gastroenterol* 2000; **6**: 20-31

3 **Sakai T,** Ogura Y, Narita J, Suto T, Kimura D, Ainai S, Fujita H, Kamada M. Simultaneous early adenocarcinoma and mucosa-associated lymphoid tissue (MALT) lymphoma of the stomach associated with *Helicobacter pylori* infection. *Gastric Cancer* 2003; **6**: 191-196

4 **Satoh K,** Sugano K. Causal relationship between *Helicobacter pylori* infection and upper gastroduodenal diseases. *Nippon Rinsho* 2001; **59**: 239-245

5 **Muller S,** Seifert E, Stolte M. Simultaneous MALT-type lymphoma and early adenocarcinoma of the stomach associated with *Helicobacter pylori* gastritis. *Z Gastroenterol* 1999; **37**: 153-157

6 **Ren Z,** Pang G, Musicka M, Dunkley M, Batey R, Beagley K, Clancy R. Coccoid forms of *Helicobacter pylori* can be viable. *Microbios* 999; **97**: 153-163

7 **Willen R,** Carlen B, Wang X, Papadogiannakis N, Odselius R, Wadstrom T. Morphologic conversion of *Helicobacter pylori* from spiral to coccoid form. Scanning (SEM) and transmission electron microscopy (TEM) suggest viability. *Ups J Med Sci* 2000; **105**: 31-40

8 **Mizoguchi H,** Fujioka T, Nasu M. Evidence for viability of coccoid forms of *Helicobacter pylori*. *J Gastroenterol* 1999; **11**(Suppl 11): 32-36

9 **Saito N,** Konishi K, Sato F, Kato M, Takeda H, Sugiyama T, Asaka M. Plural transformation-processes from spiral to coccoid *Helicobacter pylori* and its viability. *J Infect* 2003; **46**: 49-55

10 **Janas B,** Czkwianianc E, Bak-Romaniszyn L, Bartel H, Tosik D, Planeta-Malecka I. Electron microscopic study of association between coccoid forms of *Helicobacter pylori* and gastric epithelial cells. *Am J Gastroenterol* 1995; **90**: 1829-1833

11 **Mizoguchi H,** Fujioka T, Kishi K, Nishizono A, Kodama R, Nasu M. Diversity in protein synthesis and viability of *Helicobacter pylori* coccoid forms in response to various stimuli. *Infect Immun* 1998; **66**: 5555-5560

12 **Mao HY,** Fang PC, Ye SJ, You JF, Zhu YL, Yu JG. Analysis of babA2 cagA and vacA genotypes of *Helicobacter pylori* in chronic gastritis and peptic ulcer. *Zhejiang Daxue Xuebao Yixueban* 2003; **32**: 29-32

13 **Oleastro M,** Gerhard M, Lopes AI, Ramalho P, Cabral J, Sousa Guerreiro A, Monteiro L. *Helicobacter pylori* virulence genotypes in portuguese children and adults with gastroduodenal pathology. *Eur J Clin Microbiol Infect Dis* 2003; **22**: 85-91

14 **Debets-Ossenkopp YJ,** Reyes G, Mulder J, Aan De Stegge BM, Peters JT, Savelkoul PH, Tanca J, Pena AS, Vandenbroucke-Grauls CM. Characteristics of clinical *Helicobacter pylori* strains from Ecuador. *J Antimicrob Chemother* 2003; **51**: 141-145

15 **Bravo LE,** van Doom LJ, Realpe JL, Correa P. Virulence-associated genotypes of *Helicobacter pylori*: do they explain the African enigma? *Am J Gastroenterol* 2002; **97**: 2839-2842

16 **Kusters JG,** Gerrits MM, Van Strijp JA, Vandenbroucke-Grauls CM. Coccoid forms of *Helicobacter pylori* are the morphologic manifestation of cell death. *Infect Immun* 1997; **65**: 3672-3679

17 **Narikawa S,** Kawai S, Aoshima H, Kawamata O, Kawaguchi R, Hikiji K, Kato M, Iino S, Mizushima Y. Comparison of the nucleic acids of helical and coccoid forms of *Helicobacter pylori*. *Clin Diagn Lab Immunol* 1997; **4**: 285-290

18 **Costa K,** Bacher G, Allmaier G, Dominguez-Bello MG, Engstrand L, Falk P, de Pedro MA, Garcia-del Portillo F. The morphological transition of *Helicobacter pylori* cells from spiral to coccoid is preceded by a substantial modification of the cell wall. *J Bacteriol* 1999; **181**: 3710-3715

19 **Sato F.** *Helicobacter pylori* in culture: an ultrastructural study. *Hokkaido Igaku Zasshi* 2000; **75**: 187-196

20 **Nakamura A,** Park A, Nagata K, Sato EF, Kashiba M, Tamura T, Inoue M. Oxidative cellular damage associated with transformation of *Helicobacter pylori* from a bacillary to a coccoid form. *Free Radic Biol Med* 2000; **28**: 1611-1618

21 **Monstein HJ,** de la Cour CD, Jonasson J. Probing 23S ribosomal RNA cleavage sites in coccoid *Helicobacter pylori*. *Helicobacter* 2001; **6**: 100-109

22 **Rabelo-Goncalves EM,** Nishimura NF, Zeitune JM. Acute inflammatory response in the stomach of BALB/c mice challenged with coccoidal *Helicobacter pylori*. *Mem Inst Oswaldo Cruz* 2002; **97**: 1201-1206

23 **Wang X,** Sturegard E, Rupar R, Nilsson HO, Aleljung PA, Carlen B, Willen R, Wadstrom T. Infection of BALB/c A mice by spiral and coccoid forms of *Helicobacter pylori*. *J Med Microbiol* 1997; **46**: 657-663

24 **Cao J,** Li ZQ, Borch K, Petersson F, Mardh S. Detection of spiral and coccoid forms of *Helicobacter pylori* using a murine monoclonal antibody. *Clin Chim Acta* 1997; **267**: 183-196

25 **Sisto F,** Brenciaglia MI, Scaltrito MM, Dubini F. *Helicobacter pylori*: ureA, cagA and vacA expression during conversion to the coccoid form. *Int J Antimicrob Agents* 2000; **15**: 277-282

26 **Monstein HJ,** Jonasson J. Differential virulence-gene mRNA expression in coccoid forms of *Helicobacter pylori*. *Biochem Biophys Res Commun* 2001; **285**: 530-536

Edited by Xia HHX **Proofread by** Xu FM

PO Box 2345, Beijing 100023, China
Fax: +86-10-85381893
E-mail: wjg@wjgnet.com www.wjgnet.com

World J Gastroenterol 2004;10(23):3514-3517
World Journal of Gastroenterology
Copyright © 2004 by The WJG Press ISSN 1007-9327

• BRIEF REPORTS •

Real-time determination of human telomerase reverse transcriptase mRNA in gastric cancer

Li-Hua Hu, Feng-Hua Chen, Yi-Rong Li, Lin Wang

Li-Hua Hu, Feng-Hua Chen, Yi-Rong Li, Department of Transfusion, Union Hospital, Tongji Medical College, Huazhong University of Science and Technology, Wuhan 430022, Hubei Province, China
Lin Wang, Life Science College, Wuhan University, Wuhan 430070, Hubei Province, China
Supported by the Key Program of Science and Technology Foundation of Hubei Province, No. 2002AA304B10
Correspondence to: Dr. Li-Hua Hu, Department of Transfusion, Union Hospital, Tongji Medical College, Huazhong University of Science and Technology, Wuhan 430022, Hubei Province, China. xhhlh@126.com
Telephone: +86-27-85726312
Received: 2004-01-15 **Accepted:** 2004-04-13

Abstract

AIM: To set up a real-time fluorescent quantitative reverse transcription-polymerase chain reaction (RT-PCR) assay, to detect human telomerase reverse transcriptase (hTERT) messenger RNA in gastric carcinomas, and to evaluate quantitative determination of hTERT mRNA in the diagnostic value of gastric carcinomas, and to analyze the correlation between the expression level of hTERT mRNA and clinicopathological parameters in patients with gastric cancer.

METHODS: A real-time quantitative RT-PCR (RQ-PCR) based on TaqMan fluorescence methodology and the LightCycler system was used to quantify the full range of hTERT mRNA copy numbers in 35 samples of gastric carcinomas and corresponding adjacent non-cancerous tissues. The normalized hTERT (NhTERT) was standardized by quantifying the number of GAPDH transcripts as internal control and expressed as 100× (hTERT/GAPDH) ratio. Variables were analyzed by the Student's *t*-test, χ^2 test and Fisher's exact test.

RESULTS: NhTERT from gastric carcinomas and corresponding adjacent non-cancerous tissues was 6.27±0.89 and 0.93±0.18, respectively (t = 12.76, P<0.001). There was no significant association between gastric cancer hTERT mRNA expression level and patient's age, gender, tumor size, location and stage ($_P$TNM), but a significant correlation was found between hTERT mRNA expression level in gastric carcinomas and the degree of differentiation.

CONCLUSION: Quantitative determination of hTERT mRNA by RQ-PCR is a rapid and sensitive method. hTERT might be a potential biomarker for the early detection of gastric cancer.

Hu LH, Chen FH, Li YR, Wang L. Real-time determination of human telomerase reverse transcriptase mRNA in gastric cancer. *World J Gastroenterol* 2004; 10(23): 3514-3517
http://www.wjgnet.com/1007-9327/10/3514.asp

INTRODUCTION

Telomerase is a reverse transcriptase that adds telomeric repeats to chromosomal ends to compensate for sequence loss during DNA replication. Telomerase activity has been detected in about 85% of human cancer samples and is associated with cell immortalization and the acquisition of malignancy, but most normal tissues have low or no telomerase activity[1]. Telomerase is one of the most widespread tumor markers at present. To date, the main assay to detect telomerase activity is telomere repeat amplification protocol (TRAP). TRAP is a qualitative or semi-quantitative assay, and can not accurately exhibit telomerase expression level, and needs functional ribonucleoproteins, including both reverse transcriptase activity and undegraded RNA. The presence of telomerase inhibitors, Taq polymerase inhibitors, proteases, or RNases in tissue extract may influence its detection and subsequently lower its sensitivity. With the cloning of both genes coding for human telomerase RNA (hTR) and human telomerase reverse transcriptase (hTERT), hTERT becomes the catalytic subunit of telomerase and is a rate-limiting determinant of the enzymatic activity of human telomerase, and only the expression of hTERT is closely associated with telomerase activity[2-5], whereas the expression of hTR is widespread. The close relationship between hTERT mRNA expression and telomerase activity suggests that quantification of the mRNA expression of the hTERT gene could be used as an alternative to measure telomerase activity. In this study, we used real-time quantitative reverse transcription-polymerase chain reaction (RQ-PCR) to detect and quantify hTERT mRNA in samples of gastric carcinoma and corresponding non-cancerous tissues, and to evaluate the quantitative determination of hTERT mRNA in the diagnostic value of gastric carcinomas, and to analyze the correlation between the expression level of hTERT mRNA and clinicopathological parameters in patients with gastric cancer.

MATERIALS AND METHODS

Patients and samples

We analyzed tissues (gastric cancer and corresponding non-cancerous tissues) from surgically removed primary gastric cancer in Union Hospital and Tongji Hospital of Tongji Medical College of Huazhong University of Science and Technology from October 2002 to May 2003. All patients (25 males and 10 females, mean age 55.2 years, range 34-73 years) were at initial presentation and had no radiotherapy or chemotherapy history before surgery. All samples were examined histopathologically to confirm the diagnosis. Control tissues were the corresponding non-cancerous mucosa from the stomach of cancer patients, and excised beyond 5 cm from neoplastic lesions. Samples were stored at -80 ℃ until further analysis.

Reagents and instruments

TRIzol was the product of Omega. The reagents used for reverse transcription were purchased from Promega. The reagents used for PCR and PCR product purification, glyceraldehydes 3-phosphate dehydrogenase (GAPDH) quantification, and the primers and TaqMan probe of hTERT were all purchased from Shanghai Shenyou Company. Both T4 DNA ligase and PMD18-T vector were the products of TaKaRa. The other chemical reagents used in this study were ACS reagents of China. The fluorescent quantitative PCR instrumentation was the LightCycler system of Roche.

Real-time quantitative RT-PCR

We used a RQ-PCR assay based on TaqMan fluorescence methodology to quantify the full range of hTERT mRNA copy numbers[6,7]. This method used a dual-labeled nonextendable oligonucleotide hydrolysis (TaqMan) probe in addition to the two amplification primers. The probe contained 6-carboxy-fluorescein (FAM) as a fluorescent reporter dye, and 6-carboxytetramethyl-rhodamine (TAMRA) as a quencher for its light emission spectrum. During the extension phase of PCR, the probe hybridized to the target sequence and was then cleaved due to the 5' to 3' exonuclease activity of *Taq* polymerase. The increase in the fluorescence signal of the reporter was proportional to the amount of specific PCR products, providing highly accurate and reproducible quantification. The number of PCR cycles to reach the fluorescence threshold was the cycle threshold (Ct). The Ct value for each sample was proportional to the log of the initial amount of input cDNA. By plotting the Ct value of an unknown sample on the standard curve, the amount of target sequences in the sample could be calculated.

To normalize the hTERT mRNA expression for sample-to-sample differences in RNA input, RNA quality, and reverse transcriptase efficiency, we amplified the housekeeping gene GAPDH. According to each standard curve, we got the copy numbers of GAPDH and hTERT, respectively. The ratio between copy numbers of hTERT and GAPDH represented the normalized hTERT (NhTERT) for each sample and could be compared with that of other samples[8].

NhTERT = (hTERT mRNA $copies_{sample}$/GAPDH mRNA $copies_{sample}$) ×100.

Primers and probes

According to GAPDH quantification reagents and the reference[9], the nucleotide sequences of oligonucleotide TaqMan probes and primers are shown in Table 1.

RNA extraction and cDNA synthesis

According to the manufacturer's instructions, total RNA from frozen tumor and corresponding non-cancerous tissue specimens was isolated by disruption of 50-100 mg tissues in 1 mL of TRIzol. RNA was quantified spectrophotometrically, and its quality was determined by agarose gel electrophoresis and ethidium bromide staining. Only samples that were not degraded and showed clear 18 S and 28 S bands under ultraviolet light were used for real-time RT-PCR.

All samples were denatured for 10 min at 60 ℃ to melt secondary structure with the template and cooled immediately on ice for 5 min to prevent secondary structure from reforming. Total RNA (1-2 μg) was reverse transcribed in a total volume of 25 μL containing 1×RT buffer (Promega), 200 U of Moloney murine leukemia virus Reverse Transcriptase (M-MLV RT) (Promega), 20 U of RNasin (Promega), 0.2 μg random primer (Promega) and 1 mmol/L deoxynucleotides. The reaction was performed for 10 min at 25 ℃, for 60 min at 42 ℃ and for 10 min at 70 ℃. cDNA was stored at -20 ℃ until use.

Construction of recombinant plasmid calibrator

Pure hTERT fragments from classical RT-PCR were joined to PMD18-T vector by T4 DNA ligase, resulting in recombinant plasmid PMD18-hTERT. The recombinant plasmids were confirmed in including hTERT target fragments by sequencing, and extracted and purified. The recombinant plasmid DNAs at 10^7 copies/mL were stored at -20 ℃ until use. GAPDH standard template was from the GAPDH quantification reagents.

LightCycler real-time PCR amplification

All PCR reactions were performed using the LightCycler System (Roche Diagnostics, Switzerland) in a total volume of 20 μL containing 1×*Taq* polymerase buffer, 4 mmol/L $MgCl_2$, 200 μmol/L deoxynucleotides, 300 nmol/L each primer, 150 nmol/L probe, 1 U *Taq* polymerase and 20 ng cDNA. Water instead of cDNA template was used for the negative controls. Both GAPDH and hTERT amplification were done in duplicate for each sample. The thermal cycling conditions were 5 min at 94 ℃, followed by 40 cycles, each at 94 ℃ for 15 s and at 60 ℃ for 1 min for GAPDH or at 65 ℃ for 1 min for hTERT (two-step PCR). The number of GAPDH and hTERT transcripts in samples was calculated with the LightCycler software, using these standard curves.

Statistical analysis

Data were expressed as mean±SD. The Student *t*-test, χ^2 test and Fisher's exact test were used in this study. $P<0.05$ was considered statistically significant.

RESULTS

Standard curve construction

We used different concentrations of GAPDH and hTERT standard templates including 10^4, 10^5, 10^6 and 10^7 copies/mL to perform quantitative PCR and calculate the standard curves, respectively. The standard curves were: Ct_{GAPDH} = -3.86 log (GAPDH copies) +46.60; and Ct_{hTERT} = -3.42 log (hTERT copies) +37.31. The correlation coefficients were both -1.00 (Figure 1A, B).

hTERT mRNA expression levels in gastric cancer and corresponding adjacent non-cancerous tissues

The expression of hTERT mRNA in gastric carcinomas was analyzed by a highly sensitive RQ-PCR assay. HTERT mRNA expression was detectable not only in all 35 gastric carcinomas, but also in the corresponding non-cancerous gastric tissues (Figure 2). For each experimental sample, the amount of hTERT and GAPDH was determined from the appropriate standard curve. Then, hTERT amount was divided by the GAPDH amount to obtain NhTERT. NhTERT was significantly higher (t = 12.76, $P<0.001$) in tumor tissues (6.27±0.89) than in the corresponding non-cancerous tissues (0.93±0.18).

Table 1 Sequences of primers and probes used in this study

Gene and oligonucleotide	Sequence	PCR product size (bp)
GAPDH		
Upper primer	5'-GAAGGTGAAGGTCGGAGTC-3'	
Lower primer	5'-GAAGATGGTGATGGGATTTC-3'	226
Probe	5'-(FAM) CAAGCTTCCCGTTCTCAGCC (TAMRA)-3'	
hTERT		
Upper primer	5'-TGACACCTCACCTCACCCAC-3'	
Lower primer	5'-CACTGTCTTCCGCAAGTTCAC-3'	95
Probe	5'-(FAM) ACCCTGGTCCGAGGTGTGTCCCTGA (TAMRA)-3'	

The primers placed in different exons, were tested to ensure that they did not amplify the contaminated genomic DNA.

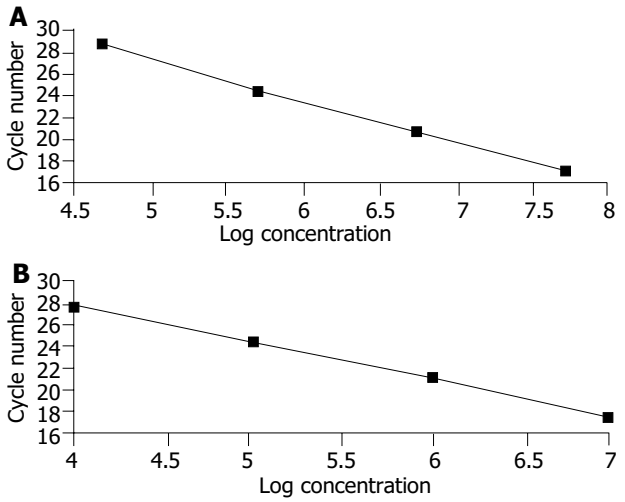

Figure 1 Standard curve of GAPDH and hTERT A: Standard curve of GAPDH: slope = -3.86, intercept = 46.60, r = -1.00. B: Standard curve of hTERT: slope = -3.42, intercept = 37.31, r = -1.00.

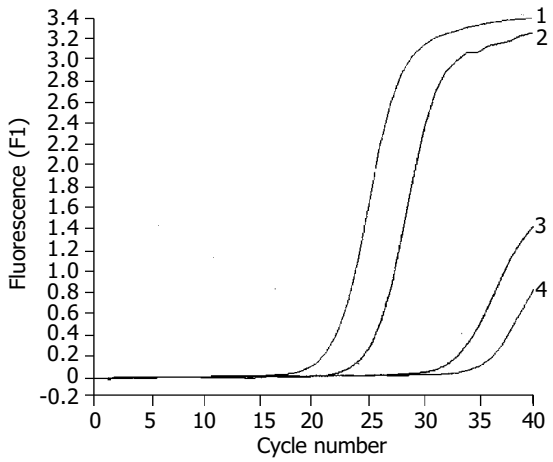

Figure 2 hTERT mRNA expression in samples of gastric cancer and corresponding non-cancerous tissues. Lanes 1, 2: Gastric cancer; Lanes 3, 4: Corresponding non-cancerous tissues.

Correlation between hTERT mRNA expression level and clinicopathological parameters

The data obtained by RQ-PCR were analyzed in relation to clinicopathological parameters of the patients. All 35 corresponding non-cancerous gastric tissue samples expressed low detectable NhTERT, ranging from 0.06 to 2.11. In the 35 gastric carcinomas, NhTERT varied greatly, ranging from 0.28 to 90.55. NhTERT was categorized as low or high, using a cutoff at 5.39, which was the value that represented the median value of the expression distribution. Thus, 17 tumors (48.6%) showed low hTERT expression, whereas 18 tumors (51.4%) had high hTERT expression. We observed the statistical links between hTERT mRNA expression levels and the degree of differentiation (P = 0.007). Seventy-three point six percent (14 of 19) of poorly differentiated and undifferentiated tumors showed high NhTERT expressions, whereas 75% (12 of 16) of well and moderately differentiated tumors exhibited low NhTERT expressions. Poorly differentiated and undifferentiated tumors had higher hTERT mRNA expression levels than well and moderately differentiated tumors. No relationship was found between hTERT mRNA expression level and patients' age, gender, tumor size, tumor location and stage (pTNM). The results obtained are shown in Table 2.

Table 2 Relationship between hTERT mRNA expression level and clinicopathological parameters in patients with gastric cancer

Parameter	n	NhTERT		P
		Low (n = 17)	High (n = 18)	
Age (yr)				
<50	13	7	6	
⩾50	22	10	12	0.73
Gender				
Male	25	13	12	
Female	10	4	6	0.71
Size of diameter (cm)				
<5	19	11	8	
⩾5	16	6	10	0.31
Location				
Cardia	14	8	6	
Body and antrum	21	9	12	0.50
Degree of differentiation				
Well and moderately differentiated	16	12	4	
Poorly differentiated and undifferentiated	19	5	14	0.007
Lymph node metastasis				
N_0	8	4	4	
N_1	13	8	5	
N_2	14	5	9	0.40
Depth of invasion				
T_1 and T_2	24	13	11	
T_3 and T_4	11	4	7	0.43
Metastasis				
M_0	20	12	8	
M_1	15	5	10	0.17

DISCUSSION

We used RQ-PCR based on TaqMan methodology for the accurate quantification of hTERT mRNA expression in gastric carcinomas. This assay has several marked advantages over the TRAP assay for cancer detection. It needs only a 95-bp fragment of hTERT mRNA, making the assay less sensitive to RNase activity and insensitive to proteases and protein inhibitors. The assay output is numerical rather than qualitative, allowing appropriate diagnostic statistics to be applied. It uses endogenous controls (GAPDH in this study) which allow correction for parameters like RNA input, RNA degradation, or RT inhibitors. Real-time PCR makes RNA quantification much more precise and reproducible, based on Ct values established in the early exponential phase of the PCR reaction (when none of the reagents is rate-limiting) rather than end point quantification of the amount of accumulated PCR product. It does not require post-PCR sample handling and the closed-tube method minimizes the risk for cross-contamination. These suggest that quantitative determination of hTERT mRNA by RQ-PCR is a powerful method to investigate the telomerase status and superior in specificity and sensitivity to the evaluation of telomerase activity by the TRAP assay. In addition, we used recombinant hTERT plasmid DNA to calculate the external standard curves, and found it was better for the quantification of mRNA than the recombinant RNA calibrator or endogenous standards[10,11]. Theoretically, the slope of the standard curve should be -3.3 if 10-fold dilutions are used, but in practice a slope between -3.0 and -3.9 is probably acceptable as long as the correlation coefficient is >0.95. The standard curves we obtained in this study had acceptable slopes and correlation coefficients.

In this study, the level of hTERT mRNA estimated with RQ-PCR procedure was the average amount of transcripts in a whole

tissue sample and mainly depended on the number of hTERT-positive cells present in the tissue. hTERT mRNA was detected in 100% of gastric carcinoma RNAs, and also in all the corresponding non-cancerous gastric mucosa RNAs. The highest NhTERT was detected in gastric cancer, whereas the lowest NhTERT was found in non-cancerous gastric tissues. However, NhTERT in samples of non-cancerous tissues was only approximately 14.8% of those found in the cancerous samples, and NhTERT was significantly higher (t = 12.76, P<0.001) in tumor tissues (6.27±0.89) than in the corresponding non-cancerous tissues (0.93±0.18). We believed that these were not in contradiction to the findings using TRAP with which telomerase activity could not be detected in most non-malignant gastric tissues and the positive rate of hTERT mRNA expression by means of *in situ* hybridization or classical RT-PCR in gastric carcinoma[12-15]. The difference could be explained by the increased sensitivity of the RQ-PCR assay and the presence of residual malignant cells, inflammatory lymphocytes or tumor infiltrating activated cells. Our results showed real-time measurement of hTERT expression could discriminate gastric carcinoma from nonmalignant gastric tumors. This discrimination would be more distinct if the percentage of tumor cells was higher in the selected tissues.

No relationship was found in our study between hTERT mRNA expression level and patients' age, gender, tumor size, location and tumor stage (pTNM) (P>0.05) and there were statistical links between hTERT mRNA expression levels and the degree of differentiation (P = 0.007). These suggest that the up-regulation of hTERT appeared to be an early event in gastric carcinogenesis. HTERT may play a critical role in gastric carcinogenesis and have potential as a biomarker in the telomerase status for the early detection of gastric cancer. Real-time quantitative analysis of hTERT mRNA in tissues, cancer cells in the blood, and plasma or serum of the patients with cancer before and after surgery, radiotherapy or chemotherapy may be helpful for early detection and diagnosis of cancer, and find out therapeutic effect and estimate prognosis[16-21]. hTERT may become a target in gene therapy of cancer and inaugurate a new approach for cancer therapy.

In conclusion, monitoring hTERT mRNA expression with RQ-PCR analysis appears to be a new effective and sensitive method to better differentiate gastric cancer from nonmalignant gastric tumors. HTERT mRNA expression status may be used as a molecular marker of gastric cancer. These findings must be confirmed in a larger series of gastric cancer patients.

REFERENCES

1 **Shay JW,** Bacchetti S. A survey of telomerase activity in human cancer. *Eur J Cancer* 1997; **33**: 787-791

2 **Meyerson M,** Counter CM, Eaton EN, Ellisen LW, Steiner P, Caddle SD, Ziaugra L, Beijersbergen RL, Davidoff MJ, Liu Q, Bacchetti S, Haber DA, Weinberg RA. hEST2, the putative human telomerase catalytic subunit gene, is up-regulated in tumor cells and during immortalization. *Cell* 1997; **90**: 785-795

3 **Lingner J,** Hughes TR, Shevchenko A, Mann M, Lundblad V, Cech TR. Reverse transcriptase motifs in the catalytic subunit of telomerase. *Science* 1997; **276**: 561-567

4 **Feng J,** Funk WD, Wang SS, Weinrich SL, Avilion AA, Chiu CP, Adams RR, Chang E, Allsopp RC, Yu J, Le S, West MD, Harley CB, Andrews WH, Greider CW, Villeponteau B. The RNA component of human telomerase. *Science* 1995; **269**: 1236-1241

5 **Nakamura TM,** Morin GB, Chapman KB, Weinrich SL, Andrews WH, Lingner J, Harley CB, Cech TR. Telomerase catalytic subunit homologs from fission yeast and human. *Science* 1997; **277**: 955-959

6 **Bustin SA.** Absolute quantification of mRNA using real-time reverse transcription polymerase chain reaction assays. *J Mol Endocrinol* 2000; **25**: 169-193

7 **PE Biosystems.** DNA/RNA real-time quantitative PCR. Available from: http://www.wzw.tum.de/gene-quantification/pe-realtimeoverview-1.pdf

8 ABI Prism 7700 Sequence detection System User Bulletin #2 (2001) Relative quantification of gene expression. Available from: http://docs.appliedbiosystems.com/pebiodocs/04303859.pdf

9 **Bièche I,** Noguès C, Paradis V, Olivi M, Bedossa P, Lidereau R, Vidaud M. Quantitation of *hTERT* gene expression in sporadic breast tumors with a real-time reverse transcription-polymerase Chain reaction assay. *Clin Cancer Res* 2000; **6**: 452-459

10 **Pfaffl MW,** Hageleit M. Validities of mRNA quantification using recombinant RNA and recombinant DNA external calibration curves in real-time RT-PCR. *Biotechnol Lett* 2001; **23**: 275-282

11 **Ke LD,** Chen Z, Yung WK. A reliability test of standard-based quantitative PCR: exogenous *vs* endogenous standards. *Mol Cell Probes* 2000; **14**: 127-135

12 **Yoo J,** Park SY, Kang SJ, Kim BK, Shim SI, Kang CS. Expression of telomerase activity, human telomerase RNA, and telomerase reverse transcriptase in gastric adenocarcinomas. *Mod Pathol* 2003; **16**: 700-707

13 **Miyachi K,** Fujita M, Tanaka N, Sasaki K, Sunagawa M. Correlation between telomerase activity and telomeric-repeat binding factors in gastric cancer. *J Exp Clin Cancer Res* 2002; **21**: 269-275

14 **Okusa Y,** Ichikura T, Mochizuki H, Shinomiya N. Clinical significance of telomerase activity in biopsy specimens of gastric cancer. *J Clin Gastroenterol* 2000; **30**: 61-63

15 **Yao XX,** Yin L, Sun ZC. The expression of hTERT mRNA and cellular immunity in gastric cancer and precancerosis. *World J Gastroenterol* 2002; **8**: 586-590

16 **Dasi F,** Lledo S, Garcia-Granero E, Ripoll R, Marugan M, Tormo M, Garcia-Conde J, Alino SF. Real-time quantification in plasma of human telomerase reverse transcriptase (hTERT) mRNA: a simple blood test to monitor disease in cancer patients. *Lab Invest* 2001; **81**: 767-769

17 **Buttitta F,** Pellegrini C, Marchetti A, Gadducci A, Cosio S, Felicioni L, Barassi F, Salvatore S, Martella C, Coggi G, Bosari S. Human telomerase reverse transcriptase mRNA expression assessed by real-time reverse transcription polymerase chain reaction predicts chemosensitivity in patients with ovarian carcinoma. *J Clin Oncol* 2003; **21**: 1320-1325

18 **Miura N,** Shiota G, Nakagawa T, Maeda Y, Sano A, Marumoto A, Kishimoto Y, Murawaki Y, Hasegawa J. Sensitive detection of human telomerase reverse transcriptase mRNA in the serum of patients with hepatocellular carcinoma. *Oncology* 2003; **64**: 430-434

19 **de Kok JB,** Ruers TJM, van Muijen GNP, van Bokhoven A, Willems HL, Swinkels DW. Real-time quantification of human telomerase reverse transcriptase mRNA in tumors and healthy tissues. *Clin Chem* 2000; **46**: 313-318

20 **Chen XQ,** Bonnefoi H, Pelte MF, Lyautey J, Lederrey C, Movarekhi S, Schaeffer P, Mulcahy HE, Meyer P, Stroun M, Anker P. Telomerase RNA as a detection marker in the serum of breast cancer patients. *Clin Cancer Res* 2000; **6**: 3823-3826

21 **Tchirkov A,** Rolhion C, Kemeny JL, Irthum B, Puget S, Khalil T, Chinot O, Kwiatkowski F, Perissel B, Vago P, Verrelle P. Clinical implications of quantitative real-time RT-PCR analysis of hTERT gene expression in human gliomas. *Br J Cancer* 2003; **88**: 516-520

Edited by Chen WW and Wang XL **Proofread by** Xu FM

PO Box 2345, Beijing 100023, China
Fax: +86-10-85381893
E-mail: wjg@wjgnet.com www.wjgnet.com

World J Gastroenterol 2004;10(23):3518-3521
World Journal of Gastroenterology
Copyright © 2004 by The WJG Press ISSN 1007-9327

• BRIEF REPORTS •

NDRG2 expression and mutation in human liver and pancreatic cancers

Xiao-Lan Hu, Xin-Ping Liu, Shu-Xin Lin, Yan-Chun Deng, Na Liu, Xia Li, Li-Bo Yao

Xiao-Lan Hu, Xin-Ping Liu, Yan-Chun Deng, Na Liu, Xia Li, Li-Bo Yao, Department of Biochemistry and Molecular Biology, Fourth Military Medical University, Xi'an 710032, Shaanxi Province, China
Shu-Xin Lin, Department of Pathophysiology, Fourth Military Medical University, Xi'an 710032, Shaanxi Province, China
Supported by the National Natural Science Foundation of China, No. 30370315, No. 30171044 and Medical and pharmaceutical Research Fund of PLA, No. 01MA185
Correspondence to: Li-Bo Yao, Department of Biochemistry and Molecular Biology, Fourth Military Medical University, 17 Changle West Road, Xi'an 710032, Shaanxi Province, China. bioyao@fmmu.edu.cn
Telephone: +86-29-83374513 **Fax:** +86-29-83374513
Received: 2004-03-18 **Accepted:** 2004-04-05

Abstract

AIM: To investigate the expression of NDRG2 and mutation of the entire coding region of NDRG2 in human liver and pancreatic cancers, and to further discuss the possible causes of NDRG2 distinct expression patterns.

METHODS: Reverse transcription-polymerase chain reaction (RT-PCR) was used to analyze the expression of NDRG2 mRNA in 37 fresh cancer specimens (including 8 cases of pancreatic cancer and 29 cases of liver cancer) and adjacent normal tissues collected from clinical operation. In addition, mutation analysis of the whole coding region of NDRG2 in these cancers was examined by polymerase chain reaction-single strand conformational polymorphism (PCR-SSCP).

RESULTS: Compared with adjacent normal tissues, the expression levels of NDRG2 mRNA in corresponding cancer tissues reduced significantly (pancreatic cancer: 0.680±0.112 *vs* 2.089±0.214, $P<0.01$) (liver cancer: 0.894±0.098 *vs* 1.345±0.177, $P<0.05$). Using PCR-SSCP, the mutation of the whole coding region of NDRG2 was not found in those cancer tissues where the expression of NDRG2 mRNA reduced markedly.

CONCLUSION: *NDRG2* gene might express differently between normal tissues and cancer tissues, and might play an important role in the development of pancreatic cancer and liver cancer. Low expression of NDRG2 might be unrelated to the mutation of coding region of NDRG2.

Hu XL, Liu XP, Lin SX, Deng YC, Liu N, Li X, Yao LB. NDRG2 expression and mutation in human liver and pancreatic cancers. *World J Gastroenterol* 2004; 10(23): 3518-3521
http://www.wjgnet.com/1007-9327/10/3518.asp

INTRODUCTION

NDRG2, a new member of the N-Myc downstream-regulated gene (NDRG) family including NDRG1-4, was first discovered and cloned from normal human whole brain cDNA library by subtractive hybridization in our laboratory[1]. NDRG2 is located on chromosome 14q11.2, including 16 exons and 15 introns, and its cDNA is 2 024 bp in length[2]. Studies from our laboratory and others have shown that NDRG2 was highly expressed in many normal tissues, especially in the brain, heart, skeletal muscle, and kidney, whereas low expressed or not detected in various tumors and tumor cell lines[3,4]. This suggests that NDRG2 inactivation might play an important role in some tumor genesis or evolution, and NDRG2 might be a new cancer suppressor gene candidate. To date, no report on mutation analysis of NDRG2 in a variety of tumors has been presented. This study was conducted to determine whether the distinct expression of NDRG2 was related to gene mutation as most cancer suppressor genes. The expression of NDRG2 mRNA in 37 patients with liver cancer and pancreatic cancer was detected, and the mutation of the whole coding region of NDRG2 in normal and cancer specimens was analyzed by PCR-SSCP.

MATERIALS AND METHODS

Patients and tissue specimens

Thirty-seven fresh cancer specimens (including 8 cases of pancreatic cancer and 29 cases of liver cancer) and corresponding adjacent normal tissues were collected from patients who underwent surgery at First Affiliated Hospital of Xi'an Jiaotong University, Tangdu Hospital and Xijing Hospital between May 2003 and September 2003. All specimens were examined by microscope after haematoxylin and eosin (H&E) staining.

RNA isolation and RT-PCR

Total RNA was extracted from tissue specimens using TRIzol reagent (GIBCO BRL, USA) according to the manufacturer's instructions. Reverse transcription reaction was set up according to Promega's reverse transcription system protocol. cDNAs were then amplified by PCR using specific primers for human NDRG2: upstream primer 5'- GC GGA TCC ATG GCG GAG CTG CAG GAG GTC -3'; and downstream primer 5'- GC GAA TTC AAC AAG GGC CAT TCA ACA GGA GAC -3', about 1 200 bp. The primer sequences of glyceraldehyde-3-phosphate dehydrogenase (GAPDH) which was used as an internal quantitative control for the amplification were as follows: upstream primer 5' -GCC TCA AGA TCA GCA AT- 3'; downstream primer 5' -AGG TCC ACC ACT GAC ACG TT- 3', 310 bp. Cycling condition for NDRG2 was at 94 ℃ for 5 min, followed by 32 cycles of 94 ℃ for 40 s, 59 ℃ for 50 s, and 72 ℃ for 60 s, and the cycling condition for GAPDH was at 94 ℃ for 5 min, followed by 30 cycles of 94 ℃ for 30 s, 57 ℃ for 30 s, and 72 ℃ for 30 s, and finally for 10 min at 72 ℃. The PCR products were then analyzed and visualized on 12 g/L agarose gel containing 5 g/L ethidium bromides. Results were normalized by the ratio of band density of NDRG2 mRNA to GAPDH mRNA.

PCR-SSCP silver staining

According to cDNA sequence of *NDRG2* gene, we designed by DNAstar analysis software and synthesized 6 pairs of primers covering the whole coding region of *NDRG2* gene, with length of each PCR product around 150 to 370 bp, and PCR reaction

Table 1 Primer sequence, annealing temperature and PCR product size for PCR-SSCP

	Primer	Sequence	Annealing temperature (℃)	PCR product size (bp)
A	Upstream	5'-ATGGCGGAGCTGCAGGAGGTC-3'	54	186
	Downstream	5'-ATTTATAGTTGAGTCCCACATC-3'		
B	Upstream	5'-CACCATACGGCTCTGTCACTTTCACT-3'	58	188
	Downstream	5'-CTCTTCCATTCCAGGGGCATCCAC-3'		
C	Upstream	5'-GCCAGCGATCCTTACCTACC-3'	58	365
	Downstream	5'-GGCTGCCCAATCCATCCAACC-3'		
D	Upstream	5'-CCGGACACTGTTGAAGGT-3'	55	364
	Downstream	5'-GGGTCCAGTTTGAGTTACATT-3'		
E	Upstream	5'-CTGTGATGCTGGTGGTAGGAGA-3'	58	286
	Downstream	5'-TGGGACAGGTGCGAGAG-3'		
F	Upstream	5'-GTCCGGTCTCGTACAGCCTCTC-3'	56	153
	Downstream	5'-AACAAGGGCCATTCAACAGGAGAC-3'		

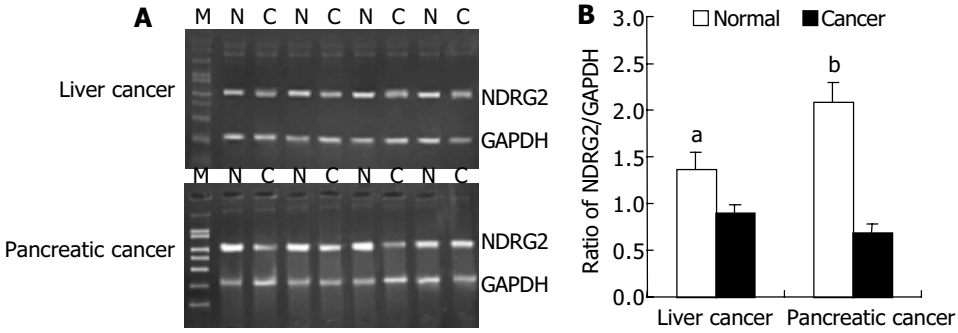

Figure 1 Expressions of NDRG2 mRNA in human liver cancer and pancreatic cancer. A: Representative agarose gels of RT-PCR-amplified NDRG2. M: DNA molecular weight marker; N: Normal tissue; C: Cancer tissue; B: Relative amount of NDRG2 mRNA was evaluated by the ratio of band optical density of NDRG2/GAPDH and the expression was significantly decreased in cancer (n=29 for liver cancer, and 8 for pancreatic cancer respectively) *vs* normal tissues. $^aP<0.05$, $^bP<0.01$ *vs* normal.

conditions are described in Table 1. The PCR products were separated by electrophoresis on 12 g/L agarose gel to check the specificity of each PCR reaction. The products were mixed with the same amount of formamide-loading buffer (950 g/L formamide, 10 mmol/L EDTA, and 0.5 g/L bromophenol blue, 0.5 g/L xylene cyanol) and heated at 100 ℃ for 5 min, and loaded on 80 g/L non-denaturing polyacrylamide gel in 1× TBE buffer for 8-12 h at 40 V. After electrophoresis, the gel was fixed, silver-stained, and finally developed, photographed and analyzed. The sample was considered normal if the band position was the same as that of the normal tissue. Otherwise, it was abnormal.

Statistical analysis

Statistical analysis was performed by SPSS version 10.0. Data were expressed as mean±SD, and analyzed by Student's *t* test. $P<0.05$ was considered statistically significant.

RESULTS

RT-PCR data

We investigated the expression patterns of NDRG2 mRNA by RT-PCR in 37 cases of human cancers including 29 liver cancers and 8 pancreatic cancers. Figure 1A shows PCR products of representative agarose gels for NDRG2 and GAPDH in human liver cancer and pancreatic cancer. The size of the RT-PCR products was as predicted, 1 200 bp for NDRG2 and 310 bp for GAPDH. The levels of NDRG2 mRNA expression were quantified by the ratio of band optical density of NDRG2/GAPDH (Figure 1B). Compared with adjacent normal tissues, there were marked decreases in NDRG2 mRNA expression in liver cancer (0.894±0.098 *vs* 1.345±0.177, $P<0.05$) and pancreatic cancer (0.680±0.112 *vs* 2.089±0.214, $P<0.01$).

PCR-SSCP analysis

The PCR products, which were amplified by 6 pairs of primers covering the whole coding region of *NDRG2* gene, were separated by electrophoresis on 12 g/L agarose gel to check the specificity of each PCR reaction (Figure 2). PCR products with only one specific band of right size in the gel can further be used for SSCP assay. Figure 3 shows representative results of SSCP silver staining of the PCR products amplified by 6 pairs of primers covering the whole coding region of NDRG2. By SSCP, all the PCR products from the cancer tissues of 27 patients of NDRG2 low-expression confirmed by RT-PCR, did not show any mutation.

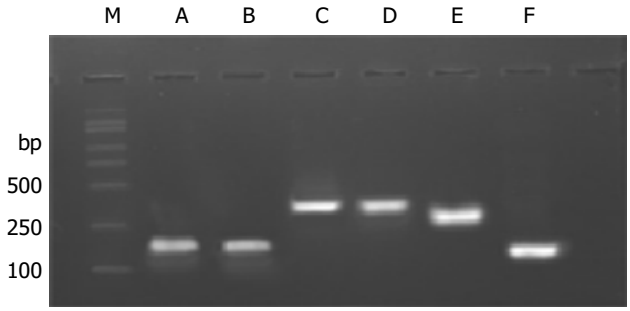

Figure 2 Agarose gel analysis of PCR products amplified by 6 pairs of primers covering the whole coding region of NDRG2. M: DNA molecular weight marker, PCR product size was 186 bp for A, 188 bp for B, 365 bp for C, 364 bp for D, 286 bp for E and 153 bp for F.

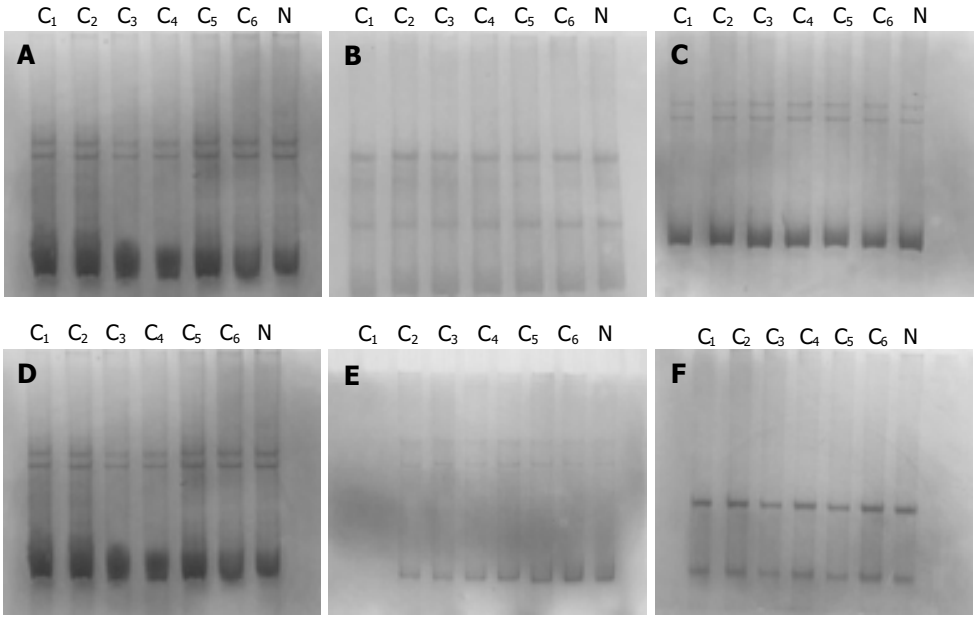

Figure 3 Representative results of SSCP silver staining of the PCR products (186 bp for A, 188 bp for B, 365 bp for C, 364 bp for D, 286 bp for E, and 153 bp for F) amplified by 6 pairs of primers covering the whole coding region of NDRG2. C: cancer tissue; N: normal tissue.

DISCUSSION

NDRG2, together with NDRG1, NDRG3 and NDRG4, constitute *NDRG* gene family. The four members, which share 53-65% amino acid identity, belong to the alpha/beta hydrolase super family[5]. Phylogenetic analysis of the family demonstrated that human NDRG1 and NDRG3 belong to a subfamily, and NDRG2 and NDRG4 to another. Expression of the fusion proteins showed that all of them were cytosolic proteins. Northern and dot blot analysis showed that NDRG gene family was evidently expressed in adult brain and almost not detected in some human cancer lines[6-8]. In addition, NDRG2 is highly expressed in adult skeletal muscle and brain, NDRG3 remarkably expresses in brain and testis, and NDRG4 evidently expresses in brain and heart, suggesting that they might display different specific functions in distinct tissues[9,10]. Although *NDRG* gene family is believed to be involved in cell differentiation, the exact molecular and cellular function of members of this family is still unknown.

In 2000, our laboratory first discovered and successfully cloned human NDRG2 cDNA from normal human whole brain cDNA library by subtractive hybridization. Our previous studies showed that the expression level of NDRG2 mRNA was very high in brain, salivary gland, skeletal muscle and mammary gland, and low in bone marrow, testis, peripheral blood and placenta, and not detectable in leukocyte, colon and some tumor cell lines. Other studies have also shown similar result[11,12], suggesting that NDRG2 inactivation might play an important role in some cancer genesis or evolution, and NDRG2 might be a new cancer suppressor gene candidate.

A recent study showed that over expression of NDRG1 in tumor cells decreased the proliferation rate, enhanced differentiation, and suppressed metastasis potency of cancer cells. More interestingly, a nonsense mutation in *NDRG1* gene may be the cause of hereditary motor and sensory neuropathy-Lom (HMSNL)[13].

The activation of oncogene and inactivation of cancer suppressor gene can lead to uncontrolled cell proliferation and occurrence of cancer. The inactivation of most cancer suppressor genes has been confirmed to relate to gene mutation such as *p53*, *p16* and *Rb* gene[14]. To the authors' knowledge, we first investigated the expression patterns of NDRG2 mRNA by RT-PCR in 37 cases of human cancers including 29 liver cancers and 8 pancreatic cancers. The results showed that there was marked decrease in NDRG2 mRNA expression in human liver cancer ($P<0.05$) and pancreatic cancer ($P<0.01$), compared with adjacent normal tissue. We speculated that different expression pattern of NDRG2 might relate to gene mutation. The designed 6 pairs of primers covering the whole coding region of *NDRG2* gene to amplify the cancer tissue of 27 patients of NDRG2 low-expression were confirmed by RT-PCR, but no mutation was found.

In conclusion, our results indicate that *NDRG2* gene expresses differently between normal tissues and cancer tissues, and it might play an important role in the development of pancreatic cancer and liver cancer. The low expression of NDRG2 might be unrelated to mutation of the coding region of NDRG2. In addition, whether a mutation exists in the upstream sequence of transcription initial site of NDRG2, deserves further investigation.

ACKNOWLEDGEMENTS

We are grateful to Dai-Hua Yu, Bang-Yong Sun, Wei Lin, and Jiang-Wei Liu for the collection of tissue specimens and Jiang-Tian Yu, Li-Hu Wu, and Li-Feng Wang for digital photographs.

REFERENCES

1 **Deng YC,** Yao LB, Liu XP, Nie XY, Wang JC, Zhang XG, Su CZ. Exploring a new gene containing ACP like domain in human brain and expression it in *E.coli*. *Prog Bichem Biophys* 2001; **28**: 72-76

2 **Okuda T,** Kondoh H. Identification of new genes *ndr2* and *ndr3* which are related to Ndr1/RTP/Drg1 but show distinct tissue specificity and response to N-myc. *Biochem Biophys Res Commun* 1999; **266**: 208-215

3 **Qu X,** Zhai Y, Wei H, Zhang C, Xing G, Yu Y, He F. Characterization and expression of three novel differentiation-related genes belong to the human NDRG gene family. *Mol Cell Biochem* 2002; **229**: 35-44

4 **Deng Y,** Yao L, Chau L, Ng SS, Peng Y, Liu X, Au WS, Wang J, Li F, Ji S, Han H, Nie X, Li Q, Kung HF, Leung SY, Lin MC. N-Myc downstream-regulated gene 2 (NDRG2) inhibits glioblastoma cell proliferation. *Int J Cancer* 2003;

106: 342-347

5 **Shaw E,** McCue LA, Lawrence CE, Dordick JS. Identification of a novel class in the alpha/beta hydrolase fold superfamily: the N-myc differentiation-related proteins. *Proteins* 2002; **47**: 163-168

6 **Zhou RH,** Kokame K, Tsukamoto Y, Yutani C, Kato H, Miyata T. Characterization of the human NDRG gene family: a newly identified member, NDRG4, is specifically expressed in brain and heart. *Genomics* 2001; **73**: 86-97

7 **van Belzen N,** Dinjens WN, Diesveld MP, Groen NA, van der Made AC, Nozawa Y, Vlietstra R, Trapman J, Bosman FT. A novel gene which is up-regulated during colon epithelial cell differentiation and down-regulated in colorectal neoplasms. *Lab Invest* 1997; 77: 85-92

8 **Piquemal D,** Joulia D, Balaguer P, Basset A, Marti J, Commes T. Differential expression of the RTP/Drg1/Ndr1 gene product in proliferating and growth arrested cells. *Biochim Biophys Acta* 1999; **1450**: 364-373

9 **Boulkroun S,** Fay M, Zennaro MC, Escoubet B, Jaisser F, Blot-Chabaud M, Farman N, Courtois-Coutry N. Characterization of rat NDRG2 (N-Myc downstream regulated gene 2), a novel early mineralocorticoid-specific induced gene. *J Biol Chem* 2002; **277**: 31506-31515

10 **Zhao W,** Tang R, Huang Y, Wang W, Zhou Z, Gu S, Dai J, Ying K, Xie Y, Mao Y. Cloning and expression pattern of the human NDRG3 gene. *Biochim Biophys Acta* 2001; **28**: 134-138

11 **Nichols NR.** Ndrg2, a novel gene regulated by adrenal steroids and antidepressants, is highly expressed in astrocytes. *Ann N Y Acad Sci* 2003; **1007**: 349-356

12 **Choi SC,** Kim KD, Kim JT, Kim JW, Yoon DY, Choe YK, Chang YS, Paik SG, Lim JS. Expression and regulation of NDRG2 (N-myc downstream regulated gene 2) during the differentiation of dendritic cells. *FEBS Lett* 2003; **553**: 413-418

13 **Kalaydjieva L,** Gresham D, Gooding R, Heather L, Baas F, de Jonge R, Blechschmidt K, Angelicheva D, Chandler D, Worsley P, Rosenthal A, King RH, Thomas PK. N-myc downstream-regulated gene 1 is mutated in hereditary motor and sensory neuropathy-Lom. *Am J Hum Genet* 2000; **67**: 47-58

14 **Wunderlich V,** Rajewsky MF. "Tumor suppressor gene" concept of carcinogenesis. *Lancet* 1995; **345**: 1570-1571

Edited by Chen WW **Proofread by** Zhu LH and Xu FM

PO Box 2345, Beijing 100023, China
Fax: +86-10-85381893
E-mail: wjg@wjgnet.com www.wjgnet.com

World J Gastroenterol 2004;10(23):3522-3527
World Journal of Gastroenterology
Copyright © 2004 by The WJG Press ISSN 1007-9327

• BRIEF REPORTS •

Involvement of extracellular signal-regulated kinase/mitogen-activated protein kinase pathway in multidrug resistance induced by HBx in hepatoma cell line

Jian Guan, Xiao-Ping Chen, Hong Zhu, Shun-Feng Luo, Bin Cao, Lei Ding

Jian Guan, Xiao-Ping Chen, Hong Zhu, Shun-Feng Luo, Bin Cao, Lei Ding. Hepatic Surgery Center, Tongji Hospital, Tongji Medical College, Huazhong University of Science and Technology, Wuhan 430030, Hubei Province, China
Supported by the Key Clinic Programs of Ministry of Public Health, No. 2001-2003
Correspondence to: Xiao-Ping Chen, M.D., Professor and Chairman, Department of Surgery, Tongji Hospital, Tongji Medical College, Huazhong University of Science and Technology, Wuhan 430030, Hubei Province, China. chenxp_53@163.com
Telephone: +86-27-83662599 **Fax:** +86-27-83662851
Received: 2004-04-24 **Accepted:** 2004-05-13

Abstract

AIM: To investigate the molecular mechanism of the influence of HBx protein on multidrug resistance associated genes: multidrug resistance 1 (MDR-1), multidrug related protein (MRP-1), lung resistance related protein (LRP) in hepatoma cells and the potential role of extracellular signal-regulated kinase/mitogen-activated protein kinase (ERK/MAPK) pathway in this process.

METHODS: A cell model stably expressing the HBx protein was established by liposome-mediated transfection of HBx gene into HepG2 cell line. The expression of multidrug resistance associated genes and proteins was detected by RT-PCR and Western blot. AnnexinV-FITC/PI assay was used to confirm the multidrug resistance (MDR) phenotype of transfected cells by fluorescence cytometry (FACS). The ERK/MAPK pathway activation was measured by Western blot through comparing the ratio of phosphorylation of ERK/MAPK to total ERK/MAPK protein. After treated with the ERK/MAPK pathway inhibitor U0126, the HBx-expressing cells were harvested. Then RT-PCR, Western blot and FACS were used to analyze the alterations in the expression of multidrug resistance associated genes and the MDR phenotype after exposure.

RESULTS: Compared with the control group, the transfected cells showed a higher expression of MDR associated genes and proteins. Marked elevations in MDR-1 (64.3%), MRP-1 (87.5%) and LRP (90.8%) were observed in the transfected cells ($P<0.05$). RT-PCR revealed that the over-expression of MDR associated proteins was due to amplification of such genes (MDR1 2.9 fold, MRP1 1.67 fold, LRP1.95 fold). Furthermore, we found that the ERK/MAPK activity was remarkably high in the HBx-expressing cells. The activation of ERK/MAPK, as measured by the ratio of phosphorylated ERK bands normalized to the total ERK bands, was increased by 2.3-fold in HBx-transfected cells compared with cells transfected with the empty vector. After treated with the ERK/MAPK pathway inhibitor, the level of MDR associated genes and proteins in the transfected cells decreased to some extent. Compared with controls, a significant decrease in MDR-1 mRNA (53.3%), MRP-1 mRNA (59.7%) as well as LRP mRNA (56.4%) was observed in the U0126 treated transfected cells after 12 h. Western blot also demonstrated that the protein expression of these MDR associated genes slightly reduced after treated with U0126 for 12 h (MDR-1 40.1%, MRP-1 29.4%, LRP35.7%). This change was accompanied with the rise of cell apoptosis ratio confirmed by Annexin V-PI detection. The apoptosis index of U0126-treated cells increased by 1.28 fold, compared with that of transfected cells. Obviously, the MDR phenotype of these cells was obviously related with increased activities of the ERK/MAPK pathway.

CONCLUSION: HBx protein might be one of the causes for the occurrence of MDR in HCC, and ERK/MAPK pathway might be involved in this change.

Guan J, Chen XP, Zhu H, Luo SF, Cao B, Ding L. Involvement of extracellular signal-regulated kinase/mitogen-activated protein kinase pathway in multidrug resistance induced by HBx in hepatoma cell line. *World J Gastroenterol* 2004; 10(23): 3522-3527

http://www.wjgnet.com/1007-9327/10/3522.asp

INTRODUCTION

Hepatocellular carcinoma (HCC) is one of the most common cancers in China and approximately 90% of HCC cases in this region are associated with hepatitis B virus (HBV) infection[1,2]. The mechanism underlying the development of HCC is still unclear. X gene, a unique open reading frame of HBV, codes for a 16.5 kd protein (X protein, HBx)[3]. There is evidence that HBx is an essential viral protein with pleiotropic activity that might act directly or indirectly on development of hepatocellular carcinoma during chronic hepadnavirus infection[4,5]. Over-expression of HBx induces transformation of some cell types[6].Additionally, it has been reported that HBx is involved in the arrest of cell cycle progression and the modulation of apoptosis [7,8]. HBx protein also interacts with the tumor suppressor *p53*, resulting in a loss of its function[9]. Due to its cytosolic localization, HBx has been shown to participate in a wide range of cellular signal transduction cascades, including Ras-Raf-mitogen-activated protein kinase, *c-Jun N*-terminal kinase, NF-kB and Janus kinase (*JAK*) -signal transducer and activator transcription factor (STAT) pathway[10-12]. It is well-known that tumor cells may avoid the death fate because apoptotic signals generated by the chemotherapeutic agents fail to activate the necessary pathways required to initiate apoptosis. Therefore, such survival signal pathways whose activation has been shown to play an anti-apoptotic role after treatment with various chemotherapeutic drugs have become the focus of recent researches. The mitogen-activated protein kinase (MAPK) family has emerged as one of such important membrane-to-nucleus signaling mechanisms of HBx, functioning as a mediator of cellular responses to a variety of cellular stimuli[13]. The MAPK family has been classified into 3 distinct subfamilies: the extracellular signal-relulated protein

kinases (ERKs) including ERK1 and ERK2, the stress-activated *c-Jun N*-terminal protein kinase (JNKs) and *p38* kinase[13]. Resistance to a broad spectrum of chemotherapeutic agents in cancer cells is called MDR[15]. The MDR phenotype is associated with the increased drug efflux from cells that is mediated by an energy-dependent mechanism and the blockade of the apoptosis-inducing pathway, the latter is the highlight of research nowadays. The results of experiments aiming at exploring the role of HBx on apoptosis pathways, however, are controversial and thence disappointed[15,16]. So we became more interested in determining whether these signal pathways were involved in the development of MDR, and investigated the potential role of MAPK pathways in multidrug resistance induced by HBx in hepatoma cells.

MATERIALS AND METHODS

Reagents

Dulbecco's modified Eagle's medium (DMEM), fetal bovine serum (FBS), lipofectamine 2 000 and G418 were purchased from Invitrogen Inc. ERK/MAPK pathway inhibitor U0126, was purchased from Alexis Inc. Anti-phospho-ERK_1/ERK_2 rabbit polyclonal antibody was purchased from RD systems. Anti-ERK_1/ERK_2 rabbit polyclonal antibody was purchased from Biovision Inc. Polyclonal antibody to multidrug related protein (MRP-1), was from Alexis Inc. Lung resistance-related protein (LRP) mouse antibody, multidrug resistance 1 (MDR-1) mouse antibody and pan actin antibody-5 were provided by Neomarker Inc. Dimethyl sulfoxide (DMSO) was purchased from Sigma.

Cell lines and cell culture

Human hepatocellular carcinoma cell line, HepG2 (GDC024) was purchased from the China Center for Type Culture Collection (Wuhan University, Hubei). Cells were maintained in DMEM supplemented with 100 mL/L heat-inactivated FBS at 37 ℃ in a humid atmosphere containing 50 mL/L CO_2.

Plasmids and stable transfection

The expression vector pcDNA3-HBx (a kindly gift from Lian-Rui Zhao, PhD; Thomas Jefferson University, USA) was constructed by inserting HBx DNA fragments between the *Hin*dIII and *Kpn*1 cloning sites of the pcDNA3 vector. After amplification in *DH-5*α, we used the EZNA plasmid maxiprep kit (OMEGA, USA) to purify the plasmids. HepG2 cells at 70-80% confluence were transfected with plasmids, using lipofectamine 2 000 (Life Technologies, Inc.). Plasmid transfections were performed according to protocols supplied with the reagents. At 48 h post-transfection, cells were split at a 10:1 ratio and cultured in the presence of 800 g/L G418. After 21 d in selective medium, individual G418-resistant colonies were isolated. Expression of HBx in various cell lines was verified by RT-PCR and Western Blot. The control cell line (HepG2/pcDNA) was generated from cells transfected with the vector alone and selected using G418. After isolation of resistant clones, the concentration of G418 was changed to 400 μg/mL

Reverse transcriptase-PCR

Total cellular RNA of the stably transfected HepG2 cells was extracted with Trizol (Life Technologies, Grand Island, NY) according to the manufacturer's instructions and reverse transcribed into cDNA with 2 units of Moloney murine leukemia virus reverse transcriptase (MMLV-RT; MBI Fermentas Inc., Amherst, New York, USA), 4 μL of 10 mmol/L dNTPs (Fermentas, Inc.), 2 μL of oligo (dT),10 μL of 5X reaction buffer (Fermentas Inc.), 2 μL of ribonuclease inhibitor and 26 μL of deionized water for 90 min at 37 ℃. PCR was performed with 100 ng of cDNA in a 50 mL reaction volume containing 20 mmol/L Tris, pH 8.0, 50 mmol/L KCl, 2 mmol/L MgCl2, 10 mmol/L of each dNTP, 20 pmoL of each primer, and 1.25 units of *Taq* DNA polymerase (Fermentas, Inc.). The profile was 94 ℃ for 5 min before 25 cycles at 94 ℃ for 45 s, at Ta for 45 s, at 72 ℃ for 55 s, and a final extension at 72 ℃ for 10 min. All amplification products were separated on agarose gels and visualized by ethidium bromide staining under *uv* transillumination.

The primers used for semi-quantitative PCR were: sense 5'-TCT CCG TCT GCC GTT CCA -3'and antisense 5'-TCG GTC GTT GAC ATT GCT G-3' for HBx; sense 5'-TGA AGG ACT TCG TGT CAG CC-3 and antisense 5'-GTC CATGAT GGT GTT GAG CC-3' for MRP-1; sense 5'- CAT TGG TGT GGT GAG TCA GG-3' and antisense 5'-CTC TCT CTC CAA CCA GGG TG-3' for MDR-1;sense 5'-TAA GGG CTT CCA GCA CCA AC-3' and antisense 5'-GGA GTT CTC GCT TCT CGT CC -3' for LRP and sense 5'-GTG CGT GAC ATT AAG GAG-3' and antisense 5'-CTA AGT CAT AGT CCG CCT-3' for β-actin.

Protein preparation and Western blot analyses

Stably transfected HepG2 cells were rinsed with 0.01 mol/L PBS, and then lysed in a lysis buffer containing 50 mmol/L Tris-HCL (pH 8.5), 150 mmol/L NaCL, 0.2 g/L NaN3, 0.1 g/L SDS, 100 μg/mL PMSF, 1 μg/mL aprotinin, 10 mL/L NP-40, 5 g/L sodium deoxycholate. The products were centrifuged at 14 000 *g* for 15 min to remove the cellular debris. Protein concentrations were determined by the Bradford methods. A total of 50-100 μg of protein was separated by electrophoresis using 60 g/L or 100 g/L sodium dodecyl sulfate-polyacrylamide gels (according to the molecular mass of target protein), transferred to a immuno-blot NC membrane, blocked with degreased milk for 12 h and hybridized with polyclonal antibodies for MRP-1, LRP, MDR-1, p-ERK and ERK (each diluted to 1:1000) at 4 ℃ overnight. The membranes were then washed 4 times for 15 min incubation with TBST (10 mmol/L Tris-Cl, pH 7.4, 150 mmol/L NaCl, 10 mL/L Tween 20 and hybridized with peroxidase (HRP) -conjugated secondary antibodies corresponding to each primary antibody. Protein banding specifically to the antibodies was visualized by ECL-associated fluorography (Pierce Inc.).

Cell viability and apoptosis analysis by fluorescence cytometry (FACS)

Cells were plated and grown overnight until they reach 80% confluence, then the cells were treated with 20 μg/mL 5-Fu. Subsequently, detached cells in the medium were collected, and the remaining adherent cells were released by trypsinization. The cells were washed with phosphate-buffered saline (PBS) and resuspended in 250 μL binding buffer (annexinV-FITC kit; BD) containing 5 μL of annexin V-FITC stock and 10 μL of 20 μg /mL propidium iodide (PI) for the determination of phosphatidylserine (PS) exposure on the outer plasma membrane. After incubated for 10 min at room temperature in a light protected area, the samples were analyzed by a Becton Dickinson fluorescence cytometer using CellQuest software. We could discriminate intact cells ($annexin^-/PI^-$) from apoptotic cells ($annexin^+/PI^-$) and necrotic cells ($annexin^+/PI^+$) after treatment with 5-Fu.

Statistical analyses

The results were expressed as mean±SE. Student's *t* test was used to compare data. $P<0.05$ was considered statistically significant. All data were processed by SPSS10.0.

RESULTS

Isolation and identification of HBx-expressing cells

As shown in Figure 1, the restriction enzyme digestions demonstrated that the digestion products had exactly the expected size (about 500 bp). We also requested Shanghai Bioasia Biotechnology Inc to sequence the whole plasmid kindly gifted by Lian-Rui Zhao (Ph.D), and the result of sequencing was consistent with the sequence of V0866 in GeneBank.

After stable transfection, the cells of different groups were confirmed for the expression of HBx by using PCR and immunoprecipitaion. The identification of the successful transfection at mRNA and protein levels is shown in Figure 2 and Figure 3, respectively. The expected bands could be seen in the HBx-expressing cells and the groups treated with ERK/MAPK signal pathway inhibitors. There was no detectable band in the control group. These results indicated that HBx was successfully transferred and expressed in HepG2 cells.

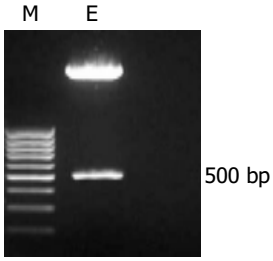

Figure 1 Restriction enzyme digestions of the plasmids. Lane M: markers (the brightest band of the marker presents the 500 bp); lane E: one of the split bands emerged at the exact position of 500 bp, and the other was the empty pcDNA3.0 vector as expected.

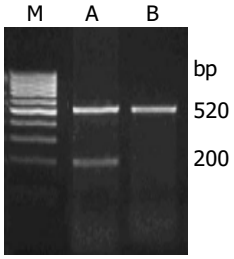

Figure 2 Confirmation of the successful transfection of HBx into HepG2 cells by RT-PCR. Lane M: markers (the brightest band of the marker presents the 500 bp); lane A: transfected cells; lane B: transfected cells treated with U0126; lane C: the control.

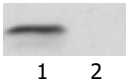

Figure 3 Western blot analysis of HBx protein in samples isolated from HepG2 cells with or without HBx transfection. Lane 1: the sample transfected with HBx; lane 2: the sample transfected with vector only.

Verification of MDR phenotype in HBx-expressing cells

To evaluate the effect of HBx introduction on the chemosensitivity of HepG2 cells, we initially used a FACS analysis of cells stained with PI and annexinV-FITC assay to compare the survival and apoptosis ratio of HepG2 cells transfected with empty pcDNA3.0 with *HBx*-transfected cells, i.e., HepG2/pcDNA and HepG2/pcDNA-HBx, after their exposure to 5-Fu (20 μg/mL) for 12 h and then cultured in normal medium for 6 h. Apoptosis index was quantified by a Becton Dickinson fluorescence cytometer. The apoptosis ratio in transfected cells (9.83±1.5%) analyzed by CellQuest software after administration of 5-Fu was significantly lower than that of the control (17.79±1.7%) (Figure 4). MTT assay also demonstrated that the inhibitory concentration 50% (IC_{50}) of adriamycin in the transfected cells was higher than that of the control (data not shown). The multidrug resistance transporter MDR-1, MRP-1, and LRP were associated with multidrug resistance. Western blot analysis was performed to examine whether the resistance to 5 Fu-induced apoptosis in HBx-expressing cells was due to the alterations of such proteins. Marked elevations in MDR-1 protein (64.3%), MRP-1 (87.5%) and LRP (90.8%) proteins were observed in the transfected cells (Figure 5 and Tables 1-2), which were well correlated with the degree of resistance. Furthermore, semi-quantitive RT-PCR revealed that over-expression of MDR-associated proteins was due to amplification of such genes (1.9-fold MDR-1, 0.67-fold MRP-1, 0.95-fold LRP) (Figure 6). Taken together, these data suggested that reintroduction of HBx contributed to the development of MDR phenotype.

Table 1 Protein level of MDR associated genes (mean±SD)

Group	MDR-1	MRP-1	LRP
transfected	0.23±0.04	0.15±0.03	0.17±0.03
control	0.14±0.03	0.08±0.03	0.09±0.02
P	0.036	0.046	0.018

Table 2 mRNA level of MDR associated genes (mean±SD)

Group	MDR-1	MRP-1	LRP
Transfected	0.29±0.06	0.62±0.11	0.82±0.15
Control	0.10±0.03	0.37±0.09	0.42±0.07
P	0.038	0.012	0.014

ERK/ MAPK pathway levels and activities in transfected cells

To assess the role of ERK/MAPK in HBx-induced activation of *MDR*1 expression, we measured the phosphorylation of ERK/MAPK in cells transfected with HBx. As shown in Figure 6, the phosphorylation of ERK/MAPK as measured by the ratio of the phosphorylated ERK bands (Figure 7A) normalized to the total ERK band (Figure 7B), was increased by 2.3-fold in HBx-transfected cells compared with control cells. These results suggested that the MDR phenotype induced by HBx was accompanied with the activation of ERK/MAPK pathways.

Effect of ERK/MAPK pathway inhibitors on MDR of HBx-expressing hepatpma cells

Based on the constitutive activation of ERK/MAPK, we determined whether U0126, a specific ERK inhibitor, could give rise to alterations in the expression of MDR associated genes and increase the transfected cell sensitivity to the cytotoxicity of 5-Fu .Treatment of transfected cells with U0126 decreased the levels of MDR-1 mRNA, as well as LRP and MRP-1 mRNA (Tables 3-4). Compared with controls, a significant decrease in MDR-1 mRNA (53.3%), MRP-1 mRNA (59.7%) as well as LRP mRNA (56.4%) was observed in U0126 treated transfected cells after 12 h. Western blot also demonstrated that the protein expression of these MDR associated genes was slightly reduced after treated with U0126 for 12 h (MDR-1 40.1%, MRP-1 29.4%, LRP35.7%).The apoptosis index of U0126-treated cells increased by 1.28 fold, compared with that of transfected cells. All these observations proved that U0126 could impair the MDR phenotype induced by HBx and sensitize cells to the toxicity of 5-Fu.

Table 3 Changes of MDR related genes after treated with U0126 (mean±SD)

Group	MDR-1	MRP-1	LRP
Transfected	0.15±0.03	0.62±0.11	0.78±0.13
Treated with U0126	0.08±0.02	0.37±0.09	0.44±0.09
P	0.028	0.040	0.020

Table 4 Changes of MDR related proteins after treated with U0126 (mean±SD)

Group	MDR-1	MRP-1	LRP
Transfected	0.22±0.04	0.17±0.02	0.14±0.02
Treated with U0126	0.13±0.04	0.12±0.02	0.09±0.02
P	0.04	0.038	0.04

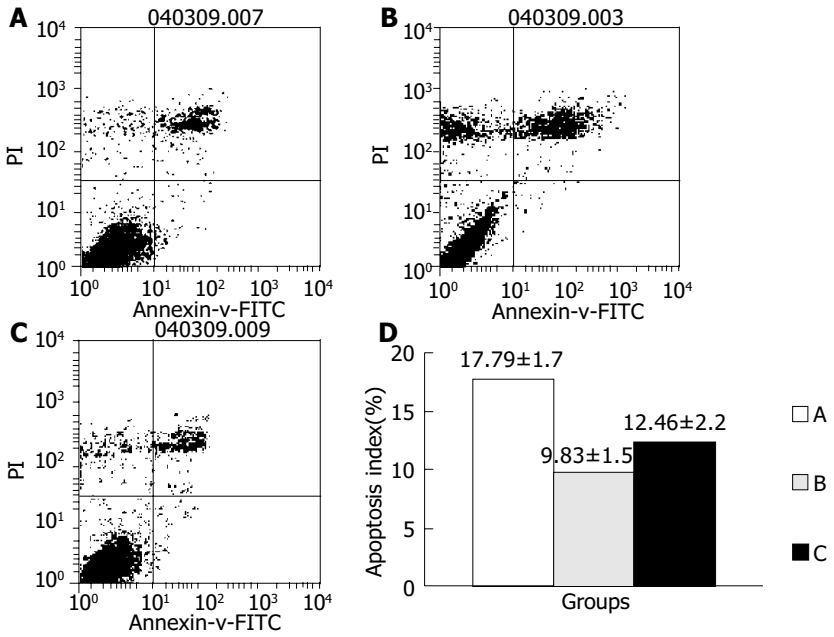

Figure 4 Apoptosis index of three different groups of cells after treatment with 5-Fu. A: HepG2/pcDNA3 cells; B: HepG2/pcDNA3-HBx cells; C: U0126 pretreated transfected cells. D: Apoptotic index quantitated by FACS.

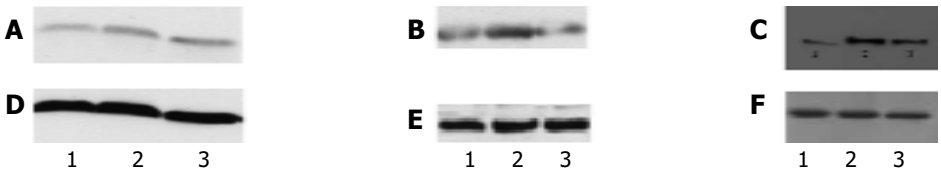

Figure 5 Protein levels of MDR associated genes in different groups of cells. Lane1: HepG2/pcDNA3 cells; lane2: HepG2/pcDNA3-HBx cells; lane3: transfected cells treated with U0126. The primary antibody for A, B, C, D was β-actin, MDR-1, MRP-1 and LRP respectively.

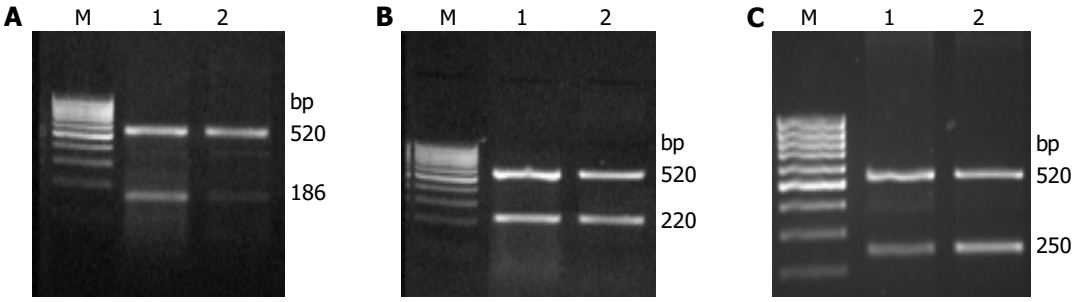

Figure 6 RT-PCR analysis of the expression of MDR associated genes in transfected and control cells. Lane 1: HBx-expressing cells; lane 2: control cells; lane M: markers. A: Specific primers to amplify MDR-1 gene; B: Specific primers to amplify MRP-1 gene; C: Specific primers to amplify LRP gene.

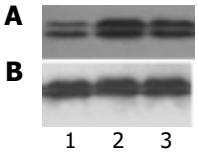

Figure 7 Increased phosphorylation of ERK induced by HBx in hepatoma cells analyzed by Western blot. Lane 1: transfected cells after treated with U0126; lane 2: HBx-expressing cells ; lane 3: control cells. A: Specific antibody for phosphorylated-ERK; B: Specific antibody for total ERK.

DISCUSSION

MDR was the leading cause of failure to comprehensive therapy of HCC[17]. Although the detailed molecular mechanisms of MDR remain to be explored, the disorder of anti-apoptotic and pro-apoptotic signal pathways and the over-expression of certain efflux proteins are generally believed to be due to MDR phenotype[18]. HBV infection is known as one of the most important risk factors in HCC development. Among the proteins coded by HBV genome, HBx has been proved to play a central role in virus duplication and carcinogenesis[2]. According to previous study, HBx could participate in several pathological processes of the generation and growth of HCC[2,4]. Apart from interfering with the suppressing function of *p53*, HBx could act as a multi-functional transcriptional transactivator to stimulate some important signal pathways. The effects of HBx on such signal pathways as ERK/MAPK, JNK, NF-kB and Src have been well-documented, especially in the aspect of apoptotic signals[16,19]. However, the pathological implications of these complex interactions in the evolvement of HCC malignant phenotypes have not been fully understood.

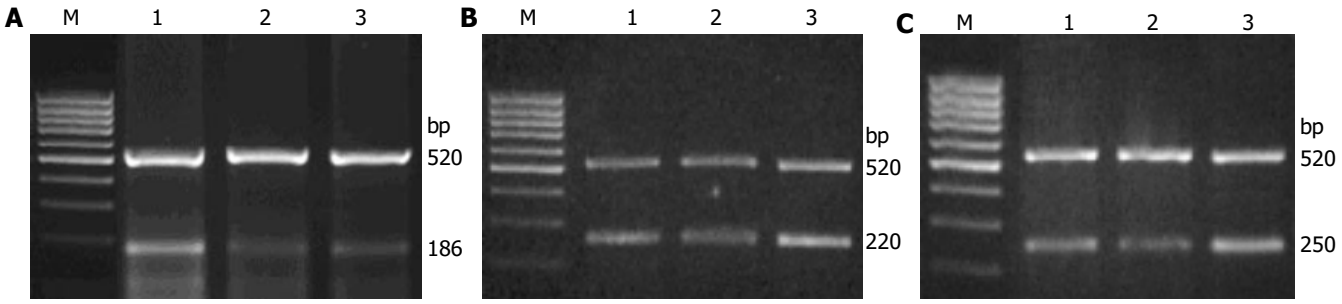

Figure 8 RT-PCR analysis of the expression of MDR associated genes in HBx-expressing cells in response to treatment of U0126. Lane 1: HBx-expressing cells; lane 2: control cells; lane 3: transfected cells treated with U0126; lane M: marker. A: Specific primers to amplify MDR-1 gene; B: Specific primers to amplify MRP-1 gene; C: Specific primers to amplify LRP gene.

In this study, we investigated the influence of HBx protein on MDR associated proteins and the potential role of ERK/ MAPK pathways in this process. Our data provided the evidence that HBx up-regulated the expression of MDR associated genes. Similar changes were witnessed in protein level. Our results indicated that HBx protein was a survival factor that could protect transfected cells from death induced by anti-tumor drugs in a constitutive expression system. Subsequent studies showed that HBx protein contributed to the MDR phenotype which was confirmed by apoptosis detection through FCAS. Furthermore, we demonstrated that the ERK/MAPK pathway worked as a downstream effector of HBx, mediating the MDR phenotype in the ERK/MAPK signal transduction pathway which was activated in HBx-expressing cells. To further confirm our previous hypothesis that the MAPK signal pathway played an important role in the MDR phenotype induced by HBx protein, we examined whether MAPK inhibited by U0126 (20 μmol/L, 12 h) could alter the phenotype of MDR. The experimental results showed that P-glycoprotein (product of the *MDR-1* gene) mediated MDR of transfected cells is reduced by the treatment of such inhibitors, which supports corroborated our presumption.

Among the myriads of intracellular signaling molecules regulated by HBx, ERK/MAPK plays an important role in regulating several cellular processes, such as proliferation and differentiation[20]. Several studies suggested that ERK/MAPK was involved in the acquired resistance of cancer cells to cytostatic drugs[22,23]. Kisucka *et al.* reported that the effect of PD98059 and UO126 on vincristine resistance of L1210/VCR cells, suggesting that both substances were reversing agents of P-glycoprotein-mediated MDR, and the role of ERK-mediated phosphorylation cascades in the occurrence of MDR should be considered. Dent *et al*.[25] also demonstrated that the activation of the ERK/ MAPK pathway played a critical role in leukemia cell survival after treatment with chemotherapeutic drugs and ionizing radiation. As shown in our experiment, the up-regulation of P-glycoprotein expression might be one of the mechanisms by which HBx induces the MDR phenotype. This result was consistent with the data reported by Chen *et al*.[26], who pointed out in his recent paper that inhibitors of the ERK/MAPK signal pathway could remarkably inhibited the expression of MDR-1. Barancik *et al*.[27]also suggested that SB203580, a specific inhibitor of the *p38*/MAPK pathway, could reverse the resistance of L1210/VCR cells mainly via P-glycoprotein dependent mechanisms. However, we could not exclude the possibility that ERK/MAPK activated by HBx could enhance the activity of P-glycoprotein (product of the *MDR-1* gene) by phosphorylation. P-glycoprotein is a phosphorylation substrate for a number of protein kinases including protein kinase C (PKC), MAPK, phospholipase C (PLC) *etc*[28,29]. Therefore, phosphorylation of such MDR related proteins might be another function of ERK/MAPK pathwayd during MDR induced by HBx protein. The influence of phosphorylation by such protein kinases as PKC or MAPK on the activity of MDR-1 protein and other MDR associated proteins is the target of our ensuing experiments in order to obtain a thorough understanding of the molecular mechanisms of interactions between HBx and MDR associated proteins.

In summary, MAPK pathway is involved in generation of MDR phenotype in hepatoma cells. The findings reported in this work might contribute to the understanding of pathogenic mechanisms involved in malignant phenotypes of HBV-associated hepatocellular carcinoma.

ACKNOWLEDGEMENTS

We thank Professor Lian-Rui Zhao (Ph.D, Thomas Jefferson University, USA) for his gift of plasmids and useful suggestions during the whole experiment. We are also grateful to Dr. Ji-Xiong Chen and Miss Shan-Shan Huang for their kind help and critical discussion.

REFERENCES

1 **Block TM,** Mehta AS, Fimmel CJ, Jordan R. Molecular viral oncology of hepatocellular carcinoma. *Oncogene* 2003; **22**: 5093-5107

2 **Birrer RB,** Birrer D, Klavins JV. Hepatocellular carcinoma and hepatitis virus. *Ann Clin Lab Sci* 2003; **33**: 39-54

3 **Koike K,** Tsutsumi T, Fujie H, Shintani Y, Kyoji M. Molecular mechanism of viral hepatocarcinogenesis. *Oncology* 2002; **62** (Suppl 1): 29-37

4 **Murakami S.** Hepatitis B virus X protein: a multifunctional viral regulator. *World J Gastroenterol* 2001; **36**: 651-660

5 **Wang T,** Wang Y, Wu MC, Guan XY, Yin ZF. HBsAg and HBx knocked into the p21 locus causes hepatocellular carcinoma in mice. *Hepatology* 2004; **39**: 318-324

6 **Jung EY,** Kang HK, Chang J, Yu DY, Jang KL. Cooperative transformation of murine fibroblast NIH3T3 cells by hepatitis C virus core protein and hepatitis B virus X protein. *Virus Res* 2003; **94**: 79-84

7 **Oh JC,** Jeong DL, Kim IK, Oh SH. Activation of calcium signaling by hepatitis B virus-X protein in liver cells. *Exp Mol Med* 2003; **35**: 301-309

8 **Li D,** Chen X, Zhang W. The inhibition of apoptosis of hepatoma cells induced by HBx is mediated by up-regulation of survivin expression. *J Huazhong Univ Sci Technol Med Sci* 2003; **23**: 383-386

9 **Wang XW.** Microinjection technique used to study functional interaction between p53 and hepatitis B virus X gene in apoptosis. *Mol Biotechnol* 2001; **18**: 169-177

10 **Yun C,** Cho H, Kim SJ, Lee JH, Park SY, Chan GK, Cho H. Mitotic aberration coupled with centrosome amplification is induced by hepatitis B virus X oncoprotein via the Ras-mitogen-activated protein/extracellular signal-regulated kinase-mitogen-activated protein pathway. *Mol Cancer Res* 2004; **2**: 159-169

11 **Diao J,** Khine AA, Sarangi F, Hsu E, Iorio C, Tibbles LA, Woodgett JR, Penninger J, Richardson CD. X protein of hepatitis B virus inhibits Fas-mediated apoptosis and is associated with up-regulation of the SAPK/JNK pathway. *J Biol Chem* 2001; **276**: 8328-8340
12 **Yoo YG,** Oh SH, Park ES, Cho H, Lee N, Park H, Kim DK, Yu DY, Seong JK, Lee MO. Hepatitis B virus X protein enhances transcriptional activity of hypoxia-inducible factor-1alpha through activation of mitogen-activated protein kinase pathway. *J Biol Chem* 2003; **278**: 39076-39084
13 **Nijhara R,** Jana SS, Goswami SK, Rana A, Majumdar SS, Kumar V, Sarkar DP. Sustained activation of mitogen-activated protein kinases and activator protein 1 by the hepatitis B virus X protein in mouse hepatocytes *in vivo*. *J Virol* 2001; **75**: 10348-10358
14 **Hilger RA,** Scheulen ME, Strumberg D. The Ras-Raf-MEK-ERK pathway in the treatment of cancer. *Onkologie* 2002; **25**: 511-518
15 **Fojo T,** Bates S. Strategies for reversing drug resistance. *Oncogene* 2003; **22**: 7512-7523
16 **Terradillos O,** de La Coste A, Pollicino T, Neuveut C, Sitterlin D, Lecoeur H, Gougeon ML, Kahn A, Buendia MA. The hepatitis B virus X protein abrogates Bcl-2-mediated protection against Fas apoptosis in the liver. *Oncogene* 2002; **21**: 377-386
17 **Schuster R,** Hildt E, Chang SF, Terradillos O, Pollicino T, Lanford R, Gerlich WH, Will H, Schaefer S. Conserved transactivating and pro-apoptotic functions of hepadnaviral X protein in ortho- and avihepadnaviruses. *Oncogene* 2002; **21**: 6606-6613
18 **Huesker M,** Folmer Y, Schneider M, Fulda C, Blum HE, Hafkemeyer P. Reversal of drug resistance of hepatocellular carcinoma cells by adenoviral delivery of anti-MDR1 ribozymes. *Hepatology* 2002; **36**(4 Pt 1): 874-884
19 **Tsuruo T.** Molecular cancer therapeutics: recent progress and targets in drug resistance. *Intern Med* 2003; **42**: 237-243
20 **Shih WL,** Kuo ML, Chuang SE, Cheng AL, Doong SL. Hepatitis B virus X protein activates a survival signaling by linking SRC to phosphatidylinositol 3-kinase. *J Biol Chem* 2003; **278**: 31807-31813
21 **Chang F,** Steelman LS, Lee JT, Shelton JG, Navolanic PM, Blalock WL, Franklin RA, McCubrey JA. Signal transduction mediated by the Ras/Raf/MEK/ERK pathway from cytokine receptors to transcription factors: potential targeting for therapeutic intervention. *Leukemia* 2003; **17**: 1263-1293
22 **Ding S,** Chamberlain M, McLaren A, Goh L, Duncan I, Wolf CR. Cross-talk between signalling pathways and the multidrug resistant protein MDR-1. *Br J Cancer* 2001; **85**: 1175-1184
23 **Fan M,** Chambers TC. Role of mitogen-activated protein kinases in the response of tumor cells to chemotherapy. *Drug Resist Updat* 2001; **4**: 253-267
24 **Kisucka J,** Barancik M, Bohacova V, Breier A. Reversal effect of specific inhibitors of extracellular-signal regulated protein kinase pathway on P-glycoprotein mediated vincristine resistance of L1210 cells. *Gen Physiol Biophys* 2001; **20**: 439-444
25 **Dent P,** Jarvis WD, Birrer MJ, Fisher PB, Schmidt-Ullrich RK, Grant S. The roles of signaling by the p42/p44 mitogen-activated protein (MAP) kinase pathway; a potential route to radio- and chemo-sensitization of tumor cells resulting in the induction of apoptosis and loss of clonogenicity. *Leukemia* 1998; **12**: 1843-1850
26 **Chen B,** Jin F, Lu P, Lu XL, Wang PP, Liu YP, Yao F, Wang SB. Effect of mitogen-activated protein kinase signal transduction pathway on multidrug resistance induced by vincristine in gastric cancer cell line MGC803. *World J Gastroenterol* 2004; **10**: 795-799
27 **Barancik M,** Bohacova V, Kvackajova J, Hudecova S, Krizanova O, Breier A. SB203580, a specific inhibitor of p38-MAPK pathway, is a new reversal agent of P-glycoprotein-mediated multidrug resistance. *Eur J Pharm Sci* 2001; **14**: 29-36
28 **Miao ZH**, Ding J. Transcription factor c-Jun activation represses mdr-1 gene expression. *Cancer Res* 2003; **63**: 4527-4532
29 **Ros JE,** Schuetz JD, Geuken M, Streetz K, Moshage H, Kuipers F, Manns MP, Jansen PL, Trautwein C, Muller M. Induction of Mdr1b expression by tumor necrosis factor-alpha in rat liver cells is independent of *p53* but requires NF-kappaB signaling. *Hepatology* 2001; **33**: 1425-1431

Edited by Wang XL and Kumar M **Proofread by** Xu FM

PO Box 2345, Beijing 100023, China
Fax: +86-10-85381893
E-mail: wjg@wjgnet.com www.wjgnet.com

World J Gastroenterol 2004;10(23):3528-3530
World Journal of Gastroenterology
Copyright © 2004 by The WJG Press ISSN 1007-9327

• BRIEF REPORTS •

Effect of environmental hyperthermia on gastrin, somatostatin and motilin in rat ulcerated antral mucosa

Feng-Peng Sun, Yu-Gang Song

Feng-Peng Sun, Yu-Gang Song, Department of Gastroenterology, Nanfang Hospital, First Military Medical University, Guangzhou 510515, Guangdong Province, China
Supported by Guangdong Provincial Natural Science Foundation, No.010578, Key Technological Program of Guangzhou, No.2002Z3-E0131 and Key Program in Social Development of Guangdong Province, No.2002C31210
Correspondence to: Dr. Feng-Peng Sun, Department of Gastroenterology, Nanfang Hospital, First Military medical University, Guangzhou 510515, Guangdong Province, China. phd@china.com
Telephone: +86-20-61648215 **Fax:** +86-20-61648216
Received: 2003-05-12 **Accepted:** 2003-06-07

Abstract

AIM: To study the effect of environmental hyperthermia on gastrin, somatostatin and motilin in rat ulcerated antral mucosa.

METHODS: Forty-two Wistar rats were equally divided into six groups, according to the room temperature (high and normal) and the treatment (acetic acid, normal saline and no treatment). Levels of gastrin, somatostatin and motilin in rat ulcerated antral mucosa were measured with a radioimmunoassay method.

RESULTS: The average temperature and humidity were 32.5 ℃ and 66.7% for the high temperature group, and 21.1 ℃ and 49.3% for the normal temperature group, respectively. Gastric ulcer model was successfully induced in rat injected with 0.05 mL acetic acid into the antrum. In rats with gastric ulcers, the levels of gastrin and motilin increased, whereas the somatostatin level declined in antral mucosa, compared with those in rats treated with normal saline and the controls. However, the change extent in the levels of gastrin, motilin and somatostatin in antral mucosa was less in the high temperature group than in the normal temperature group.

CONCLUSION: The levels of gastrin, somatostatin and motilin in rat ulcerated antral mucosal tissue remain relatively stable in a high temperature environment, which may relate to the equilibration of the dynamic system.

Sun FP, Song YG. Effect of environmental hyperthermia on gastrin, somatostatin and motilin in rat ulcerated antral mucosa. *World J Gastroenterol* 2004; 10(23): 3528-3530
http://www.wjgnet.com/1007-9327/10/3528.asp

INTRODUCTION

The abnormal secretion of gastrointestinal hormones such as gastrin, somatostatin, motilin may affect the function of alimentary tract[1,2]. In a high temperature living environment, body could develop adaptation reaction to hyperthermia, meanwhile induces a series of compensatory regulations in the central nervous system and endocrine system[3-8], the content of gastrointestinal hormones could be changed accordingly. Our experiment investigated the influence of ambient temperature on gastrin, somatostatin, motilin in rat ulcerated antral mucosa and their biological significance.

MATERIALS AND METHODS

Animals and preparation

We used healthy adult male Wistar rats weighing 200-260 g (purchased from Experimental Animal Center, Sun Yat-Sen University of Medical Sciences). The rats were raised in our Experimental Animal Center and fed with standard rat chow. The rats were randomly divided into six groups of seven rats each, respectively. They were high temperature ulcer group, normal temperature ulcer group, high temperature saline group, normal temperature saline group, high temperature control group, normal temperature control group. The room temperature of the hyperthermia group was not interfered, but that of the normal group was controlled by airconditioning.

Radioimmunoassay kits of gastrin and motilin were purchased from Tianjin Qianye Biotech Co. Ltd, and the kits of somatostatin from Department of Neurobiology of Second Military Medical University.

The temperature of the animal houses was measured by catathermometer (produced by Shanghai Medical Instrument Factory) at 8:00 and 20:00 everyday, the relative humidity was converted through the scale at the base of the catathermometer, and average values of dry bulb temperature and relative humidity were recorded. The dry bulb temperature (℃) in houses on the d 0, 1, 2, 3 after model-making and the day of rat sacrifice was 31.7, 32.5, 33.0, 32.8, 32.4 (average 32.5±0.5) for the high temperature group, and 21.2, 21.1, 21.0, 21.3, 21.1 (average 21.1±0.1) for the normal temperature group, respectively. The relative humidity (%) was 58.0, 65.5, 69.0, 76.0, 65.0 (average 66.7±6.6) for the high temperature group and 46.5, 48.0, 51.5, 53.0, 47.5 (average 49.3±2.8) for normal temperature group, respectively.

Establishment of rat model and measurement of gastrin, somatostatin and motilin

The rats of high temperature ulcer group and normal temperature ulcer group were anesthetized with 30 g/L sodium pentobarbital intraperitoneally. The abdomen was opened and 0.05 mL acetic acid was injected into the antral tissues. Omentum majus and antral tissue of the injection site were stitched. The peritoneum, parietal abdomen and ventral muscle, and skin were stitched continually. The rats of high temperature saline group and normal temperature saline group were injected with 0.05 mL saline instead of acetic acid at the same site. The rats of control group did not receive any treatment. After operation, the model-making rats were raised separately, and fasted overnight with free access to water one day before sacrifice. No treatment was given to normal control group. The rat stomach was separated and split from the greater curvature, and mucosa of gastric antrum was scraped about 0.1 g to be boiled after weighed on electronic analytical balance. The boiled tissue was homogenized into homogenates in a homogenizer with 1 mL of 1 mol/L acetic acid and neutralized

with 1 mL of 1 mol/L NaOH, the liquid of homogenates was centrifuged at 3 500 r/min for 15 min to obtain supernatant, and the samples were then stored at -70 ℃ until assay. Gastrin, somatostatin and motilin were measured by using radioimmunoassay (RIA) method, measurement procedures were performed according to the instructions attached to the kits. The unit of result was transformed to ng/g.

Statistical analysis

Data among the groups were analyzed with factorial analysis of variance by SPSS 10.0 software. The comparison between the two means of different groups was analyzed by Student-Newman-Keuls. $P<0.05$ was considered statistically significant.

RESULTS

Observation of gross specimens

Gastric contents of the rats in high temperature and normal temperature ulcer groups obviously increased, the diameter of round shape ulcers on the frontal wall of gastric antrum was about 0.5-0.7 cm, the center of the ulcer was pale covered with offwhite membrane, the base was flat with clear verge, and the mucosa around the ulcer had hyperemia and edema. Gastric contents of the rats in the other groups were suitable, mucosa plica of gastric antrum was obvious, and its color was pale red without hyperemia and edema. There was no ulcer on the surface.

Level of gastrin in rat antral mucosa of each group

The difference of gastrin level in antral mucosa between ulcer group and nonulcer group was significant (F = 9.500, $P = 0.000$), gastrin levels in ulcer group (average 5.99 ng/g) were higher than those in control group (3.68 ng/g) and saline group (3.98 ng/g). But the differences in gastrin levels among the groups were insignificant in high and normal temperature groups (F = 1.465, $P = 0.234$). There was no mutual effect between the two treatment factors of ulcer and temperature (F = 0.980, $P = 0.385$). The gastrin level in ulcerated antral mucosa increased significantly ($P<0.01$). But the level of gastrin in antral mucosa in the high temperature ulcer group increased less than that in the normal temperature ulcer group ($P<0.05$) (Table1).

Table 1 Gastrin in rat antral mucosa (n=7, ng/g, mean±SD)

Group	Ulcer	Normal saline	Control
HT	5.24±1.65	3.91±1.31	3.64±1.15[b]
NT	6.73±2.29[a]	4.04±1.28	3.71±1.13

[a]$P<0.05$, *vs* high temperature ulcer group [b]$P<0.01$ *vs* ulcer group.

Level of somatostatin in rat antral mucosa of each group

The difference of somatostatin level in antral mucosa between ulcer group and nonulcer group was significant (F=15.087, $P = 0.000$), somatostatin levels in ulcer group (average 0.62 ng/g) were less than those in control group (1.37 ng/g) and saline group (1.24 ng/g). But the differences of somatostatin levels were insignificant in high and normal temperature groups (F = 2.789, $P = 0.104$). There was no mutual effect between the two treatment factors of ulcer and temperature (F = 1.416, $P = 0.256$). The level of somatostatin in gastric ulcerated antral mucosa declined significantly ($P<0.01$). But the level of somatostatin in antral mucosa in the high temperature ulcer group declined less than that in the normal temperature ulcer group ($P<0.05$) (Table2).

Level of motilin in rat antral mucosa of each group

The difference of motilin level in antral mucosa between ulcer group and nonulcer group was significant (F = 18.178, $P = 0.000$), motilin levels in ulcer group (average 8.04 ng/g) were higher than those in control group (4.27 ng/g) and saline group (4.58 ng/g). But the differences of motilin levels were insignificant in high and normal temperature groups (F = 3.632, $P = 0.065$). There was no mutual effect between the two treatment factors of ulcer and temperature (F = 2.611, $P = 0.087$). The level of motilin in gastric ulcerated antral mucosa increased significantly ($P<0.01$). But the level of motilin in antral mucosa in the high temperature ulcer group increased less than that in the normal temperature ulcer group ($P<0.05$) (Table3).

Table 2 Somatostatin in rat antral mucosa (n = 7, ng/g, mean±SD)

Group	Ulcer	Normal saline	Control
HT	0.86±0.30	1.28±0.46	1.39±0.50[b]
NT	0.37±0.15[a]	1.19±0.41	1.36±0.41

[a]$P<0.05$, *vs* high temperature ulcer group [b]$P<0.01$ *vs* ulcer group.

Table 3 Motilin in rat antral mucosa (n = 7, ng/g, mean ± SD)

Group	Ulcer	Salt	Cont
HT	6.58±2.04	4.46±1.30	4.22±1.24[b]
NT	9.50±2.98[a]	4.70±1.43	4.31±1.40

[a]$P<0.05$, *vs* high temperature ulcer group [b]$P<0.01$ *vs* ulcer group.

DISCUSSION

Our experiment established the model of rat gastric ulcer. Gastrin, somatostatin and motilin were measured with the RIA method. The result revealed that gastrin and motilin in antral mucosa tissue increased, and somatostatin declined when the rats had gastric ulcer. Compensative changes of gastrointestinal tract and other organs took place to accommodate hyperthermia. Our experiment detected the level of gastrin, somatostatin and motilin in antral mucosa tissue of gastric ulcer rats in high and normal temperature environments. We discovered that the level of gastrin and motilin in antral mucosa in the high temperature ulcer group increased less than that in the normal temperature ulcer group, the level of somatostatin in the high temperature ulcer group declined less than that in the normal temperature ulcer group.

Complex changes of many cytokines in body occurred in heat stress environment[9-15]. Hyperthermia could change heat stress proteins (HSP), atrial natriuretic factor (ANF), angiotensin, nerve growth factor (NGF), cortisol and plasma protein, blood sugar, serum lipoprotein, microelement as well as body immune system correspondingly[16-20]. The system of neuroendocrine, cytokine and heat stress constituted an organic network, in which a chain in dynamic action could make internal milieu stable[21,22]. The result of this experiment indicates that the levels of gastrin, somatostatin and motilin in antral mucosa tissue remain relatively stable in a high temperature environment. This may relate to the equilibration of the dynamic system.

REFERENCES

1 **Kaminska B,** Kozielska E, Korzon M, Czaja M, Banach P. Bleeding from alimentary tract in pseudo Zollinger-Ellison syndrome. *Med Sci Monit* 2000; **6**: 596-601

2 **Ku SK,** Lee HS, Lee JH. An immunohistochemical study of endocrine cells in the alimentary tract of the red-bellied frog, Bombina orientalis. *J Vet Med Sci* 2000; **62**: 589-594

3 **de Freitas MS,** Spohr TC, Benedito AB, Caetano MS, Margulis B, Lopes UG, Moura-Neto V. Neurite outgrowth is impaired on HSP70-positive astrocytes through a mechanism that requires NF-kappaB activation. *Brain Res* 2002; **958**: 359-370

4 **Pacheco-Lopez G,** Espinosa E, Zamorano-Rojas HM, Ramirez-Amaya V, Bermudez-Rattoni F. Peripheral protein immuniza-

tion induces rapid activation of the CNS, as measured by c-Fos expression. *J Neuroimmunol* 2002; **131**: 50-59

5 **Deng X,** Jayanthi S, Ladenheim B, Krasnova IN, Cadet JL. Mice with partial deficiency of c-Jun show attenuation of methamphetamine-induced neuronal apoptosis. *Mol Pharmacol* 2002; **62**: 993-1000

6 **Fernandez F,** Aguerre S, Mormede P, Chaouloff F. Influences of the corticotropic axis and sympathetic activity on neurochemical consequences of 3,4-methylenedioxymethamphetamine (MDMA) administration in Fischer 344 rats. *Eur J Neurosci* 2002; **16**: 607-618

7 **Watanabe YG.** Immunohistochemical study on the fetal rat pituitary in hyperthermia-induced exencephaly. *Zoolog Sci* 2002; **19**: 689-694

8 **Khan VR,** Brown IR. The effect of hyperthermia on the induction of cell death in brain, testis, and thymus of the adult and developing rat. *Cell Stress Chaperones* 2002; **7**: 73-90

9 **Nelson EA,** Wong Y, Yu LM, Fok TF, Li K. Effects of hyperthermia and muramyl dipeptide on IL-1beta, IL-6, and mortality in a neonatal rat model. *Pediatr Res* 2002; **52**: 886-891

10 **Mearow KM,** Dodge ME, Rahimtula M, Yegappan C. Stress-mediated signaling in PC12 cells-the role of the small heat shock protein, Hsp27, and Akt in protecting cells from heat stress and nerve growth factor withdrawal. *J Neurochem* 2002; **83**: 452-462

11 **Henderson RF,** Barr EB, Blackwell WB, Clark CR, Conn CA, Kalra R, March TH, Sopori ML, Tesfaigzi Y, Menache MG, Mash DC. Response of rats to low levels of sarin. *Toxicol Appl Pharmacol* 2002; **184**: 67-76

12 **Suganuma T,** Irie K, Fujii E, Yoshioka T, Muraki T. Effect of heat stress on lipopolysaccharide-induced vascular permeability change in mice. *J Pharmacol Exp Ther* 2002; **303**: 656-663

13 **Nambiar MP,** Fisher CU, Enyedy EJ, Warke VG, Kumar A, Tsokos GC. Oxidative stress is involved in the heat stress-induced downregulation of TCR zeta chain expression and TCR/CD3-mediated [Ca(2+)](i) response in human T-lymphocytes. *Cell Immunol* 2002; **215**: 151-161

14 **Wang Y,** Li C, Wang X, Zhang J, Chang Z. Heat shock response inhibits IL-18 expression through the JNK pathway in murine peritoneal macrophages. *Biochem Biophys Res Commun* 2002; **296**: 742-748

15 **DuBose DA,** Balcius J, Morehouse D. Heat stress and/or endotoxin effects on cytokine expression by human whole blood. *Shock* 2002; **17**: 217-221

16 **Hildebrandt B,** Wust P, Ahlers O, Dieing A, Sreenivasa G, Kerner T, Felix R, Riess H. The cellular and molecular basis of hyperthermia. *Crit Rev Oncol Hematol* 2002; **43**: 33-56

17 **Roigas J,** Wallen ES, Loening SA, Moseley PL. Estramustine phosphate enhances the effects of hyperthermia and induces the small heat shock protein HSP27 in the human prostate carcinoma cell line PC-3. *Urol Res* 2002; **30**: 130-135

18 **van den Berg AP,** van den Berg-Blok AE, Kal HB, Reinhold HS. A moderate elevation of blood glucose level increases the effectiveness of thermoradiotherapy in a rat tumor model II. Improved tumor control at clinically achievable temperatures. *Int J Radiat Oncol Biol Phys* 2001; **50**: 793-801

19 **Afek A,** Keren G, Harats D, George J. Whole body hyperthermia accelerates atherogenesis in low-density lipoprotein receptor deficient mice. *Exp Mol Pathol* 2001; **71**: 63-72

20 **Ben-Hur T,** Cialic R, Itzik A, Barak O, Yirmiya R, Weidenfeld J. A novel permissive role for glucocorticoids in induction of febrile and behavioral signs of experimental herpes simplex virus encephalitis. *Neuroscience* 2001; **108**: 119-127

21 **Michael GJ,** Priestley JV. Differential expression of the mRNA for the vanilloid receptor subtype 1 in cells of the adult rat dorsal root and nodose ganglia and its downregulation by axotomy. *J Neurosci* 1999; **19**: 1844-1854

22 **Dux M,** Sann H, Schemann M, Jancso G. Changes in fibre populations of the rat hairy skin following selective chemodenervation by capsaicin. *Cell Tissue Res* 1999; **296**: 471-477

Edited by Ma JY and Wang XL **Proofread by** Xu FM

PO Box 2345, Beijing 100023, China
Fax: +86-10-85381893
E-mail: wjg@wjgnet.com www.wjgnet.com

World J Gastroenterol 2004;10(23):3531-3533
World Journal of Gastroenterology
Copyright © 2004 by The WJG Press ISSN 1007-9327

• BRIEF REPORTS •

Effects of selenium on peripheral blood mononuclear cell membrane fluidity, interleukin-2 production and interleukin-2 receptor expression in patients with chronic hepatitis

Shui-Xiang He, Bing Wu, Xin-Ming Chang, Hong-Xia Li, Wen Qiao

Shui-Xiang He, Xin-Ming Chang, Hong-Xia Li, Wen Qiao, Department of Gastroenterolgy, First Hospital of Xi'an Jiaotong University, Xi'an 710061, Shaanxi Province, China
Bing Wu, Editorial Department of Journal of Xi'an Jiaotong University, Xi'an 710061, Shaanxi Province, China
Correspondence to: Dr. Shui-Xiang He, Department of Gastroenterolgy, First Hospital of Xi'an Jiaotong University, Xi'an 710061, Shaanxi Province, China. hesx123@163.net
Telephone: +86-29-5324001 **Fax:** +86-29-85221659
Received: 2003-12-19 **Accepted:** 2004-01-12

Abstract

AIM: To study the effect of selenium on peripheral blood mononuclear cell (PBMC) membrane fluidity and immune function in patients with chronic hepatitis.

METHODS: PBMCs were pretreated with selenium (1.156×10^{-7} mol/L) for 6 h *in vitro* or extracted directly from patients after administration of selenium-yeast continuously for 8-12 wk (200 μg/d), and then exposed to Con-A for 48 h. The membrane fluidity, interleukin-2 (IL-2) production and interleukin-2 receptor (IL-2R) expression in PBMCs and malondialdehyde (MDA) concentration in medium and lipid peroxide (LPO) in plasma were determined.

RESULTS: The PBMC membrane fluidity, IL-2 production and IL-2R expression in patients with chronic hepatitis were significantly lower than those in healthy blood donators (particle adhesive degree R, 0.17±0.01 *vs* 0.14±0.01, $P<0.01$; IL-2, 40.26±9.55 *vs* 72.96±11.36, $P<0.01$; IL-2R, 31.05±5.09 *vs* 60.58±10.56, $P<0.01$), and the MDA concentration in medium in patients with chronic hepatitis was significantly higher than that in healthy blood donators (1.44±0.08 *vs* 0.93±0.08, $P<0.01$). Both *in vitro* and *in vivo* administration of selenium could reverse the above parameters.

CONCLUSION: Supplement of selenium can suppress lipid peroxidation, and improve PBMC membrane fluidity and immune function in patients with chronic hepatitis.

He SX, Wu B, Chang XM, Li HX, Qiao W. Effects of selenium on peripheral blood mononuclear cell membrane fluidity, interleukin-2 production and interleukin-2 receptor expression in patients with chronic hepatitis. *World J Gastroenterol* 2004; 10(23): 3531-3533
http://www.wjgnet.com/1007-9327/10/3531.asp

INTRODUCTION

Hepatic viruses attack immune cells thus leading to cell immune functional disorders, which is one of the major mechanisms of chronic hepatitis[1-4]. It is currently believed that the damage of immune cells caused by lack of the minor elements of selenium, proliferation of free particles and peroxidization of lipid are probably associated with cell immune functional disorders in patients with chronic hepatitis[5-9]. The use of anti-oxidants could contribute to improving the psychopathologic process of chronic hepatitis, suppress cell immune functional disorders and accelerate the recovery of liver functions[10-112]. The minor elements of selenium have anti-oxidizing effects, and have been utilized in the immune regulation of many diseases, but the effect of selenium treatment on peripheral blood mononuclear cell (PBMC) functions in patients with chronic hepatitis is still unclear[13-15]. We found during our early work that using selenium in the periphery could improve the inlerleukin-2 production of PBMCs and IL-2R expression in patients with chronic hepatitis[16]. By examining the changes of PBMC membrane fluidity, interleukin-2 (IL-2) and its receptor system in patients with chronic hepatitis before and after using selenium, We further explored the effects and mechanism of selenium treatment on the cell immune functions in patients with chronic hepatitis.

MATERIALS AND METHODS

Patients

A total of 45 patients with chronic hepatitis were inpatients of our hospital from 1995 to 1997, among them 38 were males and 7 females, aged 21-52 years. The HBsAg of 30 patients with chronic hepatitis and 15 patients with cirrhosis was positive. The diagnosis was in accordance with the readjust standards of the National Academic Conference of Viral Hepatitis held in Shanghai in 1990. Besides, ten healthy blood donators were chosen as the control group.

Peripheral experiment

Elbow venous blood was taken from fasting healthy blood donators. Then PBMCs were routinely separated and floated in the RPMI-1640 culture medium. Then cell density was adjusted to 1×10^6/L and 1 mL of cell suspension was added into each well of 24-well culture plates, and randomly divided into control group, tBHP damage inducing group, and selenium treatment group. In addition, PBMCs were taken and divided into 4 patient control group and 5 patient selenium group. $NaSeO_2$ (final density, 1.156×10^{-7} mol/L) was added into groups 3 and 5, each of the rest groups was added with the same amount of culture liquid followed by incubation for 6 h, and con A (5 mg/L) were added. Meanwhile, lipoperoxide inducing agents tBHP (20 μmol/L) were added into groups 2 and 3, and cultured at 37 ℃ for 48 h in a humidified atmosphere containing 50 mL/L CO_2.

Clinical treatment and survey

The patients were divided into two groups. The normal group was given bifendate pills and Fufangyiganling. Some individual patients were given compound ammonium glycyrrhetate injection and Qinkailing injection intravenously. Selenium treatment group, on the basis of the routine treatment, was given selenium yeast or selenium amylase (200-300 μg/d) orally for 8 to 12 wk. At the beginning of and after the treatment, blood was collected from the patients to separate PBMCs and to measure the blood plasma.

Measurement of induced IL-2 production and its activation

Each group of PBMCs was added with con-A (5 mg/L, Sigma) and cultured at 37 ℃ in a humidified atmosphere containing 50 mL/L CO_2. IL-2 activation expressed in 1×10^3 U/L was measured.

Measurement of IL-2R expression

The cells of each group, after induction and production of IL-2, were collected to measure IL-2R expression by indirect immune fluorescence and the positive rate was expressed as percentage of positive cells.

Measurement of lipid peroxidation

The supernatant from each group or patients' blood plasma was subjected to the measurement of MDA or LPO content by using microflorescence technique.

Measurement of membrane fluidity

The cells of each group were suspended in the RPMI-1640 culture medium to a cell density of 1×10^6/L. The same amount of 2×10^{-6} mol/L fluorescence probing agents DPH (sigma product) was added and cultured at 25 ℃ for 30 min. The polarization deviation degree (P) was measured under the condition of 432 nm (transmitting light) /362 nm (irritating light) on MPF-4 polarization meter and the particle adhesive degree (R) was calculated. The value of R and membrane fluidity were in inverse proportion.

Statistical analysis

All the data were expressed as mean±SD, and analyzed by *t*-test and ANOVA analysis. $P<0.05$ was considered statistically significant.

RESULTS

Effects of selenium on IL-2 activation and IL-2R expression in human PBMCs

As shown in Table 1, after PBMCs in normal group were treated with tBHP, both IL-2R expression and IL-2 secreting activity were significantly declined, which was similar to those of the patient group. Six hours after addition of selenium, the above-mentioned changes in the cells of these two groups were obviously inhibited.

Table 1 Influence of selenium on IL-2 and IL-2R expression (mean±SD)

Groups	Cases	IL-2 activation (1×10^3 U/L)	IL-2R expression (%)
Normal control group	10	72.96±11.36	60.58±10.56
+tBHP	10	42.12±12.06[b]	37.05±8.06[b]
+Selenium+tBHP	10	53.26±18.15[a]	52.12±9.68[a]
Patient control group	22	40.26±9.55[b]	31.05±5.09[b]
Patients+selenium	23	60.32±15.24[c]	54.06±5.22[c]

[b]$P<0.01$ *vs* normal control group; [a]$P<0.05$ *vs* tBHP inducing damage group; [c]$P<0.05$ *vs* patient control group.

Influence of selenium on PBMC membrane fluidity

As shown in Table 2, after PBMCs in normal group were treated with tBHP, the amount of MDA increased and the membrane fluidity obviously lowered. The PBMC membrane fluidity of the patient group was also significantly lower than that of the normal control group. Six hours after addition of selenium, the above-mentioned changes could be obviously inhibited.

Changes in IL-2R expression and IL-2 secreting activity of PBMCs of patients before and after selenium treatment

As shown in Table 3, after treatment with selenium, both the IL-2R expression and IL-2 secreting activity of PBMCs were significantly increased, while the content of MDA in the culture media was obviously decreased compared with the groups without selenium treatment ($P<0.05$).

Table 2 Influence of selenium on PBMC membrane fluidity (mean±SD)

Groups	Cases	R	MDA (μmol/L)
Normal control group	10	0.14±0.01	0.93±0.08
+tBHP	10	0.19±0.02[b]	2.32±0.25[b]
+Selenium+tBHP	10	0.16±0.02[a]	1.36±0.09[a]
Patient control group	22	0.17±0.01[b]	1.44±0.08[b]
Patients+selenium	23	0.15±0.01[c]	1.21±0.09[c]

[b]$P<0.01$ *vs* normal control group; [a]$P<0.05$ *vs* tBHP inducing damage group; [c]$P<0.05$ *vs* patient control group.

Table 3 IL-2 and IL-2R expression in PBMCs of patients before and after selenium treatment (mean±SD)

Groups	Cases	IL-2 activation (1×10^3U/L)	IL-2R expression (%)
Before treatment			
Normal control group	22	43.22±9.25	31.24±5.20
Selenium treated group	23	42.26±9.55	31.05±5.09
After treatment			
Normal control group	18	49.45±15.25	35.12±6.49
Selenium treated group	17	60.32±13.28[a]	46.05±4.46[b]

[b]$P<0.01$ *vs* before treatment.

Changes in PBMC membrane fluidity of patients before and after selenium treatment

As shown in Table 4, the PBMC membrane fluidity recovered remarkably and the content of MDA in blood plasma decreased strikingly, whereas no significant changes were observed in the control group. The result was similar to that *in vitro* experiment.

Table 4 Effect on PBMC membrane fluidity of patients before and after selenium treatment (mean±SD)

Groups	Cases	R	Lipid peroxide (nmol/L)
Before treatment			
Normal control group	22	0.17±0.01	7.36±4.15
Selenium treated group	23	0.17±0.01	7.36±4.08
After treatment			
Normal control group	18	0.16±0.01	6.15±3.85
Selenium treated group	17	0.15±0.01[b]	5.02±2.50[b]

[b]$P<0.01$ *vs* before treatment.

DISCUSSION

Previous studies have shown that the activating oxidation or the organic peroxidation of the external chemical system could influence various functions of immune cells[15,17-19]. Our previous study demonstrated that PBMCs from the patients with chronic hepatitis showed significantly increased production of IL-2 and expression of IL-2R after warmed with selenium for 6 h[16]. In this experiment, our results showed that human PBMC producing IL-2 activation and IL-2R expression percentage obviously decreased after being induced by tertiary butyl peroxides. The content of lipoperoxide MDA in the culture liquid greatly increased, which was similar to the changes in PBMCs from chronic hepatitis B patients cultured *in vitro*. It was further reported that free particles and lipoperoxide receptor system probably associated with lipoperoxide reaction of

tertiary butyl peroxide could induce PBMC membranes, and thus resulting in changes of the normal structure and nature of PBMC membranes. Besides, some abnormal changes took place in receptors, enzymes and particle passages associated with the membranes, cell energy metabolism, signal transmission, proliferation, differentiation, *etc*, thereby finally leading to the organic disorder of PBMCs[20,21].

Fluidity, one of the basic characteristics of the membranes, is the basic precondition of cells showing various functions. In many pathologic cases, excessive free particles and initiating lipoperoxide could affect membrane fluidity and lead to disorder of cell immune functions[22-25]. Our results showed that PBMC membrane fluidity in normal group obviously decreased after treated with peroxide, and was accompanied by MDA increase in the culture supernatant. Moreover, PBMC membrane fluidity decreased and its IL-2-producing activity as well as IL-2R expression percentage changed unanimously, which was identical with the result of the cultured PBMCs from patients with chronic hepatitis. Abnormally strengthened lipoperoxide reactions could lead to decrease of PBMC membrane fluidity, which might be one of the causes of immune function disorder of patients with chronic hepatitis.

Studies shown that selenium influences immune cell functions through two ways[13-16,26]. On the one hand, selenium can affect the mRNA expression of some immune cell surface receptors, such as IL-2R, iron transporter protein receptor (TfR). On the other hand, it is associated with the functions of selenium anti-oxidization. Free particles can directly damage lymphocyte membranes and destroy their completeness and fluidity, thus restraining the expressions of their surface markers and immune functions. Selenium and enzymes in combination with selenium can inhibit cell membrane peroxidization damage and defend membrane fluidity as well as functional expression. In our experiment, the degree of membrane fluidity, IL-2 secretion and IL-2R expression of PBMCs caused by selenium still remained high. Meanwhile, the content of MDA in the culture supernatant was greatly decreased, suggesting that selenium might defend human PBMC membrane fluidity and its normal functional expression through lipoperoxidization damage induced by anti-tertiary butyl peroxide.

PBMCs and IL-2 system play an essential role in cell immune system of patients with chronic hepatitis, maintaining PBMC functions and correcting IL-2 system disorder, which is of great significance in treatment of chronic hepatitis[1-3]. It has been found that internal or external selenium can improve PBMC functions and increase Il-2 secretion and IL-2R expression percentage in patients with chronic hepatitis. It has been initially proved that selenium treatment is helpful to correct dysfunction of PBMCs in patients with chronic hepatitis, which is of great significance in the complete recovery of hepatic functions of patients.

REFERENCES

1 **Reshetnyak VI**, Sharafanova TI, Ilchenko LU, Golovanova EV, Poroshenko GG. Peripheral blood lymphocytes DNA in patients with chronic liver diseases. *World J Gastroenterol* 2001; **7**: 235-237

2 **Reshetnyak VI**, Sharafanova TI, Ilchenko LY, Poroshenko GG. DNA structure in peripheral blood lymphocytes from patients with chronic viral liver damages. *Bull Exp Biol Med* 2002; **133**: 399-400

3 **Wang JP**, Li XH, Zhu Y, Wang AL, Lian JQ, Jia ZS, Xie YM. Detection of serum sIL-2R, IL-6, IL-8, TNF-α and lymphocytes subsets, mIL-2R in patients with chronic hepatitis B. *Shijie Huaren Xiaohua Zazhi* 2000; **8**: 763-766

4 **Tulek N**, Saglam SK, Saglam M, Turkyilmaz R, Yildiz M. Soluble interleukin-2 receptor and interleukin-10 levels in patients with chronic hepatitis B infection. *Hepatogastroenterology* 2000; **47**: 828-831

5 **Yu MW**, Horng IS, Hsu KH, Chiang YC, Liaw YF, Chen CJ. Plasma selenium levels and risk of hepatocellular carcinoma among men with chronic hepatitis virus infection. *Am J Epidemol* 1999; **150**: 367-374

6 **Loguercio C**, De Girolamo V, Federico A, Feng SL, Crafa E, Cataldi V, Gialanella G, Moro R, Del Vecchio Blanco C. Relationship of blood trace elements to liver damage, nutritional status, and oxidative stress in chronic nonalcoholic liver disease. *Biol Trace Elem Res* 2001; **81**: 245-254

7 **Hatano R**, Ebara M, Fukuda H, Yoshikawa M, Sugiura N, Kondo F, Yukawa M, Saisho H. Accumulation of copper in the liver and hepatic injury in chronic hepatitis C. *J Gastroenterol Hepatol* 2000; **15**: 786-791

8 **Loguercio C**, Federico A. Oxidative stress in viral and alcoholic hepatitis. *Free Radic Biol Med* 2003; **34**1: 1-10

9 **Hoek JB**, Pastorino JG. Ethanol, oxidative stress, and cytokine-induced liver cell injury. *Alcohol* 2002; **27**: 63-68

10 **Naghii MR**. Sulfur mustard intoxication, oxidative stress, and antioxidants. *Mil Med* 2002; **167**: 573-575

11 **Marotta F**, Safran P, Tajiri H, Princess G, Anzulovic H, Ideo GM, Rouge A, Seal MG, Ideo G. Improvement of hemorheological abnormalities in alcoholics by an oral antioxidant. *Hepatogastroenterology* 2001; **48**: 511-517

12 **Cui YH**, Wang XL, Liu Q, Liu P. Influences of anti-oxidation of salvianolic acid B on proliferation of rat cultured hepatic stellate cells. *Shijie Huaren Xiaohua Zazhi* 2002; **10**: 317-319

13 **Kiremidjian-Schumacher L**, Roy M. Effect of selenium on the immunocompetence of patients with head and neck cancer and on adoptive immunotherapy of early and established lesions. *Biofactors* 2001; **14**: 161-168

14 **Jahnova E**, Horvathova M, Gazdik F, Weissova S. Effects of selenium supplementation on expression of adhesion molecules in corticoid-dependent asthmatics. *Bratisl Lek Listy* 2002; **103**: 12-16

15 **Lee CY**, Wan JM. Immunoregulatory and antioxidant performance of alpha-ocopherol and selenium on human lymphocytes. *Biol Trace Elem Res* 2002; **86**: 123-136

16 **He SX**, Chang XM, Zhou QS, Li HX, Wu YE. Effects of selenium on the IL-2 production and IL-2R expression of PBMC from patients with chronic active hepatitis B. *Shijie Huaren Xiaohua Zazhi* 1999; **7:** 658

17 **Lushpaeva IuA**, Medvedeva IV, Fadienko GR. Changes in clinical and laboratory findings on oxidation metabolism in lymphocyte membranes of rheumatoid arthritis patients on synchronous programmed intensive therapy. *Klin Med* 2002; **80**: 39-42

18 **Dey A**, Parmar D, Dhawan A, Dash D, Seth PK. Cytochrome P450 2E1 dependent catalytic activity and lipid peroxidation in rat blood lymphocytes. *Life Sci* 2002; **71**: 2509-2519

19 **Jobin N**, Garrel DR, Champoux J, Bernier J. Improved immune functions with administration of a low-fat diet in a burn animal model. *Cell Immunol* 2000; **206**: 71-84

20 **Maccarrone M**, Manca-di-Villahermosa S, Meloni C, Massoud R, Mascali A, Guarina R, Finazzi-Agro A, Taccone-Gallucci M. Arachidonate cascade, apoptosis, and vitamin E in peripheral blood mononuclear cells from hemodialysis patients. *Am J Kidney Dis* 2002; **40**: 600-610

21 **Azenabor AA**, Hoffman-Goetz L. Effect of exhaustive exercise on membrane estradiol concentration, intracellular calcium, and oxidative damage in mouse thymic lymphocytes. *Free Radic Biol Med* 2000; **1**: 84-90

22 **Gornicki A**, Gutsze A. Erythrocyte membrane fluidity changes in psoriasis: an EPR study. *J Dermatol Sci* 2001; **27**: 27-30

23 **Ferrante MC**, Meli R, Mattace Raso G, Esposito E, Severino L, Di Carlo G, Lucisano A. Effect of fumonisin B1 on structure and function of macrophage plasma membrane. *Toxicol Lett* 2002; **129**: 181-187

24 **Garcia JJ**, Reiter RJ, Karbownik M, Calvo JR, Ortiz GG, Tan DX, Martinez-Ballarin E, Acuna-Castroviejo D. N-acetylserotonin suppresses hepatic microsomal membrane rigidity associated with lipid peroxidation. *Eur J Pharmacol* 2001; **428**: 169-175

25 **Gornicki A**, Gutsze A. *In vivo* and *in vitro* influence of etretinate on erythrocyte membrane fluidity. *Eur J Pharmacol* 2001; **423**: 127-134

26 **Zhao R**, Zhang GC, Yu BM, Zheng MH, Li DH, Zhu YM, Hu BY. Effect of selenium on T lymphocyte against colonic cancer cells. *Shijie Huaren Xiaohua Zazhi* 2000; **8**: 80-83

Edited by Kumar M and Wang XL **Proofread by** Xu FM

PO Box 2345, Beijing 100023, China
Fax: +86-10-85381893
E-mail: wjg@wjgnet.com www.wjgnet.com

World J Gastroenterol 2004;10(23):3534-3536
World Journal of Gastroenterology
Copyright © 2004 by The WJG Press ISSN 1007-9327

• BRIEF REPORTS •

Successful management of a benign anastomotic colonic stricture with self-expanding metallic stents: A case report

Yong-Song Guan, Long Sun, Xiao Li, Xiao-Hua Zheng

Yong-Song Guan, Long Sun, Xiao Li, Xiao-Hua Zheng, Department of Radiology Huaxi Hospital, Sichuan University, Chengdu 610041, Sichuan Province, China
Correspondence to: Dr. Yong-Song Guan, Department of Radiology, Huaxi Hospital, Sichuan University, 37 Guoxuexiang, Chengdu 610041, Sichuan Province, China. yongsongguan@yahoo.com
Telephone: +86-28-85421008 **Fax:** +86-28-85421008
Received: 2004-02-11 **Accepted:** 2004-02-21

Abstract

AIM: To assess the effectiveness of and complications associated with metallic stent placement for treatment of anastomotic colonic strictures.

METHODS: A 46-year-old man underging two procedures of surgery for perforation of descending colon due to a traffic accident presented with pain, abdominal distention, and inability to defecate. Single-contrast barium enema radiograph showed a severe stenosis in the region of surgical anastomosis and the patient was too weak to accept another laparotomy. Under fluoroscopic and endoscopic guidance, we placed two metallic stents in the stenosis site of the anastomosis of the patient with anastomotic colonic strictures.

RESULTS: In this case of postsurgical stenosis, the first stent relieved the symptoms of obstruction, but stent migration happened on the next day so an additional stent was required to deal with the stricture and relieve the symptoms.

CONCLUSION: This case confirms that metallic stenting may represent an effective treatment for anastomotic colonic strictures in the absence of other therapeutic alternatives.

Guan YS, Sun L, Li X, Zheng XH. Successful management of a benign anastomotic colonic stricture with self-expanding metallic stents: A case report. *World J Gastroenterol* 2004; 10(23): 3534-3536
http://www.wjgnet.com/1007-9327/10/3534.asp

INTRODUCTION

Self-expandable metallic stent treatment for colorectal diseases was falling behind that for other organs. Recently, however, there have been many reports on the use of self-expanding metallic stents in colorectal diseases, mainly from the West. Self-expanding metallic stent is generally used as a palliative treatment for malignant strictures of the colon and rectum and before bridge as a surgery for obstructing colorectal cancers[1-3]. Some investigators have reported on the usefulness of self-expanding metallic stents for strictures of benign diseases[4,5]. Management of narrow (<5-mm) colonic anastomotic stricture mainly is performed endoscopically by repeated balloon dilation, often ineffectively[6]. The use of metallic self-expanding stents in malignant and benign strictures of the large bowel has been suggested only recently, and is still being debated[7,8]. In this report we proposed a single-stage procedure that we developed to manage narrow anastomotic colonic strictures.

CASE REPORT

A 46-year-old man underging two procedures of surgery for perforation of descending colon due to a traffic accident presented with pain, abdominal distention, and inability to defecate. Single-contrast barium enema radiograph showed a severe stenosis in the region of surgical anastomosis. The patient was too weak to accept another laparotomy. He reached us with a significant stricture of the descending colon anastomoses (smaller than 5 mm in diameter).

With the patient in supine position and two knee joints reflexing, a catheter was inserted over a hydrophilic guide-wire through the anus to the lesion targeted under fluoroscopic and endoscopic guidance. An 85-cm 6-F catheter (Cook) and a 180-cm 0.35-inch guide wire (Bard) were used. The guide wire was maneuvered passing the stricture and the catheter was advanced. This guide wire was then replaced with another guide wire (Amplatz super stiff Guide Wire) for stent delivery and insertion. The stent was then positioned precisely across the lesion and released. The symptoms were released immediately, but on the next day the patient manifested abdominal distention, and inability to defecate. Anteroposterior radiographs from a follow-up barium study showed the stent migrated and a second stent was needed. The second stent was deployed with the same stent placement techniques. Radiographs obtained after a water-soluble enema on the day after the second stent deployed showed that the stents expanded to provide an adequate lumen (Figures 1-4). The first coated stent (Nanjing MicroTech, China) was 12-cm in length, 32-mm in diameter. The second uncoated stent (Nanjing MicroTech, China) was 20-cm in length, 32-mm in diameter. At the time of this writing, ie, 18 mo of follow-up evaluation, the patient could defecate without any difficulty.

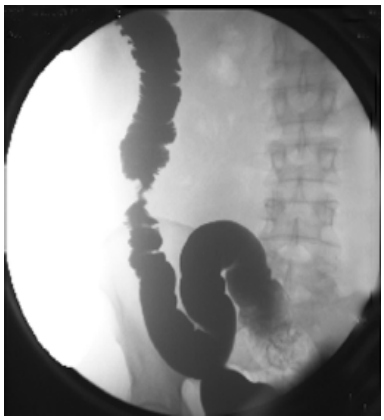

Figure 1 Stenosis at the segment of descending colon, less than 5 mm in diameter.

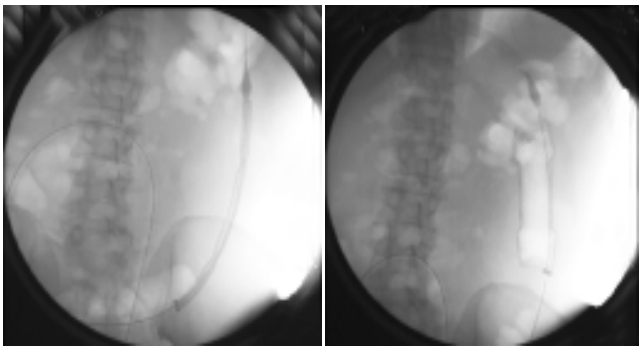

Figure 2 The first stent was appropriately positioned and deployed by withdrawing the enveloping membrane under fluoroscopic control to ensure that the lesion was adequately covered, thus relieving the obstruction.

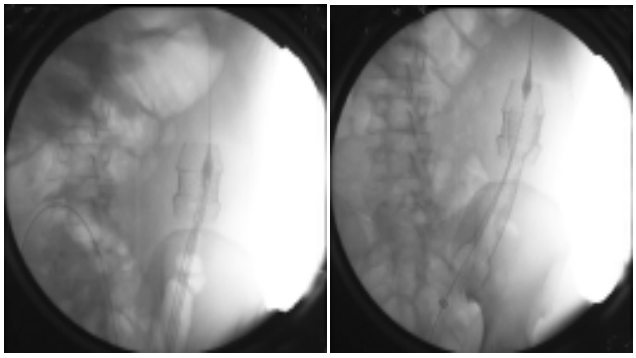

Figure 3 Clinical symptoms of obstruction recurred the next day. Anteroposterior radiographs showed the stent migrated above the lesion and a second stent was needed. Second stent was deployed with the same stent placement techniques through the lumen of the first stent.

Figure 4 Radiograph obtained after a water-soluble enema on the day after the second stent was deployed shows that the stents expanded to provide an adequate lumen.

DISCUSSION

Benign postoperative anastomotic strictures are frequent[9]. Several methods of treatment for benign anastomotic strictures after previous resection have been described, including microwave coagulation therapy, balloon and endoscopic bougie dilation, *etc*[10-14]. Placement of self-expanding metallic stents across narrower anastomotic colonic strictures is a viable alternative to colostomy and, by avoiding emergent surgery, could potentially lower morbidity and mortality[15-17]. The method of stent placement for treatment of benign colonic disorders is the same as that used in cases of malignant strictures, but few experiences with the placement of metallic stents for benign colonic disorders have been reported in the literatures. The indications for stenting were failure to establish dilatation therapy and/or refusal of surgical treatment, in high-risk patients[4-6].

In this case, the patient underwent two times of surgery and he was too weak to accept another surgery. Stenting might represent a therapeutic alternative, in cases of anastomotic strictures of esophageal carcinoma[18,19]. Endoprostheses may have a more lasting dilating effectiveness than balloons or endoscopic bougies, and the ease of recovering the stent when it has fulfilled its purpose could make treatment of the stenosis last for months or years[4-6].

Stent migration may be one of the most complications in treatment of anastomotic strictures. The stent tended to migrate once the stenosis was widened to a diameter at which it could no longer hold the prosthesis in place, and this phenomenon was followed by a recurrence of the clinical symptoms a few days later, which necessitated a series of interventions in these patients. The first stent migration happened and the second stent was needed to be placed in this case[20-22].

We conclude that the application of self-expandable metallic stents in benign stenosis of the gastrointestinal tract may be a possible therapeutic tool in selected patients. Further trials with a greater number of patients dealing with the questions of duration of stay of self-expandable metallic stents and choice of stent type are needed.

REFERENCES

1 **Saida Y,** Sumiyama Y, Nagao J. Self-expandable metallic stent in the treatment of colorectal obstruction. *Nippon Geka Gakkai Zasshi* 2003; **104**: 554-557

2 **Mainar A,** De Gregorio Ariza MA, Tejero E, Tobio R, Alfonso E, Pinto I, Herrera M, Fernandez JA. Acute colorectal obstruction: treatment with self-expandable metallic stents before scheduled surgery-results of a multicenter study. *Radiology* 1999; **210**: 65-69

3 **Miyayama S,** Matsui O, Kifune K, Yamashiro M, Yamamoto T, Kitagawa K, Kasahara Y, Asada Y, Iida Y, Miura S. Malignant colonic obstruction due to extrinsic tumor: palliative treatment with a self-expanding nitinol stent. *Am J Roentgenol* 2000; **175**: 1631-1637

4 **Paul L,** Pinto I, Gomez H, Fernandez-Lobato R, Moyano E. Metallic stents in the treatment of benign diseases of the colon: preliminary experience in 10 cases. *Radiology* 2002; **223**: 715-722

5 **Dormann AJ,** Deppe H, Wigginghaus B. Self-expanding metallic stents for continuous dilatation of benign stenoses in gastrointestinal tract-first results of long-term follow-up in interim stent application in pyloric and colonic obstructions. *Z Gastroenterol* 2001; **39**: 957-960

6 **Piccinni G,** Nacchiero M. Management of narrower anastomotic colonic strictures. Case report and proposal technique. *Surg Endosc* 2001; **15**: 1227

7 **Morgan R,** Adam A. Use of metallic stents and balloons in the esophagus and gastrointestinal tract. *J Vasc Interv Radiol* 2001; **12**: 283-297

8 **Chevallier P,** Baque P, Benchimol D, Bernard J, Souci J, Chevallier A, Bourgeon A, Padovani B. Treatement of colorectal obstruction with self-expanding metallic stents under fluoroscopic guidance. *J Radiol* 2002; **83**(4 Pt 1): 473-477

9 **Schlegel RD,** Dehni N, Parc R, Caplin S, Tiret E. Results of reoperations in colorectal anastomotic strictures. *Dis Colon Rectum* 2001; **44**: 1464-1468

10 **Takeuchi K,** Tsuzuki Y, Ando T, Sekihara M, Hara T, Kori T, Nakajima H, Asao T, Kuwano H. Usefulness of flexible colonoscopic microwave coagulation therapy for a colorectal anastomotic stricture. *Dis Colon Rectum* 2003; **46**: 1430-1435

11 **Luck A,** Chapuis P, Sinclair G, Hood J. Endoscopic laser stricturotomy and balloon dilatation for benign colorectal strictures. *ANZ J Surg* 2001; **71**: 594-597

12 **Chia YW,** Ngoi SS, Tung KH. Use of the optical urethrotome

knife in the treatment of a benign low rectal anastomotic stricture. *Dis Colon Rectum* 1991; **34**: 717-719

13 **Araki Y,** Kishimoto Y, Sato Y, Torigoe S, Kido K, Matono K, Shirouzu K. Transanal dilation using circular stapling for benign rectal stenosis: report of a case. *Kurume Med J* 2002; **49**: 149-151

14 **Brandimarte G,** Tursi A, Gasbarrini G. Endoscopic treatment of benign anastomotic colorectal stenosis with electrocautery. *Endoscopy* 2000; **32**: 461-463

15 **Wholey MH,** Levine EA, Ferral H, Castaneda-Zuniga W. Initial clinical experience with colonic stent placement. *Am J Surg* 1998; **175**: 194-197

16 **Mainar A,** Tejero E, Maynar M, Ferral H, Castaneda-Zuniga W. Colorectal obstruction: treatment with metallic stents. *Radiology* 1996; **198**: 761-764

17 **Kang SG,** Jung GS, Cho SG, Kim JG, Oh JH, Song HY, Kim ES. The efficacy of metallic stent placement in the treatment of colorectal obstruction. *Korean J Radiol* 2002; **3**: 79-86

18 **Wengrower D,** Fiorini A, Valero J, Waldbaum C, Chopita N, Landoni N, Judchack S, Goldin E. EsophaCoil: long-term results in 81 patients. *Gastrointest Endosc* 1998; **48**: 376-382

19 **Song HY,** Park SI, Do YS, Yoon HK, Sung KB, Sohn KH, Min YI. Expandable metallic stent placement in patients with benign esophageal strictures: results of long-term follow-up. *Radiology* 1997; **203**: 131-136

20 **Friedland S,** Hallenbeck J, Soetikno RM. Stenting the sigmoid colon in a terminally ill patient with prostate cancer. *J Palliat Med* 2001; **4**: 153-156

21 **Harris GJ,** Senagore AJ, Lavery IC, Fazio VW. The management of colorectal obstuction with colonicendolumenal stenting devices. *Am J Surg* 2001; **181**: 499-506

22 **Law WL,** Choi HK, Chu KW, Tung HM. Radiation stricture of rectosigmoid treated with self-expanding metallic stent. *Surg Endosc* 2002; **16**: 1106-1107

Edited by Wang XL **Proofread by** Zhu LH and Xu FM

PO Box 2345, Beijing 100023, China
Fax: +86-10-85381893
E-mail: wjg@wjgnet.com www.wjgnet.com

World J Gastroenterol 2004;10(23):3537-3541
World Journal of Gastroenterology
Copyright © 2004 by The WJG Press ISSN 1007-9327

• BRIEF REPORTS •

Cyclooxygenase 2, pS2, inducible nitric oxide synthase and transforming growth factor alpha in gastric adaptation to stress

Shi-Nan Nie, Hai-Chen Sun, Xue-Hao Wu, Xiao-Ming Qian

Shi-Nan Nie, Hai-Chen Sun, Xue-Hao Wu, Xiao-Ming Qian, Emergency Department, Nanjing General Hospital of Nanjing PLA Command Area/Clinical School of Medical college of Nanjing University, Nanjing 210002, Jiangsu Province, China
Correspondence to: Shi-Nan Nie, M.D., Emergency Department, Nanjing General Hospital of Nanjing PLA Command Area, 305 Eastern Zhongshan Road, Nanjing 210002, Jiangsu Province, China. shnnie630504@.sohu.com
Telephone: +86-25-80860143
Received: 2004-03-06 **Accepted:** 2004-04-16

Abstract

AIM: To determine the role of mucosal gene expression of cyclooxygenase 2 (COX-2), pS_2 (belongs to trefoil peptides), inducible nitric oxide synthase (iNOS) and transforming growth factor alpha (TGFα) in gastric adaptation to water immersion and restraint stress (WRS) in rats.

METHODS: Wistar rats were exposed to single or repeated WRS for 4 h every other day for up to 6 d. Gastric mucosal blood flow (GMBF) was measured by laser Doppler flowmeter-3. The extent of gastric mucosal lesions were evaluated grossly and histologically and expressions of COX-2, pS2, iNOS and TGFα were determined by reverse transcriptase polymerase chain reaction (RT-PCR) and Western blot.

RESULTS: The damage to the surface of gastric epithelium with focal areas of deep haemorrhagic necrosis was induced by repeated WRS.The adaptative cytoprotection against stress was developed with activation of cell proliferation in the neck regions of gastric glands. The ulcer index (UI) in groups II, III and IV was markedly reduced as compared with group I (I: 47.23±1.20; IV: 10.39±1.18, P<0.01). GMBF significantly decreased after first exposure to WRS with an adaptive increasement of GMBF in experimental groups after repetitive challenges with WRS. After the 4th WRS, the value of GMBF almost restored to normal level (I: 321.87±8.85; IV: 455.95±11.81, P<0.01). First WRS significantly decreased the expression of pS2 and significantly increased the expressions of COX-2, iNOS and TGFα. After repeated WRS, pS2 and TGFα expressions gradually increased (pS2: I: 0.37±0.02; IV: 0.77±0.01; TGFα: I: 0.86±0.01; IV: 0.93±0.03, P<0.05) with a decrease in the expressions of COX-2 and iNOS (COX-2: I: 0.45±0.02; IV: 0.22±0.01; iNOS: I: 0.93±0.01; IV: 0.56±0.01, P<0.01). Expressions of pS2, COX-2, iNOS and TGFα showed regular changes with a good relationship among them.

CONCLUSION: Gastric adaptation to WRS injury involves enhanced cell proliferation,increased expression of pS2 and TGFα, and reduced expression of COX-2 and iNOS. These changes play an important role in adaptation of gastric mucosa after repeated WRS.

Nie SN, Sun HC, Wu XH, Qian XM. Cyclooxygenase 2, pS2, inducible nitric oxide synthase and transforming growth factor alpha in gastric adaptation to stress. *World J Gastroenterol* 2004; 10(23): 3537-3541
http://www.wjgnet.com/1007-9327/10/3537.asp

INTRODUCTION

Gastric mucosa can enhance resistance to injury after exposure to repeated insults of noxious agents,such as aspirin, alcohol, stress or *H pylori*-related gastrotoxins. This phenomenon is called gastric adaptation[1]. It has been postulated that gastric adaptation involves enhancement of gastric blood flow and increased mucosal cell proliferation mediated by some growth factors,such as epidermal growth factor (EGF) or TGFα. The fact that the adaptation to stress is associated with increased cell proliferation let us to hypothesize that this process might be mediated by pS2, COX-2, iNOS and TGFα.

It is now well established that trefoil peptides have cytoprotective functions in protecting the gastrointestinal tract against ongoing damage from agents as diverse as ethanol, non-steroidal anti-inflammatory drugs and restraint stress[2]. The mechanism for this action is unclear. The pronounced and protracted increase in trefoil peptide expression in the inflamed and ulcerated stomach, intestine and colon implicates peptides in reparative processes of the injury gut. Studies reported that pS2 took part in the protracted phase of glandular renewal (marked by proliferation, differentiation and migration) [3]. TGFα, a 50 amino acid polypeptide produced in normal gastric mucosa, promotes cell proliferation, inhibits gastric acid secretion and exhibits gastroprotective activity against acute damage induced by topical irritants or stress[4]. In addition, an increased TGFα mRNA expression has been detected during healing of chronic experimental ulcers and acute damage of gastric mucosa in rats, suggesting its important role in gastric mucosal repair. Previous studies showed that COX-2 was an inducible enzyme. Recently, studies have suggested that COX-2 is a constitutive enzyme expressed in gastrointestinal tract also, even plays a more important role than COX-1 for mucosal integrity[5]. Gut epithelial COX-2 is rapidly induced by inflammatory stimuli, interleukin and TGFα. Suppression of COX-2 could result in exacerbation of inflammation-associated colonic injury, and impair the healing of gastric ulcer. It is generally accepted that nitric oxide (NO) plays an important role in gastric ulcer healing. NO production is highly increased by iNOS.

The aim of the present study was to determine the role of the expression of pS2, COX-2, iNOS and TGFα, and the relationship among them in gastric adaptation to WRS in rats.

MATERIALS AND METHODS

Induction of gastric adaptation to WRS

Thirty male Wistar rats, weighing 210-250 g and fasted for 24 h with free access to water, were used. The animals were deprived of water 1 h before the experiment and devided into: normal control group (n = 6) and experimental control group (n = 24). After fasted for 24 h, the rats of normal control group were lightly anesthetized with ether and tied up on the rat board, the abdomen was opened, the stomach was exposed and GMBF

was measured in the oxyntic gland area, and then gastric mucosa was sampled. The rats of experimental control group were devided into four subgroups (n = 6 in each group) and exposed to repeated WRS[3]. The rats of group I were lightly anesthetized with ether, tied up on the rat board and exposed to WRS for 4 h by placing in the water at 20-23 ℃ to the rat's xyphoid level at 10:00 am on the 1st d. Then the rats were anesthetized with pentobarbital (30 mg/kg ip), GMBF was measured and gastric mucosa was sampled. The rats of group II were treated similarly except that after WRS they were removed from the water, placed at room temprature, and refed with food and water until 10:00 am on the next day, at which time they were starved again for 24 h, and WRS was repeated. The rats of groups III and IV were exposed to the 3rd or 4th WRS as described above.

Measurement of GMBF

GMBF was measured by using laser Doppler flowmetry (LDF-3 flowmeter, Nankai University, Tianjin, China). In brief, the rats were anesthetized with pentobarbital (30 mg/kg ip), the abdomen was opened, the stomach was exposed and transected, and the gastric contents were gently evacuated to the exterior through the cut made in the stomach. Then, an optical probe was placed gently 0.5 mm above and perpendicular to the mucosal surface in the oxyntic gland area to monitor GMBF displayed in mV (value of Doppler signal voltage) on the digital panel of the flowmeter. After GMBF was stable, four points were selected for measurement (one point for 1 min) and the average value was calculated and expressed as *U/mV*.

Appreciation of UI

Mucosal lesions were evaluated by the score systems reported by Nie *et al*.[3]. Briefly, after the measurement of GMBF, the stomach was dissected out and opened along the greater curvature, then examined with a 10× magnifier for the presence of erosions and scored as follows: 1 point for small round hemorrhagic erosions; 2 points when the length of hemorrhagic erosions was less than 1 mm; 3 points when the length was 1-2 mm; 4 points when the length was 2-3 mm; 5 points when the length was longer than 4 mm; and the score value multiplied 2 when the width of erosions was larger than 1 mm.

Detection of mRNA in pS2,COX-2, iNOS and TGFα by RT-PCR

The stomachs were removed from rats with intact gastric mucosa and from those exposed to a single stress or repeated stresses. Mucosal specimens (about 100 mg) were scraped off using a slide glass and immediately snap frozen in liquid nitrogen and stored at -80 ℃ until analysis. Total RNA was isolated from mucosal samples using a guanidium isothiocyanate/phenol chloroform single step extraction kit from Stratagene (Gibco BRL, USA). Following precipitation, the RNA was resuspended in RNAse-free buffer and the concentration was estimated by absorbance at 260 nm wavelength. Furthermore, the quality of each RNA sample was determined by running the agarose fomaldehyde electrophoresis. RNA samples were stored at -80 ℃ until analysis.

Single-stranded complementary DNA (cDNA) was generated from 5 μg of total cellular RNA using StrataScript™ reverse transcripase (Gibco BRL, USA) and oligo (dT) primers (Gibco BRL, USA). Briefly, 5 μg of total RNA was used as the template to synthesize complementary DNA with 2.5 units of Maloney murine leukemia virus reverse transcriptase in 5 μL of buffer containing 10 mmol/L Tris-HCl (pH 8.3), 50 mmol/L KCl, 5 mmol/L $MgCl_2$,1 mmol/L of each deoxyribonucleaside triphospate, 2.5 mmol/L of oligo (dt) primers and 1.4 U/μL RNase blocker. Reverse-transcription was performed at room temperature for 20 min, then at 37 ℃ for 15 min, at 90 ℃ for 5 min and at 5 ℃ for min. The resulting cDNA was used as a template for subsequent PCR.

A 124-base pair (bp) fragment of pS2 was amplified from single-stranded DNA by PCR using two oligonucletide primers to pS2 sequence: sense primer, 5'-CCATGGAGCACAAGGTGA CCTG-3' and antisense primer, 5'-GGGAAGCCACAATTTAT TCT-3'. A 230-base pair (bp) fragment of COX-2 was amplified from single-stranded DNA by PCR using two oligonucletide primers to COX-2 sequence: sense primer, 5'-GCCACCTCTGCG ATGCTCTT-3' and antisense primer, 5'-GTGTTTGGGGTGGGC TTCAG-3'. A 576-base pair (bp) fragment of iNOS was amplified from single-stranded DNA by PCR using two oligonucletide primers to iNOS sequence: sense primer, 5'-GTGTTCCACCAGG AGATGTTG-3' and antisense primer, 5'-CTCCTGCCCACTGA GTTCGTC-3'. A 246-base pair (bp) fragment of TGFα was amplified from single-stranded DNA by PCR using two oligonucletide primers to TGFα sequence: sense primer, 5'-TCTGGGTACGTGGGTGTTCG-3'and antisense primer, 5'-AGAGTGGCAGCAGGCAGTCC-3'. Concomitantly, amplification of the 521 bp fragment of rat β-actin was performed on the same RNA samples to assess RNA integrity using two oligonucletide primers to β-actin sequence: sense primer, 5'-TGGGACGATATGGAGAAGAT-3' and antisense primer, 5'-ATTGCCGATAGTGATGACCT-3'. The nucleotide sequences of the primers for pS2, COX-2, iNOS and TGFα were based on the published cDNA sequences encoding pS2, COX-2, iNOS and TGFα[3,6,7]. The primers were synthesized by Bo-Ya Biotechnical Co. Ltd, Shanghai, China.

Reaction mixture for PCR contained cDNA template (2 μL), 50 pmoL of each primer, and 2.5 U of Termus aquaticus DNA (Promega) in 10 mmol/L Tris-HCl (pH 8.8), 50 mmol/L KCl, 1.5 mmol/L $MgCl_2$, 0.5 mmol/L dNTPs in a volume of 50 μL. RT blanks (no RNA included) were incubated in each analysis. The mixture was overlaid with 25 μL of mineral oil to prevent evaporation. Amplification was performed using a DNA thermal cycler for 35 cycles, each cycle consisting of denaturation for 2 min at 94 ℃, annealing for 45 s at 55 ℃ (pS2), 52 ℃ (COX-2 , iNOS) and 60 ℃ (TGFα), and extension for 1 min at 72 ℃. The final cycle included an extension for 5 min at 72 ℃ to ensure a full extension of the product. The number of amplification cycles was previously determined to keep amplification in the linear to avoid the "plateau effect" associated with increased number of PCR cycles.Eight microliters of each PCR product was electrophoresed on 16 g/L agarose gel stained with ethidium bromide, and then visualized under *uv* light. Location of predicted PCR products was confirmed by using DNA digest phix 174/Hae III as a stained size marker. The gel was then photographed under *uv* transillumination. In addition to size analysis by agarose gel electrophoresis, specificity of the primer pairs for pS2, COX-2, iNOS and TGFα was assessed by sequencing PCR products. For quantification, we determined the intensity of PCR products on the negative film of gel photographs according to Morrissey *et al*.[6]. Expression of the products was quantified using a video image analysis system (Tanon GIS-1000, Tanon Technical Co, Ltd, Shanghai, China). An index of mRNA expression was determined in each sample according to Konturek *et al*.[8].

Western blot analysis of pS2, COX-2, iNOS and TGFα proteins

Gastric tissues for the analysis of protein expressions of pS2, COX-2, iNOS and TGFα were homogenized in a proteinase inhibitor buffer containing 50 mmol/L Tris HCl (pH 7.5), 150 mmol/L NaCl, 5 g/L β-cholate sodium, 1 g/L SDS, 2 mmol/L EDTA, 10 mL/L Triton X-100, 100 g/L glycerol, 1 mmol/L PMSF and aprotinin, and then centrifuged at 10 000 *g* for 15 min at 4 ℃. The supernatant was collected and the protein content was determined with the dye-binding (Bio-Rad) method. Thirty micrograms of total protein was loaded onto SDS-polyacrylamide

gel and blotted onto hybrid C membranes (Amersham Life Science, Little Chalfont, Buckinghamshire, England) by electrophoresis. Pre-stained rainbrow recombinant protein molecular mass markers (Amersham International plc, Little Chalfont, Buckinghamshire, England) were used for molecular mass determinations. Membranes were blocked with blocking buffer containing 50 g/L fat free milk powder, 10 mmol/L Tris-HCl (pH 7.5), 100 mmol/L NaCl and 1 mL/L Tween 20 for 1 h at room temperature. The blots were incubated overnight at 4 ℃ with 1∶1 000 dilution of polycolonal antibodies against pS2 and TGFα (Stress-Gen, Victoria, Canada), monoclonal antibody against iNOS (Transduction Lab, Lexington, Kentucky, USA), polyclonal antibody against COX-2 (Santa Cruz Biotechnology INC, Santa Cruz, California, USA). After washed in washing buffer for 30 min, the membranes were treated with HRP conjugated secondary antibody (1∶4 000 dilution) (Bio-Rad) for 1 h at room temperature, followed by another 30 min of washing. The ECL Western blotting system (Amersham Life Sciences) was used in accordance with the manufacturer's instructions for chemiluminescence of proteins, and the blots were then exposed to photographic films.

Statistical analysis

Results were expressed as mean±SD. Statistical comparisons were made by Student's *t* test. Linear correlation analysis was used to analyse the relationship between two variants. *P* values less than 0.05 were considered statistically significant.

RESULTS

Damage to the surface of gastric epithelium with focal areas of deep haemorrhagic necrosis was induced by repeated WRS. The adaptative cytoprotection against stress was developed with activation of cell proliferation in the neck regions of gastric glands. The UI in groups II, III and IV was markedly reduced as compared with group I (I: 47.23±1.20; IV: 10.39±1.18, $P<0.01$). GMBF significantly decreased after the first exposure to WRS with a adaptive increasement of GMBF in experimental groups after repetitive challenges with WRS. After the 4th WRS, the value of GMBF almost restored to normal level (I: 321.87±8.85; IV: 455.95±11.81, $P<0.01$). The first WRS significantly decreased the expression of pS2 and significantly increased the expression of COX-2, iNOS and TGFα. After repeated WRS, pS2 and TGFα expressions gradually increased (pS2: I: 0.37±0.02; IV: 0.77±0.01; TGFα: I: 0.86±0.01; IV: 0.93±0.03, $P<0.05$) with a decrease in the expression of COX-2 and iNOS (COX-2: I: 0.45±0.02; IV: 0.22±0.01; iNOS: I: 0.93±0.01; IV: 0.56±0.01, $P<0.01$). The expressions of pS2, COX-2, iNOS and TGFα showed regular changes with a good relationship among them (decrease of COX-2 and iNOS was accompanied by an increased expression of pS2 and TGFα after 4 consecutive WRS). (Figure 1,Table 1).

DISCUSSION

The cytoprotective functions of pS2, COX-2, iNOS and TGFα in the gastrointestinal tract against ongoing damage may be accomplished in several ways, and there evidence is that thes factors participate in both the early phase of epithelial repair known as restitution (marked by increased cell migration but no proliferation), and in the subsequent protracted phase of glandular renewal (marked by proliferation, differentiation and migration)[9-11].

In this study, when WRS was applied once,it produced numerous gastric mucosal erosions, the adaptative cytoprotection against stress was developed after repeated stresses,and mucosal lesions were reduced markedly after the 2nd, 3rd and

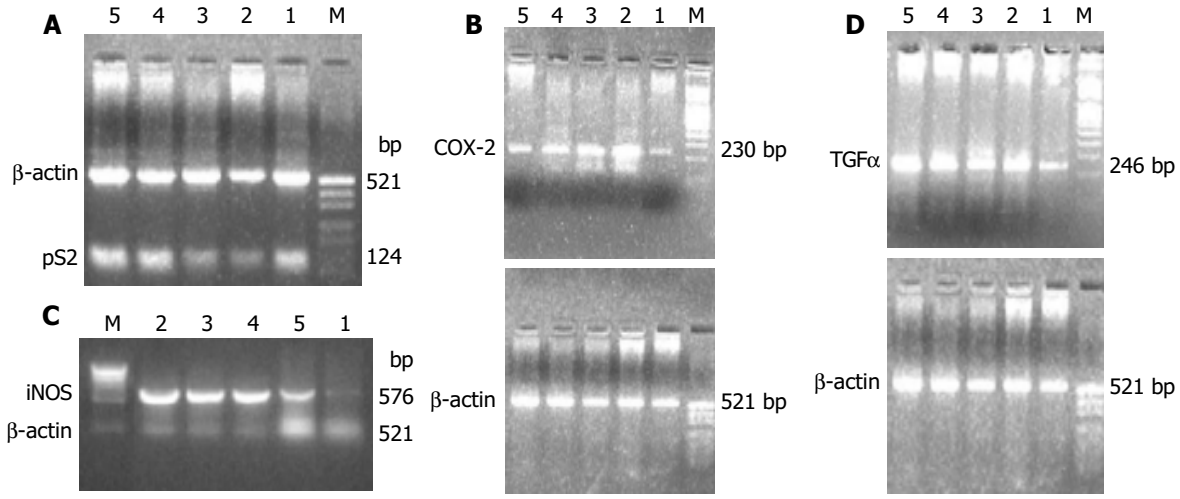

Figure 1 Expression of pS2 mRNA and β-actin (A), COX-2 mRNA and β-actin (B), iNOS mRNA and β-actin (C),TGFα mRNA and β-actin (D) in gastric mucosa of rats after repeated exposure to WRS and in control intact rats. Lane M: PCR size marker; Lane 1: control group; Lane 2-5: groups I-IV.

Table 1 Changes of gene expression of pS2, COX-2, iNOS, TGFα and GMBF, UI in gastric mucosa after repeated exposure to WRS

Group	GMBF (*U*/mV)	UI	iNOS	pS2	TGFα	COX-2
Control	484.01±10.97	0.00	0.16±0.01	0.63±0.01	0.26±0.01	0.10±0.01
Experimental						
I	321.87±8.85[b]	47.23±1.20	0.93±0.01[b]	0.37±0.02[b]	0.86±0.01[a]	0.45±0.02[b]
II	418.35±7.94[bd]	30.54±1.12[d]	0.78±0.01[bd]	0.42±0.01[bd]	0.87±0.02[ad]	0.38±0.02[bd]
III	446.09±10.98[bd]	20.75±1.54[d]	0.67±0.02[bd]	0.72±0.02[bd]	0.88±0.01[ad]	0.29±0.01[bd]
IV	455.95±11.81[bd]	10.39±1.18[d]	0.56±0.01[bd]	0.77±0.01[bd]	0.93±0.03[bc]	0.22±0.01[bd]

[a]$P<0.05$, [b]$P<0.01$ *vs* experimental control group; [c]$P<0.05$, [d]$P<0.01$ *vs* group I.

4th WRS. The expressions of COX-2, iNOS and TGFα were all up-regulated, but that of pS2 was down-regulated after the first stress in rats with WRS-induced ulcers. But the major finding of this study was the gastric adaptation to WRS involving a gradually decrease of overexpression of COX-2 and iNOS, and a gradually increase of expression of pS2 and TGFα, and an increased rate of cell proliferation in the gastric mucosa.

Members of the trefoil peptide family, including pS2, share a common structural feature, which is a motif of six cysteine residues termed a trefoil or a P domain. There is increasing evidence that trefoil peptides are important in maintaining the integrity of gastric mucosae and involved in the repair of ulcerated areas in the gastrointestinal tract[12-16]. This is supported by an observation that an increased expression of trefoil peptides was found in the ulcer-associated cell lineage (UACL), which is a glandular structure adjacent to the ulcerated mucosa[17], and by the findings from *in vitro* studies showing that trefoil peptides exhibited a mitogenic effect on different cell lines[18,19]. It has also been reported that the trefoil peptide family could contribute to gastric mucosal defence and repair by affecting cell proliferation[1,20].

It has been found that NO produced from inflammatory cells by the inducible isoforms of NOS has antimicrobial, antitumor and cytotoxic effects, but an excessive amount may lead to peroxynitrite formation, protein tyrosine nitration, hydroxyl radical production and tissue damage[21]. The present study also demonstrated that overexpression of iNOS on d 1 after the first stress was accompanied with the enlargement of ulcer crater. The expression of iNOS protein was declined when the ulcer began to heal. High expression and enzymatic activity of COX at the late ulcer healing stage were observed in stress. The changes of COX activity might be mainly due to the changes of protein level and activity of COX-2. Since tissue remodeling including reepithelization of gastric mucosa, maturation of granulation tissue, and reconstruction of extracellular matrix mainly occurs at the late ulcer healing stage, COX-2 plays an essential role in these remodeling processes[5,22-31].

There may be interactions among pS2, COX-2, iNOS and TGFα. In the present study, after the 4th WRS, GMBF almost restored to normal level, and during the process of tolerant cytoprotection, GMBF, UI and expressions of pS2, COX-2, iNOS and TGFα showed regular changes and a good relationship among them. A dramatic decrease of COX-2 and iNOS was accompanied with an increase expression of pS2 and TGFα after the 4th stress. This inverse relationship between COX-2, iNOS and pS2, TGFα expressions support the existence of a close interaction among these factors.

Trefoil peptides are a new class of regulatory peptides involving mucosal protection and repair in the gastrointestinal tract. NO and epithelium-associated mucin have important roles in sustaining mucosal integrity in the gastrointestinal tract,and trefoil peptide modulate epithelial NO production via the iNOS pathway[32-35].

Treatment with COX-2 inhibitors and COX-2 antisense oligonucleotides could suppress these responses induced by TGFα, suggesting the involvement of COX-2 in proliferation of gastric mucosal epithelium,and the synergistic stimulation of COX-2 expression by TGFα. Gut epithelial COX-2 could be rapidly induced by inflammatory stimuli, interleukin and TGFα[4,36-40].

We confirmed that WRS-adapted mucosae exhibited an augment action of GMBF, but it is not clear whether COX-2, iNOS and pS2 could directly or indirectly account for the mucosal adaptation, or what is the mechanism of this mucosal hyperemia in the stomach. TGFα has been shown to increase GMBF[41], while trefoil peptides could promote synthesis of TGFα[42-48]. Hence, we believe that hyperaemia observed during the development of adaptation might be mediated by the release of COX-2, iNOS and pS2.

In summary, different expressions of pS2, COX-2, iNOS and TGFα occur during gastric ulceration and healing. COX-2 and iNOS may contribute to tissue inflammation during ulcer formation, while pS2 and TGFα may promote ulcer healing by proliferation, since their expressions are correlated with the protracted phase of glandular renewal of ulcer tissues.

REFERENCES

1 **Konturek PC.** Physiological, immunohistochemical and molecular aspects of gastric adaptation to stress, aspirin and to *H pylori*-derived gastrotoxins. *J Physiol Pharmacol* 1997; **48**: 3-42

2 **Nie S,** Li Z, Zhan X, Tu Z, Xu G, Gong Y, Man X. Role of the pS (2) in gastric mucosa adaptative cytoprotection from stress. *Zhonghua Yixue Zazhi* 2002; **82**: 172-175

3 **Nie SN,** Qian XM, Wu XH, Yang SY, Tang WJ, Xu BH, Huang F, Lin X, Sun DY, Sun HC, Li ZS. Role of TFF in healing of stress-induced gastric lesions. *World J Gastroenterol* 2003; **9**: 1772-1776

4 **Konturek SJ,** Brzozowski T, Majka J, Dembinski A, Slomiany A, Slomiany BL. Transforming growth factor alpha and epidermal growth factor in protection and healing of gastric mucosal injury. *Scand J Gastroenterol* 1992; **27**: 649-655

5 **Franco L,** Talamini G, Carra G, Doria D. Expression of COX-1, COX-2, and inducible nitric oxide synthase protein in humangastric antrum with *Helicobacter pylori* infection. *Prostaglandins Other Lipid Mediat* 1999; **58**: 9-17

6 **Morrissey JJ,** McCracken R, Kaneto H, Vehaskari M, Montani D, Klahr S. Location of an inducible nitric oxide synthase mRNA in the normal kidney. *Kidney Int* 1994; **45**: 998-1005

7 **Brzozowski T,** Konturek PC, Konturek SJ, Stachura J. Gastric adaptation to aspirin and stress enhances gastric mucosal resistance against the damage by strong irritants. *Scand J Gastroenterol* 1996; **31**: 118-125

8 **Konturek PC,** Brzozowski T, Pierzchalski P, Kwiecien S, Pajdo R, Hahn EG, Konturek SJ. Activation of genes for spasmolytic peptide, transforming growth factor alpha and for cyclooxygenase (COX)-1 and COX-2 during gastric adaptation to aspirin damage in rats. *Aliment Pharmacol Ther* 1998; **12**: 767-777

9 **Podolsky DK.** Mucosal immunity and inflammation. V. Innate mechanisms of mucosal defense and repair: the best offense is a good defense. *Am J Physiol* 1999; **277**(3 Pt 1): G495-499

10 **Wright NA.** Aspects of the biology of regeneration and repair in the human gastrointestinal tract. *Philos Trans R Soc Lond B Biol Sci* 1998; **353**: 925-933

11 **Podolsky DK.** Healing the epithelium: solving the problem from two sides. *J Gastroenterol* 1997; **32**: 122-126

12 **Farrell JJ,** Taupin D, Koh TJ, Chen D, Zhao CM, Podolsky DK, Wang TC. TFF2/SP-deficient mice show decreased gastric proliferation, increased acid secretion, and increased susceptibility to NSAID injury. *J Clin Invest* 2002; **109**: 193-204

13 **Ulaganathan M,** Familari M, Yeomans ND, Giraud AS, Cook GA. Spatio-temporal expression of trefoil peptide following severe gastric ulceration in the rat implicates it in late-stage repair processes. *J Gastroenterol Hepatol* 2001; **16**: 506-512

14 **Longman RJ,** Douthwaite J, Sylvester PA, Poulsom R, Corfield AP, Thomas MG, Wright NA. Coordinated localisation of mucins and trefoil peptides in the ulcer associated cell lineage and the gastrointestinal mucosa. *Gut* 2000; **47**: 792-800

15 **McKenzie C,** Thim L, Parsons ME. Topical and intravenous administration of trefoil factors protect the gastric mucosa from ethanol-induced injury in the rat. *Aliment Pharmacol Ther* 2000; **14**: 1033-1040

16 **Cook GA,** Thim L, Yeomans ND, Giraud AS. Oral human spasmolytic polypeptide protects against aspirin-induced gastric injury in rats. *J Gastroenterol Hepatol* 1998; **13**: 363-370

17 **Alison MR,** Chinery R, Poulsom R, Ashwood P, Longcroft JM, Wright NA. Experimental ulceration leads to sequential expression of spasmolytic polypeptide, intestinal trefoil factor, epidermal growth factor and transforming growth factor alpha mRNAs in rat stomach. *J Pathol* 1995; **175**: 405-414

18 **Chinery R,** Coffey RJ. Trefoil peptides: less clandestine in the intestine. *Science* 1996; **274**: 204

19 **Mashimo H,** Wu DC, Podolsky DK, Fishman MC. Impaired defense of intestinal mucosa in mice lacking intestinal trefoil factor. *Science* 1996; **274**: 262-265

20 **Modlin IM,** Poulsom R. Trefoil peptides: mitogens, motogens, or mirages? *J Clin Gastroenterol* 1997; **25**(Suppl 1): S94-100

21 **Fischer H,** Huber V, Boknik P, Luess H, Neumann J, Schmitz W, Domschke W, Konturek JW. Effect of *Helicobacter pylori* eradication on cyclooxygenase 2 (COX-2) andinducible nitric oxide synthase (iNOS) expression during gastric adaptation toaspirin (ASA) in humans. *Microsc Res Tech* 2001; **53**: 336-342

22 **Brzozowski T,** Konturek PC, Moran AP, Kwiecien S, Pajdo R, Konturek SJ, Drozdowicz D, Ptak A, Pawlik W, Hahn EG. Enhanced resistance of gastric mucosa to damaging agents in the rat stomach adapted to *Helicobacter pylori* lipopolysaccharide. *Digestion* 2003; **67**: 195-208

23 **Helmer KS,** Cui Y, Chang L, Dewan A, Mercer DW. Effects of ketamine/xylazine on expression of tumor necrosis factor-alpha, inducible nitric oxide synthase, and cyclo-oxygenase-2 in rat gastric mucosaduring endotoxemia. *Shock* 2003; **20**: 63-69

24 **Slomiany BL,** Slomiany A. Platelet-activating factor modulates gastric mucosal inflammatory responses to *Helicobacter pylori* lipopolysaccharide. *Biochem Biophys Res Commun* 2003; **306**: 261-266

25 **Slomiany BL,** Slomiany A. Suppression of gastric mucosal inflammatory responses to *Helicobacter pylori* lipopolysaccharide by peroxisome proliferator-activated receptor gamma activation. *IUBMB Life* 2002; **53**: 303-308

26 **Yang R,** Gallo DJ, Baust JJ, Watkins SK, Delude RL, Fink MP. Effect of hemorrhagic shock on gut barrier function and expression of stress-related genes in normal and gnotobiotic mice. *Am J Physiol Regul Integr Comp Physiol* 2002; **283**: R1263-1274

27 **van der Woude CJ,** Jansen PL, Tiebosch AT, Beuving A, Homan M, Kleibeuker JH, Moshage H. Expression of apoptosis-related proteins in Barrett's metaplasia-dysplasia-carcinoma sequence: a switch to a more resistant phenotype. *Hum Pathol* 2002; **33**: 686-692

28 **Shen X.** Effects of cyclooxygenase-2 on formation and healing of acetic acid-inducedgastric ulcer in rats. *Zhonghua Yixue Zazhi* 2001; **81**: 1380-1383

29 **Yamamoto H,** Tanaka A, Kunikata T, Hirata T, Kato S, Takeuchi K. Inducible types of cyclooxygenase and nitric oxide synthase in adaptive cytoprotection in rat stomachs. *J Physiol Paris* 1999; **93:** 405-412

30 **Fu S,** Ramanujam KS, Wong A, Fantry GT, Drachenberg CB, James SP, Meltzer SJ, Wilson KT. Increased expression and cellular localization of inducible nitric oxidesynthase and cyclooxygenase 2 in *Helicobacter pylori* gastritis. *Gastroenterology* 1999; **116**: 1319-1329

31 **Ferraz JG,** Sharkey KA, Reuter BK, Asfaha S, Tigley AW, Brown ML, McKnight W, Wallace JL. Induction of cyclooxygenase 1 and 2 in the rat stomach during endotoxemia: rolein resistance to damage. *Gastroenterology* 1997; **113**: 195-204

32 **Zhang BH,** Yu HG, Sheng ZX, Luo HS, Yu JP. The therapeutic effect of recombinant human trefoil factor 3 on hypoxia-inducednecrotizing enterocolitis in immature rat. *Regul Pept* 2003; **116**: 53-60

33 **Tan XD,** Liu QP, Hsueh W, Chen YH, Chang H, Gonzalez-Crussi F. Intestinal trefoil factor binds to intestinal epithelial cells and inducesnitric oxide production: priming and enhancing effects of mucin. *Biochem J* 1999; **338**(Pt 3): 745-751

34 **Wolfe MM.** Future trends in the development of safer nonsteroidal anti-inflammatory drugs. *Am J Med* 1998; **105**: 444S-452S

35 **Modlin IM,** Hunt RH. Critical reappraisal of mucosal repair mechanisms. *Scand J Gastroenterol Suppl* 1995; **210**: 28-31

36 **Konturek PC,** Brzozowski T, Kwiecien S, Drozdowicz D, Harsch IA, Meixner H, Stachura J, Hahn EG, Konturek SJ. Effect of *Helicobacter pylori* on delay in ulcer healing induced by aspirin in rats. *Eur J Pharmacol* 2002; **451**: 191-202

37 **Akiba S,** Hatazawa R, Ono K, Kitatani K, Hayama M, Sato T. Secretory phospholipase A2 mediates cooperative prostaglandin generation bygrowth factor and cytokine independently of preceding cytosolic phospholipase A2expression in rat gastric epithelial cells. *J Biol Chem* 2001; **276**: 21854-21862

38 **Sawaoka H,** Tsuji S, Tsujii M, Gunawan ES, Kawai N, Sasaki Y, Hori M, Kawano S. Involvement of cyclooxygenase-2 in proliferation and morphogenesis induced bytransforming growth factor alpha in gastric epithelial cells. *Prostaglandins Leukot Essent Fatty Acids* 1999; **61:** 315-322

39 **Takahashi S,** Shigeta J, Ishikawa M, Kobayashi N, Okabe S. Role of thromboxane A2 in healing of gastric ulcers in rats. *Jpn J Pharmacol* 1999; **79**: 101-107

40 **Bamba H,** Ota S, Kato A, Matsuzaki F. Nonsteroidal anti-inflammatory drugs may delay the repair of gastric mucosa by suppressing prostaglandin-mediated increase of hepatocyte growth factor production. *Biochem Biophys Res Commun* 1998; **245**: 567-571

41 **Tepperman BL,** Soper BD. Effect of epidermal growth factor, transforming growth factor alpha and nerve growth factor on gastric mucosal integrity and microcirculation in the rat. *Regul Pept* 1994; **50**: 13-21

42 **Taupin D,** Pedersen J, Familari M, Cook G, Yeomans N, Giraud AS. Augmented intestinal trefoil factor (TFF3) and loss of pS2 (TFF1) expressionprecedes metaplastic differentiation of gastric epithelium. *Lab Invest* 2001; **81**: 397-408

43 **Kato K,** Chen MC, Nguyen M, Lehmann FS, Podolsky DK, Soll AH. Effects of growth factors and trefoil peptides on migration and replication inprimary oxyntic cultures. *Am J Physiol* 1999; **276**(5 Pt 1): G1105-1116

44 **Jones MK,** Tomikawa M, Mohajer B, Tarnawski AS. Gastrointestinal mucosal regeneration: role of growth factors. *Front Biosci* 1999; **4**: D303-309

45 **Cook GA,** Yeomans ND, Giraud AS. Temporal expression of trefoil peptides in the TGF-alpha knockout mouse aftergastric ulceration. *Am J Physiol* 1997; **272**(6 Pt 1): G1540-1549

46 **Goldenring JR,** Poulsom R, Ray GS, Wright N, Meise KS, Coffey RJ Jr. Expression of trefoil peptides in the gastric mucosa of transgenic miceoverexpressing transforming growth factor-alpha. *Growth Factors* 1996; **13**: 111-119

47 **Sarraf CE,** Alison MR, Ansari TW, Wright NA. Subcellular distribution of peptides associated with gastric mucosal healing andneoplasia. *Microsc Res Tech* 1995; **31**: 234-247

48 **Poulsom R,** Wright NA. Trefoil peptides: a newly recognized family of epithelial mucin-associatedmolecules. *Am J Physiol* 1993; **265**(2 Pt 1): G205-213

Edited by Wang XL and Kumar M **Proofread by** Xu FM